CHAPTER 1.
INTRODUCTION

1.1. PURPOSE, LOCATION, AND MAJOR PHYSIOGRAPHIC AND GEOLOGIC FEATURES

1.1.1. Purpose

The purpose of this report is to provide state-of-practice information on the hydrogeologic* framework of an area of New Mexico, Trans-Pecos Texas, and Chihuahua (MEX) that is informally named the Mesilla Basin region (MBR) herein (**Figs. 1-1** and **1-2**). The MBR includes a group of large intermontane basins that are linked by the valleys and canyons of the Rio Grande/Bravo (RG/RB) fluvial system. The report is the latest in a series of NM Water Resources Research Institute (NM WRRI)-supported hydrogeologic investigations in the MBR (e.g., Hawley et al. 2000, Hawley and Kennedy 2004, Hawley et al. 2005 and 2009). Emphasis is on advances in the development of hydrogeologic-framework models (conceptual and digital) in a 3,350-mi^2 (8,675-km^2) NM WRRI Study Area (Fig. 1-3),

Hydrogeology (hydrogeologic): The branch of geology that deals with the distribution and movement of groundwater* in the soil and rocks of the Earth's crust (commonly in aquifers – See **Table 1-2**).*
https://en.wikipedia.org/wiki/Hydrogeology

The format of the Report is designed to convey basic hydrogeologic information on (1) the hydrostratigraphy and lithologic character of basin-fill deposits, and (2) geohydrologic-boundary conditions at levels of detail appropriate for ongoing development of basin-scale (~1:100,000) numerical models of groundwater (GW)-flow and hydrochemical systems. The more than 1000 source documents that are cited in the body of the Report and its 8 Appendices provide a robust scientific foundation for the hydrogeologic interpretations made herein. Geohydrologists and hydrochemists comprise only part of a diverse audience that includes water-resource managers and water-law specialists, and all others who rely on GW resources for their water uses. Because of *target-audience* diversity, a glossary (**APNDX. G**) of more than 220 *geospecialty* terms is also included.

1.1.2. Location

Figure 1-3 (page-size **PL. 2A**) is a Study Area index map on a hydrogeologic DEM base, with 10,000 m UTM-Zone 13 NAD83 and latitude/longitude coordinates (*cf.* **PL. 1**). Its UTM Zone 13N (NAD 1983) boundary coordinates are respectively 3,504,000 m and 3,611,000 m northing, and 302,000 m and 367,000 m easting. The Mesilla, Southern Jornada, and El Parabién groundwater (GW) basins (MeB, SJB, and EPB) are outlined in green, orange and red, respectively (*cf.* **Figs. 1-8** and **1-9**). Locations of Hydrogeologic Cross-Sections **A-A'** to **S-S' (PLS. 5a** to **5s**) are shown, as are the El Paso/Ciudad Juárez and Las Cruces metropolitan centers (2020 pop. >2 million). Major fluvial-terrain features include the Mesilla Valley (MeV), Selden Canyon (SCyn), and El Paso del Norte (EPdN) of the Rio Grande.

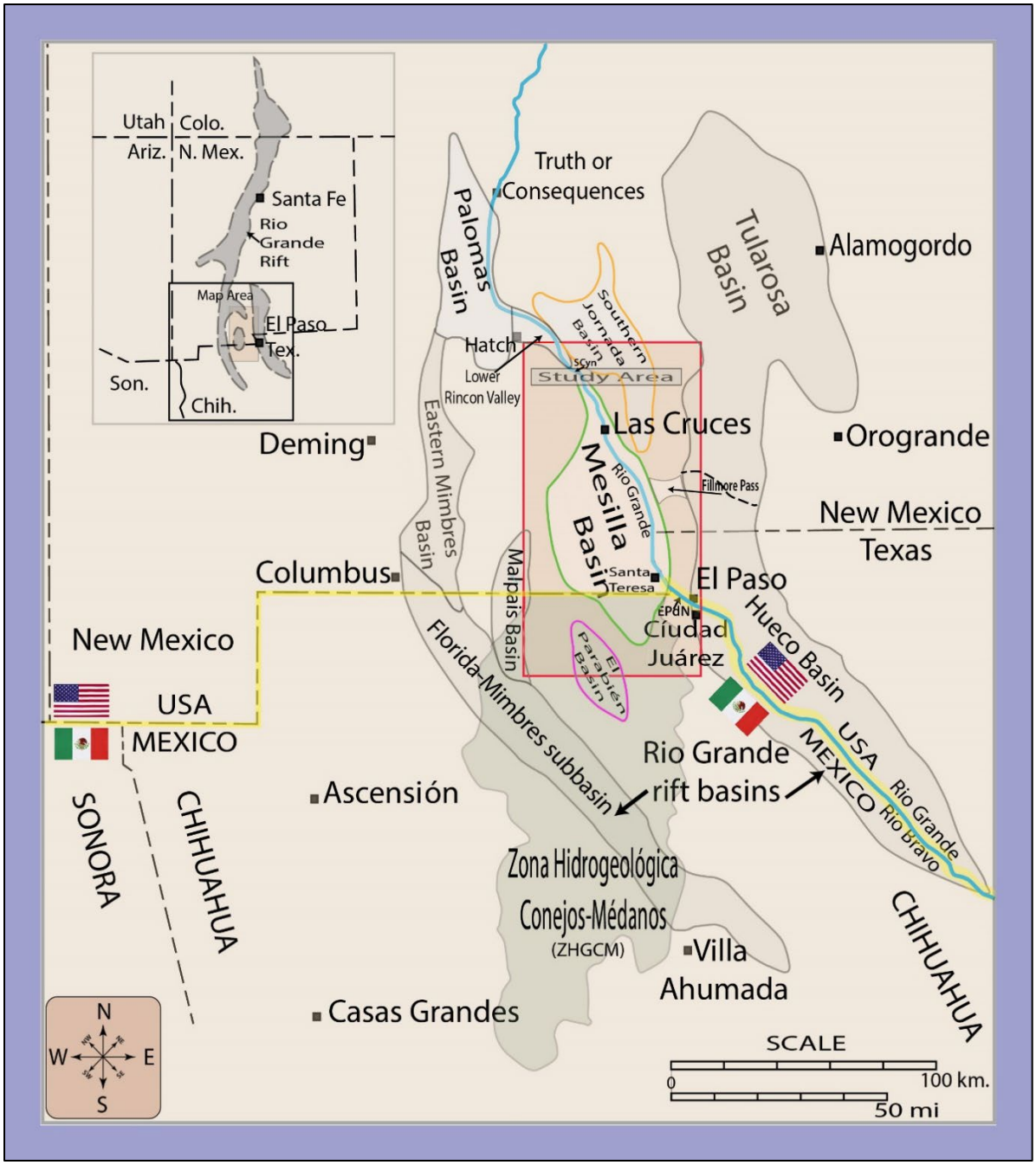

Figure 1-1. Index map for the United States-Mexico borderlands region that covers parts of southern New Mexico, western Texas, northern Chihuahua, and northeastern Sonora. Major political boundaries and selected population centers are shown, respectively, with black dashed lines and small squares. The blue line shows the general position of the Rio Grande/Bravo channel; and the NM WRRI Study Area (**Fig. 1-3**) is outlined in magenta. The small inset map in the upper-left corner shows the location of the Rio Grande rift (RG-rift) tectonic province. Outlines of major structural basins in the southern RG-rift province are based on Seager and Morgan (1979, Fig. 1); and names and outlines of the El Parabién Basin, Malpais Basin, and Florida-Mimbres subbasin are from Jiménez and Keller (2000), Seager (1989), and Averill and Miller (2013), respectively. The southern Mesilla GW Basin extends into Chihuahua's "Zona Hidrogeológica de Conejos Médanos (ZHGCM)," which is shown with light-gray shading.

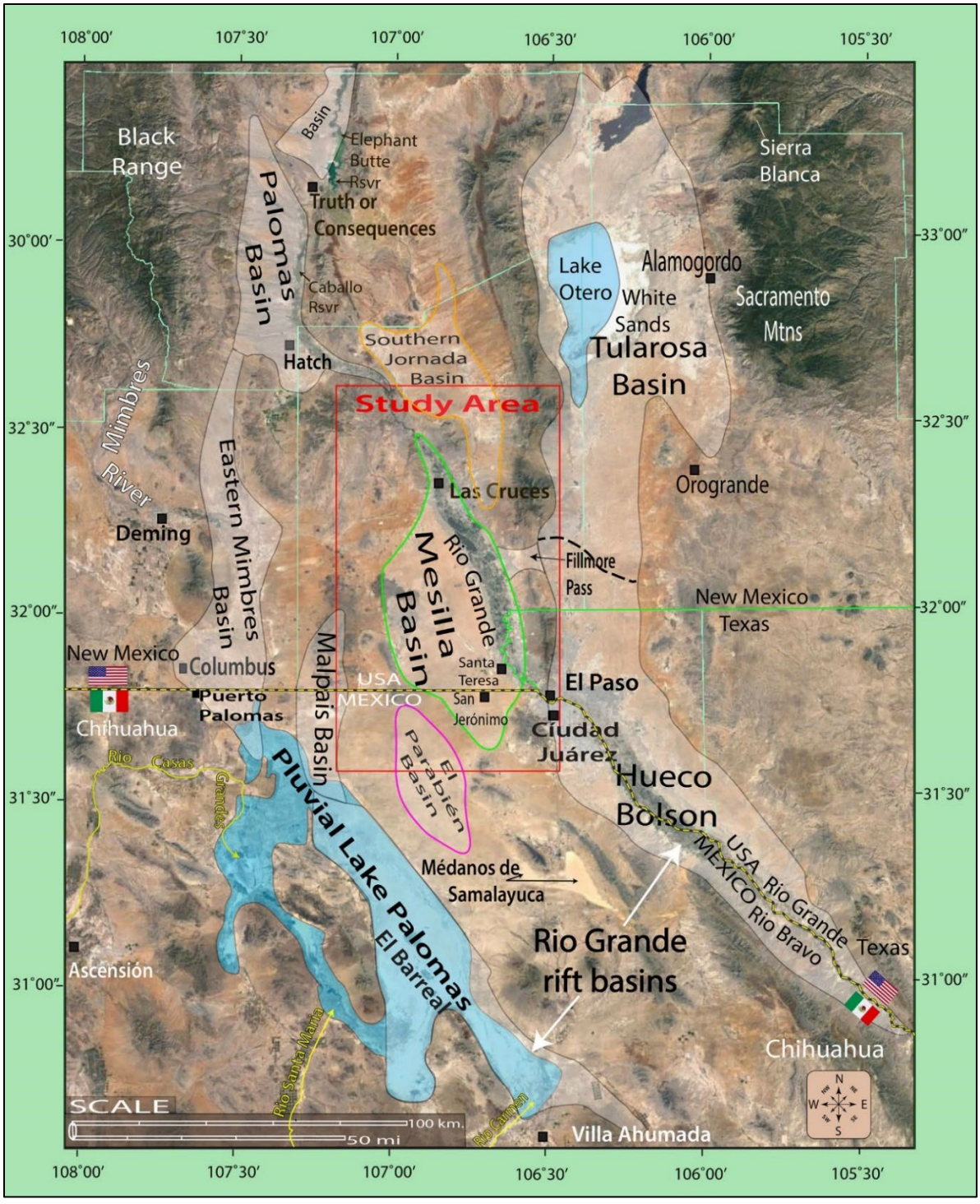

Figure 1-2 (Frontispiece)**.** Index map of the Mesilla Basin region (MBR) showing locations of the Study Area (**Fig. 1-3**, red outline), major landscape features in the northern Mexican Highland section of the B&R province, and basins of the southern RG-rift province (**Fig. 1-1**). Blue shading shows the approximate extent of the areas inundated by pluvial-Lakes Palomas and Otero at their respective Late Pleistocene high stands in the Zona Hidrogeológica de Conejos Médanos/El Barreal basin complex, and the Tularosa Basin. Swanson Geoscience, LLC compilation on a 2017 Google Earth® image-base. EPdN=El Paso del Norte.

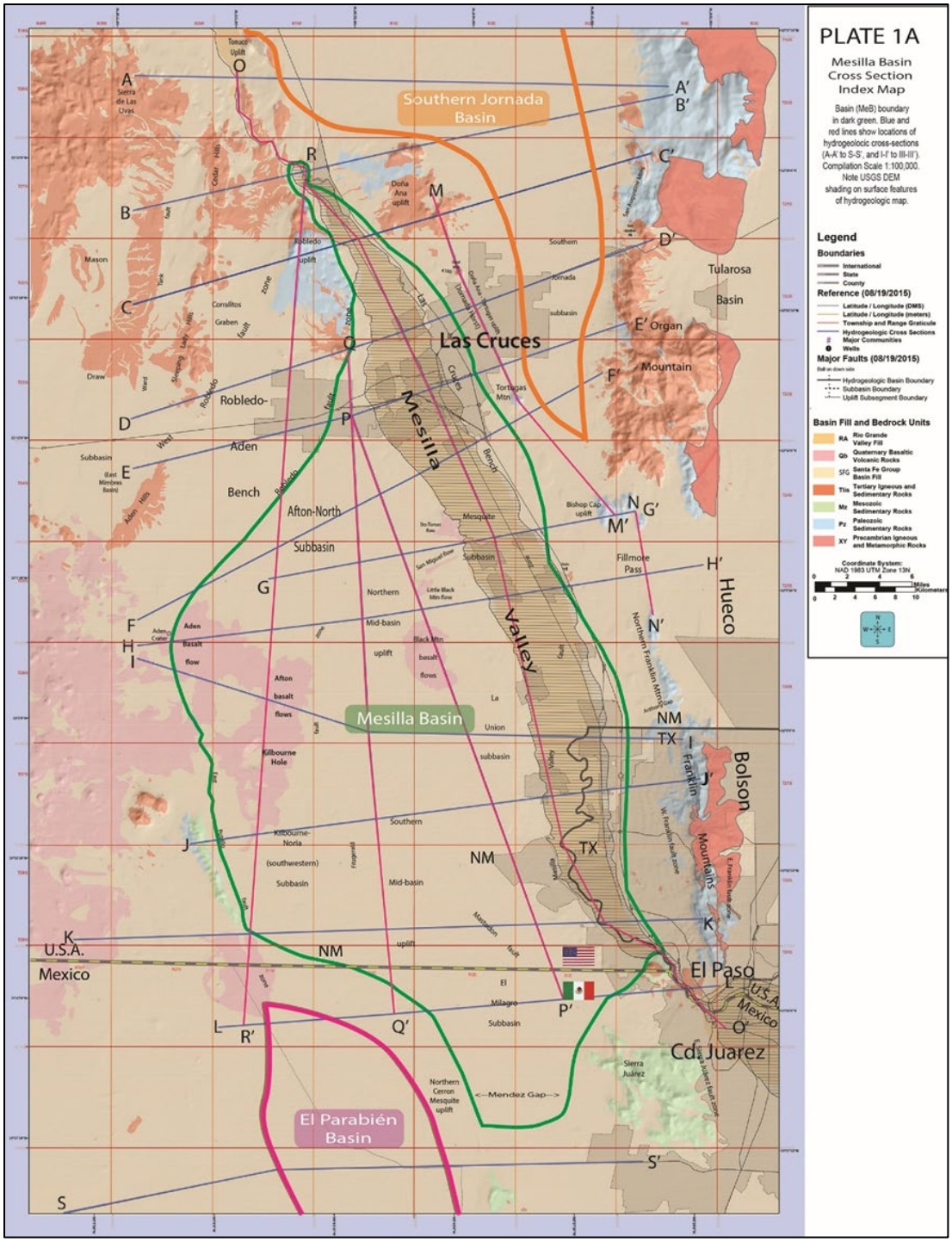

Figure 1-3. Study Area index map showing locations of the Mesilla, Southern Jornada, and El Parabién groundwater (GW) basins (MeB, SJB and EPB; outlined in green, orange, and red, respectively). Also shown are the locations of hydrogeologic cross-section **A-A'** to **S-S' (**Report **PLATES 5a** to **5s**), major terrain features (incl. the Mesilla Valley, Selden Canyon and El Paso del Norte of the Rio Grande), and the Las Cruces and El Paso/Ciudad Juárez metropolitan centers. USGS DEM base, with UTM-NAD83 SI-system and latitude/longitude coordinates.

1.1.3. Major Physiographic and Geologic Features

The MBR is in the southern Rio Grande (RG) rift tectonic province of south-central New Mexico, western Texas, and northern Chihuahua (**Figs. 1-1, 1-2** and **1-4**). It is also in the Mexican Highland section of the eastern Basin and Range (B&R) physiographic province, and the northern part of the arid to semiarid Chihuahuan Desert ecoregion (**Fig. 1-4**, **Parts 3.2** and **3.3**). Acronym codes for major B&R terrain features and RG-rift basins shown on **Figure 1-4** are listed in **Table 1-1**.

The 2017 Google Earth® image-base for **Figure 1-2** facilitates portrayal of major terrain features in the MBR of the RG-rift tectonic province. The NM WRRI Study Area (**Fig. 1-3**) is in the beige rectangle, and RG-rift basins shown on **Figures 1-1** to **1-4** are identified. The Mesilla Valley (MeV) of the Rio Grande occupies much of the eastern Mesilla Basin. Blue shading shows the approximate extent of the areas inundated by pluvial-Lakes Otero and Palomas at their respective high stands in the Tularosa Basin and the Los Muertos Basin area of Chihuahua during the last Pleistocene glacial-pluvial interval (~29 to 12 thousand years ago [ka]). The maximum extent of Lake Otero is estimated to have been about 745 mi^2 (1,930 km^2), and that of Lake Palomas about 3,000 mi^2 (7,770 km^2) (*cf.* **Part 3.3.2**).

Because of the need for proactive GW-resource conservation,* detailed characterization of aquifer systems in the RG-rift basins has been of primary concern. Upper Cenozoic Santa Fe Group (SFG) fill of RG-rift basins, and Late Quaternary alluvial deposits of the inner Rio Grande Valley form the MBR's only significant GW reservoirs. The hydrogeologic-framework of these systems is defined in terms of (1) the lithologic and hydrostratigraphic properties, (2) the primary bedrock foundation components (lithologic and structural) of rift-basin boundaries, and (3) the quantity and quality of the surface- and subsurface-water regimes.

**A careful preservation and protection of something, especially planned management of a natural resource to prevent exploitation, destruction, or neglect—e.g., water conservation.*
https://www.merriam-webster.com/dictionary/coservation

1.2. GROUNDWATER BASINS: HYDROGEOLOGIC AND NM OFFICE OF THE STATE ENGINEER ADMINISTRATIVE

1.2.1. Groundwater (GW) Basins Defined in a Hydrogeologic Context

The USGS-WRD Regional Aquifer-Systems Analysis (RASA)—Southwest Alluvial Basins (SWAB) Program has had a major impact on development of new-generation conceptual and digital models of intermontane-basin hydrogeologic systems throughout the eastern Basin and Range and Rio Grande-rift provinces (*cf.* Gates et al. 1984**,** Freethey et al. 1986). The following selections from (**1.**) Wilkins (1986, p. 2), and (**2.**) Frenzel and Kaehler (1992, p. iii), summarize the RASA program's purpose and scope (*cf.* **APNDX. C5.3**):

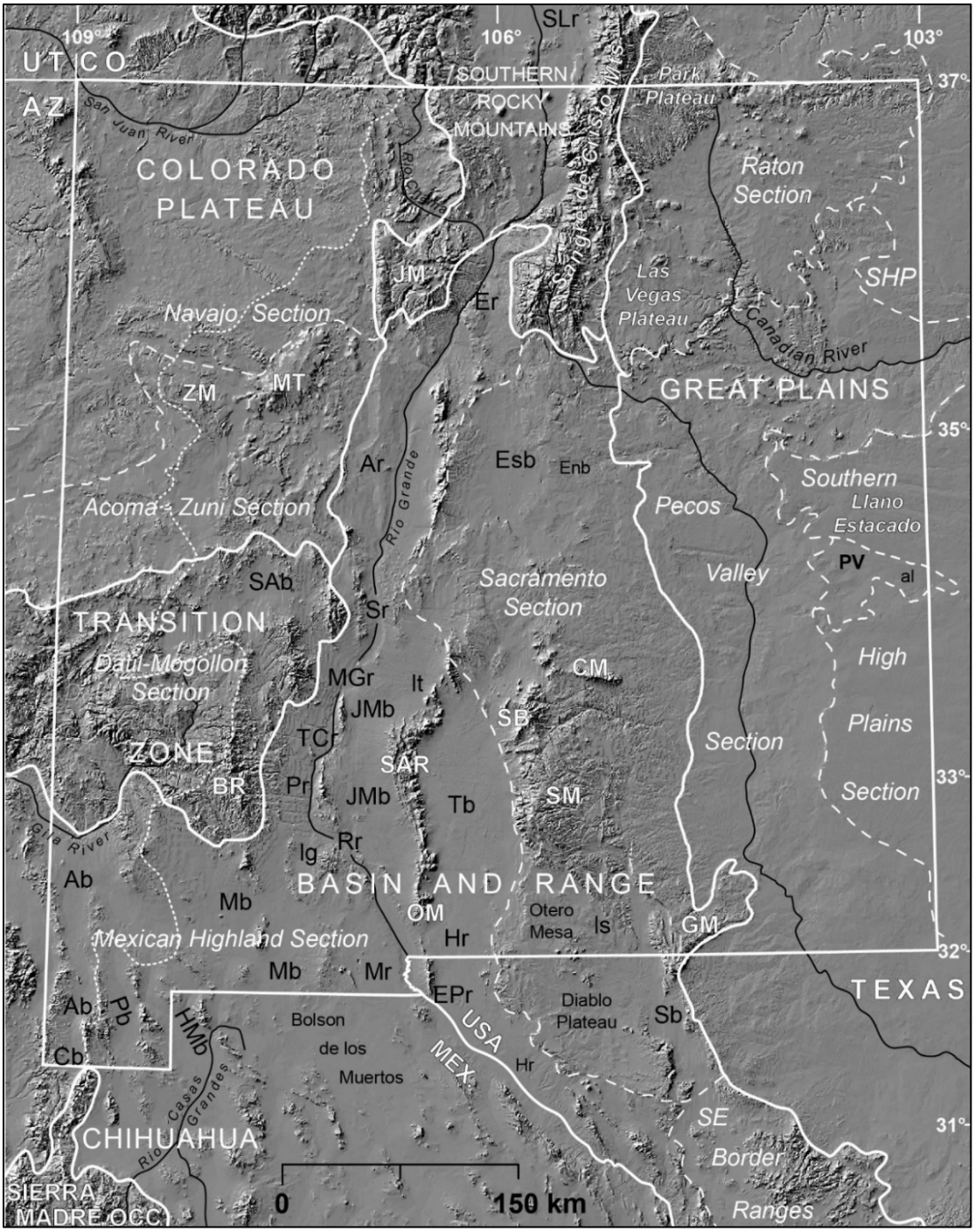

Figure 1-4 (Hawley 2005, FIG. 1)**.** Index map showing locations of physiographic provinces and their section subdivisions, and major landscape features in the binational New Mexico region. Province and political boundaries are shown by bold-white lines. A section of the Sierra Madre Occidental province in Chihuahua and Sonora is in the map's SW corner. Dashed-white lines show physiographic-section borders; the dotted-white line is the Continental Divide, and major rivers are delineated in black. Letter codes keyed to **Table 1-1** show locations of *Basins with Pluvial Lakes*, RG-rift Basins, and Mountains and Ranges (*cf.* **Fig. 3-1**). USGS 250-m DEM base.

Table 1-1. (Modified from Hawley 2005, TBL. 1) Index to (1) Physiographic and Tectonic Provinces, and (2) Major Terrain and Landform Features that are shown on Figure 1-4

Symbol	Basins and Physiographic Features		Physiographic Province & Section/Tectonic Province
	Basins with *Pluvial Lakes*		
SAb	San Agustín Plains	*San Agustín*	Transition Zone/Datil-Mogollon
Ab	Animas	*Animas*	Mexican Highland
Cb	Cloverdale (San Luis)	*Cloverdale*	
	Bolson del los Muertos*	*Palomas*	Mexican Highland/Rio Grande rift
Pr	Palomas	*Goodsight*-**lg**	Mexican Highland/Rio Grande rift
HMb	Hachita-Moscos	*Hachita*	Mexican Highland
JMb	Jornada del Muerto	*Trinity*-**lt**	Mexican Highland/Rio Grande rift
Mb	Lower Mimbres River	*Palomas*	
Pb	Playas	*Playas*	Mexican Highland
Tb	Tularosa	*Otero*	Mexican Highland/Rio Grande rift
Esb	Estancia	*Estancia*	Sacramento
Enb	Encino	*Encino*	Sacramento
	Lower Sacramento Rv	*Sacramento*-**ls**	Sacramento
Sb	Salt	*King*	Sacramento
PV	Portales Valley	*Arch*-**al**	Great Plains/Southern High Plains
	Rio Grande Rift Basins/Canyons/Narrows		
SLr	San Luis		Southern Rocky Mountains/ Rio Grande rift
Er	Española		Mexican Highland/Rio Grande rift
Ar	Albuquerque (Santo Domingo & Belen subbasins)		Mexican Highland/Rio Grande rift
Sr	Socorro		Mexican Highland/Rio Grande rift
MGr	Milligan Gulch basin		Mexican Highland/Rio Grande rift
TCr	Truth or Consequences "narrows"		Mexican Highland/Rio Grande rift
Pr	Palomas		Mexican Highland/Rio Grande rift
Rr	Rincon-Valley		Mexican Highland/Rio Grande rift
Mr	Mesilla		Mexican Highland/Rio Grande rift
EPr	El Paso del Norte "canyon"		Mexican Highland/Rio Grande rift
Hr	Hueco Bolson		Mexican Highland/Rio Grande rift
	Mountains and Ranges		
BR	Black Range		Transition Zone/Datil-Mogollon
CM	Capitan Mountains		Sacramento
JM	Jemez Mountains & Valles caldera		Southern Rocky Mountains
MT	Mount Taylor		Colorado Plateau/Acoma-Zuni
OM	Organ Mountains		Mexican Highland
SAR	San Andres Range		Mexican Highland
SB	Sierra Blanca		Sacramento
SM	Sacramento Mountains		Sacramento
ZM	Zuni Mountains		Colorado Plateau

*****_Note on use of terms "Bolson de los Muertos (BdLM)" and "Los Muertos Basins:" C.C. Reeves (1969, p. 147) informally proposed the name "Bolson del los Muertos" for a structural-basin complex in the Puerto Palomas-El Barreal area of the Zona Hidrogeológica de Conejos Médanos (ZHGCM). It is here recomended that, in the future, the terms "Bolson de los Muertos" and/or "Los Muertos Basin" should only be used in a Rio Grande-rift tectonic province context (e.g., **Figs. 1-1** to **1-2**; cf. **Part 3.3.1).**_

> **1.** The objectives of Regional Aquifer-Systems Analysis (RASA) are: (1) to describe the water-resource system, (2) to analyze changes in the system, (3) to develop a data base from existing information, and (4) to simulate the hydrologic system using mathematical models.
>
> Hydrologic data, geologic descriptions of basin boundaries, and aquifer properties presented in this report were compiled from the many previous studies completed in the regional study area. Regional interpretations resulting from analysis of existing data are also presented in this report.
>
> The study area encompasses parts of Colorado, New Mexico, and Texas and is structurally and hydrologically divided into 22 surface-water open and closed basins. The Rio Grande is the primary hydrologic connection through the open basins of southern Colorado, New Mexico, and western Texas. Closed basins in southwestern New Mexico and western Texas make up the rest of the area. . . .
>
> **2.** The Regional Aquifer-System Analysis (RASA) program was started in 1978 after a congressional mandate to develop quantitative appraisals of the major ground-water systems of the United States. The RASA program represents a systematic effort to study a number of the Nation's most important aquifer systems that, in aggregate, underlie much of the country and that represent important components of the Nation's total water supply. In general, the boundaries-of these studies are identified by the hydrologic extent of each system and accordingly transcend the political subdivisions to which investigations have often arbitrarily been limited in the past. The broad objective for each study is to assemble geologic, hydrologic, and geochemical information; to analyze and develop an understanding of the system; and to develop predictive capabilities that will contribute to the effective management of the system. The use of computer simulation is an important element of the RASA studies, both to develop an understanding of the natural, undisturbed hydrologic system and any changes brought about by human activities as well as to provide a means of predicting the regional effects of future pumping or other stresses. . . .

A significant contribution of the first major RASA-SWAB Project completed in New Mexico involved making a formal distinction between the deep, structural, Mesilla "groundwater basin (MeB)," and the areally more-extensive, physiographic- and hydrographic-basin categories, with the latter being defined, respectively, in terms of Basin and Range topography and surface-watershed divides (**Fig. 1-5**; Frenzel and Kaehler 1990, 1992). The selected MeB boundaries were designed specifically for an initial-phase "digital model of the Mesilla Basin ground-water flow system (1992, p. C2, Fig. 4)." Except for its southern extension into Chihuahua, these boundaries closely match mapped positions of the Study Area's major Basin and Range/RG-rift basin-border fault zones (e.g., L. Woodward et al. 1978). Frenzel and Kaehler were also the first to show the approximate position of the MeB's "West Mesa," the large basin-floor remnant west of the Mesilla Valley that (1) occupies more than half of the MeB area, and (2) has no surface-flow connection with the river (*cf.* **Part 3.5**). MeB boundary locations in most subsequent hydrogeologic-framework characterizations and derivative GW flow-models in the USA part of the MBR also remain in close agreement with those defined Frenzel and Kaehler (e.g., Hawley and Lozinsky 1992, Nickerson and Myers 1993, Hawley and Kennedy 2004, Hanson et al. 2018).

Figure 1-5 (Frenzel and Kaehler 1992, Fig. 4)**.** 1990 USGS index map showing locations of the Mesilla "groundwater" Basin (MeB-dashed outline), the Mesilla Valley (MeV-shaded area), the "West Mesa," major bedrock uplifts (Mountains, Sierras), and "El Paso (del Norte) Narrows."

1.2.2. "Declared Groundwater Basin"–NM Office of State Engineer Definition

> A declared groundwater basin [aka Underground Water Basin] is an area of the state proclaimed by the [OSE] State Engineer to be underlying by a groundwater source having reasonably ascertainable boundaries. By such proclamation the State Engineer assumes jurisdiction over the appropriation and use of groundwater from the source (https://www.ose.state.nm.us/WR/groundWater.php; *cf.* NMOSE-GIS [ND]).

Most of the New Mexico part of the Study Area (**Fig. 1-3**) is in the "Lower Rio Grande Underground Water Basin." Its respective south and north sections were "Declared" by the State Engineer on 9/10/1980 and 9/16/1982 (*cf.* Harris 2012, p. 239-240). The southwestern Study Area also includes much of the "Mount Riley Groundwater Basin," which was "declared" by the State Engineer on 9/22/2005. The eastern edge of the Study Area, also includes small parts of two other "declared basins": (1) the southwestern "Tularosa (declared on July 6, 1982)" and (2) the western "Hueco (no declaration date)". It is also important to note that the criteria used by the NM OSE in establishing "reasonably ascertainable boundaries" of a given "declared groundwater basin" are conceptually different than those used in the much more-detailed hydrogeologic-framework characterization of GW Basins.

1.3. MAJOR HYDROGEOLOGIC AND CULTURAL FEATURES OF THE MESILLA BASIN REGION

Major hydrogeologic and cultural features of the NM WRRI Study Area and surrounding parts of the Mesilla Basin region (MBR) include:

1. The 934-mi^2 (2,419-km^2) Mesilla groundwater basin (MeB), and parts of five other GW basins, with (1) one major valley section and two canyon reaches of the Rio Grande, (2) ten interbasin bedrock highlands, (3) six "corridors" with interbasin groundwater-underflow potential, and (4) more than twenty RG-rift basin-boundary fault zones (*cf.* **Fig. 1-8**, and **Tbls. 1-3** and **1-4**).
2. A Mesilla Valley (MeV) floor area, including the RG channel and floodplain, of about 215 mi^2 (137,600 acres or 55,687 hectares [~557 km^2]).
3. The fluvial-deltaic plain of the Plio-Pleistocene Ancestral Rio Grande (ARG) in the MeB-West Mesa area that (1) overlies a SFG aquifer system with very large reserves of stored GW in the 500 to 3,000 mg/L TDS range (*cf.* **Part 8.3.3**), and (2) essentially unlimited potential for future solar energy production (*cf.* **Figs. 1-12** to **1-14**; *cf.* **Fig. 3-14** and **Part 8.6.3**).
4. The very productive agricultural lands of the Rio Grande Project in the Mesilla and Rincon Valleys of the Rio Grande that include large areas of high groundwater consumption *(cf.* **Fig. 1-6**; e.g., Bulloch and Neher 1980, Maker et al. 1980, Lansford et al. 1997, Esslinger 1996 and 1998, Walton et al. 1999, SSURGO 2002/2003, Tillery et al. 2009, USBOR 2011).
5. Large areas of domestic-commercial-municipal-industrial (DCMI) activity in the MeV and binational Santa Teresa-San Jerónimo area where (1) groundwater consumption is high, and (2) significant water-supply issues exist (e.g., Pacheco 2010a, b, Pacheco 2017a, b, Villagran 2017, Kocherga 2017, 2018a to e, ABQ Jrnl. 2019, Pacheco 2019b and 2020c, Hamway 2020, Pacheco 2021b, Robinson-Avila 2021c and 2022c, Lee 2022, Pacheco 2022a-c, Stevenson 2022, Robinson-Avila and Narvaiz 2023; *cf.* **Figs. 1-3** and **1-11** to **1-13**).

6. Campuses of the region's two major state research universities: NM State University (NMSU) and University of Texas at El Paso (UTEP), and the Universidad Autónoma de Ciudad Juárez (UACJ). Other water-resources research sites in the El Paso area include the Texas A & M University (TAMU) Texas AgriLife Research Center, and the El Paso Water TecH_2O Center.

Since completion of Elephant Butte Dam in 1916 much of the region's GW-resource base has been used conjunctively with "Rio Grande Project (RGP)" surface water for irrigation-agricultural (I-Ag) in the Rincon and Mesilla Valleys (**Fig. 1-6**; *cf.* Esslinger 1998, Kelley et al. 2007, J.P. King 2022). Except for recharge from the Rio Grande (perennial to intermittent) and a few high-mountain areas (seasonal), GW resources in most of the MBR are now replenished by three primary local sources: (1) RGP irrigation return flow, (2) treated municipal wastewater, and (3) groundwater in basin-fill storage. Accelerating disruption of "RGP Water" deliveries reflects the complex contemporary realities of (1) global climate change and related seasonal shifts in temperature and precipitation maxima, (2) increasing water-user demands throughout the Upper Rio Grande watershed, (3) competition between I-Ag, and municipal and industrial (M&I) users for the limited fresh-GW reserves, and (4) interstate and binational challenges facing equitable sharing of surface- and subsurface water resources (*cf.* **APNDS. E** and **H**).

1.4. SCOPE OF WORK

The PI's primary responsibility has been to take the lead in preparation of a Project Completion Report that would (1) serve as a state-of-practice hydrogeologic characterization of basin-fill aquifer systems in the MBR, and (2) capture the essence of the region's 130-yr history of hydro-scientific investigations. The complex nature of the system being characterized, however, dictates that the endeavor will always remain a work-in-progress. Project work involved substantial revision of the provisional digital model of the hydrogeologic framework model developed by Hawley and Kennedy (2004), and Hawley and others (2005). This activity has continued during the past decade in collaboration with Report co-authors Baird Swanson, Steve Walker, and Heather Glaze. Most of the digital-cartographic work related to illustration preparation has been a joint effort by the PI and Baird Swanson of Swanson Geoscience, LLC (SGL), a former NM WRRI contractor. Essentially all of the electronic-file compilation for Report illustrations was also done by SGL. Former NM WRRI GIS Coordinators Heather Glaze and Steve Walker assisted, respectively, in the time-consuming tasks of hydrogeologic base-map digitation and key-well data-base compilation (e.g., **PL. 1** map series and **TBL. 1**; *cf.* **Part 2.3**).

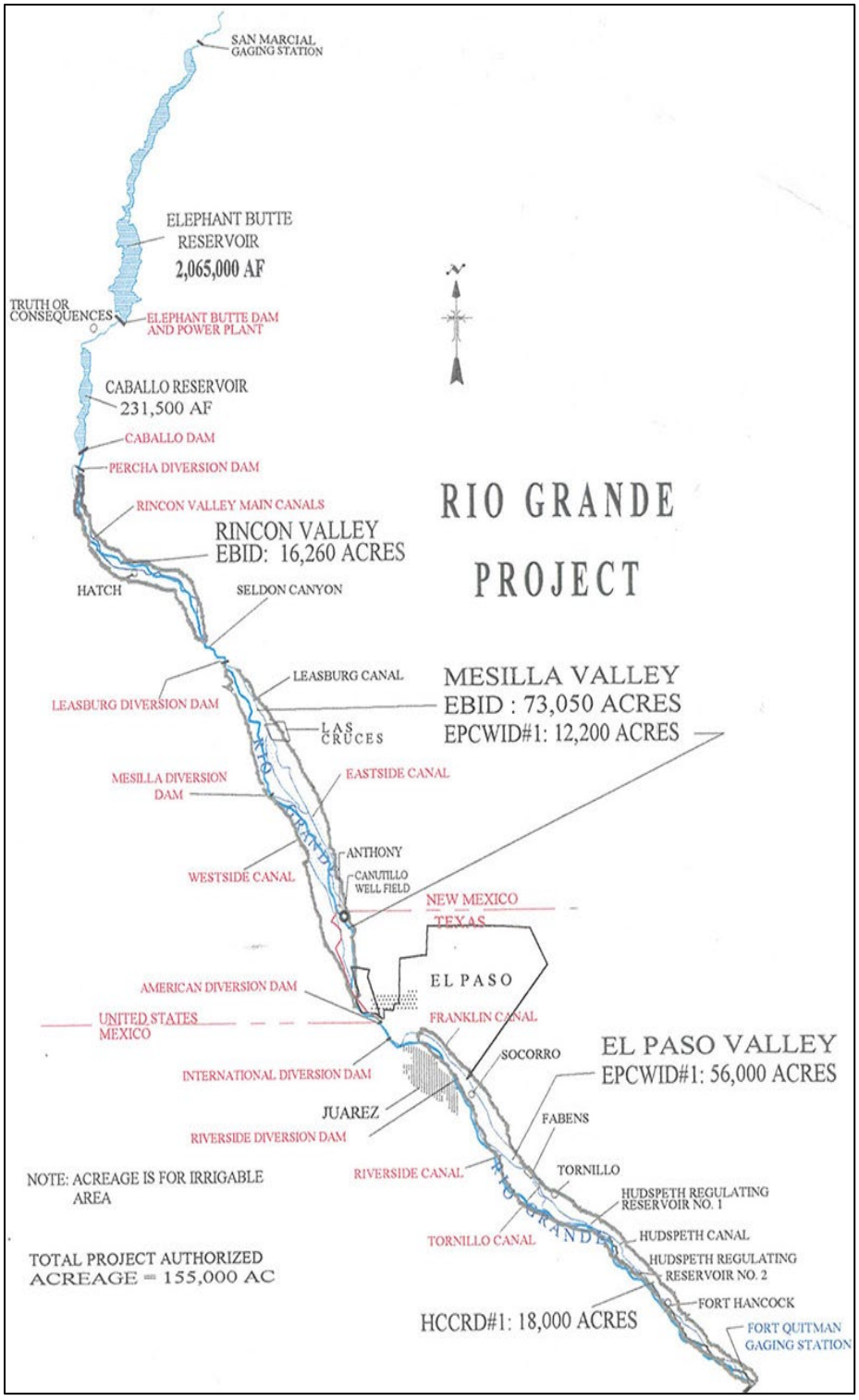

Figure 1-6. U.S. Bureau of Reclamation Map showing locations of major surface-water management structures of the Rio Grande Project between the San Marcial (removed 1964) and Fort Quitman Gaging Stations. EBID indicates Elephant Butte Irrigation District operations (courtesy of Rhea Graham; *cf.* USBOR 2011).

The untimely death of NM WRRI Associate Director, Dr. Bobby J. Creel in February 2010 coincided with a recession-related downturn in the availability of research funding at both federal and state levels. Absence of his effective leadership had a particularly negative impact on the effectiveness of Transboundary Aquifer Assessment Program (TAAP) activities that were initiated in 2007 (*cf.* **Part 1.8.1, APNDX. A2.2.3**). Nonetheless, continued support from the NM WRRI and several other entities (governmental, research-university and NGOs) has allowed the following topics to be addressed and the related tasks to be completed with only a few years delay:

1. Investigation related to the binational Transboundary Aquifer Assessment Program (TAAP) that are summarized in **Part 1.8** and covered in detail in **APPENDIX H**.
2. Description of the geologic and geomorphic setting from four hydrogeologic perspectives:
   a. Study Area location in the Basin and Range (B&R) physiographic and southern Rio Grande rift tectonic provinces, and the Chihuahuan Desert ecoregion (**CHPT. 3**).
   b. Middle- to Late-Cenozoic (~30 million yrs) of RG-rift basin development and Santa Fe Group (SFG) basin-fill deposition (**CHPTS. 3** and **6**).
   c. Middle- to Late-Quaternary (~750 thousand yrs [ka]) of development of the present RG valley and canyon system and its alluvial-aquifers (**CHPT. 3**).
   d. The role of Late Quaternary pluvial-Lakes Otero and Palomas in the Tularosa and Los Muertos Basins as regional GW-flow system recharge source (**CHPTS. 3** and **7**).
3. Introducing conceptual models of hydrogeologic-framework controls on GW-flow and chemistry in the MBR, with emphasis on three aquifer-system components:
   a. Lithofacies-assemblages (LFAs) in intermontane basin deposits (**CHPTS. 4** and **6**)
   b. Hydrostratigraphic units (HSUs). The latter include extensive and thick SFG basin fill, and the thin alluvial fill of the inner RG Valley (**CHPTS. 4** and **6**).
   c. Bedrock/structural-boundary conditions in GW Basins and interbasin Uplifts (**CHPTS. 5** and **7**).
4. Describing hydrogeologic-framework on GW flow and chemistry from the perspective of the last 30 million years (Ma) of geologic time (**CHPTS. 3** and **7**; *cf.* **Tbl. 1-3**, **Fig. 3-5**). Emphasis is on: (1) MeB GW-flow-system components that discharge at El Paso del Norte (EPdN), and (2) the role played by pluvial-Lake Palomas as a significant source of underflow-recharge to the Transboundary Aquifer system of the SE Mesilla Basin area.
5. Review progress in characterization of the Mesilla Basin region's hydrogeologic framework, and summarize options for long-term groundwater-resource development in SFG basin-fill aquifers in the United States part of the Study Area (**CHPT. 8**). More than 950 cited publications are listed in the Report's annotated "Cited References" section (*cf.* **APNDX. B**).

1.5. REPORT ORGANIZATION

While always a work-in-progress, each stage of report-text preparation, table compilation, and illustration design has continued to allow identification and filling of major gaps in needed baseline information. Report content is based on research initiated by the PI in 1963, most of which was completed between 1983 and 2010 (e.g., Hawley 1965, Hawley et al. 1969, King et al. 1971, Seager and Hawley 1973, Hawley 1975 and 1978, Hawley 1984, Seager et al. 1987, Hawley and Lozinsky 1992, Hawley et al. 2000, Hawley and Kennedy 2004, Hawley et al. 2005 and 2009; *cf.* **APNDX. A**):

1. Each iterative stage of hydrogeologic-framework characterization has involved time-consuming preparation of supporting graphic and tabular materials in appropriate digital and electronic-folder formats (**Part 2.3.1**).
2. Most of the digital map and cross-section products were originally compiled at 1:100,000 scale, and the base elevation for most hydrogeologic cross-sections is mean sea level (msl; e.g., **PLS. 5a** to **5s**). Emphasis on subsurface conditions has required acquisition and interpretation of a large borehole database (e.g., 395 entries in **TBL. 1** as of 9/2021).
3. Lithologic- and structural-framework components record still-active RG-rift tectonic processes, which for Santa Fe Group deposition lasted about 30 million years (Ma).
4. Work, including preparation of the 8 Report Appendices found in **Part 1.6**, was completed in the context of ongoing binational and multi-institutional groundwater-resource assessments.

1.5.1. Chapter Content Summaries

The **EXECUTIVE SUMMARY-CONTENTS-INDEX** section that precedes the body of the Report includes an expanded ACKNOWLEDGEMENTS section, and an acronym-abbreviation list. Most of the series of larger-format **PLATES** and **TABLES** are designed for optimum 11-in by 17-in print reproduction, and all are organized in electronic-file folders (pdf binders) in the Report DVD, which is also available online at https://nmwrri.nmsu.edu/publications/technical-reports/tr-reports/tr-363.html.

CHAPTER 1 provides general background information about the investigation, while the emphasis of much of the rest of the Report is on specific details of hydrogeologic-framework controls on groundwater-flow and hydrochemistry at various spatial and temporal scales. Brief Chapter summaries follow:

CHAPTER 2. METHODS. It includes (1) an explanation of well numbering systems, (2) GIS-related sections on feature location, and digital hydrogeologic-framework map and cross-section compilation, and (3) information on data compilation, analysis, and interpretation. Supplemental material is included in **APPENDIX A**.

CHAPTER 3. PHYSIOGRAPHIC AND GEOLOGIC SETTING OF THE MESILLA BASIN REGION—A HYDROGEOLOGIC PERSPECTIVE. Detailed geological- and geophysical-based information on the basic hydrogeologic framework components is presented in seven parts: (1) Basin and Range physiographic-province, (2) Chihuahuan Desert ecoregion, (3) Rio Grande rift tectonic province and Santa Fe Group rift-basin fill, (4) Ancestral Rio Grande (ARG) and La Mesa surface, (5) Major rift-basin components, (6) Stages of rift-basin evolution and SFG deposition, and (7) Mid-to-Late Quaternary evolution of Rio Grande valleys and canyons, and endorheic rift-basin areas. Deep-seated bedrock- and structural-boundary controls on both basin-fill composition and aquifer-system properties are illustrated with maps, cross-sections, and block diagrams (e.g., **PLS. 1A**, **1B**, **1C**, and **5**). The Chapter concludes with an introduction to the paleohydrology of an interlinked pluvial-Lake Palomas—Paso del Norte GW-flow system.

CHAPTER 4. BASIC CONCEPTS OF HYDROGEOLOGIC-FRAMEWORK CONTROLS ON GW-FLOW AND CHEMISTRY IN BASIN AND RANGE, AND RIO GRANDE-RIFT PROVINCE AQUIFER SYSTEMS. Basic concepts on hydrogeologic-framework controls on basin-fill aquifer composition, and groundwater flow and chemistry are presented in two map-scale contexts: Basin & Range provincial and Study Area. Framework controls are first discussed in terms of conceptual models of GW-flow systems in basin-fill deposits of intermontane structural basins. Basic concepts of basin *closure* in a topographic sense, and intra-basin/extra-basin GW flow classes are introduced. Rift-basin and RG-valley fills are defined in terms of both lithofacies-assemblages (LFAs) and hydrostratigraphic units (HSUs) at 1:100,000 map scale.

CHAPTER 5. BEDROCK- AND STRUCTURAL-BOUNDARY COMPONENTS OF INTERBASIN UPLIFTS. This part of the Report, and the following chapter (**6**) form its core sections. Emphasis is on the major lithostratigraphic- and structural-framework elements that are exposed in the basin-bounding highlands or are buried at shallow depth**s** beneath the RG-rift basin fill. They comprise: (1) Uplifts—exposed highland and shallowly buried bedrock terranes, (2) Benches—areas of structural transition between basins and bordering uplifts that are covered in Chapter 6, and (3) Corridors—large gaps in basin-bounding Uplifts with potential for significant amounts of interbasin underflow exchange.

CHAPTER 6. GROUNDWATER BASINS OF THE STUDY AREA AND THEIR PRIMARY HYDROGEOLOGIC SUBDIVISIONS. Emphasis here is on the internal hydrostratigraphic and structural composition of the Study Area's three major groundwater (GW) basins (Mesilla, El Parabién, and Southern Jornada) and their respective hydrogeologic subdivisions (**PLS. 1** to **7**, **TBLS. 1** to **5**). How to best characterize the complex lithofacies, stratigraphic, and structural

framework components in the three GW basins is a recurring theme in **CHAPTERS 5** and **6**. This is especially true for Mesilla Basin (MeB) with its 15 distinctive hydrogeologic map-unit subdivisions (**Fig. 1-10)**.

CHAPTER 7. HYDROGEOLOGIC CONTROLS ON GROUNDWATER FLOW AND CHEMISTRY IN AQUIFER SYSTEMS OF THE MESILLA BASIN REGION. Emphasis is on known and inferred hydrogeologic controls on components of the regional GW-flow system throughout the Study Area. Special attention is given to flow regimes in the "International Boundary Zone (IBZ)" that are directed toward the southeastern MeB-Lower MeV area (**Fig. 1-9, PL. 4**).

CHAPTER 8. PROGRESS IN HYDROGEOLOGIC-FRAMEWORK CHARACTERIZATION, AND OPTIONS FOR LONG-TERM GROUNDWATER-RESOURCE DEVELOPMENT IN THE MESILLA BASIN REGION. Study purpose and scope, and Report content are summarized in **Part 8.2**, and the history of RG-rift evolution, SFG basin-fill deposition, and river-valley/canyon development is outlined in **Parts 8.3 and 8.4.** The latter includes overviews of (1) the GW-flow system evolution that followed initial development of the through-going Rio Grande/Bravo fluvial system, and (2) the Late Quaternary history of pluvial lakes that formed in hydraulically linked endorheic rift basins. **Part 8.5** offers a contemporary perspective on GW-resource management concerns in the Mesilla Basin region. It includes reviews of the rather nebulous concepts of "resilience" and GW "sustainability" in the context of climate-change and resource-management realities. Prospects for long-term GW-resource in the United States part of the Mesilla GW Basin (MeB) aquifer systems are reviewed in **Part 8.6,** with emphasis on areas of the MeV and MeB-West Mesa where viable opportunities for long-term GW-resource development exist, especially those related to (1) brackish-GW (BGW) desalination and concentrate disposal, and (2) managed-aquifer recharge (MAR) operations. **Part 8.7** comprises a short "Concluding Remarks."

1.5.2. Appendix Content Summaries

The scope and format of the body of the Report did not permit inclusion of large amounts of relevant background information. The addition of the below listed **APPENDICES (A** to **H)** addresses the need to recognize the significant contributions to hydrogeology-related research in the binational Mesilla Basin region by many agencies and individuals. Each, with cited references, has been compiled in a separate electronic file in the final section of the Report DVD, which is also available online at https://nmwrri.nmsu.edu/publications/technical-reports/tr-reports/tr-363.html.

APPENDIX A is primarily a **CHAPTER 4** addenda that includes background material on development of conceptual models and digital methods for hydrogeologic-framework characterization. Much of its content was extracted from the following NMBG&MR and NM WRRI publications: King et al. 1971, Gile et al. 1981, Hawley and Lozinsky 1992, Hawley and Kernodle 2000, Hawley et al. 2000, Hawley and Kennedy 2004, and Hawley et al. 2009.

APPENDIX B is an expanded bibliography of more than 2,200 publications on topics related to hydrogeologic controls on groundwater-flow and hydrochemical systems in the western US-Mexico Boundary region. The 9 major topic and 31 subtopic alphanumeric codes assigned to each entry are designed to facilitate cross-referencing and EndNote® compilation. Its compilation was initiated in 2007 in collaboration with the Universidad Autónoma de Ciudad Juárez as part of the Transboundary Aquifer Assessment Program (TAAP).

APPENDIX C reviews major contributions to the hydrogeology, geohydrology, and hydrochemistry of the MBR (1890-2010), with emphasis on collaborative investigations by federal, state, and local agencies and organizations.

APPENDIX D includes facsimile reproductions of selections from published work on the Cenozoic geology, hydrogeology, geomorphology, and physical and cultural geography of the New Mexico-Chihuahua border region.

APPENDIX E is a **CHAPTER 8** addenda that provides background information on conservation of GW resources in the United States part of the MBR. Topics covered include: (1) "Sustainable" GW Development, (2) the rather nebulous concept of "resilience" in a groundwater-resource-management context, (3) GW mining, (4) Rio Grande Project water management, (5) potential impacts of climate change on water-resource availability, (6) vulnerability to aquifer and vadose-zone contamination, and (7) challenges facing future GW-resource conservation.

APPENDIX F is a compilation of selected images and photographs (satellite, aerial, and ground) of the New Mexico-Texas-Chihuahua border region: (1) Apollo, Gemini, and Landsat photographs and images, (2) aerial-photo views of Study Area landscapes, and (3) ground-photos of major Hydrostratigraphic Units and Lithofacies Assemblages in Santa Fe Group basin fill and alluvial deposits of the Rio Grande Valley.

APPENDIX G is a glossary of more than 240 scientific and technical terms. The compilation is designed to provide ready access to definitions of a large number of specialized geologic and hydrologic terms, most of which are in common usage in reports on basin-fill aquifer systems in the Basin and Range physiographic province.

APPENDIX H supplements found in **Part 1.5** contain detailed background information on (1) the 1680 to present history of water-resource development, and (2) the conservation of shared GW resources in Transboundary aquifer systems of the Paso del Norte region. Binational research collaborations, many of which have had NM WRRI support since 1964, get special attention. The most recent of these postdate 1994 implementation of EPA-La Paz Agreement Title XXI. It also includes a UACJ translation of selections on the geohydrology of northern Chihuahua from Estudio Hidrológico del Estado de Chihuahua (INEGI 1999).

1.6. INTRODUCTION TO ILLUSTRATION PREPARATION AND CONTENT

The Report's primary graphic component is a series of twelve **PLATES**. Their content and methods of preparation are summarized in **Part 2.4**, and more-background information on the conceptual development of hydrogeologic-mapping units is in summarized **APPENDIX A. PLATES 1** to **9** were initially compiled at a map scale of 1:100,000, and each is designed for electronic-file access in the Report DVD, as well as 11 x 17-inch printing. The 10,000 m (100 km^2) UTM-SI grid system is used in combination with latitude/longitude-degree and township-range (USA) coordinates for feature location.

Much of the baseline information used in hydrogeologic-map and cross-section preparation was obtained from the following publications of the NM Bureau of Mines [Geology] and Mineral Resources and Texas Bureau of Economic Geology: Seager and others (1982, 1987), Seager (1995), and Collins and Raney (2000). A primary source of information on deep-subsurface was a report by Jiménez and Keller (2000) by the University of Texas-El Paso (UTEP) Geophysical Research Center on the "Rift Basin Structure of the Border Region . . ." (*cf.* **Parts 1.7.2** and **3.6**). In previous hydrogeologic investigations, syntheses of available hydrogeologic information on the MBR were primarily presented from a geology-based perspective (e.g., Hawley and Lozinsky 1992, Hawley et al. 2000, Hawley and Kennedy 2004, Witcher et al. 2004). For example, maps and cross-sections in the Hawley and Kennedy (2004) report retained much of the cartographic detail present in their 1:100,000-1:125,000 scale geologic-map sources (**Fig. 1-7**; *cf.* **APNDX. A, Parts A2.3** and **A5**; Seager et al. 1987, Seager 1995, Collins and Raney 2000). Because of inherent map-unit complexities, however, this approach has proven to be inappropriate for the development of digital hydrogeologic-framework characterizations that mesh as effectively as possible with contemporary geohydrologic and hydrochemical numerical modeling platforms (*cf.* **Part 2.4**; Sweetkind 2017, 2018, Sweetkind et al. 2017, Teeple et al. 2017, Hanson et al. 2018).

A distinctive feature of the cartographic products in this report is their reduced complexity and expanded-graphic display of the basic hydrogeologic features that form the basic framework components of intermontane-basin and river-valley aquifer systems (*cf.* **Fig. 1-8, Part 2.3.1 and APNDX. A3**). Accordingly, lithofacies-assemblage (LFA), hydrostratigraphic-unit (HSU), and structural-boundary elements are now combined in less complex hydrogeologic-unit categories that are designed to be

compatible with current MODFLOW-compatible software like Leapfrog®. New hydrogeologic map and cross-section products include structure-contour maps of HSU-bounding surfaces (3), a pre-development potentiometric-surface approximation, and isopleth (voxel-equivalent) maps showing the primary LFA composition of the three major SFG aquifer-system subdivisions: Upper, Middle, Lower Santa Fe HSUs (*cf.* **Fig. 3-6**, **Part 4.2**). Lithofacies, hydrostratigraphic, and structural details are schematically portrayed to mean sea-level (msl) depth in 19 hydrogeologic cross-sections (**PL. 5a** to **5s**).

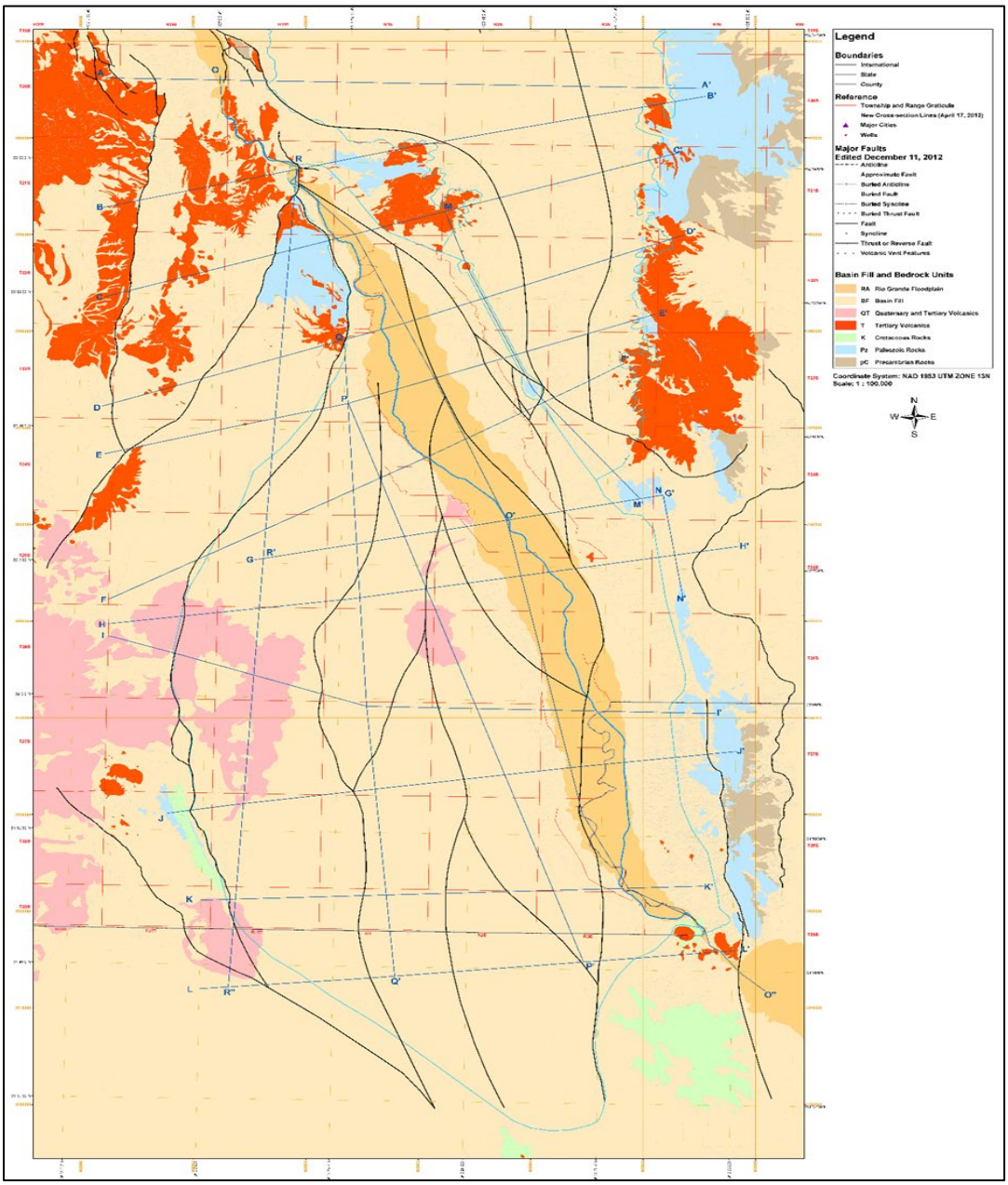

Figure 1-7. Provisional hydrogeologic index map of the 2001-2006 NM WRRI Study Area (Hawley and Kennedy 2004, Hawley et al. 2005). Blue lines show locations of Hydrogeologic Cross-Sections A-A' to O-P' (*cf.* **APNDX. A**, **Parts A2.3** and **A5**).

1.7. INTRODUCTION TO HYDROGEOLOGIC-FRAMEWORK CHARACTERIZATION

1.7.1. Basic Hydrogeologic Concepts and Terminology

Hydrogeologic investigations of aquifers and groundwater-flow systems in the B&R province can be approached from several vantage points. Emphasis of this study is on geologic and geomorphologic controls on *subsurface-water* flow and chemistry in a multi-component complex of *geologic* (i.e., solid-earth)-*material* units that typify intermontane-basin aquifer systems throughout the Basin and Range and Rio Grande-rift provinces. Definitions of commonly used *geologic*, *geohydrologic* and *hydrogeologic* terms are included in **Table 1-2** *(cf.* **APNDX**. **G—Glossary**).

The *geologic-material* components of a hydrogeologic framework comprise an integrated system of basin-fill deposits and bedrock types, and associated structural-boundary conditions (*cf.* **Part 4.2**):

1. Lithofacies assemblage (LFA) composition of the Upper, Middle, and Lower Santa Fe Group Hydrostratigraphic Units (HSUs) that comprise the bulk of the RG-rift basin fill.
2. Bedrock composition and internal structural framework of major inter-basin RG-rift uplifts.
3. Basin-border and intra-basin structural-boundary elements (primarily RG-rift fault-zones).

Both *geologic materials* and *subsurface water* are dynamic entitities when considered from appropriate *geologic-time* perspectives. Accordingly, geochronology and chronostratigraphy are essential elements of any conceptual hydrogeologic-framework model (**Table 1-3**; *cf.* **Fig. 3-5**).

Subsurface Water is defined in terms of the degree of saturation of available pore-space or fracture openings in the geologic-material media. It comprises two distinctive hydrologic units that are separated by a dynamic *water table* or *potentiometric surface*s: (1) a largely unsaturated "vadose zone," which may contain disconnected bodies of saturated earth material, and (2) an underlying *saturated* or *phreatic* zone, where a*quifers* comprise another truly dynamic framework component (*cf.* **Fig. 4-1**; Meinzer 1923, p. 5). In order to develop a functional hydrogeologic-framework model, however, factors related to the *movement* of *subsurface water* must be added to the *geologic-material* and RG-rift structural classes. From a 0.75 Ma time perspective, the ultimate driving force for the *movement* of *subsurface water* relates to the highly variable nature of (1) Rio Grande/Bravo discharge in a throughgoing fluvial system that drains to the Gulf of Mexico, and (2) GW-flow contributions from Late Pleistocene pluvial lakes in *endorheic* basins that recently had hydraulic linkage with the throughgoing fluvial system (**Fig. 1-2**).

Table 1-2. Definitions of Common Geologic, Geohydrologic, and Hydrogeologic Terms

Aquifer	A *saturated* geologic unit that is permeable enough to transmit significant quantities of water under ordinary hydraulic gradients (Deming 2002, p. 429).
Aquiclude	A rock layer that completely excludes fluid flow through it. Geologic aquicludes are rare (Deming 2002, p. 429).
Aquitard	A stratum that transmits quantities of water that are very significant for a variety of geologic problems, but is inadequate for supplying economic quantities of water to wells (Deming 2002, p. 429).
Brackish Groundwater (BGW):	There are two classes of BGW: (1) slightly saline—1,000-3,000 mg/L TDS, and (2) moderately saline—3,000 to 10,000 mg/L TDS (Stanton et al. 2017, Tbl. 1).
Endorheic	Pertaining to a closed surface-drainage basin (*cf. exorheic*).
Exorheic	Pertaining to an open surface-drainage basin (*cf. endorheic*).
Geology	The study of the planet Earth, the materials of which it is made, the processes that act on these materials, the products formed, and the history of the planet and its life forms since its origin (Neuendorf et al. 2005, p. 267).
Geomorphology	The science that treats the general configuration of the earth's surface; specifically, the study of the classification, description, nature, origin, and development of landforms and their relationships to underlying structures, and of the history of geologic changes as recorded by these surface features.
Groundwater	*Subsurface water* that is in the *saturated* zone (Neuendorf et al. 2005, p. 286).
Hydrology	The study of the occurrence and movement of water at and beneath the surface of the Earth, the properties of water, and its relationship with living and material components of the environment (Hornberger et al. 2005, p. 282).
Hydrogeology	The branch of geology that deals with the distribution and movement of groundwater in the soil and rocks of the Earth's crust (commonly in aquifers). https://en.wikipedia.org/wiki/Hydrogeology
Hydrostatic Level	The level to which water will rise in a well under its full [hydrostatic] pressure head. It defines the *potentiometric surface* (Neuendorf et al. 2005, p. 313).
Hydrostatic Pressure	The pressure exerted by the water at any given point in a body of water (Neuendorf et al. 2005, p. 313).
Phreatic Water	(1) A term that was originally applied to only to the water that occurs in the upper part of the saturated zone under water-table conditions (syn. of *unconfined groundwater*), but (2) has come to be applied to all water in the saturated zone (i.e., groundwater [and/or *phreatic zone*]) (Neuendorf et al. 2005, p. 489).
Potentiometric Surface	A surface that depicts the distribution of hydraulic heads in a *confined aquifer*; the water [level] in a well or piezometer penetrating the *confined aquifer* defines that surface (Hornberger et al. 1998, p. 286).
Saturated Zone	A region of the subsurface where pores are completely filled with water; it is bounded at the top by the water table (Hornberger et al. 1998, p. 287).
Subsurface Water	A non-specific term commonly applied to all water below the land surface.
Vadose Zone	The zone in soils or rocks between the Earth's surface and the *water table*; pores are partly filled with water and partly filled with air (Hornberger et al. 1998, p. 291).
Water Table	A surface separating the *saturated* and *unsaturated* zones . . . , [that is] defined as a surface at which the fluid pressure is atmospheric (Hornberger et al. 1998, p. 292).

Table 1-3. Divisions of Geologic Time Referred to in this Report (*cf.* Fig. 3-5, TBL. 2)

ERA	Period	Epoch (**u/m/l***)	Age (years**)
CENOZOIC (Cz**)**			
	Post-Quaternary	Anthropocene***	Future to 1950 CE
	Quaternary (**Q**)		1950 CE-2.6 Ma
		American SW Historic	*Present-1540 CE*
		Holocene (Qu)	1950 CE-11,700
		Pleistocene	11,700-2.6 Ma
		Late (**Qu**)	11,700-126 ka
		Middle (**Qm**)	126 ka-780 ka
		Early (**Ql**)	780 ka-2.6 Ma
	Tertiary (**T**)		2.6 Ma-65.5 Ma
		Late: Neogene	
		Pliocene (**Tu**)	2.6-5.3 Ma
		Late	2.6-3.6 Ma
		Early	3.6-5.3 Ma
		Miocene (**Tu**)	5.3-23 Ma
		Late	5.3-11.6 Ma
		Middle	11.6-16 Ma
		Early	16-23 Ma
		Early: Paleogene	
		Oligocene (**Tm**)	23-34 Ma
		Eocene (**Tl**)	34-55.8 Ma
		Paleocene (**Tl**)	55.8-65.5 Ma
MESOZOIC (**Mz**)			
	Cretaceous (**K**)		65.5-145.5 Ma
	Jurassic (**Jr**)		145.5-199.6 Ma
	Triassic (**Tr**)		199.6-251 Ma
PALEOZOIC (Pz)			
	Permian (**P**, **Pzu**)		251-299 Ma
	Pennsylvanian (Pn, Pzu)		299-318 Ma
	Mississippian (M, Pzu)		318-359 Ma
	Devonian (D, Pzl)		359-416 Ma
	Silurian (S, Pzl)		416-444 Ma
	Ordovician (O, Pzl)		444-488 Ma
	Cambrian (C, Pzl)		488-542 Ma
PRECAMBIAN-PROTEROZOIC (**XY**)			Ma-2.5 Ga
PRECAMBIAN-ARCHAEN (**Z**)			2.5-3.85 Ga

Modified from Koning and Read (2010, Table 2; cf. Gibbard et al. 2010, Gradstein et al. 2012)
**u/m/l = upper/middle/lower –lithostratigraphic units*
***Ga=billion years, Ma=million years, and ka=thousand years*
****Anthropocene: A provisional Epoch proposed by Crutzen and Stoermer 2000 (cf. Zalasiewicz et al. 2021);*
https://www.nytimes.com/2024/03/05/climate/anthropocene-epoch-vote-rejected.html?unlocked_article_code=1.aU0.Yoaa.8m5-c7KcfueD&smid=em-share

1.7.2. Framework Characterization in a RG-Rift Provincial Context

The inherent complexity and deep-seated nature of the major structural components of Rio Grande rift basins and their bordering bedrock uplifts requires that their characterization in a detailed hydrogeologic context be based on a variety of direct and indirect methods of surface and subsurface investigation (e.g., surface mapping, borehole-sample logging, and geophysical and geochemical surveys; *cf.* **PL. 1** to **PL. 7** series; Seager et al. 1987, and Seager 1995). Former Head of the UTEP Geophysical Laboratory, G.R. Keller describes some aspects of this multi-disciplinary process in a seminal 2004 review paper titled, "Geophysical constraints on the crustal structure of New Mexico (p. 450):"

> Seismic reflection, gravity, and drilling data have delineated the many large, deep basins that form the upper crustal expression of the [RG] rift. Initially, the primary emphasis was on gravity studies (e.g., Cordell, 1976, 1978; Ramberg et al., 1978; Birch, 1982). However, the petroleum industry has released a considerable amount of seismic reflection data for research purposes, and [a] series of papers that focus on the [RG-] rift basins and include many seismic reflection profiles is [cited] in Keller and Cather (1994). In general, the basins are asymmetrical and more complex structurally than their surface expression would suggest [*cf.* **Part 3.6**].

A large body of published information on subsurface conditions in the MBR supports G.R. Keller's observation that RG-rift basins are "more complex structurally than their surface expression would suggest" (e.g., Chapin and Seager 1975b, Seager and Morgan 1979, C. Wilson et al. 1981, Seager et al. 1987, Seager 1995, Jiménez and Keller 2000).

Synthesis of geophysical and deep-borehole information has permitted identification and subdivision of the Study Area's major GW basins at a level of detail that has heretofore not been possible (*cf.* **CHPTS. 3** and **6**, **TBL. 1**). **Figure 1-8** is an index map showing locations of the major hydrogeologic subdivisions that have been defined in the context of the MBR's RG-rift tectonic setting. The Mesilla GW Basin (MeB) is in blue shades, and the Mesilla Valley of the Rio Grande is in dark blue. The Southern Jornada and El Parabién GW Basins (SJB and EPB) are in light green and pink, respectively. SCyn and EPdN show the respective locations of Selden Canyon and El Paso del Norte. Solid and dashed black lines mark the boundaries of interbasin-uplift and intrabasin subdivisions. Acronyms for hydrogeologic-subdivision categories, including fault zones (lines with bar and ball symbols), are listed in **Tables 1-4** and **1-5 [TBLS. 2** and **3**].

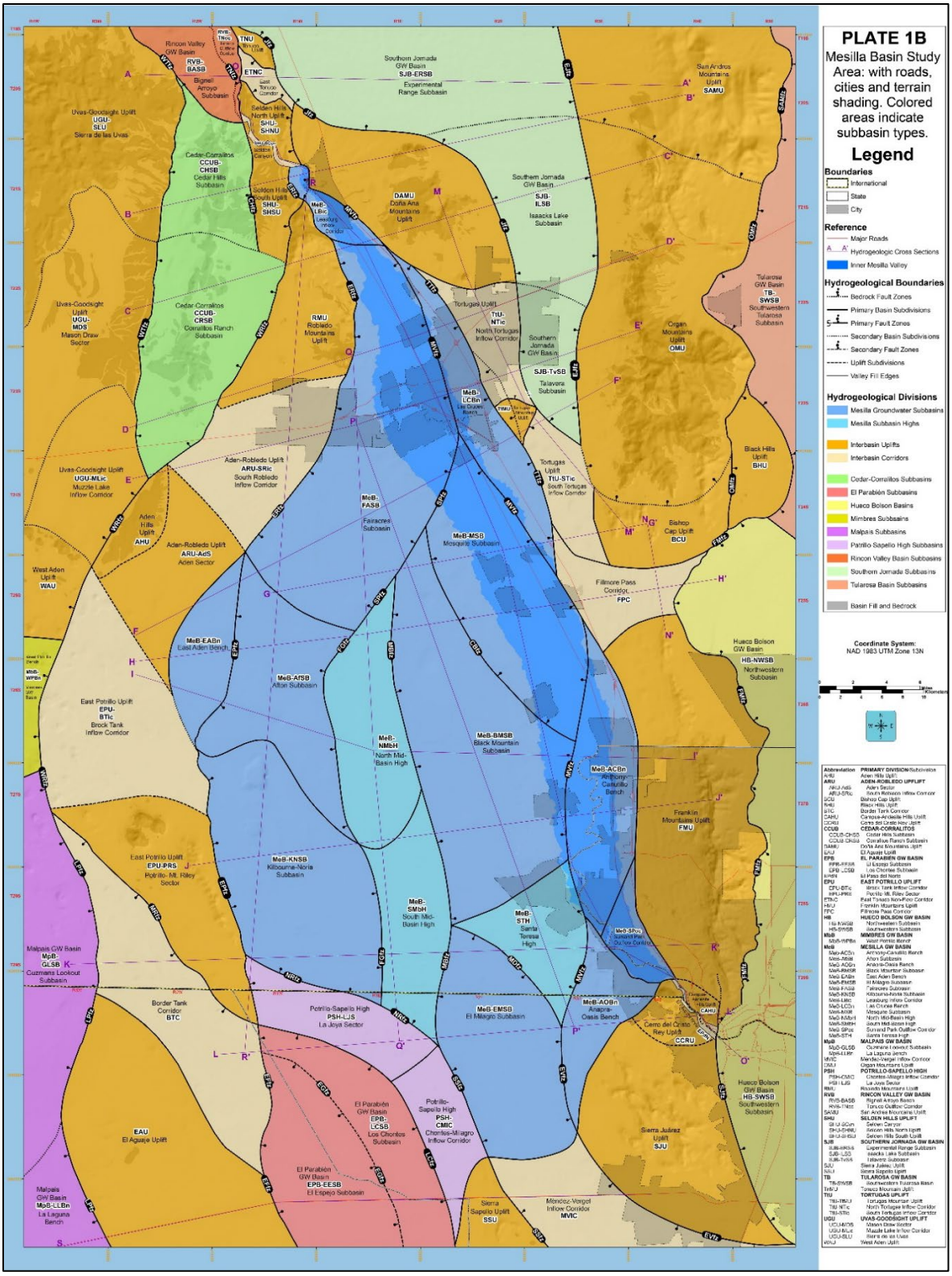

Figure 1-8 (page-size **PL. 1B).** Index map for major hydrogeologic subdivisions of the Study Area (**Fig. 1-3** and **Tbls. 1-4** and **1-5**; **Fig. 1-4**). The Mesilla, Southern Jornada, and El Parabién GW Basins are in blue, lime-green and beige, respectively. Interbasin (RG-rift) Uplifts are in brown. USGS DEM base.

Table 1-4. Names and Acronyms of Hydrogeologic Subdivisions shown on Maps, Cross-Sections, and the Well-Information Spreadsheet (PLS. 1 to 8, TBLS. 1 to 3, and Fig. 1-8 and Tbl. 1-5)

ACRONYM	RIO GRANDE (RG) VALLEY AND CANYONS (NARROWS)	
EPdN	El Paso del Norte (Cyn)	
MeV	Mesilla Valley	
SCyn	Selden Canyon (Cyn)	
EPJV	El Paso-Juárez Valley	
ACRONYM	**MESILLA GW BASIN (MeB)**	**SUBDIVISION (2,419: area in km²)**
MeB-ACBn	Mesilla Basin	Anthony-Canutillo Bench (138)
MeB-AfSB	Mesilla Basin	Afton Subbasin (180)
MeB-AOBn	Mesilla Basin	Anapra-Oasis Bench (72.7)
MeB-BMSB	Mesilla Basin	Black Mountain Subbasin (353)
MeB-EABn	Mesilla Basin	East Aden Bench (70.7)
MeB-EMSB	Mesilla Basin	El Milagro Subbasin (203)
MeB-FASB	Mesilla Basin	Fairacres Subbasin (382)
MeB-KNSB	Mesilla Basin	Kilbourne-Noria Subbasin (278)
MeB-LBic	Mesilla Basin	Leasburg Inflow Corridor (25.4)
MeB-LCBn	Mesilla Basin	Las Cruces Bench (97.5)
MeB-MSB	Mesilla Basin	Mesquite Subbasin (228)
MeB-NMbH	Mesilla Basin	North Mid-Basin High (143)
MeB-SMbH	Mesilla Basin	South Mid-Basin High (121)
MeB-STBn	Mesilla Basin	Santa Teresa High (89.5)
MeB-SPoc	Mesilla Basin	Sunland Park Outflow Corridor (33.4)
ACRONYM	**OTHER GW BASINS (B)**	**SUBDIVISION**
EPB	El Parabién Basin (N-part—Drains to MeB)	
EPB-EESB	El Parabién Basin	El Espejo Subbasin (157)
EPB-LCSB	El Parabién Basin	Los Chontes Subbasin (126)
HB	Hueco Bolson (W-edge—Receives inflow from MeB through EPdN)	
HB-NWSB	Hueco Bolson	Northwestern Subbasin
HB-NWSB	Hueco Bolson	Southwestern Subbasin
MbB	Mimbres Basin (No-flow boundary with MeB; surface and subsurface flow to Zona Hidrogeológica Conejos Médanos (ZHGCM)	
MbB-WPBn	Mimbres Basin	West Potrillo Bench
MpB	Malpais GW Basin (E-edge—connects with BTC, MbB, and LMB)	
MpB-GLSB	Malpais Basin	Guzmans Lookout Subbasin (SB)
MpB-LLBn	Malpais Basin	La Laguna Bench (Bn)
RVB	Rincon Valley GW Basin (Drains to MeB through SCyn)	
RVB-BASB	Rincon Valley Basin	Bignell Arroyo Subbasin (47.2)
RVB-TNoc	Rincon Valley Basin	Tonuco Outflow Corridor (5)
SJB	Southern Jornada GW Basin (495-Drains to MeB and RVB)	
SJB-ERSB	Southern Jornada Basin	Experimental Range Subbasin (264)
SJB-ILSB	Southern Jornada Basin	Isaacks Lake Subbasin (164)
SJB-TvSB	Southern Jornada Basin	Talavera Subbasin (68.2)
SWTB	Southwestern Tularosa Basin	
ACRONYM	**UPLAND GW BASIN**	**SUBDIVISION**
CCUB	Cedar-Corralitos Upland Basin (UB)	
CCUB-CHSB	Cedar-Corralitos	Cedar Hills Subbasin (96.2)
CCUB-CRSB	Cedar-Corralitos	Corralitos Ranch Subbasin (205)

Table 1-4 (concluded). Names and abbreviations of Hydrogeologic Subdivisions

ACRONYM	INTERBASIN HIGH (IBH)	SUBDIVISION
PSH	Potrillo-Sapello High (163)	
PSH-LJS		La Joya Sector (93.5)
PSH-CMIC		Chontes-Milagro Inflow Corridor (69.5) (EPB-LCSB to MeB-EMSB)
ACRONYM	**INTERBASIN UPLIFT (U)**	**SUBDIVISION**
AHU	Aden Hills Uplift	
ARU	Aden-Robledo Uplift	
ARU-AdS	Aden-Robledo Uplift	Aden Sector (S)
ARU-SRic	Aden-Robledo Uplift	South Robledo Inflow Corridor (145)
BCU	Bishop Cap Uplift	
BHU	Black Hills Uplift	
CAHU	Campus-Andesite Hills Uplift	
CCRU	Cerro del Cristo Rey Uplift	
CMU	Camel Mountain Uplift	
DAMU	Doña Ana Mountains Uplift	
EAU	El Aguaje Uplift (310)	
EPU	East Potrillo Uplift	
EPU-BTic	East Potrillo Uplift	Brock Tank Inflow Corridor (227)
EPU-PRS	East Potrillo Uplift	Potrillo-Mt. Riley Sector (S)
FMU	Franklin Mountains Uplift	
OMU	Organ Mountains Uplift	
RMU	Robledo Mountains Uplift	
SAMU	San Andres Mountains Uplift	
SHU	Selden Hills Uplift	
SJU	Sierra Juárez Uplift	
SSU	Sierra Sapello Uplift (41)	
TNU	Tonuco Uplift	
TtU	Tortugas Uplift	
TtMU	Tortugas Uplift	Tortugas Mountain Uplift (U)
TtU-NTic	Tortugas Uplift	North Tortugas Inflow Corridor (63.5)
TtU-STic	Tortugas Uplift	South Tortugas Inflow Corridor (59.2)
UGU	Uvas-Goodsight Uplift	
UGU-SLU	Uvas-Goodsight Uplift	Sierra de las Uvas (U)
UGU-MDS	Uvas-Goodsight Uplift	Mason Draw Sector (S)
UGU-MLic	Uvas-Goodsight Uplift	Muzzle Lake Inflow Corridor (ic, to Mimbres Basin-MbB)
WAU	West Alden Uplift	

ACRONYM	MAJOR INTERBASIN GROUNDWATER-FLOW CORRIDORS
BTC	Border Tank Corridor (214) (Malpais Basin to El Parabién Basin GW flow)
ETNC	East Tonuco Corridor (13.5) (Jornada Basin to Rincon Valley Basin GW flow)
FPC	Fillmore Pass Corridor (73.7) (Mesilla Basin-Hueco Bolson—potential inter-basin GW flow)
MVIC	Méndez-Vergel Inflow Corridor (115) (possible Hueco Bolson to Mesilla Basin GW flow)

Table 1-5. Basin- and Subbasin-Boundary Fault Zone Acronyms and Names on Fig. 1-8

I. Groundwater Basin/Intrabasin-Boundary Fault Zones (fz)
- A. Mesilla and El Parabién Basins
  - 1. Mesilla Basin (MeB)
    - CBfz—Chamberino fz
    - EVfz—El Vergel fz
    - EPfz—East Potrillo fz
    - ERfz—East Robledo fz
    - FGfz—Fitzgerald fz
    - MBfz—Mid-Basin fz
    - MDfz—Mastodon fz
    - MVfz—Mesilla Valley fz
    - NRfz—Noria fz
    - SPfz—San Pablo fz
    - SSfz—Sierra Sapello fz
    - TTfz—Tortugas fz
  - 2. El Parabién Basin (EPB)
    - EFfz—El Faro fz
    - EGfz—El Girasol fz
    - LCfz—Los Cuates fz
- B. Southern Jornada and Rincon Valley Basins
  - 1. Southern Rincon Valley Basin (SJB)
    - TNfz—Tonuco fz
    - WTfz—Ward Tank fz
  - 2. Southern Jornada Basin (SJB)
    - EJfz—East Jornada fz
    - Jfz—Jornada fz
- C. Hueco Bolson and Tularosa Basin
  - 1. Northwestern Hueco Bolson (NWHB)
    - FMfz—Franklin Mountains fz
    - SJfz—Sierra Juárez fz
  - 2. Southwestern Tularosa GW Basin (SWTB)
    - OMfz—Organ Mountains fz
    - SAMfz—San Andres Mountains Fz
- D. Western-Border Basins
  - 1. Cedar-Corralitos Upland Basin (CCUB)
    - CHfz—Cedar Hills fz
    - WRfz—West Robledo fz
    - WTfz—Ward Tank fz
  - 2. Northeastern Mimbres Basin (MbB)
    - WTfz—Ward Tank fz
    - WRfz—West Robledo fz
  - 3. Malpais Basin (MpB)
    - LPfz—La Peña fz

II. Inter-basin Uplift Fault Zones (fz)—Boundary and Interior
- A. Aden-Robledo Uplift (ARU)
  - 1. ERfz—East Robledo fz
  - 2. WRfz—West Robledo fz
- B. Doña Ana Mountain Uplift (DAMU)
  - 1. Jfz—Jornada fz
  - 2. MVfz—Mesilla Valley fz
  - 3. TTfz—Tortugas fz
- C. East Potrillo Uplift (EPU)
  - 1. EPfz—East Potrillo fz
  - 2. MRfz—Mount Riley fz
- D. El Aguaje Uplift (EAU)
  - 1. EFfz—El Faro fz
  - 2. LPfz—La Pena fz
- E. Franklin Mountains Uplift (FMU)
  - 1. FMfz—Franklin Mountains fz
  - 2. WFfz—West Franklin fz
- F. Organ Mountains Uplift (OMU)
  - 1. EJfz—East Jornada fz
  - 2. OMfz—Organ Mountains fz
- G. Robledo Mountain Uplift (RMU)
  - 1. ERfz—East Robledo fz
  - 2. WRfz—West Robledo fz
- H. Sierra Juárez Uplift (SJU)
  - 1. SJfz—Sierra Juárez fz
  - 2. EVfz—El Vergel fz
- I. Sierra Sapello Uplift
  - 1. SSfz—Sierra Sapello fz
  - 2. LCfz—Los Cuates fz
- J. Southern San Andres Mtns (SAMU)
  - 1. EJfz—East Jornada fz
  - 2. SAMfz—San Andres Mountains fz
- K. Tortugas Uplift (TtU)
  - 1. Jfz—Jornada fz
  - 2. TTfz—Tortugas fz

III. Inter-basin Corridor Boundary-fault zones (fz)
- A. Border Tank Corridor (BTC)
  - 1. LPfz—La Peña fz
  - 2. MRfz—Mount Riley fz
- B. Fillmore Pass Corridor (FPC)
  - 1. FMfz—Franklin Mountains fz
  - 2. MVfz—Mesilla Valley fz
- C. Méndez-Vergel Corridor (MVC)
  - 1. EVFZ—El Vergel fz
  - 2. SSfz—Sierra Sapello fz

The primary RG-rift structural components delineated on **Figures 1-3** and **1-8** are rift *basins* and interbasin bedrock *uplifts*, with the details of the latter described in **CHAPTER 5**, and the former in **CHAPTER 6**. Major gaps (erosional and/or structural) that disrupt *uplift* continuity and potentially permit interbasin GW flow are here referred to as *corridors*. Since study emphasis is on basin-fill aquifers and associated GW-flow systems (**CHAPT. 7**), Rift *basins* are characterized in much-more detail than the *uplifts*, parts of which may be shallowly buried by basin-fill deposits. Deeply buried analogs of *uplifts*, which are within or border the Mesilla GW Basin (MeB) are designated structural *highs* herein. Because of their significant influence on deeper parts of the regional GW-flow system, they have received special attention in this Study (**CHAPTS. 6** and **7**). Informally named *benches* are shallowly buried structural platforms that are transitional between central *basins* and *uplifts* (**Fig. 1-8**, **Tbl. 1-4**).

1.7.3. Major Geohydrologic Features in the Study Area

Figures 1-9a and **1-9b** (page-size **PLS. 4a** and **4b**) are index maps on a hydrogeologic-map base (**Fig. 1-7**) for the primary geohydrologic features in the NM WRRI Study Area (**Fig. 1-7**). The respective Mesilla, southern Jornada, and El Parabien GW Basin boundaries are in green, orange and violet. The approximate pre-development (1976) potentiometric-surface altitude (amsl) is shown with thin-blue lines (20- and 100-ft contours) on **Figure 1-9a,** and with orange lines (5-, 10-, and 30-m contours) on **Figure 1-9b**. Major surface-watershed divides are shown by solid and dashed thick blue lines (USA database from Wilson et al. 1981). The dashed blue line with arrows in the map's SW corner shows the approximate position of the predevelopment, regional GW-flow divide between (1) flow directed toward the lower MeV and EPdN, and (2) flow directed toward El Barreal in the Zona Hidrogeológica de Conejos Médanos (ZHGCM; *cf.* **Part 7.1**). The surface-watershed position is shown with a solid blue line.

Figures 1-9a and **1-9b** on following pages. Index maps for the Study Area's primary geohydrologic features on a **PLATE 1** hydrogeologic-map base (**Fig. 1-7**). The approximate pre-development (~1976) potentiometric-surface altitude (amsl) is shown on **Figure 1-9a** with 20- and 100-ft contours, and on **Figure 1-9b** with 5-, 10-, and 30-m contours. Major surface-watershed divides are shown by solid and dashed thick blue lines. The dashed blue line with arrows in the map's SW corner marks the approximate boundary between EPdN- and Los Muertos Basin-directed GW flow.

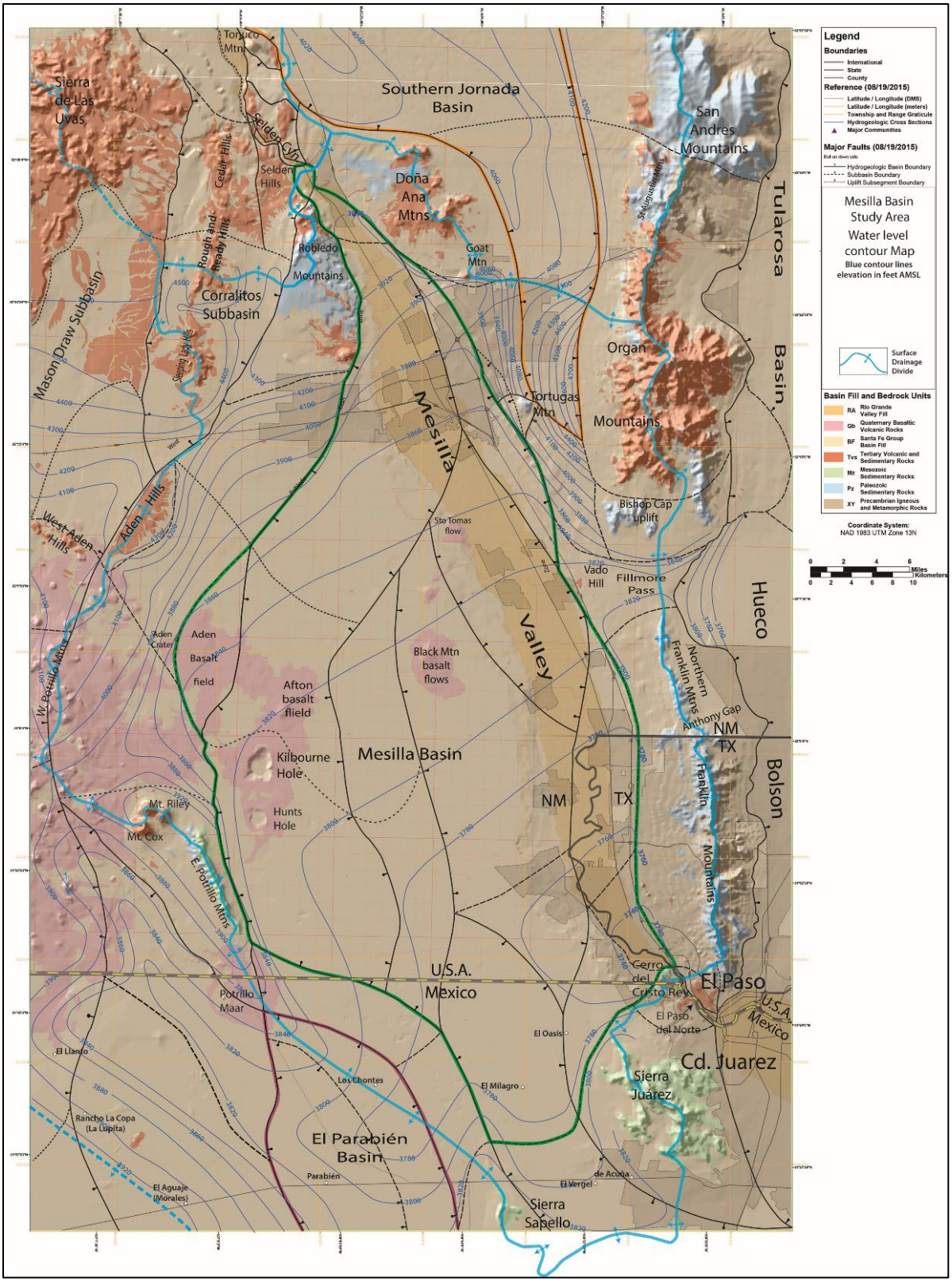

Figure 1-9a (page-size **PL. 4A).** Index map to major geohydrologic features of the NM WRRI Study Area (~1976 potentiometric-surface altitude in feet).

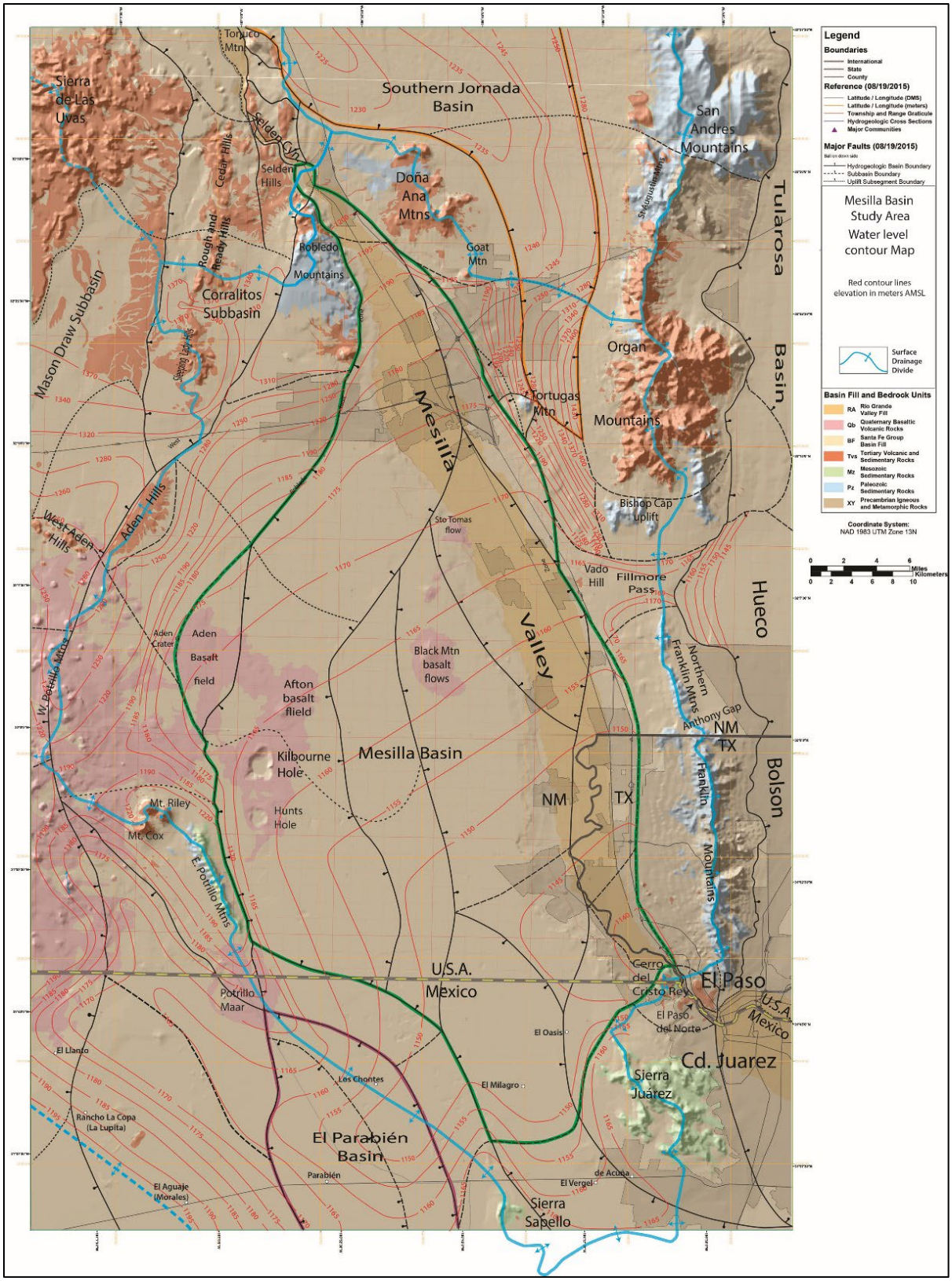

Figure 1-9b (page-size **PL. 4B).** Index map to major geohydrologic features of the NM WRRI Study Area (~1976 potentiometric-surface altitude in meters).

1.8. INTRODUCTION TO INVESTIGATIONS IN THE SOUTHERN MESILLA BASIN REGION

1.8.1. The Transboundary Aquifer Assessment Program (TAAP)

The Transboundary Aquifer Assessment Program (**TAAP**) originated in the United States-Mexico Transboundary Aquifer Assessment Act that was signed by President George W. Bush on December 22, 2006 (US-MX TAA 2006; Alley 2013). Even though the TAAP has not been adequately funded, the overall Scope of Work (**Part 1.3**) of this investigation conforms to the "Purpose" of "Act Sections 2 and 4" that require "systematically assessing priority transboundary aquifers" in the "Hueco Bolson and Mesilla aquifers underlying parts of Texas, New Mexico, and Mexico (S. 214-1 and 3)." The act specifically authorizes:

> The Secretary of the Interior to cooperate with the States on the border with Mexico and other appropriate entities in conducting a hydrogeologic characterization, mapping, and modeling program for priority transboundary aquifers, and for other purposes (S.214-1).

Primary NM WRRI hydrogeologic study "tasks" are outlined in **Tasks 2** and **4** in the "Updated U.S. Joint Work Plan for Mesilla Basin/Conejos Médanos:"

Task 2: Identify, review and evaluate previous studies on the Mesilla Basin [region] (e.g., **Tbl. 1-6**; **APNDX. B**).

Task 4: Initiate update of the Mesilla Basin hydrogeologic-framework model to adequately define aquifer characteristics and further support development of scientifically sound groundwater-flow models (e.g., **CHPTS. 3** to **7**; *cf.* **APNDX. H6**).

Figure 1-10 (page-size **PL. 11**) is an index map for GW-management and geohydrologic units in the United States and Mexico south of 32° N latitude. The El Parabién and southern Mesilla GW Basins are outlined in violet and green, respectively, and the Study Area border is in black. The back-dash white line is the "delineación oficial" of the "Acuífero Conejos-Médanos" as defined by the Instituto Nacional de Estadística, Geografía e Informática (INEGI 2012; *cf.* IBWC 2011). The larger "Zona Hidrogeológica de Conejos Médanos (ZHGCM)" is bounded with a solid yellow line (**Fig. 1-1**). Key-well sites are shown with red dots, and the dark red dots show locations of 23 production wells in the new Ciudad Juárez Junta Municipal de Agua y Saneamiento (JMASCJ) well field (*cf.* **Figs. 1-12** and **1-13**; **PL. 3, TBL. 1**). The surface-watershed boundary of the southern MeB is in blue, and the area inundated by pluvial-Lake Palomas during its Late Pleistocene high stands has light-blue shading. The dashed-blue line shows the approximate position of the present GW-flow divide between NE-directed flow toward the lower MeV and EPdN, and SW-directed flow toward El Barreal ("laguna intermitente") in the ZHGCM (*cf.* **Figs. 1-9** and **1-11**, and **Parts 1.6.3** and **7.6.2**).

Table 1-6. Sources of Published Information on the Hydrogeologic Framework of the International Boundary Zone (IBZ), many of which were used in Report preparation

A. Published information on the hydrogeologic framework of basin-fill aquifers in the United States part of the International-Boundary zone has four primary sources:

1. Government documents on the geology and groundwater conditions in Mesilla GW Basin (e.g., Lee 1907, Sayre and Livingston 1945, Leggat et al. 1962, W. King et al. 1971, C. Wilson et al. 1981, Hawley and Lozinsky 1992, Nickerson and Myers 1993, and Nickerson 2006).
2. Surficial-geologic mapping at a detailed-reconnaissance level, with limited deep-borehole control (e.g., Hoffer 1976, Drewes and Dyer 1993, Seager et al. 1987, Seager 1995, Collins and Raney 2000, and Hoffer 2001).
3. Reconnaissance-level geophysical surveys (gravity and seismic), with limited deep-borehole control (e.g., Daggett and Keller 1987 and 1995, Adams and Keller 1993, and Klein 1995).
4. Reconnaissance-level geothermal-resource surveys, with some deep-borehole-log control (e.g., Henry 1979, Henry and Gluck 1981, Henry and Price 1985, and Snyder 1986).

B. Available published information on the hydrogeologic framework of basin-fill aquifers in the Mexican part of the International-Boundary zone is of a less detailed nature, and has four primary sources:

1. Geological and geophysical field investigations of a reconnaissance nature published by Mexican federal agencies, universities and binational geoscientific societies, with facsimile copies of some reports included in **APPENDIX D** (e.g., Hawley 1969, Diaz-G and Navarro 1974, Tovar et al. 1978, Cantú-Chapa et al. 1985, SGM 1985, Araurjo-Mendieta and Casar-González 1987, Limón-González 1986, Márquez-Alameda 1992, Zwanzinger 1992, Monreal and Longoria 1999, Lawton 2004, Seager 2004).
2. Map-based reports on the geology and hydrogeology of northern Chihuahua by Mexican Federal agencies, primarily the Secretaria de Recursos Hidráulicos (SRH) and Instituto Nacional de Estadistíca, Geográfica e Informática (INEGI) published between 1982 and 2012 (e.g., Flores Mata et al. 1973, INEGI 1983a-b, 1999, 2012; *cf.* IBWC 2010). The INEGI (1983) data base for 17 wells inventoried in 1982 provided a source of information on aquifer type, static water level, and water chemistry that was essential for the compilation of **TABLE 1** and **PLATE 4** and overall framework-model development (*cf.* SRH 1988, Gutiérrez-Ojeda 2001).
3. Reports with maps on the geology and geomorphology of Chihuahua by universities located in both Mexico and the United States, with some investigations involving collaboration with U.S. federal and state agencies. Most were published between 1969 and 1993 (e.g., Berg 1969, Córdoba 1969a-b, Webb 1969, Córdoba et al. 1970, Reeves 1965 and 1969, Flores Mata 1970, Schmidt 1973, Lovejoy 1976a and 1979, Schmidt and Marston 1981, Gómez 1983, Dyer 1987, Reyes Cortés 1992, Schmidt 1992, Drewes and Dyer 1993, Haenggi 2001 and 2002, Granados Olivas 2000).
4. Reports on oil and gas exploration drilling, which in this case only involved one deep borehole in the Study Area, the 16,218-ft (4.943-m) Pemex No. 1-Moyotes Well (Thompson et al. 1978, Tovar et al. 1978).
5. Three 1:50,000-scale—15 x 20-min. topographic maps (INEGI Cartas topográficas) that cover the area between the International Boundary and 31°30′ N latitude, and 106°30′ and 107°30′ W longitude: Hoja Nos. H13A25-Cuidad Juárez, H13A24-Los Chontes, and H13A23-Nuevo Cuauhtémoc. Even with a minimum-contour interval of 10 m and general absence of ephemeral drainageways on the nearly level basin floors, these maps still allowed approximate delineation of major hydrographic boundaries, particularly where supplemented by Google Earth® imagery.

C. Published information on the geologic framework of the International-Boundary zone that is based on work in both nations, and includes reports on oil and gas exploration, geophysical surveys (gravity and seismic) and hydrogeology (e.g., Reeves and DeHon 1965, Morrison 1969, Lovejoy 1976b, Thompson et al. 1978, Woodward et al. 1978, Thompson 1982, Hibbs et al. 1999, Jiménez and Keller 2000, Hawley et al. 2000 and 2005, Hoffer 2001b, Heywood and Yager 2003, Lawton 2004, Seager 2004, Eastoe et al. 2008, Hawley et al. 2009, Averill and Miller 2013, Hibbs et al. 2015).

Figure 1-10 (page-size **PL. 11**)**.** Index map for major GW-management and geohydrologic units in Mexico and the United States south of 32° N latitude. 2018 Google Earth® image-base. The symbols are discussed in the text.

The "Acuífero Conejos-Médanos" area delineated on **Figure 1-10** is shown in detail on **Figure 1-11**, which is a facsimile copy of the "2011 Binational Waters Map" of the International Boundary and Water Commission (IBWC). CONAGUA has also published the official aquifer delineation for Chihuahua, which can be assessed at:

https://sigagis.conagua.gob.mx/gas1/Edos_Acuiferos_18/chihuahua/DR_0823.pdf

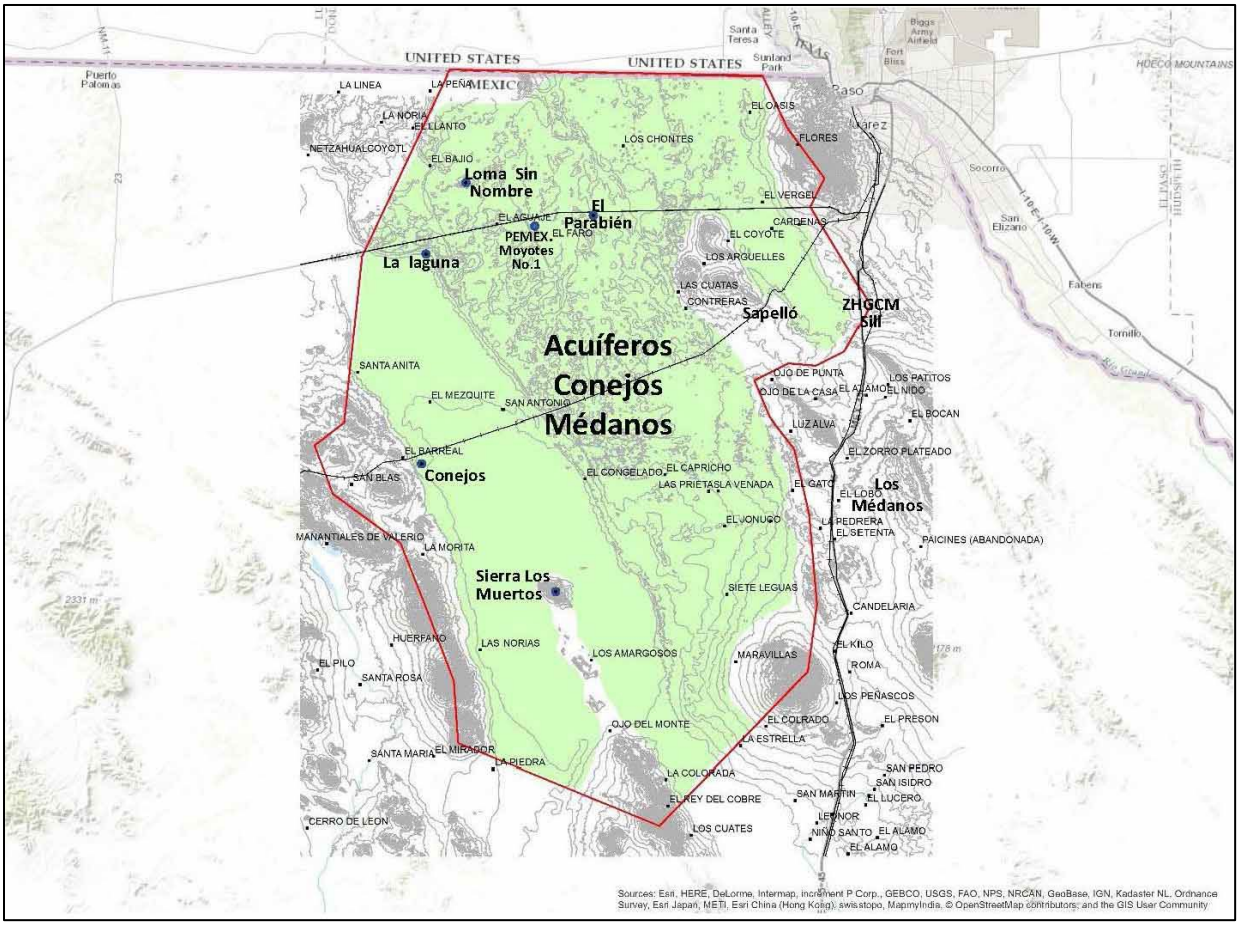

Figure 1-11. IBWC (2011) Acuífero Conejos-Médanos: Binational Waters map.
https://www.ibwc.gov/wp-content/uploads/2022/12/Conejos_Medanos_Aquifer.jpg

1.8.2. Introduction to Hydrogeologic Investigations in the "International Boundary Zone"

Figure 1-12 shows the extent of the 6,565 mi^2 (17,000 km^2) "International-Boundary Zone (IBZ)" as it is provisionally defined in this study. The IBZ is located between the 31° and 32° N Parallels and the 106°30' and 108° W Meridians, and it extends westward from the eastern edge of the Hueco Bolson to the lower Mimbres River and Rio Casas Grandes basins near Columbus, NM and Puerto Palomas, Chihuahua. The southern Study Area is within the black rectangle, and the Mesilla and El Parabién GW Basins are outlined in green and orange. Northern boundaries of the Acuífero Conejos-Médanos and the Zona Hidrogeológica de Conejos Médanos (ZHGCM) are shown, respectively, by back-

dash white and solid yellow lines (*cf.* INEGI 2012, **Fig. 1-10**). Small red dots mark Key-Wells locations (**Fig. 2-3**, **TBL. 1**), and 23 producing wells in the new JMASCJ well-field are shown by dark-red dots within the white oval. Parts of the IBZ inundated by pluvial-Lake Palomas during its Late Pleistocene high stands have blue-gray shading. The MeB's southern watershed boundary of the MeB is in solid blue in **Figure 1-11**, and the approximate position of the its southern GW-flow system boundary is shown with a dashed-blue line. Most of the boundary segment SE of the Camel Mountain Uplift also forms the contemporary GW-flow divide between NE-directed flow toward the lower MeV and EPdN, and SW-directed flow toward El Barreal in the west-central ZHGCM (*cf.* **Figs. 1-2** and **1-10**).

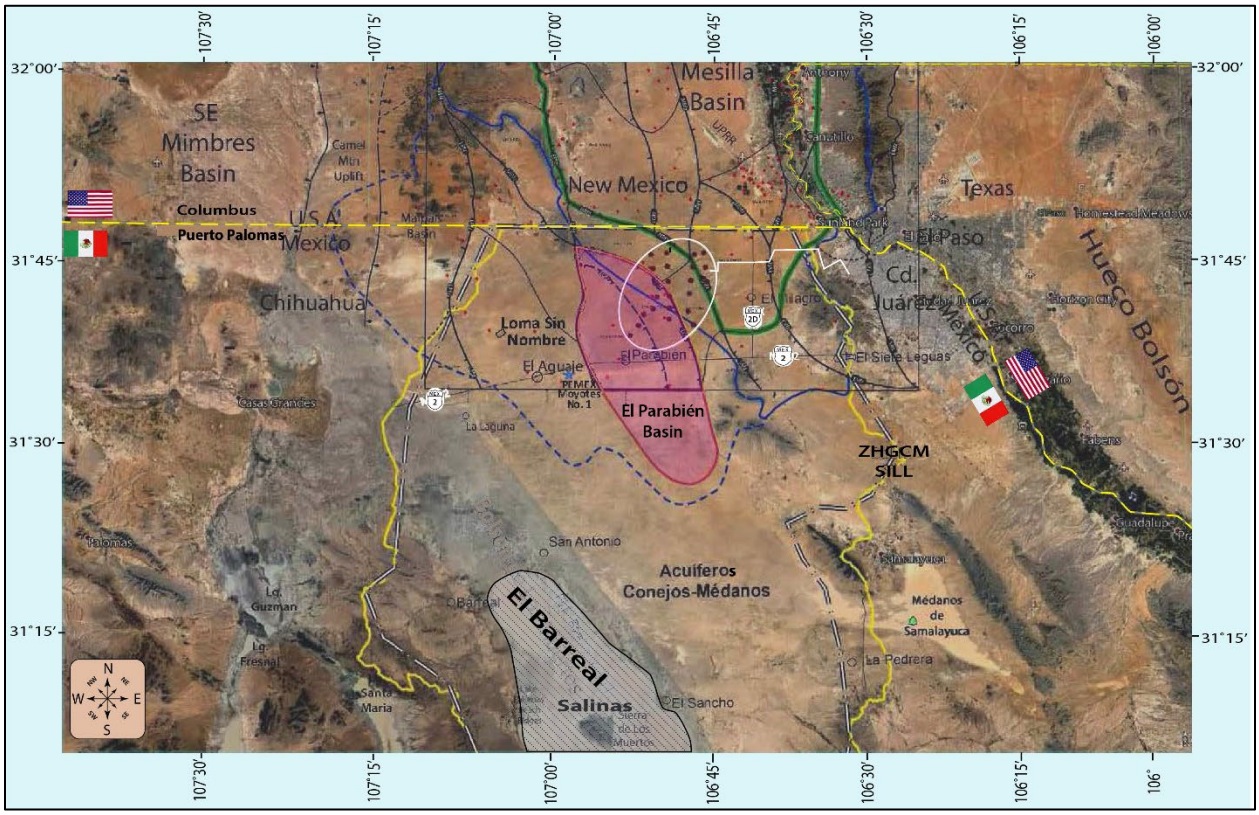

Figure 1-12 (PL 12). Index map of the "International-Boundary Zone (IBZ)" as provisionally defined in this investigation. It is located between the 31° and 32° N Parallels and the 106°30' and 108° W Meridians (*cf.* **Fig. 1-10**). 2018 Google Earth® image base.

The extent of increased GW-production now occurring west of Ciudad Juárez is shown in more detail in **Figure 1-13** (ABQ Jrnl 2019; Pacheco 2019b and 2022a-b; Robinson-Avila 2020f, 2021d, and 2022). The northeast edge of the Los Muertos Basin inundated by high stands of pluvial-Lake Palomas has blue-gray shading in the southwest corner of the map. Small red dots show locations of key wells (**Fig. 2-3**, **TBL. 1**), and black and white dots within the orange oval mark locations of 23 producing wells in the new JMASCJ well-field. The 42-inch water-transmission line that connects the well field with

central Ciudad Juárez is shown with a red-solid and dashed line. GW production is also increasing at three nearby locations: (1) Foxconn complex south of the San Jerónimo-Santa Teresa Port of Entry, (2) Santa Teresa Industrial Park, and (3) near the UPRR Intermodal Terminal and Refueling Station (**Figs. 1-10** and **1-11**; *cf.* **Part 6.3.4b**; ABQ Jrnl 2019; Pacheco 1919b and 2022a-b; and Robinson-Avila 2020f, 2021d, and 2022). The northeast edge of the Los Muertos Basin that was inundated by high stands of pluvial-Lake Palomas is shown with blue-gray shading.

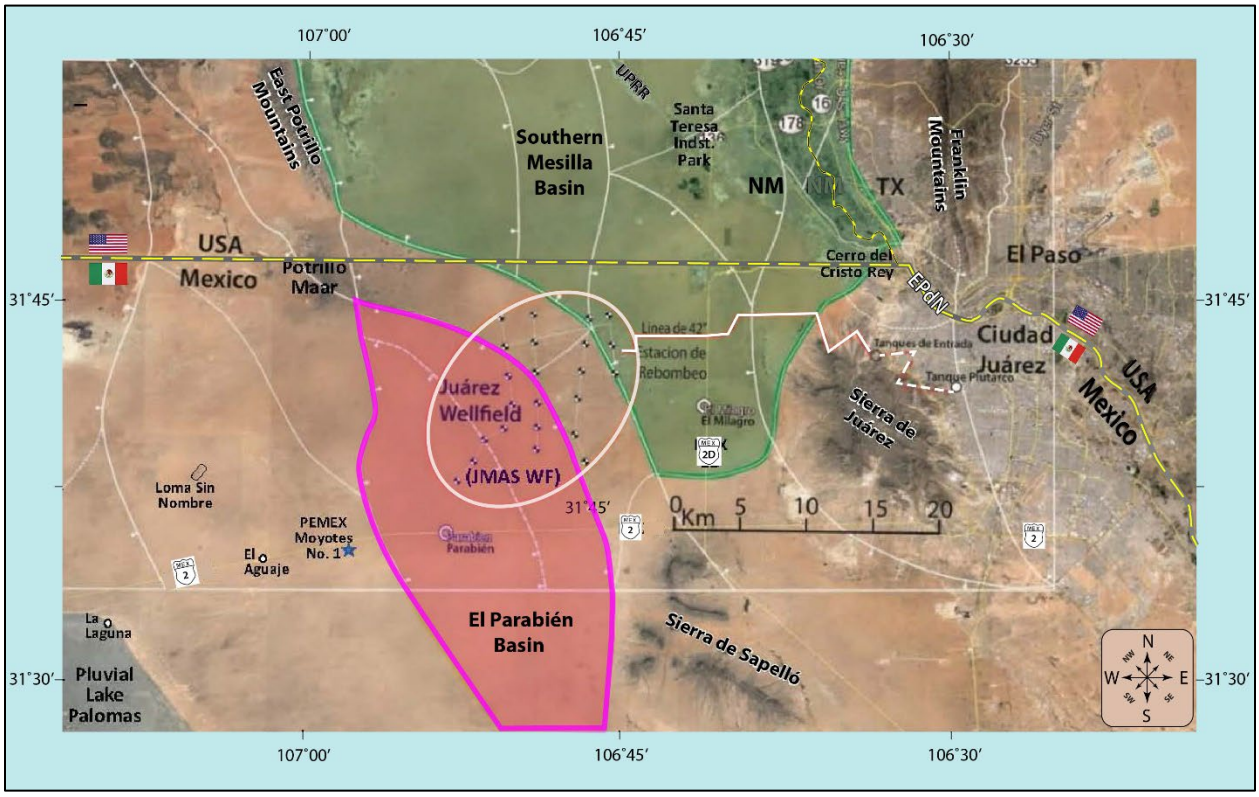

Figure 1-13. Detailed index map for the new JMASCJ well field and the 42-inch (~1.1 m) water-transmission line (red-solid and dashed) that connects it with central Ciudad Juárez. (**Figs. 1-10** and **1-11**). The International Boundary is shown with a yellow line. The white rectangle outlines the southern part of the Study Area, and the Mesilla and El Parabién GW Basins are shown in green and magenta, respectively. 2017 Google Earth® image base.

1.8.3. Border-Wall Construction and Infrastructure-Operation Concerns

The new Border Wall is a 30-ft (9.14 m) high steel-bollard structure that is sited on the International Boundary (**Fig. 1-14**; *cf.* **APNDX. H3.3.2**). It is paralled in most places with a hard-suface roadway for maintence and Border-security activities (**Fig. 1-13**). The Wall's length along the 31° 47' N Parallel west of the MeV is about 85 mi (137 km); and the section in the Study Area is about 35 mi (56 km) long (**Figs. 1-12** and **1-13**). The view across the southern Mesilla Basin from the photo site near the 107° W Meridian depicts a typical Chihuahuan Desert landscape in southwestern Doña Ana County, and

northwestern Municipio de Juárez (**Part 3.3**). El Paso del Norte is on the eastern horizon between the Franklin Mountains and Sierra Juárez Uplifts (**Figs. 1-3**, **1-12** and **1-13**; *cf.* **5.1.3** and **5.1.5**).

The fluvial-deltaic plain of the Ancestral Rio Grande (ARG) in the primary landform, and it forms the Mesilla Basin-West Mesa in this part of the MeB (**Fig. 1-5**). Saturated ARG-channel deposits in the Upper Santa Fe Group (SFG) form the most productive part of the Transboundary basin-fill aquifer system (*cf.* **Parts 6.3.3e**, **6.3.4d**, and **7.6**). SFG-ARG deposits are capped by base-surge tuff ejecta from the Late Pleistocene Potrillo Maar volcanic center is in the foreground (**Fig. 1-3**; Hoffer 2001a; *cf.* **Part 5.6.3**). The long-term impacts of the wall and its infrastructure operation on the land-surface enviroment, and on GW-flow and chemistry have yet to be evaluated **(**Banergee et al. 2018; Attanasio and Galvan 2019; Bixby and Smith 2020; Galvan 2020; Reisen 2020; Spagat 2020, 2021; Turner 2020).

Figure 1-14. (courtesy of PBS-New Mexico in Focus—Our Land) Fall 2019 aerial photograph of a newly completed section of the US-Mexico Border Wall in the southern Mesilla basin at the 31° 47' N Parallel (*cf.* **Fig. 1-15**). El Paso del Norte is on the eastern horizon between the Franklin Mountains and Sierra Juárez Uplifts. The photo site near the 107° W Meridian depicts a typical Chihuahuan Desert landscape in southern Doña Ana County, and northern Municipio de Juárez.

Figure 1-15 is an oblique 2017 Google Earth® image of the International Boundary area west of Paso del Norte. The new (fall 2019) Border Wall follows the 31° 47' N alighnment that was established by the Gadsden Treaty of 1853-1854 (Rebert 2001 and 2005; *cf.* **APNDX. H3.4**). El Cerro del Cristo Rey is in the center foreground, and the East Potrillo Mountains and the Mount Riley-Cox are on the western

skyline beyond the southern Mesilla Basin. Sierra Alta in north-central Chihuahua SW of Columbus NM is on the left of center horizon. The oval feature in the right foreground is the Sunland Park Racetrack. It is near the southern end of the Mesilla Valley (MeV) and northeast of the Rio Grande channel. The Colonia of Anapra occupies a large borderland area of Chihuahua southwest of the Cristo Rey Uplift (CRU), and south of the Union Pacific RR tracks. The Santa Teresa/San Jerónimo Port of Entry and the Santa Teresa Industrial are located north of the Boundary near the eastern edge of the ARG fluvial-deltaic plain (aka West Mesa, **Fig. 1-5**), and the trace of the 42-inch (~1.1 m) water-transmission line leading from the new JMASCJ well field can be seen on the West Mesa surface to the south (**Fig 1-13**).

Figure 1-15. Oblique 2017 Google Earth® image that is centered on the International Boundary between Paso del Norte and the East Potrillo Uplift (**Fig. 12**). Cerro del Cristo Rey and the southern Mesilla Valley of the Rio Grande are in the center-right foreground. The new Border Wall (**Fig. 1-13**) follows a 22 mi (35.4 km) section of the Boundary that crosses the West Mesa area of the southern Mesilla GW Basin (**Fig. 1-5**).

CHAPTER 2.
METHODS

2.1. OVERVIEW

The hydrogeologic-framework characterization that preceded this investigation occurred in several phases (**APNDS. A**, **C to F**, and **H**):

1. Early-stage data collection and interpretation of *field-based* information (e.g., deep-borehole logging, mapping, and cross-section design) combined with use of non-digital cartographic and illustration-drafting methods in preparation of project-completion reports (e.g., W.E. King et al. 1969 and 1971, Hawley 1984, Peterson et al. 1984, Hawley and Lozinsky 1992).
2. Use of early-stage conceptual models and digital methods in development of GIS-based graphics products on which most of the interpretations and conclusions presented herein are based (Hawley et al. 2000 and 2001, Hawley and Kennedy 2004, Witcher et al. 2004, Hawley et al. 2009).

Topics covered include methods used in collection and interpretation of borehole and well records, feature-location/elevation verification (mainly well-site) using best-available field-survey/GPS/GIS platforms, spreadsheet compilation of information on key wells (**TBL. 1**), and construction and electronic-compilation of general base maps, cross-sections, structure-contour and isopleth maps, and block-diagrams.

An addendum to **CHAPTER 4** (**APNDX. A)** includes a detailed-background discussion of basic concepts used in the 1980 to 2010 development of digital methods for hydrogeologic characterization of basin-fill systems throughout the southeastern B&R provinces. It is designed to supplement the information presented herein with more-detailed historical summaries of methods used in earlier stages of graphic and digital hydrogeologic-framework characterization. Some of this essential background information dates back to the field-based investigations of the 1962-1992 period that were funded primarily by the U.S. Soil Conservation Service (USDA-SCS), NM WRRI, N.M. Bureau of Mines & Mineral Resources (NMBMMR), N.M. Tech Hydrology Research group, and the USGS-Water Resources Division (WRD) (*cf.* **APNDS. A** and **C2**-**C4**).

The Report is illustrated by new digital cartographic products, and it includes an updated compilation of well-database information in Excel® spreadsheet format (**TBL. 1**). The iterative process involved in preparation of the current set of hydrogeologic maps (8), cross-sections (19), and block diagrams (2) has been very labor intensive and time-consuming (at least 3,000 hours). Before these products could be developed, moreover, the relevant geological, geophysical, and hydrochemical information (some dating back more than a century) had to be compiled and interpreted in a research environment marked by (1) rapid scientific and technological advances in computer-based modeling and

GIS platforms, as well as (2) uncertain socio-economic and binational-political conditions. The current study phase would certainly not have been possible in the absence of the scientific, technical, and general-knowledge input of dozens of individuals over the preceding five decades.

In 2012 and 2013, seed funding from the U.S. Geological Survey-104b "GIS for Water Resources Research Planning" grant program greatly facilitated the process of editing, and partial redrafting and digital scanning of the provisional maps and cross-sections completed prior to 2012. This collaborative effort included major contributions by co-authors Heather Glaze and Steve Walker (then with the NM WRRI GIS staff), and Lauren Breitner and Sarah Falk of the USGS New Mexico Water Science Center (NMWSC). Subsequently, "Professional Service Contract" funding support from the NM WRRI to the PI (*dba* HAWLEY GEOMATTERS) and Baird Swanson (*dba* Swanson Geoscience, LLC) allowed all early-stage map and cross-section drafts to be updated and recompiled, followed by rescanning and final digitization. Between 2013 and 2018, substantial *pro-bono* support was also provided to the NM WRRI by HAWLEY GEOMATTERS in all aspects of Report preparation. Activity of the latter entity was terminated on 12/31/2018, however, due to the PI's cancer-related inability for full-time work.

The above-described support for digital hydrogeologic map and cross-section preparation has played a key role in ultimate completion of a series of cartographic products in a format that, for the first time, is truly amenable to upgrading as new subsurface information, GIS platforms, and computer-graphic systems become available. Incorporation of less-detailed and more-interpretive hydrogeologic baseline information for the 700 mi^2 (1,815 km^2) part of the Study Area in Mexico also reinforced the need for framework-model simplification and standardization (e.g., Jiménez and Keller 2000, Haenggi 2002, Averill 2007, INEGI 1999 and 2012, Servicio Geológico Mexicano 2011, Averill and Miller 2013; **Figs. 1-1** and **1-9**, **Part 1.2**, **Tbl. 1-3**; *cf.* **Figs. 3-7** and **3-8**; **APNDS. B** to **D** and **H**). Because they were the only published work available at the time, the provisional digital characterizations of regional hydrogeologic framework developed by Hawley and Kennedy (2004) have been utilized by USGS Water-Science Center hydrologists in their most-recent hydrogeologic, hydrochemical, and groundwater-flow models for TAAP-related investigations (*cf.* **Parts 1.2** and **7.3.2**; Sweetkind 2017 and 2018, Sweetkind et al. 2017, Teeple 2017, Hanson et al. 2018, Kubicki et al. 2021).

Background information on place names referred to in the Report (e.g., major landscape features and population centers) is chiefly contained in the following source references: New Mexico—R. Julyan (1996); Texas—Sonnichsen (1968), and Chihuahua—Almada (1968), Márquez-Alameda (1992). Standardized spelling of Hispanic-American geographic names is sometimes uncertain because of the region's complex socio-political history that dates back to 1598, (e.g., bolson-bolsón, Picacho Peak, and the Rio Grande/Bravo River (*cf.* R.T. Hill 1896, 1900, Ordóñez 1936, Tamayo 1968, Hawley 1969, Márquez-Alameda 1992, INEGI 1999; *cf.* **Parts 3.2** to **3.5**, and **APNDS. B** to **D, G** and **H**).

2.2. FEATURE-LOCATION CLASSIFICATIONS

Advances in GPS technology and Google Earth® mapping-base capabilities during the past decade require continued upgrading of well-location records, particularly in the binational parts of the Study Area that are essentially inaccessible by conventional means of transportation. In such places, information on well-head elevation that is needed for preparation of accurate potentiometric-surface maps remains incomplete, and derivative groundwater-flow direction are provisional at best. Boundaries of the 2,700 mi^2 (7,000 km^2) Study Area were initially selected (~2010) on the basis of the need to provide basemap coverage of the then-known extent of the surface-water and groundwater-flow systems that affected subsurface inflow/outflow conditions to and from the Mesilla GW Basin (**PLS. 1** to **4**, **Figs. 1-3**, **1-8**, and **1-11**). The 10,000 m (100 km^2) UTM-SI grid system is used in combination with latitude/longitude-degree and township-range (USA) coordinates for most feature locations. Note, however, that the selected UTM-Zone 13N—NAD-83 boundary coordinates (290,000 m to 360,000 m-easting, and 3,500,000 m to 3,600,000 m-northing) do not extend far enough to the south and west to incorporate the entire regional GW-flow system (*cf.* **Figs. 1-9** and **1-11**; INEGI 2012).

Use of all available, well-location coordinate systems, and recognition of the provisional nature of certain database elements is an important component of **TABLE 1**, an Excel ® spreadsheet containing records of 395 selected (*key*) wells in the Study Area (*cf.* **Fig. 2-1**; **PL. 3**-well-location map). The ongoing compilation now includes baseline data and hydrogeologic interpretations for 319 wells in Doña Ana County, NM, 37 wells in El Paso County, TX, and 39 wells in Chihuahua's Acuífero Conejos-Médanos GW-administrative district (INEGI 2012; *cf.* **APNDX. H**). **TABLE 1** compilation has been a collaborative effort with Report co-author Steve Walker, and its format was designed specifically for present and future binational studies. Its expandable-spreadsheet format facilitates entry of new or modification of existing information on well location and construction, hydrostratigraphic interpretations, and reference sources.

The UTM-SI (metric, NAD-83) coordinate system for feature-location control was adopted by the NM WRRI-GIS Laboratory in the mid-1990s for all project-completion reports with a transboundary-aquifer component (e.g., Hibbs et al. 1997, Hawley et al. 2000; **APNDX. H**). Standard latitude/longitude coordinates (degree-minute-second and/or decimal) have been also used since 1990 in federal and state reports on groundwater resources of the United States part of the Study Area (e.g., Frenzel and Kaehler 1992, Woodward and Myers 1997, Nickerson 2003). While still common in land surveys in the United States part of the Study Area, the State-Plane (ft-unit) coordinate system is not used in **TABLE 1**.

The NM Office of State Engineer (NM OSE) and the USGS have long used the U.S. Public-Lands Survey system of township-range-section (TRS) subdivisions as their primary location-index units for many geographic features including wells. Because it provides the only viable cross-referencing tool

for accessing critical well-site information published before 1990, the TRS alpha-numeric code (**Fig. 2-1a**) is retained as a secondary well-location identifier in **TABLE 1** (e.g., Lee 1907, Darton 1916, Meinzer and Hare 1916, Dunham 1935, Conover 1954, King et al. 1971, Wilson et al. 1981, and Seager et al. 1987). The unique latitude/longitude/quadrangle well-location system developed for use in Texas is shown on **Figure 2-1b**.

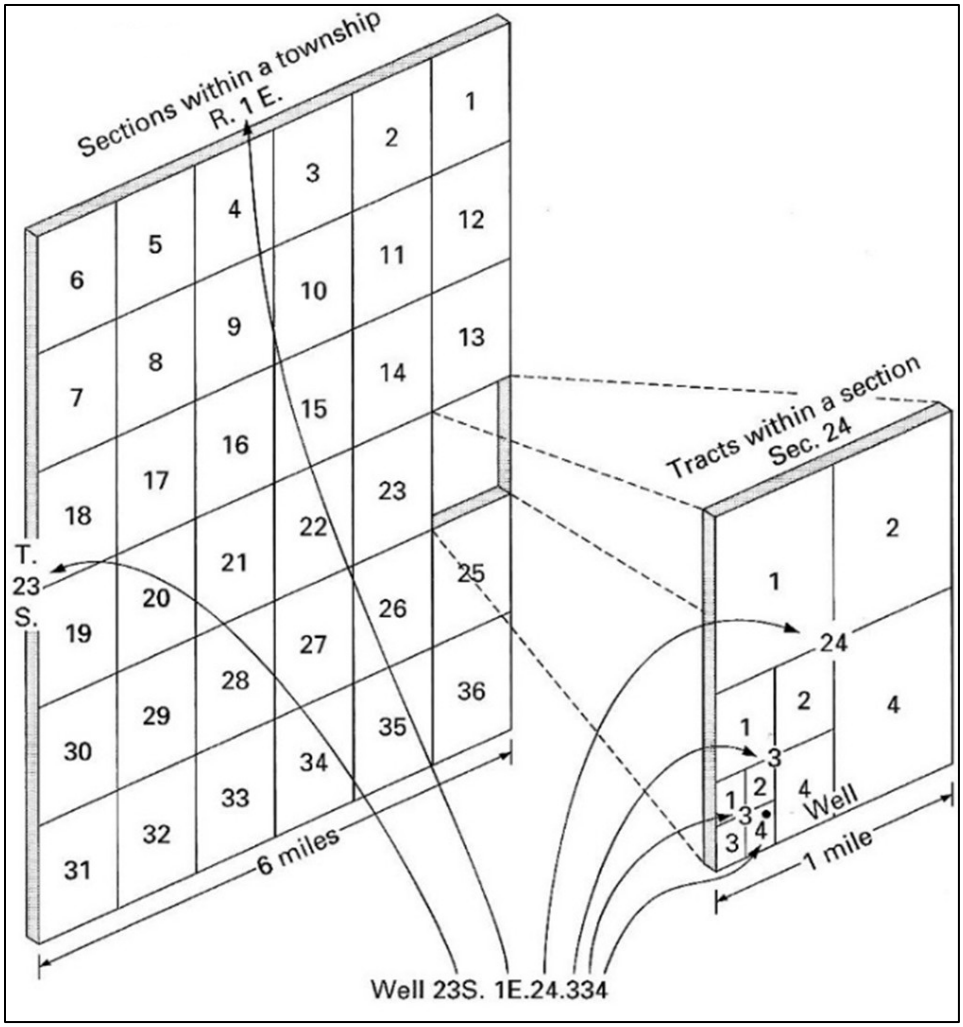

Figure 2-1a. New Mexico well-numbering system.

In New Mexico, the TWS well-location number consists of four segments separated by periods that correspond to the township, range, section, and tract within a section (**Fig. 2-1a**). Townships and ranges are numbered according to their location relative to the NM Base Line and the NM Principal Meridian. The smallest division, represented by the third digit of the final sequent, is a 10-acre (4 ha) tract. If a well has not been located precisely enough to be placed within a particular section or tract, a zero is used for that part of the location number.

Wells in Texas are assigned a number consisting of five parts. The first part of this numbering system is a two-letter prefix used to identify the county, with El Paso County being represented by JL (**Fig. 2-1b**). The second part of the number has two digits indicating the 1-degree quadrangle (here the west part of the El Paso 2-degree sheet). Each 1-degree quadrangle is divided into 64 7.5-minute quadrangles. This is the third part of the well number. The first digit of the fourth part indicates the 2.5-minute quadrangle, and the last two digits comprise a sequence number that identifies the well from others in the same 2.5-minute quadrangle. As an example (**Fig. 2-1b**), well JL-49-04-501 is in El Paso County (JL), in 1-degree quadrangle 49, in 7.5-minute quadrangle 04 (Canutillo), in 2.5-minute quadrangle 5, and was the first well inventoried in this 2.5-minute quadrangle.

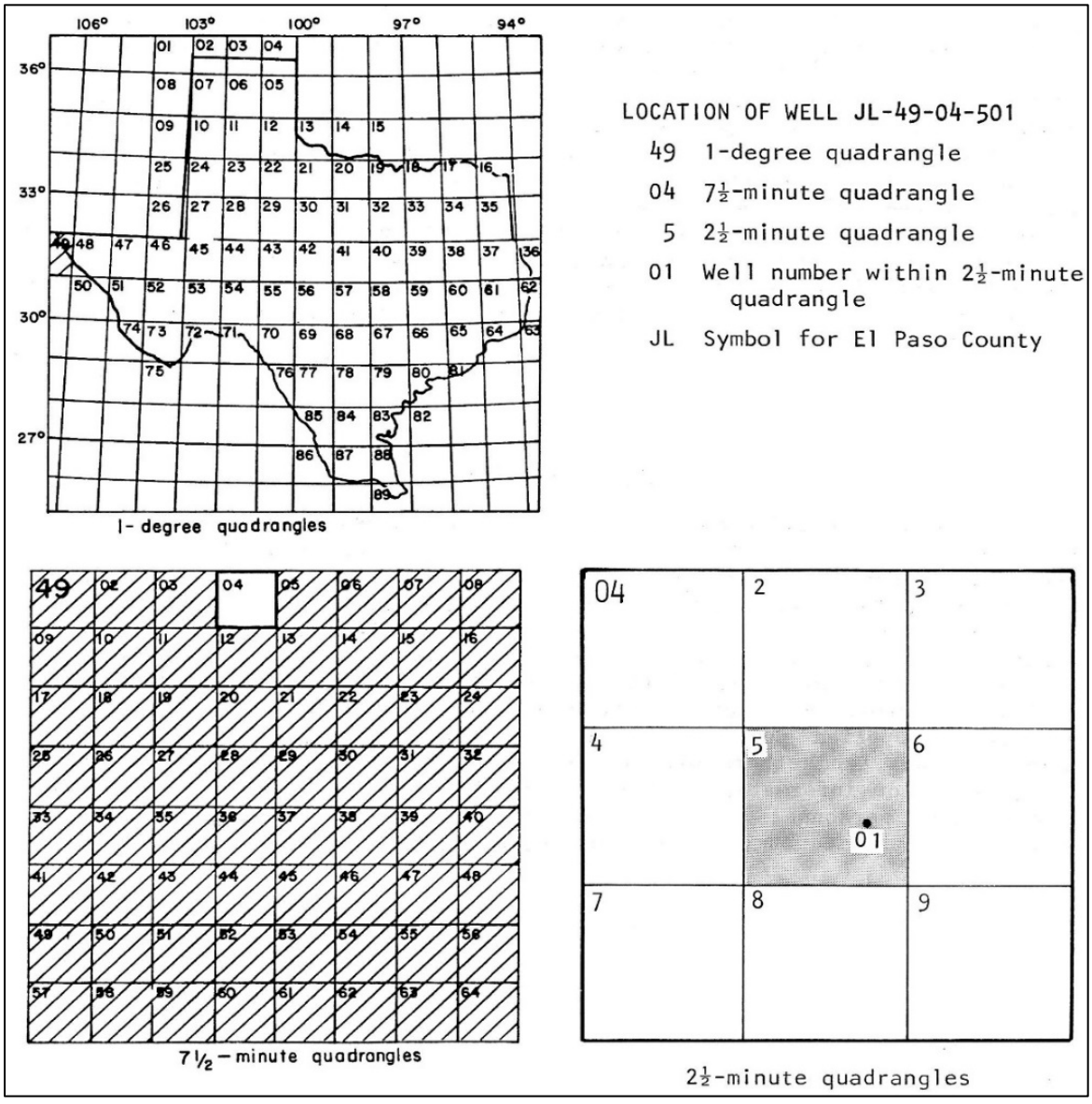

Figure 2-1b. Texas well-numbering system.

2.3. PREPARATION AND CONTENT OF TABLES AND PLATES

2.3.1. Background on the Tradition of Merging Art with Science

1. There is a long tradition of merging art with science, originating from both fields of study, with good reason. The idea that truth can be made visible has a long history directly affecting both disciplines. For example, in the rise of the natural sciences in the nineteenth century, vision was understood as a primary avenue to knowledge, and sight takes precedence over the other senses as a primary tool in the analysis and ordering of living things-opening doors to collaborations between artists and scientists even then. Communication in both art and science is dependent on cooperative and collaborative methods in lab-, field-, virtual-, and three-dimensional space and time. Finally, art is perfectly positioned to bring science to the world beyond scientists, filling a crucial need for more effective science communication to the public.*

**Bringing art to your science and thus your science to the people: Joining visual culture and scientific evidence (Gámez, Ranis, and Eppes, 2021, p. 11).*

2. The idea that people have different thinking patterns is not new. Francis Galton [1886, 1911], in *Inquiries into Human Faculty and Development*, wrote that while some people see vivid mental pictures, for others "the idea is not felt to be mental pictures, but rather symbols of facts. In people with low pictorial imagery, they would remember their breakfast table but they could not see it."

It wasn't until I went to college that I realized some people are completely verbal and think only in words. . . . When I invent things, I do not use language. Some other people think in vividly detailed pictures, but most think in a combination of words and vague generalized pictures.

For example, many people see a generalized generic church rather than specific churches and steeples when they read or hear the word steeple. Their thought patterns move from a general concept to specific examples. I used to become very frustrated when a verbal thinker could not understand something I was trying to express because he or she couldn't see the picture that was crystal clear to me. Further, my mind constantly revises general concepts as I add new information to my memory library. It's like getting a new version of software for the computer. My mind readily accepts the new "software," though I have observed that some people often do not readily accept new information.*

**Temple Grandin (2006, p. 11) Different ways of thinking,* in *Thinking in Pictures.*

3. A heuristic or heuristic technique (Ancient Greek: εὑρίσκω, heurískō, 'I find, discover'), is any approach to problem solving or self-discovery that employs a practical method that is not guaranteed to be optimal, perfect, or rational, but is nevertheless sufficient for reaching an immediate, short-term goal or approximation. Where finding an optimal solution is impossible or impractical, heuristic methods can be used to speed up the process of finding a satisfactory solution. Heuristics can be mental shortcuts [aka rules-of-thumb] that ease the cognitive load of making a decision.

**https://en.wikipedia.org/wiki/Heurisic; cf. Kahneman and Tversky (1974 and 1996), Lewis (2017, p. 183), and J.B. Miller and Gelman (2020)*

2.3.2. Background on the Compilation and Content of TABLES 1 to 3

An especially challenging task involved compilation of a robust subsurface database on hydrogeologic-framework characterization that is based on available records of *key wells* in the NM WRRI Study Area (*cf.* **Parts 2.4** and **4.2**). *Key well* selection was based primarily on the depth and quality subsurface information on (1) hydrostratigraphy, (2) hydrochemistry, and (3) the accuracy of predevelopment static water-level data. **TABLE 1** is a compilation of information on 395 *key wells* in

Excel® spreadsheet format. Published and unpublished database sources are listed in **TABLE 1A**, and **TABLE 1B** includes an index to the acronyms for the hydrogeologic-map subdivisions in which the wells are located (**Fig. 2-2**, and **Tbl. 1-4**). Specific information on feature-location, stratigraphic-unit composition, and fault-zone categories on maps and cross-sections is also compiled in **TABLES 2** and **3**.

2.3.3. Background on the Compilation and Content of PLATES 1 to 8

Preparation of the Report's maps (8), cross-sections (19), and block diagrams (2) has involved merging geoscience with artistic expression (e.g., **PLS. 1** to **8**). The effort has required the scientific and technical input of dozens of individuals, including skilled cartographers and GIS specialists, over an interval of more 50 years. Concepts and assumptions used in map, cross-section, and derivative block-diagram preparation have been derived from the large body of Earth-science information in the public-domain, most of which has been adequate for basin-scale hydrogeologic-framework characterization (*see* **APNDS. A-D**). Major components of this database include information on (1) surficial geomorphic and geologic relationships, (2) subsurface stratigraphy and structure, and (3) geophysical and hydrochemical conditions. With respect to just the remote-sensing interpretation of geomorphic processes and landscape features, the current generation of space-platform imagery (e.g., Google Earth®) has played an essential role in illustration preparation, particularly in parts of the MBR in Mexico.

Geologic processes and their lithologic-material and structural products are inherently deterministic in nature, and sampled populations of representative types are relatively small in many cases. As such, many illustrations had to be initially designed and manually compiled by the PI, whose field-based experience in the American West dates back to the 1950s. Accordingly, detailed field-based mapping efforts, such as those by W.R. Seager and associates, with maps in the 1:24,000 to 1:125,000 scale range, will never lose their essential value for hydrogeologic investigations throughout the MBR (e.g., Seager and Hawley 1973, Seager et al. 1971, 1975, Seager 1981, Kelley and Matheny 1983, Seager et al. 1987, Seager and Mack 1991, 1994, and Seager 1995). Otherwise valuable stochastic-statistical tools like ArcGIS® kriging functions are rarely appropriate for 2-D or 3-D portrayals of hydrogeologic-framework components at a wide range of map scales in the MBR.

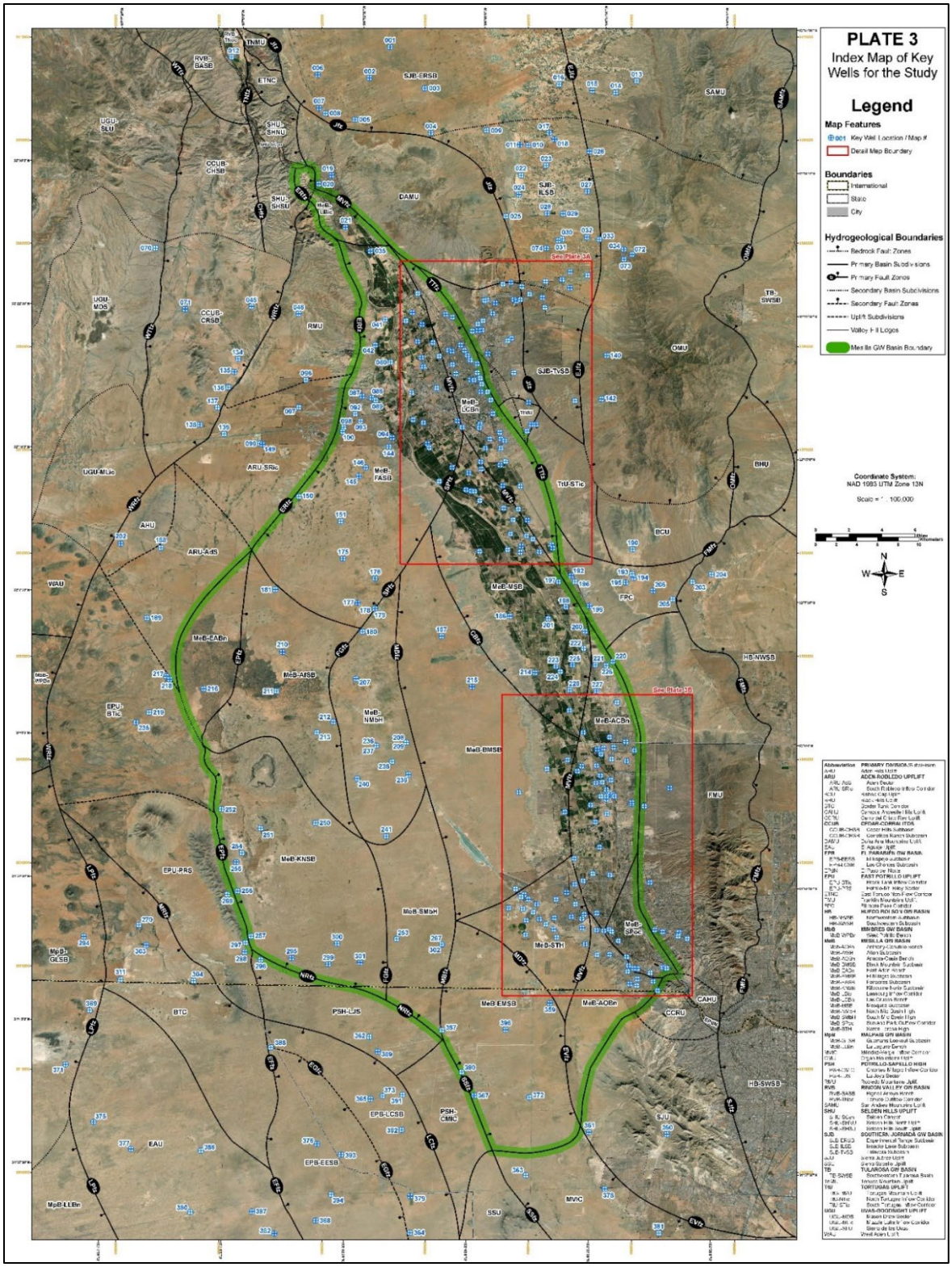

Figure 2-2 (PL. 3). Index map showing locations of the 395 key wells (blue) that were the primary sources of the subsurface hydrogeologic information used in this study. The Mesilla GW Basin is outlined in green. Well locations are shown in more detail within red rectangles.

PLATES 1 to **8** comprise some of the study's most innovative cartographic products, and represent an important advance over previous work (e.g., Hawley and Kennedy 2004, Hawley et al. 2005 and 2009). These illustrations include updated sets of hydrogeologic maps and cross-sections **(PLS. 1** to **7**) that have been redesigned to allow much more precision in definition of (1) basin-fill and bedrock composition, and (2) lithologic and rift-structural boundary conditions. Except for the block diagrams (**PLS. 8A** and **8B**), each item has been designed to portray as effectively as possible the geomorphic, lithologic and structural properties of the hydrogeologic framework that directly or indirectly control GW flow and chemistry to depths of as much as 4,000 ft (1,220 m) below ground surface (bgs). These illustrations were initially compiled at a map scale of 1:100,000, and each is designed for both 11 x 17-inch format printing and electronic-file access in the Report DVD.

Basin-boundary bedrock units are primarily grouped on the basis of geohydrologic and lithologic commonality rather than on chrono- [time-] stratigraphy. Major geology-based (RG-rift) structural subdivisions include (1) groundwater (GW) basins, (2) internal GW-basin subunits, (3) basin-bounding bedrock uplifts (U) and their lithostratigraphic composition, (4) inter-basin/intrabasin underflow corridors, and (5) major boundary-fault zones (**Tbl. 1-5**, **TBL. 3**). Locations of the Rio Grande Valley floor and hydrogeologic cross-sections A-A' to S-S' are also shown (**PL. 5a to 5s)**. Map-unit subdivision nomenclature also facilitates depiction of parts of the Study Area where GW-basin boundaries do not coincide with the positions of surface- and/or subsurface-watershed divides (**Figs. 1-8**, **1-9, 1-10** and **2-2**).

The new hydrogeologic map compilations in this Report show major framework components (lithologic, stratigraphic, and structural) on digital terrain-model or 2017-18 Google Earth® image backgrounds (e.g., **PLS. 1** to **4**, **6, 7** and **9**). Expanded explanations of stratigraphic map-unit categories and their hydrostratigraphic- and lithostratigraphic-framework components are also included in **TABLES 1** and **2**. **Figure 1-7** (**Part 1.6**) is representative of an early stage in **PLATE 1** series compilation. The provisional map, which was completed in December 2012, shows the surficial distribution of primary bedrock and RG-rift structural components of the NM WRRI Study Area (*cf.* **APNDX. A3**).

Hydrogeologic characterization of basin-fill deposits in the 700 mi^2 (1,815 km^2) part of the Study Area in Mexico is more general in nature, however, and most of the mapping units have been defined at a 1:100,000 scale (e.g., INEGI 1983a, b 1999; SGM 2004, CONAGUA 2022; *cf.* **APNDS. H4** to **H7**). As also noted in **Part 1.2.2,** much of the information on the northern "Zona Hidrogeológica Conejos-Médanos (**Fig. 1-9**)" used in the preparation of **PLATES 1** to **5** maps and cross-sections is based on 1990s detailed-reconnaissance work by the University of Texas-El Paso (UTEP) Geophysical Research Center on the "Rift Basin Structure of the Border Region . . ." (e.g., Jiménez and Keller 2000; *cf.* **Figs. 3-7** and **3-8**).

2.3.4. PLATE-Content Summaries

PLATE 1A (**Fig. 1-3**) is a Study Area index map showing locations of the Mesilla, Southern Jornada, and El Parabién GW basins (MeB, SJB and EPB), which are outlined in green, orange and red, respectively. Also shown are the locations of hydrogeologic cross-section **A-A'** to **S-S' (PLS. 5a** to **5s**), major terrain features, and the Las Cruces and El Paso/Ciudad Juárez metropolitan centers. **PLATE 1B (Fig. 1-8)** is an index map that shows the names, locations, and areas in km² of the primary hydrogeologic map-unit subdivisions that form 7 GW basins (B), 10 major and 9 minor inter-basin bedrock uplifts (U), and 5 inter-basin underflow corridors (C) (**TBL. 2**, Tbls. **1-3** and **6-1**). Emphasis is on three GW Basins: (1) Mesilla - MeB, (2) Southern Jornada - SJB, and (3) El Parabién - EPB.

PLATE 2A (**Fig. 3-7**) is provisional composite hydrogeologic and Bouguer [isostatic-residual] gravity map that covers the Study Area south of 32°30′ north latitude. It comprises a hydrogeologic-map overlay on the original Bouguer gravity compilation of Jiménez and Keller (Fig. 4; *cf.* **Part 3.4**; **Figs. 3-6** and **3-7**). **PLATE 2B** (*cf.* **Fig. 3-10**) is a schematic representation of basin-fill subcrop topography with its primary lithostratigraphic and structural components displayed on a 2017 Google Earth® image-base. The variable structure contour interval is 25-, 50-, and 100-m amsl (*cf.* **Fig. 4b**). W-E red lines show locations of geologic cross-sections I-I′ to III-III′ (*cf.* **Fig. 3-11**). **PLATE 2C** (*cf.* **Fig. 3-11**) is a set of three schematic cross-sections that show major stratigraphic and RG-rift structural features in the northern, central, and southern parts of the Study Area. Base elevation is 10,000 ft (3 km) below mean sea level (msl), and vertical exaggeration (VE) is about 2.5 (*cf.* **Part 3.4**). Section locations are shown on **Figure 3-12 PL. 5**), and stratigraphic-units are defined on **Table 3-2**.

PLATE 3 (**Fig. 2-2**) is an index map showing locations of the 395 key wells (blue) that were the primary sources of the subsurface hydrogeologic information used in this study. **TABLE 1** (includes a detailed entry for each well (*cf.* **Part 2.3.2**). The Mesilla, Southern Jornada, and El Parabién GW Basins are outlined in green, orange, and violet, respectively, and explanations of names and acronyms of hydrogeologic mapping units, including fault zones (fzs) are included in **Tables 1-4** and **1-5**. Inset maps **PLATES 3A** and **3B** (red boxes on **PL. 3**) show well-location details in the Las Cruces (3A) and El Paso (**3B**) areas.

PLATES 4A and **4B** (page size **Figs. 1-9a** and **1-9b**) are maps of major geohydrologic features of the Study Area. For water-resource administrative purposes, intermontane “alluvial basins” of the eastern Basin and Range province are typically defined in terms of surface-watershed units, with map-unit boundaries most commonly based on combinations of watershed-divide positions and locations of diversion-dam sites in river-canyon reaches (*cf.* **Fig. 1-5**). Thin blue lines (20 and 100-ft contours on **PL. 4A**, and orange 5, 10 and 30-m contours on **PL. 4B**) show the approximate pre-development (~1976-1982) potentiometric-surface altitudes (*cf.* **TBL. 1**).

The nineteen hydrogeologic cross-sections in the **PLATE 5 (5a** to **5s)** series form a fence-diagram array, with section locations shown on **Figure 1-3**. Thirteen sections have a transverse basin/river-valley orientation (**PLS. 5a-5l** and **5s**) and six sections follow general basin and mountain-range trends (**PLS. 5m-**5r; **Part 2.3.2**). **PLATE 5o** (Section O′-O" O"-O"" O″′O"' series) was compiled to better illustrate the hydrologic linkage (via Selden Canyon and El Paso del Norte) between major hydrogeologic-framework components in the Rincon Valley Basin (RVB) with those in the binational western Hueco Bolson (e.g., Hawley and Kennedy 2004, and Hawley et al. 2005, 2009 (*cf.* Witcher et al. 2004, Eastoe et al. 2008, 2010, Hibbs et al. 2003, 2015, Kubicki et al. 2021). Initial section drafting was done at 1:100,000 plan-scale with no vertical exaggeration [VE] to ensure that basic geologic-structural relationship are portrayed. A VE of 5x was used in the final digital compilation, however, in order to allow more-schematic illustration of the basic subsurface hydrostratigraphic and structural relationships to Mean Sea-Level (msl) elevation. As described in detail in **APPENDIX A**, the iterative process of cross-section design in the MBR, started with work done in support of early-stage GW-flow modeling efforts in the Mesilla GW Basin (MeB) by Khaleel et al. 1983, Peterson and others (1984), and Frenzel and Kaehler (1990, 1992) (e.g., Hawley 1984, Hawley and Lozinsky 1992, and Nickerson and Myers 1992; *cf.* **Part 7.3.1**).

Figures 2-3 and **2-4** are half-page reproductions of down-RG valley/canyon and transverse hydrogeologic cross-sections (**PLS. 5o**, and **5i-5l** and **5s)**. They extend, respectively, from (1) the Lower Rincon Valley Basin to the western Hueco Bolson, and (2) across the northern and central parts of the International Boundary Zone (IBZ – **Figs. 1-11** and **7-9**; Sections O-O'-O"-O"', I-I' to L-L' and S-S'). Inset index maps on the left end of individual sections show their specific locations (*cf.* **Fig. 1-3**). The approximate pre-development water-table/potentiometric-surface altitude (**Fig. 7-2**) is shown by a blue line in each section's upper part. The most-productive upper and middle parts of the SFG basin-fill aquifer system are shown with lighter shades of yellow. Thin (<30 m) Rio Grande alluvial deposits of Later Quaternary age (RA [RG]) are in orange (*cf.* **Parts 3.4** and **4.2**). Santa Fe Group (SFG) Hydrostratigraphic Units (HSUs USF/MSF/LSF) are shown with yellow shading, with lighter hues indicating best groundwater-production potential. Underlying bedrock units, in order of increasing age, comprise the following lithostratigraphic sequence (*cf.* **TBL. 2**): Tlvs-Eocene volcaniclastic, epiclastic and volcanic rocks of intermediate composition (gray), Tli-Eocene intrusive igneous rocks of intermediate composition (red), Tls-Lower Tertiary siliciclastic sedimentary rocks (tan), K-Cretaceous marine sedimentary rocks (light green), Pzu/Pzl-Upper and Lower Paleozoic marine sedimentary rocks (dark and light blue), and XY-Proterozoic (Precambrian) igneous and metamorphic rocks (light brown).

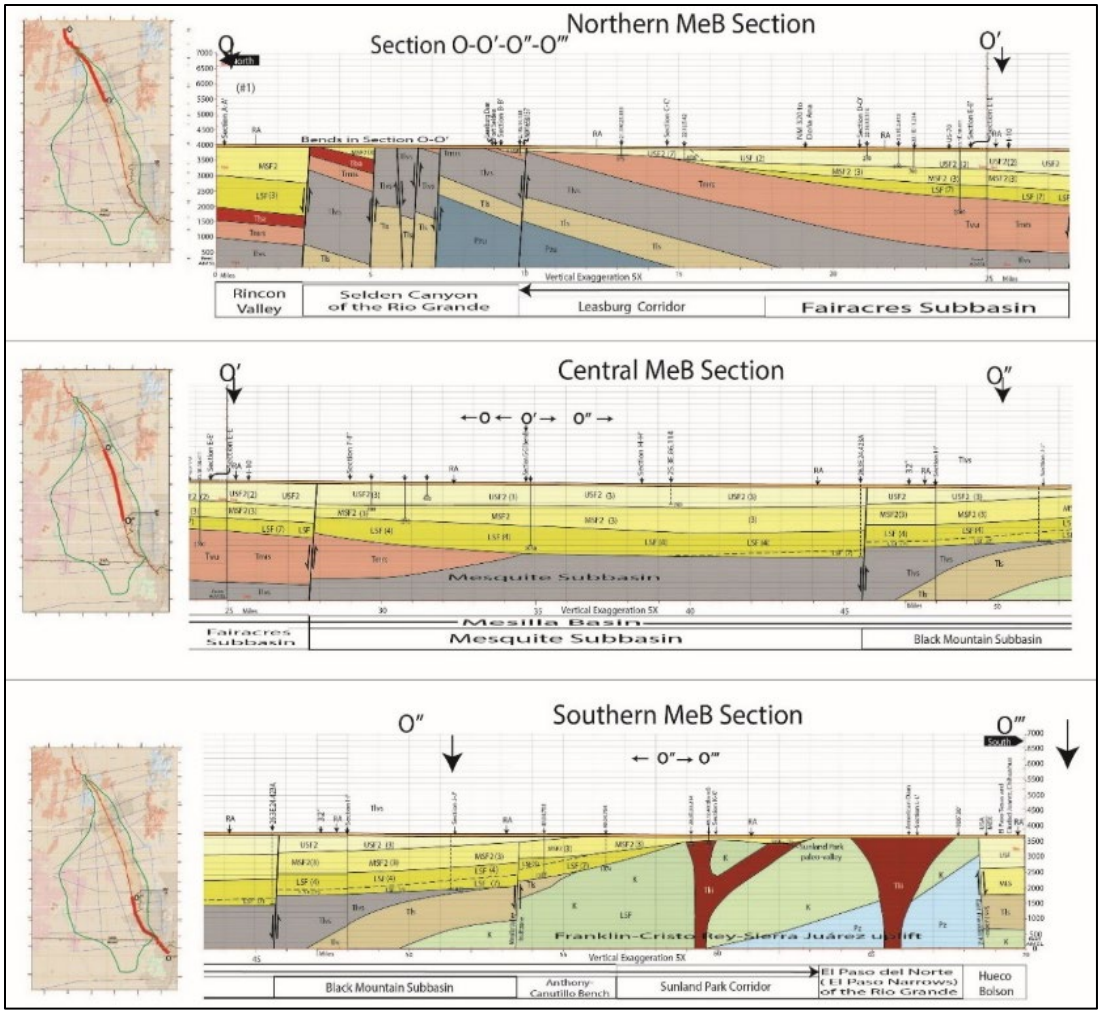

Figure 2-3. Page-size reproduction of **PLATE 5o** series of down RG Valley/Canyon (NNW to SSE) hydrogeologic cross-sections O-O'-O'-O"', with locations on shown on inset index maps **(Fig. 1-3**). Base elevation-msl and VE-5x. The approximate pre-development water-table/potentiometric-surface altitude is indicted by the blue line in the upper part of each section (**Fig. 1-9a,b**). Santa Fe Group (SFG) Hydrostratigraphic Units (HSUs) are shown with yellow shading.

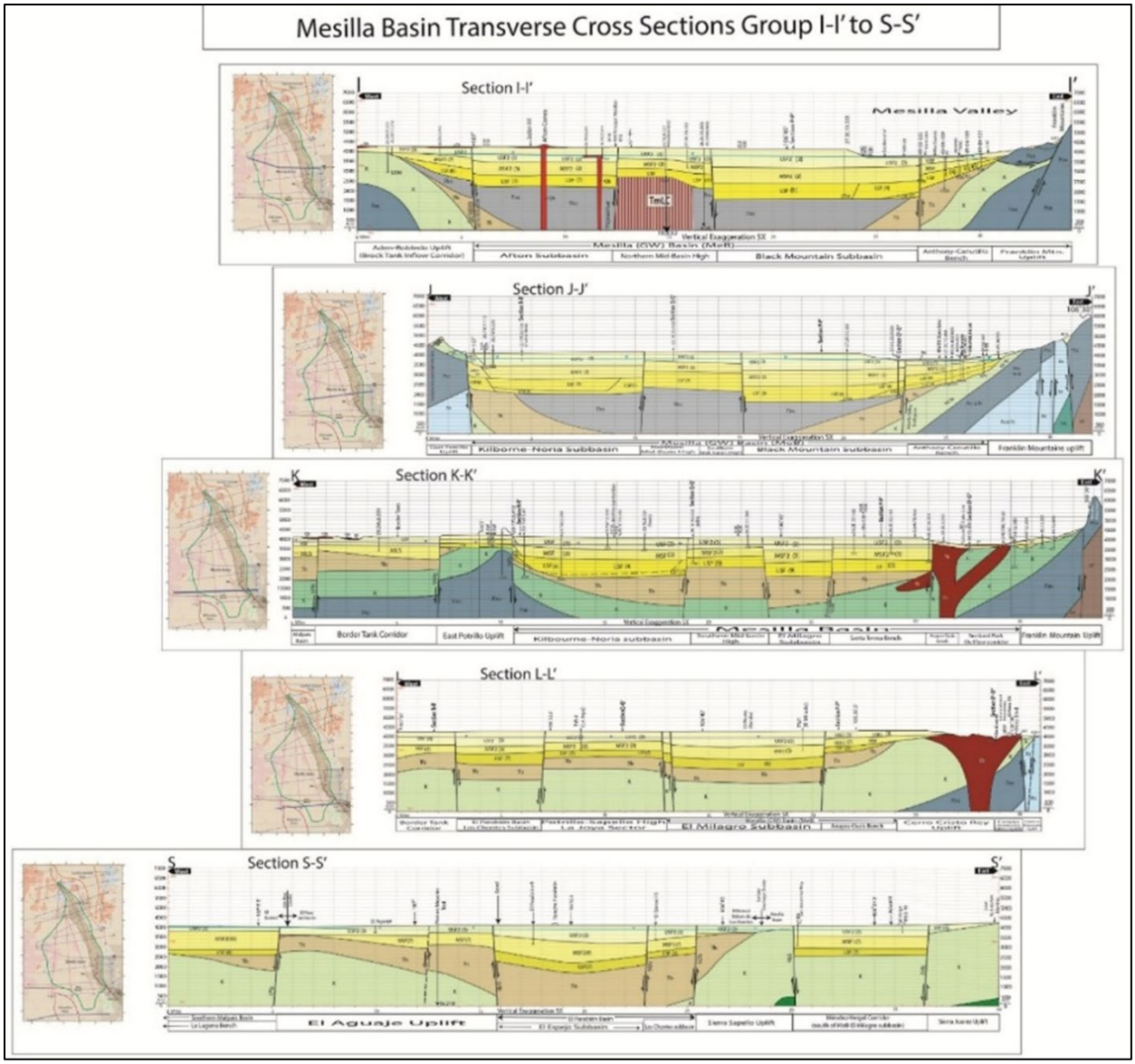

Figure 2-4 (page-size reproduction of **PLATE 5i** to **5l** and **5s** panel)**.** Transverse (W to E) hydrogeologic cross-sections I-I' to L-L' and S-S' that span the northern and central parts of the International Boundary Zone (IBZ–**Fig. 1-11**).

PLATES 6A to **6C** are structure-contour maps of the basal-bounding surfaces of the SFG Hydrostratigraphic Units (HSUs) that form the primary components of the basin-scale hydrogeologic-framework (**Fig. 2-5** [**PL. 6C-2**]). They represent state-of-practice interpretations of the topography and structural-boundaries of HSU basal surfaces for (1) the rift-basin fill bedrock boundary (e.g., **Fig. 3-11** and **Tbl. 3-2**), (2) Middle/ Lower Santa Fe HSU boundary surface, and (3) Upper/ Middle Santa Fe HSU boundary surface. The primary contour interval is 100-ft amsl on **PLATE 6C-1**, but to facilitate its use in ongoing TAAP activity (**Part 1.5.1**), the topography of the mostly buried bedrock surface is also contoured at 25-, 50-, and 100-m intervals on **PLATE 6C-2** (**Fig. 2-5**).

PLATE 7 comprises three new volumetric (isopleth) maps (**PLS. 7A** to **7C**) that show the primary lithofacies-assemblage (LFA – **Part 4.2**) composition of the saturated parts of each member of the SFG Hydrostratigraphic Unit (HSU-USF/MSF/LSF) sequence in the major GW basins of the Study Area (**Fig. 2-6**; *cf.* **CHAPT. 6).** They are general equivalents of the volume-element or "voxel" units of Sweetkind (2017, 2018; *cf.* Ahmed 2009, Journel and Huijbregts 1978, Geosoft 2016). They are designed for use in ongoing groundwater-flow model development. Each map was initially manually constructed from electronic overlays of potentiometric-surface and HSU-bounding surface and maps (**PLS. 4** and **6**). **Figure 2-6** (**PL. 7A**) is page-size isopleth map of the saturated part of HSU-USF that schematically depicts composition and thickness of the unit's primary LFAs.

PLATES 8A and 8B are northeast-facing block diagrams of the central (**8A**) and southern (**8B**) Mesilla Basin that schematically portray major RG-rift stratigraphic and structural features at no VE and a base elevation of 25,000 ft (7.6 km) below msl (2017 Google Earth® image-base; compilation scale 1:100,000; *cf.* **3-9** and **3-10**). For the purposes of this study, these illustrations provide a basin-scale interpretation of available information on deep-seated hydrogeologic relationships from a southern Rio Grande rift-tectonic perspective. Both show the inferred superposition of north-trending, mid- to Late Cenozoic RG-rift extensional features onto the northwest-trending compressional-structural fabric of the Laramide Potrillo and Rio Grande uplift and basin complex of Paleocene-Eocene age (*cf.* Lawton 2004, Seager 2004, Averill and Miller 2013).

PLATE 9-series maps comprise facsimile copies of historic water-table/depth-to-water maps from the following Federal and State publications. **PLATE 9A** (*cf.* **Fig. 7-11**) is a copy of Plate 1 *in* Conover (1954) that shows approximate 1947 groundwater-level contours in central and southern Doña Ana County, New Mexico. **PLATE 9B** (*cf.* **Fig. 7-12a, b**) is a 1969 groundwater-level map based on data collected from 1965 to 1968 by W.E. King and others (1969 [Pl. 1 *in* King et al. 1971]). **PLATE 9C** (*cf.* **Fig. 7-13**) is a map showing approximate water-level contours in the New Mexico and Texas parts of the Mesilla GW Basin (Frenzel and Kaehler 1992, Pl. 1).

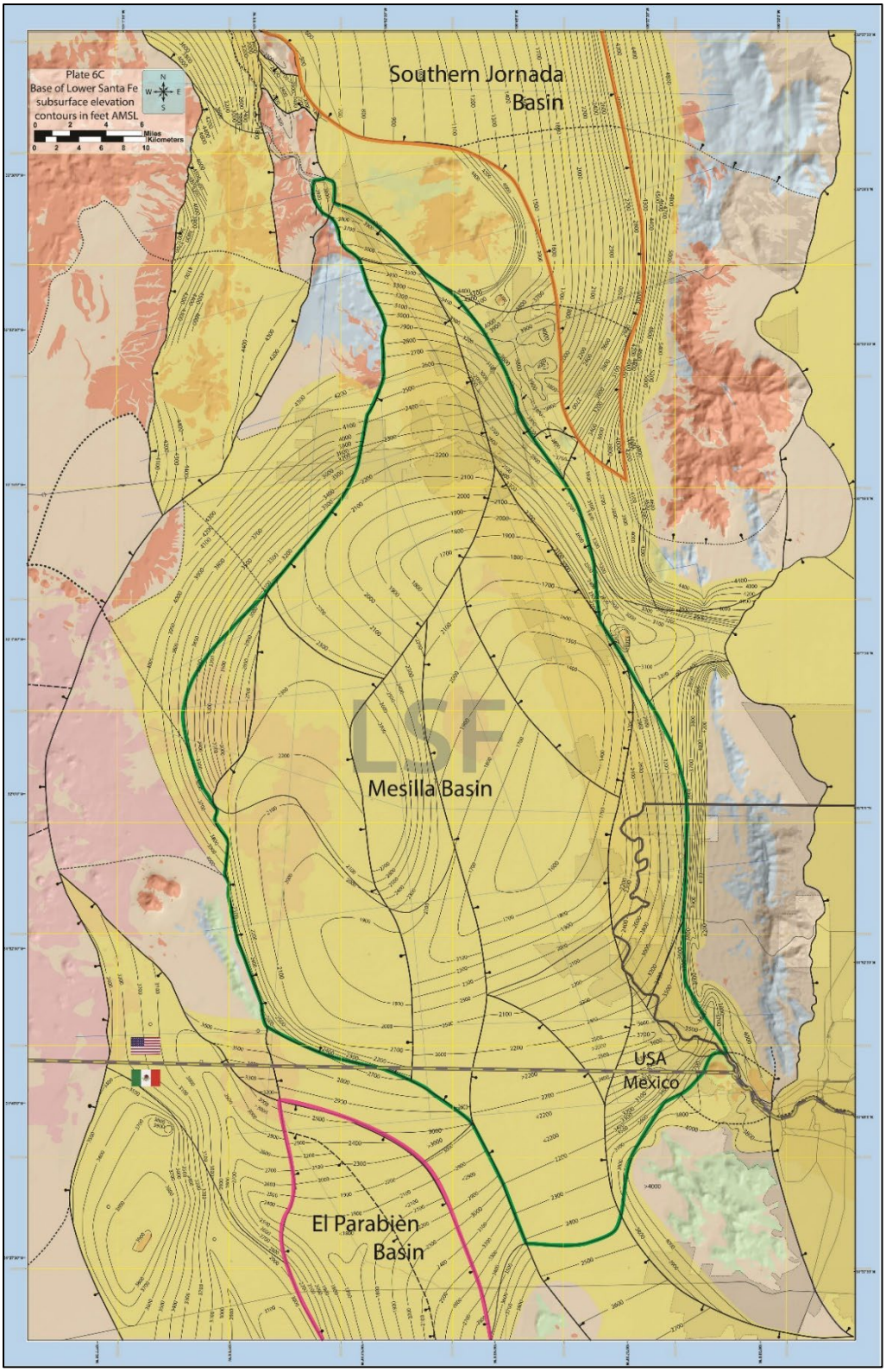

Figure 2-5 (**PL. 6C-2** page-size reproduction)**.** Schematic representation of the Study Area's basal basin-fill topography and primary structural components, with the MeB outlined in green. Variable structure-contour interval at 25, 50, and 100 m amsl (*cf.* **Figs. 1-9, 2-5** and **3-12**).

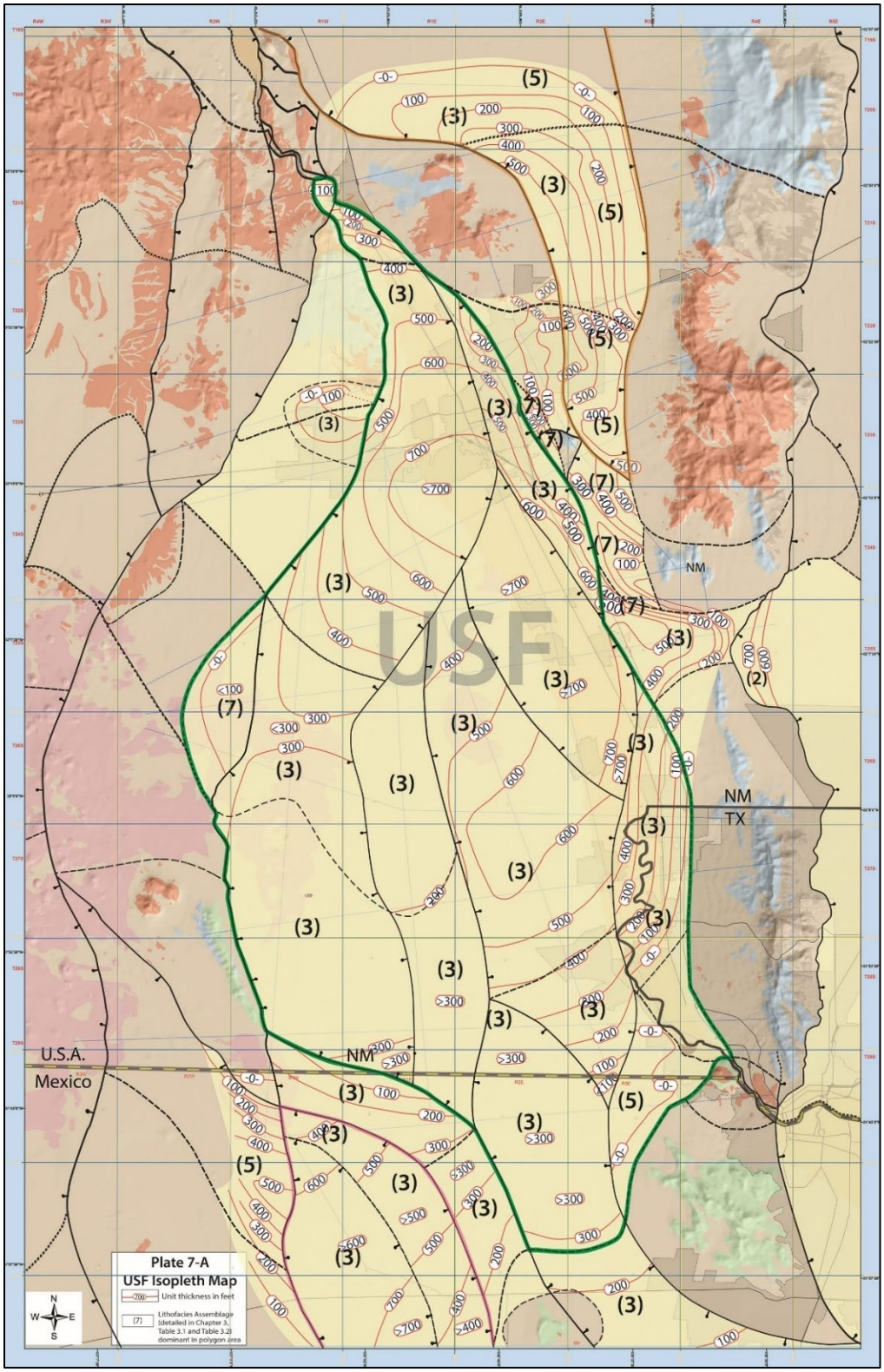

Figure 2-6 (page-size **PL. 7A).** Study Area isopleth map of the saturated part of HSU-USF that schematically depicts its LFA composition and thickness. 2017 Google Earth® image-base.

PLATE 10 is an electronic reproduction of a groundwater-quality map for the "Transboundary Aquifers of the El Paso/Ciudad Juárez/Las Cruces Region," which was compiled by the Texas Water Development Board (TWDB) and included as a back-cover insert (with CD-ROM) in Hibbs and others (1997). Water quality information is presented in a Stiff-diagram format for more than 200 wells in El Paso and Hudspeth Counties (TX), Doña Ana and Otero Counties (NM), and adjacent parts of Chihuahua (*cf.* **APNDX. H5.3**). A page-size reproduction of the map's west-central part is included in **Part 7.6.1** as **Figure 7-18.**

PLATE 11 (**Fig. 1-9**) is an index map for aquifer-management units in Mexico and major hydrographic boundaries in the United States south of 32° N latitude on a 2018 Google Earth® image-base. The Acuífero Conejos-Médanos "delineación oficial" and the Zona Hidrogeológica de Conejos Médanos boundary are bounded, respectively, by dash-dot gray and solid yellow lines (INEGI 2012). The dashed-blue line shows the general position of the Historic GW-flow divide between NE-directed underflow toward the lower Mesilla Valley, and SW-directed underflow toward the present ephemeral-lake plain (El Barreal) in the eastern Bolsón de los Muertos (*cf.* **Part 1.7.3**, **Figs. 1-9** and **1-10**).

PLATE 12 is an index map of the "International-Boundary Zone (IBZ)" as provisionally defined in this investigation (*cf.* **Figs. 1-10** to **1-12**). It is located between the 31° and 32° N Parallels and the 106°30' and 108° W Meridians, and is compiled on 2018 Google Earth® image base.

2.4. PROGRESS IN DEVELOPMENT OF DIGITAL PLATFORMS FOR DISTANCE EDUCATION AND TELECONFERENCING

Even before the onset of the COVID-19 pandemic in early 2020, all Report illustrative materials had been compiled in a format designed for use in Power Point (PPT)® presentations, both for *in house* and *distance education*. The pandemic's global extent and quarantine measures with which it is associated, however, have accelerated the use of the Zoom Video Communications, Inc. cloud-based, peer-to-peer software technology for a variety of teleconferencing activities. For example, the Zoom-PPT® platform has already been used in this Study (11/2020) for a workshop on the potential for brackish-GW resource development in the Santa Teresa Industrial Park area of the IBZ that utilized graphic material in Report **CHAPTER 8** and **APPENDIX H**.

CHAPTER 3.
PHYSIOGRAPHIC AND GEOLOGIC SETTING OF THE MESILLA BASIN REGION— A HYDROGEOLOGIC PERSPECTIVE

3.1. OVERVIEW

Due to its hydrogeologic perspective, the range of topics covered in this chapter is limited to introductory descriptions of the major components Mesilla Basin region's (MBR's) physiographic and geologic setting with respect to both surface and subsurface hydrogeologic conditions. Emphasis is on four distinctive, but still overlapping classes of geologic features: physiographic, geomorphic, tectonic-structural, and stratigraphic-sedimentologic (**Figs. 3-1** to **3-3**). Short descriptions of the Chihuahuan Desert ecoregion and hydrologically related soil-geomorphic processes are also included to emphasize the essential roles played by vegetative cover and pedogenic features in many vadose-zone and GW-flow processes. **Figure 3-1** is an index map to physiographic subdivisions and major landforms of the south-central New Mexico border region, and shows the location of the 1957-1977 USDA-SCS, Desert Soil-Geomorphology Project (blue rectangle; *cf.* **Fig. 3-2**; Hawley 1975a, b; **APNDX. D**). **Figure 3-2** is a schematic block diagram of the Desert Project area in the northeastern Mesilla and Southern Jornada del Muerto RG-rift basins. It is a 1999 adaption of Gile and others (1981) FIGURE 1 by H. Curtis Monger of NMSU (*cf.* Monger et al. 2009).

In a "physiographic" or "regional geomorphologic" context (e.g., Fenneman and Johnson 1946, Thornbury 1965), the Mesilla Basin region is located in the northern Mexican Highland section (MHS) of the Basin and Range (B&R) physiographic province (Hawley et al. 1976; Gile et al. 1981; Hawley 1986 and 2005; *cf.* Dickinson 2002). With respect to earth-crustal structure and Santa Fe Group (SFG) hydrostratigraphy, basin-fill deposits and bordering bedrock uplifts are in the southern Rio Grande-rift (RG-rift) tectonic province (Chapin and Seager 1975b; Hawley 1978; Seager and Morgan 1979; Keller and Cather 1994; Hudson and Grauch 2013; Ricketts et al. 2021; **Part 3.4**). In contrast to the fixed position of physiographic- and tectonic-province boundaries on a Late-Quaternary time scale, the extent of the Chihuahuan Desert ecoregion is primarily determined by global-climate controls on surficial-geomorphic processes that reflect an ever-increasing anthropogenic impact (Buffington and Herbel 1965; Gile 1966a, 1967; Gile and Hawley 1966; York and Dick-Peddie 1969; Schmidt 1979, 1992; Gile et al. 1981; Van Devender 1990; Dick-Peddie 1993; Douglas et al. 1993; Swetnam and Betancourt 1998; Gile et al. 1998, 2007; Monger et al. 2009; Williams et al. 2020a; **Part 3.3**).

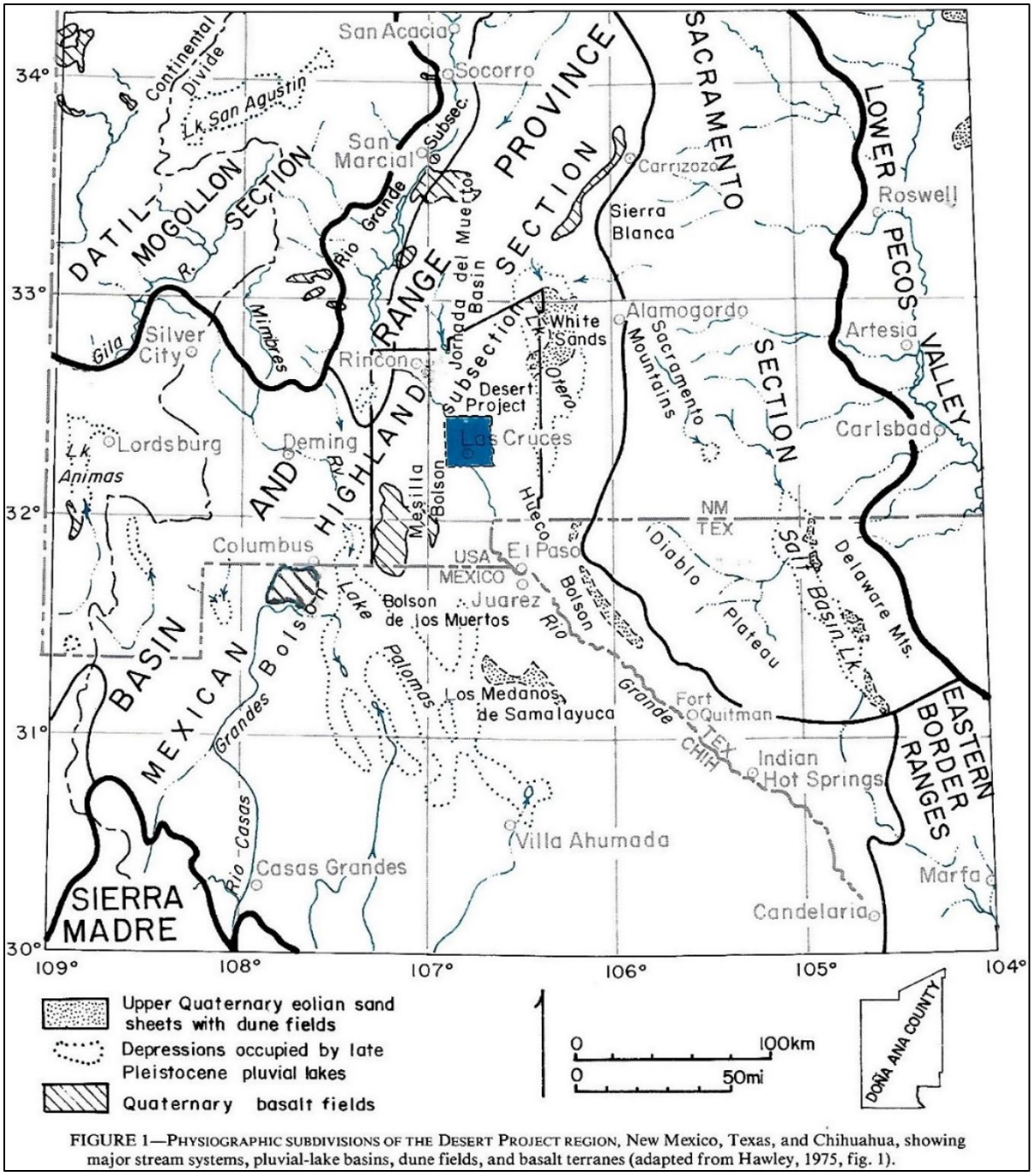

FIGURE 1—PHYSIOGRAPHIC SUBDIVISIONS OF THE DESERT PROJECT REGION, New Mexico, Texas, and Chihuahua, showing major stream systems, pluvial-lake basins, dune fields, and basalt terranes (adapted from Hawley, 1975, fig. 1).

Figure 3-1 (Gile et al. 1981, FIG.1; modified *from* Hawley 1975, Fig. 1)**.** Index map to physiographic subdivisions and major landforms in southeastern Basin and Range province region of New Mexico, Trans-Pecos Texas, and Chihuahua (*cf.* Hawley 1969, Underwood 1980, Gile et al. 1981). The Study Area (**Figs. 1-1** to **1-4**) in central Doña Ana County includes the 1957-1977 Soil-Geomorphology Project of the USDA-NRCS Soil Survey Investigations program. The RG-rift "Bolson de los Muertos" complex of Chapin and Seager (1975) is located in the "Acuifero Conejos Médanos" section of the northern Zona Hidrogeológica de Conejos Médanos (**Figs. 1-10** to 1-**12**).

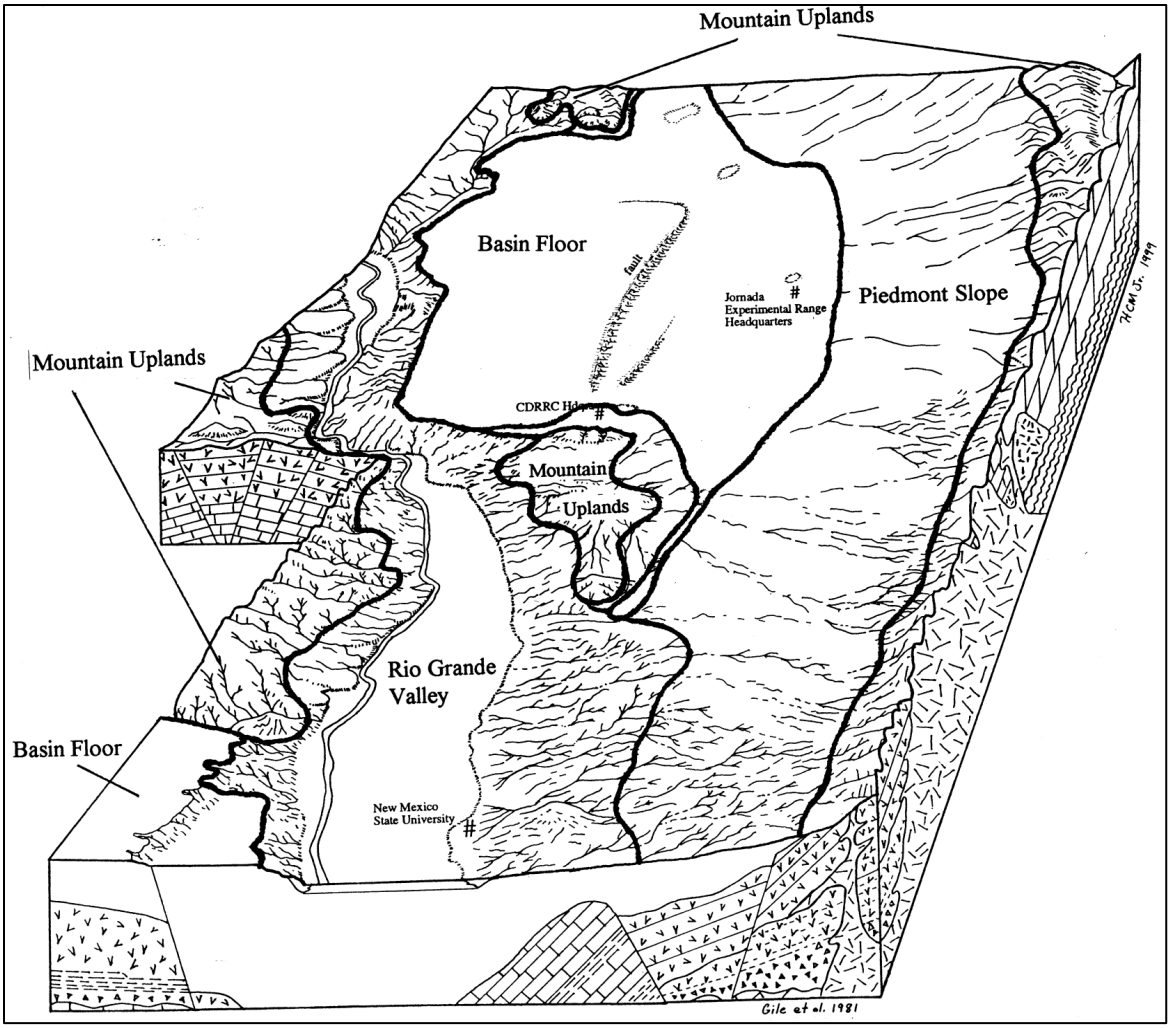

Figure 3-2 (adapted by H.C. Monger [1999] *from* Gile et al. 1981, FIG. 1)**.** Schematic block diagram of the Desert Soil-Geomorphology Project and USDA-ARS Jornada Experimental Range areas of the northeastern Mesilla and Southern Jornada RG-rift basins (**Figs. 1-1** to **1-3**, and **3-2**). Thin, surficial eolian/alluvial deposits and soils of the intermontane-basin floors and piedmont slope, and inner Rio Grande Valley are underlain by Santa Fe Group basin fill. Major components RG-rift fault-block structure and litho-stratigraphy are depicted in the diagram's south-and east-facing side panels (*cf.* **Figs. 3-8** and **3-9**; **Tbl. 3-1**).

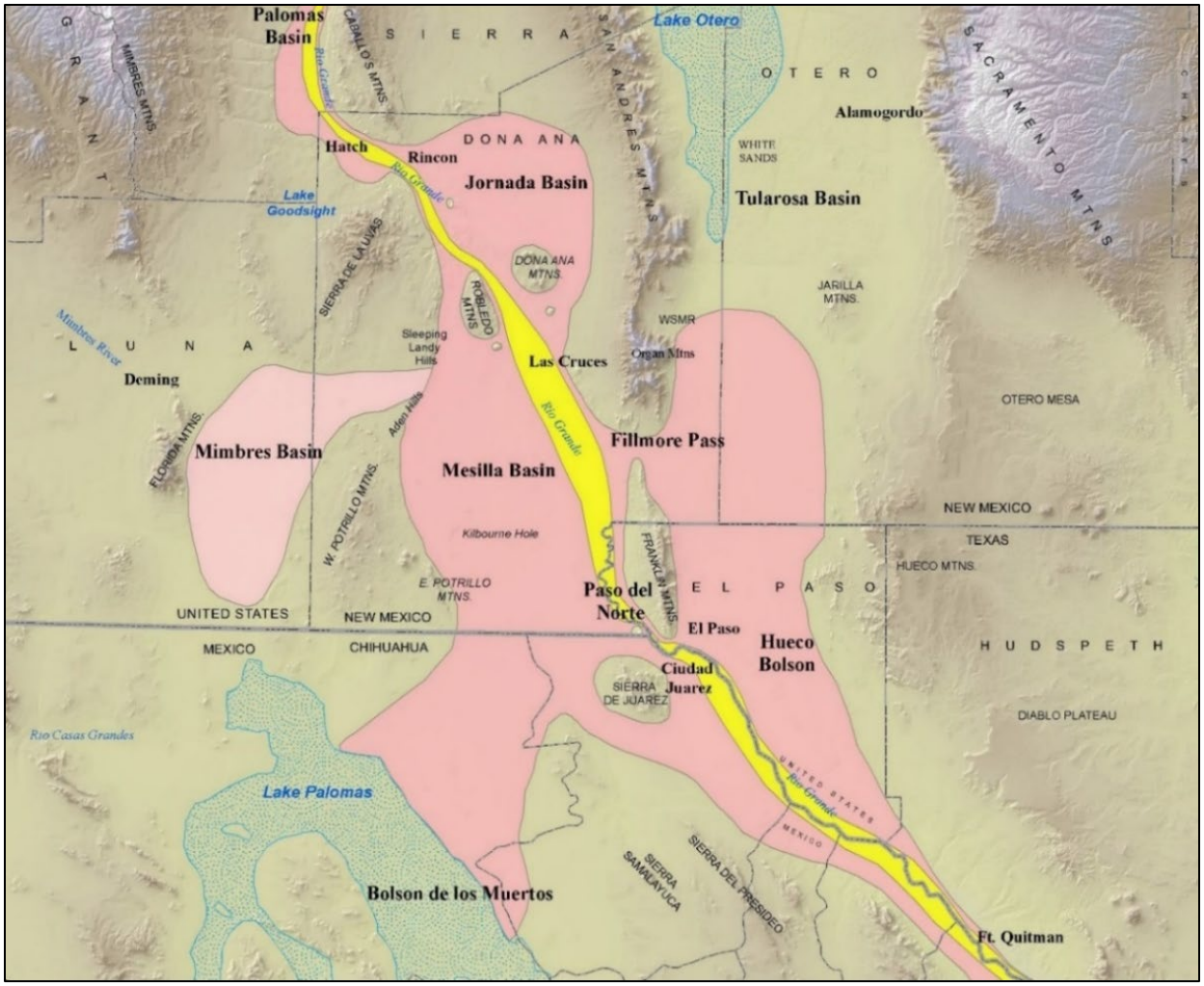

Figure 3-3 (Hawley et al. 2009, Fig. 10; *cf.* **Fig. 3-6).** Schematic depiction of major Quaternary-landscape features of the Mesilla Basin region on USGS-DEM base. The approximate area covered by the Ancestral Rio Grande (ARG) distributary drainage network that spread out from a trunk-ARG channel system in the Palomas Basin is in pink. The deeply entrenched Rio Grande/Bravo Valley and Canyon system is in yellow. The stipple pattern covers the basin-floor areas occupied by deepest Late Pleistocene stages of two large pluvial lakes: Palomas (NW Chihuahua) and Otero (Tularosa Basin). Remnants of the Early Pleistocene ARG fluvial-deltaic plain comprise parts of the "La Mesa geomorphic surface (Hawley and Kottlowski 1969)." The RG-rift "Bolson de los Muertos/Los Muertos Basin" complex of Chapin and Seager (1975) is located in the "Acuifero Conejos Médanos" section of the northern Zona Hidrogeológica de Conejos Médanos (**Figs. 1-10**, **1-11**, and **3-3**).

The Chapter's three-section—eight-part organization is designed to provide a reasonably balanced overview of the key roles played by an integrated system of hydrogeologic-framework components on GW flow and chemistry (the primary topic of **CHAPTERS 5** to **7**):

Section I. Surficial geomorphic processes: **Part 3.2**—Basin and Range physiographic province, and **3.3**—Chihuahuan Desert ecoregion.

Section II. Hydrogeologic-Framework Development: **Part 3.4—**Background on the Rio Grande (RG)-rift and the Santa Fe Group (SFG); **3.5**—Ancestral Rio Grande and La Mesa surface; **3.6—**Introduction to RG-rift basin development; **3.7—**Stages of rift-basin evolution and SFG deposition, and **3.8—**Mid- to Late-Quaternary evolution of RG-valleys and canyons, and endorheic rift-basin areas.

Section III. GW-flow system development: **3.9—**Introduction to the paleohydrology of the pluvial-Lake Palomas—Paso del Norte GW-flow system.

3.2. BASIN AND RANGE (B&R) PHYSIOGRAPHIC PROVINCE

3.2.1. B&R-Mexican Highland Section

Figure 3-3 is a schematic depiction of major Quaternary-landscape features of the Mesilla Basin region on a USGS-DEM base. Deep-valley and canyon reaches of the Rio Grande that developed during Middle and Late Pleistocene time are in yellow (**3.5**). The stipple patterns show approximate basin-floor areas inundated by the deepest Late Pleistocene stages of pluvial lakes Palomas in NW Chihuahua and Otero in the central Tularosa Basin (**Part 3.3.2**). Pink shading shows the approximate extent of the Ancestral Rio Grande (ARG) distributary drainage network that spread out from a trunk-ARG system in the Palomas Basin in Pliocene and early Pleistocene time (*cf.* **Parts. 3.5** and **3.7.2**; **Figs. 3-6**, **3-13** and **3-14**; Mack et al. 1997, and Connell 2005 [FIG. 11]). Remnants of the Early Pleistocene ARG fluvial-deltaic plain form parts of the "La Mesa geomorphic surface" (**Part 3.5**; *cf.* Ruhe 1964 and 1967, Hawley 1965, Gile 1967, Hawley and Kottlowski 1967, Hawley 1975, Gile et. al. 1981).

Throughout its drainage basin, the Grande/Bravo fluvial system and its perennial to intermittent tributaries have been the primary travel corridors and water-supply sources for the Native American population long before the arrival of first group of Spanish colonists at El Paso del Norte in late April 1598 (Fergusson 1933; Hammond and Rey 1953, 1966; Pérez de Villagrá 1962 [1612]; Almada 1968; Weber 1982; Márquez-Alameda 1992; Adorno and Pautz 1999; Sálaz Márquez 2004; **APNDX. H2.1.2**). Early Hispanic cultural primacy is reflected in the names of cultural and geographic features throughout the American Southwest, and most of the "descriptive topographic terms" in this part of "Spanish America" were initially defined from a river-valley and intermontane-basin perspective (e.g., Rio, arroyo, valle, bolson, and mesa [e.g., Hill 1896, Julyan 1996]; *cf.* **APNDX. G** and **Part 3.5**).

Ezequiel Ordóñez (1867-1950), was a prominent geologist and academic, who is regarded as the "creador de la geología petrolera mexicana. . . ." (https://es.wikipedia.org/wiki/Ezequiel_Ordóñez). The following selections are from Ordóñez' paper titled: "Principal Physiographic Provinces of Mexico," which was published in the October 1936 issue of the Bulletin of the American Association of Petroleum Geologists (AAPG; v. 20, no. 10):

> [p. 1290b] . . . the topographic elements of the [intermontane] basin or 'bolson' are the mountain slope, the alluvial fans, the gentle alluvial plain, and the silty bottom land called 'the barrial [barreal],' which is temporarily occupied by water immediately after infrequent, but torrential rains.
>
> [p.1290a] . . . In some of these basins, the [alluvial-fan] bases of the sierras extend toward the middle of the plain like a very gently inclined plane [piedmont-slope] which ends at the "barrial]," improperly called "playa"* by the American geologists and geographers.
>
> *Ordóñez only used the term "playa" for a shoreline feature of large permanent body of water (e.g., "beach").*

The Mesilla and Hueco "Bolsons" were named and defined in both physiographic and structural-geologic contexts by Robert T. Hill (1896, 1900; **Figs. 1-1** to **1-3**, **3-1** and **3-2**; *cf.* Tight 1905). The term "Jornada del Muerto" dates back to the Spanish Colonial era (Gregg 1844 [Moorhead 1954], p. 271; Julyan 1996; Kludt et al. 2018), and its basic structural framework was initially described by C.R. Keyes (1905) and N.H. Darton (1922). Together with the Zona Hidrogeológica de Conejos Médanos (ZHGCM) and the recently identified El Parabién Basin in Chihuahua, the Hueco-Jornada-Mesilla RG-rift basin system forms the largest topographic and structural-basin complexes in the eastern B&R province (**Figs. 1-1** to **1-3**; *cf.* **Part 3.2.2**; Reeves 1969, Hawley et al. 1976, Woodward et al. 1978, and Schmidt 1992). In terms of regional groundwater flow, aquifer systems in the Tularosa-Hueco and the Los Muertos-El Parabién-Mesilla rift-basin groups also made substantial underflow contributions to alluvial aquifers of the inner RG Valley during glacial-pluvial stages of the Late Pleistocene (*cf.* Hawley and Kennedy 2004; **Part 3.9** and **7.6**).

Based on long-term field observations in the American Southwest, Stanford University Professor Cyrus F. Tolman (1873-1943) was the first to make a clear geomorphic and hydrogeologic distinction between depositional systems in aggrading intermontane basins with topographic closure (*bolsons*) and those that are open in terms of both surface and subsurface flow (*semibolsons*). He recognized three basic classes of lithofacies assemblages in the continuum of closed and open basin landforms (Tolman 1909; **APNDX. C1.2**). Piedmont-slope facies (e.g., coalescent alluvial-fan) occur along the margins of both basin types, while basin floors in topographically *closed* (*endorheic*) systems include alluvial flats that grade to terminal ephemeral-lacustrine plains (e.g., *playas* and *salinas*). Floors of basins that are linked with external (*open* or *exorheic*) fluvial systems, in marked contrast, include alluvial flats and fluvial plains (*cf.* Deming [2002, p. 414-415], Hawley and Kernodle [2008, p. 511]). Tolman's early distinction

between *bolson* vs. *semibolson* hydro-geomorphic systems was later expressed in better-defined conceptual models of Basin and Range groundwater flow regimes (e.g., Mifflin 1988, Hawley and Kernodle 2000, Hibbs and Darling 2006 [*cf.* **Part 4.1** and **APPENDIX C2**]). Tolman is probably most noted as the author of the first hydrogeology textbook on "Ground Water" (1937), and as a distinguished academic (Deming [2002, p. 414-415]). For example, the research of his student, Joseph Fairfield Poland (1908-1991) on land subsidence due to depletion of hydrostatic pressure in confined aquifers is recognized as a seminal contribution to the practice of engineering geology (e.g., Poland et al. 1975).

3.2.2. Major Landscape Features and Geomorphic Processes

Desert and semi-desert landscapes of the Mesilla Basin region (MBR) are topographically and hydrogeologically characterized by (1) the large extent of closed (endorheic) intermontane basins that have no surface-drainage connection with the valleys and canyons of the throughgoing (exorheic) Rio Grande/Bravo fluvial system, and (2) the low-relief topographic expression of many of the interbasin hydrographic boundaries. In marked contrast to the massive Sangre de Cristo and San Juan Mountain ranges of the Rio Grande headwaters region, crests of the mountain ranges that separate the Jornada-Mesilla and Tularosa-Hueco basins (San Andres-Organ-Franklin-Juárez Uplifts) are narrow and low (maximum altitude-9,012 ft, 2,747 m) (**Figs. 1-2**, **1-3**, **3-1** and **3-2**; *cf.* Pazzaglia and Hawley 2004 [Fig. 1], Smith 2004).

Intermontane basins of the B&R-Mexican Highland Section have three major landscape components and a wide variety of associated geomorphic processes: piedmont slopes, basin floors, and river valleys (**Figs. 3-4a** and **3-4b**; Gile et al. 1981, Fig. 4). Piedmont slopes comprise (1) narrow erosional surfaces (rock pediments) adjacent to mountain fronts, and (2) broad fan-piedmont surfaces formed by coalescent alluvial fans, or by alluvial slopes without distinctive fan morphology (Gile et al. 1981; *cf.* Smith 2000). The central parts of basin (aka "bolson plains") are commonly very large in comparison to the size of flanking mountain uplifts and their proximal piedmont slopes. They include extensive remnants of relict fluvial-deltaic plains constructed by the Pliocene-Early Pleistocene Ancestral Rio Grande (ARG; *cf.* **Part 3.5**; **Figs. 3-6**, **3-13** and **3-14**; Hawley et al. 1969 and 1976). Basin floors comprise a variety of landforms depending on (1) whether or not a given basin has topographic closure, and (2) the regional climate/geomorphic-process setting. Basin-floor landforms in endorheic basins include alluvial plains that terminate in ephemeral-lake plains (e.g., playas and barreals; *cf.* **Parts 3.3** and **3.8**). As noted in **1.2.1**, Frenzel and Kaehler (1990, Fig 4) were also the first to show the approximate position of the MeB's "West Mesa," the large basin-floor remnant west of the Mesilla Valley that (1) occupies about two-thirds of the MeB area and (2) has no surface-flow connection with the river.

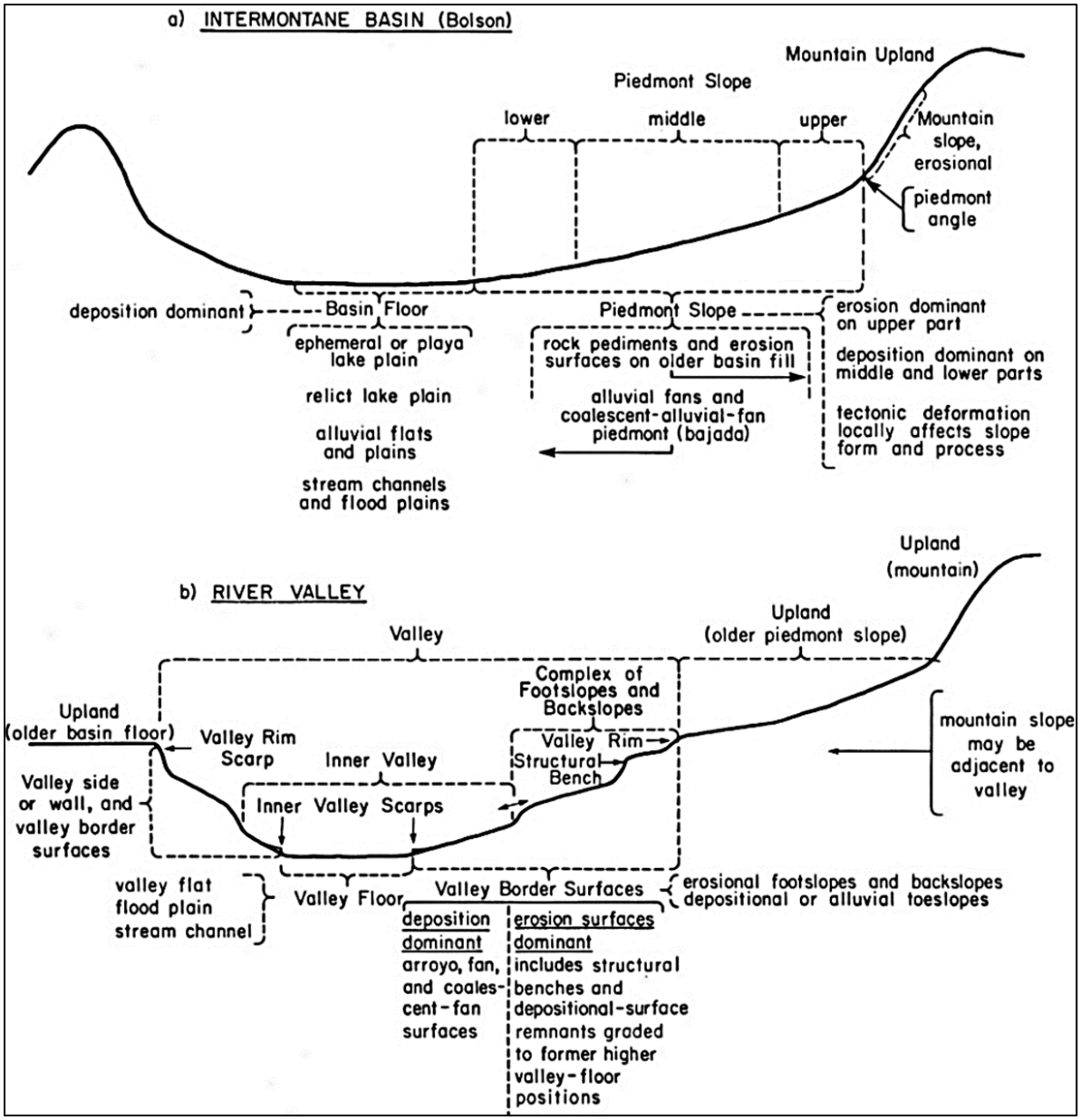

Figure 3-4 (Gile et al. 1981, Fig. 4)**.** Schematic profiles of major landform types and outline of dominant geomorphic processes in the Mexican Highland section of the Basin and Range province and the southern Rio Grande rift tectonic province: **3-4a**—Intermontane basin, and **3-4b**—River valley (**Fig. 3-3**).

The present river valley/canyon landscape is the product of the latest Quaternary stage of fluvial incision, and valley widening, and partial back-filling in a RG-rift area that extends from the Albuquerque Basin to the Presidio Bolson (**Figs. 1-1** to **1-4,** and **3-1**; *cf.* **Part 3.8**). The following observations by Hawley and Kottlowski (1969, p. 98) are especially relevant with respect to the evolution of the river's valleys and canyons downstream from Elephant Butte:

> The maximum stage of entrenchment of the Rio Grande in latest Pleistocene time . . . may be represented by a buried surface occurring at relatively shallow depths below the present floodplain surface (Lee, 1907b; Kottlowski, 1958; Hawley, 1965). Information from well drillers, examination of cuttings from several wells, and review of published information on local ground-water conditions . . . indicate that the late Quaternary river deposits extend no more than 80 feet (24 meters) below the floodplain level [Sayre and Livingstone 1945, Conover 1954, Davie and Spiegel 1967]. This depth represents the approximate thickness of unconsolidated sediments over bedrock at the International Dam Site in El Paso Canyon (Slichter, 1905) and over Tertiary volcanics and sediments in the lower Selden Canyon area.

3.2.3. Valleys and Canyons of the Rio Grande

The Rio Grande is the only surface-water resource in the MBR, and its "sustainability" is dependent on the effectiveness of future management practices on river flow in the face of climate change (*cf.* Ikard et al. 2023). The river's course through the Study Area traverses two bedrock "canyons" or "narrows:" the Mesilla Valley, and two valley reaches in neighboring RG-rift basins: The lower Rincon Valley Basin, Selden Canyon (SCyn), El Paso del Norte (EPdN), and the upper El Paso Valley/Valle de Juárez in the western Hueco Bolson (**Figs. 1-2** to **1-6**). The following quote is from Dr. Jerry Mueller's* "Restless River – International Law and the Behavior of the Rio Grande (1975, p. 1):"

**Former NMSU Earth Science Dept. Chair (based on Johns Hopkins University dissertation research).*

> A true exotic stream, like all major rivers of the arid zones, the Rio Grande is fed by spring snow melt in its headwaters, traverses desert through most of its length, eventually making its way to the sea with the aid of a few major tributaries and summer thunderstorm runoff [*cf.* **Part 7.3.2**]. Were it not for the high discharge received from the Rio Conchos at Ojinaga, Chihuahua, the Rio Grande would not be a perennial stream. Another major tributary is the Pecos River, which drains the east slope of the Rockies in southeastern New Mexico, severs the Stockton Plateau from the Edwards Plateau in West Texas, and joins the Rio Grande upstream of Del Rio. The Rio Salado drains the northern portion of the Mexican State of Nuevo Leon and joins the Rio Grande at Falcon Reservoir midway between Laredo and Rio Grande City. Just above Rio Grande City[1], the Rio San Juan contributes the discharge it collects from central Nuevo Leon [[1]~125 mi (200 km) from the Gulf of Mexico].
>
> [Elephant Butte and Caballo] Reservoir construction and irrigation in the last sixty years have reduced the Rio Grande's flow to only a fraction of pre-1900 discharges [**Fig. 1-6**]. The upper basin, defined here as that portion which lies north of El Paso and the international boundary, now has numerous dams and reservoirs and practically no spring flooding from snow melt; some minor flooding is associated with local summer thunderstorm runoff. At Fort Quitman, approximately 80 miles [130 km] downstream of EI Paso, mean annual discharge has been reduced by 95 percent as a result of reservoir storage and redistribution of waters in the upper basin.

The Frenzel and Kaehler (1992) "simulation of ground-water flow in the Mesilla Basin (p. C38)" included an assumption, based on 1898-1904 measurements by W.T. Lee (1907, p. 32) of a pre-Elephant Butte Dam average river flow through Selden Canyon of 700 cfs (506,774 ac-ft/yr, 625 hm^3/yr). However, peak discharge during floods in 1904 and 1905 in the San Marcial-El Paso reach of the river

ranged from 50,000 cfs [122.33 x 10^6 m^3/d] at San Marcial (10/11/1904) to 24,000 cfs [58.72 x 10^6 m^3/d] at El Paso (6/12/1905). Post-dam average-annual discharges at Caballo, Leasburg, and American (EPdN) Dams have been reported, respectively, at about 615,791, 506,774, and 362,230 ac-ft/yr (759.6, 625, and 446.8 hm^3/yr), and maximum daily discharge has usually been less than 5,000-10,000 cfs (141-283 m^3/s) since dam completion and the onset of Rio Grande Project operations in 1916 (USGS Surface Water Branch 1961, 1965; http://water.usgs.gov/nm/nwis/sw).

3.2.3a. Selden Canyon (SCyn)

Selden Canyon (SCyn) of the Rio Grande links the lower Rincon Valley Basin (RVB) with the Mesilla Valley (MeV) section of MeB (**Fig. 1-3**; **APNDX. F: Pls. F3-1c** and **F4-1d** to **1g**). It is about 5 mi (8 km) long and is cut mainly in Tertiary bedrock units of the Selden Hills Uplift (**Part 5.2.2**; *cf.* Hawley et al. 1975, Mack and McMillan 1998, Seager et al. 2021). Minimum width of the canyon floor is about 330 ft (100 m), and the river-floodplain altitude ranges in from 4,000 to 3,960 ft (1,213-3,960 m) above msl. Maximum thickness of inner-canyon alluvial fill (HSU-RA) is about 80 ft (25 m).

3.2.3b. Mesilla Valley (MeV)

The head of the Mesilla Valley (MeV) is at Leasburg Dam, which is located at the mouth of SCyn near the site of Fort Selden (1865-1890) and the Village of Radium Springs (**Figs. 1-3**, **1-6** and **3-6**; **Tbl. 1-1**, **PLS. 2** to **4, and 5o**; **APNDX. F: Pls. F2-8, F3-1c** to **1j**, **F4-1h to 4-1l**, and **F5-3h**; *cf.* **Parts 5.2.2** and **6.2**). The dam (crest alt. 3,960 ft /1,207 m) was constructed in 1908, and it is one of the oldest irrigation-diversion structures on the river (Julyan 1996, p. 201). The area of its upstream watershed is about 28,000 mi^2 (72,520 km^2) and includes parts of Colorado's San Luis Basin (**Figs. 1-4** and **1-6**, and **Tbl**. **1-1**).

The MeV is 60 mi (100 km) long, and as much 5 mi (8 km) wide (**Figs. 1-2** to **1-6** and **3-3**). Valley floor area, including the river channel and floodplain, is about 215 mi^2 (557 km^2, 137,600 acres or 55,687 hectares). The floodplain is 300 to 350 ft (90-107 m) below adjacent parts of the West Mesa (La Mesa) surface (**PLS. 5d** to **5k**), with valley-floor altitude decreasing from 3,960 ft (~1,207 m) at Leasburg dam to about 3,725 ft (~1,135 m) at the head of El Paso del Norte near Courchesne Bridge (**PL. 5o**). Average floodplain gradient is about 0.001 (4.5 ft/mi, 1 m/km). The slope of the pre-1865 meandering-river channel was as low as 1.4 feet per mile, and its maximum sinuosity (ratio of channel or thalweg length to meander-wave length) was about 2.5 (U.S. Reclamation Service 1914; Hawley and Gile 1966a, p. 62).

Although the area continues to urbanize, much of the valley floor continues to be utilized for intensive-irrigation agriculture (Richardson et al. 1972; Bulloch and Neher 1980; Wilson et al. 1981; Peterson et al. 1984; Wilson and White 1984; Frenzel and Kaehler 1992; Esslinger 1996, 1998; Walton et

al. 1999; SSURGO 2002/2003; Tillery et al. 2009; USBOR 2011). As such, the area is occupied by a network of canals, ditches, laterals, and drains that now replace much of the floodplain's initial hydrologic function in terms of recharge to, storage in, and discharge from the MeV's shallow-aquifer system (*cf.* **Parts 7.3** and **8.5**). In addition to the reports on pioneering geohydrologic studies by Slichter (1905) and Lee (1907) (**APNDX. C1**), key historic-baseline documents on the fluvial geomorphology and soils of the RG Valley floor include: (1) "Maps of Mesilla Valley, showing various known river channels" (U.S. Reclamation Service 1914) and (2) the 1912 USDA Bureau of Soils "Soil Survey of the Mesilla Valley, New Mexico-Texas" (Nelson and Holmes 1914). The latter map shows details of soil-texture classes to a depth of about 6 feet (1.83 m), and printed on a 1:63,360 scale, 2-ft contour interval plane-table topographic base. It is also essential to note that the water-table throughout almost all to the surveyed area was within 6 feet (1.83 m) of the river-floodplain surface in 1912.

3.2.3c. El Paso del Norte (EPdN)

El Paso del Norte (EPdN) or the "El Paso Narrows" is the short (~4-mi/6.5-km) "canyon" or "water gap" reach of the Rio Grande that links the MeB-Sunland Park Outflow Corridor (SPoc) with the El Paso Valley/Valle de Juárez in the westernmost Hueco Bolson (WHB-SWHB; **Fig. 1-8**, SE end of **PL. 5o** and E end of **PL. 5l**; **APNDX. F: Pls. F2-7**, **F3-1j**, and **F4-1l**; *cf.* **Parts 5.1.4**, **6.3.5d**, and **7.5**). The head of EPdN is located near Sunland Park Race Track and the Courchesne Bridge gaging station, and it is immediately downstream from the Lower MeV area that includes the discharge zone for the pre-development binational-regional GW-flow (**Figs. 1-8**, **1-9** and **1-14**; **APNDX. F: Pl. F4-1m**).

EPdN is incised in Cretaceous and Tertiary bedrock units of the Cerro Cristo Rey Uplift and Campus-Andesite Hills (**Part 5.1.4**). River-channel altitude decreases from about 3,725-ft (1,135-m) amsl near Courchesne Bridge to 3,705-ft (1,126-m) amsl at the western edge of Hueco Bolson, with an average down-valley gradient of about 0.003. Minimum river-channel/floodplain width is less than 330 ft (100 m), and maximum thickness of alluvial fill (RA) is about 80 ft (25 m; Slichter 1905b). The last interval of canyon incision occurred during the Late Pleistocene-Wisconsinan Glacial Stage sometime between 29 and 11.7 ka (*cf.* **Parts 3.8** and **5.1.4**; **3-5**, **3-16** and **3-17**). Downstream from EPdN the "rectified" Rio Grande/Bravo channel forms the International Boundary (Mueller 1975; **APNDX. H2.6**).

3.3. CHIHUAHUAN DESERT ECOREGION

Ecoregions are dynamic biogeographical entities, which are sensitive to changes in atmosphere/hydrosphere-related geomorphic processes that have periodicities in the decadal to multi-millennial range (Omernik 2004). Unlike the relatively fixed temporal boundary criteria for physiographic or tectonic provinces, their transitional borders are determined by subcontinental-scale climatic, hydrographic, and biogeographic conditions with an ever-increasing anthropogenic component (*cf.*

Gutzler 2005, 2020, Meixner et al. 2016, Overpeck and Udall 2020, Allen 1922). It is also important to note that accelerating global-scale climate and associated regional-environmental changes during the past century may have already marked the end of the well-documented glacial-interglacial cycles of Quaternary Period (i.e., past 2.6 Ma; *cf.* **Figs. 3-5** and **3-18**). If so, a new *Anthropocene Epoch** of uncertain duration and character is well underway, and planning horizons for prudent water-resource management now appear to be in multi-decade range in arid/semiarid basins of the American Southwest (**Tbl. 1-3**; **Part 8.2**; **APNDX. E4**).

**Anthropocene (provisional name proposed by Crutzen and Stoermer 2000 [cf. Zalasiewicz et al. 2019 and 2021]); https://www.nytimes.com/2024/03/05/climate/anthropocene-epoch-vote-rejected.html?unlocked_article_code=1.aU0.Yoaa.8m5-c7KcfueD&smid=em-share*

In terms of its climate and biogeography, much of the B&R Mexican Highland Section below altitudes of about 5,000 ft (1,525 m) is currently part of the arid to semiarid Chihuahuan Desert ecoregion (Schmidt 1973, 1979, 1986, 1992; Spaulding et al. 1983; Van Devender 1990; Douglas et al. 1993; Metcalfe et al. 1997; Dick-Peddie et al. 2000; Nordt 2003; Hall 2005; Castiglia and Fawcett 2006). Tamayo (1968, p. 162) includes much of this area in the northern part of the "Chihuahua-Potosinense Provincia biótica." Under present-day vegetative-cover conditions, desert-scrub flora occupy a much-larger part of the Chihuahua Desert landscape than do grasslands (York and Dick-Peddie 1969). On the other hand, prior to large-scale introduction of livestock after the Civil War, grasslands appear to also have been a major Middle Holocene to Historic land-cover component (Buffington and Herbel 1965; Dick-Peddie 1965; Herbel and Gile 1973; Gile and Grossman 1979; Gile et al. 1981; Dick-Peddie 1993; Gile 1999, Gile et al. 2007; Monger et al. 2009; Bestelmeyer et al. 2013, 2018).

In striking contrast with climate/vegetative-cover conditions of the Mid-Holocene to present Chihuahuan Desert ecoregion, Late Pleistocene glacial maxima in the B&R-MHS were characterized by greater cool-season snow-fall and less-intense warm-season (monsoon-type) precipitation, with significantly lower evapotranspiration in both upland and lowland terrains (e.g., Hawley et al. 1976, Gile et al. 1981, Barry 1983, Smith and Street-Perrott 1983, Spaulding and Graumlich 1986, Van Devender et al. 1987, Betancourt et al. 1990, Ortega-Ramírez et al. 1998, Metcalfe et al. 2002, Palacios-Fest et al. 2002, Allen 2005, Wagner et al. 2010, Jasechko et al. 2015, Eastoe and Towne 2018, Hunt and Lucas 2022, McDonald 2022). This relatively short interval of geologic time occurred in the mid- to later-part of the marine oxygen-isotope stage (OIS) 2, which lasted from about 29 to 12 ka (Lisiecki and Raymo 2005; *cf.* Stein et al. 2006, Fig. 2; **Parts 3.3.2** and **3.8**; *cf.* **Figs. 3-5** and **3-17**). Montane-forests extended to lower altitudes in many but not all terrains, and the desert-shrub and grassland communities of Chihuahuan Desert's central-basin plains were replaced by savanna-type grasslands analogous to those now present on the semiarid to subhumid Southern High Plains (Spaulding et al. 1983; Van Devender

1995; Monger et al. 1998; Nordt 2003; Pazzaglia and Hawley 2004; Hall 2005; Holliday and Miller 2013).

The resulting increases in effective precipitation and much-lower evapotranspiration during the mid- to late-Quaternary glacial-pluvial intervals of the past 0.75 Ma led, in turn to vegetative cover and surface- and subsurface-water flow conditions that were conducive to: (1) river-valley incision and widening, (2) soil formation on stable geomorphic surfaces, and (3) flooding of low-lying parts of the endorheic Zona Hidrogeológica de Conejos Médanos (ZHGCM) and Tularosa Basin to form large intermittent to perennial lakes (**Figs. 1-2**, **1-10**, **3-1** and **3-3**; *cf.* **Parts 3.3**, **3.9**, **7.5**, and **7.6**). Basin-floor surfaces that were inundated by pluvial-Lakes Palomas and Otero during the most-recent Quaternary glacial/pluvial interval are now the sites of large intermittent lakes (**Figs. 1-2, 1-10**, **1-11**, **3-1** and **3-3**). The latter include (1) El Barreal and Salinas de Unión, and the Médanos de Samalayuca dune field in the Bolsón de los Muertos area, and (2) Lake Lucero-Alkali Flats and White Sands in the central Tularosa Basin (*cf.* **Part 7.6.2**; Herrick 1904, Meinzer and Hare 1915, Kottlowski 1958b, Hawley 1969, Morrison 1969, Reeves 1969, Schmidt 1992, Hawley et al. 2000, 2009, Allen 2005, Castiglia and Fawcett 2006, Allen et al. 2009, Bustos et al. 2018, Love et al. 2020, Bennett et al. 2021).

3.3.1. Background on the "Regiones Hidráulicas-Cuencas Cerradas del Norte" of Chihuahua

The Zona Hidrogeológica de Conejos Médanos (ZHGCM) occupies much of the lowland areas in the western part of Mexico's endorheic "Regiones Hidráulicas-Cuencas Cerradas del Norte" (RH34–INEGI 1999, Fig. 5.3A, B; **Fig. 3-5**; *cf.* **APNDX. H4.5**). RH34 has an area of about 35,366 mi^2 (91,597 km^2), and almost all of it is in Chihuahua. The New Mexico part of this basin complex has an area of about 5,020 mi^2 (13.000 km^2), and includes all of the Mimbres and Hachita-Moscos Basins, and a small section of the southern Playas Basin (Hawley et al. 2000, p. 2-3). Accordingly, the areal extent of this enormous, binational endorheic system is about 40,390 mi^2 (104,699 km^2). By way of comparison, the area of the Upper Rio Grande basin above Leasburg Dam (at the head of the Mesilla Valley) is 28,000 mi^2 (72,520 km^2) (USGS 1961, 2017).

The western RH34 includes the Sierra Madre Occidentál headwaters for three major fluvial systems that drain to the ZHGCM intermontane-basin complex: Río Casas Grandes, Rio Santa Maria, and Rio del Carmen (respectively, Cuencas D, C, and B; INEGI 1999, **Figs. 3-5a** and **3.5b**). Jorgé Tamayo in his description of "Las regiones geomorphícas de México (1968, p. 61-64)," reports the following watershed areas that contribute direct-surface and subsurface flow to the terminal *sinks* of the three "Rios:" Casas Grandes-16,600 km^2 (6,410 mi^2)—*Laguna Guzman*; Santa Maria-10,680 km^2 (4,124 mi^2)—*Laguna Santa Maria*; and Del Carmen-11,880 km^2 (4,587 mi^2)— *Laguna Patos*. Because it also includes a number of small endorheic subbasins, the 25,050 mi^2 (65,000 km^2) area INEGI (1999) "B-D Cuenca" group is much larger than that of the combined drainage basins of the 3 "Ríos." The Mimbres River, with a watershed

area of about 11,423 km^2 (4,410 mi^2) contributes a small amount of surface and subsurface flow to the northern parts of "Cuencas C and D" (Darton 1916, p. 111; Hanson et al. 1994, p. 2).

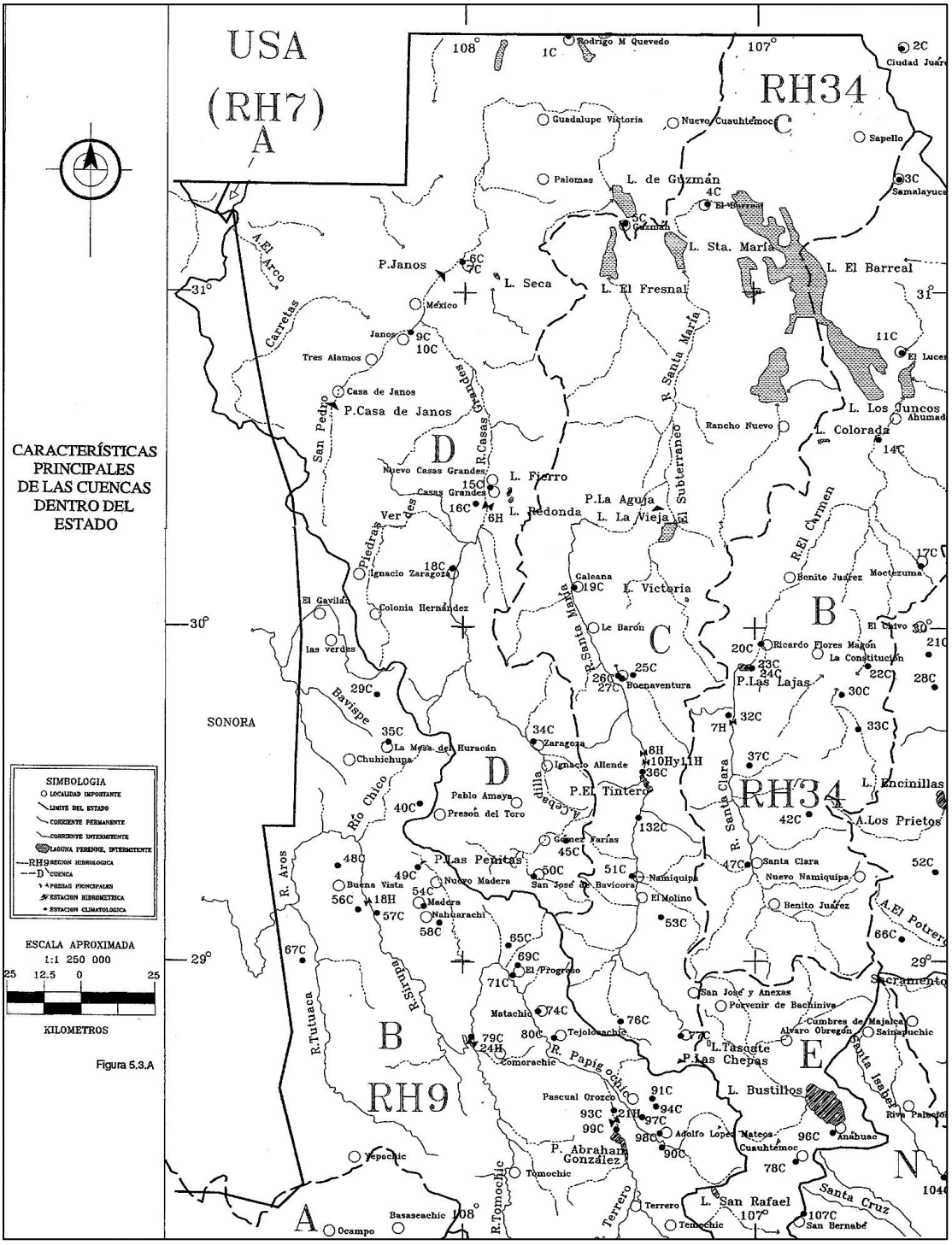

Figure 3-5a (INEGI 1999, Fig. 5.3.A)**.** Index map to hydrographic units/fluvial systems in the western part of Región Hidrologíca (Hydrologic Region) RH34—Cuencas Cerradas del Norte (endorheic basins of the north) in northwestern Chihuahua.

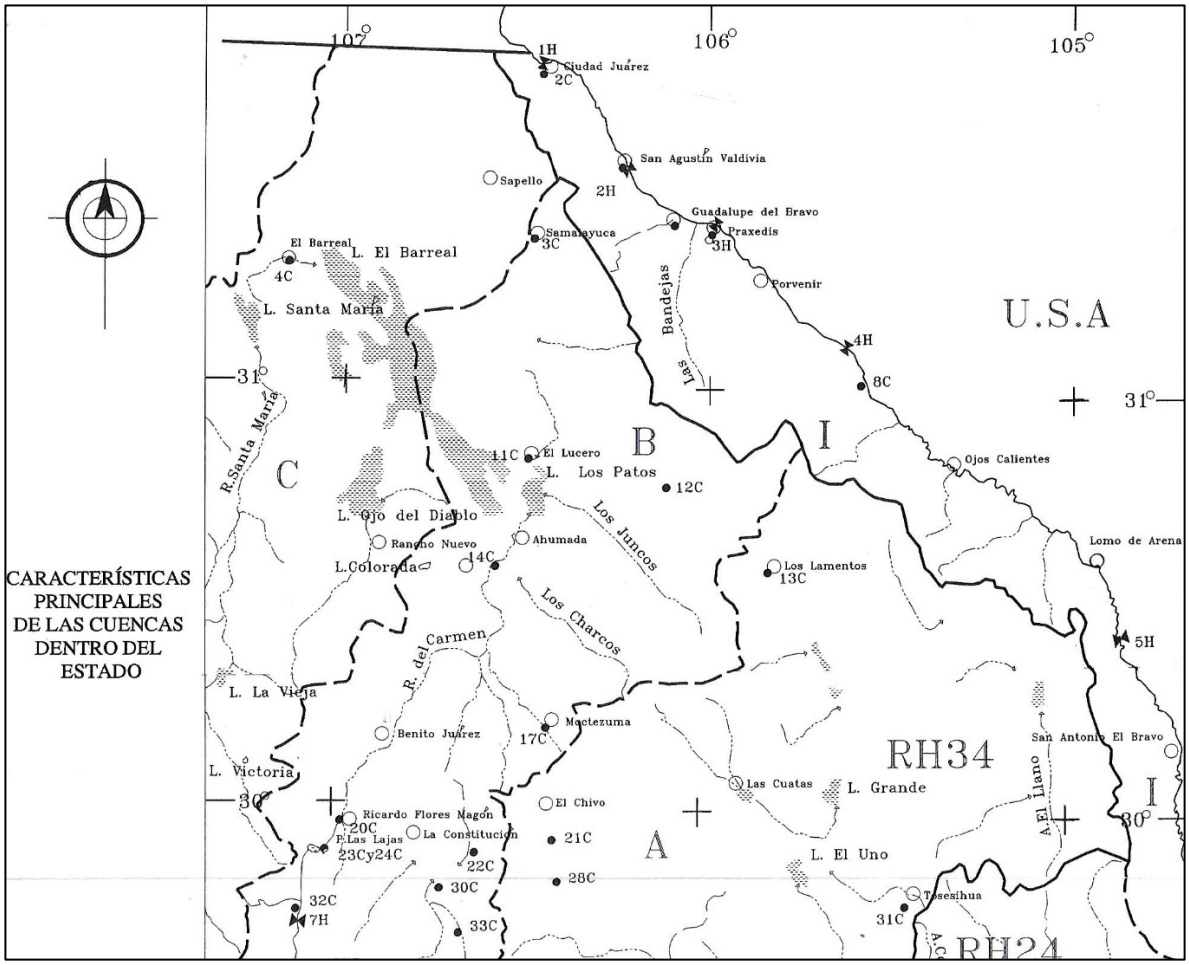

Figure 3-5b (INEGI 1999, Fig. 5.3.B)**.** Index map to hydrographic units/fluvial systems in the northeastern part of Región Hidrologíca (Hydrologic Region) RH34—Cuencas Cerradas del Norte (endorheic basins of the north) in northern Chihuahua.

The altitude of the lowest part of HG34-ZHGCM at the southern end of El Barreal is between 1,175- and 1,180-m (3,855-3,872-ft) amsl (CONAGUA 2020). The phreatic (GW-ET) discharge) area for that part of the ZHGCM is located between Sierrita Amargosa and Salina[s] de Unión. The head of a flowing-well head near the northeastern base of Sierrita Amargosa is about 1,182 m (3,878 ft) (*cf.* **APNDX. H6.3** [**Fig. H6-4**]). There is no geohydrologic evidence, however, of any present-day hydraulic linkage between the Salina[s] de Unión area and the Transboundary GW-flow system in the northernmost part of RG34-ZHGCM section. The no-flow divide that separates NE (EPdN)-directed GW flow from SW (El Barreal)-directed flow is located between La Laguna and El Aguaje at altitude of about 1,195 m (3,925 ft) (**Figs. 1-9**, **1-10** and **1-12**; *cf.* **Part 7. 3**).

"**ZHGCM SILL**" on **Figures 1-10** and **1-l2** marks the approximate location of the lowest part of the surface-drainage divide that forms boundary between the endorheic RG34-ZHGCM and the exorheic southwestern Hueco Bolson. The site is about 3.2 km (2 mi) north of Sierra del Presidio, and 2.5 km (1.6

mi) south of Sección Tierra Blanca on the Ferrocarriles Nacionales de México; and its altitude is about 1,245-m (4,085-ft) amsl (**Figs. 1-11,** and **3-5b**). Precise determination of its location, however, is hampered by the absence of distinct drainage features on a nearly level terrain. The estimated altitude of the potentiometric surface in the area of the "SILL" was about 1,165 m (3,822 ft) in 2007 (CONAGUA 2020, Figs. 4 and 5). In the San Elizario (Clint)-San Isidro reach of the Rio Grande/Bravo, 20 km (12 mi) to the northeast, the static water level in the shallow alluvial aquifer remains at about 1,100-m (3,610-ft) amsl (Heywood and Yager 2003; *cf.* Hutchison 2006). In this case, it is important to note that the two sites are separated by the Sierra Juárez fault zone (SJfz), which forms the primary structural boundary of the southwestern Hueco (RG-rift) basin (**Figs. 1-1**, **1-2**, **1-8**; **Tbl. 1-5**; *cf.* **APNDX. H5.5**, and Hawley et al. 2009 [PLS. 2g and 2h]).

3.3.2. Bolsón de los Muertos (BdLM)

Texas Tech Professor of Geology, C.C. Reeves (1931-2013) proposed the name "Bolson de los Muertos (BdLM)" in the following one-sentence statement:

> Laguna de Palomas and "El Barreal" occur along the axis of the floor of a large basin complex, termed Bolson de Los Muertos in this report, . . . [Reeves 1969, p. 147].

Except for three preliminary ground-based gravimeter surveys, Reeves' work in the area was reconnaissance in nature, much of which involved light plane overflights. The feature name was taken from Sierra de los Muertos, a small outlier of Lower Cretaceous sedimentary and Tertiary igneous-intrusive rocks in the south-central part of El Barreal (**Fig. 1-10**; IBWC 2011; CONAGUA 2020, Fig. 2); and specific boundaries were never established (e.g.,1969, FIG. 1; *cf.* **APNDX. H4.2.5c**). Most of Reeves' *conceptual*-BdLM area is in the endorheic Zona Hidrogeológica de Conejos Médanos (ZHGCM **[Fig. H1-1]**, with the northern half of the latter including the Acuífero Conejos-Médanos, both of which are delineated on maps in INEGI (2012) (https://www.inegi.org.mx/inegi/contacto.html).

"Bolson de los Muertos" is not mentioned in any publication on the hydrology of Mexico (e.g., INEGI 1999 and 2012, and CONAGUA 2020). Its only mention is in the following selection from a review paper titled "Chihuahua, tierra de contrastas geográficos: Geografía" by Robert H. Schmidt, Professor of Geography at the University of Texas-El Paso (*cf.* Rpt. **APNDX. D3**). The paper was included as a Chapter in the "Historía general de Chihuahua I – Geología, geografía y arqueología" that was published in 1992 by the Universidad Autónoma de Ciudad Juárez y Gobierno del Estado Chihuahua (Márquez-Alameda [coordinador del volumen]):

> [p. 64] El Bolsón de los Muertos [Reeves 1969], a menos de 75 kilómetros al suroeste de Ciudad Juárez, es la playa* más grande en el estado y en Mexico. . . . La superficie actual de la playa contigua cubre 1,245 km^2, su longitud de norte a sur es de 69 kilómetros y tiene poco mas de 24 kilómetros de ancho. Las enormes grietas formadas al secarse el lodo, también llamadas

> grietas de desecación, llegan a ser de hasta tres metros de ancho; algunas de estas grietas se encuentran en la parte noroeste de la playa [El Barreal herein]. . . .

Note Schmidt's use of "playa" as the term is defined by geographers and geologists in descriptions of various-sized ephemeral and intermittent lakes throughout the western United States. With respect to "Las enormes grietas…, de desecación," identical features were described by W.B. Lang in a 1943 paper in *Science* titled "Gigantic drying cracks in the Animas Valley, New Mexico." Such large-scale desiccation cracks in fine-grained sediments of bolsón floors and bordering piedmont slopes are attributed to two types of water-table drawdown conditions that have occurred in many "deep alluvial basins" of the Basin and Range province during the Late Quaternary: (1) Natural—desiccation of pluvial lakes and incision of nearby by stream valleys; and (2) Anthropogenic—overdrafts (mining) of groundwater reservoirs (e.g., Reeder et al. 1957, Willden and Mabey 1961, Chico 1968, Neal et al. 1968, Fleischhauer and Stone 1982, Haneberg and Friesen 1995, Krider 1998, and Carpenter 1999).

Initial use of the "BdLM" or "Los Muertos Basin" was primarily in reference to a complex of structural basins in the southwesternmost RG-rift province (e.g., **Fig. H4-1** and **H4-6**; Chapin and Seager 1975b, L. Woodward et al. 1978, and Seager and Morgan 1979). In light of the provisional nature of the term's introduction (with no binational peer review), it is here recomended that "Los Muertos Basin" should no longer be used in any RG-rift basin context (e.g., **Figs. 1-1, 1-2, 1-4**, and **Fig. 3-4**). As noted by Averill and Miller (2013, Figs. 1 and 2), the currently accepted name for the feature is the "Florida-Mimbres subbasin" of the Mimbres Basin (*cf.* Hawley et al. 2000 [p. 35]).

3.3.3. Pluvial-Lake Palomas

During the cooler and wetter intervals of the last Pleistocene glacial stage (about 29,000 to 12 ka) parts of the ZHGCM and contiguous lowland areas below a present altitude of about 3,970 ft (1,210 m) were inundated by pluvial-Lake Palomas (Reeves 1969; Castiglia and Fawcett 2006; *cf.* **Figs. 1-10**, **1-11**, **3-1** and **3-3**). Its high-stand surface area, which is shown with light-blue shading on **Figure 1-10**, is estimated to have been at least 2,900 mi^2 (7,000 km^2; Castiglia and Fawcett 2006, p. 114). By way of comparison, the present areal extent of Lake Erie is about 9,940 mi^2 (25,745 km^2). The source watershed of pluvial-Lake Palomas and its ephemeral-lake remnants [barreals-lagunas-salinas] has an area of at least 70,000 km^2 (27,000 mi^2), which is about the same as the 28,000 mi^2 (72,520 km^2) area of the Rio Grande drainage basin above Leasburg Dam (alt. 3,960 ft/1,207 m; USGS 1961, 2017; **Figs. 1-4** and **1-6**; **Part 3.1.3a**). Note, however, that Castiglia and Fawcett (2006, Fig. 1A) do not include most of Mimbres River basin (about 10,000 km^2 / 3,860 mi^2) in their estimates of the contributing-basin size (*cf.* Darton 1916, Love and Seager 1996). The other large pluvial lake in the Mesilla Basin region, Lake Otero in the west-central Tularosa Basin, was of much smaller size, but it still covered a basin-floor area of about 745 mi^2 (1,930 km^2) at its 3,950 ft (1,204 m) Late Pleistocene high stand (**Figs. 1-3** and **3-3**; Allen et al. 2009).

The geochronologic and paleohydrologic interpretations of Lake Palomas history that are described here are based primarily on intensive (MS-thesis) field research by Peter Castiglia (2002) in the Laguna [El] Fresnal, Guzman, and Santa María subbasins of the Lake Palomas basin (**Figs. 1-10** and **1-11**; *cf.* **Fig. 3-5**). Well-preserved fossil clams (*Pyganodon grandis*) that Castiglia discovered in high-level beach-ridge deposits of the Lagunas Fresnal and Santa María subbasins proved to be ideal for ^{14}C age determinations. This allowed him to establish a relatively precise chronology of Holocene and latest Pleistocene "lake-level variation" that (1) applies throughout the Los Muertos Basin area, and (2) documents the close correlation of early to middle Holocene episodes of increased precipitation with pluvial-lake high stands (Castiglia and Fawcett 2006, p. 113-114). Two excerpts from the Castiglia and Fawcett report summary are included here because of their special relevance in this study:

> (p. 113) Laguna El Fresnal and Laguna Santa Maria are two remnants of a multibasin, hydrologically closed lake system that drained a combined area of 60,000 km^2 in northern Mexico. Reeves (1969) described these as part of the pluvial Lake Palomas basin, comprising four interconnected subbasins: El Barreal, Laguna Guzman, Laguna Santa María, and Laguna El Fresnal [Lg. Fresnal – **Figs. 1-10**, **1-11** and **3-3**]. Shoreline features located above an internal sill (1,197 m) indicate that these four subbasins formed much larger contiguous lakes in the past. The maximum lake highstand in the Palomas basin during the [mid-] Holocene (~5,600 km^2) was spatially more extensive than many other pluvial lakes in the southwestern United States during the late Pleistocene.
>
> (p. 113-114) Lacustrine features preserved in the interior basins of the pluvial Lake Palomas system include wave-cut benches, spits, lacustrine sediments, and constructional beach ridges. Three major constructional beach ridges, first identified and described by Reeves (1969), are located on the eastern flank of Laguna El Fresnal, where sediments of the lower two shorelines contain multiple sites with well-preserved freshwater pelecypods . . . . In Laguna El Fresnal, a partially eroded beach ridge composed predominately of poorly sorted fine-grained sands to gravels is preserved at an elevation of 1,210 m (. .). This high shoreline (beach ridge I) can be found in all other subbasins as a wave-cut bench marking a change in slope above the playa margins. No pelecypods were found in the sediment exposures of this shoreline, and no reliable age could be obtained. Based on its position and degree of preservation, however, beach ridge I must be older than the lower shorelines and is probably late Pleistocene in age. The lake represented by this shoreline was >7,000 km^2 in area, and a 20-km-long spit associated with this beach ridge is at the mouth of the Rio Casas Grandes at the northern end of Laguna Guzman.
>
> Beach ridge II (1,202 m above sea level) is 5 m above an internal sill separating Laguna Guzman from Laguna El Fresnal (. .). In an escarpment on the western side of Laguna Guzman, we measured the altitude of three wave-cut benches with a differentially corrected GPS instrument. A prominent bench at 1203 m corresponds to the constructional beach ridge in El Fresnal, within the vertical resolution of the GPS. Two dates, 8456 ± 97 ^{14}C yr B.P. and 8269 ± 64 ^{14}C yr B.P. (. .)*, obtained from pelecypods collected from a silt deposit in the shoreface on the southeastern side of El Fresnal subbasin (. .) show that beach ridge II formed during the early Holocene.
>
> **Using the CALIB 5.0 model of Stuiver and Reimer (1993), the calibrated calendar-year age range of these ^{14}C dates is 9,139 to 9,032 cal-yr BP)*

As noted in **Part 3.3.2**, the only area of surface discharge for the RG34-ZHGCM groundwater-flow system is located in the lowest part of El Barreal in the Salina de Unión area (alt. 1,175-1,180 m [3.855-3,872 ft]; **Figs. 1-2**, **1-10** and **3-3**). Based on field- and aerial reconnaissance of the Lake Palomas area, Reeves (1969, p. 153-154) provided this summary of the local hydrochemical setting of the Salinas de Unión (**Fig. 1-10**):

> Because the basin of pluvial Lake Palomas has always been closed, surrounded by volcanics, and was the terminal reservoir for at least three large rivers [Casas Grandes, Santa Maria, and Mimbres], it satisfies several of the requisites listed by [G. I.] Smith (1966) for accumulation of continental salines. The high, abandoned shorelines show that evaporation of vast quantities of water took place and the bordering volcanics and stream influents from these terranes have undoubtedly supplied the salts.
>
> Salines la Unión S. A., with general offices in Villa Ahumada, has been producing sodium sulfate for several years at Salinas [de Unión] about 27 miles [43.5 km] northwest of Villa Ahumada [**Fig. 1-2**]. Production is from of confined brines of 13° Beaume which rise to nearly the playa surface, are concentrated by evaporation, and then pumped to concrete evaporation pits. The brine is then pumped, after additional concentration by solar evaporation, over an ammonia cooler which causes precipitation of the sodium sulfate. Production of several tens of thousands of tons per month is easily attained (personal communication, R. C. Ponsford, Jr.).
>
> Extent of the Salinas sodium sulfate deposit is not known; however, waters in other areas show high concentrations of various ions necessary for other salt deposits. Because of the resemblance of the basin of pluvial Lake Palomas to Searles Lake, California [Smith 1966], one may suggest that exploration for continental salines will be highly successful in certain areas of the basin.

3.4. INTRODUCTION TO THE RIO GRANDE RIFT TECTONIC PROVINCE AND SANTA FE GROUP (SFG) RIFT-BASIN FILL

The RG-rift tectonic province comprises a group of north-trending block-faulted mountain ranges and intermontane-structural basins that are connected by valleys and canyons of the Rio Grande fluvial system (**Figs. 1-1**, **1-2**, **1-4**, **3-1** and **3-3**; **Tbl. 1-1**; *cf.* **Parts 3.6 and 3.7**). Mid- to Late Cenozoic sedimentary fill of some of the deeper RG-rift basins exceeds 10,000 ft (3 km) in thickness (Woodward et al. 1978). Extensive silicic to basaltic volcanic fields are commonly present throughout the province (*cf.* Chapin 1971 and 1979, Hawley 1978, Seager and Morgan 1979, Keller and Cather 1994, Mack 2004, Pazzaglia and Hawley 2004, Connell et al. 2005, and Hudson and Grauch 2013). Kirk Bryan (1938, p. 197-225) initially named this continental-scale crustal-extensional feature the Rio Grande "depression." Chapin (1971) introduced "rift" as a much-more appropriate term for use in a modern plate-tectonic context (*cf.* Stewart 1971, Chapin and Seager 1975b, Seager and Morgan 1979, Gries 1980, Keller et al. 1990, Stewart 1998, Keller 2004, Averill and Miller 2013, Dickerson 2013, Ricketts et al. 2021).

The Santa Fe Group (SFG) forms the primary intermontane basin-fill component throughout the RG-rift province (**Figs. 1-1**, **3-1** and **3-5**). This major Cenozoic lithostratigraphic unit is described from a hydrogeologic perspective in **Part 3.7** and **CHAPTER 6**. Kirk Bryan (1938, p. 205-215) included most

of what he designated as “Rio Grande depression” fill in an undivided “Santa Fe formation” geologic-mapping unit (*cf.* Hayden 1873, Cope 1884, Dunham 1935, p. 175, Kelley and Silver 1952, p. 123, and Conover 1953, p. 21; *cf.* **APNDX. C1.7**). Brewster Baldwin (1956) proposed that Bryan’s (1938) “Santa Fe formation” be redefined as a “Group (Gp)” of mappable “Formations (Fms).” The “Santa Fe group” as redefined by Baldwin (1963, p. 38-39) includes all Rio Grande-rift basin fill that was deposited prior to initial incision of the valleys and canyons of the through-flowing Rio Grande/Bravo fluvial system (Hawley et al. 1969, p. 52-53; Hawley 2020, p. 67).

The large number of formation-rank lithostratigraphic subdivisions that are now mapped throughout the RG rift has led to informal subdivision of the SFG into Lower (L), Middle (M), and Upper (U) hydrostratigraphic units (HSUs) for hydrogeologic mapping purposes (*cf.* **Part 4.4.2**). Past and ongoing work using geochronology now shows that the SFG in the southern RG-rift region ranges from Mid-Oligocene to Early Pleistocene in age (about 30 to 0.75 million years [Ma], **Fig. 3-6**; *cf.* Hawley 1978, Chart 1; Tedford 1981, Chapin and Cather 1994, Mack 2004, Connell et al. 2005, Mack et al. 2018a).

Figure 3-6 shows general correlations between major Cenozoic time-rock classes, lithostratigraphic units, and their hydrostratigraphic-unit (HSU) equivalents in the southern RG-rift region. SFG formation-rank subdivisions comprise the Hayner Ranch Formation, Rincon Valley Formation, Fort Hancock Formation, and the Camp Rice and Palomas Formations (*cf.* **Part 3.7.2**). The Hayner Ranch and Rincon Valley Formations were named and mapped by Seager and others (1971) in their Rincon Valley type area (**Fig. 1-3** and **Tbl. 1-1**). The Palomas Formation was defined by Lozinsky and Hawley (1986) based on mapping by Lozinsky (1986) in the unit’s Palomas Basin type area (**Figs. 1-1** to **1-3** and **3-3**). **Part 3.7.2b** includes more-detailed information on initial field research by W.S. Strain (1966) in the Hueco Bolson type area of the Camp Rice and Fort Hancock Formations.

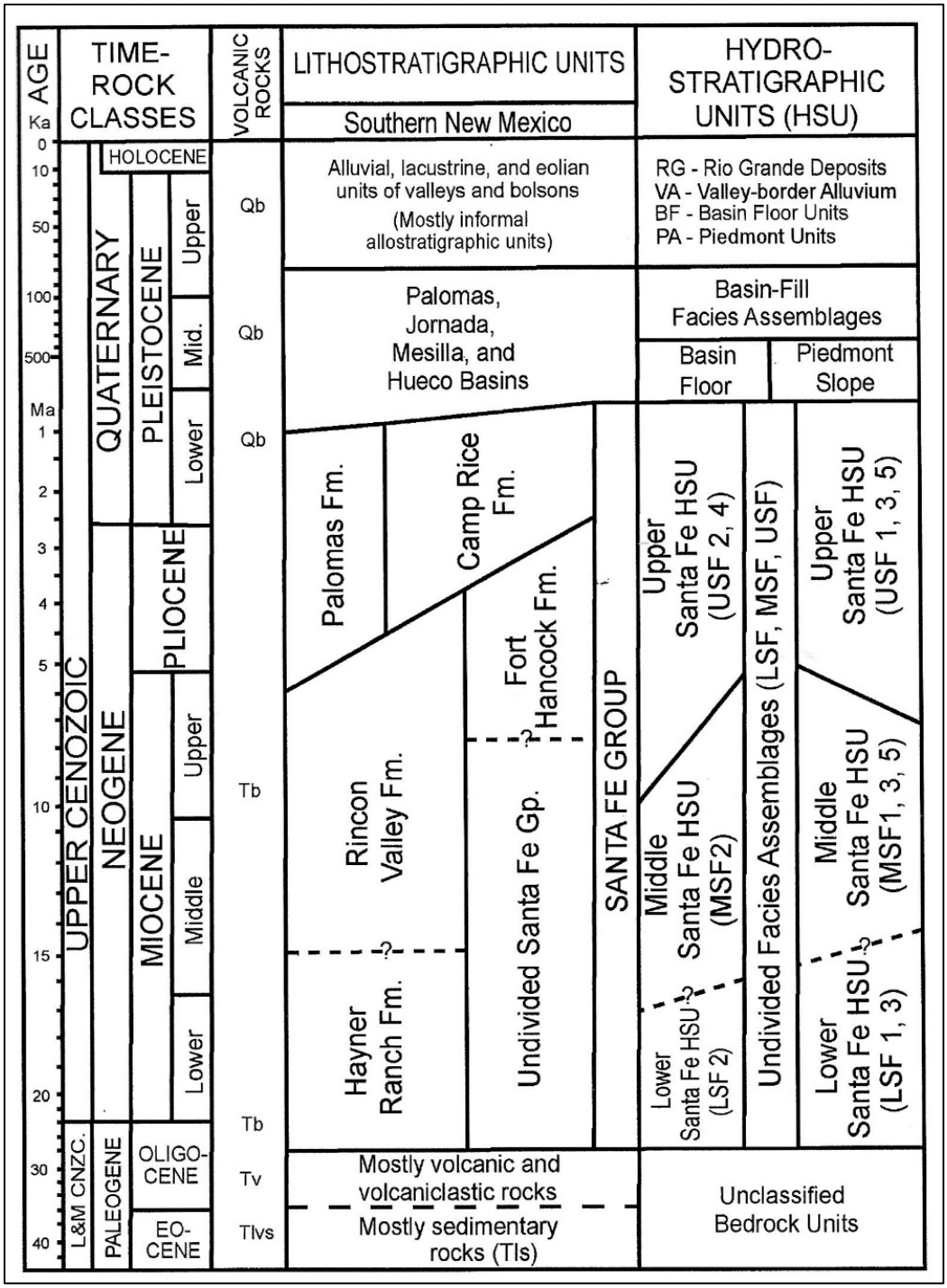

Figure 3-6 (modified from Hawley et al. 2009, Fig. 6; *cf.* **Tbl. 1-3**, **TBL. 2).** Correlation diagram of major time-rock (chronostratigraphic) classes, lithostratigraphic, allostratigraphic, and hydrostratigraphic units (HSU) of Cenozoic age in the southern RG-rift region (*cf.* NACOSN 2005, **APNDX. G**). Even numbered HSUs are basin floor deposits and odd numbered HSUs are piedmont slope deposits. Bedrock units: Qb–Quaternary basalt, Tb–Tertiary mafic volcanics, Tv–older Tertiary intermediate and silicic volcanics with associated plutonic-igneous and sedimentary rocks, and Tlvs are volcanic and epiclastic sedimentary rocks.

3.5. UPPER SFG BASIN FILL, THE ANCESTRAL UPPER RIO GRANDE (ARG), AND LA MESA GEOMORPHIC SURFACE

Fluvial and fluvial-deltaic facies of the Late Miocene to Early Pleistocene Ancestral Rio Grande (ARG) are the distinguishing component of Upper SFG deposits in the Mesilla Basin region (**Fig. 3-7**). ARG basin development upstream from the Rio Grande/Bravo canyons in the Trans-Pecos Texas/Big Bend region has been the product of fluvial-geomorphic processes in two transitional physiographic and tectonic settings: (1) a Southern Rocky Mountains headwaters area that was partly glaciated during Early Pleistocene Ice-Ages, and (2) a distal semiarid to arid endorheic-basin interior (*cf.* Schumm 1965, p. 700-792, Connell et al. 2005, Fig. 11, J.R.L. Allen 1965, Fig. 1).

Figure 3-7 (Hawley et al. 2009, Fig. 9) is a schematic depiction of the general area occupied by the Ancestral Rio Grande's (ARG's) terminal distributive-drainage network (**Figs. 3-3**; *cf.* **Part 3.7.3**). The approximate area occupied by the primary distributary-drainage network that spread out from an apex area at the end of the trunk ARG channelbelt in the Palomas Basin above Hatch is in dark pink, and a secondary ARG spill-out fluvial fan in eastern Mimbres Basin is in light pink. Numbers in **Ma** on **Figure 3-7** show provisional million-year age ranges of major distributary channelbelts based on geochronologic information available in 2008. This distributary network terminated in fluvial-deltaic transition zones that bordered a large complex of intermittent to perennial lakes that UTEP Geology Professor William S. Strain (1966, 1971) *collectively* named "Lake Cabeza de Vaca (LCdV)" in honor of Álvar Núñez Cabeza de Vaca, leader of the first Hispanic party that traversed the Chihuahua part of the MBR in late 1535 (Adorno and Pautz 1999; Flint and Flint 2019; *cf.* **APNDX. H3.1**). This paleo-lake occupied basin-floor areas below a present altitude of about 4,050 ft (1,235 m) in Tularosa Basin, Hueco Bolson and Zona Hidrogeológica Conejos Médanos (Strain 1971, Gustavson 1991a). ARG fluvial-plain remnants preserved in the present landscape comprise parts of the "La Mesa geomorphic surface" (Gile et. al. 1981).

The extent and approximate age range of an "ancient Rio Grande [ARG]" fluvial system in the Mesilla-Jornada Basin region was initially recognized by Willis T. Lee (1907; *cf.* Kues 2014b). Lee (1907) introduced the term "La Mesa–Sp. *tableland*" in reference to the MeB-West Mesa area (**Fig. 1-6**, **APNDX. C1.3**), and he correctly inferred "that the ancient Rio Grande flowed through the Jornada and La Mesa into the interior basin of Mexico [BdlM], and that in comparatively recent geologic time changes occurred which turned it out of its valley [West Mesa area] and away from the interior [Los Muertos] basin toward the Gulf of Mexico (p. 22)." N.H. Darton (1932, p. 132] also noted the presence of "earlier stage" Rio Grande deposits in "many fine exposures of gravel and sand" along the SP[UP]RR between Anapra and Strauss [present Santa Teresa Industrial Park site] (*cf.* **Part 6.3.4c**, **APNDX. C1.5)**.

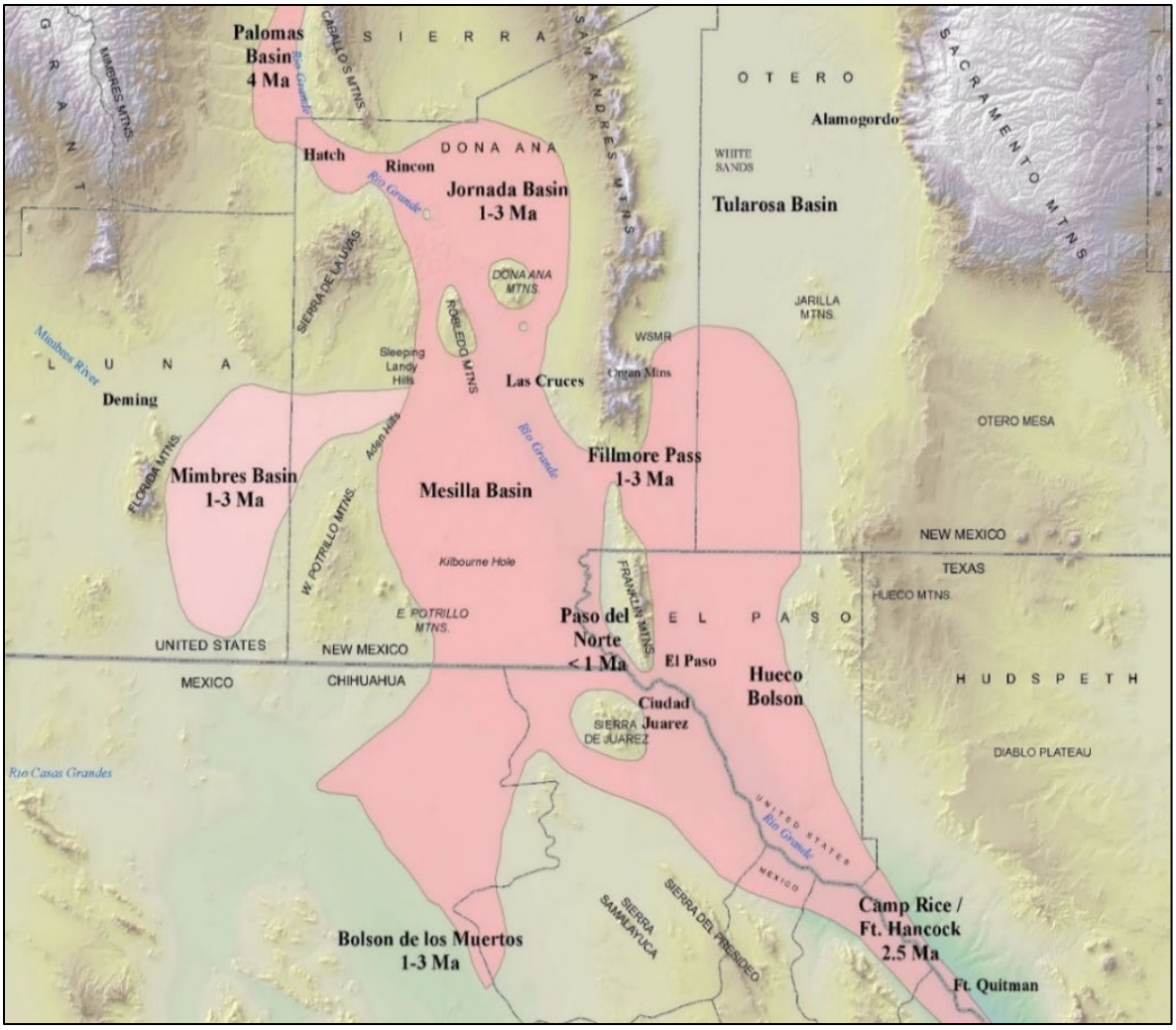

Figure 3-7 (Hawley et al. 2009, Fig. 9)**.** Schematic depiction of the approximate area where fluvial and fluvial-deltaic deposits of the Ancestral Rio Grande (ARG) form the dominant Upper SFG basin-fill component. The primary distributary-channel network that spread out from an apex at the end of a trunk ARG channelbelt in the Palomas Basin northwest of Hatch is in dark pink. Million-yr (Ma) age ranges of major distributary channelbelts are based on geochronologic information available in 2008. The network terminated in fluvial-deltaic transition zones that bordered the paleo-Lake Cabeza de Vaca (LCdV) system of Strain (1966; *cf.* **Part 3.7.2**). The "Bolson de los Muertos" rift-basin complex of Chapin and Seager (1975) is located in the "Acuifero Conejos Médanos" section of the northern ZHGCM (**Figs. 1-10**, **1-11**, and **3-3**).

K.C. Dunham (1935, p. 178), was the first to formally use the term "ancestral Rio Grande (ARG)" in reference to upper Santa Fe "formation" deposits in the Doña Ana County region. The current conceptual model of ARG evolution in the northern Rio Grande basin was proposed by Hawley (1975), who initially used the drainage-network classification system of British sedimentologist J.R.L. Allen (1965, Fig. 1; **Figs. 3-3** and **3-6**; *cf.* **Figs. 3-13 and 3-14**). According to Connell and others (2005, p. 130, FIG. 11):

> Drainage of the [Ancestral] Rio Grande can be considered in terms of the contributive and distributive drainage nets of Allen (1965), where drainage is collected through a contributive network of tributary streams, transferred through a trunk river, and eventually emptied across a distributive drainage network. Headwater basins contain tributaries that form the up-stream contributory (or contributary) section. The San Luis, Española, and Albuquerque basins represent the northern contributory section, defined by the presence of rather large tributary drainages that feed into the main-stem ancestral Rio Grande. A relatively short trunk section is present where drainage is confined within narrow and elongate half-graben basins containing few large tributaries. The Socorro, San Marcial, Engle, and Palomas basins generally represent the central trunk-river section and contain deposits typical of half-graben basins; however, this trunk-river distinction is not clear everywhere. The southern distributary system is recognized by repeated occupation of adjacent basins by the axial river across relatively low-relief topographic (and structural) divides. Below the Rincon area (between Truth or Consequences and Las Cruces, . .), the river forms a quasi-distributary drainage pattern that episodically spills laterally into adjacent basins ([Seager 1981], Mack et al., 1997 [*cf.* **Figs. 3-15** and **3-16**]).

Most early workers followed Lee in using "La Mesa" as a specific name for the Mesilla GW Basin's (MeB's) West Mesa area (e.g., Dunham 1935, Bryan 1938, Sayre and Livingstone 1946, Conover 1954, and Kottlowski 1958 and 1960). R.V. Ruhe (1964) and Hawley (1965) subsequently proposed that the term "La Mesa" be formally redefined as the "La Mesa geomorphic surface" to designate the constructional top of ARG deposits in SFG basin fill throughout the MBR (**Fig. 3-7)**.

The MeB-West Mesa north of the International Boundary has an area of about 500 mi^2 (1,300 km^2); its average southward slope rarely exceeds 0.0005 (2.5 ft/mi), and the land-surface altitude ranges from about 4,300 to 4,100 ft (1,310-1,120 m). Upper SFG-ARG deposits have a thin veneer of eolian sand in most places, and the West Mesa plain contains hundreds of shallow depressions of complex deflational, fluvial and/or structural origin (Gile 1966a and 1967; Gile et al. 1981; Seager et al. 1987; Seager 1995). Several prominent fault scarps, a variety of volcanic-vent features and locally extensive basalt flows of Pleistocene age also disrupt and/or cap the West Mesa (Seager et al. 1987; Seager 1995; Dunbar 2005; **Parts 6.3.3c** and **6.3.3e**; *cf.* **APNDS. F3-4** and **F7**).

The complex mixture of thin eolian and fluvial deposits that is associated with the La Mesa geomorphic surface (aka "La Mesa surface") form the parent materials for a wide variety of calcic soils with profiles that are usually less than ten feet (3 m) thick (Gile 1967; Bulloch and Neher 1980; Gile et al. 1981, 1995). Zones of soil-carbonate (primarily calcite) accumulation are at least partly indurated, and common names used for this pedogenic feature American Southwest include: caliche, caprock caliche, and pedogenic calcrete (*cf.* Gile 1961, Gile et al. 1966, Flores Mata 1970, Gile and Grossman 1979, Machette 1985, Monger et al. 1991, 2009; **APNDS. F3-4** and **F7: Pls. F7-1c** to **1f**).

The primary pedogenic mechanism for soil-carbonate accumulation involves downward movement from upper-soil horizons by eluvial/illuvial and solution/reprecipitation processes. In advanced stages, it results in complete cementation and disruption of the initial soil parent-material matrix (*cf.*

APNDX. F7-1). There is a direct correlation of geomorphic-surface age, and the morphological complexity and thickness of associated zones of secondary-carbonate accumulation. Dust-trap data, and aerosol and bulk-precipitation analyses demonstrate that atmospheric additions have made a significant contribution to pedogenic processes in many arid to subhumid temperate regions (Junge and Werby 1958; Feth and Whitehead 1964; Hoidale et al. 1967; Gile et al. 1981; Reheis et al. 1995; Monger et al. 2009; McFadden 2013). Saturated-zone diagenetic processes have not played a significant role in the above-described mechanisms of soil-carbonate accumulation.

3.6. MAJOR STRUCTURAL COMPONENTS OF RG-RIFT BASINS AND UPLIFTS

3.6.1. Background

As noted in **Part 1.3.2**, the internal complexity and deep-seated nature of many structural components of RG-rift basins and their bordering bedrock uplifts requires that hydrogeologic-framework characterization be based on a wide variety of direct and indirect methods of surface and subsurface investigation (e.g., detailed mapping, borehole-sample logging, and geophysical and geochemical surveys. The Bouguer [isostatic-residual] gravity maps and cross-sections of Jiménez and Keller (2000, Figs. 4 and 7) have served as an essential source of information on the locations of major deeply buried bedrock and structural-boundary features in southern MBR (*cf.* **CHPTS. 5** and **6**). Map and cross-section compilation is described in more detail in **Part 2.3.3** and **APPENDIX A3**.

Figure 3-8 is a provisional Study Area base map produced by digital superposition of the Study Area's hydrogeologic-basemap (**PL. 1A**) on a section of the Bouguer isostatic-residual gravity map of Jiménez and Keller (2000, Fig. 4, 4-milligal contour interval; *cf.* Jiménez 1999). The Southern Jornada Basin (SJB), Mesilla Basin (MeB), and El Parabién Basin (EPB) are outlined in orange, green, and violet, respectively (*cf.* **Figs. 1-3** and **1-7**). Identification of the heretofore unrecognized EI Parabién basin by Jiménez and Keller (Fig. **3-9a, b**) is of special hydrogeological significance, because it helps explain unsuspected anomalies in Transboundary GW-flow and chemistry between the ZHGCM-El Barreal area and the southern MeB (*cf.* **Part 7.6.2**). According to Jiménez and Keller (2000, p. 80):

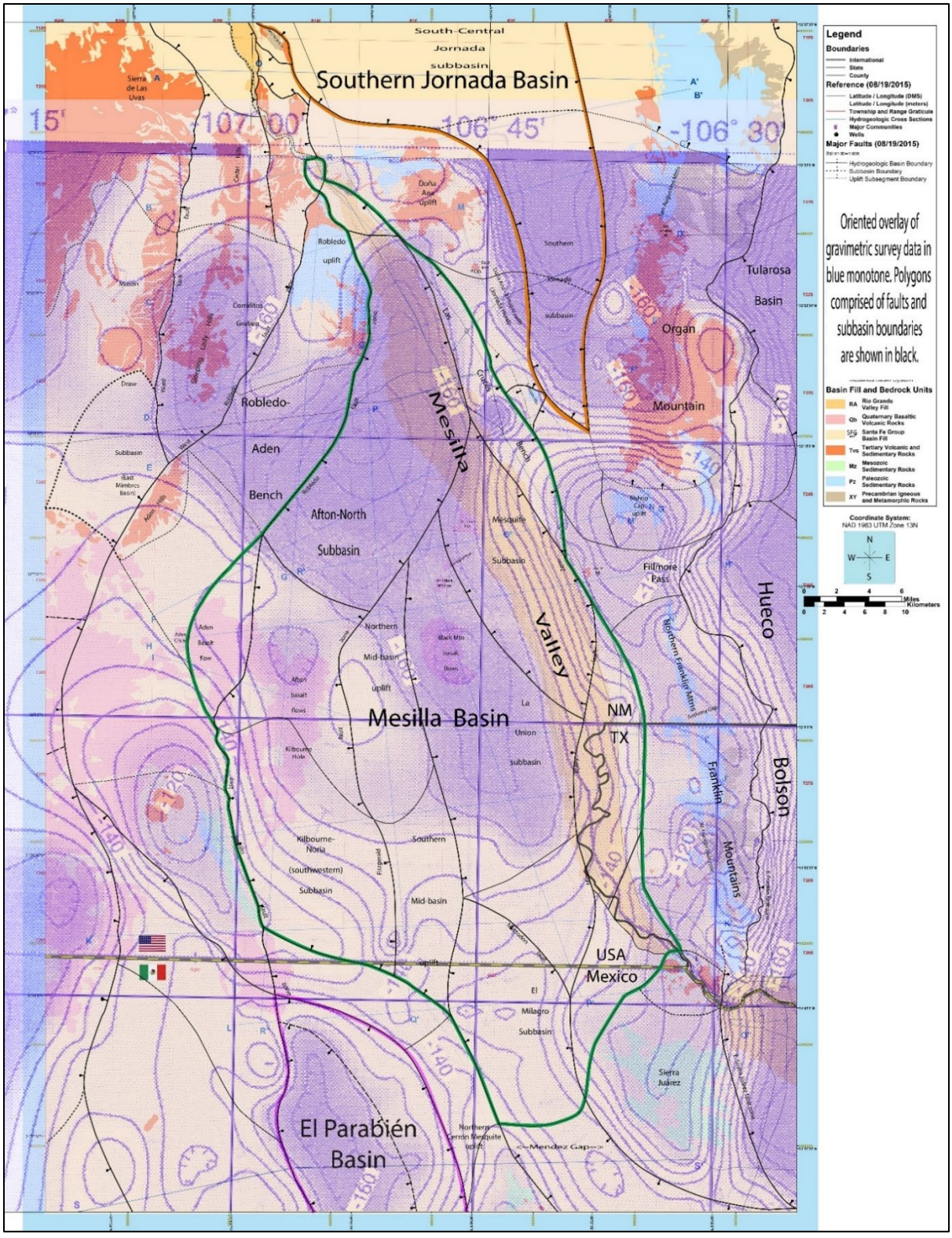

Figure 3-8 (page-size **PL. 2A**)**.** Digital overlay of Bouguer isostatic-residual gravity map (4 milligal contour interval) on the Study Area's hydrogeologic-basemap (**Fig. 1-8 [PL. 1B**]). The MeB and parts of the Southern Jornada and El Parabién GW Basins outlined in green, orange and dark red, respectively.

Gravity data provide an economical source of information on earth structure. In the Rio Grande rift, gravity data have contributed significantly to the, location of normal faults, definition of basement structure, and delineation of basin geometry (e.g., Cordell 1978, Ramberg et al. 1978, Daggett et al. 1986, Adams and Keller 1994). The negative anomalies are associated with basin fill that has low density, while the positive anomalies are associated with uplifts (Decker and Smithson 1975). In the deepest portions of the basins, the thickness of Cenozoic sediments typically ranges from 2 to 3 km based on gravity modeling; . . . .

The region of primary interest is situated immediately west of Ciudad Juárez [**Figs 1-3 and 3-3**]. The definition and investigation of the gravity lows in this area was the chief aim of this study. These gravity lows correspond to a series of basins west of the EI Paso-Ciudad Juárez metroplex that may contain important water resources [p. 80]. . . .

The gravity model was constructed using all available geological and geophysical data as controls [,] and should be considered to be geophysically constrained geologic cross section. The [Pemex] Moyotes 1 well [**Fig. 3-8b**] was a particularly important constraint [p. 81].

The gravity profile and resulting model are shown in Figure 6 [*cf.* **Fig. 3-8a, b**]. Relatively low gravity values (-160 to -170 [milligals] obtained in the El Parabién Ranch area indicate the presence of a deep basin containing sedimentary fill with a thickness of 2.2 km [7,218 ft – SFG/Tls; *cf.* **Figs. 3-11** and **3-12**, **Tbl. 3-2**]. Here we name this feature as the El Parabién basin [p. 81-82, Figs. 6 and 7] . . . .

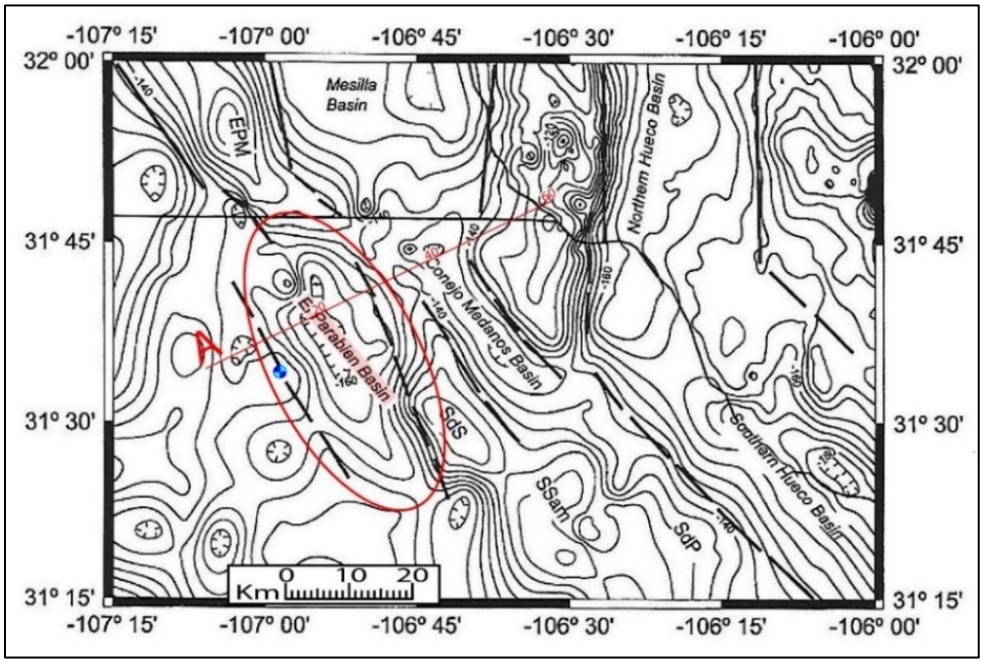

Figure 3-9a (modified from Jiménez and Keller (2000, Fig. 7, p. 82); reproduced with permission from the New Mexico Geological Society, Inc.; *cf.* **Fig. 3-8).** Gravity map (4 milligal contour interval) with an interpreted extent of the major RG-rift basins in the border region that is "based on the integrated analysis of gravity, drilling, geologic, and remote-sensing data." (**Part 6.4**), El Parabién Basin-red outline, Profile A- red line (**Fig. 3-9b**), and Pemex Moyotes No. 1-blue circle **(5.6.4**). The "Conejo Medanos Basin" comprises most of the Méndez-Vergel Inflow Corridor and MeB-El Milagro Subbasin as defined herein (*cf.* **5.1.6** and **6.3.4d**). EPM-East Potrillo Mountains SdS-Sierra de Sapello, Ssam-Sierra Samalayuca, and SdP-Sierra del Presidio.

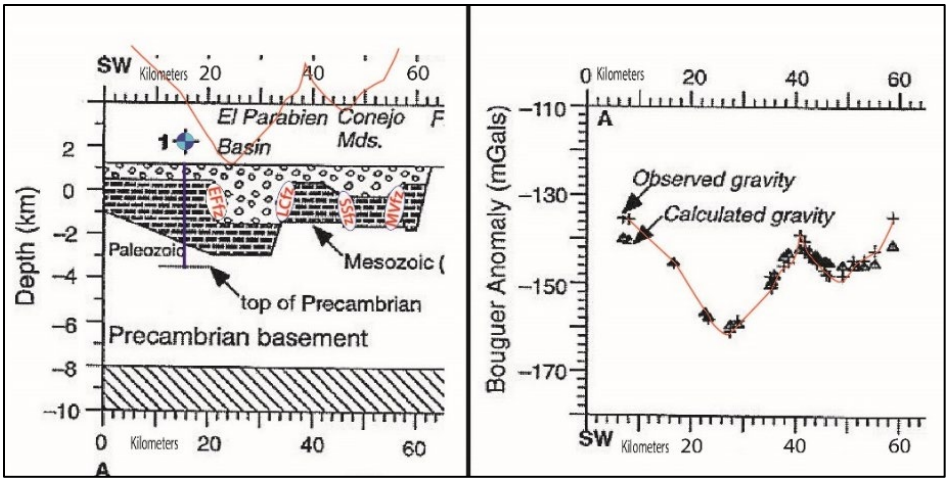

Figure 3-9b (modified from Jiménez and Keller (2000, Fig. 6)); reproduced with permission from the New Mexico Geological Society, Inc.)**.** Western part of computer model of gravity profile A-A' (right; and red line, right and left), and schematic geologic section (left), with Cenozoic Laramide and RG-rift basin fill shown with open polygons (SFG/Tls – **Tbl. 3-2**). Location of Profile A shown on **Fig. 3-9a**. Pemex Moyotes No.1-blue circle (*cf.* **Parts 5.6.4** and **6.5**). Fault zones (**Tbl. 1-3**): Effz-El Faro, LCfz-Los Cuates, SSfz-Sierra Sapello, and MVfz-Mesilla Valley.

3.6.2. Basin-Scale Characterization of the Buried Bedrock Terrane

Figures 3-10 and **3-11** (**PLS. 8A** and **8B**) are block diagrams that schematically portray basin-scale interpretations of available information on deep-seated structural and stratigraphic relationships in the central and southern Mesilla Basin area of the RG rift (*cf.* **Figs. 3-11** and **3-12**). Information sources include reports on surface-geologic mapping, deep-borehole logging, and surface-geophysical surveys. Initial diagram-compilation scale was 1:100,000, with no vertical exaggeration (VE), and diagram bases are at 25,000 ft (7.6 km) bmsl. Each diagram faces northeast, and both have north-facing and east-facing borders. Their geographic position is shown on an oval-shaped section of 2017 Google Earth® image, which allows portrayal of the surrounding landscape features of the MBR (**Fig. 3-1**). The WRRI Study Area is outlined in blue on the Figure 11 image base.

Middle- to Late-Cenozoic extensional features of the Rio Grande rift have general north-south trend. They are superimposed on the northwest-southeast trending compressional fabric of the Paleocene-Eocene, "Laramide" Potrillo basin and Rio Grande uplift complex (*cf.* Gries 1979, 1980, Seager et al. 1986, Jiménez and Keller 2000, Lawton 2004, Seager 2004, Averill and Miller 2013). Summary descriptions of mapping units are included in **Table 3-1**. Deep-subsurface conditions in the southern MeB and EPB area also suggest that these structural-depressions are superimposed on pre-existing tectonic features with a NW-SE trend that have existed since the formation of the Bisbee basin and Chihuahua trough during Mesozoic time (**TBL. 2**; *cf.* Gries 1979 and 1980, Dickinson et al. 1986, Seager et al. 1986, Haenggi 2002, Lawton 2004, Seager 2004).

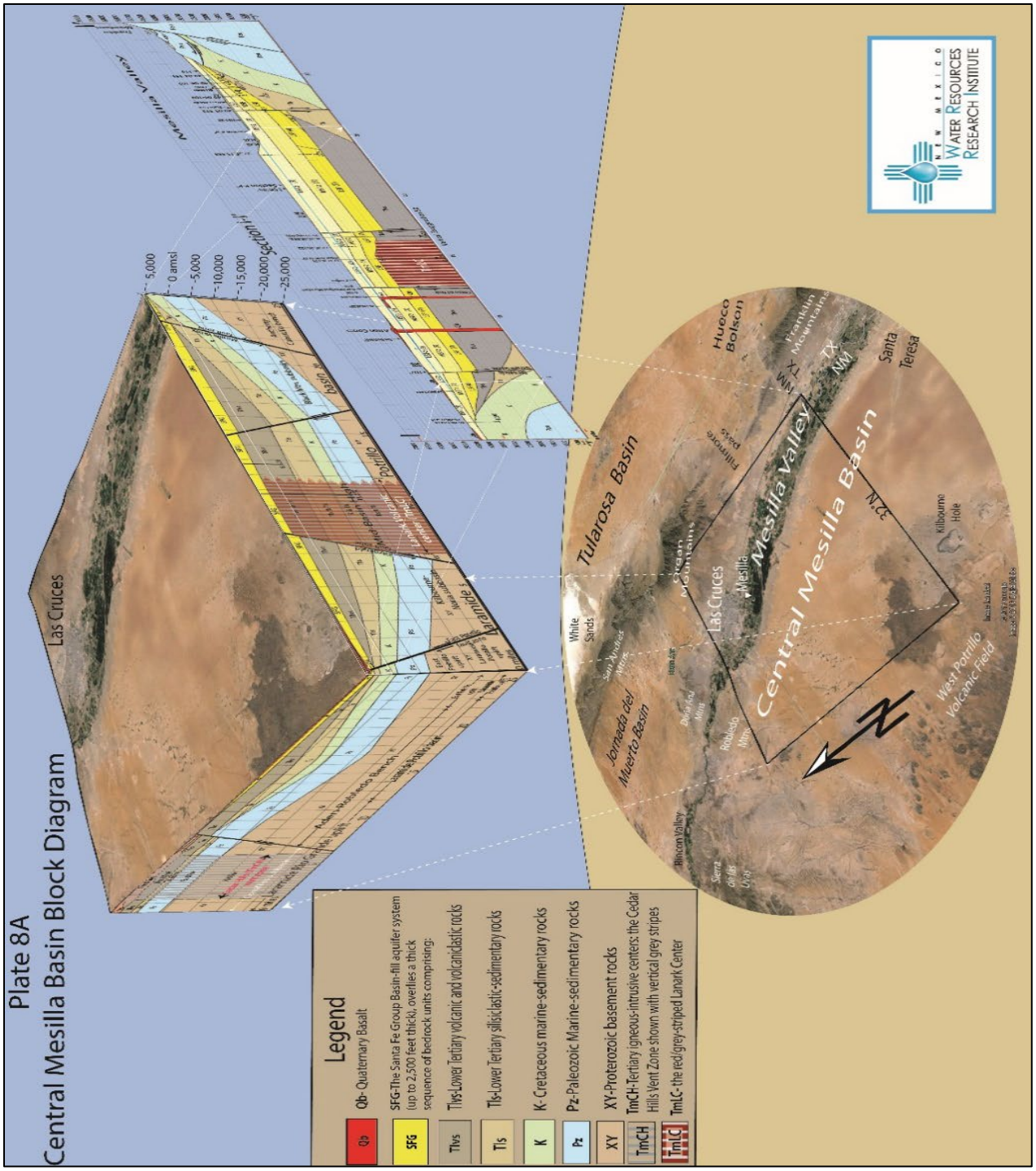

Figure 3-10 (page-size **PLATE 8A,** with stratigraphic-unit definitions on **Table 3-1**)**.** Block diagram of the central Mesilla Basin that schematically portrays major RG-rift stratigraphic and structural features at 1x vertical exaggeration (VE) and a base elevation of 25,000 ft (7.6 km) below mean sea level. Inset cross-section I-I′ (msl base, 5x VE) is one of 19 hydrogeologic sections that show lithofacies, hydrostratigraphic, and structural relationships at levels of detail appropriate for groundwater-flow and hydrochemical modeling. Major components of the mid-Tertiary Lanark igneous-intrusive complex in the central Mid-Basin High are also shown. 2017 Google Earth® image base.

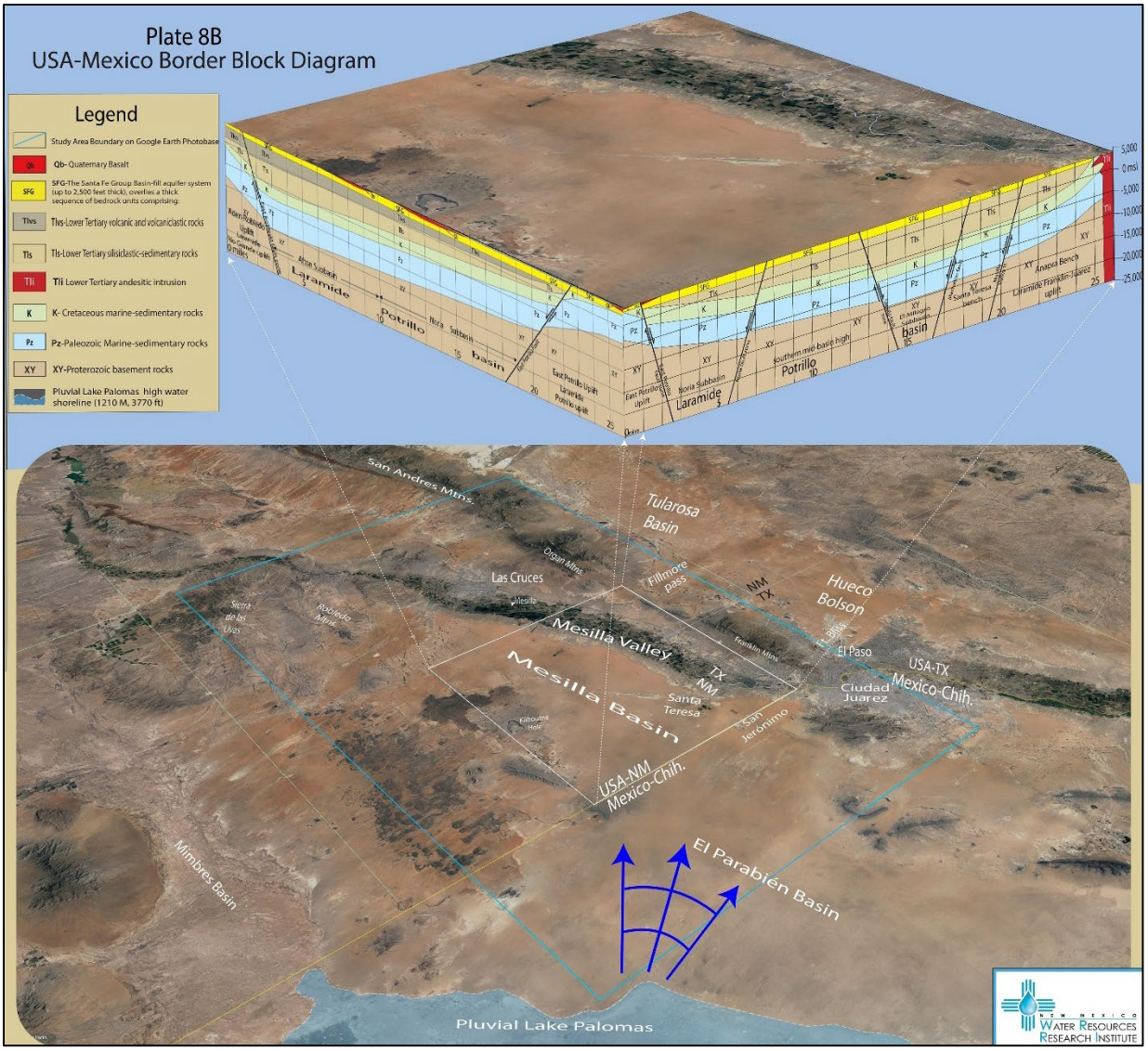

Figure 3-11 (page-size **PL. 8B).** Northeast-facing block diagram of the southern Mesilla Basin, with its southern panel at the International-Boundary and stratigraphic-unit definitions on **Table 3-1**. It schematically portrays major RG-rift stratigraphic and structural features, including the Eocene Cristo Rey igneous-intrusive complex to a base elevation of 25,000 ft (~7.6 km) below mean sea level (msl). The pale-blue shading at the base of the circular 2017 Google Earth® image show the part of the NE Los Muertos Basin floor that was inundated by Late Pleistocene pluvial-Lake Palomas stands between about 28,000 and 12,000 years ago (**Figs. 1-9** and **1-10**). Blue arrows show Mesilla Valley-directed outflow component of GW discharge during Lake Palomas high stands (3,940-3,970-ft / 1,201-1,210-m amsl).

Table 3-1. Explanation of Basin-fill and Bedrock Mapping Units on Figures 3-10 and 3-11 (PLS. 8A and 8B). Time-Rock Class, Lithostratigraphic and Hydrostratigraphic Unit, and Fault-Zone Category Definitions on Figure 3-5, and Tables 1-2 and 1-3 (*cf.* **TBL. 2**).

RA Channel and overbank-floodplain deposits of the Rio Grande—Late Quaternary, as much as 100 ft (30 m) thick and mostly in the saturated zone

Qb Alkali-olivine basalt flows and cinder cones associated with volcanic centers in the Mesilla Basin-West Mesa and West Potrillo Mountains areas—Pleistocene

SFG Rio Grande-rift basin fill-undivided—mostly Santa Fe Group: HSU's USF/MSF/LSF (LFAs *1-10*)—Late Oligocene to Early Pleistocene; thickness locally up to 3,600 ft (1100 m), but less than 2,500 ft (760 m) in the MeB

Tmrs Silicic pyroclastic and volcaniclastic rocks—Oligocene; mainly rhyolite and dacitic ashflow tuffs and tuffaceous sandstones, with some capping basaltic-andesite flows

TmCH Cedar Hills vent zone (Seager and Clemons 1975; Mack et al. 1994, 1998). N-S aligned series of flow-banded rhyolite domes and feeder conduits (unit Tmrs) that are intruded into the Tlvs/Tls/Pz/XY stratigraphic sequence in the Cedar-Corralitos Upland Basin (**PL. 2,** and **PL. 5a** and **5d**)

TmLC Lanark igneous-intrusive complex (Clemons 1993, Report **Part 6.3.2a**). Mixed felsic intrusive-rock varieties (Tmi), and contact-altered volcanic and sedimentary rocks of the intruded-bedrock sequence (Tlvs/Tls/K/P-**TBL. 2**). The "complex" is located in southern part of the Northern Mid-Basin High, where it is buried by at least 1,500 ft (455 m) of SFG basin fill near UPRR **Lanark Siding (**no. 237 oil test, **TBL. 1**; **PLS. 1B**, **1C**, **3, 5i** and **5q**, and **8A**)

Tmi Intermediate to silicic (felsitic) plutonic rocks in the Organ and Dona Ana Mountains, and Mt. Riley-Cox and **TmLC** areas, including monzodiorite to syenite stocks— Oligocene and Late Eocene (Seager et al. 1987, Clemons 1993, Seager 1995)

Tlvs Volcaniclastic and epiclastic-sedimentary rocks, local basal gypsite beds, and some andesite flows and breccias. Palm Park-Rubio Peak correlative of Eocene age. The unit is locally buried by as much as 1,450 ft (442 m) of SFG basin fill and is about 3,880 ft (1,183 m) thick in no. 180 oil test (**TBLS. 1** and **2; PLS. 5h** and **5q**).

Tli Intrusive igneous rocks of intermediate composition; porphyritic and generally fine grained, and intercalated with Tlvs clastic rocks. Eocene age

Tls Mostly sedimentary rocks, sandstones, mudstones and conglomerates with minor or no volcanic constituents (non-marine). General Love Ranch/Lobo Formation correlative of Paleocene and Early Eocene age. The unit is about 7,000 ft (2,134 m) thick in no. 180 oil test (**PLATE 5h** and **5q**). An inferred correlative sequence of siliciclastic rocks is at least 1,000 ft (330 m) thick in no.397 oil test (**TBL. 1**, **PL. 5s**).

K Sandy to shaly limestone, pelecypod-coquina limestone, silty shale, calcareous sandstone, and limestone-pebble conglomerate, with local gypsite interbeds (marine). Early Cretaceous age, and subject to major Laramide tectonic deformation. Approximately 1550 to 2200 ft (470-670 m) thick in the East Potrillo Mountains. The unit is about 1,050 ft (320 m) thick in no. 180 oil test, and 5,512 ft (1,680 m) thick in no. 397 oil test (**TBL. 1**)

Pz Primarily limestone, with shale, sandstone, redbed mudstones, and local gypsite beds (mostly marine)—Paleozoic age rocks-undivided

XY Igneous and metamorphic rocks, undivided. Proterozoic (Precambrian) age

The north-facing (W-E) panel of **Figure 3-10** has a 32º N latitude alignment, and extends across the MeB-West Mesa and the Anthony area of the MeV between the East Potrillo and Franklin Mountains Uplifts. The west-facing panel crosses the East Potrillo-East Robledo fault system that forms the western edge of the MeB, and the southern part of the Cedar Hills igneous-intrusive complex of mid-Tertiary age (TmCH; Seager and Clemons 1975; Clemons 1976a; Mack et al. 1994b). The north-facing panel of **Figure 3-11**) has an International Boundary (latitude 31º47' N) alignment; and it extends across the Mesilla Basin between the East Potrillo Uplift (Late Miocene) and the Early Tertiary andesitic-intrusive centers of Cerro del Cristo Rey and El Paso del Norte (*cf.* **PL. 5k** and **5l**; **Fig. 3-5**). Pale-blue shading at the southern edge of the Google Earth® image base shows the approximate area of the northeastern ZHGCM-El Barreal basin area that was inundated by pluvial-Lake Palomas high stands (**Part 3.3.2**). Blue arrows show Mesilla Valley-directed outflow component of GW discharge during Lake Palomas high stands of 3,940-3,970-ft (1,201-1,210-m) amsl.

Figure 3-12 (page-size **PL. 2B**) schematically portrays the topography, and primary stratigraphic and structural components of the bedrock terrane that is buried by basin-fill deposits within the Study Area (**Fig. 1-4**). The Mesilla GW Basin boundary is in green, with map-unit subdivisions defined in **Table 1-4**. The general position of the deeply buried "Lanark igneous-intrusive complex (TmLC)," which forms the central part of the Mid-Basin High, is also shown (**Figs. 3-10**, **3-12**and **3-13**; *cf.* **PLS. 5i** and **5q**; **Part 6.3.2a**; Clemons 1993). The map represents the first effort to create an approximation of the base of the RG-rift basin fill and associated aquifer systems in the Study Area (*cf.* **Part 1.5**). It is based on a synthesis of available geological and geophysical information that has been acquired by the PI since the start of his MBR work in 1962. The structure-contour intervals on the bedrock surface are 25, 50 and 100 m, and the red lines show locations of three schematic geologic cross-sections (I-I′ to III-III′) on **Figure 3-13** (**PL. 2C**). The latter shows general subsurface relationships to a depth of 10,000 ft (3 km) bmsl at about 2.5 VE. Stratigraphic-unit names and acronyms are also listed on **Table 3-2**.

Section I-I′ shows basic bedrock geologic relationships in the northern MeB/MeV and southern part of the Southern Jornada Basin (SJU).

Section II-II′ illustrates these basic geologic relationships in a central MeB area that includes the deeply buried Lanark intrusive complex (TmLC) that forms much of the central Mid-Basin High (MeB-MBH; **Part 6.3.2a**).

Section III-III′ shows basic geologic relationships in an area located about 5 mi (8 km) south of the International Boundary.

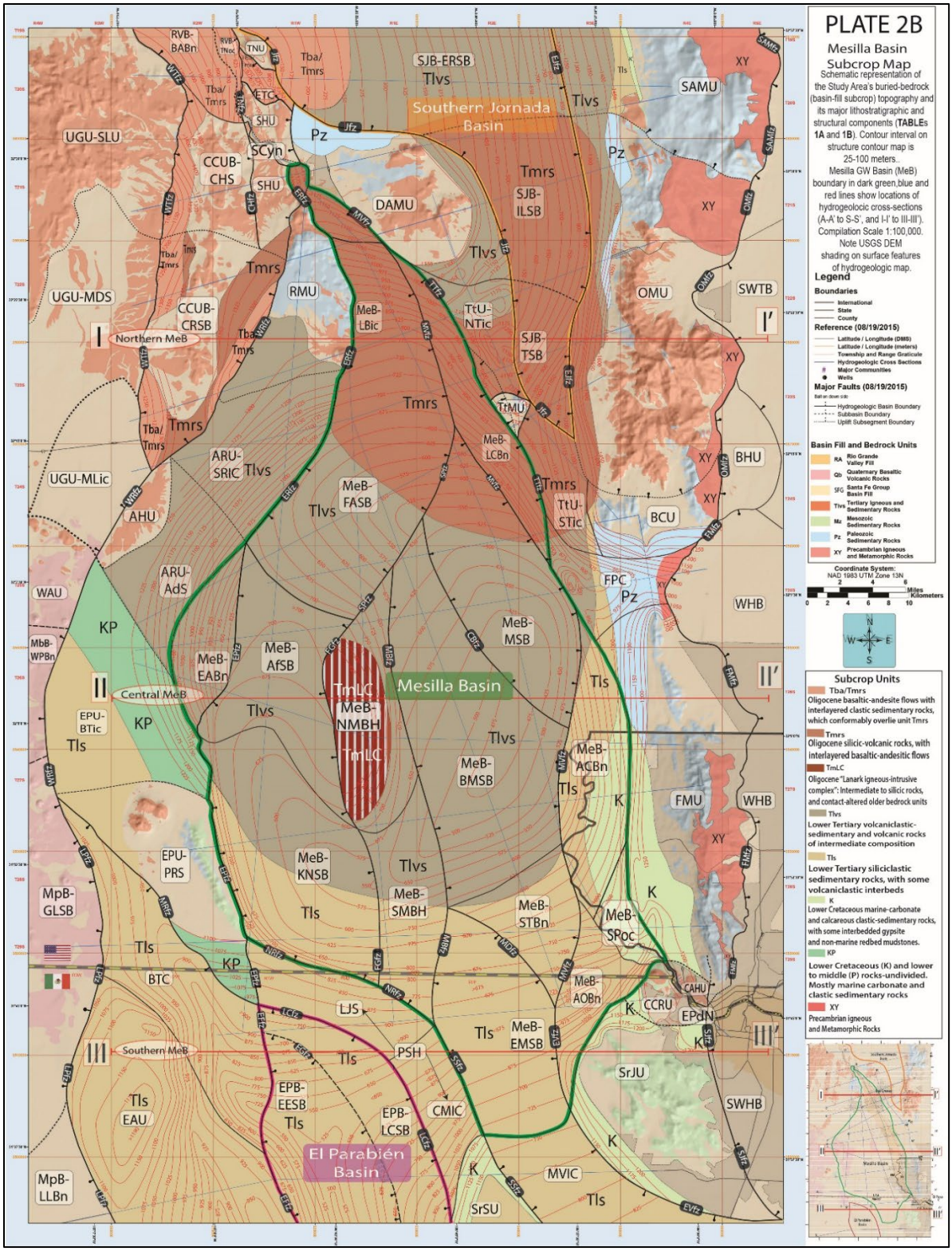

Figure 3-12 (page-size **PL. 2B).** Schematic depiction of basin-fill subcrop topography, and primary lithostratigraphic and structural components in the Study Area (25, 50, and 100 m contour intervals), with explanation on **Tables 1-4 and 3-2**. W-E red lines show locations of geologic cross-sections I-I′ to III-III′ (**Fig. 3-13**). **PLATE 1** hydrogeologic-map base.

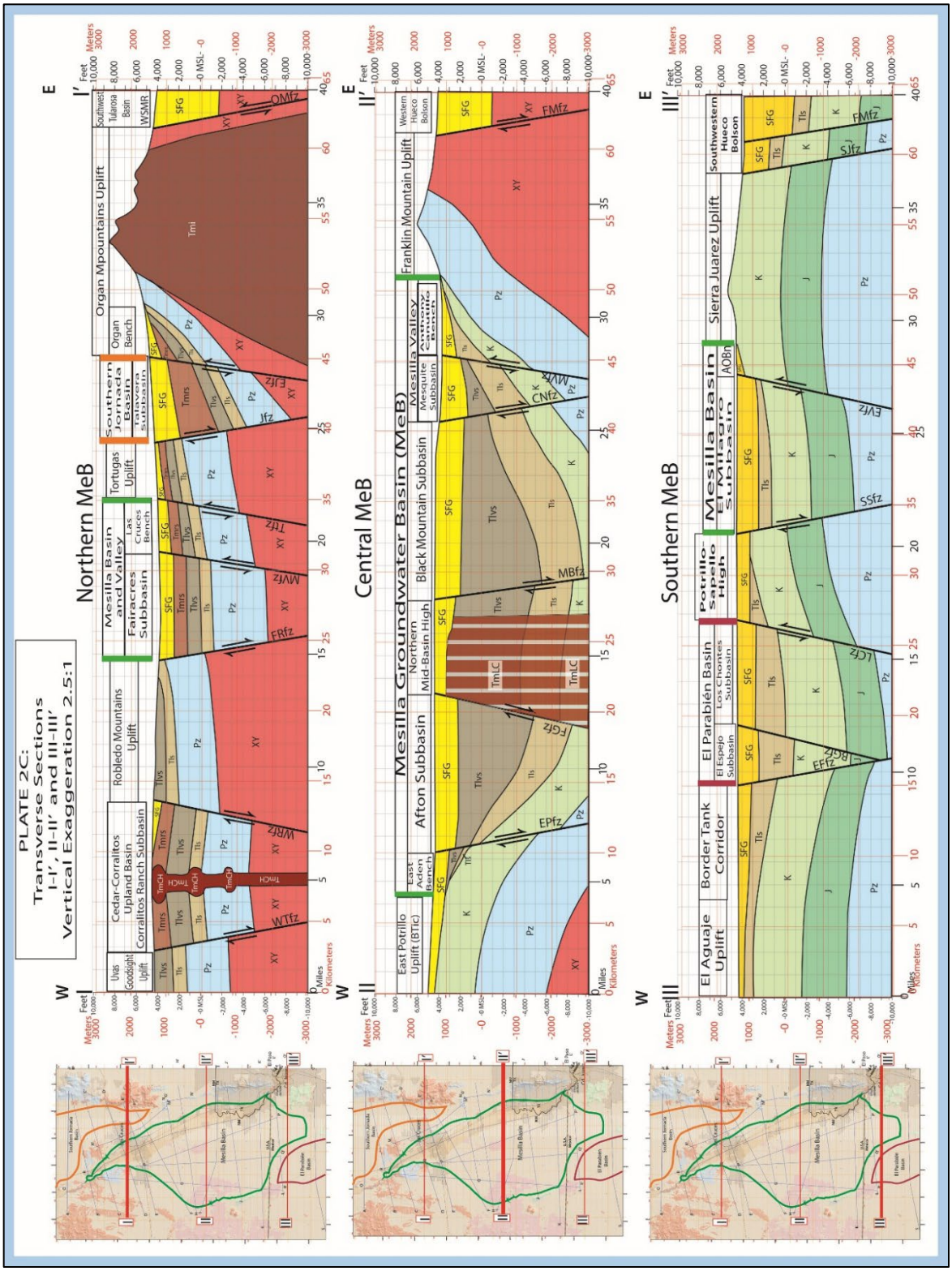

Figure 3-13 (page-size **PL. IIC**)**.** Schematic geologic cross-sections I-I' to III-III' that show major subsurface stratigraphic and structural relationships in the central and southern parts of the Study Area. Explanation on **Table 3-2**, with geologic-section locations on **Figure 3-12.**

Table 3-2. Explanation of Lithostratigraphic Units on Figures 3-12 and 3-13

Rio Grande Rift Basin Fill (Upper Oligocene to Lower Pleistocene)

SFG Santa Fe Group Hydrostratigraphic Units (HSUs)-Undivided. Post-**SFG** HSUs-not shown. Includes alluvial deposits of the inner Rio Grande Valley (**RA**), and thin, but locally extensive basaltic volcanics (**Qb**). Mostly middle to late Quaternary age

Middle to Lower Tertiary Igneous Extrusive/Intrusive and Non-marine Sedimentary Rocks

Tba Basaltic andesite lava flows and vent-zone units, with interlayered mudstones, sandstones and conglomerates volcanic rocks—late Oligocene Uvas Basaltic Andesite correlative

Tmrs Silicic pyroclastic and volcaniclastic rocks—Oligocene; mainly rhyolite and dacitic ashflow tuffs and tuffaceous sandstones, with some capping basaltic-andesite flows (**Tba**)

TmCH Cedar Hills vent zone. N-S aligned series of flow-banded rhyolite domes and feeder conduits intruded into the Cedar-Corralitos Upland Basin stratigraphic sequence—Oligocene

TmLC Lanark Complex—Intermediate to silicic igneous-intrusive complex that forms central part of the Northern Mid-Basin High and is buried by at least 1,500 ft (455 m) of SFG basin fill—Oligocene (*cf.* **PLS. 1A, 1B, 3, 5i** and **5q**; Phillips-Sunland oil test: **TBL. 1,** no. 237; Clemons 1993)

Tmi Intermediate to silicic (felsitic) plutonic rocks in the Organ and Dona Ana Mountains, and Mt. Riley-Cox and **TmLC** areas, including monzodiorite to syenite stocks—Oligocene and Late Eocene (Seager et al. 1987, Clemons 1993, Seager 1995)

Tlvs Volcaniclastic and epiclastic-sedimentary rocks, and local basal gypsite beds, with andesitic to dacitic flows and breccias—Eocene Palm Park and Rubio Peak Formation correlative that is exposed in uplifts flanking much of the northern and central Study Area. The unit is about 3,880 ft (1,183 m) thick in the Mobile-Grimm oil test (**PLs 5q**, **TBL. 1**, no. 180; Clemons 1993).

Tls Mostly siliciclastic sedimentary rocks, sandstones, mudstones and conglomerates with minor or no volcanic constituents. General correlative of lower Eocene/Paleocene Love Ranch/Lobo Formations. The unit is about 7,000 ft (2,134 m) thick in the Mobil-Grimm oil-test well (**TBL. 1**, no. 180). An inferred correlative sequence of siliciclastic rocks is at least 1,000 ft (330 m) thick in the Pemex-Moyotes oil-test well (**PL. 5s**, **TBL. 1**, no. 397; Clemons 1993; Jiménez and Keller 2000)

Mesozoic Sedimentary Rocks-Mostly Marine, and Commonly Structurally Deformed

K Lower Cretaceous marine rocks-undivided. Sandy to shaly limestone, coquina limestone, silty shale, calcareous sandstone, and limestone-pebble conglomerate, with local occurrences of gypsite beds. Approximately 1550 to 2200 ft (470-670 m) thick were exposed in the Sierras Juárez and Sapello, Cerro Cristo Rey, and the East Potrillo Mountains. 1,050 ft (320 m) penetrated in the Grimm oil-test well (**TBL. 1**, no. 180). In the Pemex-Moyotes oil-test well, the Lower Cretaceous section is 5,512 ft (1,680 m) thick (**PL. 5s**, **TBL. 1**, no. 397)

J Jurassic marine rocks-undivided: limestone, shale, and gypsite, with local occurrences of halite beds beneath the southeastern-most part of the Study Area. Present in the shallow subsurface but nor exposed in Sierra Sapello. A 3,380 ft (1,130 m) thick Jurassic section was penetrated in the Pemex-Moyotes oil-test well between Permian (**P**) and Lower Cretaceous (**K**) rocks (**PL. 5s**, **TBL. 1**, no. 397)

Paleozoic Sedimentary Rocks-Mostly Marine, and Commonly Structurally Deformed

Pz Paleozoic rocks, **Pzu/Pzl**-undivided

Pzu Upper Paleozoic (Pennsylvanian and Permian) rocks-undifferentiated: primarily limestone and redbed mudstones, with shale, sandstone and some gypsite

Pzl Middle and Lower Paleozoic rocks-undivided: Middle Paleozoic (Devonian and Mississippian) —primarily limestone, with shale. Lower Paleozoic (Cambrian-Ordovician-Silurian)—primarily limestone and dolomite, with thin basal sandstone

Proterozoic (Precambrian) Rocks

XY Igneous and metamorphic rocks-undivided

3.7. STAGES OF RIFT-BASIN EVOLUTION AND SANTA FE GROUP DEPOSITION

3.7.1. Early and Middle Stages of Basin Formation and SFG Deposition

Earth-crustal extension, with differential displacement and rotation of basin and mountain blocks, and associated igneous activity, are the primary deep-seated processes that are reflected in the composition of SFG aquifer systems throughout the RG-rift tectonic province. During early stages of basin filling, the initially separate Mesilla-El Parabién-ZHGCM and Hueco-Tularosa basin groups received a major influx of fine- to medium-grained sediments from nearby upland areas that had been sites of Laramide uplift and basin formation, as well as late Eocene and Oligocene volcanic activity (Henry and Price 1985; Seager 1987; Clemons 1993; Mack et al. 1998; Mack 2004; Seager 2004). It is here inferred that the Mesilla-El Parabién-ZHGCM rift-structural trend probably served as the primary terminal-discharge site for regional surface- and subsurface-water flow during the entire period of SFG deposition, and possibly even earlier during the Paleocene-Eocene (Laramide) interval (**Tbl. 1-3** and **Fig. 3-6**; *cf.* **Parts 3.6** and **6.4**).

In contrast with the high-relief basin-boundary terrain of the present landscape, uplifts like the Robledo and East Potrillo Mountains had little or no significant topographic expression until the later part of Miocene Epoch (5 to 10 Ma). High-relief basin-border areas during Oligocene to mid-Miocene stages of SFG deposition appear to have been limited to the Organ and Doña Ana calderas, the Mount Riley-Cox intrusive center, Sierra de las Uvas, and parts of the San Andres, Franklin, and Sierra Juárez ranges (**Figs. 1-3** and **1-8**; *cf.* **CHPT. 5**). According to this interpretation of the Miocene basin and upland topography, the dominant lower and middle SFG depositional environments comprised alluvial and ephemeral-lake plains, with down-wind eolian sand tracts on eastern-basin margins. Because of their deep burial in most parts of the region, lithostratigraphic-unit (Formation rank) names have not been assigned to the lower and middle parts of the SFG. They are, however, general correlatives of with the respective Lower and Middle Santa Fe-Hayner Ranch and Rincon Valley Formations that are well exposed Rincon-Hatch Valley area (**Fig. 3-5**; Seager et al. 1982, 1987; Collins and Raney 2000).

The most striking lower SFG lithofacies in the southeastern MeB comprises thick deposits of well-sorted, fine to medium sand that forms a very productive “deep-aquifer” zone beneath the southern Mesilla Valley (*cf.* **Parts 4.2.1** and **6.3.5**). However, the nature of their role as active parts of the present-day GW-flow regime remains enigmatic (*cf.* **7.2.1**). The lower SFG-LFA4 unit was first identified by Leggat and others (1962) in in the EPWU-Canutillo well field and later by Wilson and others (1981) beneath the central Mesilla Valley area (*cf.* Cliett 1969, W.E. King et al. 1971, Hawley 1984, Cliett and Hawley 1996; **APNDX. C2**). These partly consolidated eolian sediments, which are as much as 600 ft (183 m) thick in the Canutillo Well Field area, have long been interpreted as deposits of an ancient dune-field complex that has contemporary analogs in the Great Sand Dunes area of Colorado’s San Luis Basin,

and the Médanos de Samalayuca of north-central Chihuahua (**Figs**. **1-3**, **1-4**, **3-1** and **3-3**; *cf.* **APNDX. H1.5.2**; Schmidt and Marsden 1981, Valdez and Zimbelman 2020).

Most of the Middle SFG was deposited during middle- to late-Miocene time when maximum differential movement occurred between the central rift-basin blocks and flanking mountain uplifts. In the Mesilla Basin east of the present location of the MeV, the primary basin-fill component of the Middle SFG comprises coarse-grained fan-piedmont alluvium derived from the rapidly rising southern Organ and Franklin uplifts. The developing Robledo and East Potrillo Uplifts contributed similar piedmont-alluvial facies to westernmost parts of the Mesilla Basin during the Late Miocene. Beneath the MeB's broad West Mesa area, however, the predominant Middle SFG lithofacies is a thick sequence of interbedded sand and silt-clay beds also forms the basin's most extensive aquifer zone (HSU-MSF2−LFA *3*, **Part 4.2**). The unit is locally as much as 1000 ft (305 m) thick (**Pls. 3f**, **4a-d**, **5c**), and analyses of driller and sample logs suggest a major component intertonguing of distal-piedmont-slope and basin-floor facies, with the latter including interbedded playa-lake, alluvial-flat, and eolian-sandsheet deposits.

3.7.2. Late-Stage Rift-Basin Development and Culmination of SFG Deposition

3.7.2a. Evolution of the ARG Fluvial-Deltaic System

All major structural components of the basin and bedrock uplifts of the present regional landscape had formed by Late Miocene time (10 to 5 Ma), with the Robledo and East Potrillo uplifts being the most recent to emerge as prominent mountain landforms (Seager and Mack 1994, Seager et al. 2008). There is no stratigraphic or geomorphic evidence, however, to suggest that surface-drainage systems exited the Mesilla Basin region during the 20 to 25 Ma interval of Lower and Middle SFG deposition. Early basins in the southern RG-rift region appear to have existed as a slowly aggrading, poorly integrated group of structural depressions until a sediment-loaded Ancestral Rio Grande (AGR), with headwaters in the Southern Rocky Mountains, entered the Palomas Basin as early as 5 Ma (Mack et al. 1997; Mack 2004; Connell et al. 2005; Mack et al. 2006, 2009; Hawley et al. 2009; Koning et al. 2018).

ARG deposits of Early Pleistocene age mark the culmination of SFG basin-fill deposition throughout the southern New Mexico border region (Hawley et al. 1969; Gile et al. 1981; Seager et al. 1987; Mack et al. 2006; **Figs. 3-6** and **3-7**; *cf.* **3-14** and **3-15**, and **Part 3.6.2**). The Upper SFG-ARG distributary-channel and fluvial-deltaic complex that underlies most of the basin-floor parts of the Study Area may be as much as 5 Ma old at its base (Seager et al. 1984 and 1987; Mack et al. 2006; Koning et al. 2018). During a 3 to 4 Ma interval of Pliocene and Early Pleistocene time, the ARG fluvial system delivered enormous quantities of water and sediment to two groups of then-interlinked endorheic rift basins: the Southern Jornada-Mesilla-El Parabién-Los Muertos group on the west, and the Tularosa Basin-Hueco Bolson group on the east (**Part 3.4.2**; **Figs. 1-2**, **3-1** and **3-3**; Stuart and Willingham 1984; Seager et al. 1984; Gustavson 1991a; Collins and Raney 2000). Fillmore Pass between the Organ and

Franklin Mountains formed the primary corridor that connected the two basin groups (**Part 5**.**1.2**; *cf.* **Fig. 3-15**, Strain 1966, p. 11). Saturated parts of the Upper SFG-ARG facies, which are locally more than 600 ft (180 m) thick, form the most productive aquifer unit in the Mesilla Basin and Hueco Bolson region (Hawley and Kennedy 2004; Hawley et al. 2009; *cf.* **Parts 4.2.3**, **6.3.2-6.3.5**, and **7.3.3**). According to Hawley and others (1969, p. 58):

> The origin of the early- to mid-Pleistocene [ARG] sand and gravel deposits, interpreted as fluvial sediments [herein], has been debated. . . . Since this time-transgressive unit in the upper Santa Fe [Gp] section occurs on both side of the Rincon Hills, the Tonuco-Selden Hills uplands, and the Robledo, Doña Ana, and Franklin Mountains (…), it is certainly not a single channel deposit of an ancestral river, as described by Bryan and associates in basins north of Socorro (Bryan [1938]; Denny, 1941; Wright [1946]). Evidence that these are fluvial deposits and not lacustrine gravel and sand, . . ., follows: (1) The wide-spread deposits of gravel and sand are confined to the ancient, often very broad, basin floors and do not occur as fringing [beach-ridge] bars on piedmont slopes. (2) The deposits tend to thicken toward basin axes and slope to the south. (3) The sediments contain some rock types, exotic to the particular basin, that are derived from areas to the north. (4) Sedimentary structures within the deposits (such as trough sets of cross beds and armored mud balls) are generally indicative of fluvial sedimentation. (5) Similar high-level gravel and sand deposits, at relatively constant altitudes above the present river floodplain, are preserved in many places along the Rio Grande trough from central New Mexico to western Texas (DeBrine, Spiegel, and Williams, 1963; Davie and Spiegel, 1967; Hawley, 1965; Strain**,** 1966; and Weber, 1963). Thus, the ancestral Rio Grande in the south-central New Mexico border region might best be characterized as a time-transgressive system of distributary channels, with shifting loci of deposition, that spread out from a more confined channel system in the Palomas Basin above Rincon [*cf.* **Figs. 3-6**, **3-13** and **3-14**]. Before integration with the lower Rio Grande system southeast of the Quitman Mountains and initiation of valley entrenchment, the upper Rio Grande at various times fed large lakes in the border region (Lee, 1907; King [P.B., 1935]; Brand, 1937; Bryan [1938]; Sayre and Livingston [1948]; Kottlowski, 1958; Reeves [1965]; Strain, 1966).

With respect to the occurrence of "exotic" gravel clasts in the Upper SFG, the following description of a "caliche-pit" exposure along Mexico Federal Highway 2 and near Rancho del Parabién is of special note (Córdoba et al. 1969, Km 58; **Fig. 1-11**, **APNDX. D1a**):

> Caliche pit on north side of highway. Partly indurated caliche and underlying sands contain scattered rounded pebbles of mixed, generally siliceous composition. Rock types include rhyolite (welded tuff and trace of obsidian*), granite, quartz, chert, and basalt. The gravel reflects the composition of bedrock and older basin-fill deposits north of the 32nd Parallel, and is not from local sources. The lithology of surficial basin fill in this area is identical to that of the Camp Rice Formation in the Mesilla Basin and further north [*cf.* **Part 3.5**].
>
> **Closest source-rock exposures are near Mount Taylor or in the Jemez Mountains!*

3.7.2b. Fort Hancock and Camp Rice Formations, and Paleo-Lake Cabeza de Vaca

William S. Strain (1966) formally introduced "Camp Rice Formation" and "Fort Hancock Formation" as the lithostratigraphic names for the respective, fluvial and lacustrine deposits of the ARG

and paleo-Lake Cabeza de Vaca (LCdV) that he had mapped in the formation's type localities (**Part 3.5**; **Figs. 3-5** and **3-6**). He inferred that the disconformable Camp Rice /over/ Fort Hancock Formation sequence** was a time-transgressive, succession of fluvial, fluvial-deltaic and lacustrine facies that were deposited by shifting ARG distributary channelbelts that terminated in a then endorheic basin complex located in the Mesilla and Tularosa Basins, Bolsón de los Muertos, and Hueco Bolson, (**Figs. 3-13** and **3-14**).**

Subsequent advances in biostratigraphy, tephrochronology, and magneto-stratigraphy, have led to significant revisions in age estimates for the ARG fluvial-deltaic system (e.g., **Fig. 3.6; cf. Strain 1971, Tedford 1981, Izett and Wilcox 1982, Vanderhill 1986, Collins and Raney 1991, Gustavson 1991a, Gile et al. 1995, Connell et al. 2005, Mack et al. 2006).*

***Gustavson (1991a) inferred that LCdV occupied basin-floor areas below a present altitude of 4,050 ft (1,235 m) in the Tularosa Basin, Hueco Bolson, Mesilla Basin, and* Bolsón de los Muertos.

According to Hawley (1975, p. 145):

> The major facies of the Camp Rice [Fm] is fluvial sand and gravel deposited by the ancestral Rio Grande during times when the river terminated in, or flowed through bolsons southwest and southeast of EI Paso. The broad (diagrammatic) pattern of river distributaries in the Doña Ana County area shown on Figure 2 [**Fig. 3-13**] indicates the broad zone where fluvial beds constitute most of the formation. To the south in Chihuahua, and probably also in the Tularosa and Hueco bolsons, these deposits grade to fine-grained, dominantly [LCdV] lacustrine units with gypsiferous evaporites (Hawley 1969 [b]; Hawley et al. 1969). The latter deposits include the Fort Hancock Formation of Strain (1966, [**Fig. 3-5**]) . . . .

Gile and others (1981, 33-34) also noted that:

> Sandy to gravelly river-channel deposits are the dominant component of the [Camp Rice Fm] fluvial facies. Thin, fine-grained units that represent overbank (floodplain) deposits are also locally present. . . . Gravel clasts are relatively well rounded and mainly of pebble size. They include a mixture of resistant rock types from distant (upstream) as well as local sources. Clasts of carbonate rocks are rare, and beds containing cobble-size [armored] mudballs are common. Sands are quartz-rich, feldspathic [arkosic], and usually free of silt-clay matrix. Sand and gravel units are well bedded, and contain very thick sets of cross-stratification. . . .

3.7.3. Background on the Distributive Fluvial System (DFS) Model

The ARG "distributive drainage network" shown in **Figure 3-13** is representative of early efforts to describe a very common depositional environment in "continental sedimentary basins." It was designed to more accurately portray the very large watersheds of the paleo-Lake Cabeza de Vaca's five major contributing ancestral-river systems: ARG, Mimbres, Casas Grandes, Santa Maria, and Carmen (*cf.* Hawley 1969 [FIG. 1], Hawley 1975 [Fig. 2]). Most of the Upper SFG was deposited by ARG fluvial and fluvial-deltaic distributaries that terminated in the four most actively subsiding southern RG-rift depressions: Mesilla Basin, Tularosa Basin, Hueco Bolson, and "Bolsón de Los Muertos" (**Figs. 1-1** to **1-2**, **3-1**, **3-3** and **3-7**). Of these, only parts of the Mesilla Basin and Hueco Bolson are now connected with

the through-going Rio Grande/Bravo system in terms of both surface and subsurface flow (Bedinger et al. 1989b, Hawley et al. 2009).

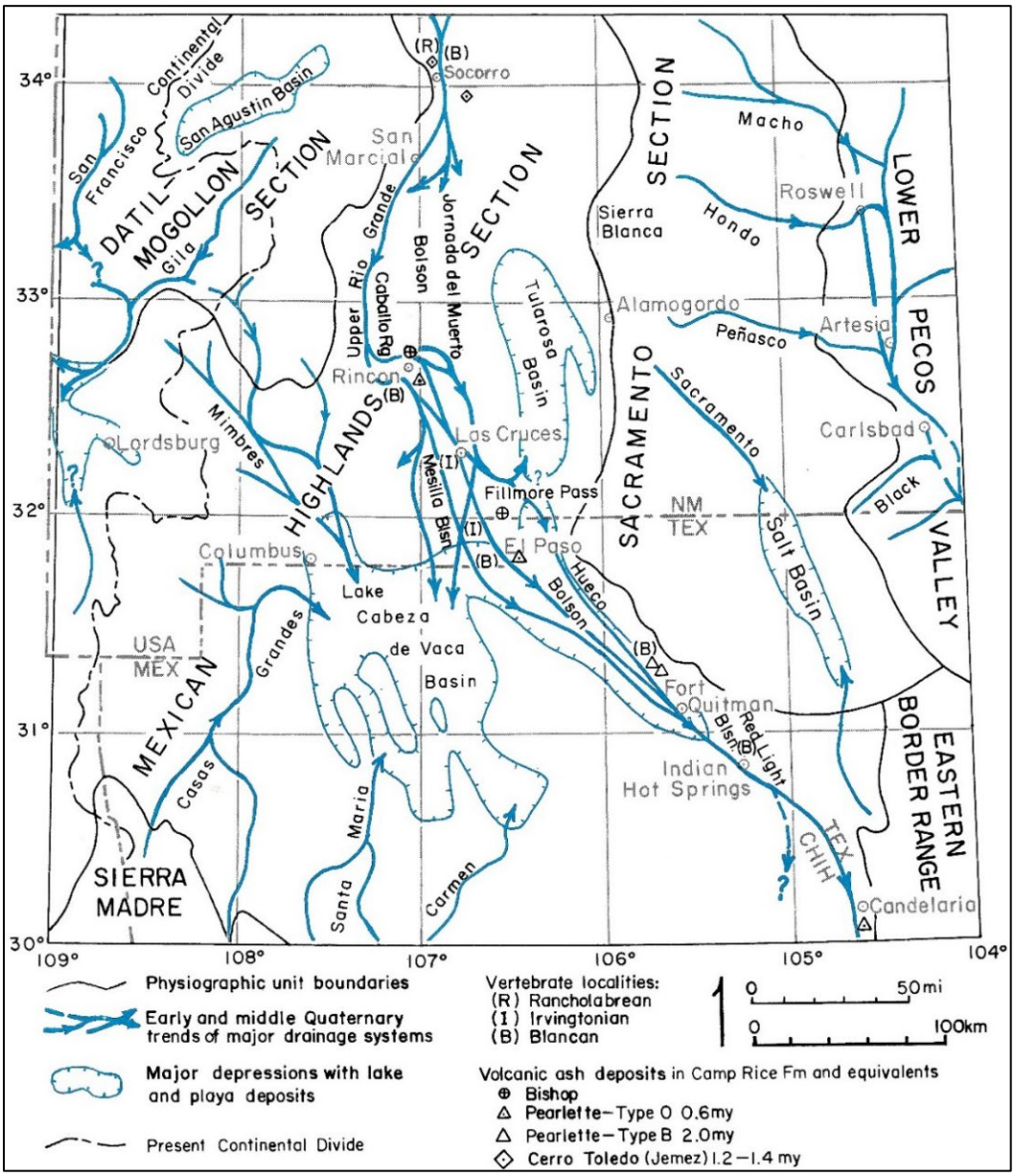

Figure 3-14 (Gile et al. 1981, Fig. 5 [modified from Hawley 1975, Fig. 2])**.** Schematic depiction of the general area occupied by the distributive drainage network of the upper ARG during much of Pliocene and Early Pleistocene time (*cf.* Connell et al. 2005, Fig. 11b and 11c). The network's apex was located near the present site of Caballo Dam about 20 mi (32 km) NW of Rincon, and it terminated in the paleo-Lake Cabeza de Vaca (LCdV) basin complex in the Mesilla-El Parabién-Los Muertos and Tularosa-Hueco structural depressions of the southern RG-rift region (Strain 1966, 1971). Four of the five large-river systems that discharged to the Los Muertos Basin section of LCdV remain as major components of the fluvial landscape: Rios Casas Grandes, Santa maria and Carmen, and the Mimbres River (**Figs. 3-1**, **3-7** and **3-15**).

This type of distal-fluvial aggradational pattern is now referred to as a "distributive fluvial system (DFSs)" (e.g., Hartley et al. 2010, Davidson et al. 2013). Weissmann and others (2011, p. 327) describe the basic genetic and compositional features of a DFS in the following selection from a review paper titled "Alluvial facies distribution in continental sedimentary basins−distributive fluvial systems:"

> Fluvial depositional patterns in modern continental sedimentary basins from different tectonic settings are dominated by distributive fluvial systems (DFSs). A review of satellite imagery from over 700 modern continental sedimentary basins from different tectonic and climatic settings shows that rivers on DFSs are generally not confined to valleys and have a clear apex from which active and abandoned channelbelts radiate outward to form a positive topographic feature centered on this apex. Channels have no tributaries on the DFSs and commonly decrease in size downstream on the DFSs due to bifurcation, infiltration, and evaporation. In contrast, fluvial systems in sedimentary basins that are confined within a valley, such as those held between adjacent or opposing DFSs [e.g., channel and floodplain deposits of the inner RG Valley], incised into the DFSs, or that lie in an axial position in a basin, typically have less area for floodplain development and display coarse-grained dominated facies. These confined rivers appear to be more similar to tributary rivers that are commonly described for present fluvial facies models. Because sediments deposited in continental sedimentary basins are those that constitute the rock record, this work suggests that many of the fluvial rocks observed may have formed in DFSs [e.g., HSUs USF2/MSF2−LFAs *1-3*; **Part 4.2**]. . . .

British sedimentologist Gary Nichols describes DFSs in terms that directly apply to the ARG fluvial-deltaic deposits of Mesilla Basin region in his superbly illustrated "Stratigraphic architecture of fluvial distributive systems in basins of internal drainage (2015, p. 1):"

> Stratigraphic models of fluvial* successions tend to focus on the 'incised valley' model, which assumes that a marine base level exerts a strong control on the distribution of sandstones deposited by river channels. However, not all rivers flow to the sea and in basins of internal drainage there is no control exerted on river profiles by fluctuations in marine base level. Internal drainage basins are the sites of approximately half of the actively depositing fluvial systems today . . . . In relatively humid endorheic basins a deep basin-center lake may act as a partial downstream control on fluvial successions. However, in temperate through to arid settings, rivers terminate in a shallow, perhaps ephemeral lake, dry out on an alluvial* plain or interfinger with aeolian environments. In these settings the level of the downstream termination is related to aggradation in the basin, which is itself determined by sediment supply via the rivers. The fluvial system, its depositional patterns, and the stratigraphic architecture are hence controlled by just discharge and sediment supply. A distributive fluvial pattern** seems to be dominant in modern and modern and ancient endorheic basins. The fluvial successions formed by these systems in endorheic basins have a fundamentally different architecture to the 'incised valley fill' model commonly used in fluvial stratigraphy.
>
> **While the distinction between "alluvial" and "fluvial" processes is rarely clear, the former are most often associated with ephemeral and intermittent streams, and the latter relate to perennial streams or rivers (cf. Schumm 1965, 1968, 1977; Bull 1977; Leeder 1998).*
>
> ***As in many analogs in nature (e.g., organic branching structures), DFSs have the property of anabranching fractality (Mandelbrot 1982): That is, exhibiting a "repetition of geometric patterns at different scales, revealing smaller and smaller versions of themselves. Small parts resemble, to some degree, the whole (Taleb 2010, p. 257)."*

During an interval of at least three million years, the northern ARG basin with headwaters in the Southern Rocky Mountains (**Fig. 1-4**) contributed enormous quantities of sediment and water to the two major southern rift-basin groups that were linked by the Fillmore Pass Corridor between the Organ and Franklin Mountains: the Southern Jornada-Mesilla-El Parabién-ZHGCH group on the west, and the Tularosa Basin-Hueco Bolson group on the east (**Figs. 1-2**, **3-7**, and **3-13** to **3-15**; **Parts 5.1.2** and **7.7.1b**; *cf.* Mack et al. 2006, Connell et al. 2005 [Fig. 11c]; Hawley et al. 2009 [Pl. 1, p. 30-33]).

The 2018 Google Earth® image base for **Figure 3-15** provides a more-detailed, but still schematic portrayal of the DFSs of the five ancestral rivers that terminated in the western part of the paleo-LCdV basin: Rio Grande and Mimbres River (USA); and Rios Casas Grandes, Santa Maria, and Carmen (Mexico). Red lines show major ARG channelbelt locations; and DFS-Apex locations are show with red lower-case letters. "a" marks the head of the ARG-DFS in the southern part of the Palomas RG-rift Basin between the present sites of Caballo Reservoir and Hatch (**Figs. 1-2**, **3-3**, and **3-7**). **Figure 3-5** color codes for the ancestral Mimbres River, Rio Casas Grandes, Rio Santa Maria, Rio Del Carmen fluvial-deltaic systems are, respectively, yellow. Purple, pink, and orange. Summary explanations for the color-coded alpha-numeric **a** (**a1-a10**) to **e** (**e1-e3**) series of DFS apices and channel belts are included in **Table 3-3.**

The iterative process of designing **Figure 3-15** included use of information from the following sources: (1) initial biostratigraphic work of Strain (1966), (2) reconnaissance field studies by Hawley (1975, Fig. 2), (3) detailed geologic mapping by Seager (1981) and Seager and others (1987), (4) detailed basin-fill stratigraphic studies by Gustavson (1991a), (5) basin-fill stratigraphic and tephrochronlogic studies by Mack and others (1996 and 1997), (6) detailed geologic mapping by Collins and Raney (2000), and (7) hydrogeologic-map and cross-section compilations by Hawley and Kennedy 2004, and Hawley and others 2009. During an interval of at least three million years, the ARG basin upstream from the Caballo Reservoir area contributed enormous quantities of sediment and water to the two major southern rift-basin groups that were linked by the Fillmore Pass Corridor between the Organ and Franklin Mountains: the Southern Jornada-Mesilla-El Parabién-Los Muertos group on the west, and the Tularosa Basin-Hueco Bolson group on the east (**Figs. 1-2**, **3-7**, and **3-13** to **3-15**; **Parts 5.1.2** and **7.7.1b**; *cf.* Mack et al. 2006, Connell et al. 2005 [Fig. 11c], Hawley et al. 2009 [Pl. 1, p. 30-33]).

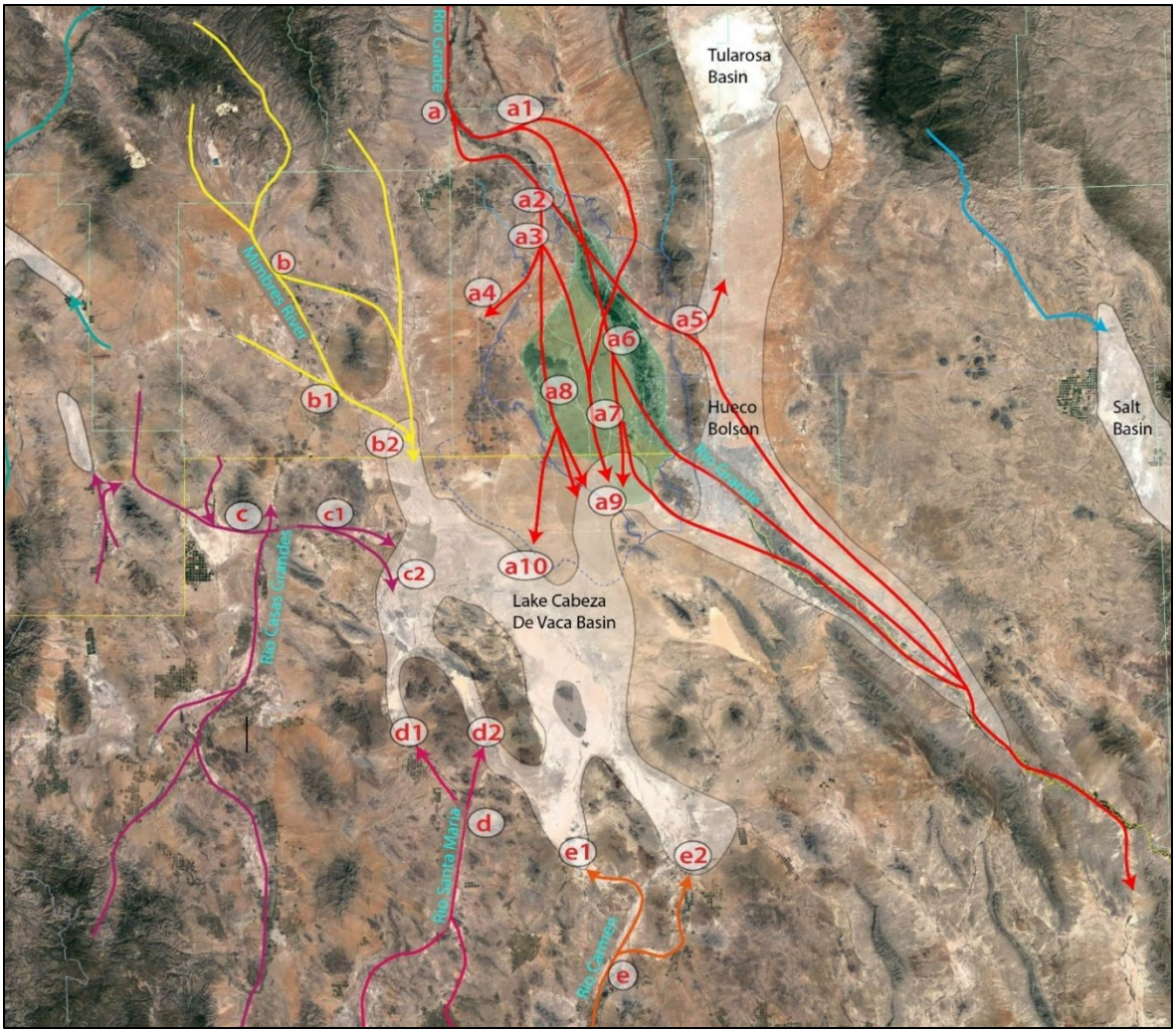

Figure 3-15 (adapted from Hawley 1975, Fig. 2)**.** Pliocene and Early Pleistocene depositional setting of the ARG distributive fluvial system (DFS-red lines) that terminated in the paleo-Lake Cabeza de Vaca (LCdV) complex of W.S. Strain (1966, 1971). The Mesilla GW Basin is shown in green. ARG deposits in the Upper SFG Hydrostratigraphic Unit (HSU-USF2) comprise a large part of the region's most-productive aquifer system (*cf.* **Fig. 4-3**). Explanations of symbols for general positions of distributive-fluvial system (DFS)-apices, ancestral-river channelbelt-segments, and LCdV fluvial-deltaic termini are in **Table 3-3**. The location of Fillmore Pass and the DFS apex of the ARG "Camp Rice Fan Delta" of Seager (1981, Fig. 84) is shown with an **a5** (*cf.* **Fig. 3-16**). The Rios Casas Grandes (violet), Santa Maria and Carmen (pink and orange), and the Mimbres River (yellow) remain as the primary surface- and subsurface-flow contributors to ephemeral lake-plain remnants of pluvial-Lake Palomas in the Zona Hidrogeológica de Conejos Médanos (ZHGCM) area: Lagunas Guzman, Santa Maria and Patos, and El Barreal-Salinas de Uníon. Only small parts of the Mesilla Basin and Hueco Bolson have surface-flow connection with Rio Grande at present (Hawley et al. 2000, 2009). 2018 Google Earth® image base.

Table 3-3. Explanation of Figure 3-15 Alpha-Numeric Symbols for Pliocene and Early Pleistocene Distributive Fluvial Systems (DFSs) of Ancestral Rivers with Fluvial-Deltaic Termini in the Paleo-Lake Cabeza de Vaca (LCdV) Complex

---

A. APEX AREA OF THE ANCESTRAL RIO GRANDE-CAMP RICE FM DFS (ARG-DFS) IN THE SOUTHERN JORNADA BASIN, HUECO BOLSON, AND LOS MUERTOS BASIN (BdLM) —RED LINES

A1. Eastern Rincon Valley head of the ARG-DFS distributary-channel complex in the Southern Jornada Basin.

A2. Upper Selden Canyon head of the ARG-DFS distributary-channel complex in the central and eastern Mesilla Basin area.

A3. Lower Selden Canyon head of the ARG-DFS distributary-channel complex in the western Mesilla Basin area.

A4. Cedar-Corralitos Basin head of the ARG-DFS distributary-channel complex in the northwestern Mesilla and northeastern Mimbres Basin areas.

A5. Fillmore Pass head of the ARG-DFS distributary-channel complex in the western Tularosa Basin and northwestern Hueco Bolson area (**Fig. 1-15**, Seager 1981 [Fig. 84]).

A6. South-central Mesilla Basin head of the ARG-DFS distributary-channel complex in the El Parabién Basin-Paso del Norte area.

A7. Southeastern Mesilla Basin head of the ARG-DFS distributary-channel complex in the El Parabién Basin, Méndez-Vergel Corridor, and southwestern Hueco Bolson area.

A8. Southwestern Mesilla Basin head of the ARG-DFS distributary-channel complex in the El Parabién Basin and the northeastern LCdV-BdLM.

A9. South-central termini of ARG-DFS fluvial-deltaic distributaries in the northeastern LCdV-BdLM.

A10. Southwestern termini of ARG-DFS fluvial-deltaic distributaries in the northwestern LCdV-BdLM.

B. APEX AREA OF THE ANCESTRAL RIO MIMBRES-UPPER GILA GP DFS (ARM-DFS—YELLOW LINES) IN THE NORTHERN LCdV-BdLM

B1. Southeastern Mimbres Basin head of the ARM-UGDFS fluvial-deltaic distributaries.

B2. Southern termini of ARM-DFS fluvial-deltaic distributaries in the northern LCdV-BdLM.

C. APEX AREA OF THE ANCESTRAL RIO CASAS GRANDES-BOCA GRANDE DFS (ARCG-DFS—VIOLET LINES) IN THE NORTHWESTERN LCdV-BdLM

C1. Head of ARCG-BGDFS fluvial-deltaic distributaries in the northwestern LCdV-BdLM

C2. Eastern termini of ARCG-DFS fluvial-deltaic distributaries in the northwestern LCdV- BdLM

D. APEX AREA OF THE ANCESTRAL RIO SANTA MARIA DFS (ARSM-DFS—PINK LINES) IN THE SOUTHWESTERN LCdV-BdLM

D1. Eastern termini of ARSM-DFS fluvial-deltaic distributaries south of Laguna Santa Maria.

D2. Western termini of ARSM-DFS fluvial-deltaic distributaries south of Laguna Fresnal

E. APEX AREA OF THE ANCESTRAL RIO CARMEN DFS (ARC-DFS—ORANGE LINES) IN THE SOUTHEASTERN LCdV-BdLM

E1. Eastern termini of ARC-DFS fluvial-deltaic distributaries in the southeastern LCdV-BdlM near Villa Ahumada and Laguna Patos.

E2. Western termini of ARC-DFS fluvial-deltaic distributaries northwest of Carrizal in the southeastern LCdV-BdLM

Figure 3-16 (Seager 1981, Fig. 84) is a detailed-diagrammatic portrayal of the early Pleistocene "Camp Rice Fan Delta" of the in the southwestern Tularosa Basin and northwestern Hueco Bolson area with its apex in Fillmore Pass between the Organ (N) and Franklin (S) Mountains (**Fig. 3-15**, **a5**). This feature is one of the major components of the ARG distributive fluvial system in the MBR (*cf.* **Figs. 3-7, 3-14** and **3-15**).

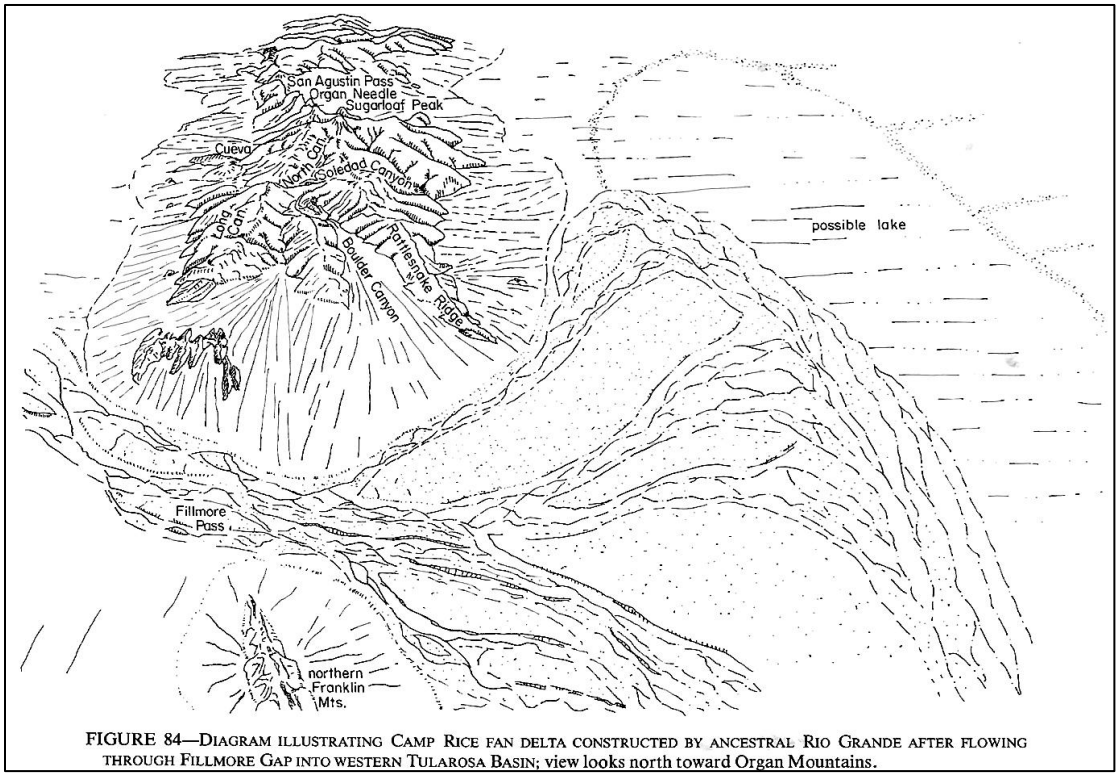

FIGURE 84—DIAGRAM ILLUSTRATING CAMP RICE FAN DELTA CONSTRUCTED BY ANCESTRAL RIO GRANDE AFTER FLOWING THROUGH FILLMORE GAP INTO WESTERN TULAROSA BASIN; view looks north toward Organ Mountains.

Figure 3-16 (Seager 1981, Fig. 84)**.** Fillmore Pass and the DFS apex of the ARG "Camp Rice Fan Delta" of Seager (1981, p. 78-84) is shown with an **a5** in **Figure 3-15.**

The best-available information on site-specific ARG-channel location in the northern Hueco Bolson area of the MBR (Fig. 1-2) is derived from "airborne-electromagnetic (aeromagnetic) surveys" that were used by Gates and Stanley (1976) as an "electrical prospecting" method "to explore for fresh groundwater southeast of El Paso (p. 1, 22-26, 32-34)." **Figure 3-17** (Gates and Stanley 1976, Fig. 5a) shows INPUT [Induced Pulse Transient] electromagnetic (EM)-response curve profiles (red) for 17 complete flight-lines, with heavy-dashed line marking the approximate borders of high-resistivity Camp Rice distributary-channel "material deposited by the ancestral Rio Grande on its course through Fillmore Pass and to the southern part of the Hueco Bolson." Note that the GW-salinity focus of the early 1970s survey methods had significant drawbacks from a hydrogeologic modeling perspective (*cf.* Paine and Collins 2002, Grauch and Hudson 2007, Grauch and Connell 2013).

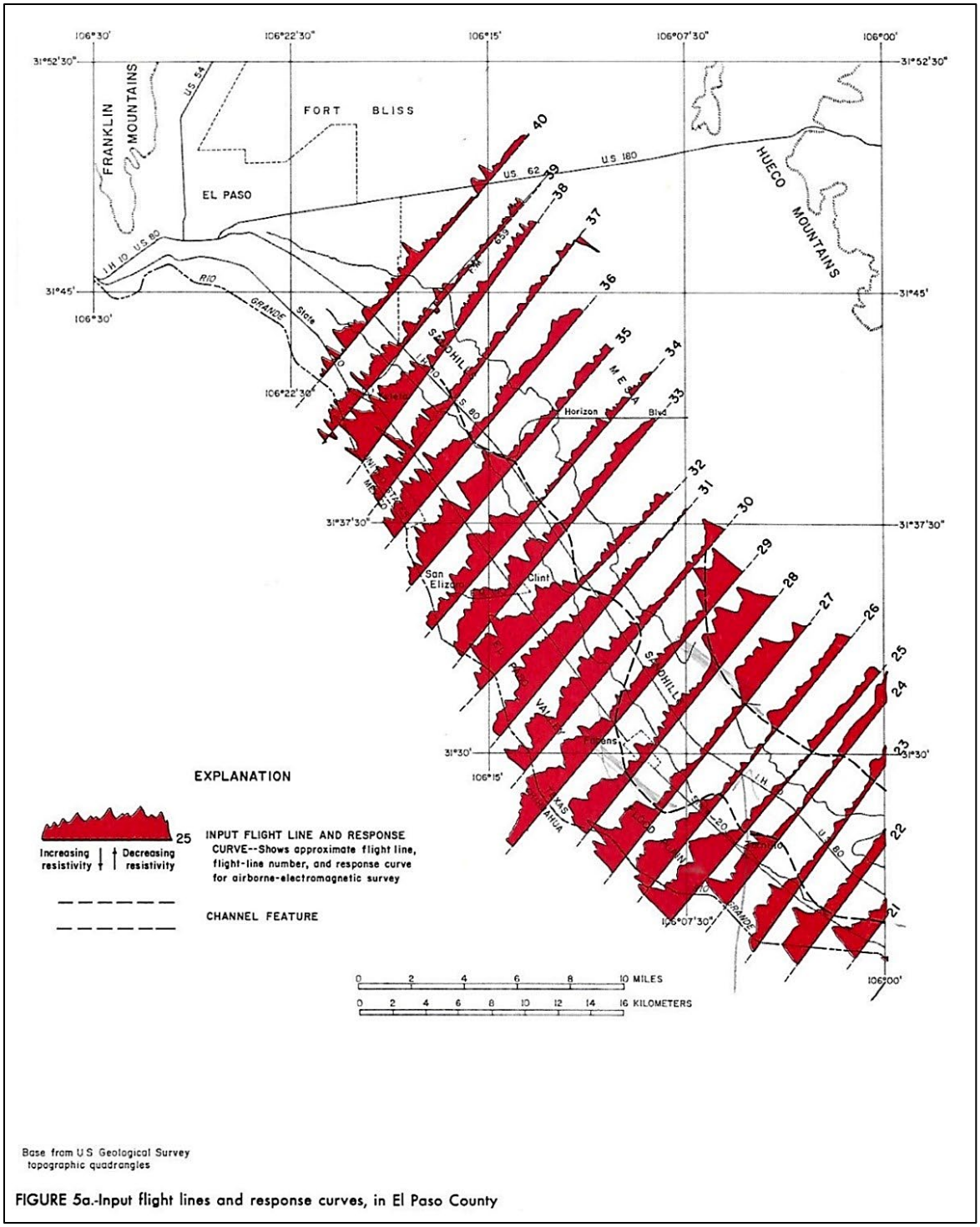

FIGURE 5a.-Input flight lines and response curves, in El Paso County

Figure 3-17 (Gates and Stanley 1976, FIG. 5a, p. 33)**.** Approximate flight line location and response curves for airborne-electromagnetic survey lines in the western Hueco Bolson. INPUT [Induced Pulse Transient] EM-response curve for 17 complete profiles in red, with heavy-dashed line showing approximate borders of high-resistivity Camp Rice distributary-channel "material deposited by the ancestral Rio Grande on its course through Fillmore Pass and to the southern part of the Hueco Bolson (**Figs. 3-15** and **16**; *cf.* Hawley et al. 2009, PL 1)."

3.8. QUATERNARY EVOLUTION OF RIO GRANDE/BRAVO VALLEYS AND CANYONS, AND CONTIGUOUS ENDORHEIC RIFT-BASINS

Continued uplift of the Organ-Franklin-Sierra Juárez mountain chain and subsidence of the Hueco-Tularosa basin complex between 1 and 2.6 Ma, resulted in a relatively short-lived shift of ARG fluvial-deltaic distributaries into parts of the southern Mesilla and Central Parabién GW Basins (MeB and EPB). The latter include three lowland areas: (1) El Paso del Norte, (2) the Méndez-Vergel Corridor between the Sierras Juárez and Sapello, and (3) the broad fluvial-deltaic plain west of Sierra Sapelló that terminates in the basins of the ZHGCM-El Barreal area (*cf.* **Figs. 1-2**, **1-3**, **1-9**, **3-3**, **3-6**, **3-13** and **3-14**).

Details are still needed on the complex tectonic and fluvial-geomorphic processes involved in integration of a Rio Grande/Bravo system that connected glaciated parts of the Southern Rocky Mountain province with the Gulf of Mexico. Nonetheless, the river has occupied its present valley and canyon positions for at least the past 0.8 Ma. Entrenchment and partial backfilling of the river's valleys and canyons during subsequent full-glacial parts of glacial-interglacial cycles resulted in diachronous cessation of Santa Fe Group deposition throughout the RG-rift province (Dethier 2001; Pazzaglia and Hawley 2004, p. 429; Connell et al. 2005 [Fig. 11c]; Galloway 2005; Mack et al. 2006; Respasch et al. 2017).

The chronology of Mid- to Late- Quaternary river-valley evolution presented in **Figure 3-18** and **Table 3-4** is based primarily on information initially compiled by Hawley (1978, Chart 2). Interpretations were supported by best-available information on the age of stratigraphic units, erosional and depositional features, fossil molluscan faunas, and paleoclimatic fluctuations recognized through to the upper Rio Grande watershed (Kottlowski 1958a; Metcalf 1967; Hawley and Kottlowski 1969; Hawley et al. 1976). The geologic-time frame of this conceptual model remains in close agreement with present-day geochronologic information. The timing of Late Pleistocene pluvials and interpluvials, for example, is in close agreement with the age ranges of glacial and interglacial intervals currently recognized in the northernmost Rio Grande basin in the Southern Rocky Mountain province (**Fig. 1-4** and **Tbl. 1-1**; *cf.* Armour et al. 2002, Pazzaglia 2005).

The fluvial-geomorphic genetic sequence of river-valley/canyon evolution also conforms closely with the 3-stage sequence initially described by Stanley Schumm (1965, p. 790-792): (1) excavation of the axial valley and at least the lower segments of tributary valleys during waxing and full-glacial intervals, (2) deposition during waning glacial and early interglacial times, and (3) relative stability during the remainder of a given interglacial interval. From a regional hydrogeologic-framework perspective, the post-SFG valley/canyon incision also resulted in progressive drainage of aquifers in contiguous endorheic intermontane basins of the MBR (**Figs. 1-2**, **1-3**, **1-13**, and **3-3**; *cf.* Hawley and Kennedy 2004; Hawley et al. 2009; **Parts 3.9** and **7.6.2**).

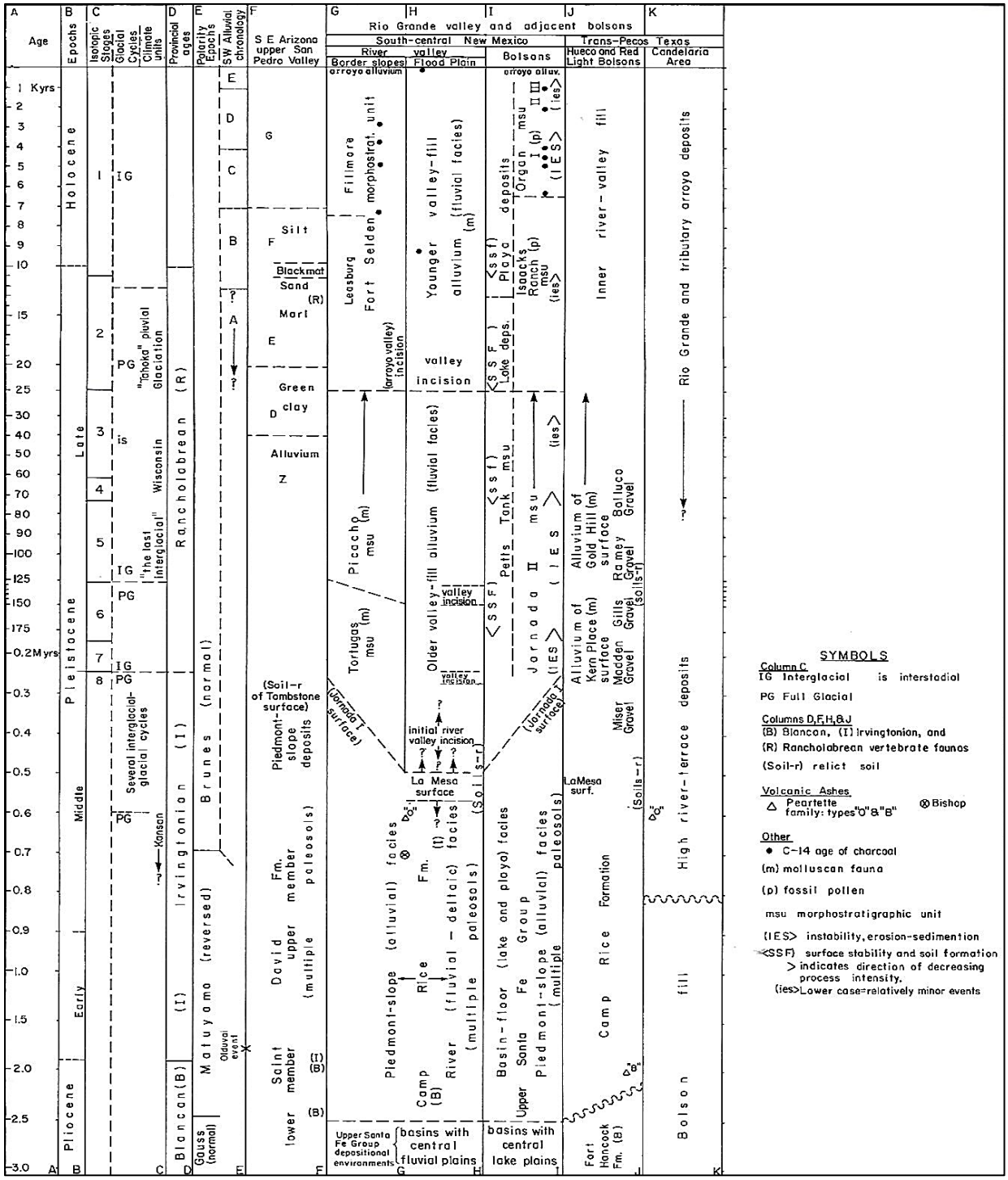

Figure 3-18 (Gile et al. 1981, Fig. 8)**.** Correlation diagram for representative stratigraphic units and geomorphic-process categories of Late Pliocene and Quaternary age in the southern Rio Grande rift region of south-central New Mexico and Trans-Pecos Texas. Adapted from Hawley (1978, Chart 1). A more-detailed explanation for Figure content, including a topical key to Cited References, is in **Table 3-4**. *See* **Figure 3-19** for a schematic cross-section view of basic hydrogeologic-framework relationships in the northern Mesilla Valley area.

Table 3-4. Explanation for Figure 3-18 Content and Key to Cited References

Column C:	Interglacial-glacial cycles—PG-full glacial; IG-interglacial, ig-interstadial
Column D, F, H and K:	North American mammalian provincial ages—Blancan (B, ~5 to 1.8 Ma). Irvingtonian (I, ~1.8 to 0.3 Ma), and Rancholabrean (R, ~0.3 Ma to 11 ka)
Column E:	Southwestern United States Alluvial Chronology of Haynes (l968a)—Depositional Units A to E
Column F:	Upper San Pedro Valley (SE AZ)—Valley-Fill Units D to G, Z of Haynes (1968b)
Columns F to K:	Soils (soil-r)-relict surface soil
Columns G to K:	Tephrochronology and Tephra (sources): "O" Lava Creek, and "B" Huckleberry Ridge (Yellowstone); **x** in circle- Bishop (Long Valley, CA)
Columns J-L:	msu-morphostratigraphic [allostratigraphic] unit; •^{14}C-dated charcoal; mf-molluscan fauna; p-pollen record
Column L:	Dominant surface-geomorphic processes (IES>, (ies> =instability, erosion-sedimentation; <SSF):-stability and soil formation > =decreasing process-intensity direction

Topical List of Cited References

Column B:	Gibbard and others (2010), Walker and others (2012)
Column C:	Berggren and others (1995), Lisiecki and Raymo (2005), Morgan and Lucas 2005), Rosholt and others (1991), Roy and others (2004). Stein and others (2005)
Column D:	Lindsey and others (1984), Vanderhill (1986), Morgan and Lucas (2003, 2005), Tedford 1981, Woodburne and Swisher (1995)
Column E:	Haynes (l968), Mack et al. (1993, 1998), Rosholt and others (1991), Smith (1994)
Column F:	Haynes (l968), Morrison (1991), Smith (1994)
Columns G and H:	Metcalf (1967, 1969), Hawley and Kottlowski (1969), Gile and others (1981, 1995), Seager and others (1984), Seager and others (1997), Connell and others (2005), Mack and others (2006)
Column I:	Gile et al. (1981, 1995), Seager and others (1987), Mack and other (1996, 1997, 1998 and 2006)
Columns J:	Albritton and Smith (1965), Strain (1966), Seager and others (1987), Collins and Raney (1991, 2000), Gustavson (1991a), Hawley and others (2009)
Column K:	Groat (1972), Hawley (1975), Henry and Price (1985)
Columns F to K – Soils:	Gile and others (1981), Machette (1985), Smith and others (1993), Mack and others (1994), Gile and others (1995), Monger and others (2009), Jochems and Morgan (2018)
Columns G to K – Tephrochronology:	Izett and Wilcox (1982), Izett and others (1988), Sarna-Wojcicki and Davis (1991)

Middle- to Late-Quaternary RG-Valley evolution resulted in the formation of the stepped sequence of graded geomorphic surfaces that are located between the present valley floors, and relict basin floors and piedmont slopes of Middle Pleistocene age (*cf.* **Figs. 3-18** and **3-19,** and **Tbl. 3-4**). Correlation of geomorphic surfaces and associated alluvial deposits fills (e.g., Tortugas, Picacho, and Fort Selden morphostratigraphic units [msus]*) is possible over long distances upstream and downstream from the Las Cruces area, thus indicating that paleoclimatic factors played a major role in the regional RG-Valley landscape genesis (e.g., Hawley 1965, Metcalf 1967 and 1969, Gile et al. 1981, Mack et al. 1998, 2006, Connell et al. 2005).

Unconformity-bounded mapping units of Quaternary age rift-basin deposits of the MAR were initially classed as "morphostratigraphic units (msus)" as defined by Frye and Willman (1962; e.g., Hawley and Kottlowski [1969], Hawley et al. [1976], Gile et al. [1981]). However, the North American Stratigraphic Code of the North American Commission on Stratigraphic Nomenclature (NACOSN 2005) now requires that most mappable deposits in the informal "msu" category need to be reclassified as "allostratigraphic Units" (e.g., Alloformations-APNDX. G**).*

The early cycles of valley entrenchment and aggradation have yet to be precisely dated in the Mesilla Basin Region. They are only known to be older than the last major episode of Rio Grande entrenchment that occurred in late Wisconsinan time (apparently during the mid-part of the 29,000- to 11,000-yr-B.P. interval). Older valley-fill deposits include those capped by basalt flows near San Miguel that have K-Ar ages of about 200,000 yrs B.P. (*cf.* Dunbar 2005; **PL. 5g**; **Part 6.3.4**). These fills are definitely younger than the 640,000 ka, Lava Creek B [type-O Pearlette] ash described by Seager and others (1975) in the (post-Camp Rice Formation) Ash Mine Mesa deposit in Selden Canyon (Table 10, columns G-H [*cf.* Hawley et al. 1969, p. 75-76, Izett and Wilcox 1982, Gile et al. 1995, p. 36]).

Work to date, however, suggests that the youngest part of the Tortugas morphostratigraphic unit (msu—Alloformation) was deposited during the first part of the interglacial-glacial cycle preceding the Wisconsinan cycle (**Fig. 3-18**), column C, 245,000-130,000-yr interval). However, the Tortugas msu may include still-older deposits (e.g.,) as early as marine oxygen-isotope stage (OIS 12). From a regional geomorphic-history and GW-flow perspective, it is also important to note that the high stand of Paleo-Lake Alamosa and its subsequent spillout (*circa* 452-427 ka) described below generally correlates with an early phase of deep RG-Valley/Canyon entrenchment that is now recognized in both the Mesilla and Albuquerque Basins (*cf.* Hawley and Kottlowski 1969, Connell 2013). For example, the erosional base (strath surface) of the basal part of the Tortugas msu is within 33 ft (10 m) of the Historic floodplain level in the upper MeV (**Fig. 3-19** and **PLS. 5c** to **5f**).

Most of the Picacho msu (Alloformation) was probably deposited during the last interglacial (OISs 3 to 5) and the waning part of the preceding full glacial ([OIS 6) stages. This depositional interval is tentatively considered to have started between 130,000 and 150,000 yrs ago (**Fig. 3-18**, columns C and H). Well-developed calcic soils with some morphological features formed under conditions significantly

moister than those of the present are preserved in surficial deposits of the Picacho msu. These pedogenic features clearly started forming during a long interval of relative-surface stability prior to late Wisconsinan (OIS 2) valley entrenchment. The Fort Selden (*Alloformation*) and present valley-floor msus are associated with the last major interval of valley incision and partial backfilling (OIS 2/1).

On the basis of ^{14}C dating of charcoal in younger valley-fill deposits, deep entrenchment below a late Picacho base level and initial backfilling took place in late Wisconsinan time prior to 12,000 yrs BP (Hawley and Kottlowski 1969, Metcalf 1969, **Fig. 3-19**). River-valley incision during this interval was of regional extent, occurring from the Albuquerque Basin at least as far south as the southern Hueco Bolson (Hawley 1965, Davie and Spiegel 1967, Hawley and Kottlowski 1969). Fillmore msu (Alloformation) deposits make up the bulk of the younger valley-border alluvium and contain charcoal with ^{14}C ages that range from approximately 7,300 to 2,600 yrs BP.

Ongoing field USGS field investigations in the Rio Grande's Southern Rocky Mountain headwaters region, moreover, now demonstrate that the uppermost Rio Grande basin was not integrated with downstream reaches in north-central and southern New Mexico until after about 430,000 years ago (Machette et al. 2013, Ruleman 2019). The triggering event was overflow of Paleo-Lake Alamosa in the San Luis Basin of south-central Colorado (Machette et al. 2013, p. 1, 2; **Figs. 1-1** and **1-4**):

> . . . . Lake Alamosa persisted for ~3 m.y. [Ma], expanding and contracting and filling the [San Luis] valley with sediment until ca. 430 ka, when it overtopped a low sill and cut a deep gorge through Oligocene volcanic rocks in the San Luis Hills and drained to the south. As the lake drained, nearly 100 km^2 (81 x 10^6 acre-ft or more) of water coursed southward and flowed into the Rio Grande, entering at what is now the mouth of the Red River. The key to this new interpretation is the discovery of ancient shoreline deposits, including spits, barrier bars, and lagoon deposits nestled among bays and in backwater positions on the northern margin of the San Luis Hills, southeast of Alamosa, Colorado.
>
> Alluvial and lacustrine sediment nearly filled the basin prior to the lake's overflow, which occurred ca. 430 ka as estimated from ^3He [helium] surface-exposure ages of 431 ± 6 ka and 439 ± 6 ka on a shoreline basalt boulder, and from strongly developed relict calcic soils on barrier bars and spits at 2330-2340 m (7645-7676 ft), which is the lake's highest shoreline elevation. Overtopping of the lake's hydrologic sill was probably driven by high lake levels at the close of marine oxygen-isotope stage (OIS*) 12 (452-427 ka), one of the most extensive middle Pleistocene glacial episodes on the North American continent. . . .
>
> **Lisiecki and Raymo 2005 [cf. Ruleman et al. 2019].*

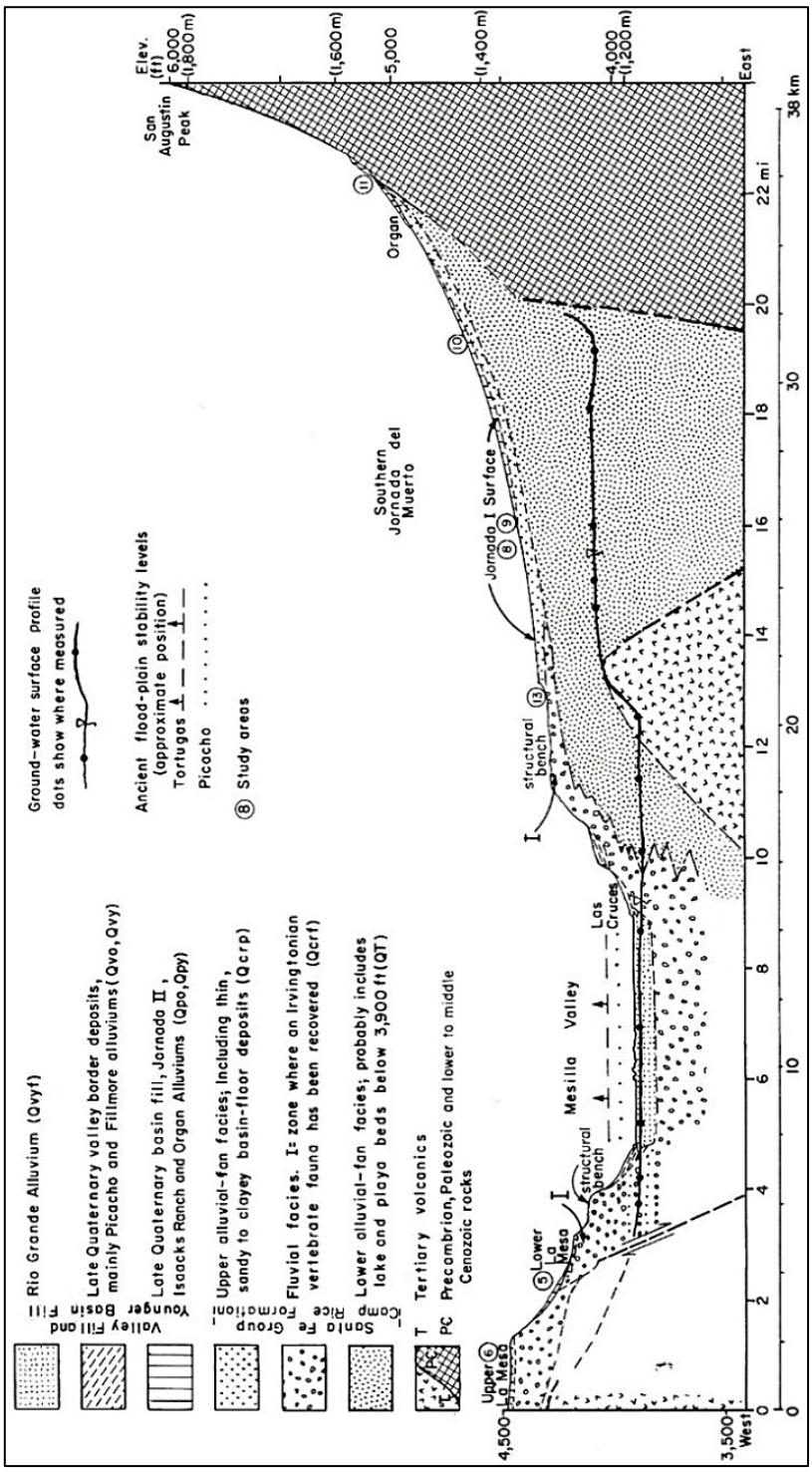

Figure 3-19 (Gile et al. 1981, FIG. 6)**.** Hydrogeologic cross-section of the northern Mesilla and Southern Jornada groundwater Basins, which are separated by the shallowly buried Tortugas Uplift (US-70—Hydrogeologic Section DD' alignment, **PL. 5d**). Approximate former water-table profile (solid line with dots at well-control sites) and mid-Pleistocene valley-floor base-level positions are shown: Tortugas morphostratigraphic [allostratigraphic] unit (msu-dashed, >250 ka), and Picacho msu (dotted, ~120 ka) (**Fig. 3-18** and **Tbl. 3-4**, NACOSN 2005).

3.9. INTRODUCTION TO THE PALEOHYDROLOGY OF AN INTERLINKED PLUVIAL-LAKE PALOMAS—EL PASO DEL NORTE GW-FLOW SYSTEM

Groundwater-flow regimes have been materially affected by episodic valley/canyon incision during at least four Middle- to Late-Pleistocene glacial-pluvial intervals in the southern New Mexico border region's two major through-going river systems, the Gila River and the Rio Grande (e.g., Lee 1907, Schwennesen 1918, Sayre and Livingston 1945, Knowles and Kennedy 1957, Reeder 1957, Trauger and Doty 1965, Trauger 1972, Gile et al. 1981, Bedinger et al. 1989b, Frenzel and Kaehler 1992, Hawley et al. 2000, Dethier 2001, Hawley and Kennedy 2004, Mack 2004, Connell et al. 2005, Hawley et al. 2009 and 2010, Ruleman et al. 2019). Emphasis here is on the parts of the Bolson de los Muertos and Tularosa Basin that were occupied by pluvial-Lakes Palomas and Otero during the middle- to later-part of marine oxygen-isotope stage (OIS) 2, which lasted from about 29 to 11 ka (Lisiecki and Raymo 2005; and Stein et al. 2006, Fig. 2; *cf.* **Parts 3.3**, **3.8**, **7.2.3** and **7.6.2**).

One of this study's more-significant contributions is better documentation of the effects of RG-channel base-level lowering on the regional GW-flow system that has been linked to underflow-discharge from high stands of pluvial Lake Palomas that occurred most recently between 29 to 11 ka B.P. during the late Pleistocene (Wisconsinan) full-glacial stage (**Fig. 3-17** and **Tbl. 3-4**; *cf.* **Parts 3.3**.**3**, **7.2.3**, and **7.6.2**). The basic process was initially described by Kennedy and Hawley (2003, p. 181):

> During major glacial-pluvial intervals of the Late Quaternary, a complexly linked system of intermontane basin lakes and through-going streams dominated the geohydrologic setting the Paso del Norte region of southern New Mexico, Trans-Pecos Texas, and Chihuahua, Mexico. Hydrogeologic setting and fluctuating paleoclimatic conditions were the major controls on size and permanence of lakes and streams in this now arid to semiarid Chihuahuan Desert region of the Basin and Range—Mexican Highland section. Bolson complexes of the region have both *open* and *closed* topographic components, but many *closed* subbasins are *partly drained* hydrologic systems with groundwater inflow and outflow links with adjacent areas [*cf.* **Part 4.1.1**]. The entrenched Rio Grande/Bravo fluvial system formed the regional discharge zone or *sink* for large amounts of surface and subsurface flow during much of the Middle and Late Quaternary.
>
> The Mesilla and El Paso/Juárez Valleys of the Rio Grande/Bravo (1,090-1,175 m [amsl]) bisect the floors of the Los Muertos-Guzman-Santa María and Tularosa-Hueco bolson complexes (1,175-1,210 m), which are the sites of the region's two largest pluvial lakes, Palomas (Chihuahua) and Otero (NM). At highest (Wisconsinan) stages, Lakes Palomas and Otero had areas of at least 7,500 and 2,000 km^2, respectively. . . . Watersheds (~3,000-m max elev.; 63,700 km^2 area) contributing to Lake Palomas include highlands bordering the northern Sierra Madre Occidental (Rios Casas Grandes, Santa Maria and Carmen headwaters) and southeastern ranges of the Datil-Mogollon—Transition Zone province (Mimbres River source). . . . In many places, major shoreline features with good age control are visible on LANDSAT imagery; and advanced GIS technology enables basin-scale paleohydrologic and hydrogeologic reconstructions [*cf.* **Part 7.6**].

Based on more-detailed analyses of GW-flow conditions in the southern Mesilla Basin area Hawley and Kennedy (2004, p. 74-75) made the following observations:

> More work still must be done with respect to transboundary underflow conditions in the broad Mesilla Basin area between the bedrock uplifts formed by Sierra Juárez and Cerro de Muleros (del Cristo Rey), and the East Potrillo Mountains [**Figs. 6-1** and **7**-7 (**PLS. 5k** and **5l**)] (. . . .). Unpublished water-level data from several 1,000-ft [300-m] test wells [drilled by the SRH in 1988] in the Mexican part of the basin [now including the southern MeB and the EPB] indicate that, at least the shallow part of the groundwater-flow system in HSU MSF2 (mostly LFA 3) is northeastward toward the Santa Teresa area (e.g., El Mirador and La Joya [also El Girasol and El Parabién] tests; . . . [**PL. 3**; **TBL. 1**, nos. 359, 362, 364 and 359]).
>
> Current research on the Late Quaternary history of "pluvial Lake Palomas (Reeves 1969)" by Castiglia and Fawcett (2001 [2006]), and Castiglia (2002) [**Part 3.3.2**] demonstrates that the floor of Bolson de los Muertos, and adjacent parts of the Mimbres, Casas Grandes, Santa Maria, and Fresnal basins were periodically inundated by very large and deep lakes as late as early to middle Holocene time (8,400 to 6,500 ^{14}C yrs BP). The watershed contributing to these basin systems is about 12,650 mi^2. Elevations of the deep-lake stages are in the 3,940 to 3,965-ft range, or 160 to 185 ft above the "predevelopment" potentiometric surface (3,780 to 3,770 ft) in the Noria to Santa Teresa area about 30 mi to the northeast (. . . ; Wilson et al. 1981 [Pl. 9]). Furthermore, the floor of the Wisconsinan "Ice Age" bedrock channel of the ancestral Rio Grande at El Paso Narrows was scoured out to a depth of about 85 ft below present floodplain level (channel-base elev. Of ~ 3,635 ft.). Therefore, during these Lake Palomas high stands, the northeastward gradient of (at least) the shallow part of the groundwater-flow system would have been at least 5 ft/mi [0.005], with underflow discharge to the Mesilla Valley shallow aquifer system in the Anapra, Sunland Park, [and] (lower) Santa Teresa area. Since the present potentiometric surface [altitude amsl] in the north-central part of the Bolson de los Muertos is about 3,775 ft (Córdoba et al. 1969, p. 7), there may still be a slight northeast-trending pressure gradient toward the International Boundary area northwest of Cerro del Cristo Rey . . . .

With respect to hydrogeologic-framework controls on groundwater flow and chemistry in the Mesilla Basin region, the primary topic of **CHAPTER 7**, Middle- to Late- Pleistocene river-valley/canyon entrenchment produced an almost complete reversal in the dominant southward-directed GW-flow system of Pliocene and Early Pleistocene time, a process first recognized by W.T. Lee in 1907 (p. 22; *cf.* **Part 3.5**, **APNDX. C1**). The general potentiometric-surface configuration and GW-flow boundary positions shown on **Figures 1-9** and **1-11 (PLS. 4** and **12**) illustrate how saturated parts USF2-ARG distributary-channel networks now function as an enormous system of high-permeability drains that deliver large volumes of GW recharge to the shallow aquifer systems of the inner-MeV in the area between La Union and El Paso del Norte (**Figs. 1-3**, **1-8**, **3-3** and **3-14**; **PLS. 5j**, **5k** and **5o**; ***cf.*** **Parts 6.3.4b-c** and **6.3.5b-d**). In addition, these deposits are very efficient conduits for transport from residual GW reservoirs in the Study Area's Transboundary Aquifer system that were periodically replenished by groundwater discharge from pluvial-Lake Palomas and precursor intermittent to perennial lakes during Middle- to Late-Pleistocene pluvial intervals (*cf.* **Parts 7.2.2** and **7.6.2**).

CHAPTER 4.
BASIC CONCEPTS OF HYDROGEOLOGIC-FRAMEWORK CONTROLS ON GW-FLOW AND CHEMISTRY IN BASIN AND RANGE, AND RIO GRANDE-RIFT PROVINCE AQUIFER SYSTEMS

Basic concepts of hydrogeologic-framework controls on groundwater flow and chemistry in basin-fill aquifer systems are described in two regional-geologic/geomorphic contexts: (1) Basin and Range–physiographic, and (2) Rio Grande rift–tectonic. Conceptual models of framework controls on GW-flow regimes in idealized groups of hydrologically interlinked fault-block basins and mountain uplifts are first described in terms of a generic regional model initially developed by Eakin and others (1976-**Part 4.1.1**), and then in a more specific, basin-scale model developed by Anning and Konieczki (2005-**Part 4.1.2**). See **APPENDIX G** for additional information on relevant terminology.

Basic concepts at a Study Area scale (here 1:100,000), are presented in terms of the primary components of (1) basin- and valley-fill lithofacies assemblages (LFAs), and (2) SFG and valley-fill alluvial hydrostratigraphic units (HSUs) (Part **4.2**). Bedrock-lithostratigraphic and basin-boundary structural components of the basic framework model were introduced in **Part 3.5**, and at a Study Area scale these components comprise basin-border, intra-basin structures, and pre-SFG bedrock units, and tectonic features. Major bedrock components of interbasin structural uplifts are described in **CHAPTER 5**, and the emphasis of **CHAPTER 6** is on the LFA and HSU composition of SFG basin-fill and river valley-fill deposits in the Study Area's GW basins (**PL. 2** and **TBL. 2**; **Fig. 1-8**, and **Tbls. 1-4** and **1-5**).

4.1. CONCEPTUAL MODELS OF HYDROGEOLOGIC CONTROLS ON GW-FLOW IN A BASIN AND RANGE PROVINCIAL SETTING

Many of the principles of basic hydrogeologic-framework controls on aquifer-system composition and GW flow and chemistry were developed in the Great Basin section of the Basin and Range (B&R) province during the three decades following WW II (e.g., Maxey and Jameson 1948, Maxey and Eakin 1949, Maxey and Shamberger 1961, Hawley and Wilson 1965, Cohen et al. 1965, Cohen 1966, Maxey 1968, Mifflin 1968, Winograd and Thordarson 1975, and Eakin et al. 1976; *cf.* Mifflin 1988, Hibbs and Darling 2005). Adaption of these conceptual models for other sections of the B&R province, with emphasis on the B&R-Mexican Highland section, is the primary theme of the following discussion (*cf.* **Parts A1** and **A2** of **APNDX. A**).

4.1.1. Adaptions of the Eakin, Price, and Harrill (1976) Conceptual Model

Figure 4-1 is a schematic block diagram that illustrates basic hydrogeologic-framework and groundwater-flow system interrelationships that occur throughout the B&R province. It was originally designed by Eakin, Price, and Harrill (1976) for USGS-WRD "appraisals" of ground-water resources in the B&R Great Basin section. Martin Mifflin's 1988 (Fig. 8) version of the original diagram was adapted

by Hibbs and others (1997, Fig. 1.6) to include effects on subsurface flow (*drainage*) by valley and canyon incision of large through-going streams like the Rio Grande, and Colorado and Gila Rivers. This adaption has facilitated use of the original Great Basin conceptual model in the region-scale characterization of GW-flow in intermontane basins throughout the B&R-Mexican Highland section and RG-rift tectonic province (e.g., Hawley et al. 2000, 2001, Kennedy et al. 2000, *cf.* Hibbs and Darling 2005). Basin-scale RG-Rift tectonic features (1:100,000 herein), such as interbasin and intrabasin boundary faults and flexures, also play a significant localized role in groundwater-flow dynamics (**CHAPTERS 5** to **7**).

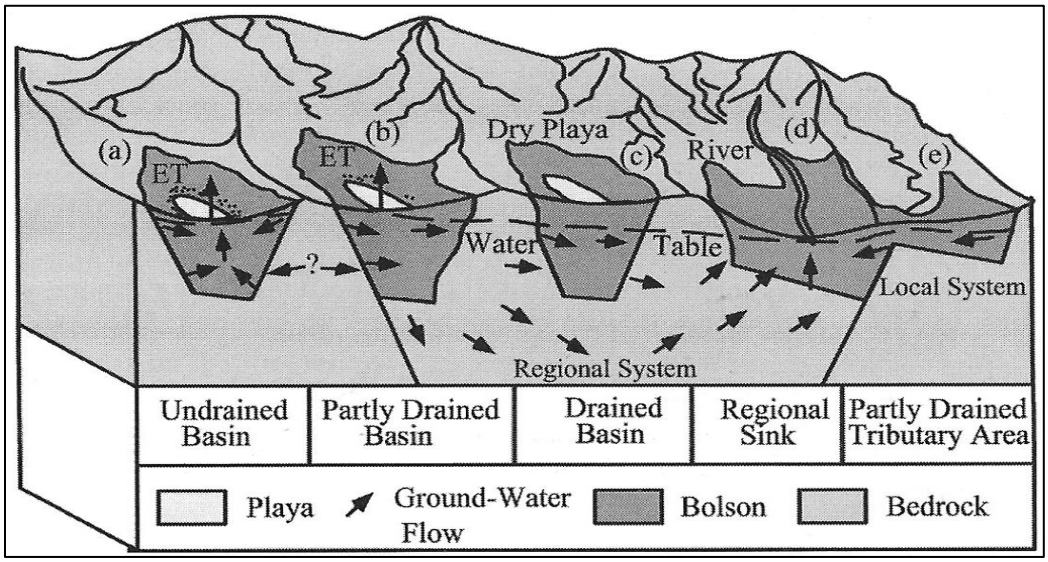

Figure 4-1 (Kennedy et al. 2000, Fig. 1; reproduced with NM Geological Society, Inc. permission)**.** Generic block diagram that illustrates basic hydrogeologic framework and groundwater-flow system interrelationships in a group of topographically *closed* and *open* (*endorheic* and *exorheic*) B&R province basins, most of which have a regional GW-flow component. There are five basin categories: **(a)** *undrained basins* with phreatic playas, **(b)** *partly drained basins* with phreatic playas, **(c)** *drained basins*, **(d)** *regional sinks*, and I complex-topographic *partly drained tributary [basin]* areas. Modified from diagram illustrating idealized GW-flow relationships in (1) the Great Basin section, and (2) the Mexican Highland section.

As illustrated in **Figure 4-1**, the terms *closed* and *open* (*endorheic* and *exorheic*) are used in this study primarily in a topographic/hydrographic context and in reference to the surface flow into, through and from intermontane basins (*cf.* **Tbl. 1-3**), whereas the terms *undrained*, *partly drained*, and *drained* refer to basin types with groundwater-flow regimes that involve intrabasin and/or interbasin movement. *Phreatic* and *vadose*, respectively, indicate saturated and unsaturated-partly saturated subsurface conditions. *Phreatic playas* (with bordering springs and seeps) are restricted to floors of *closed* basins (*bolsons [Span: bolsónes]*) that are *undrained* or *partly drained,* while *vadose playas* occur in both *closed* and *open*, *drained* basins (*cf.* Meinzer 1923, Bryan 1937, Tolman 1937).

Cienegas are wetlands located in places where the zone of saturation intersects an undissected valley- or basin-floor surface. Few intermontane basins in the eastern Basin and Range province are *undrained* in terms of groundwater discharge, whether or not they are topographically *closed* or *open* (*cf.* **APNDX. C**, **Part C1a:** *bolsons* and *semibolsons* [Tolman 1909, 1937], and **Part C2c**: **Fig. C-3** [from Bryan 1938]). In the Mesilla Basin and adjacent parts of the southern Rio Grande rift, the (intermediate) *partly drained* basin category, which is also "incompletely" *open*, is the predominant geohydrologic system (**Figs. 1-2**, **1-4**, **1-9,** and **3-3**). Only Bolsón de Los Muertos and the north-central Tularosa Basin are presently *closed, undrained basins* (**Figs. 1-2** and **3-3**). Both, however, were *partly drained* systems during latest Pleistocene and Early Holocene pluvial intervals (**Parts 3.1.2** and **3.7**).

Most recharge to basin-fill aquifers occurs by two mechanisms in the B&R province: mountain front/block where some precipitation falling on bedrock highlands contributes to the groundwater reservoir along basin margins, and tributary, where the reservoir is replenished along losing reaches of larger intra-basin streams (Kernodle 1992b; Wasiolek 1995; Waltemeyer 2001; Naus 2002; Scanlon 2004; Wilson and Guane 2004; Markovich et al. 2019, 2022). Because of the limited extent and low altitude of mountain highlands in the NM WRRI Study area, mountain-front/block-recharge processes are not major contributors to basin-fill aquifer replenishment (Frenzel and Kaehler 1992; Nickerson and Myers 1993; Hawley and Kennedy 2004; Teeple 2017; *cf.* **CHAPT. 5**). Tributary recharge is the dominant recharge process in the parts of the MBR that includes the valleys of the Rio Grande/Bravo fluvial system (Nickerson 1998; Teeple 2017; Hanson et al. 2018). Under predevelopment conditions, groundwater discharge in the region occurred mainly through (1) contributions to gaining reaches of the Rio Grande/Bravo system, (2) inter-basin subsurface flow, (3) flow from seeps and springs, (4) evapotranspiration from basin- and valley-floor wetlands (e.g., *phreatic playas* and *cienegas*), and (5) evaporation from open-water bodies, such as lakes, reservoirs, and rivers.

Mountain blocks dominated by dissolution-prone carbonate and gypsiferous sedimentary units, however, do form local sources for brackish/saline and/or geothermal aquifer systems, and deserve further detailed study (Witcher et al. 2004, Kubicki et al. 2021). Unlike many Basin and Range areas of eastern Nevada and Trans-Pecos Texas, however, there are no extensive bodies of transmissive carbonate rocks that can provide effective conduits for large regional GW-flow systems (e.g., Mifflin 1968, Maxey 1968, Winograd and Thordarson 1975, Mifflin and Hess 1979, Harrill and Prudic 1988, Sharp 2001; *cf.* **Part 5.4.1**). Groundwater production from most consolidated rocks of the region is limited to low-yield fracture zones, which occur in a wide variety of bedrock types including clastic-sedimentary, igneous intrusive and extrusive, and metamorphic rocks. The only exception are basaltic rocks and silicic tuffs that immediately underlie or are locally interlayered with SFG basin fill.

Short- and long-term climatic changes obviously have had substantial impacts on the water-resource availability in this arid to semi-arid region (Allen 2005; Gutzler 2005 and 2020; Creel 2010; Phillips et al. 2011; Meixner et al. 2016; Overpeck and Udall 2020; Paskus 2020; Davis 2021c; **APNDX. E4**). Very large quantities (millions of ac-ft, thousands of hectare-m) of fresh to slightly saline water are stored in the basin-fill aquifer system, and ongoing geohydrologic research demonstrated that most groundwater in storage is at least 12,000 years old, and was recharged during Late Pleistocene glacial/pluvial stages (e.g., Plummer et al. 2004, Sanford et al. 2004, Scanlon 2004, Darling et al. 2017, Teeple 2017, Garcia-Vásquez et al. 2022; *cf.* Zalasiewicz et al. 2021, **Parts 7.3**, **7.4** and **8.2**). As noted in **Parts 3.1.3** to **3.1.5**, climatic conditions during the cooler and wetter, glacial-pluvial intervals of Middle and Late Pleistocene were substantially different than those in the Holocene. From a groundwater-recharge perspective the floors of the larger closed depressions of the MeB West Mesa surface would have been sites of relatively long-lived ephemeral lakes that locally contributed significant amounts of seepage recharge to the regional aquifer system even through thick vadose zones (*cf.* **Part 7.5.3**).

4.1.2. Anning and Konieczki (2005) Hydrogeologic Area and Flow System Classification

Figure 4-2 illustrates a second method of "Classification of Hydrogeologic Areas and Hydrogeologic Flow Systems in the Basin and Range" province that was developed by Anning and Konieczki (2005, p. 1-2, Fig. 2). The Anning and Konieczki (A-K) method, as summarized below, provides an innovative conceptual framework for more-detailed basin-scale GW flow-system characterization than the more-generalized model illustrated in **Figure 4-1** (*cf.* **Parts 7.5** to **7.7**).

> …. A conceptual model for the spatial hierarchy of the hydrogeology was developed for the Basin and Range Physiographic Province and consists, in order of increasing spatial scale, of hydrogeologic components, hydrogeologic areas, hydrogeologic flow systems, and hydrogeologic regions. . . .
>
> Hydrogeologic areas are conceptualized as a control volume consisting of three hydrogeologic components: the soils and streams, basin fill, and consolidated rocks [**Fig. 4-2**]. The soils and streams hydrogeologic component consists of all surface-water bodies and soils extending to the bottom of the plant root zone. The basin-fill hydrogeologic component consists of unconsolidated and semiconsolidated sediment deposited in the structural basin. The consolidated-rocks hydrogeologic component consists of the crystalline and sedimentary rocks that form the mountain blocks and basement rock of the structural basin.
>
> Hydrogeologic flow systems consist of either a single isolated hydrogeologic area or a series of multiple hydrogeologic areas that are hydraulically connected through interbasin flows. A total of 54 hydrogeologic flow systems were identified and classified into 9 groups. One group consisted of single isolated hydrogeologic areas. The remaining eight groups consisted of multiple hydrogeologic areas and were distinguished on the basis of (1) whether all water is removed from the system through evapotranspiration (terminally closed) or whether some water is removed as outflow into another downgradient system (terminally open), and (2) the predominant hydrogeologic component(s) that hydraulically connected the hydrogeologic areas.

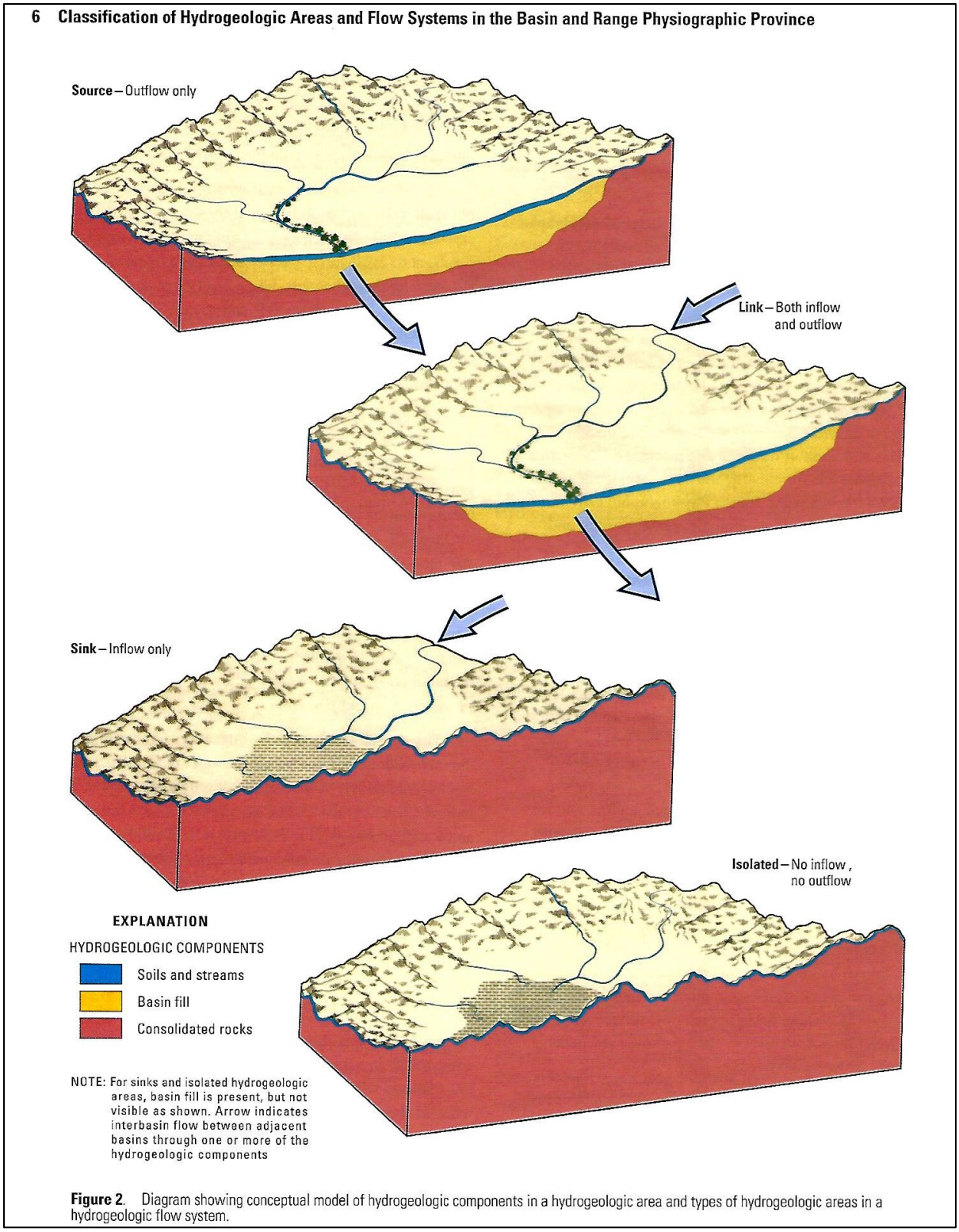

Figure 4-2 (Anning and Konieczki 2005, Fig. 2)**.** Block diagrams that schematically illustrate a "conceptual model of hydrogeologic components of a hydrogeologic area and types of hydrogeologic areas in a hydrogeologic flow system" in the B&R province.

Because Anning and Konieczki (2005) do not cover the Trans-Pecos Texas and northern Chihuahua parts of the MBR, their (A-K) classification method has not been used in this study. While not specifically identified, however, the primary GW-basins the Study Area would be best placed in the following A-K *Hydrogeologic-Area* classes:

Mesilla GW Basin (MeB)—*Group L3, Linked-Type Hydrogeologic Area [Pl. 2 and Tbl. 2, n009]*: *Hydrogeologic Area*s in this group have inflows and outflows occurring through both *soils and streams* and *basin fill*. *The predominant surface-drainage feature is a perennial stream [here the RG], which is hydraulically connected to the regional aquifer.*

Southern Jornada GW Basin (SJB)—*Group L3* [TLVB] and *Group SR2* [ILSB and ERSB] *Isolated Hydrogeologic Area classes [Pl. 2 and Tbl. 2, n006]*: *Hydrogeologic Area*s [in *Group SR2*] *lack [perennial/intermittent-stream] inflows and have outflow occurring only through the basin-fill hydrogeologic component. The predominant surface-drainage feature is a playa [or scattered small playas] that is [are] intermittently or indirectly hydraulically connected with groundwater in the regional aquifer*. Other examples of *Group SR2* GW basins in and adjacent to the Study Area include the southern Tularosa Basin (SWHB), northwestern part of the Hueco Bolson (WHB), and the Malpais Basins (MpB).

El Parabién GW Basin (EPB)—*Isolated Hydrogeologic Area*, and in a transitional *Group SR2-SR 3* class, which is located in Mexico south of the Anning and Konieczki (2005) study area. *Group SR3 Hydrogeologic Area*s *lack [perennial/intermittent-stream] inflows and have outflow occurring only through the basin-fill hydrogeologic component. The predominant surface-drainage feature is a playa [or series of small playas] that is [are] hydraulically disconnected from groundwater in the regional aquifer*. The predevelopment component of the latter drained to the shallow aquifer system at the lower end of the Mesilla Valley via the upper SFG aquifer in the southern MeB (**Part 6.3.5b-d**).

Although also located outside the Study Area, the floor of Bolsón de los Muertos (**Figs. 1-10** and **3-3**) belongs to *Group SK2*, which consists *predominantly of Sink-Type Hydrogeologic Areas* (**Fig. 4-2**), in which *inflow* occurs *through both soils and streams and basin fill hydrogeologic components, but have no outflow. The predominant surface-drainage feature is typically a playa, which is . . . hydraulically disconnected to the regional aquifer*. *In some cases, the predominant surface-drainage feature is a perennial freshwater or saline lake, which is directly connected to the regional aquifer (*Anning and Konieczki 2005, Pl. 2 *Explanation*).

4.2. LITHOFACIES AND HYDROSTRATIGRAPHIC COMPONENTS OF THE BASIN-SCALE HYDROGEOLOGIC FRAMEWORK

The basin-scale hydrogeologic framework has three primary mapping-unit components:

1. Sedimentary Lithofacies-Assemblages (LFAs) in SFG basin-fill and RG Valley-fill deposits (**Fig. 4-3**, and **Tbls. 4-1** to **4-3**).
2. Hydrostratigraphic Units (HSUs) comprising an LFA or LFA-combinations that are designed for both surface and subsurface mapping of basin- and valley-fill deposits (**Fig. 3-5**).
3. Bedrock-lithologic, and structural boundary components of GW-basins and interbasin uplifts (**Figs. 1-8**, and **3-9** to **3-12**).

LFAs and HSUs are described in the following sections **(Parts 4.2.1** and **4.2.2**). Basin-scale bedrock- and structural-boundary components of the framework (both intra-basin and basin border) were introduced in **Part 3.4** and are described in more detail in **CHAPTER 5** *(cf.* Hawley and Lozinsky 1992, Hawley and Kernodle 2000, Hawley et al. 2000 and 2001, Hawley and Kennedy 2004, and Hawley et al. 2009).

Lithofacies-assemblage and hydrostratigraphic-unit (LFA and HSU) classification systems of the type used in this Study are designed as a relatively simple, qualitative to semi-quantitative means for interpretation of how basin-scale geohydrologic systems are influenced by (1) basin-fill lithofacies distribution in sequences of hydrostratigraphic mapping units, and (2) bedrock- and structural boundary conditions (**PLS. 1**, **2**, **5** and **7**). They facilitate systematic organization of large amounts of information with wide variation in quality and scale (e.g., from general drillers observations to detailed bore-hole logs and water-quality data). GIS science and technology now allows graphical and numerical display of hydrogeologic-framework elements in 3-D formats so that basic information and inferences on geohydrologic attributes (e.g., hydraulic conductivity, transmissivity, anisotropy, and facies-distribution patterns) may be transferred to basin-scale numerical models of GW-flow and hydrochemical systems (*cf.* Siegel 2008, Yeh et al. 2015 [Part 4], Siegel and Hinchey 2019; **APNDX. A1.3**). The LFA/HSU classification scheme has been used to date in the Albuquerque, Mesilla, Hueco, and several other "alluvial basins" of the southwestern New Mexico border region (Hawley and Haase 1992; Hawley and Lozinsky 1992; Thorne et al. 1993; McCord and Stephens 1999; Hawley and Kernodle 2000; Hawley et al. 2000 and 2001; McAda and Barrow 2002; Hawley and Kennedy 2004; Witcher et al. 2004; Plummer et al. 2004; Nickerson 2006; Hawley et al. 2009; Sweetkind 2017).

4.2.1. Lithofacies Assemblages (LFAs)

In 1981, Dr. Lynn Gelhar, then head of NM Tech Geoscience Department-Hydrology Group, asked the PI to design a simplified ten-component classification of basin-fill lithofacies-assemblages

(LFAs) that could be used in a new generation of 3-D groundwater-flow models that he and his research associates were developing (e.g., Gelhar 1993, Gelhar et al. 1979, 1983, 1992; *cf.* Molz 2015). A provisional ten-component classification of LFAs was first applied by Peterson and others (1984) in the NM WRRI TCR 178 on "Quasi three-dimensional modeling of groundwater flow in the Mesilla Bolson." (*cf.* Hawley 1984, Frenzel and Kaehler 1992 [Fig. 11]; **Part 7.5.1** and **APPENDIX A1.3**).

LFAs, as defined herein, form the hydrogeologic framework's basic building blocks, and they are the primary components of SFG hydrostratigraphic units (HSUs-Part **4.2.2**). LFA classes are defined primarily on the basis of grain-size distribution, mineralogy, sedimentary structures, and degree of post-depositional alteration. Inferred environments of deposition form the secondary basis for facies-assemblage definitions (**Tbl. 4-1**). Throughout the study region, basin and river-valley fills are subdivided into thirteen major assemblages (LFAs 1-10, a-c), which are ranked in decreasing order of aquifer-production potential (**Figs. 4-3** and **4-4**, **Tbls. 4-2** and **4-3**). LFAs represent four major depositional environments (**Tbl. 4-1**): basin floors (1-3, 9, 10, c), piedmont slopes (5-8), river-valley floors (a1-a3), and river-valley borders (b). LFA 4 primarily comprises deeply buried sand-dune fields on the leeward (eastern) sides of basins and large-stream valleys, and other partly cemented sand-dominated sediments (**APNDX. F**: **Pls. F6-1a** to **1f**, and **F6-2a** to **2f**).

Figure 4-3 schematically illustrates the general distribution pattern of the major LFAs that Mesilla Basin region. **Figure 4-4** is qualitative **t**riangular diagram of dominant textural classes in LFAs 1 to 10, and it also shows the primary LFA composition of the major SFG Hydrostratigraphic Units (HSU—) - USF/MSF/LSF (*cf.* Fig, 4-3). LFAs have distinctive geophysical, geochemical and hydrologic attributes, and they provide a mechanism for showing the distribution patterns of a wide range of aquifer- and vadose-zone conditions on hydrogeologic cross-sections and isopleth maps (**PLS. 5** and **7**).

The 19 hydrogeologic cross-sections in the **PLATE 5** electronic folder (**Fig. 1-3**; **PL. 5a** to **5s**) illustrate the predominance of permeable, medium- to coarse-grained ancestral-river (ARG), and eolian-sand lithofacies assemblages (LFAs 1 to 4*)* in the Study Area's most-productive aquifers. In marked contrast, fine-grained alluvial or lacustrine sediments (LFAs 9 and 10), which were deposited in basin-floor sedimentary environments, form the primary aquitards and aquicludes in the GW-flow system. Upper SFG-ARG deposits (LFAs 1 to 3) are also distinguished by the presence of exotic clasts (pebble-gravel to coarse-sand size) derived from upper river-basin source areas. Exotic clasts are commonly characterized by subrounded resistant rock and mineral varieties, and include pumice and obsidian derived from the Mt. Taylor and Jemez Mountains volcanic centers (e.g., Baldridge 2004, Goff and Gardner 2004). Relatively soft sedimentary rock types (e.g., limestone, sandstone and mudstone clasts), on the other hand, are rare in river-channel facies of any age.

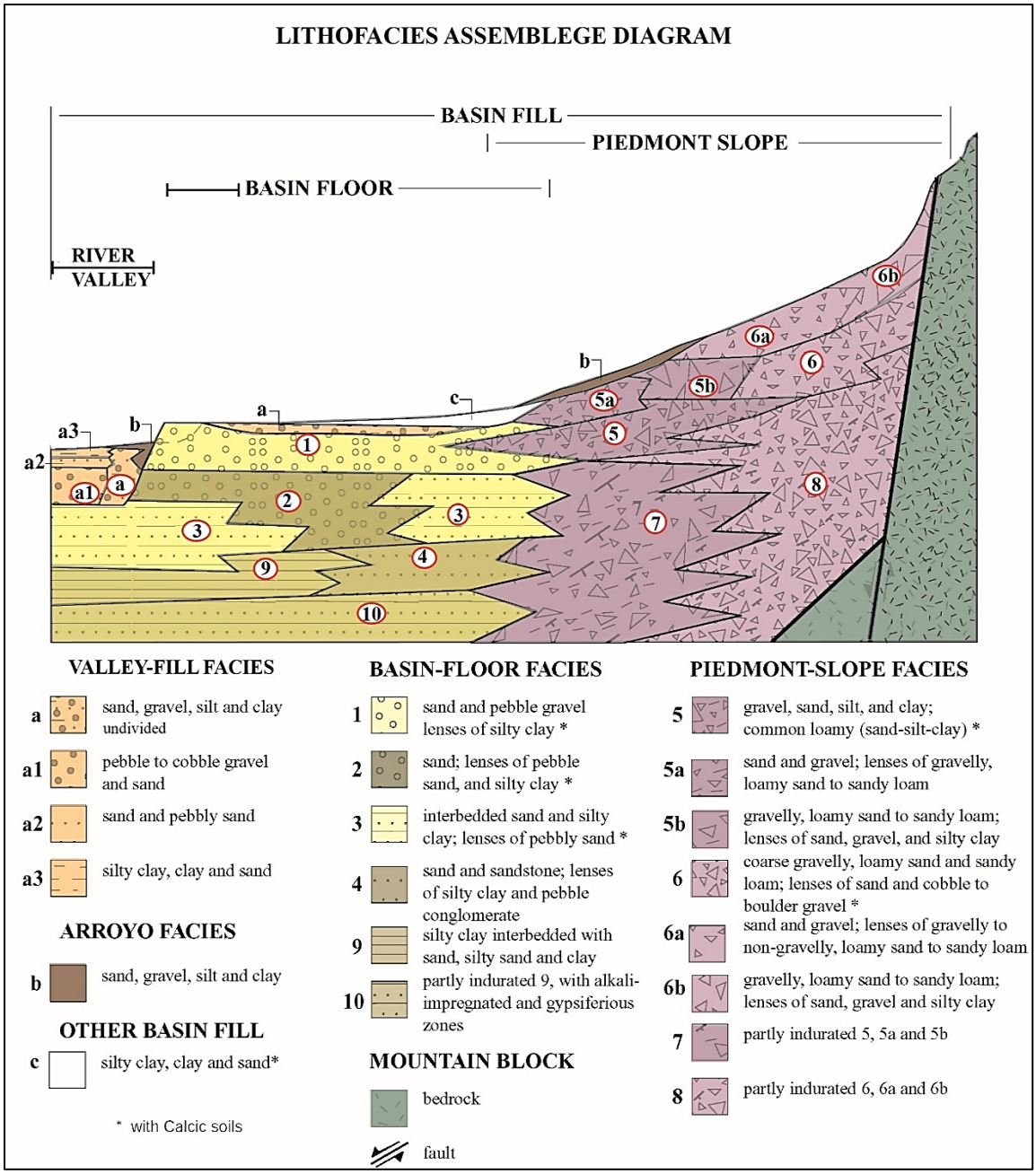

Figure 4-3 (modified from Hawley and Kernodle 2000, Fig. 5)**.** Schematic distribution patterns of major lithofacies assemblages (LFAs) in intermontane-basin and river-valley fills of the RG-rift province (*see* **Fig. 4-4** and **Tbls. 4-1** to **4-3.** Diagram designed and compiled in collaboration with Swanson Geoscience, LLC.

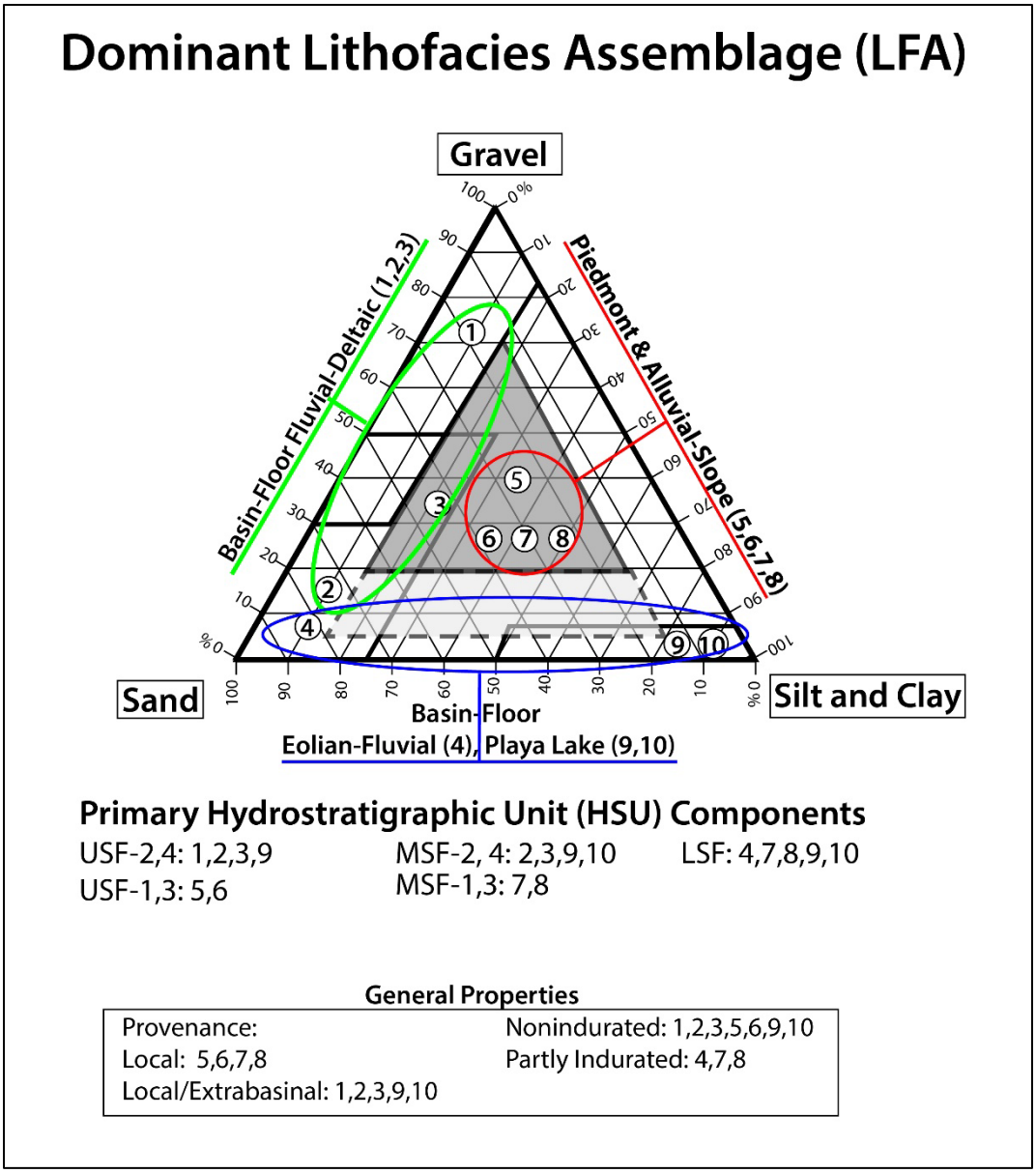

Figure 4-4. Triangular diagram of dominant textural classes in lithofacies assemblages (LFAs) 1 to 10, and primary LFA composition of SFG Hydrostratigraphic Units (HSU)–USF/MSF/LSF (*see* **Fig. 4-3** and **Tbls. 4-1** to **4-3**). Diagram designed and compiled in collaboration with Swanson Geoscience, LLC.

Table 4-1. Summary of Depositional Setting and Dominant Textures of Major Lithofacies Assemblages (LFAs) in Santa Fe Group Basin Fill (1-10) and Rio Grande Valley fill (a-c) in Intermontane Basins of the Rio Grande Rift Tectonic Province. Modified from Hawley and Kernodle (2000). *See* Figures 4-3a and 3b, and Tables 4-2 and 4-3.

Lithofacies	Dominant depositional settings and process	Dominant textural classes
1	Basin-floor fluvial plain	Sand and pebble gravel, lenses of silty clay
2	Basin-floor fluvial, locally eolian	Sand; lenses of pebbly sand and silty clay
3	Basin-floor, fluvial-overbank, fluvial-deltaic and playa-lake; eolian	Interbedded sand and silty clay; lenses of pebbly sand
4	Eolian, basin-floor alluvial	Sand and sandstone; lenses of silty sand to clay
5	Distal to medial piedmont-slope; alluvial fan	Gravel, sand, silt, and clay; common loamy (sand-silt-clay)
5a	Distal to medial piedmont-slope, alluvial fan; associated with large watersheds; alluvial-fan distributary-channel primary; sheet-flood and debris-flow secondary	Sand and gravel; lenses of gravelly, loamy sand to sandy loam
5b	Distal to medial piedmont-slope, alluvial fan; associated with small steep watersheds, debris-flow sheet-flood, and distributary-channel	Gravelly, loamy sand to sandy loam; lenses of sand, gravel, and silty clay
6	Proximal to medial piedmont-slope, alluvial-fan	Coarse gravelly, loamy sand and sandy loam; lenses of sand and cobble to boulder gravel
6a	Like 5a	Sand and gravel; lenses of gravelly to non-gravelly, loamy sand to sandy loam
6b	Like 5b	Gravelly, loamy sand to sandy loam; lenses of sand, gravel, and silty clay
7	Like 5	Partly indurated 5
8	Like 6	Partly indurated 6
9	Basin-floor-alluvial flat, playa, lake, and fluvial-lacustrine; distal-piedmont alluvial	Silty clay interbedded with sand, silty sand, and clay
10	Like 9, with evaporite processes (paleophreatic)	Partly indurated 9, with gypsiferous and alkali-impregnated zones
a	River-valley, fluvial	Sand, gravel, silt, and clay
a1	Basal channel	Pebble to cobble gravel and sand (like 1)
a2	Braided plain, channel	Sand and pebbly sand (like 2)
a3	Overbank, meander-belt oxbow	Silty clay, clay, and sand (like 3)
b	Arroyo channel and valley-border alluvial-fan	Sand, gravel, silt, and clay (like 5)
c	Basin floor, alluvial flat, cienega, playa, and fluvial-fan to lacustrine plain	Silty clay, clay, and sand (like 3,5, and 9)

Table 4-2. Summary of Major Sedimentary Properties that Influence Groundwater-Flow and Aquifer-Production Potential of Lithofacies Assemblages (LFAs) 1 to 10 in Santa Fe Group Basin Fill. Modified from Haase and Lozinsky (1992). *See* Figure 4-3, and Table 4-1.

Lithofacies	Ratio of sand plus gravel to silt plus clay[1]	Bedding thickness (meters)	Bedding configuration[2]	Bedding continuity (meters)[3]	Bedding connectivity[4]	Hydraulic conductivity (K)[5]	Groundwater production potential
1	High	>1.5	Elongate to planar	>300	High	High	High
2	High to moderate	>1.5	Elongate to planar	>300	High to moderate	High to moderate	High to moderate
3	Moderate	>1.5	Planar	150 to 300	Moderate to high	Moderate	Moderate
4	Moderate to low*	>1.5	Planar to elongate	30 to 150	Moderate to high	Moderate	Moderate
5	Moderate to high	0.3 to 1.5	Elongate to lobate	30 to 150	Moderate	Moderate to low	Moderate to low
5a	High to moderate	0.3 to 1.5	Elongate to lobate	30 to 150	Moderate	Moderate	Moderate
5b	Moderate	0.3 to 1.5	Lobate	30 to 150	Moderate to low	Moderate to low	Moderate to low
6	Moderate to low	0.3 to 1.5	Lobate to elongate	130 to 150	Moderate to low	Moderate to low	Low to moderate
6a	Moderate	0.3 to 1.5	Lobate to elongate	30 to 150	Moderate	Moderate to low	Moderate to low
6b	Moderate to low	0.3 to 1.5	Lobate	<30	Low to moderate	Low to moderate	Low
7	Moderate*	0.3 to 1.5	Elongate to lobate	30 to 150	Moderate	Low	Low
8	Moderate to low*	>1.5	Lobate	<30	Low to moderate	Low	Low
9	Low	>5	Planar	>150	Low	Very low	Very low
10	Low*	>5	Planar	>150	Low	Very low	Very low

[1]High >2; moderate 0.5-2; low <0.5

[2]Elongate (length to width ratios >5); planar (length to width ratios 1-5); lobate (asymmetrical or incomplete planar beds).

[3]Measure of the lateral extent of an individual bed of given thickness and configuration.

[4]Estimate of the ease with which groundwater can flow between individual beds within a particular lithofacies. Generally, high sand + gravel/silt + clay ratios, thick beds, and high bedding continuity favor high bedding connectivity. All other parameters being held equal, the greater the bedding connectivity, the greater the groundwater production potential of a sedimentary unit.

[5]High 10 to 30 m/day; moderate, 1 to 10 m/day; low, <1 m/day; very low, <0.1 m/day.

*Significant amounts of cementation of medium to coarse-grained beds (as much as 50%)

Table 4-3. Summary of Major Sedimentary Properties that Influence Groundwater-Flow and Aquifer-Production Potential of Lithofacies Assemblages (LFAs) a to c in Post-SFG Deposits. Modified from Hawley and Kernodle (2000). *See* Figure 4-3, and Table 4-1.

Lithofacies	Ratio of sand plus gravel to silt plus clay[1]	Bedding thickness (meters)[3]	Bedding configuration[2]	Bedding continuity (meters)[3]	Bedding connectivity[4]	Horizontal hydraulic conductivity (K)[5]	Groundwater production potential
a	High to moderate	>1.5	Elongate to planar	>300	High to moderate	High to moderate	High to moderate
a1	High	>1.5	Elongate to planar	>300	High	High	High
a2	High to moderate	>1.5	Planar to elongate	150 to 300	Moderate to high	Moderate	Moderate
a3	Moderate to low	>1.5	Planar to elongate	30 to 150	Moderate to high	Moderate to low	Moderate to low
b	Moderate to low	0.3 to 1.5	Elongate to lobate	<300	Moderate	Moderate to low	Moderate to low
c	Low to moderate	0.3 to 1.5	Elongate to lobate	30 to 150	Low	Low	Low

[1]High >2;moderate 0.5-2; low <0.5

[2]Elongate (length to width ratios >5); planar (length to width ratios 1-5); lobate (lenticular or discontinuous planar beds).

[3]Measure of the lateral extent of an individual bed of given thickness and configuration.

[4]Estimate of the ease with which groundwater can flow between individual beds within a particular lithofacies. Generally, high sand + gravel/silt + clay ratios, thick beds, and high bedding continuity favor high bedding connectivity. All other parameters being held equal, the greater the bedding connectivity, the greater the groundwater production potential of a sedimentary unit.

[5] High, 10 to 30 m/day; moderate, 1 to 10 m/day; low, <1 m/day; very low, <0.1 m/day.

4.2.2. Hydrostratigraphic Units (HSUs)

George Burke Maxey* (1964, p. 126) originally defined a hydrostratigraphic unit (HSU) as "a body of rock having considerable lateral extent and composing a geologic framework for a reasonably distinct hydrologic system." As initially applied in the Study Area: "A hydrostratigraphic unit may represent an entire [litho-] stratigraphic unit, a portion of a stratigraphic unit, or a combination of adjacent stratigraphic units with consistent hydraulic properties" (Giles and Pearson 1998, p. 322). In this report, HSUs are used as the chief mechanism for hydrogeologic mapping of RG-rift basin-fill deposits on the basis on distinctive LFA composition and well-defined lithostratigraphic-sequence positions (**Fig. 3-5**; *cf.* Hawley and Kernodle 2000, Hawley and Kennedy 2004; **APNDX. A2.1.1**).

**Dr. George Burke Maxey was the PI's research advisor at the University of Illinois from 1957 to 1962 (cf. Hawley et al. 1961, Hawley 1962, Hawley and Wilson 1965). He established Nevada's Desert Research Institute's Hydrology Program in 1961 (e.g., Maxey and Shamberger 1961), and was the recipient of the 1971 Geological Society of America O.E. Meinzer Award for his paper "Hydrogeology of Desert Basins (Maxey 1968, Hackett 1972)."*

The first step in organizing hydrogeologic information about basin-fill stratigraphy and sedimentology involved development of a provisional hydrostratigraphic classification system that is applicable throughout the eastern B&R and RG-rift provinces (**Figs. 1-4** and **3-5**). Even-numbered alphanumeric codes (e.g., HSUs, USF 2, and MSF 2) designate units composed of basin-floor lithofacies assemblages (LFAs 1-3, 9-10), and odd-numbered codes) denote units comprising piedmont-slope LFAs (5-9; e.g., USF 1, MSF 1). Refinement in HSU definitions is an ongoing process, with updates occurring during each study phase. Informal Upper, Middle, and Lower Santa Fe HSUs (USF, MSF, LSF) form the major basin-fill aquifer zones in the Mesilla Basin region, and they correspond roughly to the Camp Rice, Fort Hancock, Rincon Valley, and Hayner Ranch lithostratigraphic subdivisions of the Santa Fe Group (**Fig. 3-5**, **Part 3.5.2b**). Proper identification and correlation these lithostratigraphic units in the deeper subsurface, however, remains a significant problem in parts of many *NM OSE closed*-GW basins (**Part 1.2.2**); hence, the informal status of this hydrostratigraphic classification system.

Distribution of HSUs and their primary LFA components in Study-Area basin fill is schematically depicted in the array of 19 hydrogeologic cross-sections assembled on **PLATE 5 (PL 5a to 5s**; *cf.* **PLS. 7** to **9, TBL. 2**). Dominant sedimentary facies in the Upper Santa Fe HSU are basin-floor LFAs 1-3 and piedmont-slope LFAs 5 and 6 (**Fig. 4-3a** and **4-3b**, **Tbl. 4-1**). The Middle Santa Fe HSU is characterized by basin-floor LFAs 3 and 9, piedmont LFAs 5-8, and the transitional (mainly eolian) LFA 4. The Lower Santa Fe commonly includes LFAs 4 and 7 to 10. Basin-floor LFAs 3 and 9 are normally present throughout the Santa Fe Group section in central topographically *closed* basin areas, particularly HSUs LSF and MSF2, and sandy eolian deposits in LFAs 2 and 4, are significant SFG lithofacies components in the eastern (leeward) parts of the southern Mesilla Basin.

The other major class of hydrostratigraphic units comprises channel and floodplain deposits of the Rio Grande (HSU–RA/LFA **a)** and its larger arroyo tributaries (VA, VAY/LFA **b**). Thin (<100 ft, 30 m) HSU-RA/LFA **a)** deposits of Late Quaternary age form most of the region's most productive shallow-aquifer system (**Figs. 3-5** and **4-3a, Tbls. 4-1** and **4-3**, and **PLS. 5a** to **5k**, and **5o**). Surficial playa-lake sediments (BF, BFP/LFA c), arroyo-valley fill (VA, VAY), and piedmont-slope alluvium (PA, PAY) are usually in the *vadose* zone, but they locally form significant groundwater-recharge sites. *Phreatic* conditions still exist in the large intermittent to ephemeral remnants (e.g., lagunas, barreal123rovincnas, and alkali flats) of pluvial-Lakes Palomas and Otero that are located in nearby parts the Zona Hidrogeológica Conejos Médanos and Tularosa Basins (**Figs. 1-2**, **3-1** and **3-3**; *cf.* **Parts 3.1**, **3.3.1** and **3.3.2**).

LFAs 1 and 2 in HSU-USF2 also comprise optimum reservoir material for a variety of "subsurface-water storage and recovery" activities in both the phreatic zone and the lower part of the vadose zone, with especially favorable sites located in the western Mesilla Valley-border areas near the Las Cruces metro-area. As noted in **Part 1.3.2**, managed aquifer recharge (MAR) operations have already been successfully implemented in a similar hydrogeologic setting in the EPWU's western Hueco Bolson well field (*cf.* Garza et al. 1980, Knorr and Cliett 1985, Knorr 1988, Buszka et al. 1995, EPW-ND; *cf.* **Parts 8.5.4** and **8.6.2**, Hawley 2020, Wolf et al. 2020).

CHAPTER 5.
BEDROCK- AND STRUCTURAL-BOUNDARY COMPONENTS OF INTERBASIN UPLIFTS

Emphasis of the first of the Report's three *core* chapters (**5** to **7**) is on the bedrock uplifts that separate five of the major GW basins of the Mesilla Basin region (Mesilla, Southern Jornada, Tularosa, Hueco, and eastern Mimbres-Malpais). All of these bedrock terranes are primarily of fault-block origin, lithologically diverse, and exhibit a wide range of topographic and structural relief (**Figs. 3-9** to **3-12**; **PLS. 1** to **4**; **Part 3.6**). The names and acronyms for the major boundary-fault zones shown on hydrogeologic maps and cross-sections are listed on **Table 1-2** (**TBL. 3**). Marine-carbonate and siliciclastic rocks of Late Paleozoic (Pennsylvanian-Permian) and Early Cretaceous age are the dominant lithologic units forming the Robledo, San Andres, Tortugas, Bishop Cap, Franklin, Juárez, Sapello, and East Potrillo uplifts (**PLS. 1**, **2**, and **4** to **6**). Igneous-intrusive and volcanic rocks of large Early to Mid-Cenozoic caldera complexes are the primary components of the Doña Ana and Organ Mountains uplifts. Gypsiferous-evaporite (gypsite) strata are present in Upper Pennsylvanian rocks of the southern San Andres range and the northern Doña Ana and Franklin Mountains; they also occur in Lower Cretaceous strata in the Sierra Juárez and Sapello Uplifts (**PLS. 1**, **2**, and **5**; **Tbl. 1-3**; *cf.* Seager et al. 1987, Seager 1995, Collins and Raney 2000, Haenggi 2002).

There are two primary categories of exposed or shallowly buried bedrock terranes that form the major structural uplifts that separate four of the five-designated GW basins in the Study Area (**Part 1.2.2**, **Fig. 1-8**, **Tbl. 1-4**):

1. Basin-border Uplifts (U) that have a wide range of topographic relief and extensive areas of exposed bedrock. The latter, for the most part, are composed of rock types of relatively low permeability, and commonly form effective barriers to inter-basin GW flow. Basin-bounding highlands are the primary source terranes for local mountain-block/front recharge, and their crests form first-order watershed divides; depth of bedrock burial rarely exceeds 300 ft (90 m) in topographic lows.
2. Corridors (C) are large interbasin paleo-valleys of complex origin (erosional and tectonic) that disrupt Uplift continuity. Thickness of saturated SFG deposits in deeper segments is in the 300 to 600-ft (90-180 m) range. They allow or potentially allow significant amounts of inter-basin GW underflow (e.g., "inflow" and "outflow" classes; **PLS. 2** and **4**, **TBL. 1B**).

Deeply buried, inter-basin and intra-basin bedrock terranes that have been identified as structural-positive areas by deep test borings and geophysical surveys are designated Highs (H) in this report. They are here interpreted as remnants of early-stage RG-rift and/or Laramide, basin- or subbasin-boundary uplifts that are now buried by 1,000 to 1,800 ft (300-550 m) of SFG basin fill (primarily Middle and

Upper SF HSUs). Such features, were initially included in a broader "Uplift" category by Hawley and Lozinsky (1992) and Hawley and Kennedy (2004) (*cf.* Witcher et al. 2004, Hawley et al. 2005, Sweetkind 2017 and 2018, and Teeple 2017). Bedrock composition and structure of basin-bounding Uplifts and Highs are described in the below-listed parts of the Chapter (*cf.* **PLS. 1**, **2**, and **5**):

5.1. UPLIFTS AND CORRIDORS BETWEEN THE SOUTHERN JORNADA AND MESILLA BASINS, AND THE TULAROSA BASIN AND HUECO BOLSON.

5.2. UPLIFTS BETWEEN THE LOWER RINCON VALLEY, SELDEN CANYON AND MESILLA BASIN, AND THE SOUTHERN JORNADA BASIN.

5.3. UPLIFTS NORTHWEST OF THE MESILLA GW BASIN.

5.4. UVAS-GOODSIGHT UPLIFT AND CEDAR-CORRALITOS BASIN.

5.5. UPLIFTS BETWEEN THE MESILLA GW BASIN, AND THE EASTERN MIMBRES AND MALPAIS BASINS.

5.6. WEST POTRILLO VOLCANIC FIELD.

The southwestern Study Area also includes the easternmost parts of two adjacent RG-rift basins, both of which have large binational GW-basin components: The Mimbres and Malpais Basins (MbB and MpB; **Figs. 1-1**, **1-2** and **1-10**; and **Tbl. 1-4**; *cf.* **Part 5.7**). Neither basin has any surface-flow connection with the MeB (**Fig. 1-6**), but the northeastern MpB* does contribute a small amount of subsurface recharge to SFG aquifers in the northern El Parabién GW Basin (EPB). Prior to initial operation of the new Ciudad Juárez Junta Municipal de Agua y Saneamiento (JMAS) well field (~2009), the MpB and EPB were also hydraulically linked to the regional Transboundary GW-flow system that discharges at the lower end of the Mesilla Valley (**Figs. 1-9, 1-10** and **1-11**; *cf.* **Parts 5.7.2-7.5, 6.3.5**, **6.4**, and **7.6**).

As of 9/22/2005, most of the US part of the MpB is in the NM OSE "declared" – "Mount Riley Groundwater Basin (Part 1.1.4**)"*

5.1. UPLIFTS AND CORRIDORS BETWEEN THE SOUTHERN JORNADA AND MESILLA BASINS, AND THE TULAROSA BASIN AND HUECO BOLSON

The San Andres-Organ-Franklin-Sierra Juárez mountain chain (SAMU-OMU-FMU-CJU), which separates the Southern Jornada and Mesilla Basins (SJB and MeB) from the Tularosa Basin (SWTB) and Hueco Bolson (WHB), forms a well-defined hydrographic (surface-watershed) and geohydrologic (subsurface-watershed) boundary. Peak altitudes of Organ and Franklin Mountains (OMU and FMU), and Sierra Juárez (SJU) are, respectively, 9,012 ft, (2,747 m), 7,192 ft (2,192 m) and 5,823 ft (1,775 m). While structurally complex internally, the ranges north of EPdN have the overall form of a series of tilted fault blocks that dip westward into the Southern Jornada and eastern Mesilla Basins. Except where disrupted by the Oligocene Organ Mountains caldera, their core of Proterozoic igneous and metamorphic rocks (Precambrian-basement complex) is capped by a thick sequence of Paleozoic carbonate and

siliciclastic rocks, and Eocene volcanics (Harbour 1972, Seager 1981, Kelley and Matheny 1983, Seager et al. 1987, Collins and Raney 2000). Basic geologic-framework composition, from both surface and subsurface perspectives, is schematically illustrated in **Figures 3-9** to **3-12,** and **PLATES 1B**, **1C**, **5a-s**, **8A** and **8B**.

The structure of the SAMU-OMU-FMU-CJU mountain chain documents multiple episodes of tectonism dating back to Proterozoic time, but evidence of both Early and Late Cenozoic (Laramide and RG-rift) tectonism is most clearly expressed (Mattick 1966; Harbour 1972; Seager 1975a and 1981; Lovejoy and Seager 1978; Seager and Morgan 1979; Seager et al. 1987; Kelley and Chapin 1997; Collins and Raney 2000; Haenggi 2002; Amato et al. 2017; Creitz et al. 2018; Ramos et al. 2018c). The eastern boundary-fault system comprises, from north to south, the linked San Andres Mountain, Organ Mountains, Franklin Mountains and Sierra Juárez fault zones (SAmfz. OMfz, FMfz and SJfz; **Tbl. 1-4**; **APNDX. J: Pls. F2-7**, **F3-2i** and **2j**, and **F7-4d** and **4e**). All have down-to-the-east, normal-displacement segments (*strands*), some of which have remained active in Holocene time (Gile 1986, 1991, 1994b; Keaton 1993; Keaton and Barnes 1995; Machette et al. 1998; Collins and Raney 2000; McCalpin 2006; Avila et al. 2016).

5.1.1. Organ Mountains and Bishop Cap Uplifts (OMU and BCU)

The Organ Mountains uplift (OMU) includes the exposed parts of a large caldera complex of latest Eocene age, with igneous-intrusive rocks (granites to monzonites) forming its northern and central (**Fig. 1-8**, **Tbl. 1-4**; *cf.* Dunham 1935, Seager 1981, Rioux et al. 2016, Ramos et al. 2018c). The latter includes Organ Needle (alt. 9,012 ft, 2,747 m), the highest peak on the Mesilla (hydrographic) Basin perimeter (**Figs. 3-11** and **3-12**; **PLS. 1B** and **1C**; **APNDX. F: Pls. F2-8**; **F3-2b**, **2c**, **2e, 2f,** and **2j**). Silicic volcanics (lavas and welded tuffs) are the dominant rock types in the southern OMU. Thick sections of Paleozoic carbonate rocks, with local gypsiferous strata, are exposed at the southeastern end of the OMU and in outlying peaks of the Bishop Cap Uplift (BCU), a small remnant of the Organ Caldera's southern rim (Seager 1973, 1981). The Black Hills Uplift (BHU) is a low-relief fault-block outlier between the southwestern Tularosa GW Basin (SWTB), and the southeastern-most OMU and the BCU. Basaltic-andesite volcanics and interbedded fanglomerates of Oligocene age that form the exposed part of the BHU are partly buried by piedmont and ARG facies of the upper USF (Seager 1981; Hawley et al. 2009, Pl. 1).

5.1.2. Fillmore Pass Corridor (FPC)

The continuity of SAMU-OMU-FMU-SJU chain of uplifts is broken in only two places, the El Paso del Norte (EPdN) Rio Grande *water gap* (**Part 3.3**), and the Fillmore Pass Corridor (FPC) *wind gap* (**Fig. 1-8**, **Tbl. 1-4**). The latter is a deep paleo-valley between the Bishop Cap Uplift (BCU) and the north

tip of the Franklin Mountains (**PL. 5h** and **5n, TBL. 1**, well nos. 205 and 206; **APNDX. F: Pls. F2-1** and **2**, **F3-2g** to **F3-2j,** and **F5-3h**; *cf.* Knowles and R. Kennedy 1958, Strain 1966, p. 11, Hawley et al. 1969, Hawley 1975, Seager 1981, Wilson et al. 1981, Orr and White 1985, Seager et al. 1987, Orr and Risser 1992, Mack et al. 1996, 1997, Hawley and J. Kennedy 2004, Hawley et al. 2009). The 6-mi (10 km) long FPC connects the MeB-Mesquite Subbasin (MSB-**Part 6.3.4a**) with the northwestern Hueco Bolson (WHB). Minimum width of this fluvial-erosional feature is 2.5 mi (4 km), and its base is about 900 ft (275 m) below the constructional surface of deposits of a large USF2-ARG distributary system that flowed through the pass in Early Pleistocene (prior to ~1 Ma; Knowles and R. Kennedy 1958; Strain 1966; Mack et al. 1996 and 1997). At an altitude of about 4,200-ft (1,280-m) amsl, this La Mesa Surface remnant is about 350 ft (107 m) above the MeV floodplain surface to the west, and about 150 ft (45 m) higher than the Hueco Bolson floor (**PL. 5h** and **5n**). The potential for interbasin-groundwater discharge from the western Hueco Bolson (WHB) to the southeastern MeB and lower MeV via the FPC is discussed in **Part 7.5.2**.

5.1.3. Franklin Mountains Uplift (FMU)

The Franklin Mountains Uplift (FMU) is composed primarily of a thick sequence of Upper and Lower Paleozoic carbonate and clastic sedimentary rocks that unconformably overlies a Proterozoic (Precambrian) complex of mostly granitic and silicic meta-volcanic rocks (**Fig. 1-8** and **Tbl. 1-4**; **Figs. 3-9** to **3-12**; **PLS. 1B**, **1C** [II-II′], **5i** to **5k** and **5n**; **APNDX. F: Pls. F2-1** and **2**, and **F3-2g** to **2j**; *cf.* Harbour 1972, LeMone and Lovejoy 1976, Kelley and Matheny 1983, Dyer 1989, Lueth et al. 1998). Thick gypsum beds occur in the Upper Pennsylvanian section east of Anthony and Berino. The steep, west-tilted structure of the main part of the uplift (peak elev. 7,192 ft [2,192 m]) stands in sharp contrast with that of an extensive foothill area, which is located between the eastern MeV border and the range's western-frontal fault zone (WFfz-**Tbl. 1-5**, **Figs. 1-8**, **3-11** and **3-12**). The partly buried, and complexly faulted bedrock terrane of the western foothills comprises a series of Upper Permian and Lower Cretaceous marine carbonate and siliciclastic rocks that have been intruded by intermediate hypabyssal rocks of Eocene age (**PL. 5i** to **5k;** Hoffer 1970; Lovejoy 1973; Lovejoy and Seager 1978; Hoover et al. 1988; Collins and Raney 2000; McMillan 2004; Lucas et al. 2010).

5.1.4. Campus Andesite Hills and Cerro de Cristo Rey Uplifts

El Paso de Norte (EPdN) of the Rio Grande, which separates the FMU from the Sierra Juárez Uplift (SJU), cuts through the Campus-Andesite Hills (CAHU) and Cerro del Cristo Rey [Cerros de Muleros] Uplift (CCRU) (**Fig. 1-7**, **Tbl. 1-4**; *cf.* Córdoba 1969a, Hoffer 1970, Lovejoy 1976a, Lucas et al. 1998; **PLS. 5o** and **5l**; **Parts 3.2.3c** and **6.3.5d**; **APNDX. F: Pls. F2-6**, **F3-1j**, and **F4-1l** and **41m**). The small, but rugged peaks of the CAHU on the EPdN's eastern border occupy much of the UTEP Campus

area. The CCRU's nearly circular, domal uplift to the southwest of the EPdN is formed by a large andesitic igneous intrusion in Cretaceous marine-sedimentary rocks. Its central peak, Cerro del Cristo Rey (alt. 4,675 ft, 1,425 m) is located about 1,500 ft (455 m) north of the International Boundary, and about 0.7 mi (1.1 km) from the Rio Grande (Lovejoy 1976, Hoover et al. 1988, Lucas et al. 1998, McMillan 2004). Darton (1933, p. 131-132) describes the CCRU [his Cerros de Muleros] as follows:

> The Cerro de Muleros [del Christo Rey] consists of a mass of limestone, shale, and sandstone of [Lower] Cretaceous age penetrated and tilted by a large mass of [Eocene andesite] porphyry. The lower or quarry [Comanche] limestone in this succession is well exposed in the first railroad cut west of the river. It is overlain by nodular and slabby limestones and shales containing large numbers of Washita fossils and grading upward in to a thick mass of dark shale in which there are deep cuts extending to and beyond Brickyard siding. This shale is extensively worked for brick, hollow tile, etc., on the west bank of the river below the 2 railroad bridges. . . .

Gypsiferous beds in the Cretaceous stratigraphic sequence contribute to very poor GW quality conditions not only in the CCRU, but also in adjacent parts of the Lower Mesilla Valley (e.g., >3,000 mg/L TDS; **Parts 6.3.4c, 6.3.5c** and **6.3.5d**; **PLS. 5o, 5k** and **5l**; **TBL. 1,** well nos. 279-281, 293, 308, 312 and 316; *cf.* Villagran 2017a, Kubicki et al. 2021).

5.1.5 Sierra Juárez and Sierra Sapello Uplifts

The Sierra Juárez uplift (SJU; peak alt. 5,823 ft [1,775 m]) forms the southeastern structural boundary of the Mesilla RG-rift Basin (**Fig. 1-8**, **Tbl. 1-4**; **Figs. 3-11** and **3-12** [III-III′], **APNDX. F: Pls. F2-2, 2-6** and **2-7**, and **F4-1l**; *cf.* Córdoba 1969, Lovejoy 1979, Drewes and Dyer 1993, Haenggi 2002, McMillan 2004). High ridges of tightly folded marine-carbonate rocks of Early Cretaceous age comprise the crest of this fault-block uplift, which is bounded on the east and southwest, respectively, by the Sierra Juárez and El Vergel fault zones (SJfz and EVfz; **Fig. 1-8**, **Tbl. 1-5**). As in the Cerro del Cristo Rey [Cerros de Muleros] Uplift gypsiferous beds in lower part of the Cretaceous stratigraphic sequence are major contributors to very poor GW quality conditions not only in the SJU, but also beneath flanking piedmont-slopes and basin floors (**PLS. 1B, 1C, 5l and 5s**; **TBL. 1**, well nos. 360, 361, 378 and 381).

The Sierra Sapello Uplift (SSU [Sierra Mesquité of Córdoba 1969]) is located about 15 km (9 mi) southwest of the SJU (**Fig. 1-8**, **Tbl. 1-4**). The SSU comprises a group of low-relief ridges of tightly folded, Lower Cretaceous limestone and shale, with local andesitic-intrusive bodies of early Tertiary age (**Figs. 3-11** and **3-12**; **PLS. 1B**, **1C**, and **5s**; Córdoba 1969a; Córdoba et al. 1969; Chavez-Quirarte 1986; Hoover et al. 1988; McMillan 2004). The SSU is about 3 mi (5 km) south of the southern MeB boundary, and Mexico Federal Highway 2 crosses its shallowly buried northern tip (**PL. 5s**). The sinuous crest of the SSU is comprises the watershed divide between the Mesilla and El Parabién hydrographic basins (max. alt. 4905 ft, 1,495 m). Since the general level of the La Mesa geomorphic surface (**Part 3.5**) that forms the adjacent El Parabién Basin (EPB) floor is about 4,020-ft (1,225-m) amsl, maximum local relief is less

than 900 ft (275 m). Gypsiferous interbeds in Cretaceous limestone and shale strata, as well as in subjacent Jurassic rocks, contribute to the very poor groundwater-quality conditions in the SSU and parts of three bordering hydrogeologic subdivisions: (1) the Méndez-Vergel Inflow Corridor (MVIC), (2) El Parabién GW Basin (EPB), and (3) the deeply buried, Potrillo-Sapello High that separates the MeB and EPB (**Parts 5.1.6**, **6.4.1** and **6.4.2**; **TBL. 1**, well nos. 362, 363 and 366).

5.1.6. Méndez-Vergel Inflow Corridor

The Méndez-Vergel Inflow Corridor (MVIC) is a deep paleo-valley (wind gap) that is located between the Sierra Juárez and Sierra Sapello Uplifts and was formerly occupied by one or more distributary channels of the ARG (**Fig. 1-8**, **Tbl. 1-4**; **Figs. 3-13** and **3-14**; **Tbls. 1-1** and **3-3**; **Part 3.7.2**; **APNDX. F: Pls. F2-2, 2-6** and **2-7**). This fluvial-geomorphic analog of the Fillmore Pass Corridor (FPC) is about 5 mi (8 km) wide and 6-mi (10 km) long. In this case, the MVIC connects the southern end of the MeB with the southwestern-most Hueco Bolson. The provisional compound name comes from (1) El Méndez Station on the Chihuahua al Pacífico branch of the Mexican National Railroad, near the corridor's eastern end; and (2) El Vergel (Plazuela de Acuna) on Mexico Federal Highway 2 at the northeastern edge of the Corridor (**Fig. 1-10**, **PL. 5s**). Approximate-boundary placement is based on (1) surface gravity-survey information, (2) logs of S.A.R.H. (CONAGUA after 1987) exploration wells, and (3) GW-quality and static water-level data from these wells (**Figs. 1-8**, **1-10**, **1-11**, **3-7** and **3-8; PLS. 1A**, **1B** and **4**; **TBL. 1**, well nos. 363, 378 and 381; INEGI 1983, 2012; Jiménez and Keller 2000).

The Corridor's transitional boundary with the southernmost part of the MeB-El Milagro Subbasin (EMSB) is placed about 3.5 mi northwest of El Vergel and the Highway 2 Aduana. The eastern boundary of the MVIC is located southeast of the Méndez Station-Sapello Siding section of the Chihuahua al Pacifica RR branch. The Corridor'd border in that area follows a poorly defined 1250-m (4,101-ft) drainage divide between the southwestern Hueco Bolson (SWHB) and southeastern Mesilla hydrographic basin watersheds (**Figs. 1-3** and **1-10**; **PLS**. **2** and **4;** *cf.* **Part 6.3.4d**). The southern segment of the Mexico Federal Highway 45—Santa Teresa Port-of-Entry bypass route marks the approximate position of the MVIC's southwestern border. The MVIC has also been proposed as the location of a new Mexican National Railroad section that connects with the Union Pacific RR in the Santa Teresa Industrial Park area (Pacheco 2022b-c; *cf.* **Parts 1.1.2** and **6.3.4b-d**).

Maximum thickness of the MVIC's undivided SFG basin fill has yet to be determined by test drilling, but it locally exceeds 1,000 ft (300 m) (**PLS. 1B**, **5s**, and **7**). Thickness of the sand-dominant upper fill unit is as much as 660 ft (200 m), and is here interpreted as being composed of interbedded ARG-USF2 fluvial and eolian sediments (**TBLS. 1**, **1B**; **PL. 5s**). The Late Quaternary-age groundwater flow-system in the MVIC conducts brackish underflow to the southern end of the MeB (El Milagro Subbasin) from local recharge sources that include a large unnamed topographic depression adjacent to

the southwestern Hueco Bolson (SWHB; **Figs. 1-9** and **1-11**). The latter area is located in the northern part the "Valle Samalayuca" as defined in INEGI (1999, p. 49-50, 6.2.4; **APNDX. C6b**). It is bounded on the east by the northern Sierra del Presidio and on the south by the Sierra Sapello Uplift (SSU) and Sierra Samalayuca (**Figs. 1-3**, **1-8** and **3-3**; Berg 1969; Córdoba 1969; Chavez 1986; Zwanzinger 1990a; Molina 1997). Gypsiferous beds in Lower Cretaceous rocks in adjacent parts of the SJU and SSU are major contributors to very poor GW quality conditions, and both gypsic and halitic evaporites are present in the Jurassic strata that underlie the nearby Sierra Samalayuca area at relatively shallow depths (**TBL. 1**, wells 360, 363, 381 and 383; *cf.* **Fig. 7-17**, Araurjo-Mendieta and Casar-González 1987, Zwanzinger 1990 and 1992, Molina 1997, Haenggi 2002, Lawton 2004).

5.2. UPLIFTS BETWEEN THE LOWER RINCON VALLEY, SELDEN CANYON AND MESILLA BASIN, AND THE SOUTHERN JORNADA BASIN

5.2.1. Doña Ana Mountains Uplift

The Doña Ana Mountains Uplift (DAMU) forms the central highland component of the group of RG-rift fault-block uplifts that separate the northeastern MeB-MeV area from the western and southern parts of the Southern Jornada Basin (SJB; **Fig. 1-8** and **Tbl**. **1-4**; **PLS. 1** and **2**; **PL. 5b** and **5c**; **APNDX. F: Pls. F2-1**, F**2-8**, **F4-1h**, and **F4-3b**; *cf.* Seager et al. 1976, Mack et al. 2018b, 2018c, Ramos and Heizler 2018, Seager and Mack 2018). The DAMU is dominated by an igneous-intrusive and extrusive complex that associated with a large caldera that formed in the late Eocene, and is bordered on the northwest by thick sequence of upper Paleozoic (siliciclastic, carbonate and gypsum-bearing) sedimentary rocks. Doña Ana Mountain (peak alt. 5,835 ft, 1,778 m) is the highest point on the Mesilla Basin's northern hydrographic boundary. The uplift's northern and eastern structural border with the SJB is formed by the Jornada fault zone (Jfz-**Fig. 1-8 [PL. 2]**, **Tbl. 1-5**). Goat Mountain, at the southern edge of the DAMU (alt. 4,815 ft, 1,468 m), is the intrusive-root of a rhyolite dome of latest Eocene age.

5.2.2. Selden Hills and Tonuco Mountains Uplifts

In the northwestern part of the Study Area, the DAMU is structurally connected to the Selden Hills and the Tonuco Uplifts (SHU and TNU) that are separated by the East Tonuco Corridor (ETC), which is about 2 mi (3.2 km) in width (**PLS. 2**, **5a**, and **9**). The SHU-ETC-TNU area is bounded on the east by the Jornada fault zone (Jfz), and on west by the Tonuco fault Zone (TNfz) (**Fig. 1-8**, **Tbl. 1-5**; Seager et al. 1987, 2023). The latter feature forms a distinct eastern structural boundary for the southern end of the Rincon Valley Basin (RVB) above the head of Selden Canyon (SCyn) of the Rio Grande (**Part 3.5.2a**; Seager et al. 2023). Maximum altitude of the Selden Hills is 4,622-ft (1,409-m) amsl, while that of adjacent parts of the SCyn floor is about 3,980 ft (1,213 m). The canyon is incised primarily in Eocene andesitic volcaniclastic rocks —Tlvs - **Tbl. 3-3**), and these units along with well-indurated LSF

conglomerates are also exposed in the higher parts of the SHU (Seager 1975b, Hawley et al. 1975, Seager et al. 1975, Mack and McMillan 1998, Seager et al. 2023).

San Diego Mountain*, which forms the summit area of the Tonuco Uplift (TNU), has a peak altitude of 4,957-ft, 1,511-m) amsl, and overlooks the lower end of the Rincon Valley Basin (**Fig. 1-10** and **Tbl. 1-3**; Seager et al. 2003; *cf.* **APNDX. F: Pl. F4-1a** to **1e**). Proterozoic metamorphic and Lower Paleozoic sedimentary rocks exposed in the northeastern part of the TNU are remnants of the Laramide Rio Grande uplift (Seager et al. 1971, 1986, 1997, 2023). Most of the exposed bedrock units, however, comprise the same andesitic volcaniclastic units that crop out in the SHU (Seager 1975b, Seager et al 2023).

**The Tonuco Mountains (Dunham 1935, p. 18) are named after Tonuco Siding on the BNSFRR (cf. Morgan et al. 2017). San Diego Mountain derives its name from the historic (post-1598) San Diego paraje (camp) site near the Rio Grande about 2.5 mi (4 km) west of El Camino Real (Moorhead 1954 [p. 270], Julyan 1996, p. 311; cf. Seager et al. 1971, Mack et al. 2018b).*

A camp about 72 miles [116 Km] south of the Fray Cristóbal Range, to the west of San Diego Mountain, where the Rio Grande returns from its west[east]ward bend and resumes its southward course [Moorhead 1954, Chapt. 4, p. 270, footnote [13]].

Of special note are (1) the thick basal LSF conglomerates that form the San Diego Mountain summit area, and (2) the presence of extensive siliceous, high-temperature spring deposits of Quaternary age (Jarvis et al. 1998). The latter material is associated with a large RG-rift geothermal system that extends northwestward from the Radium Springs-Leasburg Dam area to the Rincon Hills (Seager and Morgan 1978; Reiter and Barroll 1990; Ross and Witcher 1998; Witcher 1998). The following quotation from Seager and Morgan (1978b, p. 81-82) serves as a brief introduction to the major role played by rift-associated elevated terrestrial heat flow in the north-central part of the Study Area:

The large fault blocks in the southern rift are all horsts, grabens, or tilted blocks that probably resulted from deep-seated extension (Stewart, 1971). In the San Diego Mountain-Radium Springs area, however, the Miocene-Pliocene basin deposits have been moderately rotated on low- to moderate-angle faults that probably flatten downward and suggest thin-skinned distension in this region. . . . The deformation is similar to that described by Anderson (1971) in southern Nevada and attributed by him to distension above shallow spreading plutons. The San Diego Mountain-Radium Springs area is the most geothermally active area in the region with hot springs and young travertine mounds [Jarvis et al. 1998]. The highest conductive heat-flow values in the state have been measured in boreholes at San Diego Mountain (670 ± 75 and 640±125 mWm^{-2}; 16.1±1.8 and 15.3±3.0 HFU: Reiter and others, 1978; this guidebook [Hawley 1978]); and a ground-water base reservoir temperature of near 200° C here has been estimated from geochemical data (Swanberg, 1975, and personal communication, 1978). At least some Oligocene felsic volcanic rocks have a high K_2O content (greater than 7.0 percent) and a low Na content (less than 1.0 percent) in this area; these percentages suggest cation exchange by hot water (Baptey, 1955; Orville, 1963). The thermal anomaly, as well as the structural style, suggest the emplacement of a shallow pluton in the area within the past few million years. In terms of the tectonic disruption of an early rift basin, the structural style, and the geochemical and

thermal anomalies, this part of the—rift - like the Socorro—area - is anomalous, relative to the rest of the rift in the south-central New Mexico region.*

**For additional background on this topic, see: Decker and Smithson 1975, Reiter et al. 1975, Seager and Morgan 1979, Keller et al. 1990, Witcher and Mack 2018.*

A highly deformed section of LSF conglomerates and conglomeratic sandstones, with stratal dips of as much as 45° is exposed in the East Tonuco Corridor (ETC) between the TNU and SHU. The unit's measured thickness exceeds 2,700 ft (823 m), and it is overlain by more as much as 660 ft (200 m) of fine-grained MSF2 basin-floor facies that are predominantly ephemeral-lake deposits that are moderately deformed (Hawley and Seager 1969, Seager et al. 1971, 2023). As much as 330 ft (100 m) of USF2-ARG facies cap the older RG-rift basin fill in the ETC (Morgan et al. 2017). Structural deformation of these deposits is limited to fault and fold offsets of less than 200 ft (60 m) in the immediate vicinity of the Jornada fault zone (Jfz, **Tbl. 1-5** and **PL. 5a**; **APNDX. F: Pl. 7-4c**). The "Corridor" designation is based on observations of GW-head differences in wells near I-10 in the northwestern SJB and springs in the BNSF-Tonuco Siding area of the lower RVB (~4,030 ft [1,228 m] vs 4,000 ft [1,219 m]; *See* topic-related discussions in **CHPTS. 6** and **7**).

5.2.3. Tortugas and Tortugas Mountain Uplifts

The mostly buried Tortugas Uplift (TtU) extends southeastward from the Goat Mountain silicic-intrusive center at the southern edge of the DAMU to the Bishop Cap Uplift (BCU). The TtU ("Jornada horst" of Woodward and Myers 1996) is a narrow structural uplift that separates the Southern Jornada Basin (SJB)-Talavera Subbasin (TSB) from the MeB's Las Cruces Bench (LCBn) (**Figs. 1-8**, **3-11** and **3-12** [I-I′]; **Tbl. 1-4; PLS. 5d** to **5g** and **5m**; **Parts 6.1.3** and **6.3.5a**; **APNDX. F: Pls. F2-8** and **F3-2c**). The southernmost segment of the Jornada fault zone (Jfz) forms the TtU's eastern boundary, and the "West Tortugas fault zone (WTfz)" here designates a more-poorly defined, SSE-trending series of closely spaced, down-to-west faults that form a transitional structural boundary between the TtU and the northeastern MeB border (**Tbl. 1-5**).

The Tortugas ("A") Mountain Uplift (TMU) forms the (central) exposed part of the TtU. It is located at the east edge of the NMSU Campus and has a maximum altitude 4, 931 ft (1,503 m). This small fault-block upland is primarily composed of Permian (Upper Paleozoic) carbonate rocks (W. King and R. Kelley 1980), and it is part of significant GW geothermal-resource area (Gunaji et al. 1978; Chaturvedi 1981; Gross and Icerman 1983; Icerman and Lohse 1983; Cuniff 1986; Ross and Witcher 1998; **TBL. 1**, well nos. 122-124). The TMU is bordered by two shallowly buried TtU subdivisions: (1) North-Tortugas (Alameda-Telshor) Inflow-corridor (NTIc), and (2) South-Tortugas (Telbrook-Mossman) Inflow-corridor (STIc). Bedrock topographic lows in both Inflow-corridors (**PL. 5m**) allow some high-quality GW underflow from the SJB-Talavera Subbasin (TSB) and southern Organ Mountains Uplift (OMU) to enter

the Mesquite Subbasin (MSB) of the MeB via the Las Cruces Bench (LCBn, *cf.* **Parts 6.3.5a** and **7.5.1**, and Hawley and Kennedy 2004, p. 75). Saturated thicknesses of undivided-SFG basin fill in such places, however, rarely exceeds 200 ft (60 m; **PL. 5m**; P. Mack 1985; Woodward and Myers 1997; Gunaji-Klement & Associates 2001).

5.3. UPLIFTS NORTHWEST OF THE MESILLA GW BASIN

The East Robledo fault zone (ERfz, **Tbl. 1-5**) forms the northwestern structural boundary of the Mesilla GW Basin—(MeB - **Figs. 1-8, 3-11** and **3-12**; **APNDX. F: Pls. F3-1d** to **1f**). Two bedrock highlands define the respective northern and southern limit of the broad horst-type uplift that separates the MeB from the Cedar-Corralitos Upland Basin (CCUB) and the southernmost Uvas-Goodsight Uplift to the west (**Part 5.4**): the massive Robledo Mountains Uplift (RMU) with a maximum altitude of 5,890-ft (1,795-m) amsl, and the much smaller Aden Hills Uplift (AHU-max. alt. 4,835 ft/1,473 m) (**Figs. 3-11** and **3-12**[I-I′], **PLS. 5d** to **5g** and **5p** to **5r**; Seager et al. 1987; Seager 1995; Seager et al. 2008). The piedmont-slope terrain between the RMU and the AHU, here designated the Aden-Robledo Uplift (ARU), is underlain at shallow depths by andesitic-volcanic rocks, and the thin (<200 ft, 60 m) cover of USF basin fill is composed primarily of ARG deposits. The watershed divide that forms the northwestern hydrographic boundary of MeB's surface- and subsurface-flow system is well defined by the crest of the Aden Hills and the Robledo Mountains summit area, but can only be approximately delineated elsewhere (**Fig. 1-9** [**PL. 4**]; *cf.* **Parts 7.5.3** and **7.5.4**).

5.3.1. Northwestern MeB-Boundary Uplifts

5.3.1a. Robledo Mountains Uplift

The Robledo Mountains form the exposed part of the Robledo Mountains Uplift (RMU), and comprise the western topographic and structural border of the northernmost MeB and MeV area (**Figs. 1-8**, **3-11** and **3-12**[I-I′]; **Tbl. 1-4**; **PLS. 5c**, **5d, 5r**, and **8**; Seager et al. 2008; Mack et al. 2018b). This south tilted, wedge-shaped fault block is primarily composed of Paleozoic carbonate rocks, and is bounded on the east and west, respectively, by the northern segments of East and West Robledo fault zones (ERfz and WRfz). The RMU are intruded by early- to mid-Tertiary rhyolitic sills, and Miocene basaltic plugs occur near the uplift's southern border. Picacho "Peak" (4,959 ft, 1,512 m), a prominent remnant of a late Eocene intrusive-rhyolite dome in the southeastern-most part of the RMU, overlooks the northern MeV (**Fig. 3-11**; **PLS. 5d** and **5q**).

Two deep oil and gas exploration wells provide relatively detailed stratigraphic and structural information on the southern part of the RMU (**TBL. 1**, nos. 46 and 96). The deepest of the two, Sinclair No. 1 Federal Dona Ana 18 (**TBL. 1**, no. 46), was completed in Cambrian sandstone and a Tertiary rhyolite sill at a total depth of 6,440 ft (1,963 m) on 4/7/1962 (Kottlowski et al. 1969, Thompson and

Bieberman 1975, Seager et al. 1987 [well 17]). It penetrated at least 3,590 ft (1,094 m) of Paleozoic carbonate and siliciclastic rocks (Permian to Cambrian) that are in fault contact with 2,850 ft (869 m) of overlying Lower Tertiary volcanic and volcaniclastic rocks (Tlvs). According to Thompson and Bieberman (p. 173):

> The microlog indicate permeable zones in the Pennsylvanian, Mississippian, Fusselman [Silurian], Montoya, and El Paso [Ordovician]. On the induction log, significant SP deflections in the Mississippian and older units suggest that the formation waters are salty and have not been flushed by fresh water. No drill-stem tests were taken.

5.3.1b. Aden Hills and Aden-Robledo Uplift

The small Aden Hills Uplift (AHU) has a maximum altitude of about 4,800 ft (1,463 m) and is formed on andesitic volcaniclastic rocks of Eocene age that are correlative with andesitic volcanics (Tlvs) exposed at the base of Picacho Peak (**Figs. 1-8**, **3-9**, **3-11** and **3-12**; **Tbls. 1-4, 3-2** and **3-3**; **PLS. 5d** to **5f**, and **5r**; *cf.* Seager 1995, Seager et al. 1987 and 2008). The AHU and RMU are bounded on the west by the West Robledo fault zone (WRfz-**Tbl. 1-5**), and are separated by a broad, gently sloping platform that is here informally named the Aden-Robledo Uplift (ARU). The underlying Tlvs bedrock component has a thin (<300-ft, 90 m) cover of partly saturated of Upper SFG basin fill, which includes ARG fluvial facies.

The northern part of the ARU is here named the South Robledo inflow-corridor (SRic), with that designation being based on recognition that the Corralitos Ranch Subbasin (CRSB) of the CCUB contributes at least some underflow recharge to the MeB (Conover 1954, Pl. 1; King et al. 1971; Wilson et al. 1981; Frenzel and Kaehler 1992; Nickerson and Myers 1993; *cf.* **Fig. 1-9 [PL. 4**], and **Part 7.5.3**). The Aden Sector (AdS) in the southern part of the ARU comprises a transitional piedmont area between the AHU and the southern East Robledo fault zone (ERfz), which forms much of the MeB's western boundary (**Fig. 1-10**, **Tbls. 1-3** and **1-4**; **Part 5.3.2**). General, surface and shallow-subsurface hydrogeologic relationships in the southern Aden-Robledo and West Aden Uplift areas were first described in a *railroad-log* commentary by N.H. Darton (1933), which covers SPRR-UPRR route between Kenzin siding on the ARU-AdS and the eastern edge of the Mimbres hydrographic basin (*cf.* **APNDX. C1** and **Part 5.7.1**).

5.3.2. East and West Robledo Fault Zones

The East and West Robledo fault zones (ERfz and WRfz) are the major RG-rift tectonic features in the northwestern part of the Study Area (**Tbl. 1-5**; **PLS. 1A** to **1C** and **5c** to **5f**; Seager et al. 1987; Seager 1995). The ERfz is of major importance in this investigation because it forms a distinct structural boundary to the two primary hydrogeologic subdivisions of the northwestern MeB: the Fairacres Subbasin (**Part 6.3.3b**) and the Afton Subbasin (**6.3.3c**). Together with its southern extension, the East Potrillo fault zone (EPfz-**5.5.2**), the ERfz forms one of the longest basin-boundary fault-systems in the

RG-rift province with large-scale Pleistocene activity (Gile et al. 1981, Seager and Mack 1994, Seager et al. 2015). As noted in above and in **Part 5.7.2** and **5.7.4,** the West Robledo fault zone (WRfz) merges southward with the more-poorly defined La Peña fz (LPfz) in the Chihuahua part of the Study Area (**Fig. 1-8**, **Tbl. 1-5**).

5.4. UVAS-GOODSIGHT UPLIFT AND CEDAR-CORRALITOS BASIN

5.4.1. Uvas-Goodsight Uplift (UGU)

The southern Uvas-Goodsight Uplift (UGU) is located in the northwestern part of the Study Area and has two (provisionally named) hydrogeologic subdivisions: The Mason Draw Sector (MDS) and the Muzzle Lake inflow corridor (MLic) (**Fig. 1-8**, **Tbl. 1-4**). The MDS and MLic have framework properties that are nearly identical to those of the Aden-Robledo Uplift (ARU). HSU-USF basin fill forms a thin (<200 ft, 60 m) cover on andesitic volcanic rocks of unit Tlvs (**Figs. 3-5** and **3-11**, **Tbl. 3-3** and **PLS. 5b** and **5c**). Most of the southern Uvas-Goodsight Uplift (UGU) is within the Mimbres Basin (MbB) surface and subsurface watershed.

The only deep oil and gas exploration well in the UGU-MDS is the Cities Service No. 1 Gov.-Corralitos "A" (**TBL. 1**, no. 70). It is located on the footwall block of the Ward Tank fault zone (WTfz) and was completed on 7/25/1971 in Cambrian sandstone at a total depth of 5,129 ft (1,563 m) (Thompson and Bieberman 1975). The original borehole penetrated at least 5,030 ft (1,533 m) of Paleozoic carbonate and siliciclastic rocks (Permian to Cambrian) that unconformably underlie 1,100 ft (330 m) lower Tertiary volcanic and sedimentary rocks (Tlvs/Tls?). Wilson and others (1981, p. 160-161) reported a total depth of 3,007 ft (916.5 m) and a static water level (swl) of 746 ft (227.4 m) bgs when the depth-to-water was measured by the USGS on 3/4/1972. This indicates that the exploration well was ultimately developed in the Upper Paleozoic part of the stratigraphic section as a Corralitos Ranch stock well. Wilson and others (p. 161) also reported a 3.8 gpm (0.24 L/s) production rate, a relatively low-salinity, GW specific conductance of 1,800 micro-mhos (~1,200 mg/L TDS), and a 27° C GW temperature when the well was test pumped on 6/17/73. Electric-log information for the original-borehole also suggests that high-porosity carbonate rocks in the Lower Paleozoic (Fusselman/Montoya/El Paso) sequence may have significant potential for low-salinity GW production (Thompson and Bieberman 1975, p. 171). More-detailed assessment of deep low-salinity GW resources of the Cedar-Corralitos Basin area is now being jointly planned by the NMBGMR-Aquifer Mapping Program and the NMSU-Dept. of Geological Sciences (12/1/2020 e-mail communications).

5.4.2. Cedar-Corralitos Upland Basin (CCUB)

The Cedar-Corralitos Upland Basin (CCUB) is an isolated rift basin located between the Selden

Hills, Robledo Mountain and Aden-Robledo Uplifts (SHU-RMU-ARU) on the east and the Uvas-Goodsight Uplift (UGU) on the west (**Figs. 1-9**, **3-11** and **3-12** [Sec. I-I′]**,** and **Tbls. 1-4** and **3-3**; **PLS. 5b to 5d,** and **8A**). It has two subdivisions: the Cedar Hills Subbasin (CHSB) and the Corralitos Ranch Subbasin (CRSB). The CCUB's eastern structural boundary is formed, respectively, by the Cedar Hills and West Robledo fault zones (CHfz and WRfz) (**Fig. 1-8** and **Tbl. 1-5**; **PLS. 5b-5e**). The Ward Tank fault zone (WTfz) forms the CCUB's western border with the UGU (**PLS. 5b-5e**). The north-trending Cedar-Rough and Ready-Sleeping Lady chain of "Hills" form the CCUB's topographic axis. They are primarily composed of silicic igneous-intrusive rocks of the Cedar Hills vent zone, and are locally capped by basaltic-andesite flows (map-units Tba/Tmrs and TmCH-**Tbls. 3-2** and **3-3**; **Figs. 3-11** and **3-12**; **PLS. 5b-5d, 8A**).

The CCUB comprises a distinctive part of the Study Area's hydrogeologic framework that heretofore has only been described in detail from a geologic perspective (Clemons et al. 1975; Hawley et al. 1975; Seager and Clemons 1975; Seager et al. 1975; Clemons 1976a and 1977, Mack and McMillan 1998; Mack et al. 1994 and 1998). In marked contrast to all other GW basins described herein, primary aquifer units are in basaltic and silicic volcanic and interlayered sedimentary rocks of Oligocene age (Tba/Tmrs), with only limited aquifer conditions in basal parts of a discontinuous cover of SFG basin fill (**Tbl. 3-2**, **Figs. 3-11** and **3-12** [Sec. I-I′]). The CCUB's hydrogeologic framework is analogous to that of the larger Nutt-Hockett *GW-administrative basin*, which is located west of Hatch in the Palomas Basin-Uvas Valley area (**Figs. 1-1, 1-2** and **1-4**; Clemons 1979; Hawley et al. 2005).

5.4.2a. Cedar Hills Subbasin

The Cedar Hills Subbasin (CHSB) is topographically *open* and has a maximum altitude of about 5,020-ft (1,530-m) amsl. Its geologic components have been described in detail by Seager and others (1975), and Clemons (1976a). Runoff from the CHS watershed contributes surface flow to the Rio Grande as well as recharge to the shallow aquifers of the lower Rincon Valley Basin (RVB), Selden Canyon (SCyn), and upper Mesilla Valley **(Parts 3.1.3a**, **6.2**, **6.3.1a** and **6.3.3a**). It is bordered on the west by the Ward Tank fault zone (WTfz) and the Sierra de las Uvas (SLU) section of the Uvas-Goodsight Uplift (UGU), the latter having a maximum altitude of 6,623-ft (2,019-m) amsl (**Fig. 1-8**, and **Tbls. 1-4** and **1-5**). Its eastern structural boundary with the Selden Hills and northern Robledo Mountains Uplifts (SHU and RMU) is marked by the overlapping strands of the Cedar Hills and West Robledo fault zones (CHfz and WRfz). The CHSB also contributes small amounts of GW discharge to the RG alluvial aquifer (HSU-RA) in SCyn primarily via the Broad Canyon Arroyo system (Fox 1975; Hawley et al. 1975; Seager et al. 1975; Mack and McMillan 1998).

5.4.2b. Corralitos Ranch Subbasin

The Corralitos Ranch Subbasin (CRSB) is a topographically *closed* hydrogeologic unit with complex hydrographic character (**Fig. 1-8**, **Tbl. 1-4**). The Rough and Ready Hills (N) and Sleeping Lady Hills (S), with respective maximum altitudes of 5,351 ft (1,631 m) and 5,287-ft (1,611-m) amsl, form the CRSB's axial chain of silicic-intrusive-cored uplifts at the southern end of the Cedar Hills vent zone (Clemons 1976a, Mack et al. 1994, 1998). The CRSB includes a complex drainage divide that separates the surface- and subsurface- flow systems of the Mesilla and the Mimbres GW Basins (**Figs. 1-9** and **3-11**; **Tbls. 1-2**, **1-3** and **3-3**; *cf.* Conover 1954, King et al. 1971, Wilson et al. 1981, Frenzel and Kaehler 1992, Hanson et al. 1995, Hawley et al. 2000). A relatively small component of underflow discharge crosses the South Robledo Inflow Corridor (SRIC) of the Aden-Robledo Uplift (ARU), and contributes to the recharge of the basin-fill aquifer system in the Fairacres Subbasin (FASB) of the MeB (**Part 6.3.3b**). West of the divide, an equally small underflow component moves towards the MbB interior via the Mason Draw Sector (MDS) and the Muzzle Lake Inflow corridor (MLic) at the southern end of the Uvas-Goodsight Uplift (UGU).

5.5. UPLIFTS BETWEEN THE MESILLA GW BASIN, AND THE EASTERN MIMBRES AND MALPAIS BASINS

In this study, all Uplifts of the southwestern MeB border area between the Aden-Robledo Uplift (ARU) and the International Boundary have been combined into a single hydrogeologic-map unit, the East Potrillo Uplift (EPU-**Tbl. 1-3**). Whereas Tertiary volcanics form the predominant bedrock substrate in the ARU, the shallowly buried bedrock terrane of the EPU is composed mainly of Cretaceous and Permian marine-carbonate and Lower Tertiary siliciclastic sedimentary rocks (**Figs. 3-11** and **3-12** [II-II′]; **PLS. 5j** and **5k**). RG-rift extensional structural elements with a dominant N-S trend are superimposed on NW-SE trending basin and uplift features associated with NE-directed Laramide crustal-compression (**PLS. 5i** to **5k**; *cf.* **Part 3.4** and **APNDX. H)**.

5.5.1. East Potrillo Uplift (EPU)

Several major landscape features in the local area, as well as the abandoned settlement of Potrillo (EP&SW-SPRR Siding) at the southern end of the East Potrillo Mountains, take their name from the Spanish word for "colt" (Julyan 1996). The EPU has two topographically and structurally distinct subdivisions, both of which include extensive remnants of the Laramide "Potrillo uplift and basin" bedrock terrane (Seager 2004; *cf.* Seager 1989): (1) highlands of the Potrillo-Riley Sector (PRS), and (2) the broad topographic saddle between the PRS and the Aden-Robledo Uplift (ARU), which is here provisionally named the Brock Tank Inflow Corridor (BTic) (**Figs. 1-8** and **3-11**; **Tbl. 1-4**; **PLS. 5j**, **5k**, and **8**).

5.5.1a. Potrillo-Riley Sector

The EPU Potrillo-Riley Sector (PRS) includes two major highland areas, the East Potrillo Mountains (max. alt. 5,185 ft/1,580 m) and the Mount Riley and Cox twin peaks (max. alt. 5,905 ft/1,800 m) (**Fig. 1-8** and **Tbl. 1-4**; Seager and Mack 1994; Seager 1995; **APNDX. F: Pls. F2-1**, **F2-3** to **F2-5**, **F4-1k**, **F4-3a**, and **F7-4b**). The watershed divides at the crests of the East Potrillo and Mount Riley-Cox highlands forms the southwestern boundary of the MeB's surface- and subsurface-flow system. It is the only well-defined hydrographic feature in the western part of the Study Area zone because both surface and subsurface watersheds can only be approximately delineated in the basalt-flow and cinder-cone complex of the West Potrillo volcanic field [aka "Mountains"] to the west and northwest (**Parts 5.5.1b** and **5.6**; **Figs. 1-4** and **1-6**).

The structurally complex East Potrillo Mountains are primarily composed of lower Cretaceous and middle Permian marine-carbonate and siliciclastic rocks, and strata of both ages that are locally in reverse- and detachment-fault contact (Seager and Mack 1994). Mount Riley and Mount Cox the northwest part of the PRS comprise the exposed part of a large volcanic dome and smaller intrusive bodies of intermediate to silicic composition (**Fig. 3-11**, **Tbl. 3-3**). The latter penetrate and overlap both Cretaceous/Permian (KP) and Lower Tertiary non-marine siliciclastic (Tls) rocks. The marine origin of the Cretaceous and Upper Paleozoic bedrock units (exposed and buried) contributes the moderately brackish quality of groundwater in the SFG basin-fill aquifer system along the western margin of the in the Kilbourne-Noria Subbasin (KNSB, **Part 6.3.3e**; *cf.* Anderholm *in* Nickerson and Myers 1993, p. C65-C67). Willis T. Lee (1907, Tbl. 5) describes the Potrillo (El Paso & S.W. Rwy.) Siding well at the south end of the PRS as being completed in "Sand and clay" at 240 ft, with a "Depth to water" of 220 ft and an assumed brackish quality.

Four deep exploration wells, three geothermal and one for oil and gas provide relatively detailed stratigraphic and structural information on the EPR-East Potrillo Mountains and in contiguous parts of the KNSB (**TBL. 1**, nos. 257, 269, 297 and 298). The geothermal wells (nos. 257, 297 and 298) penetrated thick sections of highly fractured carbonate and siliciclastic rocks of Middle Permian age (San Andres and Yeso Formations), with probable karstic-porosity zones, and lost-circulation problems were encountered at each site (Snyder 1984). General subsurface conditions encountered in the 7,346-ft (2,239-m) Pure Oil Co. No. 1-H Federal test well (**TBL. 1**, no. 269) were initially described by F.E. Kottlowski (1965a, p. 146):

> The Pure Oil Co. No. 1-H Federal, drilled during 1961-1962 in sec. 24, T. 28 S., R. 2 W. on the northeast flank of the East Potrillo Mountains, probably encountered steeply dipping and faulted beds along the border fault zone of the East Potrillo Mountains. Most of the strata penetrated appear to be similar to the Early Cretaceous* limestones that crop out in the range, except for

the Tertiary diorite sill at the bottom of the test. Much fresh water** was obtained from the faulted limestones.

**Now identified as middle Permian and older Paleozoic rocks by Seager and Mack (1994).*

***"3,480 ft of mud-cut water (Thompson)" and "much fresh water (Kottlowski)" is probably in the slightly to moderately brackish range (1,000 to 5,000 mg/L TDS) based on reported water-quality values in in a stock well (no. 256) that is located 3,000 ft (0.9 km) east of the Pure Oil Co test well at the western edge of the MeB-KNSB: 4,770 mg/L TDS; Cl 1,600 mg/L (Anderholm in Frenzel and Kaehler [1992, p. C67-C67, Tbl. 10]).*

A detailed description of stratigraphic and structural relationships in the Pure Oil Co. No. 1-H Federal well in Seager and Mack 1994 (p. 24) provides critical information on (1) the actual age of the carbonate-bedrock units penetrated in the borehole (Permian instead of Cretaceous), and (2) the structural framework of the East Potrillo Mountains front:

> In 1962 Pure Oil Company drilled the Pure No.1 Fe"e"al "H" test in the central part of the East Potrillo Mountains at the eastern base of the range. The well was spudded in middle Permian limestone approximately 0.6 km west of the East Potrillo boundary fault. . . . Thompson (1982) indicates a reverse fault was cut by the well at a depth of 4,405 ft, but he does not identify it as a range-boundary fault.
>
> From an examination of cuttings, Thompson (1982) interprets the following down-hole lithologies:
>
> 0-625 ft 'Lower Cretaceous rocks (. . .);' the well was actually spudded in middle Permian limestone, so this 625 ft probably is Permian.
>
> 625-3,850 ft Permian to Mississippian limestone, dolostone, chert, and mudstone.
>
> 3,850-4,060 ft [Devonian] Percha Shale, dark, radioactive mudstone.
>
> 4,060-4,405 ft [Silurian] Fusselman Dolomite, light, coarsely crystalline dolostone.
>
> [~4,405 ft—Cross major reverse-fault zone]
>
> 4,405-6,240 ft Repeat of Permian to Mississippian section.
>
> 6,240-6,815 ft Marbleized Paleozoic rocks.
>
> 6,815-TD Tertiary diorite.

5.5.1b. Brock Tank Inflow Corridor

The shallowly buried Lower Tertiary/Cretaceous bedrock terrane in the Brock Tank Inflow Corridor (BTic) area has a thin (<300 ft/90 m) cover of USF basin fill, which is capped in many places by the Pleistocene basalt flows at the eastern edge of the of the West Potrillo volcanic field (**Fig. 1-8** and **Tbl. 1-4**; Seager 1989 and 1995; Hoffer 1976 and 2001b; *cf.* **Part 5.6**). The fresh to slightly brackish quality of groundwater in basal USF deposits in the BTic suggests that at least some of the better-quality underflow contribution to the southwestern MeB GW-flow system has recharge sources in (1) in the basaltic-volcanic uplands of the West Potrillo Mountains, and (2) the northern slopes of the Mount Riley part of the Potrillo-Riley Sector (PRS).

5.5.2. East Potrillo Fault Zone (EPfz)

The EPU is bounded on the east by the East Potrillo fault zone (EPfz-**Tbl. 1-5**). The latter merges

with the southern East Robledo fault zone (ERfz) in an area (immediately south of the UPRR) where structural-framework complexities are masked by basalt flows from the Aden Crater and Afton Cones centers of the eastern Potrillo volcanic field (Hoffer 1976; Seager et al. 1987; Seager 1995; Dunbar 2005; DeHon and Earl 2018; **Parts 5.3.2** and **6.3.3c** to **6.3.3e**; **APNDX. F: Pl. F7-4b**). Middle- to late-Pleistocene activity along the entire length of the EFfz south of the Potrillo volcanic field (about 18 mi/30 km) is well documented by offsets of uppermost beds of HSU-USF and capping calcretes (indurated soil-carbonate zones) of the La Mesa (geomorphic) surface that locally exceed 60 ft (18 m) (**Figs. 1-8, 3-11** and **3-12** [III-III′], **Tbls. 1-5** and **3-3**; **PLS. 5j** and **5k**; Hawley and Lozinsky 1992, PL. 7; Seager and Mack 1994).

Detailed gravity-survey interpretations by Jiménez and Keller (2000) and limited deep test-well data indicate that the EPfz merges southward with the provisionally named El Faro fault zone (EFfz) (**Figs. 1-8**, **3-7a**, **3-7b** and **3-10**; **Tbl. 1-2**; **TBL. 1,** nos. 357, 360, 390-394, 397). The latter structure forms a deeply buried and hence poorly defined boundary between El Parabién Basin (EPB), and the Border Tank Corridor (BTC) and El Aguaje Uplift (EAU) to the west (**Figs. 3-10** and **3-11**, **PLS. 5l**, **5r**, and **5s**; *cf.* **Parts 3.4**, **5.7.3**, and **6.4**). The Jiménez and Keller (2000) gravity-survey interpretations also suggest that a SE-trending fault zone or monoclinal flexure, here informally named the Noria (NRfz), forms the southern boundary of the MeB-Kilbourne-Noria Subbasin (KNSB-**6.3.3e**).

The general subsurface-geologic and hydrochemical relationships at the southern ends of the East Potrillo Uplift (EPU) and MeB-KNSB that are schematically illustrated in **PLATES 5k** and **5r** are based on interpretations of a group of geothermal test holes drilled by Hunt Energy Corp. in 1977 (**TBL. 1**, well nos. 295-298; **PLS. 5k** and **5r**; *cf.* Snyder 1986, Hawley and Lozinsky 1992, Pl. 7, Hawley and Kennedy 2004, Pl. A4w). The westernmost well (no. 297 [H-1485]-4,230 ft/1,298 m lsd [land-surface datum]) was completed in tilted and fractured Cretaceous rocks at 2,000-ft (610-m) bgs near the edge of the East Potrillo fault-zone footwall. The basin-fill cover of undivided SFG deposits is almost 600 ft (180 m) thick, with the lower 200 ft (60 m) in the zone of saturation. The well's temperature log shows a 20°-C to almost 60°-C increase in the SFG section, and an isothermic profile (55°-C to 60°-C) in the bedrock section, which documents significant GW-circulation activity in the Cretaceous/Permian (KP) subcrop units along the MeB's southwestern border (**Figs. 3-9**, **3-11** and **3-12**; **PLS. 5k, 5j** and **5r**).

The large Late Miocene to Pleistocene displacement on the East Potrillo fault zone is best documented by the temperature log of Hunt Energy well H-1017 (**TBL. 1**, no. 296), which was drilled one mile (1.6 km) east of Well H-1485 (no. 297) on the basin floor (La Mesa surface) near the western edge of the EPfz hanging-wall block in the southwestern-most part of the Kilbourne-Noria Subbasin (*cf.* **Part 6.3.3e**, **Fig. 6-10**). This 2,000-ft (610-m) borehole is also interpreted as being completed in Cretaceous bedrock, but here the overlying SFG section is at least 1,600 ft (488 m) thick. In addition, the

EPfz down-to-the-east offset of surficial USF2-ARG facies with capping La Mesa surface calcretes (lsd 4,160 ft/1,268 m) of early Pleistocene age is at least 70 ft (21 m) (**PL. 5k** and **5r**; *cf.* Seager and Hawley 1987 [Section F-F′], Seager and Mack 1994, Seager 1995, Hawley and Kennedy 2004 [Pl. A4w]). Cretaceous rocks were not penetrated in the easternmost 2,000-ft (610-m) geothermal test well that was drilled about 1.8 mi (2.9 Km) further east on the basin floor (4,135 ft/1,260 m lsd; H-1014; **TBL. 1**, no. 295; **PL. 5k**).

5.6. WEST POTRILLO VOLCANIC FIELD

The volcanic-upland west of East Potrillo Uplift (EPU), and the West Robledo and Mount Riley fault zones (WRfz and MRfz) comprises a distinctive part of the regional hydrogeologic framework that has yet to receive any type of subsurface exploration (**Figs. 1-10**, **3-11** and **3-12; Tbl. 3-3**; **PL. 5k**; **APNDX. F: Pls. F2-3** and **F2-4**). Even though they form a prominent highland with a maximum summit altitude of 5,297-ft (1,615-m) amsl, the West Potrillo Mountains are not a RG-rift structural uplift. They are, instead a constructional upland in which an extensive cover of Pleistocene basaltic volcanics buries the (RG-rift) structural-boundaries between the eastern Mimbres and Malpais Basins (MbB and MpB) and the MeB-EPU (**Figs. 1-10** and **3-12**; **PLS. 1** and **5k**; *cf.* Hoffer 1976, Seager 1989 and 1995).

The West Potrillo volcanic field includes 124 cinder or spatter cones, two maar volcanoes with tuff rings, a number of lava flows, and associated vent conduits, all of which overlie or intrude unknown thicknesses of undivided SFG basin fill (Hoffer 1976, Hoffer et al. 1998, Hoffer 2001b). Accordingly, definition of both surface- and subsurface-watershed divides is difficult or impossible simply due to the myriad closed depressions and relatively low topography that are commonly associated with Pleistocene basaltic volcanic fields (*cf.* King et al. 1971, Seager et al. 1987, Seager 1989 and 1995, Hawley et al. 2000).

5.7. BASIN-BOUNDARY SUBDIVISIONS OF THE SOUTHWESTERN STUDY AREA*

The southwestern Study Area includes the easternmost parts of two adjacent RG-rift basins, both of which have large binational components: The Mimbres Basin and the Malpais Basin (MbB and MpB; **Figs. 1-1**, **1-2** and **1-10**, and **Tbl. 1-4**; *cf.* Seager 1989 and 1995, and Hawley et al. 2000 [Chapter 4]). While separated in a structural sense from the MeB by the East Potrillo Uplift (EPU), the eastern MpB contributes relatively small (<2.2 ac-ft/yr [2.7 hm^3/yr]) amounts of underflow discharge to the Transboundary aquifer system in the southwestern Study Area (**Figs. 1-8** and **1-12**; *cf.* **Parts 6.3.4d**, **6.3.5e**, **6.4**, and **7.5.6**).

**The United States parts of the MpB and BTC are also in the "Mount Riley Groundwater Basin" that was "Declared" by the NM State Engineer on September 22, 2005*
*(**Part 1.1.4;** see https://www.ose.state.nm.us/WR/groundWater.php).*

The MbB and MpB have been subdivided into three provisional mapping units in this study:

1. The West Aden Uplift (WAU) and the West Potrillo Bench (WPBn) at the east-central edge of the Mimbres Basin watershed (**Part 5.7.1**).
2. The Guzmans Lookout Subbasin (GLSB) and La Laguna Bench (LLBn) in the respective central and southernmost parts of the Malpais Basin (**Part 5.7.2**).
3. The Border Tank Corridor (BTC) between the EPU-Potrillo-Riley Sector (PRS) and the Malpais Basin (**Part 5.7.3**).

5.7.1. West Aden Uplift and West Potrillo Bench

The West Aden Uplift (WAU) and Mimbres Basin-West Potrillo Bench (MbB-WPBn) are structural and topographic uplands that are located almost entirely west of the watershed divide that forms the hydrographic boundary between the Mesilla and Mimbres Basin surface- and subsurface-water flow systems (**Figs. 1-8**, **1-9** and **1-13**; **Tbl. 1-4**; **PLS. 4** and **1B**; *cf.* King et al. 1971 [Pl. 1], Hanson et al. 1994 [Pl. 2], Hawley et al. 2000 [Fig. 4-4]). The WAU and WPBn are here interpreted as being in a zone of structural transition between the Uvas-Goodsight Uplift (UGU) and the northern part of the Laramide Potrillo uplift and basin complex where Lower Tertiary, Cretaceous and Permian sedimentary rocks are still buried at relatively shallow depth (Tls/KP; **Figs. 3-11** and **3-12** [II-II′]; **Tbl. 3-3**). The WAU includes a westward-aligned group of low-relief hills with well-exposed silicic to andesitic volcanic rocks of Late Oligocene to Eocene age, which are named the "Aden Hills" by Seager (1995). The surface expression of transitional boundaries between the WAU, the West Portillo Bench (WPBn) and the northern Malpais Basin (MpB) is obscured by the southward-thickening cover of Quaternary basalts of the West Potrillo volcanic field (**Parts 5.6** and **5.7.2**).

5.7.2. Malpais Basin

The Malpais Basin (MpB) is a relatively small RG-rift basin that straddles the US-Mexico Boundary at the southwestern edge of the Study Area (**Figs. 1-1** to **1-3**, **1-8** and **1-11**; **Tbl. 1-4**). The place-name Malpais (*Sp. bad land or area of basalt-lava flows*) refers to an abandoned "El Paso & S.W. Rwy." [SPRR] siding and small settlement (including 2 wells) that are located about 2 mi (3.2 km) north of the International Boundary in the central part of the Basin (Darton et al. 1933; Conover 1954 [p. 151, 192-193]; Julyan 1996; **TBL. 1**, well no. 321).

Provisional placement of the boundary between the WPBN and the northern Malpais Basin is based great part on the work of W.R. Seager (1995), and Bouguer isostatic-residual gravity map compilations by Daggett and Keller (1995) and Jiménez and Keller (2000; **Figs. 3-7**, **3-8** and **3-11**; **Tbl. 3-3**; *cf.* Averill and Miller 2013). The MpB was identified as a major RG-rift structural depression and formally named by W.R. Seager (1989). The basin's eastern edge is located west of the West Robledo-La

Peña fault system in the southwestern-most part of the Study Area (**Figs. 1-3** and **3-11**; **Tbl. 1-5**; **PL. 5k**). The Malpais fault zone forms the Basin's western boundary with the Camel Mountain Uplift. It is located about 7.5 mi (12 km) west of the Study Area (**Fig. 1-11**; *cf.* Seager 1989 and 1995). South of the International Boundary the MpB is bounded on the east by the provisionally named La Peña fault zone and the El Aguaje Uplift (**Part 5.7.5**). According to Seager (1989, p. 57):

> . . . . The Malpais structural basin has little or no surface expression. It is essentially hidden by sand and basalt.
>
> The basin is clearly revealed by gravity data (DeAngelo and Keller, 1988). It is a north-trending graben, approximately 12 mi wide, that is bounded on the east by the West Robledo fault and on the west by a steep Bouguer gravity gradient interpreted to be a fault, the Malpais fault zone . . . . The basin has more than 30 mgl and 20 mgl [milligal] relief on the east and west sides, respectively.
>
> Although there are no exposures of basin fill within the graben, uplifted and exposed fanglomerate crops out on both the western and eastern bordering uplifts, at Camel Mountain and along the western edge of the East Potrillo horst [**PL. 5k**], respectively. The deposits are tilted and faulted [lower SFG] basin-fill deposits, probably [early] Miocene in age, derived largely from Tertiary volcanic rocks. Exposed thickness in both areas is several hundred feet. Presumably the same deposits, possibly much thicker, occur in the deeper, buried parts of the Malpais basin. The older deposits within the graben, together with exposed sections of basin fill on adjacent uplifts, may constitute the fill of an early [RG-] rift basin whose original extent was greater than the modern Malpais graben [*cf.* Averill and Miller 2013 (Figs. 3 and 4)].

The northernmost of the MpB's two provisionally named subdivisions, the Guzmans Lookout Subbasin (GLSB), includes all of the United States part of the Basin as originally delineated by Seager (1989 and 1995). It takes its name from a prominent cinder-cone in the southern West Potrillo volcanic field, Guzmans Lookout Mountain (alt. 4,762 ft/1,451 m; Julyan 1996). The extent of the MpB-GLSB in Mexico is based on interpretation of the Bouger-gravity anomaly maps of Jiménez and Keller (2000, Figs. 4 and 7). In the southwestern-most corner of the Study Area, the GLSB merges southward with La Laguna Bench (LLBn), whose southern and western boundaries have yet to be defined. South of the International Boundary, the poorly defined Malpais Basin (MpB) is in the northeastern part of the Zona Hidrogeológica de Conejos Médanos (ZHGCM) (**Figs. 1-1**, **1-2**, and **1-8**). As noted in **Part 3.3.2**, the ZHGCM in the we143rovincart of Mexico's endorheic "Regiones Hidráulicas-Cuencas Cerradas del Norte" (RH34–INEGI 1999, Fi^{a}. 5.3A, B; **Fi^{a}. 3-5a**; *cf.* **APNDX. H4.5**). The latter, in turn, is part of structural- and highland complex that includes much of El Barreal (**Figs. 1-1**, **1-2, 1-8** to **1-13**, **2-' [S-S']**, **3-5a**, and **3-12**).

5.7.3. Border Tank Corridor

The Border Tank Corridor (BTC) is a large hydrogeologic subdivision with a significant Transboundary GW-flow component (**Figs. 1-3**, **1-8**, **1-9**, **1-11**, and **3-10**; **Tbl. 1-4**; *cf.* **Parts 7.5.5** and **7.6.2**). It is located on the southwestern flank of the East Potrillo Uplift (EPU), and takes its provisional

name from Border Tank, a large earthen stock tank on the Mount Riley Ranch (Mount Riley SE, 7.5-min. quad; **PL. 5k**). Interpretations of basin-scale hydrogeologic relationships are illustrated on the western segment of Hydrogeologic Section K-K′ (**PL. 5k**) and **Figure 3-10**. The "Corridor" designation of the BTC reflects the probability that parts are (or were) an important pathway for interbasin GW flow from the eastern Malpais Basin-Guzmans Lookout Subbasin (MpB-GLSB) to the interlinked-aquifer zones of the El Parabién and southern Mesilla Basins (EPB and MeB) (**Parts 5.7.2**, **6.3.4d** and **6.4**; *cf.* **Fig. 1-9** [**Pl. 4**]).

5.7.4. Uplift-Boundary Fault Systems of the Southwestern Study Area

The Mount Riley fault zone (MRfz, **Tbl. 1-5**) forms a distinct structural and hydrogeologic boundary between the East Potrillo Uplift and Border Tank Corridor (Seager 1995), but the latter's southwestern border with the El Aguaje Uplift (EAU) in the Chihuahua part of the Study Area may or may not include a large-displacement fault zone (**Part 5.7.5**). The provisionally named La Peña fault zone (LPfz), which merges northward with the West Robledo fault zone (WRfz), also forms a distinct topographic and structural boundary between the BTC and the eastern Malpais Basin (**Figs. 1-8**, **3-11** and **3-12**; **Tbl. 1-4** *cf.* **5.3.2**).

The Potrillo Maar volcanic center of latest Pleistocene age is located at the eastern edge of the BTC, and is just west of the southern tip of the East Potrillo Uplift (EPU; **Figs. 1-8** and **3-11**; **APNDX F: Pls. F3-5a**, and **F7-3f**; DeHon 1965; Reeves and DeHon 1965; Callahan and Terrazas 1971; Waggoner 1990; Hoffer 2001a; Moncada-Gutierrez 2016). This deep-seated hydromagmatic (phreatomagmatic) center "and its associated explosive deposits cover an area of around 13 km^2 [5 mi^2], and exhibit three phases of activity [Hoffer 2001a]. The first is characterized by pre-maar effusive basaltic volcanism [mid-Pleistocene?], followed by the very explosive maar formation, followed by moderately explosive formation of cinder and spatter cones (Dunbar 2005, p. 101)."

The EPU Potrillo-Riley Sector's (PRS's) western boundary-fault system comprises overlapping strands of the southern West Robledo and northwestern Mount Riley fault zones (WRfz and MRfz), with the WRfz merging southward with the La Peña fault zone (LPfz) near the International Boundary (**Figs. 1-8** and **3-11**; **Tbls. 1-4**, **1-5** and **3-3**; **PL. 5k**; *cf.* Seager 1989, 1995). Convergence of the EPfz and MRfz about 2 mi (3 km) south of the International Boundary marks the southeastern tip of the EPU-PRS, and the eastern edge of the Border Tank Corridor (**Fig. 3-12** and **3-13** [III-III′], **PLS. 2** and **5r**). The site is also about the same distance east of the El Volcan group of cinder cones of latest Pleistocene age (~18 ka) that are near the center of Potrillo Maar (107° W longitude; *cf.* Seager et al. 1987, Callahan and Terrazas 1971, Hoffer 2001a; Part **5.5.2b**). In addition, it important to note that tuff-ring deposits on the east flank of Potrillo Maar depression are offset as much as 30 ft (9 m) down-to-east EPfz displacement (**PL. 5r**).

5.7.5. El Aguaje Uplift and PEMEX No. 1–Moyotes Exploration Well

El Aguaje Uplift (EAU) takes its provisional name from El Aguaje, the site of a water well and former service-station on Mexico (Fed,) Highway 2 (**Figs. 1-8** and **1-11**; **Tbl. 1-2**; **TBL. 1**, no. 380 [INEGI 1983c]). It is located between the El Parabién GW Basin (EPB) on the east, and the Border Tank Corridor (BTC) and the Malpais Basin (MpB), respectively, on the northeast and west (**Parts 5.7.2** and **5.7.3**). Basin-scale structural and lithostratigraphic relationships in the EAU area are schematically illustrated on Hydrogeologic Section S-S′ (**PL. 5s**), which follows the general alignment of Highway 2. Because of burial by SFG basin fill, the EAU's structural boundaries are poorly defined in many places. Placement of the bounding La Peña and El Faro fault zones (LPfz and EFfz, **Tbl. 1-5**) is based primarily on interpretations of gravity-survey and deep borehole data by Jiménez and Keller (2000; *cf.* **Part 6.4**).

The only information on deep-subsurface conditions in the EAU is provided by borehole logs from the 16,218-ft (4.943-m) Petróleos Mexícanos (Pemex) Moyotes No. 1 exploration well (Thompson et al. 1978, Tovar et al. 1978; **Fig. 2-2** [**PL. 3**]; **TBL. 1**, no. 397). The well is located in the southwestern Study Area near the junction of Hwy. 2 and the access road to El Faro (**Figs. 1-11** and **3-7a**). As shown on **Plate 5s**, SFG basin fill at the well site is less than 1,000-ft (300-m) thick, and it overlies a thick sequence of Lower Tertiary/Cretaceous/Jurassic/Permian sedimentary rocks. The well penetrated Precambrian "granite-gneiss" (XY) at 15,772 ft (4,810 m) bmsl. Conglomeratic sandstone is well exposed in a low-relief ridge that is located in the central part of the EAU about 1,650 ft (500 m) east of well no. 377 (**Fig. 2.2, PL. 3**). The unit has heretofore been mapped as basaltic rock of Plio-Pliocene age (*cf.* **APNDX. H4.4** [**Fig. H4-8**]). Because it is here interpreted as a sedimentary deposit of Miocene age in the basal SFG, the area of exposures deserves detailed field study in the near future.

CHAPTER 6.
GROUNDWATER BASINS OF THE STUDY AREA AND THEIR PRIMARY HYDROGEOLOGIC SUBDIVISIONS

Emphasis of the second of the Report's three *core* chapters is on the hydrogeologic framework of the Mesilla GW Basin (MeB), and the three GW basins with which it has direct hydraulic linkage: the Southern Jornada, Rincon Valley, and El Parabién Basins (SJB, RVB, and EPB; **Fig. 6-1** and **Tbls. 6-1** and **6-2**). It also includes descriptions of each of the 24 hydrogeologic-mapping units into which the three basins have been subdivided: SJB-2, MeB-20, and EPB-2. Due to subject-matter complexity, several illustrations and tables from **CHAPTERS 1** to **3** are repeated here (e.g., **Figs. 6-1** to **6-3**). Primary framework components comprise three mapping-unit categories:

1. Subbasins (SB)—the primary hydrogeologic subdivisions of GW basins that are associated with the deepest structural depressions and thickest SFG aquifer zones.
2. Highs (H)—deeply buried, structurally positive bedrock terranes in central parts of GW basins
3. Benches (Bn)—areas of transition between the central parts of GW basins and bordering bedrock uplifts with respect to both basin-boundary structure and basin-fill lithofacies composition.

SFG basin-fill deposits in each hydrogeologic-subdivision unit on **Figure 6-2** (**PL. 1B**) are described in terms of primary hydrostratigraphic-unit (HSU) and lithofacies-assemblage (LFA) categories (**Part 4.2**; **Figs. 4-3a** and **4-3b**). The major structural- and lithostratigraphic-elements of the bedrock terrane that are commonly buried at great depth**s** below the land surface are also identified (e.g., **Figs. 6-1** and **6-2;** *cf.* **Parts 2.3.2** and **3.4)**. Basin/subbasin-boundary fault-zones names and acronyms are listed in **Table 6-2**, and compositions of bedrock lithostratigraphic units on hydrogeologic maps and cross-sections are summarized in **Table 6-3** [*cf.* **TBL. 2**]. The 19-section grid of hydrogeologic cross-sections on **PLATE 5** (**5a** to **5s**) graphically portrays information on well-location and depth, as well as the PI's interpretations of HSU identity and dominant LFA composition (cross-sections A-A' to S-S' located on **Figs. 1-4** and **6-1**). **PLATE 5o** is a schematic depiction of basin-scale hydrogeologic relationships beneath the river valley/canyon floors throughout the Study Area (*cf.* **Part 3.2.3**).

Figure 6-2 (**PL. 1B**) is a provisional interpretation of the Study Area's buried-bedrock (basin-fill subcrop) topography and latter's major lithostratigraphic and structural components. The map is a digital synthesis of surface- and subsurface-geologic, borehole-log, and geophysical-survey information that was initially compiled at a scale of 1:100,000 on a 2017 Google Earth® image base (*cf.* **Parts 2.3.3** and **3.6.2**, **Figs. 3-11** and **3-12**, and **APNDX. A3**). Contour intervals on the structure-contour map are 25, 50 and 100 m, and fault zones and lithostratigraphic mapping units are defined in **Tables 6-2 and 6-3.**

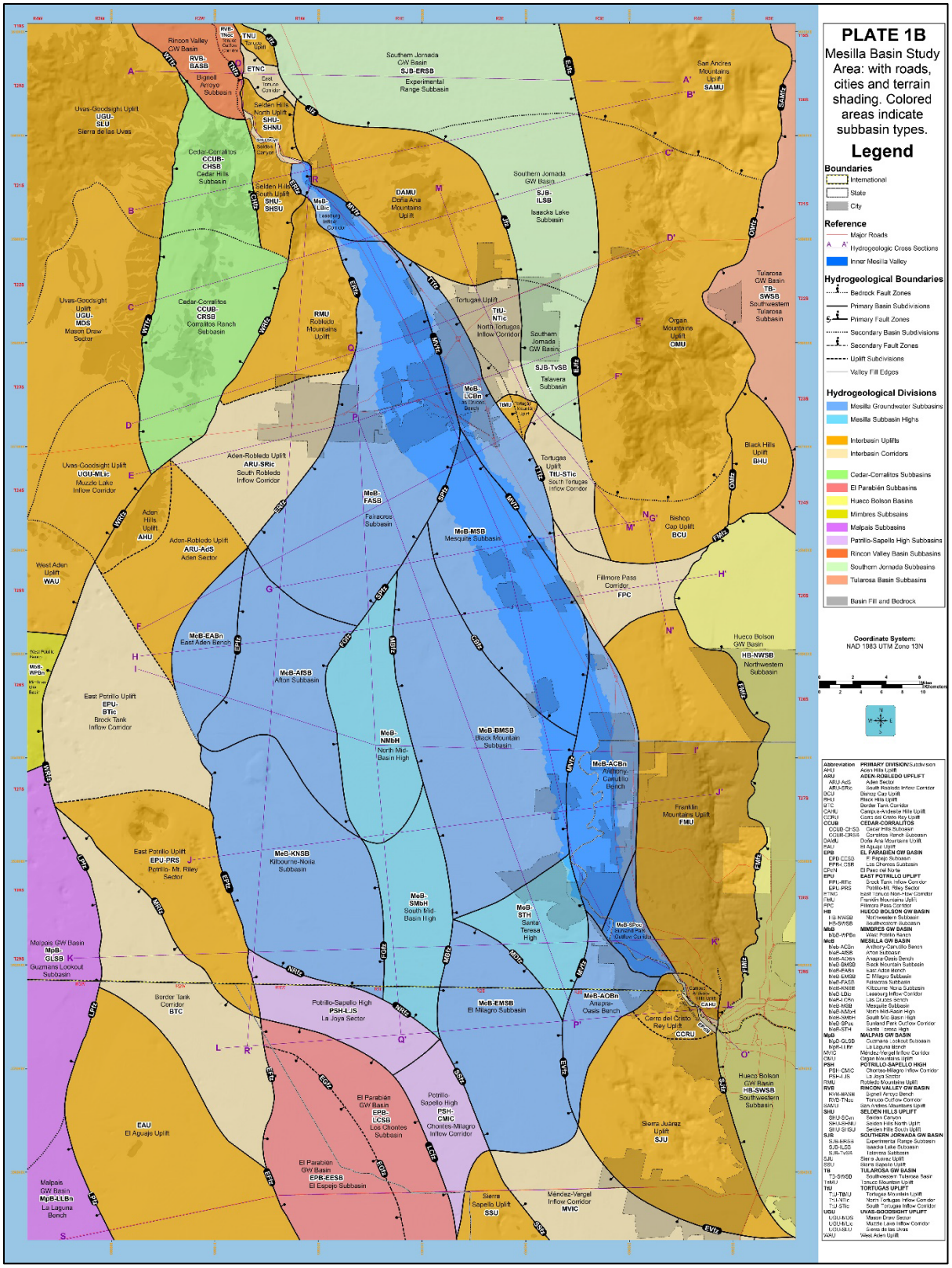

Figure 6-1 (page-size **PL. 1B).** Index map for major hydrogeologic subdivisions of the Study Area (**Tbls. 6-1 and 6-2**; *cf.* **Parts 2.3.2** and **3.4)**. **PLATE 1** (USGS DEM) base.

Table 6-1. Names and Acronyms of Hydrogeologic Subdivisions shown on Maps, Cross-Sections, and the Well-Information Spreadsheet (PLS. 1 to 8, TBLS. 1 and 2, and Fig. 6-1)

ACRONYM	RIO GRANDE (RG) VALLEY AND CANYONS (NARROWS)
EPdN	El Paso del Norte (Cyn)
MeV	Mesilla Valley
SCyn	Selden Canyon (Cyn)
EPJV	El Paso-Juárez Valley

ACRONYM	MESILLA GW BASIN (MeB)	SUBDIVISION (AREA in km²)
MeB-ACBn	Mesilla Basin	Anthony-Canutillo Bench (138)
MeB-AfSB	Mesilla Basin	Afton Subbasin (180)
MeB-AOBn	Mesilla Basin	Anapra-Oasis Bench (72.7)
MeB-BMSB	Mesilla Basin	Black Mountain Subbasin (353)
MeB-EABn	Mesilla Basin	East Aden Bench (70.7)
MeB-EMSB	Mesilla Basin	El Milagro Subbasin (203)
MeB-FASB	Mesilla Basin	Fairacres Subbasin (382)
MeB-KNSB	Mesilla Basin	Kilbourne-Noria Subbasin (278)
MeB-LBic	Mesilla Basin	Leasburg Inflow Corridor (25.4)
MeB-LCBn	Mesilla Basin	Las Cruces Bench (97.5)
MeB-MSB	Mesilla Basin	Mesquite Subbasin (228)
MeB-NMbH	Mesilla Basin	North Mid-Basin High (143)
MeB-SMbH	Mesilla Basin	South Mid-Basin High (121)
MeB-STH	Mesilla Basin	Santa Teresa High (89.5)
MeB-SPoc	Mesilla Basin	Sunland Park Outflow Corridor (33.4)

ACRONYM	OTHER GW BASINS (B)	SUBDIVISION
EPB	El Parabién Basin (N-part—Drains to MeB)	
EPB-EESB	El Parabién Basin	El Espejo Subbasin (158)
EPB-LCSB	El Parabién Basin	Los Chontes Subbasin (126)
HB	Hueco Bolson (W-edge—Receives inflow from MeB through EPdN)	
HB-NWSB	Hueco Bolson	Northwestern Subbasin
HB-SWSB	Hueco Bolson	Southwestern Subbasin
MbB	Mimbres Basin (No-flow boundary with MeB; surface and subsurface flow to Zona Hidrogeológica Conejos Médanos (ZHGCM)	
MbB-WPBn	Mimbres Basin	West Potrillo Bench
MpB	Malpais GW Basin (E-edge—connects with BTC, MbB, and LMB)	
MpB-GLSB	Malpais Basin	Guzmans Lookout Subbasin (SB)
MpB-LLBn	Malpais Basin	La Laguna Bench (Bn)
RVB	Rincon Valley GW Basin (Drains to MeB through SCyn)	
RVB-BASB	Rincon Valley Basin	Bignell Arroyo Subbasin (47.2)
RVB-TNoc	Rincon Valley Basin	Tonuco Outflow Corridor (5)
SJB	Southern Jornada GW Basin (Drains to MeB and RVB)	
SJB-ERSB	Southern Jornada Basin	Experimental Range Subbasin (264)
SJB-ILSB	Southern Jornada Basin	Isaacks Lake Subbasin (164)
SJB-TvSB	Southern Jornada Basin	Talavera Subbasin (68.2)
SWTB	Southwestern Tularosa Basin	

ACRONYM	UPLAND GW BASIN	SUBDIVISION
CCUB	Cedar-Corralitos Upland Basin (UB)	
CCUB-CHSB	Cedar-Corralitos	Cedar Hills Subbasin (96.2)
CCUB-CRSB	Cedar-Corralitos	Corralitos Ranch Subbasin (205)

Table 6-1 (concluded). Names and Abbreviations of Hydrogeologic Subdivisions

ACRONYM	INTERBASIN HIGH (IBH)	SUBDIVISION
PSH	Potrillo-Sapello High (163)	
PSH-LJS		La Joya Sector (93.5)
PSH-CMIC		Chontes-Milagro Inflow Corridor (69.5) (EPB-LCSB to MeB-EMSB)

ACRONYM	INTERBASIN UPLIFT (U)	SUBDIVISION
AHU	Aden Hills Uplift	
ARU	Aden-Robledo Uplift	
ARU-AdS	Aden-Robledo Uplift	Aden Sector (S)
ARU-SRic	Aden-Robledo Uplift	South Robledo Inflow Corridor (145)
BCU	Bishop Cap Uplift	
BHU	Black Hills Uplift	
CAHU	Campus-Andesite Hills Uplift	
CCRU	Cerro del Cristo Rey Uplift	
CMU	Camel Mountain Uplift	
DAMU	Doña Ana Mountains Uplift	
EAU	El Aguaje Uplift (310)	
EPU	East Potrillo Uplift	
EPU-BTic	East Potrillo Uplift	Brock Tank Inflow Corridor (227)
EPU-PRS	East Potrillo Uplift	Potrillo-Mt. Riley Sector (S)
FMU	Franklin Mountains Uplift	
OMU	Organ Mountains Uplift	
RMU	Robledo Mountains Uplift	
SAMU	San Andres Mountains Uplift	
SHU	Selden Hills Uplift	
SJU	Sierra Juárez Uplift	
SSU	Sierra Sapello Uplift (41)	
TNU	Tonuco Uplift	
TtU	Tortugas Uplift	
TtMU	Tortugas Uplift	Tortugas Mountain Uplift (U)
TtU-NTic	Tortugas Uplift	North Tortugas Inflow Corridor (63.5)
TtU-STic	Tortugas Uplift	South Tortugas Inflow Corridor (59.2)
UGU	Uvas-Goodsight Uplift	
UGU-SLU	Uvas-Goodsight Uplift	Sierra de las Uvas (U)
UGU-MDS	Uvas-Goodsight Uplift	Mason Draw Sector (S)
UGU-MLic	Uvas-Goodsight Uplift	Muzzle Lake Inflow Corridor (ic, to the Mimbres Basin-MbB)
WAU	West Alden Uplift	

ACRONYM	INTER-BASIN GROUNDWATER-FLOW CORRIDORS
BTC	Border Tank Corridor (214) (Malpais Basin to El Parabién Basin GW flow)
ETNC	East Tonuco Corridor (13.5) (Jornada Basin to Rincon Valley Basin GW flow)
FPC	Fillmore Pass Corridor (73.7) (Mesilla Basin-Hueco Bolson—potential inter-basin GW flow)
MVIC	Méndez-Vergel Inflow Corridor (115) (possible Hueco Bolson to Mesilla Basin GW flow)

Table 6-2. Names and Acronyms for Boundary-Fault Zones* of the Study Area's Major GW Basins (TBL. 3; PLS. 1, 2, 5 and 9, and Tbl. 6-1)

Map-Unit Acronyms and Names	Bordering Hydrogeologic-Map Subdivisions (**Fig. 6-1**, **Tbl. 6-1**)
Southern Jornada Basin (SJB)	
West Side	
Jfz—Jornada fz (**A1**, **B2**, **C1**)*	ERSB/SDMU-ETNC-DAMU, ILSB/DAMU, TSB/TtU
East side	
EJfz—East Jornada fz (**A3**, **B3**, **C2**)	ERSB/SAMU, ILSB/OMU, TSB/OM
Mesilla Basin (MeB)	
MeB Border	
West Side (N to S)	
ERfz—East Robledo fz (**A1**, **B1**, **C2**)	LBic/RMU, FASB/RMU—ARU-RS
EPfz—East Potrillo fz-S (**A1**, **B1**, **C1-2**)	KNSB/EPU-BTic, KNSB/EPU-PRS
NRfz—Noria fz (**A3**, **B3**, **C2, C4**)	KNSB/PSH-LJS, SMBH/PSH-LJS
SSfz—Sierra Sapello fz (**A3**, **B3**, **C3-4**)	EMSB/PSH-CMIC
East Side (N to S)	
MVfz—Mesilla Valley fz-N (**A3**, **B3**, **C2**)	LBic/DAMU
TTfz—Tortugas fz (**A3**, **B3**, **C2**)	LCBn/DAMU, LCBn/TtU, LCBn/FPC
MVfz—Vado Hill Segment (**A3**, **B3**, **C2**)	MSB/FPC
MeB Interior (Intra-Basin)	
North and West of Mid-Basin High (MBH)	
MVfz—Mesilla Valley fz-C (**A3**, **B4**, **C2**)	FASB/LCBn
SPfz—San Pablo fz (**A3**, **B3**, **C2**)	FASB/MSB, FASB/BMSB, FASB/NMBH
FGfz—Fitzgerald fz (**A2**, **B2**, **C2**)	AfSB/NMBH, KNSB/sMBH
EPfz—East Potrillo fz-N (**A2**, **B4**, **C2**)	AfSB/EABn.
East of Mid-Basin High (MBH)	
MVfz—Mesilla Valley fz-S (**A3**, **B4**, **C2**)	MSM/ACBn, BMSB/ACBn, STBn/ACBn, STH/AOBn
CBfz—Chamberino fz (**A2**, **B2**, **C3**)	MSB/BMSB
MBfz—Mid-Basin fz (**A3**, **B3**, **C4**)	BMSB/NMBH, BMSB/SMBH, EMSB/SMBH
MDfz—Mastodon fz (**A1**, **B2**, **C2**)	EMSB/STH
EVfz—El Vergel fz-N (**A3**, **B4**, **C2**)	EMSB/AOBn
El Parabién Basin (EPB)	
West side	
EFfz—El Faro fz (**A2**, **B4**, **C1**)	LCSB/BTC
East Side	
LCfz—Las Cuates fz (**A2**, **B2**, **C1**)	EESB/BTC, EESB/EAU
El Parabién Basin Interior (Intra-Basin)	
EGfz—El Girasol fz (**A2**, **B2**, **C2**)	EESB/LCSB

**Qualitative Fault-Zone Attributes*

A. Plio-Pleistocene (<5 Ma) Fault-Zone Activity: A1. High, A2. Moderate, A3. Low

B. Fault-Zone Topographic Definition: B1. High, B2. Moderate, B3. Low, B4. Buried

C. Fault-Zone Subsurface Definition (e.g., borehole and/or geophysics):
C1. High, C2. Moderate, C3. Low, C4. Deeply Buried

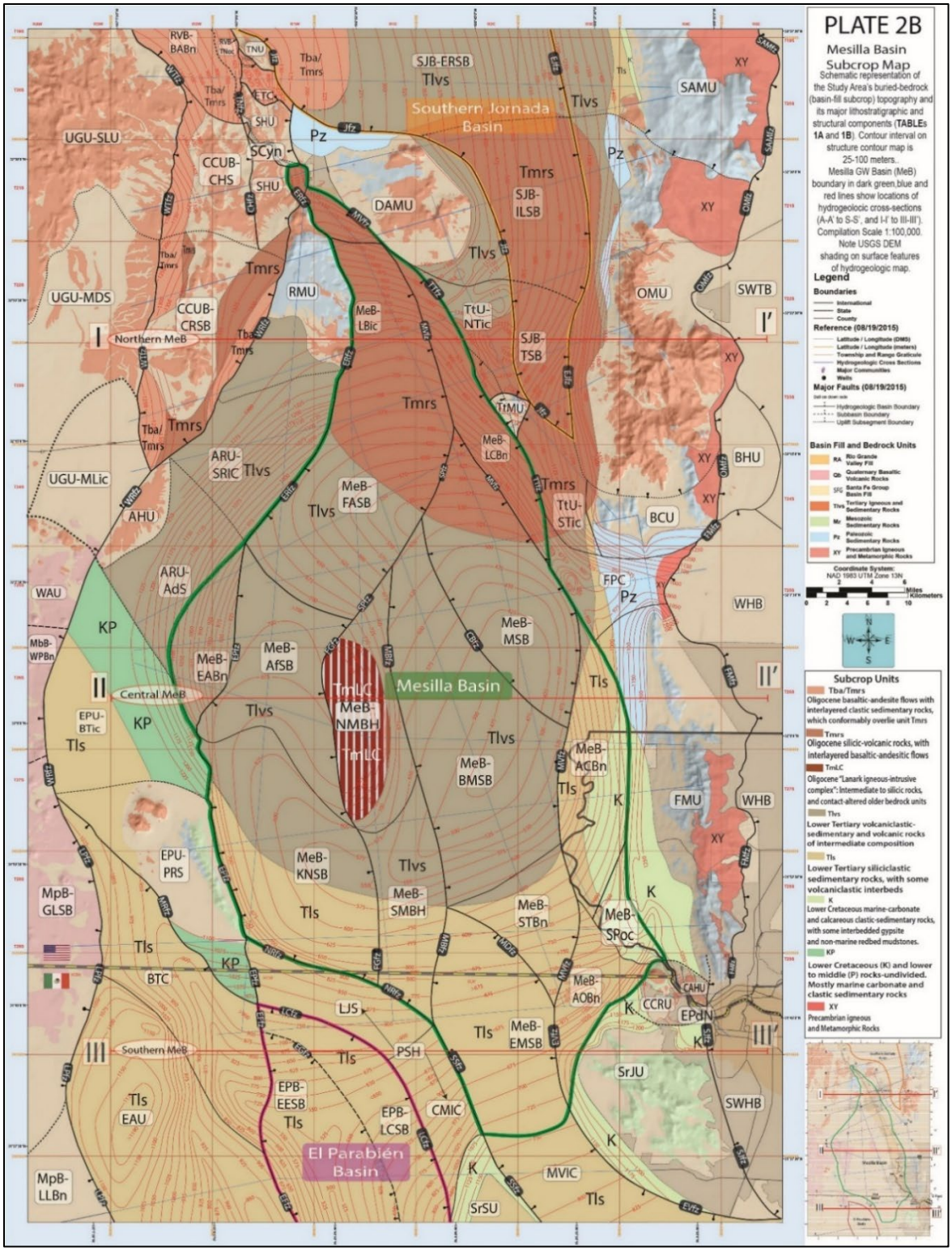

Figure 6-2 (page-size **PL. 2B).** Schematic depiction of basin-fill subcrop topography, and primary lithostratigraphic and structural components in the Study Area, with explanation on **Tables 6-1 and 6-3**. Structure contours are at 25, 50, and 100 m intervals, and W-E red lines show locations of cross-sections I-I' to III-III' (**Fig. 6-3**). **PLATE 1** Hydrogeologic-Map base.

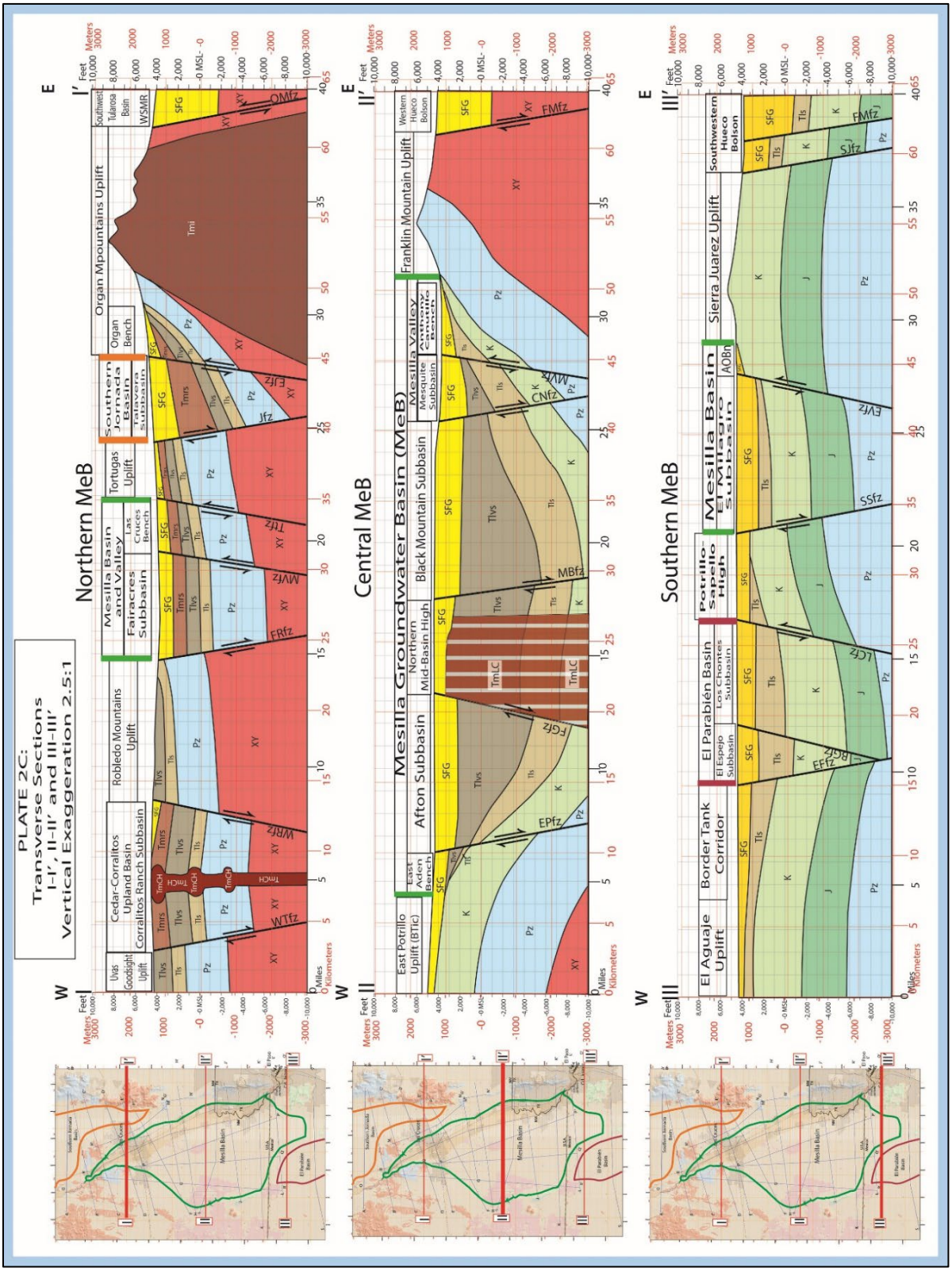

Figure 6-3 (page-size **PL. 2C**)**.** Schematic geologic cross-sections I-I' to III-III' that show major subsurface stratigraphic and structural relationships in the central and southern parts of the Study Area. Explanation on **Table 6-3**, with geologic-section locations on **Figure 6-2.**

Table 6-3. Explanation of Lithostratigraphic Units on Figures 6-2 and 6-3

Rio Grande (RG) Rift Basin Fill (Upper Oligocene to Lower Pleistocene)

SFG Santa Fe Group Hydrostratigraphic Units (HSUs)-Undivided. Includes alluvial deposits of the inner Rio Grande Valley (**RA**), and thin, but locally extensive basaltic volcanics (**Qb**). Mostly middle to late Quaternary age

Middle to Lower Tertiary Igneous Extrusive/Intrusive and Non-marine Sedimentary Rocks

Tba Basaltic andesite lava flows and vent-zone units, with interlayered mudstones, sandstones and conglomerates volcanic rocks—late Oligocene Uvas Basaltic Andesite correlative

TmCH Cedar Hills vent zone. N-S aligned series of flow-banded rhyolite domes and feeder conduits intruded into the Cedar-Corralitos Upland Basin stratigraphic sequence—Oligocene

TmLC Lanark Complex—Intermediate to silicic igneous-intrusive complex that forms central part of the Northern Mid-Basin High and is buried by at least 1,500 ft (455 m) of SFG basin fill—Oligocene (*cf.* **PLS. 2, 5i** and **5q**; Phillips-Sunland oil test: **TBL. 1,** no. 237; Clemons 1993)

Tmrs Silicic pyroclastic and volcaniclastic rocks—Oligocene, mainly rhyolite and dacitic ashflow tuffs and tuffaceous sandstones, with some capping basaltic-andesite flows (**Tba**)

Tmi Intermediate to silicic (felsitic) plutonic rocks in the Organ and Dona Ana Mountains, and Mt. Riley-Cox and **TmLC** areas, including monzodiorite to syenite stocks—Oligocene and Late Eocene (Seager et al. 1987, Clemons 1993, Seager 1995)

Tlvs Volcaniclastic and epiclastic-sedimentary rocks, and local basal gypsite beds, with andesitic to dacitic flows and breccias—Eocene Palm Park and Rubio Peak Fm correlative that is exposed in uplifts flanking much of the northern and central Study Area. The unit is about 3,880 ft (1,183 m) thick in the Mobile-Grimm oil test (**PLs 5q**, **TBL. 1**, no. 180; Clemons 1993).

Tls Mostly siliciclastic sedimentary rocks, sandstones, mudstones and conglomerates with minor or no volcanic constituents. General correlative of lower Eocene/Paleocene Love Ranch/Lobo Fms. The unit is about 7,000 ft (2,134 m) thick in the Mobil-Grimm oil-test well (**TBL. 1**, no. 180). An inferred correlative sequence of siliciclastic rocks is at least 1,000 ft (330 m) thick in the Pemex-Moyotes oil-test well (**PL. 5s**, **TBL. 1**, no. 397; Clemons 1993, Jiménez and Keller 2000)

Tli Andesitic-intrusive rocks in the El Paso de Norte-Cerro de Cristo Rey area—Eocene

Mesozoic Sedimentary Rocks-Mostly Marine, and Commonly Structurally Deformed

K Lower Cretaceous marine rocks-undivided. Sandy to shaly limestone, coquina limestone, silty shale, calcareous sandstone, and limestone-pebble conglomerate, with local occurrences of gypsite beds. Approximately 1550-2200 ft (470-670 m) thick were exposed in the Sierras Juárez and Sapello, Cerro Cristo Rey, and the East Potrillo Mountains. 1,050 ft (320 m) penetrated in the Grimm oil-test well (**TBL. 1**, no. 180). In the Pemex-Moyotes oil-test well, the Lower Cretaceous section is 5,512 ft (1,680 m) thick (**PL. 5s**, **TBL. 1**, no. 397)

J Jurassic marine rocks-undivided: limestone, shale, and gypsite, with local occurrences of halite beds beneath the southeastern-most part of the Study Area. Present in the shallow subsurface but nor exposed in Sierra Sapello. A 3,380 ft (1,130 m) thick Jurassic section was penetrated in the Pemex-Moyotes oil-test well between Permian (**P**) and Lower Cretaceous (**K**) rocks (**PL. 5s**, **TBL. 1**, no. 397)

Paleozoic Sedimentary Rocks-Mostly Marine, and Commonly Structurally Deformed

Pz Paleozoic rocks, **Pzu/Pzl**-undivided

Pzu Upper Paleozoic (Pennsylvanian and Permian) rocks-undifferentiated: primarily limestone and redbed mudstones, with shale, sandstone and some gypsite

Pzl Middle and Lower Paleozoic rocks-undivided: Middle Paleozoic (Devonian and Mississippian)—primarily limestone, with shale. Lower Paleozoic (Cambrian-Ordovician-Silurian)—primarily limestone and dolomite, with thin basal sandstone

Proterozoic (Precambrian) Rocks

XY Igneous and metamorphic rocks-undivided

Along with the fence-diagram grid of 19 hydrogeologic cross-sections on **PLATES 5a** to **5s** **Figures 6-2** and **6-3** provide the primary spatial frame of reference for the descriptions of subsurface hydrogeologic-boundary controls on the basin-scale GW-flow and hydrochemistry in **CHAPTERS 5** to **7**. The **Figure 6-3** (**PL. 1C**) cross-sections offer a general 3-D perspective to the subsurface hydrogeologic-framework map on **Figure 6-2** (**PL. 1B**). Cross-section VE is about 2.5x and the base elevation is 10,000 ft (~3,000 m) below mean sea level (bmsl). **PLATES 6** and **7** are sets of structure-contour and isopleth maps that are designed to convey essential basin-scale hydrogeologic information needed for GW-flow and hydrochemical modeling (*cf.* **Parts 2.3.2** and **7.1**). The combined lithofacies-assemblage (LFA), and hydrostratigraphic-unit (HSU) thickness and surface-area interpretations on the isopleth maps (**PL. 7**) facilitates estimations of hydraulic-property ranges for individual HSUs (*cf.* **4.2**). Basin-scale information on deep-seated (bedrock/structural)-framework components is also schematically portrayed in two block-diagram compilations to a depth of 25,000 ft (7 km) below msl (**Figs. 3-9** and **3-10** [**PLS. 8A** and **8B**]).

As noted in **Parts 1.1.3** and **1.1.4**, criteria for the basin-scale (here ~1:100,000) hydrogeologic characterization of GW Basins and their major subdivisions differ significantly from those developed by the NM OSE for determining "reasonably ascertainable boundaries" of a given "declared groundwater basin" (*see* https://www.ose.state.nm.us/WR/groundWater.php).

The MeB is hydrologically linked, directly or indirectly, with parts of the six adjacent RG-rift basins (**Figs. 1-9** and **6-1**; **Tbl. 6-1**; **PLS. 2** and **4**). In general north-south, east-west location order, they comprise the: (1) Lower Rincon Valley (RVB), (2) Southern Jornada (SJB), (3) Southwestern Tularosa (SWTB), (4) Western part of the Hueco [Bolson] (WHB, SWHB), (5) Malpais (MpB), and (6) El Parabién (EPB). All have some degree of hydraulic connection with the through-going Rio Grande (RG) fluvial system via surface and/or subsurface flow (**Figs. 1-9** and **1-13**, *cf.* **Fig. 6-21**). The MeB (**Part 6.3**) and five other GW basins with which it has, or potentially has, a significant hydraulic connection receive the most-detailed coverage in the following Chapter sections (**Parts 6.2** to **6.4**; **Fig. 6-1, Tbl. 6-1**):

1. Southern Jornada Basin (SJB): Direct inflow—third-order contribution (**Part 6.1**).
2. Rincon Valley Basin (RVB): Direct inflow—first-order contribution (**Part 6.2**).
3. El Parabién Basin (EPB): Direct inflow—first-order contribution potential (**Part 6.4**).
4. Malpais Basin: Indirect inflow, via Border Tank Corridor and El Parabién Basin (BTC and EPB)—second-order contribution potential (**Parts 5.7.2** to **5.7.4**, *cf.* **7.5.5** and **7.6.2**).
5. Western Hueco Bolson (WHB) and southwestern Tularosa Basin (SWTB): Limited direct outflow, with some potential for third-order GW flow via the Fillmore Pass Corridor (**Parts 5.1.2** and **7.5.2**).

6.1. SOUTHERN JORNADA GW BASIN (SJB)

The Southern Jornada Ground Water Basin (SJB) is located in the northeastern part the Study Area (**Fig. 6-1** and **6-2**, and **Tbl. 6-1**; **PLS. 1B, 1C** and **5a-5f;** *cf.* King et al. 1971, Wilson et al. 1981**,** Shomaker and Finch 1996, Hawley et al. 2005, Kambhammettu et al. 2010). It has three subbasin components: Experimental Range (ERSB), Isaacks Lake (ILSB), and Talavera Subbasins (TvSB). The SJB is bounded on the east by the southern San Andres and northern Organ Mountains Uplifts (SAMU and OMU) (*cf.* **Parts 5.1** and **5.1.1**; Seager et al. 1987). The partly buried bedrock uplifts that form the'basin's western border comprise (in north to south order) the Tonuco Mountains, Selden Hills, Doña Ana Mountains, and Tortugas Uplift (TNMU, SHU, DAMU and TtU/TtMU; *cf.* **5.2**). The Jornada fault zone (Jfz, **Tbl. 6-2** [**TBL. 3**]) forms the SJB's well-defined western structural-boundary with the TMU-SHU-DAMU-TtU/TtMU series of bedrock uplands. A more-poorly defined East Jornada fault zone (EJfz) separates the eastern SJB from the southern San Andres-Organ Mountains range (SAMU-OMU; Seager et al.1987, Maciejewski and Miller 1998). EJfz is also named the "West-Side fz" by Seager (1981).

6.1.1. Experimental Range Subbasin (ERSB)

The Experimental Range Subbasin (ERSB) of the SJB is a topographically *closed* structural depression with a mapped area of almost 100 mi² (260 km²) (**Figs. 6-1** and **6-2**, and **Tbls. 6-1** to **6-3**; **PLS. 1B, 2** and **5a-5b**; *cf.* Doty 1963, Seager et al.1987, Giles and Pearson 1998, Maciejewski and Miller 1998, Hawley et al. 2005). Three- to four-hundred feet (90-120 m) of mostly unsaturated HSU-USF2 deposits (LFAs 1 to 3) underlie the extensive ARG fluvial-plain (La Mesa geomorphic-surface) that occupies most of the subbasin area (**PLS. 5a** and **5b**). Fine-grained basin-floor and distal-piedmont conglomeratic sandstone lithofacies assemblages (LFAs 10 and 7) of HSUs MSF and LSF form the bulk of the saturated basin fill, and the thickness of HSU-MSF/LSF deposits is in the 1,500 to 3,500-ft (450 to 1,070-m) range (**PL. 7**). Estimated saturated-thickness of HSU-USF (LFA 3 and 5) is in the 100- to 300-ft (30-90 m) range only in the southernmost part of the ERSB, while thickness ranges for units MSF and LSF (LFA 9 and 10) are, respectively, 600 to 1,400 ft (180-425 m), and 1,500 to 2, 500 ft. (455-760 m) throughout mapped part of the subbasin (**PLS. 7B** and **7C**).

Eocene andesitic volcanic and volcaniclastic rocks (Tlvs-**Tbl. 6-3**) underlie SFG basin fill in most of the ERSB area, and are overlapped by silicic-volcanic rocks and basaltic-andesite flows of latest Eocene to late Oligocene age in its western part (**Fig. 6-2** [**PL 1B**]; Tmrs and Tba**-Tbl. 6-3**). At southern edge of the subbasin, the Tlvs-subcrop terrane includes a small area of overlapping silicic volcanic and associated epiclastic rocks of unit Tmrs, with ultimate DAMU and OMU caldera sources (**PLS. 1**, **2**, and **9**; **Tbl. 6-3** [**TBL. 2**]). The ERSB contributes small amounts of brackish-water underflow to the Rincon Valley Basin (RVB) in two places:

1. The East Tonuco Corridor (ETNC) between the Tonuco and Selden Hills Uplifts (TNU and SHU-**Part 5.2.2**).
2. An unnamed "corridor" unit between the TNU and Rincon Hills, where underflow from the westernmost ERSB discharges to the central RVB near the mouth of Rincon Arroyo and the Village of Rincon (I-25/BNSFRR-Overpass area).

6.1.2. Isaacks Lake Subbasin (ILSB)

The Isaacks Lake Subbasin (ILSB) of the SJB is also topographically *closed*, and has a surface area of about 55 mi² (140 km²) (**Figs. 6-1** and **6-2** and **Tbls. 6-1** to **6-3**; **PLS. 5b** to **5d**; **APNDX. F: Pls. F2-8**, **F3-2a, F4-3b**, and **F6-1b** to **1f**). It is named for Isaacks Lake playa (floor-alt. 4,285-ft, 1,306-m amsl), the terminal *sink* for all surface runoff, much of which is derived from ephemeral-stream watersheds in the southern San Andres, northern Organ, and Doña Ana Mountains Uplifts (SAMU, OMU, and DAMU, **Parts 5.1.1** and **5.2.1**). Piedmont slopes are the dominant landform, and, in marked contrast to ERSB, the USF2-ARG fluvial-plain (La Mesa surface) occupies a relatively small part of the subbasin (eastern **PL. 5b** to **5d**). Silicic-volcanic and volcaniclastic rocks of latest Eocene to middle Oligocene age, with caldera sources in the OMU and DAMU, underlie SFG deposits throughout the subbasin (**Fig. 6-2**; Tmrs-**Tbl. 6-3**).

Most of the SFG basin fill is composed of medium- to coarse-grained, distal- to medial-piedmont lithofacies assemblages (LFAs 5 and 7) of the USF1/MSF1/LSF Hydrostratigraphic-Unit sequence. A much smaller proportion of SFG deposits comprise fluvial-facies (mostly LFA 3) sediments in HSUs USF2 and MSF2). Basin-fill thickness is in the 1,500 to 3,000-ft (450 to 900-m) range, with upper 300 to 400 ft (90-120 m) in the vadose zone (**PLS. 4** and **7A** [upper]). Estimated saturated-thickness of HSU-USF–LFA 3 and 5 is in 100- to 500-ft (30-150 m) range, and thickness ranges for units MSF and LSF (LFA 7) are, respectively, 500 to 1,000 ft (150-300 m), and 700 to 1, 400 ft (215-430 m) (**PLS. 5b** to **5d**, **7B** [middle] and **7C** [lower]).

The SJB-ILSB contributes some fresh and brackish GW underflow northward to the SJB-ERSB. However, the significant amount of fresh water in aquifer storage has been and is being utilized (i.e. *mined*) for industrial use at the NASA White Sands Test Facility and residential-subdivision use in the Moongate-Butterfield Park-Talavera area (Doty 1963; King et al. 1971; Wilson et al. 1981; Shomaker and Finch 1996; Giles and Pearson 1998; Hawley et al. 2005).

6.1.3. Talavera Subbasin (TvSB)

The SJB's Talavera Subbasin (TvSB) is a topographically *open* and *drained* structural depression at the southernmost Jornada del Muerto Basin system of the RG rift (**Figs. 6-1** and **6-2**, and **Tbls. 6-1** to **6-3; PLS. 5d** to **5f**; **APNDX. F: Pls. F2-8**, **F3-2b** and **2c**, **F4-3a**, and **F6-1b** to **1f**; *cf.* L. Woodward et al.

1978, Keller and Cather 1994). From a hydrographic perspective, the TvSB is within the MeB's surface- and subsurface-watershed (**Fig. 1-9** [**Pl. 4**]) and has a surface area of about 23 mi² (60 km²). It takes its provisional name from the Las Cruces suburban Talavera Subdivision that is located between Tortugas Mountain and the southern Organ Mountains Uplift (TtMU and OMU). The TvSB is bounded on the east by the central and southern OMU and on the west by the Tortugas Uplift (TtU-**Part 5.1.2**), and its southern structural termination is formed by the convergence of the Jornada and East-Jornada fault zones (Jfz and EJfz, **Tbl. 6-2**).

Silicic-volcanic and volcaniclastic rocks of latest Eocene to middle Oligocene age, with a caldera source in the OMU, underlie the basin fill throughout the subbasin area (**Fig. 6-2** [**PL. 1B**]; Tmrs-**Tbl. 6-3**; Seager 1981; Seager et al. 1987; Gunaji-Klement & Associates 1994). SFG deposits in the SJB-TvSB are primarily composed of medium- to coarse-grained (distal to medial), piedmont lithofacies assemblages in the USF1/MSF1/LSF HSU sequence (LFAs 5 and 7; **PLS. 5d** to **5f** and **PLS. 7A to 7C**). Basin-fill is less than 1,500 ft (450 m) thick, and vadose-zone thickness is in the 200 to 300 ft (60 to 90 m) range. Estimated saturated-thickness of HSU-USF1–LFA 5 is in 300 to 600 ft (90-180 m) range, and thickness range for unit MSF (LFA 7) is 200 to 900 ft (60-270 m) (**PLS. 5d** to **5f**, and **7A** and **7B**). Inferred thicknesses of underlying HSU-LSF deposits (LFAs 7 and 8) range from less than 100 ft (30 m) to about 600 ft (180 m) (**Fig. 6-3**, **PLS. 5d** to **5f**, and **7C**).

Most surface-runoff from the TvSB discharges to the northeastern MeB through the valleys of larger arroyos that cross buried parts of the TtU both north and south of Tortugas Mountain (TtMU-**Figs. 6-1** and **6-2**; **PLS. 1B, 2, 5e, 5f,** and **5m**; *cf.* **Parts 5.2.3** and **7.5.1**; Woodward and Myers 1997, Hawley and Kennedy 2004). The western slopes of the OMU and parts of the TvSB contribute a significant amount of fresh GW recharge to the MeB via the North and South Tortugas Inflow Corridors (NTic and STic). The latter comprise a few shallow buried valleys cut into parts of the TtU located north and south of the TtMU (**Part 7.5.1**).

6.2. LOWER RINCON VALLEY GW BASIN (RVB)

"Rincon Valley Basin (RVB)" is the informal name for a hydrographic and structural-geologic unit that (1) includes the valley of the Rio Grande, and (2) is located between southern Palomas and Jornada del Muerto RG-rift Basins (**Figs. 6-1** and **6-2**). As defined herein, the RVB extends from near the Village of Hatch to the head of Selden Canyon (SCyn, **3.1.3a**), and the Village of Rincon is located at its north-central border (**APNDX. F: Pls. F4-1b** to **1e**). A low-gradient river-valley floor (~0.001) and steep valley-border slopes comprise the dominant terrain components, with the latter features bounded by the southern Caballo Mountain Range and Rincon Hills to the north, and Sierra de las Uvas (SLU) to the south and west (Seager and Hawley 1973; Clemons and Seager 1973; Seager et al. 1975, 2015; Hawley et al. 2005).

Basic hydrostratigraphic and structural relationships in the mapped part of the RVB are illustrated on **Figure 6-2** (**PL. 2B**), and **PLATES 5a** and **5o**. It has an area of about 20 mi² (50 km²), and Tonuco and Ward Tank fault zones (TNfz and WTfz) form the Basin's respective eastern and western structural boundaries (**Tbl. 1-5**). In north to south order, the RVB is separated from the Experimental Range Subbasin (ERSB) of the Southern Jornada Basin (SJB) by (1) an unnamed, mostly buried bedrock uplift that connects the Rincon Hills and Tonuco Uplift (TNU), (2) San Diego Mountain, (3) the East Tonuco Corridor (ETNC), and (4) the northern part of the Selden Hills Uplift (*cf.* **Part 5.2.2**; Seager and Hawley 1973, Seager 1975b). The Bignell Arroyo Subbasin (BASB), which forms the western, valley-border section of the RVB, is named after a large RG tributary that crosses its central part and has its headwaters in the eastern foothills of the Sierra de las Uvas (UGU-SLU, **Fig 6-1**; *cf.* Seager et al. 1975). The BASB is underlain by as much as 3,000 ft (900 m) of low-permeability, middle and lower SFG mudstones and conglomeratic sandstones (mostly HSU-MSF2/LSF, LFAs 9 and 7). No basin-fill aquifer units of significance are present in the 20 mi² (50 km²) mapped part of the subbasin.

The RVB's inner-valley section is provisionally named the Tonuco Outflow Corridor (TNoc) herein (**Fig. 6-1**, **Tbl. 6-1**; *cf.* **Part 3.1.3a**). It occupies about 4 mi² (10 km²) of the mapped area, and serves as the primary conduit for surface and shallow-subsurface water flow to Selden Canyon of the Rio Grande and the MeB. The TNoc is bounded on the east by the TNU, the East Tonuco Corridor (ETNC), and the northern Selden Hills Uplift (SHU). Eastward-dipping mudstones and conglomeratic sandstone, which are exposed in the BASB to the west, are buried by no more than 80 ft (25 m) of Rio Grande alluvium (HSU-RA), with the latter forming the only significant aquifer unit throughout the RVB (**PLS. 5a** and **5o**; *cf.* Hawley et al. 2005, Tillery and King 2006, Schmid et al. 2009). The inner-valley sequence of coarse- to medium-grained fluvial deposits is capped by a surficial layer of medium- to fine- grained channel and overbank sediments. The latter forms an important soil-resource base with long-term capability for irrigation agriculture within the Rio Grande Project surface-water allocation structure (**Fig. 1-8**; *cf.* Sweet and Poulson 1933, Conover 1954, Maker et al. 1980, Wilson et al. 1981, Esslinger 1996 and 1998, SSURGO 2002/2003, Tillery et al. 2009).

6.3. MESILLA GW BASIN (MeB)

The Mesilla GW Basin (MeB) comprises the largest RG-rift depression in the Study Area (**Fig. 1-4**), and saturated parts of its thick SFG basin fill form the primary integrated system of aquifers in the southern New Mexico border region (*cf.* **Figs. 6-1** and **6-2**; **PLS. 1** to **5** and **7**; **Parts 3.6** to **3.9**). Information on the MeB's hydrogeologic subdivisions in **Table 6-4** has been compiled in a manner that most effectively conveys current interpretations of basin-scale framework controls on GW flow and chemistry (*cf.* **Tbl. 6.1** and **Part 7.1**). The 30 million-year (Ma) history of RG-rift basin evolution also dictates that most of the hydraulic/hydrologic boundaries between the MeB's 15 hydrogeologic

subdivisions are, rather than discrete faults, actually narrow zones of structural transition that exhibit progressively greater offset of hydrostratigraphic units (HSUs) as their age increases (**Figs. 1-10** and **6-1** and **6-2**; **PLS. 5c** to **5l** and **5o**; ***cf.* Part 1.7.2**). Descriptions of individual MeB hydrogeologic subdivisions are presented in the following order:

6.3.1a-b. Mesilla Valley of the Rio Grande (MeV) and the Mesilla Valley Fault Zone (MVfz)

6.3.1a. Inner Mesilla Valley

6.3.1b. Mesilla Valley Fault Zone (MVfz)

6.3.2a-b. Mid-Basin High (MeB-MbH)

6.3.2a. North Mid-Basin High (NMbH)

6.3.2b. South Mid-Basin High (SMbH)

6.3.3a-e. Hydrogeologic Subdivisions North and West of the Mid-Basin High

6.3.3a. Leasburg Inflow Corridor (LBic)

6.3.3b. Fairacres Subbasin (FASB)

6.3.3c. Afton Subbasin (AfSB)

6.3.3d. East Aden Bench (EABn)

6.3.3e. Kilbourne-Noria Subbasin (KNSB)

6.3.4a-d. Hydrogeologic Subdivisions between Mid-Basin High and Mesilla Valley Fault Zone

6.3.4a. Mesquite Subbasin (MSB)

6.3.4b. Black Mountain Subbasin (BMSB)

6.3.4c. Santa Teresa High (STH)

6.3.4d. El Milagro Subbasin (EMSB)

6.3.5a-d. Hydrogeologic Subdivisions East of the Mesilla Valley fault zone (MVfz)

6.3.5a. Las Cruces Bench (LCBn)

6.3.5b. Anthony-Canutillo Bench (ACBn)

6.3.5c. Anapra-Oasis Bench (AOBn)

6.3.5d. Sunland Park Outflow Corridor (SPoc)

Table 6-4. Names and Acronyms for Major MeB Hydrogeologic Subdivisions on Maps, Cross-Sections, and the Well-Information Spreadsheet (PLS. 1 to 8, and TBLS. 1 and 1B.
***See* Tbls. 1-3 and 6-2 for Boundary-Fault Zone (fz) Names and Acronyms**

Text Part	Acronym	Hydrogeologic Subdivision (area-mi²/km²/acres)
6.3.1		Mesilla Valley of the Rio Grande[a]
6.3.1a	MeV	Mesilla Valley Floor (215/557/137,600)
6.3.1b	MVfz	Mesilla Valley fault zone
6.3.2	MeB-MBH	Mid-Basin High (102/264/65,280)
6.3.2a	MeB-NMbH	North Mid-Basin High (55.2/143/35,328)
6.3.2b	MeB-SMbH	South Mid-Basin High (46.8/121/29,952)
6.3.3		Hydrogeologic subdivisions north and west of the MeB-MBH
6.3.3a	MeB-LBic	Leasburg Inflow Corridor (9.8/25.4/6,272)
6.3.3b	MeB-FASB	Fairacres Subbasin (148/382/94,720)
6.3.3c	MeB-AfSB	Afton Subbasin (69.5/180/44,480)
6.3.3d	MeB-EABn	East Aden Bench (27.3/70.7/17,472)
6.3.3e	MeB-KNSB	Kilbourne-Noria Subbasin (107/ 278/68,480)
6.3.4		Hydrogeologic subdivisions between MBH and Mesilla Valley fault zone (fz)
6.3.4a	MeB-MSB	Mesquite Subbasin (88/ 228/56,320)
6.3.4b	MeB-BMSB	Black Mountain Subbasin (136.2/353/87,168)
6.3.4c	MeB-STH	Santa Teresa High (34.5/89.5/22,080)
6.3.4d	MeB-EMSB	El Milagro Subbasin (78.4/203/50,176)
6.3.5		Hydrogeologic subdivisions east of the Mesilla Valley fault zone (fz) [a]
6.3.5a	MeB-LCBn	Las Cruces Bench (37.6/97.5/24,064)
6.3.5b	MeB-ACBn	Anthony-Canutillo Bench (53.2/138/34,048)
6.3.5c	MeB-AOBn	Anapra-Oasis Bench (28/72.7/17,920)
6.3.5d	MeB-SPoc	Sunland Park Outflow Corridor (13/33.4/8,320)

6.3.1 Mesilla Valley of the Rio Grande (MeV) and the Mesilla Valley Fault Zone (MVfz)

The Mesilla Valley of the Rio Grande (MeV) is not part of the MeB's RG-rift structural framework (**Part 3.2.3**, **Fig. 6-1**; **APNDX. F: Pls. F2-8, F3-1c** to **1j**, **F4-1h to 4-1l**, and **F5-3h**). It is, instead, one of a series of deep valleys and canyons that are the product of multiple-major glacial/interglacial cycles of fluvial erosion, which was initiated about 0.75 million years (Ma) ago following integration of a through-going Rio Grande that discharged in the Gulf of Mexico (**3.4.1**). The MeV extends about 60 mi (97 km) between its head at the mouth of Selden Canyon (SCyn- elev. 3,960; 1,207 m) and its terminus at the upper end of El Paso del Norte (EPdN-elev. 3,725; 1,135 m; **PLATE 5o**). The 5-mi (8-km) SCyn-reach of the river above Leasburg Dam (**3.1.3a**) forms the surface-flow link with the Tonuco Outflow Corridor (TNoc) subdivision of the Rincon Valley Basin (RVB; **Part 6.2**). The minimum width of the canyon's floor is about 300 ft (90 m), and the thickness of coarse-grained RG-channel fill does not exceed 80 ft (25 m). Accordingly, the potential for significant inter-basin groundwater flow is minimal.

Rio Grande alluvial deposits of Late Quaternary age that underlie the RVB-TNoc and MeV floors (HSU-RA, LFA a), while less than 100-ft (30-m) thick, are seasonally recharged by the river and irrigation-return flow (**Fig. 6-1**; **PL. 5o**; *cf.* **Parts 3.2.3,** and **7.5**). These fluvial sediments are mainly composed of sand and pebble gravel, with saturated hydraulic conductivities (K_{hsat}) that are commonly in the 50 to 100 ft/d (15-30 m/d) range (**Tbls. 4-1** and **4-3**). They form the primary aquifer unit in the Rincon [Hatch] Valley (RVB) below Caballo Reservoir. In the MeV and parts of the upper El Paso/Juárez Valley in the Hueco Bolson, however, HSU-RA is hydraulically well connected, not only with the river and the irrigation-system network that it feeds, but also with underlying USF2-ARG deposits that are of relatively high permeability (LFAs 1 to 3, **Tbls. 4-1** and **4-2**; **PLS. 5b** to **5j** and **5o**). Note that the potential for significant recharge from tributary-arroyo discharge is very low.

The following selection from Nickerson (2006, p. 2) is equally applicable to RG-valley and canyon areas throughout the Mesilla Basin region. It represents the first formal USGS use of the basin-scale hydrogeologic-framework model developed by Hawley and Lozinsky (1992) in the southern RG-rift region (*cf.* Sweetkind 2017, Sweetkind et al. 2017, Teeple 2017, Hanson et al. 2018):

> The lower Mesilla Valley ground-water system consists primarily of a basin-fill aquifer with two main geologic units: the Santa Fe Group of Quaternary and Tertiary age and the Rio Grande flood-plain alluvium of Quaternary age (King and others, 1971). The Santa Fe Group is an intermontane basin-fill unit that extends throughout the Mesilla Basin and includes alluvial, eolian, and lacustrine deposits (Hawley and Lozinsky, 1992, p. 4). These clay, silt, sand, and gravel deposits can reach depths of more than 2,000 feet in the lower Mesilla Valley. The Rio Grande flood-plain alluvium overlies the Santa Fe Group in the Mesilla Valley and consists of channel and flood-plain deposits of clay, silt, sand, and gravel that generally are less than 125 feet thick (Wilson and others, 1981, p. 27 [*cf.* **APPENDIX A**, **Part A2**]).
>
> The hydrogeologic framework of the Mesilla Basin was established in Hawley and Lozinsky (1992). Their basinwide conceptual model delineated three hydrogeologic features: (1) bedrock and structural boundaries, (2) lithofacies assemblages, and (3) hydrostratigraphic units [**Part 4.2**]. Santa Fe Group basin fill is divided into the informal upper, middle, and lower hydrostratigraphic units based on depositional environment and age. The upper Santa Fe hydrostratigraphic unit (USF) consists primarily of ancestral Rio Grande deposits of medium to coarse sand and [pebble] gravel. The USF includes the Camp Rice and upper Fort Hancock Formations. The middle Santa Fe hydrostratigraphic unit (MSF) consists primarily of alluvial deposits with eolian and playa-lake facies.
>
> Basin-floor sediments of interbedded sand and silty clay are common. The MSF includes the Fort Hancock and Rincon Valley Formations. The lower Santa Fe hydrostratigraphic unit (LSF) consists primarily of eolian, playa-lake, and alluvial facies. Basin-floor sediments include thick-bedded dune sand. The LSF includes the Hayner Ranch and the lower Rincon Valley Formations. Detailed descriptions of the hydrostratigraphic units and associated lithofacies can be found in Hawley and Lozinsky (1992). The Mesilla Basin hydrogeologic framework was recently updated and integrated into a digital format by Hawley and Kennedy (2004).

6.3.1a. Inner Mesilla Valley

The complex of river-channel and floodplain sediments that underlies the 215 mi^2 (557 km^2) Mesilla Valley floor (HSU-RA) is less than 100 ft (30 m) thick, and was deposited within the past 26,000 yrs (**PLS. 5a** to **5l** and **5o**; *cf.* **Part 3.2.3b**). This sequence of coarse- to medium-grained fluvial deposits is capped by a surficial layer of medium- to fine-grained channel and overbank deposits, with latter forming a significant part of the State's soil-resource base with long-term capability for sustainable irrigation agriculture (Bullock and Neher 1980; Maker et al. 1971; Hibbs et al. 1997; Esslinger 1998; Walton et al. 1999; SSURGO 2002/2003).

Coarse-grained, basal-channel facies are associated with final stage of deep valley entrenchment during the last full-glacial stage of the Late Pleistocene, but much of this gravelly unit was deposited during the Holocene (past 11 ka; Hawley and Kottlowski 1969; Gile et al. 1981). High- to moderate-permeability HSU-RA and HSU-USF2 (ARG) deposits are in direct contact in parts of five of the most-extensive hydrogeologic subdivisions of the MeV (*cf.* **Part 3.1.3b**): the Fairacres Subbasin (FASB-**6.3.3b**), Las Cruces Bench (LCBn-**6.3.5a**), Mesquite Subbasin (MSB-**6.3.4a**), Black Mountain Subbasin (BMSB-6.3.4c), and Anthony-Canutillo Bench (ACBn-**6.3.4b**). This stacked sequence of poorly consolidated, medium- to coarse-grained fluvial sediment has a saturated thickness that locally exceeds 300 ft (90 m). As such, it comprises not only the primary shallow-unconfined aquifer in the northern and central parts of the MeV, but also a renewable-resource of major cultural, economic, and environmental importance (**Fig. 6-1, Tbls. 6-1** and **6-4**).

6.3.1b. Mesilla Valley Fault Zone (MVfz)

The East Robledo and East Potrillo fault zones (ERfz and EPfz) form a distinct topographic and structural boundary with adjacent bedrock uplifts at the western edge of the MeB (**Parts 5.3.2** and **5.5.2**). The Mesilla Valley fault zone (MVfz), on the other hand, is buried by river-valley fill and uppermost SFG basin fill (**PLS. 5d** to **5k**; *cf.* Seager et al. 1987, Hawley and Lozinsky 1992, Hawley and Kennedy 2004). Moreover, there is no evidence (surface or subsurface) that a significant amount of displacement has occurred along the MVfz's mapped length of about 55 mi (88 km) during the Quaternary (past 2.6 Ma).

E.M.P. Lovejoy (1976b) was the first to postulate that a shallowly buried system of closely spaced faults beneath the lower MeV floor produced a large amount of down-to-west displacement of SFG and underlying bedrock units, and he introduced the name "Mesilla Valley fault" for that RG-rift structural unit. The approximate position of the buried fault zone is marked by a prominent north-trending, down-to-west inflection on Bouguer isostatic-residual gravity maps of the eastern parts of the Fairacres, Mesquite and Black Mountain Subbasins, and the Santa Teresa High between Las Cruces and Sunland Park (**Figs. 3-7a, 3-7b**, **6-1** and **6-2** [II-II′, III-III′]; **PLS. 1A**, **1B**, **1C,** and **5e** to **5h**, and **5o**; *cf.* Ramberg et al. 1978, Daggett et al. 1986, Daggett and Keller 1987, and Jiménez and Keller 2000, Fig. 4).

Because of shallow burial by inner-MeV fill, segments of the MVfz that form the eastern structural boundary of the MeB's deepest structural depressions can only be broadly defined in many places. Accordingly, the interpretation of MVfz location and configuration presented in this report is based on a combination of detailed mapping of surficial deposits, deep borehole logging, and analysis of all available geophysical-survey information (e.g., Zohdy et al. 1976, Wilson et al. 1981, Seager et al. 1987, Hawley and Lozinsky 1992, Nickerson and Myers 1993, Reiter and Wade 1994, Wade and Reiter 1994, Jiménez and Keller 2000, Hawley and Kennedy 2004, Witcher et al. 2004, Nickerson 2006, Moore et al. 2008, and Hiebing 2016).

The MVfz borders three of the MeB's deepest structural depressions, which are here listed in north to south order: the Fairacres Subbasin (FASB-**6.3.3b**), the Mesquite Subbasin (MSB-**6.3.4a**), and the Black Mountain Subbasin (BMSB-**6.3.4b**). All three of the MeB hydrogeologic-map subdivisions that are located east of the MVfz are located in areas of structural transition with the bordering Tortugas and Franklin Mountains Uplifts (TtU and FMU). In north to south order, they comprise the southern half of the Las Cruces Bench (LCBn-**6.3.5a**), western Fillmore Pass Corridor (FPC-**5.1.2**), and northern two-thirds of the Anthony-Canutillo Bench (ACBn-**6.3.5b**).

6.3.2. Mid-Basin High (MeB-MbH)

One of the more significant modifications to MeB hydrogeologic-framework model made during course of the present investigation involved adjusting the boundaries of the deeply buried structural High (H) that separates the major eastern and western structural subdivisions of the MeB. Detailed interpretation of subsurface relationships is hampered by the ubiquitous cover of Ancestral Rio Grande (ARG) that comprises a major component of SFG basin fill throughout the MeB West Mesa area (**Fig. 1-6**; **Part 3.5**). This feature was originally named the "Mid-Basin Uplift," following its initial usage in Hawley and Lozinsky (1992, fig. 3i; *cf.* Hawley and Kernodle 2000, Hawley et al. 2001, Hawley and Kennedy 2004, Witcher et al. 2004). However, the fact that the "uplift" is everywhere buried by at least 1,500 ft (457 m) of SFG basin fill, indicates that use of the less-specific term "Mid-Basin High (MBH)" is much more appropriate (**Figs. 6-1** to **6-3**, **Tbls. 6-1** to **6-4**; **PLS. 1B**, **1C**, and **5h** to **5k**). In marked contrast to the western- and eastern-bordering parts of the MeB-West Mesa, centers of Late Cenozoic basaltic volcanism are absent on the MBH (**PL. 1***, cf.* Seager et al. 1987, Seager 1995).

The provisional MBH-boundary locations shown on **PLATE 1** (and derivative illustrations) reflect the major advances that have occurred during the past three decades in the overall understanding of RG-rift and precursor-Laramide structural features (*cf.* Keller and Cather 1994, Mack and Giles 2004, Hudson and Grauch 2013). The wide-spacing of deep boreholes and the relatively low resolution of gravity-survey data, precludes precision in boundary fault-zone placement in many places (*cf.* Seager and

Hawley 1987, Sections E-E′ to G-G′, Hawley and Lozinsky 1992, Pl. 4, Jiménez and Keller 2000, Hawley and Kennedy 2004, Pls. 4b and 4c; *cf.* **Fig. 3-5**, and **PLS. 1A** and **3**).

Current inferences on deep-subsurface relationships are primarily based on interpretations of (1) surface geophysical surveys (e.g., gravity, earth-resistivity, and seismic) and deep-well logs (geophysical and sample), and (2) review of information in the following published and unpublished sources: **TABLE 1**, well nos. 183, 184, 208, 237 and 238 (King et al. 1971; King 1973; Cordell 1975; Jackson and Bisdorf 1975; Jackson 1976; Abernathy and Small 1986; Hawley and Lozinsky 1992-Pl. 13, Tbl. 4a; Nickerson and Myers 1993-Fig. 36; Clemons 1993; Klein 1995; Jiménez and Keller 2000; Seager 2004; Hamblock et al. 2007; Khatun et al. 2007; Averill and Miller 2013). Hydrogeologic interpretations presented herein are schematiIally illustrated on **Figures 3-8** to **3-13,** and **6-1** and **6-2** (**PLS. 1B** and **1C, 5h** to **5j, 5q, 8A** and **8B**).

The MBH is bounded on the west by the Fitzgerald fault zone (FGfz, Kottlowski 1960), which has distinct topographic expression only in its northern segment (Seager et al. 1987). Even though its existence is confirmed by deep-bore sample and geophysical data, exact placement of MBH's buried eastern structural boundary remains problematic (e.g., Hawley and Lozinsky 1992, Pl. 4). It is informally designated the Mid-basin fault zone (MBfz) herein.

6.3.2a. North Mid-Basin High (NMbH)

The North Mid-Basin High (NMbH) is a deeply buried horst-block and igneous-intrusive complex that is located between the Afton and southern Fairacres Subbasins (west) and the Black Mountain Subbasin (east). It has an area of about 55 mi² (142 km²), a topographic relief of about 600 ft (180 m), and is buried by about 1,500 to 2,000 ft (455-610 m) of SFG deposits. The latter cap an erosional surface cut on a complex igneous-extrusive and intrusive terrane of early and middle Tertiary age (Tlvs and Tmi) (**Figs. 6-1** and **6-2**, **Tbls. 6-1** to **6-4**; **PLS. 1B**, **1C**, **5h**, **5i** and **5q**). Saturated-thickness of HSU-USF2 (mostly LFA 3) is about 200 ft (60 m). Respective thickness ranges of HSU-MSF2 (LFA 3) and HSU-LSF (mostly LFA 7) are 500 to 550 ft (150-165 m) and 350 ft to 850 ft (105-260 m) (**PL. 7**).

An Oligocene (?) igneous-intrusive complex of "felsic" composition, with a subcrop area of as much as 32.5 mi² (84 km²), is located in the western part of the NMbH (**Figs. 6-1** and **6-2**). Because of its position beneath the UPRR [SPRR] Lanark Siding area, it is provisionally named the Lanark igneous-intrusive complex (TmLC) herein (**TBL. 2**, **Tbl. 6-3**). Interpretations of local bedrock composition in the deep subsurface are based primarily on the detailed petrographic analysis of borehole cuttings by NMSU Professor of Geology, Russell Clemons from the two oil and gas exploration wells that have been drilled in the general Lanark area: the Grimm et al. Mobil 32 (completed in 1973, TD 21,759 ft/6,632 m), and the Phillips-Sunland Park Unit No. 1 (completed in 1986, TD 18,232 ft/5,557 m); **TBL. 1**, nos. 180 and 237). The Phillips-Sunland Park well site is actually located 2.5 mi (4 km) NW of Lanark Siding and about 22

mi (35 km) NW of the town of Sunland Park. The general deep-subsurface stratigraphic relationships at the well site are described in the following selection from Clemons (1993, p. 5):

> The [Phillips] Sunland Park well penetrated 1,530 ft of basin-fill sediments overlying Tertiary volcanic and volcaniclastic rocks. Distinctive characteristics of stratigraphic units in this well are mostly obscured by alteration and contact metamorphism adjacent to felsite intrusions encountered frequently between 1,530 and 17,150 ft depths. Eighteen hundred ft of Cretaceous section, composed of fossiliferous [marine-clastic and carbonate rocks], was penetrated at 15,100 ft. [The] Actual top of the Cretaceous is probably within the immediately overlying 4000 ft of muddy siltstones, sandstones [Tls/K-**Tbl. 3-3**], [intrusive-contact altered] skarn [and] hornfels, and felsites [Tmi-**Tbl. 3-3**]. The Cretaceous section is underlain by 1,332 ft of fossiliferous [clastic-marine sedimentary rocks] correlative with the Lower Permian Hueco Formation.*
>
> **See memorial to R.E. Clemons (d. 11/24/1994) by W.R. Seager (1994).*

In February 1986, a second test well was completed at the Phillips-Sunland Park well site (surf. alt. 4,189 ft/1,277 m). This time the purpose of the test well was for detailed analyses of hydrostratigraphy and groundwater chemistry in both SFG basin fill and subjacent bedrock units (**TBL. 1**, no. 236 [MT-2]). The well was drilled to a depth of 1,565 ft (477 m) and penetrated bedrock of intermediate-igneous composition and early to middle Tertiary age at 1,489 ft (454 m) bls. It was completed as a monitoring well in a collaborative effort by the USGS-WRD and the EPWU. The NMBMMR was responsible for the petrographic analysis of drill cuttings, and overall hydrogeologic interpretation of borehole sample logs from the Lanark well (MT-2), and three other deep test wells at representative sites central and southern parts of the MeB (Hawley and Lozinsky 1992, p. 21-29, Pls. 12-15, Tbl. 4a): Afton site (MT-1) in the FASB north of the UPRR Afton Siding (**TBL. 1**, no. 175; **Part 6.3.3b**), La Union site (MT-3) is in the Black Mountain Subbasin (BMSB) near La Union (**TBL. 1,** no. 242; **6.3.4b**), and the Noria (MT-4) site is over the Southern Mid-Basin High (SMbH) northeast of the abandoned SPRR Noria Siding (**TBL. 1,** no. 253; **6.3.2b**).

Hydrostratigraphic interpretations of the four 1986 test-well logs were initially made by John Hawley and Richard Lozinsky (NMBMMR) in collaboration with Thomas Cliett (EPWU), Kenneth Stevens (USGS-WRD), and Francis West (NMOSE). Edward Nickerson and Robert Myers (1993) of the USGS-WRD described the investigation's geohydrological phase in detail (p. 55-64, Figs. 35-42, and Tbl. 2). The geophysical and hydrochemical data, and hydrostratigraphic interpretations for the Lanark test hole, which are summarized in **Figures 6-4** and **6-5**, demonstrate that fresh-water aquifer thickness is significantly less than that initially estimated by C.A. Wilson and others (1981, Pl. 15; *cf.* **Part 6.3.3b**).

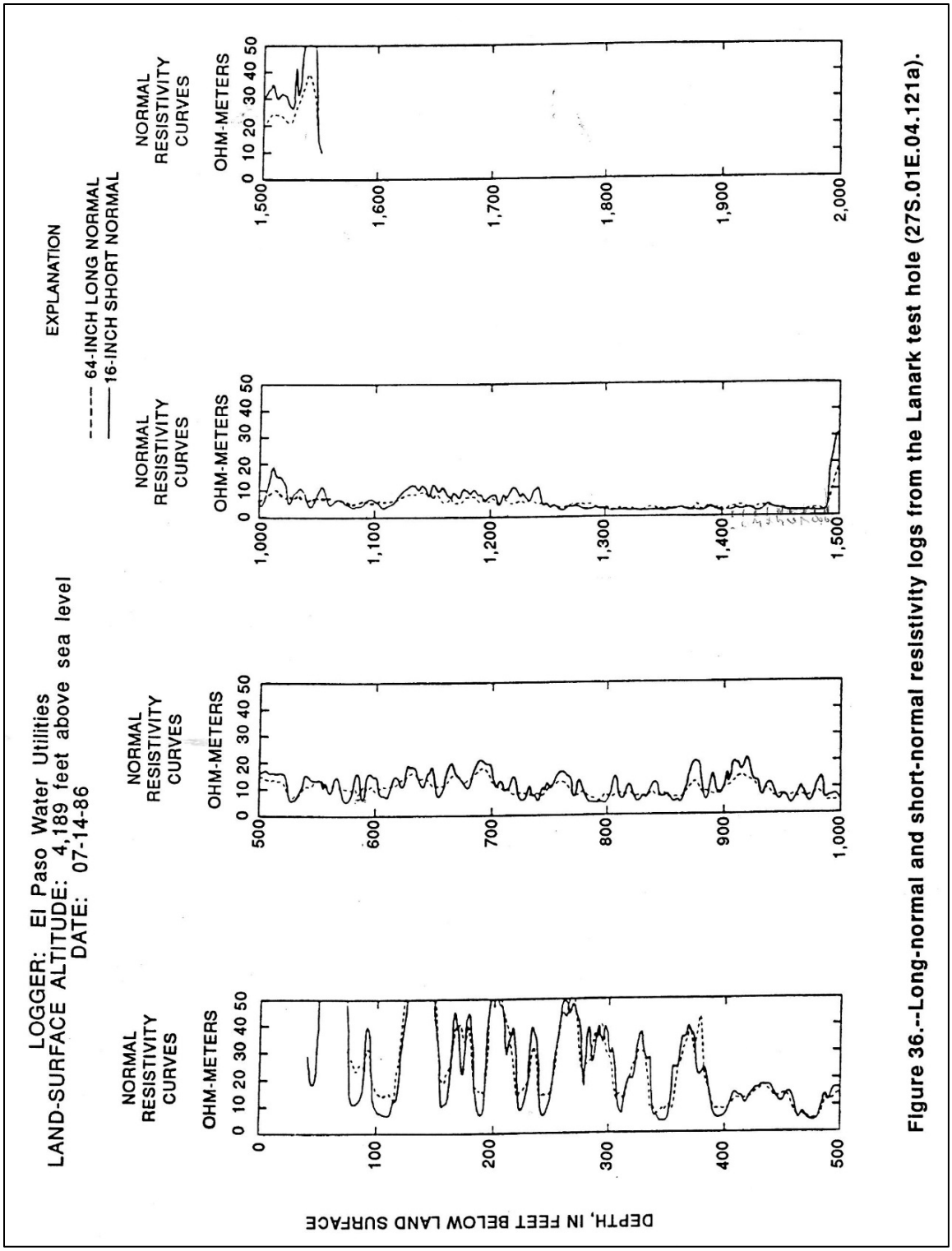

Figure 36.--Long-normal and short-normal resistivity logs from the Lanark test hole (27S.01E.04.121a).

Figure 6-4 (Nickerson and Myers 1993, Fig. 36)**.** Electrical-resistivity log of USGS-EPWU Lanark test-hole (**TBL. 1**, no. 236), with current interpretations of HSU contact depths (bgs): USF—/MSF2 - 530 ft (162 m), MS—2/LSF - 1,120 ft (340 m), and LS—/TmLC - 1,490-ft (454 m). Depth to water was 383 ft (117 m) in July 1986. *See* Hawley and Lozinsky (1992, Pls. 4, 8, 9, and 13), Hawley and Kennedy (2004, Pls. 5d, A3, and A5), and **PLATES 5i** and **5q**.

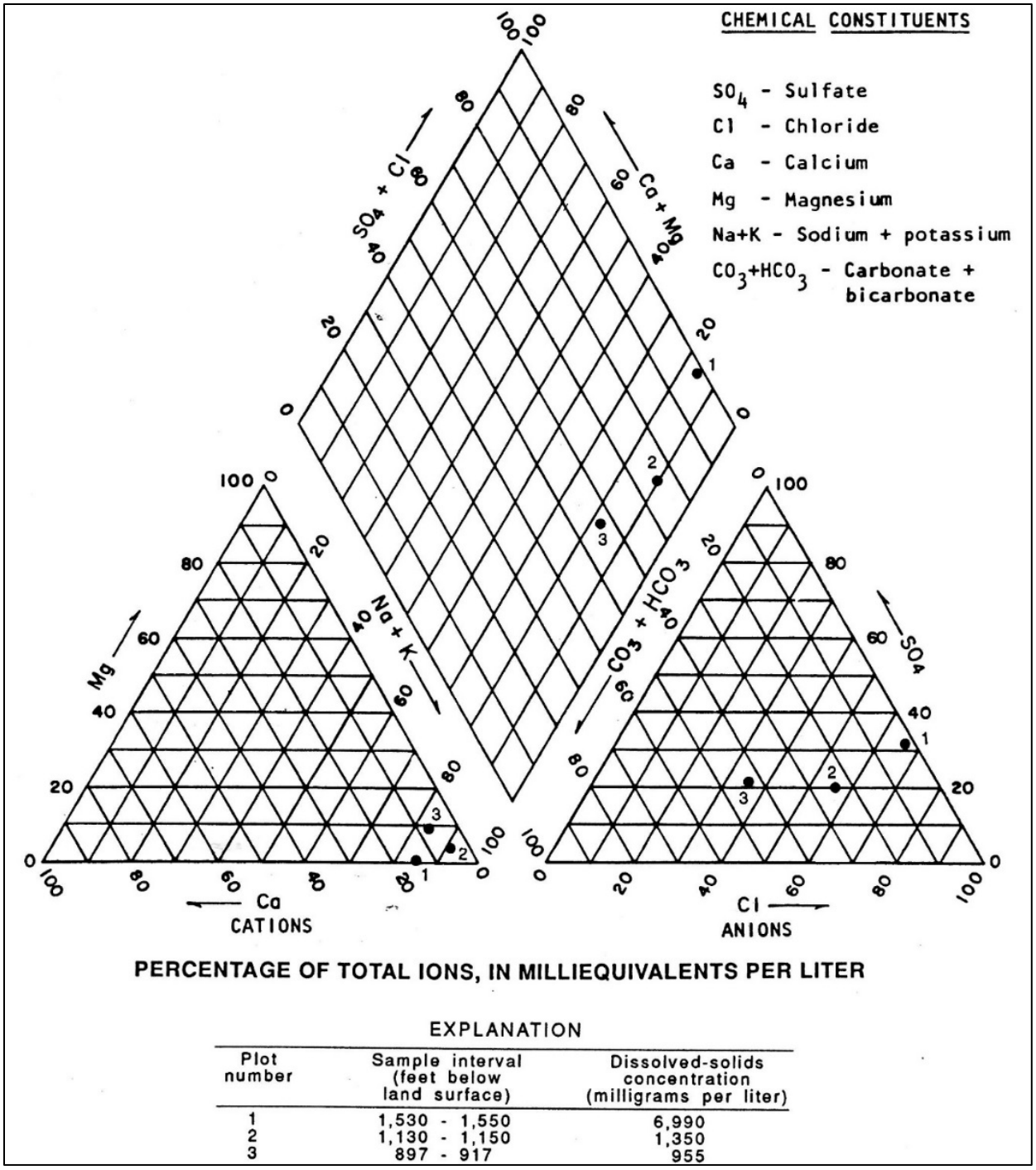

EXPLANATION

Plot number	Sample interval (feet below land surface)	Dissolved-solids concentration (milligrams per liter)
1	1,530 - 1,550	6,990
2	1,130 - 1,150	1,350
3	897 - 917	955

Figure 6-5 (Nickerson and Myers 1993, p. 62, Fig. 40)**.** Chemical analyses of water from selected depth intervals in the Lanark test hole (USGS-EPWU, **TBL. 1**, no. 236). Samples from: (1) uppermost part of the Lanark igneous-intrusive complex (**PLS. 5i**, **5q**, and **8B**: TmLC-Tmi/Tlvs), (2) upper part of HSU-LSF (LFA-7), and (3) HSU-MSF (LFA 3). Sample temperature and silica content (Celsius and mg/L): (1) 42.5° and 63, (2) 35° and 52, and (3) 31.5° and 67 (*cf.* Hawley and Lozinsky 1992, Tbl. 4a, Nickerson and Myers 1993, Tbl. 2).

The borehole electric-log and GW-chemical analyses for the USGS-EPWU Lanark test well have provided invaluable baseline information for many of the hydrogeologic interpretations presented herein (Nickerson and Myers 1993, Figs. 6-4 and 6-5). These data also provide the best evidence for the existence of a large geothermal and high groundwater-salinity source that is deeply buried by SFG basin fill in the west-central MeB (**Fig. 6-2** and **6-3** [II-II′]; **PLS. 5i** and **5q**). **Figure 6-5** (Nickerson and Myers 1993, Fig. 40) summarizes the chemical analyses of water sampled at three depth intervals in the Lanark test well (USGS-EPWU MT-2, **TBL. 1**, no. 239): (1) Top of the Lanark igneous-intrusive complex (**Fig. 6-3** [II-II′], **PLS. 5i**, **5q**, **8A**, and **9**: TmLC-Tmi/Tlvs), (2) Upper HSU-LSF (LFA 7), and (3) HSU-MSF2 (LFA 3). Here, and in other reports by Nickerson on hydrochemical conditions in the MeB, water type is illustrated with Piper diagrams (Piper 1944; *cf.* Nickerson 2006; **Figs. 6-12** and **6-16**). Water temperature and silica content (degrees C and mg/L) is (1**)** 42.5° and 63, (2**)** 35° and 52, and (3**)** 31.5° and 67. Of special note is the high TDS, and Na, Cl, and SO_4 content of water sampled from the uppermost TmLC (Fig. 6-5; 6,990, and 2,137, 1,666, and 1,471 mg/L, respectively).

6.3.2b. South Mid-Basin High (SMbH)

The MeB's Southern Mid-Basin High (SMbH) is located between the Kilbourne-Noria Subbasin (KNSB), and the Santa Teresa High and northern El Milagro Subbasin (STH and EMSB). Its provisional border with the NMbH is near the inferred southern edge of the Lanark Intrusive Complex (TmLC). The SMbH has an area of about 47 mi² (122 km²), and as in the NMbH, wide-spacing of deep borehole sites and the relatively low resolution of gravity and seismic survey data precludes precision in boundary fault-zone placement (**Part 6.3.2a**; *cf.* Seager and Hawley 1987, Section F-F′, Hawley and Lozinsky 1992, Pls. 6 and 7, Klein 1995, Jiménez and Keller 2000, Hawley and Kennedy 2004, Pls. 4d and 4e, Averill and Miller 2013, Fig. 3, p. 470). The SMbH's structural boundary with the central PSH (**Part 5.5.2**) is near the US-Mexico Border (**Figs. 6-1** and **6-2** and **Tbls. 6-2 and 6-3**; **Tbls. 6-2** to **6-4**; **PLS. 1B** and **5q**). It is buried by at least 1,500 ft (457 m) of basin fill, and coincides with the eastern segment of the Noria fault zone (NRfz). Bedrock subcrop units comprise Eocene volcanics (Tlvs) in the subbasin's northern part, with Lower Tertiary siliciclastic sedimentary rocks to the south (**Figs. 6-1** and **6-2**; **PLS. 5j**, **5k,** and **5q**). The saturated-thickness of HSU-USF2 (mostly LFA 3) is about 200 ft (60 m), and the thickness of unit MSF2 (LFA 3) is in the 350 to 550 ft (105-170 m) range. Underlying LSF basin fill (mostly LFA 7) ranges from 600 ft to 950 ft (180-290 m) in thickness (**PLS. 5j**, **5k**, **5q,** and **7**).

Figure 6-6 (Nickerson and Myers 1993, Fig. 36) is an electric log of the USGS-EPWU Noria test-hole (**TBL. 1**, no. 253), with the PI's current interpretations of HSU-USF/MSF/LSF contact depths. **Figure 6-7** (Nickerson and Myers 1993, Fig. 39) summarizes chemical analyses of groundwater sampled at three depth intervals in the Noria test well: Basal HSU-MSF2 (LFA-3/9), HSU-MSF2 (LFA 3), and Basal HSU-USF2 (LFA 3). Water temperature and silica content (Celsius and mg/L) is, (1) 31° and 34,

(2) 28° and 37, and (3) Not Sampled and 59. As in most other parts of the West Mesa area, subsequent more-detailed work has shown that fresh-water aquifers are about half as thick as they were initially estimated to be by Wilson and others (1981, Pl. 15; e.g., Nickerson and Myers 1993 p. 56; *cf.* **APNDX. C4.2**).

6.3.3. Hydrogeologic Subdivisions North and West of the Mid-Basin High

6.3.3a. Leasburg Inflow Corridor (LBic)

The Leasburg Inflow Corridor (LBic) coincides with the northern end of the MeV, and it is the northernmost hydrogeologic subdivision of the MeB (**Fig. 6-1** and **Tbl. 6-1**). It has an area of about 12 mi^2 (30 km^2) and serves as the sole conduit for surface-water inflow from a RG drainage basin area upstream from Leasburg Dam of about 28,000 mi^2 (72,520 km^2; **Part 3.2.3a**; **APNDX. F: Pls. F3-2c** and **F4-1h**). This informal hydrogeologic-map subdivision is named after the settlement of Leasburg (founded in 1866), which is located on the BNSF-RR at the eastern edge of the RG floodplain (Julyan 1996). The southern part of the LBic is bounded on the west by the East Robledo fault zone (ERfz) and Robledo Mountains Uplift (RMU), and on the east by the northern strand of the Mesilla Valley fault zone (MVfz) and Doña Ana Mountains Uplift (DAMU). The northern third of the Leasburg Inflow Corridor (LBic) includes the narrow river-valley floor near Leasburg Dam and Radium Springs that is located immediately west of Fort Selden State Monument. It is in a complex zone of structural transition between the MeB and Selden Hills Uplift (SHU), and deep-subsurface hydrostratigraphic and structural relationships are schematically illustrated on **Figs. 6-2** and **6-3** [I-I′] and **Tbls. 6-1** to **6-4**; **PLS. 5b**, **5c**, **5o**, and **5r**). As in the SCyn and lower RVB (**3.2.3** and **6.2**), the thin (<80 ft/25 m) alluvial fill of the present river-valley (HSU-RA) forms the only significant aquifer zone (*cf.* King et al. 1971, Hawley and Kennedy 2004).

About half of the LBic area is occupied by the RG floodplain and channel (MeV floor), while the remainder includes valley-border surfaces on the flanks of the Robledo and Doña Ana Mountains, and the Selden Hills (**Part 5.2.2**). The well-exposed HSU-USF and post-Santa Fe valley-border alluvial deposits are entirely in the vadose zone (Perez-Arlucea 2000; Mack et al. 2018b). On the other hand, the underlying HSU-MSF/LSF (LFA 7-8) basin fill and Tertiary volcanic rocks (Tmrs/Tlvs), while mostly saturated, have no significant aquifer potential due to their low permeability.

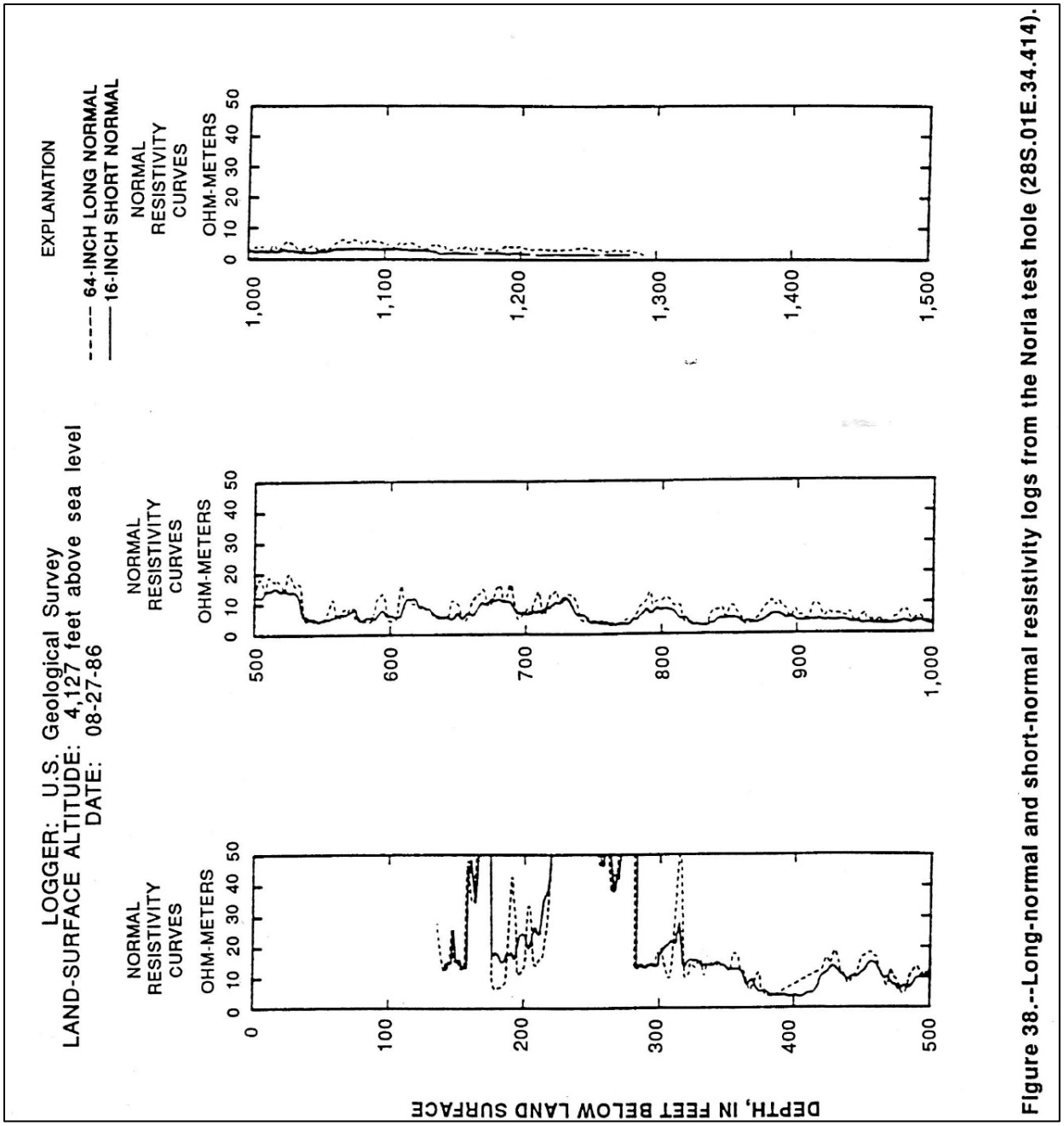

Figure 6-6 (Nickerson and Myers 1993, p. 62, Fig. 38)**.** Electrical-resistivity log of USGS-EPWU Noria test hole (USGS-EPWU, MT-4, **TBL. 1**, no. 253), with current interpretations of HSU contact depths (bgs): USF—/MSF2 - 540 ft (165 m), MS—2/LSF - 1,170 ft (357 m), and estimated L—F/Tls - 1,530-ft (466 m). Depth to water was 327 ft (100 m) in September 1986. *See* Hawley and Lozinsky (1992, Pls. 6, 7, 8, 15), Hawley and Kennedy (2004, Pls. 4e and A4), and **PLATES 5k** and **5q.**

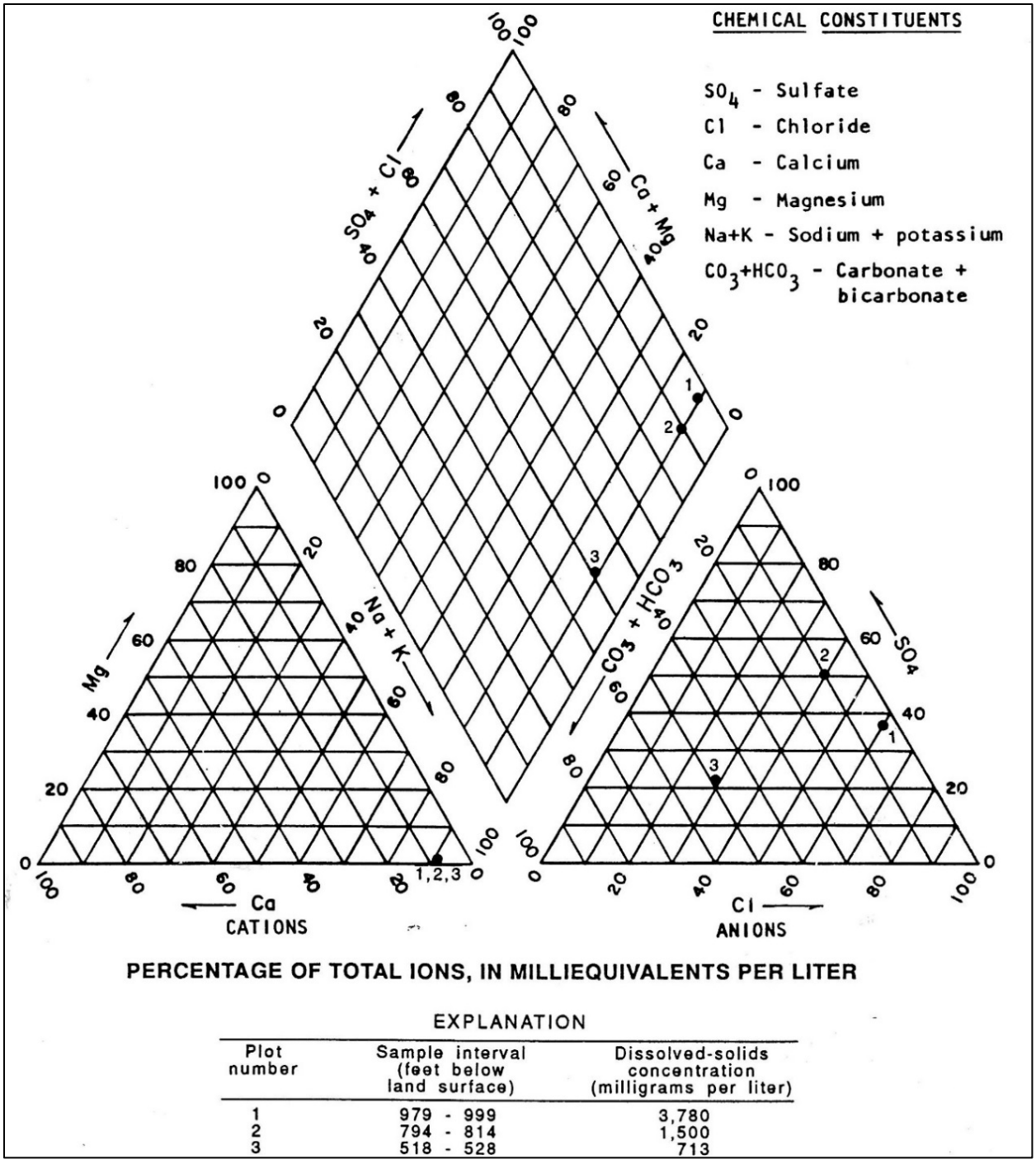

Plot number	Sample interval (feet below land surface)	Dissolved-solids concentration (milligrams per liter)
1	979 - 999	3,780
2	794 - 814	1,500
3	518 - 528	713

Figure 6-7 (Nickerson and Myers 1993, Fig. 42, p. 64)**.** Chemical analyses of water from selected depth intervals in the Noria test hole (USGS-EPWU, **TBL. 1**, no. 253). Samples from (1) lower part of HSU-MSF2 (LFA 3/9), (2) middle part of HSU-MSF2 (LFA 3), and (3) basal part of HSU-USF2 (LFA 3). Sample temperature and silica content (Celsius and mg/L): (**1**) 31° and 34, (**2**) 28° and 37, and (**3**) Not Sampled and 59 (*cf.* Hawley and Lozinsky 1992, Tbl. 4a, Nickerson and Myers 1993, Tbl. 2).

Valley-border exposures of silicic-intrusive rocks near Leasburg Dam are associated with the major intra-rift geothermal system that extends northward to Tonuco Uplift and the Rincon Hills (Ross and Witcher 1998; Witcher 1998; Witcher et al. 2004; Witcher and Mack 2018). According to Seager and Morgan (1978a, p. 78):

> Radium Springs takes its name from the hot springs at this stop [Witcher and Mack 2018]; the water at 86° C, is a manifestation of the high heat flow in the [RG-] rift (Reiter and others, 1978, this guidebook; Decker and Smithson, 1975); and this location has been classified as a Known Geothermal Resource Area (KGRA). Heat-flow value of 104±10 and 135±28 mWm^{-2} (2.48±0.23 and 3.24±0.68 HFU [Heat-Flow Units]) have been measured in deep boreholes (greater than 800 m) approximately 18 mi (30 km) east of here near the town of Organ (Reiter and others, 1978). Geothermal-gradient measurements in water wells indicate ubiquitous high heat flow in the Rio Grande Valley south of Radium Springs, [which are] locally augmented by hydrothermal systems (P. Morgan and C.A. Swanberg, unpublished data [*cf.* Swanberg 1979, and Seager and Morgan 1979]). Water geochemistry data also indicate that hydrothermal circulation systems in the valley have some structural control, because many of the high temperature samples are concentrated close to the [Mesilla] valley fault zone [MVfz—**Tbl. 6-2**], which approximately follows the line of Interstate Highways I-25 and I-10 between Radium Springs and El Paso (Swanberg, 1975 [Part 6.3.1b; *cf.* **Fig. 6-2** (**PL. 1B**)]).

6.3.3b. Fairacres Subbasin (FASB)

HSU-USF2 (ARG) deposits of the MeB's Fairacres Subbasin (FASB) form the primary geohydrologic link between Rio Grande-flow and upper GW-flow regimes in (1) the northern Mesilla Valley, and (2) all parts of the SFG basin-fill aquifer system north and west of the Mid-Basin High (MBH) (**Figs. 6-1** to **6-3** [I-I′] and **Tbls. 6-1** to **6-4**; **PLS. 5c** to **5g** and **5o**). The 230 mi^2 (600 km^2) subbasin is named after Fairacres, a small farming settlement (PO 1926-) located on US Hwy. 70 about 1 mi. (1.6 km) west of its bridge over the Rio Grande (Julyan 1969; **APNDX. F: Pls. F2-8** and **F3-1f**). The FASB's western structural- and topographic-boundary with the Robledo Mountains and mostly buried Aden-Robledo Uplifts (RMU and ARU) is well defined by the East Robledo fault zone (ERfz, **Tbl. 6-2**; **Part 5.3.2**). The northern segment of the Mesilla Valley fault zone (MVfz-**6.3.4a**), which is shallowly buried by inner-MeV fill (**6.3.1**), forms a less well-defined northeastern subbasin boundary with the Las Cruces Bench (LCBn-**6.3.5a**, **Fig. 6-1**, **Tbls. 6-1** and **6-4**).

The San Pablo fault zone (SPfz-**Tbl. 6-2**) forms a poorly defined structural boundary between FASB and the northern ends of the Mid-Basin High and the Black Mountain and Mesquite Subbasins (NMbH-**6.3.2a**, BMSB-**6.3.4b**, and MSB-**6.3.4a**). Its provisional name comes from San Pablo, a small farming settlement on NM-28 that is located near its juncture with the MVfz about 2 mi (3 km) south of Las Cruces (**PL. 5f** and **5o**-intersection area). The SPfz has no distinct topographic expression in the West Mesa-La Mesa area and is buried in the MeV, its provisional location is based on the PI's interpretation of a prominent NE-trending, down-to-NW inflection on published Bouguer isostatic-residual gravity maps

and a very-limited amount of deep-well data (e.g., Seager and others (1987, sheet 3), and Jiménez and Keller 2000, Fig. 4; *cf.* **Figs. 3-7a** and **3-7b**; **PLS. 1A**, **5f**, **5g**, and **5o**).

Thick HSU-USF2 (LFA 2-3) deposits in the northeastern third of the FASB are hydraulically well-connected with overlying HSU-RA alluvial aquifers of the inner MeV (**Figs. 4-3** and **4-4**, **Tbls. 4-1** to **4-3**). An extensive remnant of the relict USF2-ARG fluvial-plain (La Mesa geomorphic surface) occupies most of West Mesa portion of the subbasin (*cf.* **Part 3.3**). There, the vadose zone is about 350 ft (105 m) thick and composed entirely of HSU-USF2 deposits (**PLS. 5c** to **5g**). Thick HSU-USF2 (LFA 1-2) deposits of the central FASB and adjacent parts of the Mesquite Subbasin (MSB), particularly beneath the West Mesa area that borders the MeV west of Mesilla Dam, are of special interest because of their potential for future siting of large-scale aquifer storage and recovery (ASR) operations (**APNDX. F: Pls. F2-8** and **F3-1g**; *cf.* **Parts 1.3**, **4.2** and **8.5**). Saturated thickness ranges from about 300 ft (90 m) at the subbasin's northern boundary with the Leasburg Inflow Corridor (LBic) to almost 2,000 (600 m) ft at its southwestern, transitional border with the Afton Subbasin (AfSB) of the MeB (**PLS. 5e** to **5g**, **5o**, and **7**).

Estimated saturated-thickness of HSU-USF2 (mostly LFA 3) ranges from 400- to 700-ft (120-215 m), and thickness of unit MSF2 (LFA 3) in all but the subbasin's northernmost part is in the 400 to 800 ft (120-245 m) range (**PLS. 5d** to **5g** and **5o** to **5r**). Inferred thicknesses of underlying LSF basin fill (LFAs 7 and 8) range from 300 ft (90 m) to about 800 ft (245 m), except in the area of gradual HSU-MSF/LSF wedge out within 5 miles (8 km) of the LBic-FASB boundary (**PL. 5o**). Eocene andesitic volcanic, volcaniclastic, and epiclastic sedimentary rocks (Tlvs-**Tbl. 6-3**), which underlie the basin fill in the southern third of the FASB, are overlapped northeastward by Oligocene silicic-volcanic and associated epiclastic rocks (map-unit Tmrs) that have an ultimate Organ Mountains (OMU) caldera source (**Figs. 6-2** and **6-3**; **Tbl. 6-3**).

The first deep groundwater-test well in the MeB-West Mesa area was drilled to depth of 1,650-ft (503-m) in the southeastern part of the FASB for the American Smelting and Refining Company (ASARCO) in 1972 (Halpenny et al. 1972; King 1973). According to Clemons and others (1975, p. 30):

> The [ASARCO] well penetrated upper (?) Santa Fe Grp. basin fill to a depth of 1,650 ft [503 m; **TBL. 1**, no. 176]. The unit comprised alternating layers of sand, gravel, clay, and mudstone. The electric log showed about 50 percent of the interval between 350 (static water level) and 1,650 ft [107 and 503 m] as sand and gravel, . . . [*cf.* **Fig. 6-19**: log 25 S.1 E.16.111]. Twenty-four hour test pumping of a gravel-packed, perforated-casing interval between 450 and 1,650 ft [137 and 503 m] (12 3/4-inch casing above and 8 5/8-inch casing below 600 ft [183 m]) produced about 1,000 gpm at a drawdown of 26 ft [8 m]. Transmissivity was calculated from well-recovery data to be about 90,000 gpd/ft [12,000 ft^2/d, 1,080 m^2/d] (King, 1973).

C.A. Wilson and others (1981, p. 410-411) reported ASARCO-Well transmissivities in the 11,900 to 13,000 ft^2/d [1,106-1,208 m^2/d] range for an "estimated total sand thickness" of 630 ft (192 m)

in a 600 to 1,650-ft (183 to 503-m) “screened interval.” They (p. 56) also cite King (1973) in reporting a 570 mg/L TDS sampled-water quality, which is here interpreted as being produced from about the upper 600 ft (180 m) of the USF2/MSF2 aquifer zone.

The second deep groundwater-test well in the MeB-West Mesa area is a 2,470-ft (753-m) borehole located about 6.8 mi (11 km) north of the ASARCO test well in the southeastern part of the FASB. The well was drilled for the USGS in January 1975 and is listed as no. 146 in **TABLE 1** (Wilson et al. 1981, 24S.1E.08.123, p. 232-233). The well penetrates a representative 1,850-ft (564-m) section of SFG deposits (**PLS. 5p** and **5q**), and was completed in andesitic volcanic and epiclastic rocks of unit Tlvs (**Fig. 6-2**, **Tbl. 6-2**). Water-quality samples were collected at three depth zones: 568-588 and 754-774 ft (173-179 and 230-236 m) in HSU-USF2, and 1,383-1,403 ft (422-428 m) in basal HSU-MSF2, with respective TDS values of 526, 556, and 461 mg/L. This well site is at the north end of the borehole electric-log series illustrated in **Figure 6-18** (**Part 6.3.4c**), and it is located in the part of the MeB with the best-documented, still-untapped fresh-water reserves (*cf.* **APNDX. A5-Pl. EA-5**; Hawley and Kennedy 2004).

The third deep groundwater-test well in the FASB is the 2,486 ft (758 m) USGS-EPWU Afton test well (MT-1). It is located in the southern part of the FASB about 2.3 mi (3.7 km) northwest of the ASARCO test well, and was drilled in January 1986. The borehole penetrated a representative 1,900-ft (579-m) section of SFG deposits (**PLS. 5g**, **5q**, and **9**; **Part 6.3.2a**), and it was completed in andesitic volcanic and epiclastic rocks of unit Tlvs (Hawley and Lozinsky 1992, p. 21-26, Tbl. 4a, Pls. 9 and 12; *cf.* **Fig. 6-2** and **Tbl. 6-2**).

Figure 6-8 (Nickerson and Myers 1993, Fig. 35) is the electric log of the Afton test-hole (MT-4, **TBL. 1**, no. 175), with the PI’s interpretations of hydrostratigraphic contact depths (bgs) within the HSU-USF2/MSF2/LSF sequence (*cf.* Hawley and Kennedy 2004, Pls. A2, and A5). **Figure 6-9** summarizes chemical analyses of groundwater sampled at five depth intervals in the test hole (Nickerson and Myers 1993, Fig. 39*): (1) upper part of Tlvs, (2) top of Tlvs, (3) HSU-MSF2 (LFA 3*)*, and (4) and (5) base of HSU-USF2 (LFA 3). Water temperature (degrees C) and silica content (mg/L) are (1) 29.5° and 53°, (2) 28° and 57°, (3) 28.5° and 34°, (4) 32° and NS, and (5**)** 29° and 27.5°. Hawley and Lozinsky (1992, Tbl. 4a) also report on the major ion composition of a sample collected from HSU-LSF (LFA 7) at a depth of 1,585-1,605 ft (483-489 m) bgs. In that sample, TDS was 1,052 mg/L, with the following mg/L values for major anions and cations: Na+K-344, Ca-9, Mg-3.9, Cl-356, CO_3+HCO_3– 356, and SO_4 – 241.

**See Nickerson and Myers (1993) Table 2 for correct mg/L TDS values.*

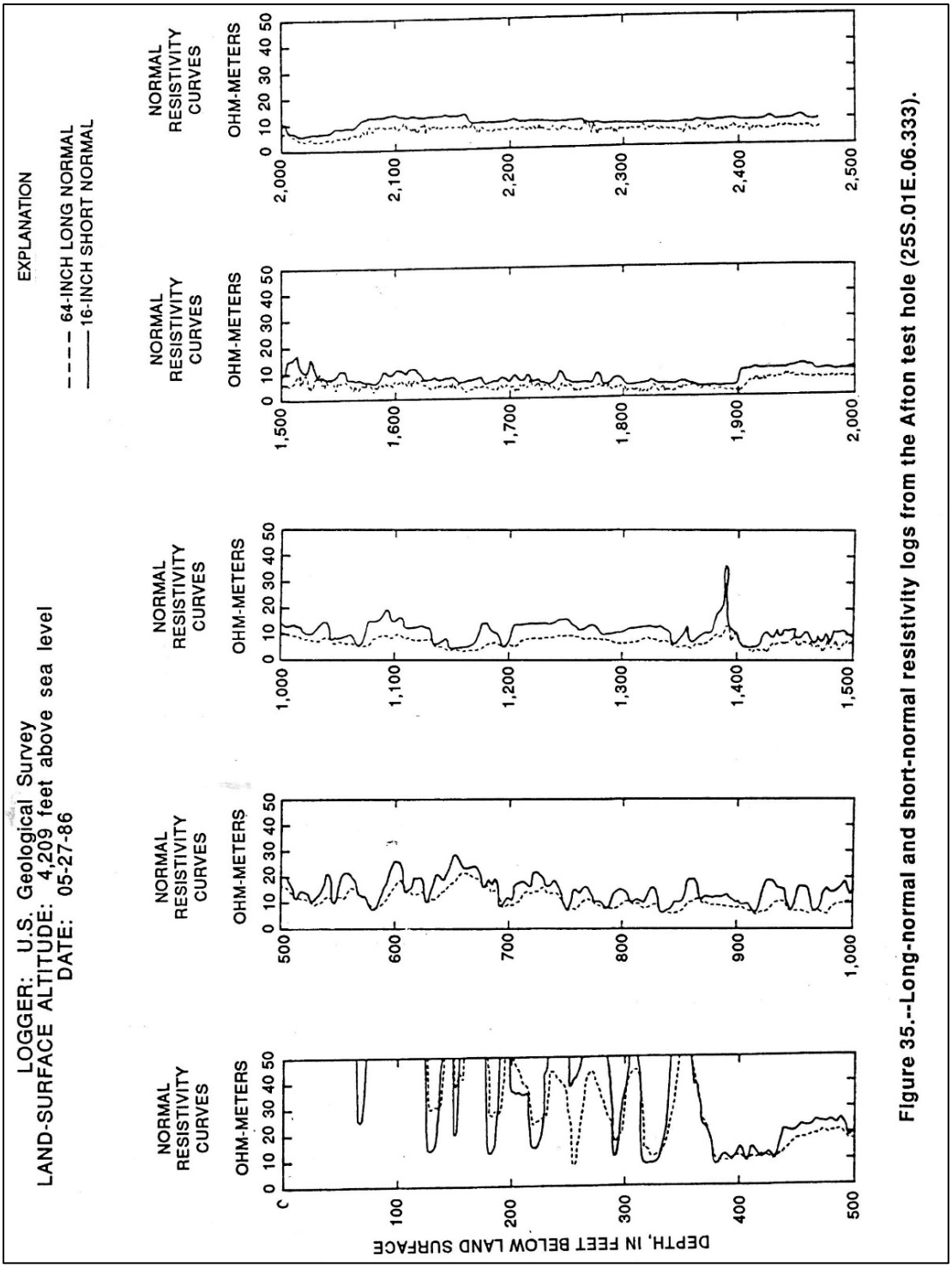

Figure 35.--Long-normal and short-normal resistivity logs from the Afton test hole (25S.01E.06.333).

Figure 6-8 (Nickerson and Myers 1993, Fig. 35)**.** Electrical-resistivity log of USGS-EPWU Afton test-hole MT-1 (**TBL. 1,** no. 175), with current interpretations of HSU contact depths (bgs): USF—/MSF2 - 690 ft (210 m), MS—2/LSF - 1,530 ft (466 m), and LS—/Tlvs - 1,900-ft (579 m). Depth to water was 366 ft (117 m) in June 1986. *See* Hawley and Lozinsky (1992, Pls. 2, 3, 8, and 13), Hawley and Kennedy (2004, Pls. 5d, A2, and A5), **Fig. 6-18**, and **PLS. 5i** and **5q.**

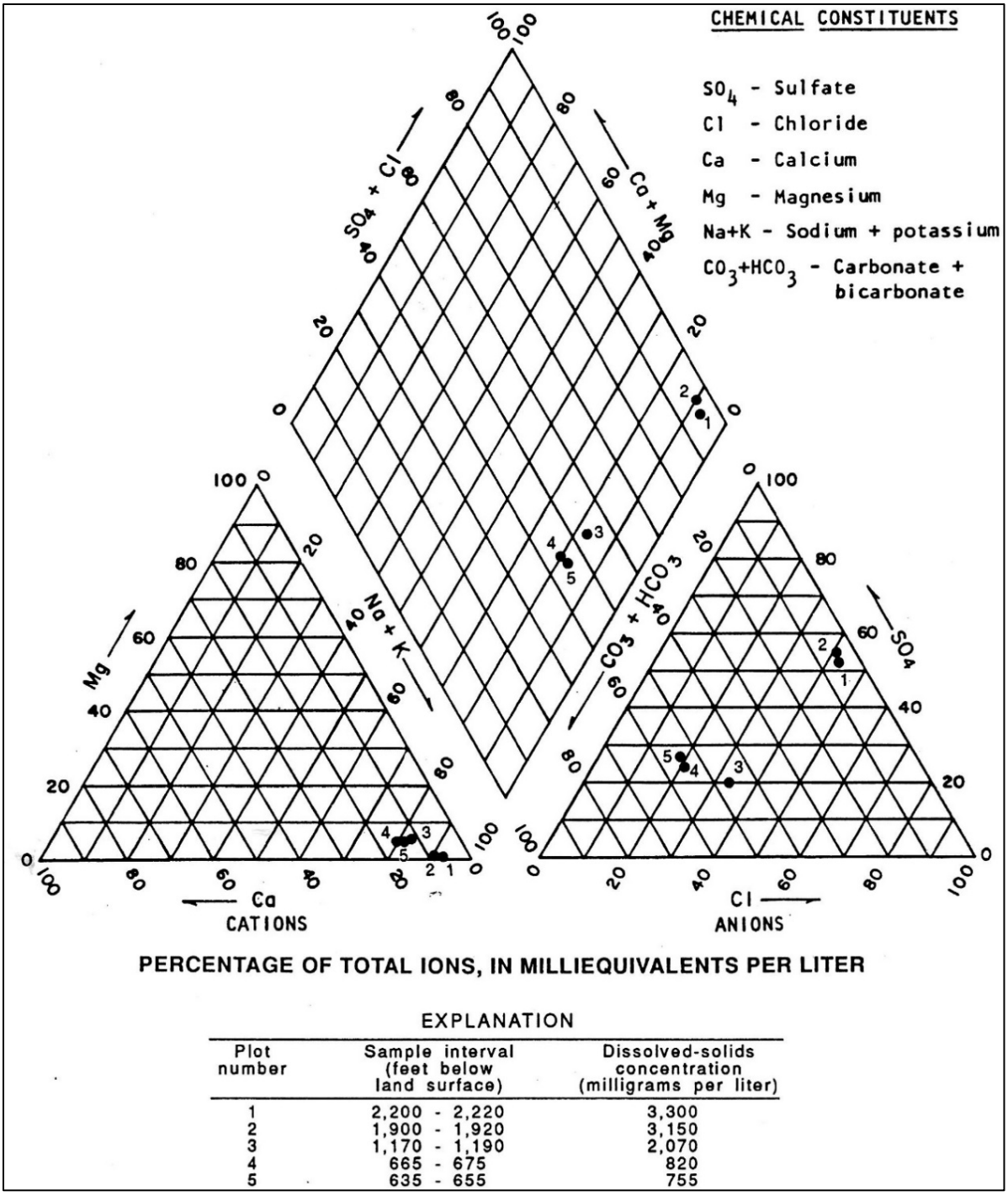

EXPLANATION

Plot number	Sample interval (feet below land surface)	Dissolved-solids concentration (milligrams per liter)
1	2,200 - 2,220	3,300
2	1,900 - 1,920	3,150
3	1,170 - 1,190	2,070
4	665 - 675	820
5	635 - 655	755

Figure 6-9 (Nickerson and Myers 1993, Fig. 39, p. 61)**.** Chemical analyses of water from selected depth intervals in the USGS-EPWU Afton test hole (MT-1, **TBL. 1**, no. 175)*. Samples from: **1**. Upper part of Tlvs, **2**. Top of Tlvs, **3.** HSU-MSF2 (LFA 3*)*, and **4** and **5**. Base of HSU-USF2 (LFA 3). Water temperature (Celsius) and silica content (mg/L) are (**1**) 29.5° and 53°, (**2**) 28° and 57°, (**3**) 28.5° and 34°, (**4**) 32° and NS, and (**5)** 29° and 27.5°.

**Note that the listed mg/L TDS values actually in specific-conductance units. See Nickerson and Myers (1993) Table 2 for the correct TDS values: i.e., 460, 1,200, 1,900, and 2,100 mg/L for the respective 635-655 ft, 1,170-1,190 ft, 1,900-1,920 ft, and 2,200-2,220 ft intervals.*

As in most other parts of the West Mesa area, freshwater-aquifer thickness is significantly less than that estimated by Wilson and others (1981, Pl. 15). Based solely on preliminary interpretations of Schlumberger (earth-resistivity) soundings, the freshwater-aquifer thickness in the Afton test-well area was initially estimated to be about 1,100 ft (335 m) (*cf.* Jackson 1976). Nickerson and R. Myers (1993, p. 56) and the PI, on the other hand, determined that the maximum freshwater-aquifer thickness in the southern part of the FASB is in the 450 to 550 ft (137-168 m) range. The borehole electric-log *signatures* for SFG deposits and subjacent Tlvs bedrock in the Afton (MT-1) test hole and the deep-test boring for Santa Teresa Estates Well-14 (**TBL. 1**, no. 261) are very similar even though they are about 22 mi (35 km) apart and are on opposite sides of the Mid-basin High (*cf.* **Parts 6.3.2** and **6.3.4c**; **Fig. 6-18**, and **APNDX. A5** [Hawley and Kennedy 2004, Pl. A5]). This suggests that at least general hydrostratigraphic continuity exists beneath much of central and southeastern part of the MeB-West Mesa area.

6.3.3c. Afton Subbasin (AfSB)

The Afton Subbasin (AfSB) borders the FASB on the southwest and has an approximate area of 70 mi² (180 km²). It is named after the Historic Afton Siding (*circa* 1881) on the Southern Pacific Rail Road—(SPRR - now Union Pacific RR, *cf.* Lee 1907, Darton 1933). In terms of landscape position, it, like all other parts of the Mesilla Basin's West Mesa area, occupies a portion of relict ARG fluvial-plain (La Mesa geomorphic surface; **Figs. 6-1** to **6-3** [II-II′]; **PLS. 1B**, **1C**, **5h, 5i** and **5r**). The northern segment of the Fitzgerald fault zone (FGfz) marks the AfSB's eastern, deeply buried structural boundary with the North Mid-Basin High and the Lanark igneous-intrusive complex (TmLC) (**Figs. 6-1** to **6-3**[I-I′] and **Tbls. 6-1** to **6-4**; **PLS. 5h, 5i** and **5r**). The southernmost segment of the East Robledo fault zone (ERfz) also forms a distinct western structural boundary between the AfSB and the MeB's East Aden Bench (EABn) (*cf.* **Part 5.3.2**).

From a deep-subsurface perspective, the AfSB is here interpreted as a moderately deep MeB hydrogeologic subdivision. This inference is primarily based on the presence of a prominent northwest-trending inflection in the 4-milligal contours located beneath its mapped northeastern boundary (**Fig. 3-6** [**PL 1A**]; *cf.* Jiménez and Keller 2000 [Fig. 4]). The latter geophysical anomaly suggests the presence of a large-displacement, deeply buried fault-zone of Laramide or early RG-rift age beneath this part of the MeB (**PLS. 1B**, **5f** and **5r**; *cf.* **Part 3.6**; Keller 2004, Seager 2004). The inference is also supported by published interpretations of the borehole-log data (geophysical and sample) from the deep exploratory wells drilled in nearby areas (**TBL. 1**, well nos. 145, 146, 175, 179, and 180; *cf.* Seager et al. 1997, Hawley and Lozinsky 1992, Nickerson and Myers 1993, Hawley and Kennedy 2004).

Surficial USF2-ARG deposits in the southwestern AfSB have an extensive basalt-flow cover of Late Pleistocene (~110 ka) age. Almost all flows are associated with the Afton sector of the Potrillo volcanic field, which had its source in the central Afton Cones vent group (**PLS. 5h** and **Pi**; Kottlowski

1960; Hoffer 1976; Seager et al. 1987; Anthony and Poths 1992; Williams 1999). The thin cover of Afton basalt flows also extends almost 10 miles (16 km) southward into the adjoining parts of Kilbourne-Noria Subbasin (KNSB), which include the large Kilbourne Hole and Hunts Hole maar-volcanic centers that are also of late-Pleistocene age (16-28 ka, Dunbar 2005; *cf.* **Part 6.3.3e**; Lee 1907, Darton 1916a, DeHon 1965, Seager 1987). Thick tuff-ring deposits associated with the maar eruptions and the extensive cover of Aden and Afton basalts prevent detailed description of continuity relationships between the two major fault zones that form the MeB's western structural boundary: the East Robledo and East Potrillo fault zones (ERfz and EPfz, **Tbl. 6-2**; *cf.* **Figs. 6-2** and **6-3** [II-II′], **Parts 5.3.2** and **5.5.2**). For example, surface expression of the northern East Potrillo fault zone south of the UP[SP]-RR-Afton Siding area is completely obscured by a basalt-flow cover in the Aden sector of the Potrillo volcanic field, the site of the youngest volcanic center in the Mesilla Basin region (**6.3.3d**; *cf.* Kahn 1987, Seager 1995, DeHon and Earl 2018).

It has been common practice in geologic mapping of the MeB West Mesa area to locate the centers of basaltic volcanism on or immediately adjacent to RG-rift faults with significant vertical displacement and estimated dips in the 65 to 75-degree range (*cf.* Clemons et al. 1975, p. 28). More than five decades of experience in the mapping of RG-rift basin fill, however, has convinced the PI that the major centers of Pleistocene basaltic volcanism like Aden, Afton, Kilbourne, Hunts, Potrillo, and Black Mountain, are more likely associated with deep-seated extensional-fracture zones without any requisite vertical-displacement component (*cf.* Cordell 1975, p. 269). With regards to groundwater flow and chemistry, moreover, except for the significant geothermal activity associated with large volcanic centers at depth, surficial volcanic materials do not play a significant role in the geohydrologic system, particularly with respect to groundwater recharge in an arid to semiarid region where vadose-zone thickness commonly exceeds 330 ft (100 m).

Nelia Dunbar's (2005) summary description of the "Potrillo Volcanic Field and Associated Areas (p. 101-102)" are included here for background-information completeness:

> The Potrillo volcanic field, in southwestern New Mexico . . ., is located in the southern portion of the RGR, near the eastern margin of the Basin and Range Province [Hoffer 1976, Baldridge 2004, Thompson et al. 2004]. This field, together with a few associated areas, has been extremely active during the Quaternary. The Potrillo field contains a total of several hundred young lava flows, cinder cones and maar craters, covering a total area of 4,600 km^2 (Williams, 1999 [*cf.* Seager et al. 1987, Seager et al. 1995, Thompson et al. 2005]). The erupted material in this field is dominantly alkali olivine basalt and basanite (Hoffer, 2001b). The West Potrillo field alone includes 124 cinder or spatter cones, two maar volcanoes and a number of lava flows (Hoffer, 2001b). Landsat imagery indicates that these features were erupted over an extended period of time, but probably all during the Quaternary (Hoffer, 2001b [Hoffer et al. 1998]). . . . The Potrillo field is well-known for well-developed and well-exposed maar volcanoes, of which the best-known is Kilbourne Hole [*cf.* Seager 1987, Maksim 2016], a maar known for its

> abundance of mantle xenoliths (Padovani, 1987). Several other well-exposed maar craters are also present in the Potrillo field, including Hunts Hole and Potrillo maar [*cf.* DeHon 1965, Reeves and DeHon 1965, Waggoner 1990, Hoffer 2001a, Moncada-Gutierrez 2016]. . . . Another well-known feature of the Potrillo field, Aden crater, sits atop a broad shield [Callahan 1973, Kahn 1987]. The 1.6 km diameter crater shows evidence of a lava lake which overflowed the crater rim. Post-shield spatter cones are found inside the crater, as well as on the flanks of the shield (Hoffer, 1976 [DeHon and Earl 2018a, b).
>
> A number of dating techniques have been used to determine the age of the volcanic features in the Potrillo volcanic field, as well as other nearby volcanic features. These include conventional K-Ar dating, $^{40}Ar/^{39}Ar$ dating, as well as [surface-exposure] cosmogenic techniques, such as ^{36}Cl (Leavy, 1987) and ^{3}He (Williams, 1999 [Williams and Poths 1994]), and soil development methods (Gile, 1987a). . . [**APNDX. F: Pls. F3-4a** to **4e**, and **F7-3a** to **3f**].

Eocene andesitic volcanic and volcaniclastic rocks underlie the entire Afton Subbasin (**Fig. 6-3** [II-II′], Tlvs-**Tbl. 6-3**), and SFG basin fill is penetrated by feeder conduits for the Afton field basalt flows in several places (**PLS. 1**, **5h** and **5i**, **7** and **8B**). Saturated basin-fill thickness ranges from about 300 ft (90 m) at the subbasin's northern boundary with the FASB to more than 1,500 ft (460 m). Estimated saturated-thickness of HSU-USF2 (mostly LFA 3) ranges from about 250- to 350-ft (75-105 m), and unit MSF2 (LFA 3) is in the 650 to 750 ft (200-230 m) thickness range (**PLS. 5h, 5g, 5r** and **7**). Inferred thicknesses of underlying LSF basin fill (mostly LFA 7) range from 450 ft (135 m) to 750 ft (230 m).

6.3.3d. East Aden Bench (EABn)

The provisionally named East Aden Bench (EABn) has a surface area of about 27.5 mi² (71 km²). It is located in a broad zone of structural and SFG-compositional transition between the deep Mesilla (structural and GW) Basin, and the shallowly buried, bedrock terrane in the Aden-Robledo Uplift (ARU) to the west (**Figs. 6-1** to **6-3** [II-II′] and **Tbls. 6-1** to **6-4**; **PLS. 5f**, and **5h**; **Part 5.3.1b**). Eocene andesitic volcanic and volcaniclastic rocks (Tlvs-**Fig. 2-3**) underlie the entire area. The most prominent geologic feature is the large Aden Crater shield volcano of latest Pleistocene age (~22 ka, Dunbar 2005), and its surrounding 29 mi² (75 km²) basalt-lava field (**PL**. **5h**; **APNDX. F: Pls. F3-4c** to **4e**, and **F7-3e**; *cf.* Callahan 1973, Hoffer 1976, Kahn 1987, Seager 1995, DeHon and Earl 2018a-b). Estimated saturated-thickness of HSU-MSF2 (LFA 7) is less than 200 ft (60 m) (see west end of **PL. 5h**) and in the 100- to 300-ft (30-90 m) range only in the southernmost part of the ERSB, while thickness ranges for units MSF and LSF (LFA 9 and 10) are, respectively, 600 to 1,400 ft (180-425 m), and 1,500 to 2, 500 ft. (455-760 m) throughout mapped part of the subbasin.

Because of its historical significance, N.H. Darton's (1933, p. 135) description of Aden Crater and its "remarkable ground sloth" inhabitant is included here and in **APPENDIX C1**:

> Aden Crater, 4 miles [6 km] south of Pronto siding and 7½ miles [12 km] southeast of Aden siding, is a cone of lava undoubtedly marking the vent from which came one of the large recent lava flows skirted by the railroad in this vicinity. In its top is a deep blowhole or steam vent in the

> lava, in which many animal skeletons have been found, including coyotes, bobcats, and other animals of the present fauna, and a remarkable ground sloth which Lull[1] has identified as *Nothrotherium shastence*. The remains were partly buried in bat guano in a sloping chamber about 100 feet [30] below the surface. The bones of the sloth were held together by the original ligaments, and some of the periosteum, patches of skin, muscle fibers, and claws remain. Most of the hide has been devoured by fellow victims, whose teeth marks are visible on the remaining fragments. The sloth and other animals had evidently fallen into this hole, which is a natural trap in the crater rim. The time was many thousands of years ago, for the sloth is a species found also in the Rancho La Brea asphalt in Los Angeles, where it occurs with bones of . . . Pleistocene age.
> [1]*Lull, R.S., 1929, A remarkable ground sloth: Yale University Peabody Museum Memoir, v. 3, part 2, 21 p.*

The paleoecological significance of fossil remains of *Nothrotherium shastence* at both Aden Crater and Bishop Cap's Shelter Cave, especially the dung (aka *coprolites*), continues to be great scientific interest (*cf.* Eames 1930, Simons and Alexander 1964, Long et al. 1974, Thompson et al. 1980, Hunt and Lucas 2022, Hunt and Morgan 2022, and McDonald 2022). McDonald (2022, TBL. 1) reports a11,060±50 yrs. B.P. radiocarbon age of sloth dung from Aden Crater. As initially reported by Eames (1930), sloth diet at Aden Crater at the onset of the Holocene interglacial stage was dominated by the woody shrubs *Atriplex* (Four-wing saltbush) and *Gutierrezia* (Snakeweed). It is important to note that both of these plants are common components of the present-day vegetation in this part of the Chihuahuan Desert (Gile et al. 1981, TBL. 4).

6.3.3e. Kilbourne-Noria Subbasin (KNSB)

The Kilbourne-Noria Subbasin (MeB-KNSB) borders the MeB on the southwest and has an approximate map area of 107 mi² (278 km²) (**Figs. 6-1** to **6-3**; **Tbls. 6-1** to **6-4**; **PLS. 5j**, **5k** and **5r**). Its compound name refers to (1) the Kilbourne Hole maar volcanic center (~20 ka), which is located at the subbasin's northern end, and (2) the site of Noria Siding on a now-abandoned section of the SPRR (Lee 1907 and 1907a, Darton 1916a and 1933).

Like other parts of the Mesilla Basin's southern West Mesa area, the KNSB includes an extensive relict-ARG fluvial-plain (La Mesa surface) that continues southward into north-central Chihuahua, where it crosses the deeply buried El Parabién Basin (EPB, Part **6.4**) and terminates at the northeastern edge of the southern Florida-Mimbres subbasin (**Fig. 1-2**; *cf.* Averill and Miller 2013). The East Potrillo fault zone (EPfz, **5.4.2a**) forms a distinct western topographic and structural boundary between the KNSB and the East Potrillo Uplift (EPU) (**Figs. 6-1** to **6-3**; **Tbl. 6-2**; **PLS. 1**, **2**, **5j**, and **5k**). The Subbasin's relatively distinct, but transitional southern boundary with the deeply buried La Joya Sector of the Potrillo-Sapello High (PSH-LJS) lacks surface expression, which in this case is due to a very thick cover of USF2-ARG deposits (**Part 6.4.1**). Its approximate location is solely based on the presence of a

prominent SE-trending, down-to-NE inflection on the detailed Bouguer isostatic-residual gravity maps compiled by Jiménez and Keller (2000; **Figs. 3-6** and **3.7a**; **PLS. 1A**, **5f**, **5g**, and **5o**).

The KNSB's structural boundary with the South Mid-Basin High (SMbH, **Part 6.3.2b**) remains poorly defined due to (1) a general lack of high-resolution gravity-and seismic survey control, and (2) the absence of topographic evidence for a southern extension of the Fitzgerald fault zone (FGfz; Seager et al. 1987; Klein 1995; Jiménez and Keller 2000; Averill and Miller 2013; *cf.* **Figs. 3-9** and **6-1** to **6-3**; **Tbls. 6-1** to **6-4**; **PLS. 7j** and **7k**). The KNSB-SMBH boundary is here provisionally located near the eastern edge of a 6-mi (10-km)-wide zone between the Noria (MT-4) monitoring well and the easternmost geothermal exploratory well drilled for Hunt Energy Corp (**Fig. 6-10**; **TBL. 1**, nos. 257, 297 and 298; *cf.* Parts **5.4.2a** and **6.3.3a**; Hawley and Lozinsky 1992, Pl. 7, Hawley and Kennedy 2004, Pl. 4e).

A thick sequence of Eocene andesitic volcanic and epiclastic and siliciclastic sedimentary rocks (Tlvs and Tls) comprise the bedrock units that immediately underlie SFG basin fill in the KNSB area (**Figs. 6-2** and **6-3**, **Tbl. 6-3**). These volcanic and sedimentary units are confined to the northeastern half of the subbasin. Unit-Tls (**Tbl. 6-3**) is present at depth throughout the area, and was deposited in the NW-trending Laramide Potrillo basin of early Cenozoic age that predated RG-rift development (**PLS. 5j**, **5k and 5r**). Saturated SFG thickness ranges from more than 1,500 ft (460 m) at the KNSB's northern boundary with the AfSB to at least 1,800 ft (550 m) in its south-central part (**PLS. 5j**, **5k**, **5r**, and **8B**). Estimated thickness of HSU-USF2 (mostly LFA 3) ranges from 250 to 350 ft (75-105 m), and unit MSF2 (LFA 3) is in the 450 to 700 ft (135-215 m) thickness range (**PLS. 5j, 5k, 5r** and **7**). Inferred thicknesses of underlying HSU-LSF deposits, here interpreted as sand/sandstone-dominant LFA 4, ranges from 600 ft (180 m) to 1050 ft (320 m). Estimated water quality is in the 1,000 to 3,000 mg/L TDS range.

PLATE 5r includes schematic cross-section depictions to msl depth of the diatreme interiors and flanking tuff rings Kilbourne and Hunts Holes, the subbasin's two large hydrovolcanic (phreatomagmatic) eruptive centers (Lee 1907a; Darton 1916a; DeHon 1965; Cordell 1975; Hoover and Tippens 1975; Jackson and Bisdorf 1975; O'Donnell et al. 1975; Podovani 1987; Seager 1987; Padovani and Reid 1989; Dunbar 2005; Maksim 2016; Vitarelli 2021; *cf.* **APNDX. F: PL. F3-4a** and **4b**, and **F3-7a** to **d**). USGS geophysicist Lindrith Cordell (1975, p. 269) was the first to describe the "Holes" hydromagmatic origin and internal structure from a contemporary geophysical perspective:

> During March 1975, in support of an evaluation of geothermal potential of federal land, the U.S. Geological Survey made gravity, air and ground magnetic, resistivity, audio-magnetotelluric, telluric, and magnetic variation studies in the vicinity of the Kilbourne Hole maar. In this paper I will state our viewpoint, summarize the geophysical findings, and then describe in particular the gravity and magnetic data. The following [1975 NMGS] guidebook papers by Jackson and Bisdorf, Hoover and Tip'ens, O'Donnell and others, and Towle and Fittermann will describe the other data sets.

Unusually well-developed maare of late Pleistocene age occur at Kilbourne and Hunts Holes and elsewhere both locally and regionally. At Kilbourne maar the crater is about 2 km in diameter, 60 m deep, and rimmed with hills of cross bedded, base-surge and air-fall material up to 60 m high on the downwind side of the crater. The maare were described by DeHon (1965). In contrast to DeHon, however, I find neither geological nor geophysical evidence to show that the maare are related to surficial geologic structure. . .

Geophysical studies in general seek to test and occasionally to evaluate a presupposed geological model. Here our model comprises about 6 km [22,000 ft] of horizontal suprabasement sedimentary and volcanic rocks broken by northwest- and northeast-trending Neogene block faults. Near Kilbourne Hole the surface unit is predominantly siltstone and sandstone about 700 m [2,300 ft] thick (Santa Fe Group) underlain by Tertiary volcanic rocks.

Geologically, we expected the maare to be underlain by a funnel-shaped breccia zone grading downward into a stem of basalt and thence into basalt dikes [*cf*. **PL. 5r**]. The geophysical data do not exactly reject this model but they do not entirely support it. We find no gravity expression of anomalous rock density nor magnetic expression of igneous rock beneath the maare. We do find anomalously high electrical conductivity [*cf.* Hoover and Tippens 1975, Jackson and Bisdorf 1975, O'Donnell et al. 1975]. Unfortunately, the conductivity data tell less about the rocks than about the condition of their contained waters. In any case the electrical data indicate that a vertical pipe of some kind extends beneath the craters across major stratigraphic boundaries to a depth of at least 2 km [6,562 ft]. The water within this zone must be unusually hot, or saline, or contain a large amount of clay related to hydrothermal alteration.

This zone could be a diatreme choked with basalt and large blocks plucked out of underlying sedimentary and volcanic layers [*cf.* Vespermann and Schmincke 2000]. In terms of the magnetic and gravity data, however, the maare are indistinguishable from adjacent sandstone and siltstone of the Santa Fe Group. Although the gravity data are subject to an unusual operational uncertainty, the restrictions provided by the magnetic data are fairly severe. Therefore, for 1 km or so beneath the maare two alternative models are 1) Santa Fe Group sandstone and siltstone having high electrical conductivity because of brecciation, chemical alteration or invasion from below by hot or saline water; or 2) a breccia zone containing exotic fragments which are sufficiently jumbled that magnetic moments cancel, and containing enough increased pore volume to offset the addition to the system of denser rock. The first alternative, which seems to me the more likely, implies that the flux of solid or incandescent material through shallow levels was small in volume and that the erupting material was primarily hot gas.

Figure 6-10 is a page-size reduction of **Plate A-A4w** in **APPENDIX A-5 (**Hawley et al. 2005). This hydrogeologic index section shows six key-well sites in the southern KNSB area, which also includes parts of the southern East Potrillo Uplift (EPU-PRS; Part **5.5.1**) and the South Mid-Basin High (SMbH, **Part 6.3.2b**). The cross-section's general **PLATE 5k** (**K-K'**) alignment approximates that of NM Hwy 9 and an abandoned section of the SPRR route (Darton 1933, **APNDX. C1c**). Cross-section base altitude is 1,500-ft (457-m) amsl, vertical exaggeration (VE) is 10x, and respective borehole electric-log color codes are: long-normal—blue, and short-normal or single-point—red. Hydrostratigraphic, lithofacies, and structural interpretations were made by Hawley and Lozinsky (1992, Pl. 7; **APNDX. A**, **Tbl. A-5**). The PI's current interpretations are shown on **PLATES 5k** and **8B**.

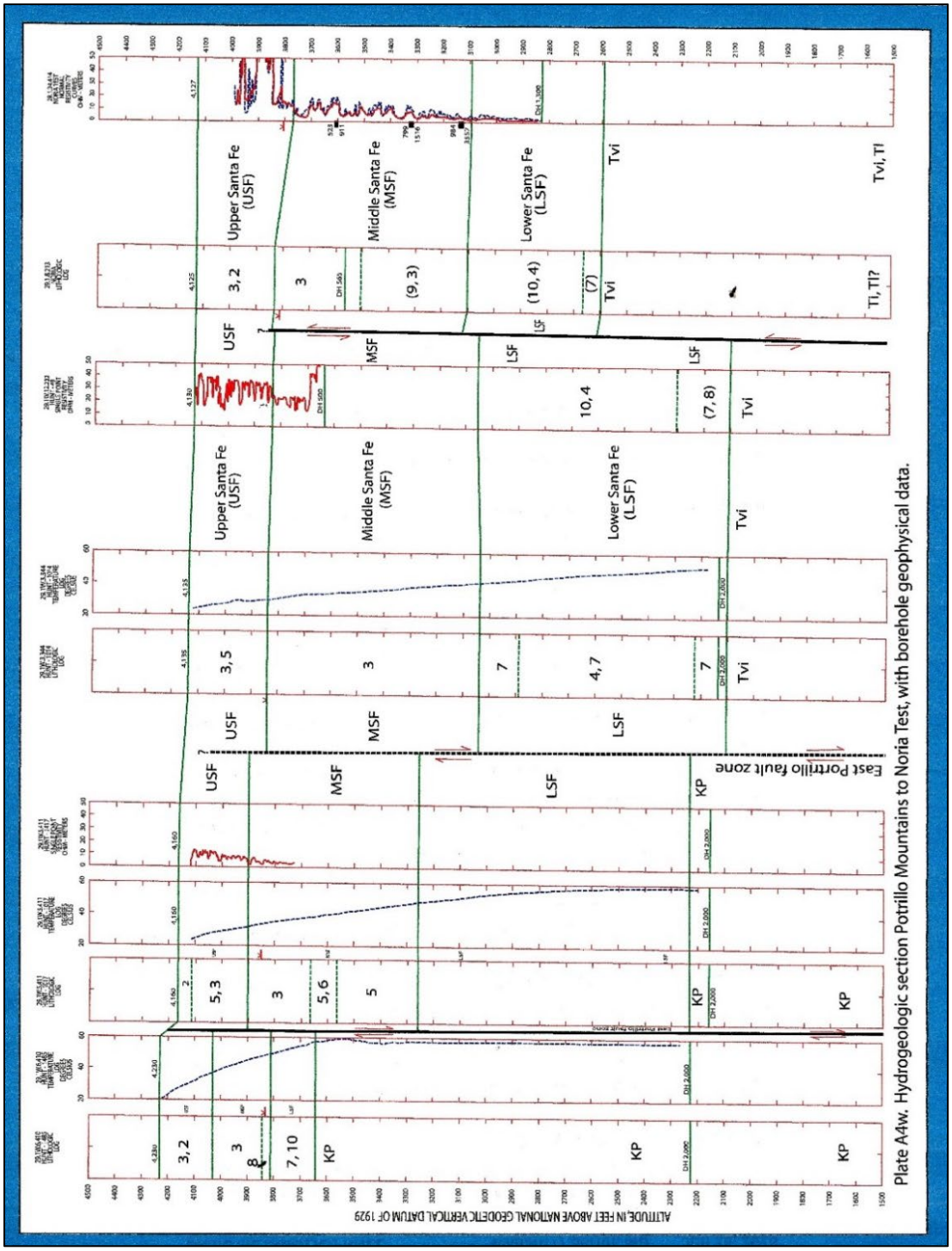

Figure 6-10. Index hydrogeologic section showing six key-well sites in the Kilbourne-Noria Subbasin (KNSB) and adjacent parts of the southern East Potrillo Uplift (EPU-PRS, **5.4.1a**) and the South Mid-Basin High (SMbH, **6.3.2b**). **PLATE 5k** (**K-K'**) alignment west of **PLATE 5q.** E-logs: long normal-blue, short normal and single point-red. Temperature logs are shown as black dots. The main strand of the East Potrillo fault zone (EPfz) is located between Hunt-test holes 1485 and 1017. Tl=Lower Tertiary sedimentary rocks, Tvi=Lower and Middle Tertiary volcanic and igneous-intrusive rocks, and KP=Cretaceous and Permian marine-sedimentary rocks.

The Noria well is in the eastern part of the **Figure 6-10** group (**TBL. 1**, no. 301). It was drilled in 1916 as a water-supply well at Noria Siding for steam engines on the El Paso to Douglas (AZ) route of the El Paso & Southwestern Rail Road (EP&SWRR). The well has a high-quality cable-tool driller's log, and is now USGS observation well no. 154. The EP&SWRR line was later purchased and then abandoned by the SPRR in the 1960s (Darton et al. 1933, **APNDX. C1.5**). Four of the wells were drilled in the late 1970s for a Hunt Energy Corporation geothermal energy exploration project (**TBL. 1**, nos. 295-297 [Hunt-1014, 1017 and 1485—temperature logs], and no. 298 [Hunt-49—e-resistivity log]; *cf.* **Part 5.5.2**). The easternmost well in the group, USGS-EPWU MT-4, is located above the southwestern edge of the MeB-SMbH (**TBL. 1**, no. 253; **6.3.2b**).

Two significant revisions to the interpretations of structure and hydrostratigraphy shown on **Figure 6-10** have been made during the course of this study: (1) The SPRR-Noria Well site (no. 301) is within the KNSB, and (2) the East Potrillo fault zone (EPfz-**Part 5.5.2**) is located between Hunt-test holes 1485 (no. 297) and 1017 (no. 296). With respect to the initial placement of the HSU-LSF/KP contact at about 2,230-ft [680-m] amsl in test hole no. 297 (Hunt-1097), current interpretations of isothermic (near vertical) temperature-log segments for the Hunt test holes indicates that all were completed in relatively high-porosity/permeability zones associated with dissolution of fracture zones in Cretaceous and/or Permian carbonate rocks. Accordingly, the LSF/KP contact near test-hole 297 is now placed at about 2,600-ft [790-m] amsl (*cf.* **PL. 5k**).

6.3.4. Hydrogeologic Subdivisions between Mid-Basin High and Mesilla Valley Fault Zone

The following discussion covers the three MeB hydrogeologic subdivisions that are located south of the Fairacres Subbasin (FASB-**6.3.3b**), and between the Mid-Basin High (MBH-**6.3.2**) and the Mesilla Valley fault zone (MVfz-**6.3.1b**): **3.4a**-Mesquite Subbasin (MSB), **3.4b**-Black Mountain Subbasin (BMSB), and **3.4c**-Santa Teresa High (STH). It also includes El Milagro Subbasin (EMSB-**4d**), which comprises the southernmost part of the MeB and is mostly in Mexico (6.3.4d; **Fig. 6-1**; **Tbl. 6-4; PLS. 5k** and **5l**). The hydrogeologic subdivisions between the MVfz and the MeB's eastern-boundary bedrock uplifts are described in **Part 6.3.5**.

6.3.4a. Mesquite Subbasin (MSB)

The 88 mi² (228 km²) Mesquite Subbasin (MeB-MSB) takes its name from the farming community of Mesquite located on the BNSFRR near the east edge of MeV about 12 mi (20 km) SSE of Las Cruces. The town was named in 1882 by SPRR officials for the local abundance of "mesquite bushes" (Julyan 1996). Thick HSU-USF2 deposits (mostly LFA 2-3) in the eastern third of the subbasin coarsen northward toward their upstream-ARG source area. They are hydraulically well-connected with the overlying HSU-RA (LFA a) alluvial aquifers of the inner MeV, and form the primary hydraulic link

between the river-sourced irrigation infrastructure and the shallow-aquifer system in almost all parts of the MeV-floor area south of the Fairacres Subbasin (FASB) (**Figs. 4-3a**, **4-3b** and **6-1**; **Tbls. 4-1** to **4-3** and **6-4**; **PLS. 5f** to **5h** and **5o**; **APNDX. F: Pls. F2-8**, and **F3-1g** and **1h**). The westernmost part of the MSB extends out of the valley onto a remnant of the relict USF2-ARG (La Mesa) fluvial-plain the eastern edge of the West Mesa (**PLS. 5g** and **5h**). The vadose zone in that area is 300 to 400 ft (90-120 m) thick and composed entirely of HSU-USF2 deposits (mostly LFAs 1 and 2).

Because of burial by HSU-RA deposits, the approximate position of the MVfz and the eastern structural boundary of the MSB is defined on the basis of interpretations of surface geophysical-survey data and borehole-log information from a small number of wells (**Part 6.3.1**; **Figs. 3-6**, **6-2** and **6-3** [II-II′]; **PLS. 5f** to **5h**, and **5o**; **TBL. 1**, nos. 224 to 234). Three hydrogeologic-map subdivisions border the MSB on the east (**Fig. 6-1**): southern Las Cruces Bench (MeB-LCBn, **6.3.5a**), Fillmore Pass Corridor (FPC, **Part 5.1.2**), and northern Anthony-Canutillo Bench (MeB-ACBn, **6.3.5b**). The buried San Pablo fault zone (SPfz-**6.3.3b**), which is identified primarily by gravity-survey information, forms the structural boundary between the northwestern MSB and the FASB (**Fig. 3-8** [**PL. 1A**], **Tbl. 6-2**). Offset of uppermost HSU-USF2 beds is probably less than 30 ft (10 m) (**PLS. 5f** and **5o**).

The MSB's southwestern structural and topographic-boundary with the MeB-Black Mountain subbasin (BMSB) is marked by the NW-trending Chamberino fault zone (CBfz-**Tbl. 6-2**), which is only exposed in a small valley-border area of deformed USF2 beds located northwest of the village of Chamberino (**PLS. 1B**, **2**, **5g** and **5h**; *cf.* Seager et al. 1987). The CBfz is elsewhere more broadly defined by a series of downwarped La Mesa surface remnants that are locally capped by mid- to late-Pleistocene basalt flows of the northern Santo Tomas-Black Mountain volcanic field (Hoffer 1971; Seager et al. 1987; Gile 1990; Williams and Poths 1994; and Dunbar 2005, Tbl. 2). Only one of the field's five cinder-cone source vents, Santo Tomas "Mountain," is located in the MSB, while the rest are in adjacent parts of BMSB, and all are sites of aggregate-resource mining activity.

The southern half of the MSB occupies the structurally deepest part of the Mesilla RG-rift basin, with a minimum SFG/Tlvs contact-elevation of about 1,350 ft (410 m). Eocene andesitic volcanic, volcaniclastic, and epiclastic sedimentary rocks (Tlvs-**Tbl. 6-3**), which underlie the basin fill in the southern three-quarters of the MSB, are overlapped northeastward by Oligocene silicic-volcanic and an associated epiclastic rocks (map-unit Tmrs) that have an ultimate Organ Mountains (OMU) caldera source (**Fig. 6-3** [**PL. 1B**]; **Tbl. 6-3**; *cf.* **5.1.1**). Saturated SFG thickness ranges from about 1,600 ft (490 m) at the subbasin's northern boundary with the FASB to almost 2,300 ft (700 m) at its southern and western borders with the Black Mountain Subbasin (BMSB) (**PLS. 5f** to **5h**, **5o**, and **7**). Estimated saturated-thickness of HSU-USF2 (mostly LFA 3) is about 700 ft (210 m), and thickness of unit MSF2 (also LFA 3) is in the 600 to 950 ft (180-290 m) range (**PLS. 5f** to **5h**, **5o**, and **7**). HSU-LSF has an

estimated thickness range of 400 ft (120 m) to 850 ft (260 m), and partly indurated eolian-sand deposits (LFA 4) are here inferred to be the dominant lithofacies assemblage (**PLS. 5o** and **7**). Limited deep well control in the western third of the MSB, however, does suggest that much of the lower part of HSU-LSF in that area is composed of fine-grained basin-floor facies (primarily LFA 9).

Nickerson (2006) provides essential background information on recent EPWU-USGS cooperative efforts in the general MSB area. Due to its definitive commentary on two of the deepest wells in adjacent parts of the MSB and BMSB (LVB-2 and LVB-3), and because the report is not cited in Teeple 2017, extended passages on hydrostratigraphic, hydrochemistry, and groundwater-age relationships are included here, and information on the third piezometer set at the LMV-1 site is presented in Part **6.3.5b** (ACBn):

> [p. 1] In 2003, El Paso Water Utilities installed six deep piezometers at three sites in the lower Mesilla Valley. This report, which was written in cooperation with El Paso Water Utilities, presents . . . piezometer-location and completion information, selected borehole-geophysical logs, water-level data, water-quality data, and water-quality characteristics, including the interpretation of isotope data to estimate the source and apparent age of ground water. . . .
>
> [p. 7] The LMV-2 site [**PL. 1,** no. 229] is located in the lower Mesilla Valley approximately 3 miles northwest of Anthony, New Mexico. The borehole was drilled to a total depth of 2,300 feet below land surface. Piezometer LMV-2A is completed in the MSF unit; the screened interval is from 680 to 690 feet below land surface. Piezomet—r LMV - 2B is completed in the LSF unit; the screened interval is from 1,860 to 1,870 feet below land surface. Dissolved-solids concentrations in water samples from the LMV-2 site range from 362 mg/L at 1,080 to 1,100 feet below land surface to 5,900 mg/L at 1,990 to 2,010 feet below land surface [**Figs. 6-11** and **6-12**]. The freshwater zone is estimated to extend from the water table to about 1,900 feet below land surface. Slightly saline to saline water extends from the base of the freshwater zone to the bottom of the borehole. Water type varies with aquifer depth from shallow sodium bicarbonate water to deep sodium sulfate water. The dissolved fluoride concentration in LMV-2B exceeded the USEPA primary drinking-water standard. Dissolved arsenic concentrations in LMV-2A and LMV-2B exceeded the proposed USEPA primary drinking-water standard. . . .
>
> [p. 10] The LMV -3 site [**PL. 1,** no. 248] is located on the west side of the lower Mesilla Valley approximately 0.8 mile southeast of La Union, New Mexico. The borehole was drilled to a total depth of 1,820 feet below land surface. . . [*cf.* **Part 6.3.4b**].
>
> Water-quality samples collected by the USGS from the LMV [1-3] piezometers were analyzed for the stable isotopic ratios of $\delta^{2}H$, $\delta^{18}O$, and $\delta^{l3}C$. The isotopic composition of sample LMV-1A [280-290 ft / 85.3-88.4 m piezometer] may represent source water from precipitation as mountain-front recharge along the Franklin Mountains [*cf.* **6.3.5b**]. The deep inner-valley samples from LMV-2A, LMV-2B, and LMV-3B are isotopically lighter (hydrogen depleted). The sources of recharge water to these piezometers are unknown. The $\delta^{l3}C$ compositions in samples from LMV-1A, LMV-2A, LMV-2B, and LMV-3B ranged from -13.71 to -4.99 per mil. The range in values indicates that different processes have affected carbon compositions and may represent differences in recharge origin and chemical reactions along the ground-water flow path ….
>
> Analytical results for the radioactive isotopes tritium (^{3}H) and carbon-14 (^{14}C) were used to estimate the age of ground water in the LMV piezometers. The small tritium values (less than 0.5 pCi/L) are indicative of ground water that was isolated from the atmosphere prior to 1954 atmospheric nuclear weapons testing and that has received no post-1954 contribution from recharge. The ^{14}C values ranged from 2.61 to 8.42 pmC [percent modern carbon, **Table 6-5**].

Geochemical reactions, including the dissolution of carbonate minerals and carbon isotopic exchange, can substantially decrease carbon composition in ground water. The extent of these chemical reactions in the lower Mesilla Valley and the degree to which they affect carbon composition are unknown. The uncorrected apparent ages [**Tbl. 6-5**] ranged from 10,400 to 30,100 years before present and represent maximum calculated ages. The corrected apparent ages ranged from 4,670 to 24,400 years before present and represent minimum calculated ages (maximum carbonate dissolution). The larger ^{14}C composition of 28.42 pmC in the LMV-3B sample resulted in a younger corrected apparent age of 4,670 years, which is inconsistent with the conceptual model of the ground-water flow system.

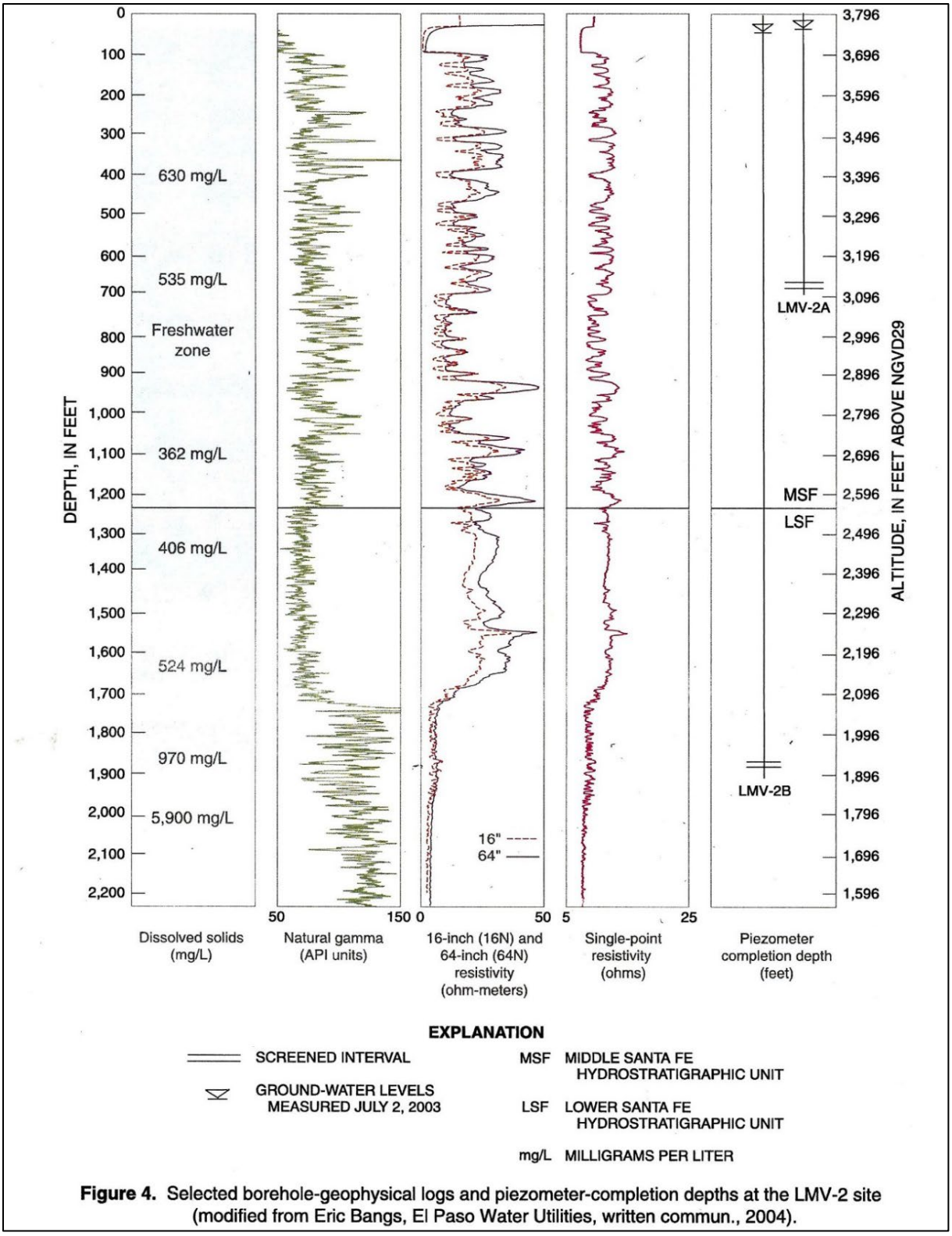

Figure 4. Selected borehole-geophysical logs and piezometer-completion depths at the LMV-2 site (modified from Eric Bangs, El Paso Water Utilities, written commun., 2004).

Figure 6-11 (Nickerson 2006, Fig. 4)**.** Selected borehole-geophysical logs and piezometer-completion depths at the LMV-2 site (**TBL. 1**, no. 229). The LFA 4/3-9 contact depth in HSU-LSF is about 1,720 ft (525 m) bgs.

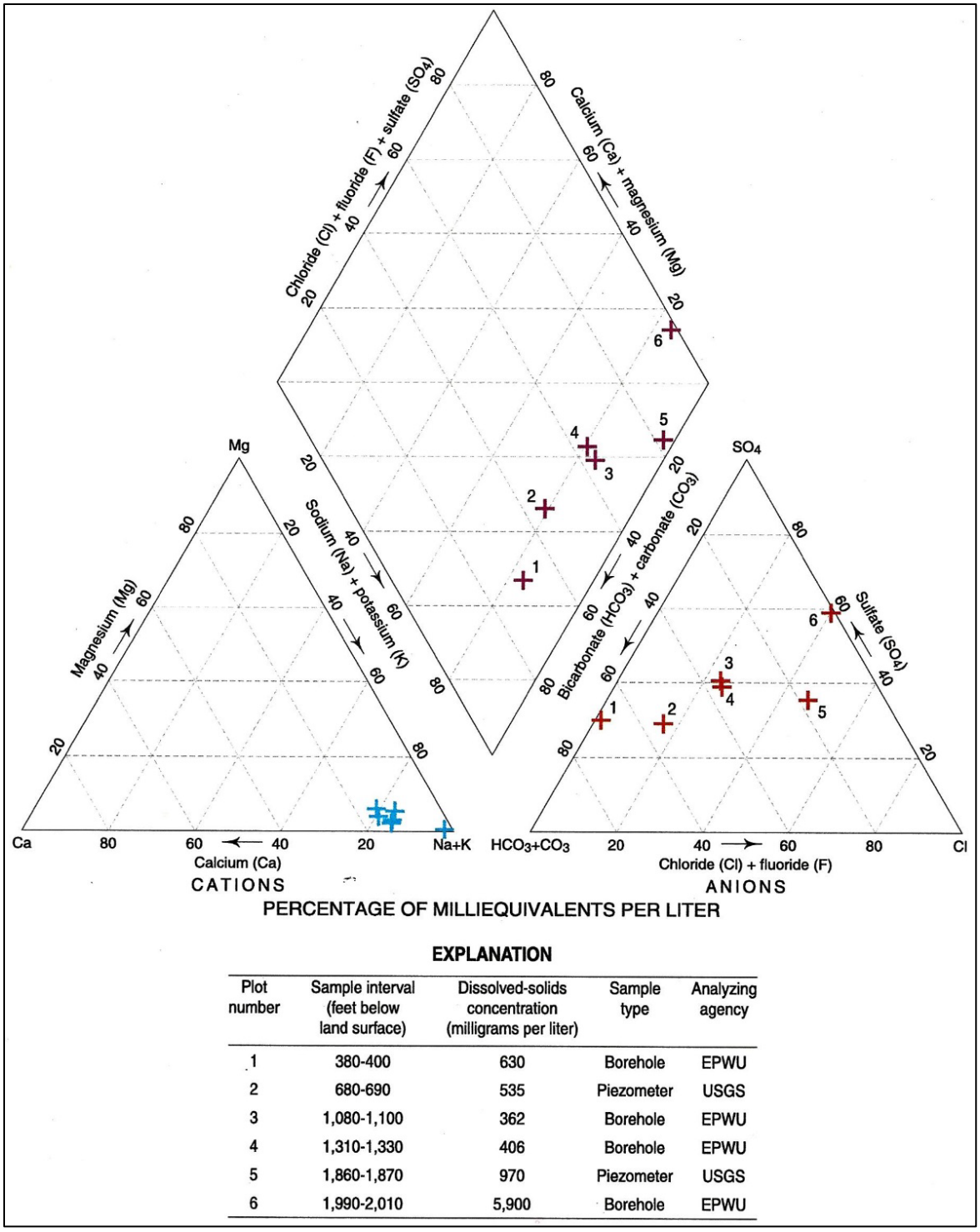

EXPLANATION

Plot number	Sample interval (feet below land surface)	Dissolved-solids concentration (milligrams per liter)	Sample type	Analyzing agency
1	380-400	630	Borehole	EPWU
2	680-690	535	Piezometer	USGS
3	1,080-1,100	362	Borehole	EPWU
4	1,310-1,330	406	Borehole	EPWU
5	1,860-1,870	970	Piezometer	USGS
6	1,990-2,010	5,900	Borehole	EPWU

Figure 6-12 (Nickerson 2006, Fig. 5)**.** Distribution of major constituents in groundwater-quality samples from selected depth intervals at the LMV-2 site (**TBL. 1**, no. 229). Sampled intervals by HSU and LFA: (1) 380-400 ft (116-122 m)−USF2 (LFA 3); (2) 680-690 ft (207-210 m)−MSF2 (LFA 3); (3) 1,080-1,100 ft (116-122 m)−MSF2 (LFA 3); (4) 1,310-1,330 ft (399-405 m)−LSF (LFA 4); (5) 1,860-1,880 ft (567-573 m)−LSF (LFA 3?), and (6) 1,990-2,010 ft (607-613 m)−LSF (LFA 9). GW silica content (mg/L): (1) 50; (2) 38.8; (3) 15.3; (4) 31.7; (5) 15.3, and (6) 16.7 (*cf.* Nickerson 2006, Appendix Table 2, p. 22).

With reference to piezometers LMV-2A and 2B (**Table 6-5**), which were installed at the respective depths of 680 to 690 ft (207-210 m) and 1,860 to 1,880 ft (567-573 m), Nickerson (2006, Tbl. 4) notes that: 1. ^{14}C in percent modern carbon (pmC) in sample LMV-2A is 15.54, and the "Corrected apparent [GW] age" is 9,600 years before present (BP), and 2. ^{14}C in pmC in sample LMV-2B is 2.61, and the "Corrected apparent [GW] age" is 24,400 years BP.

Table 6-5. (Nickerson 2006, Tbl. 4) Measured ^{14}C Composition, Partial Pressure of Carbon Dioxide, Saturation Index for Calcite, and Apparent Age of Groundwater Sampled in 2003 at Piezometer Sites LMV-1A [Part 6.3.5b], LMV-2A and 2B [6.3.4a], and LMV-3 [6.3.4b]

[pmC, percent modern carbon]

Piezometer name (fig. 1)	^{14}C, in pmC	Partial pressure of carbon dioxide, in atmospheres	Saturation index, calcite	Uncorrected apparent age assuming Ao equals 100 pmC, in years before present	Corrected apparent age assuming Ao equals 50 pmC, in years before present
LMV-1A	6.74	-2.43	-0.03	22,300	16,600
LMV-2A	15.54	-2.53	0.17	15,400	9,660
LMV-2B	2.61	-3.54	0.09	30,100	24,400
LMV-3B	28.42	-3.90	0.39	10,400	4,670

6.3.4b. Black Mountain Subbasin (BMSB)

The 136 mi^2 (350 km^2) Black Mountain Subbasin (MeB-BMSB) occupies much of the east-central West Mesa between the Mid-Basin High (MBH) and the Gadsden-La Union area of the Lower Mesilla Valley. A large remnant of the relict ARG fluvial-plain (La Mesa surface) comprises most of the subbasin area, and only a small portion is located in the Mesilla Valley (<20 mi^2 /52 km^2; **Figs. 6-1** to **6-3** [II-II′]; Tbl. 6-2 to 6-4; **PLS. 1B**, **1C**, **5g** to **5j**, and **5p**). The BMSB takes its provisional name from Black Mountain, the central cinder-cone vent for the largest expanse of basalt flows (~9 mi^2 /23 km^2) in the Black Mountain-Santo Tomas volcanic field of mid- to late- Pleistocene age (**APNDX. F: Pls. F2-2,** and **F3-1h** and **1i**). The field extends across the eastern West Mesa floor into the southwestern part of the Mesquite Subbasin (MSB), and includes the vents for the less-extensive Little Black Mountain, San Miguel, and Santo Tomas basalt flows (**Part 6.3.4a**; *cf.* Kottlowski 1960, Hoffer 1971, Seager et al. 1987, Gile 1990, Dunbar 2005). The poorly defined Mid-basin fault zone (MBfz) forms the deeply buried structural boundary between the western BMSB and the Mid-Basin High (MbH), and a short segment of the San Pablo fault zone (SPfz) marks the Fairacres-Black Mountain subbasin boundary (**Figs. 6-1** to **6-3**;

Tbls. 6-1 to **6-4**; **PLS. 1B, 1C**, **5g** to **5j**, **5o** and **5p**). The NW-trending Chamberino fault zone (CBfz) forms the BMSB's northeastern boundary with the MSB.

Together with the southern Mesquite Subbasin (MSB), the east-central Black Mesa Subbasin (BMSB) occupies the structurally deepest part of the MeB, with a minimum SFG/Tlvs-bedrock contact-altitude of about 1,550-ft (470-m) amsl (**PL. 1B**, **Fig. 3-11**). SFG basin fill is unconformably underlain by Eocene andesitic volcanic, volcaniclastic, and epiclastic sedimentary rocks (Tlvs) throughout the subbasin (**PLS. 1B**, **1C**, **5g** to **5j**, and **5p**; **Figs. 3-11** and **3-12**, **TBL. 2** and **Tbl. 3-3**). Its transitional southern boundary with the Santa Teresa High is marked by (1) significant thinning of SFG deposits, and (2) wedging out of Tlvs volcanics over underlying siliciclastic sedimentary rocks unit Tls (**PLS 5o** and **5p**). Available deep-borehole sample and geophysical data from this area indicates that the upper Oligocene to mid-Miocene, HSU-LSF has two primary lithofacies-assemblage (LFA) components: (1) an extensive fine-grained basin-floor facies (LFA 9) on the west, and (2) eolian-sand (dune-field) component (LFA 4) along the MeB's eastern border (**PLS. 5g-5j**, **5o**, **7C**; *cf.* Wilson et al. 1981, Wilson and White 1984, Hawley and Lozinsky 1992, Hawley and Kennedy 2004). This suggests that much of the BMSB-MSB area was a closed structural depression during early to middle stages of RG-rift basin formation. As such, it included (1) a large ephemeral to intermittent lake plain, and (2) a flanking dune-field analog of the present Médanos de Samalayuca (*cf.* **Fig. 1-13**; **Part 3.3.2**; **APNDX. H1.5.2**).

The vadose zone in the West Mesa area of the BMSB is from 300 to 400 ft (90-120 m) thick and composed entirely of HSU-USF2 (ARG) deposits (mostly LFAs 2 and 3). Saturated SFG thickness ranges from 1,600 ft to 1,700 ft (488-518 m) at the subbasin boundaries with the FASB and the Santa Teresa High (STH) to 2,200 ft (670 m) at its eastern border with the MSB (**PLS. 2, 5h, 5j**, and **5p**). Estimated saturated-thickness of HSU-USF2 (LFA 3) ranges from about 350 to 650 ft (105-200 m), and the thickness range of HSU-MSF2 (also LFA 3) is 650 to 900 ft (200-275 m) (**PLS. 5g** to **5j**, **5p**, and **7A**). The inferred thickness of the fine-grained basin-floor facies HSU-LSF (LFA 9) is between 500 and 550 ft (150-168 m). The upper 230 ft (70 m) of the HSU-USF2 interval (upper Camp Rice Formation correlative) is well exposed along the western border of the MeV between the Village of Chamberino and Anapra-Sunland Park (*cf.* **Parts 6.3.4b** and **6.3.5c**; **Fig. 6-17**). An Early Pleistocene age of these ARG sediments has been established by the detailed sedimentologic, biostratigraphic and magneto-stratigraphic work near La Union by Vanderhill (1986), Mack and others (1998b, and Morgan 2022). The Ancestral Rio Grande (ARG) origin of these sediments was first recognized by N.H. Darton (1933, p. 132) in his description of the SPRR (now UPRR) route between Anapra and Strauss (**APNDX. C1.5**).

The new UPRR Intermodal Terminal and Refueling Station, which opened in 2014, is located near the original SPRR Vevay Siding site (alt. 4,135 ft/1,260 m). It is centered in a heretofore undeveloped part of the Black Mountain Subbasin about 5 mi (8 km) southwest of USGS-EPWU test-

well MT-3 (*cf.* **Fig. 6-13**) and the same distance northwest of the Santa Teresa Industrial Park (**Part 6.3.4c**). Development in this part of the International Boundary Zone (IBZ) for municipal and industrial (M&I) uses is projected to ultimately result in a major increase in fresh- and brackish-GW production throughout the southeastern MeB (**Figs. 1-4** and **2-2**, *cf.* Pacheco 2011 and 2012, Quigley 2011, Robinson-Avila and Villagran 2014). The scope of the activity is illustrated by following selections from two Albuquerque Journal articles (1) The Associated Press in the 12/25/2013 BUSINESS section, and (2) Journal Staff in its 5/5/2019 JOURNAL AND WIRE REPORTS seon:

> (1) SANTA TERESA - A $400 million Union Pacific railroad facility near a young New Mexico border town could open next year, according to the company.
>
> Union Pacific spokesman Aaron Hunt said Tuesday that construction near Santa Teresa is ahead of schedule and the facility could be operational in 2014. It had been slated to open in 2015. "The second phase of construction (which began in July 2012) will finish the yard to include all the mechanical, electrical, architectural, utilities, track and civil engineering portions of the project," Hunt said in a statement. . . .
>
> The Santa Teresa-San Jeronimo region is still young and development there only started after the Santa Teresa Port of Entry opened in 1993. The New Mexico Border Authority said last year that the port of entry processed more than 81,000 commercial trucks - 13 percent higher than any year on record. The region's growth has been a keystone to plans by Gov. Susana Martinez for New Mexico economic expansion.
>
> In August, Martinez and officials from Mexico announced the creation of a 70,000-acre, master-planned community around the Santa Teresa-San Jeronimo border crossing in an effort to expand the fast-growing border region even more. Under the plan, the project would create new trade zones, joint health care programs and "quality residential living." Officials said the goal was to create an industrial powerhouse capable of transforming the area into a busy international trading zone. . . .
>
> (2) SANTA FE - State officials say Union Pacific Railroad is undertaking a $20 million project at its Santa Teresa Intermodal Terminal and Refueling Station.
>
> The New Mexico Economic Development Department announced Friday that the investment will allow the company to add container blocks to passing trains faster and more efficiently.
>
> Officials say the improvements also will mean more shipments and less downtime for customers waiting for merchandise along the railroad's 760-mile Sunset Corridor between El Paso and Los Angeles.
>
> The original 2,200-acre intermodal facility opened in 2014 as a strategic location that allows the railroad to sort and move cargo along its routes in 23 states.

The USGS-EPWU La Union test well MT-3 (**TBL. 1**, no. 242) is located in the southeastern part of the BMSB near the eastern edge of the West Mesa and about two miles (3.2 km) west of the community of La Union. It was completed in fine-grained basal HSU-LSF sediments (LFA 9) at a depth of 2,250 ft (686 m), and penetrated almost all of the thickest documented SFG section in the MeB (Hawley and Lozinsky 1992, p. 21-26, Tbl. 4a, Pls. 4, 5, 9, and 14). **Figure 6-13** (Nickerson and Myers 1993, Fig. 36) is an electric log of the MT-3 test well, with the PI's interpretations of HSU bgs contact depths (USF2/MSF2-530 ft/162 m; MSF2/LSF-1,735 ft/529 m). Chemical analyses of water sampled at

five depth intervals in the test well are summarized in **Figure 6-14** (Nickerson and Myers 1993, Fig. 41): **1.** Lower HSU-LSF (LFA 9−2,200-2,220 ft [671-667 m]), **2.** Upper HSU-LSF (LFA 9−1,900-1, 920 ft [579-585 m]), **3**. HSU-MSF2 (LFA 3−1,170-1, 190 ft [357-363 m]), **4.** Upper and middle HSU-MSF2 (LFA 3−665-675 ft [203-206 m]) and **5**. Upper HSU-MSF2 (LFA 3−635-655 ft [194-200 m]). Water temperature and sample silica content (Celsius and mg/L): (**1**) 30.5° and 45°, (**2**) 32° and 22°, (**3**) 30.5° and 42°, (**4**) 28.5° and 37°, and (**5**) 29° and 43° (*cf.* Hawley and Lozinsky 1992, Tbl. 4a).

The other deep test well in the southeastern Black Mountain Subbasin, EPWU-USGS LMV-3 (**TBL. 1**, no. 248), is located on the floor of the Lower MeV and approximately 0.8 mile (1.3 km) southeast of the Village of La Union (**Figs. 6-15** and **6-16**; *cf.* **PLS. 5i**, **5j**, and **5o**). According to Nickerson (2006, p. 10):

> Piezometer LMV-3A is completed in the MSF unit; the screened interval is from 880 to 890 feet below land surface. Because the driller was unable to develop piezometer LMV-3A, no water-level data or water-quality samples were obtained. Piezometer LMV-3B is completed in the LSF unit; the screened interval is from 1,745 to 1,755 feet below land surface [**Figs. 6-15** and **6-16**]. Dissolved-solids concentrations in water samples from the LMV-3 site range from 378 mg/L at 640 to 660 feet below land surface to 6,100 mg/L at 1,745 to 1,755 feet below land surface. The freshwater zone is estimated to extend from less than 190 to about 1,320 feet below land surface. Slightly saline to saline water extends from the base of the freshwater zone to the bottom of the borehole. Water type varies with aquifer depth from shallow sodium bicarbonate water to deep sodium chloride sulfate water. The concentration of dissolved arsenic in LMV-3B exceeded the proposed USEPA primary drinking-water standard ….

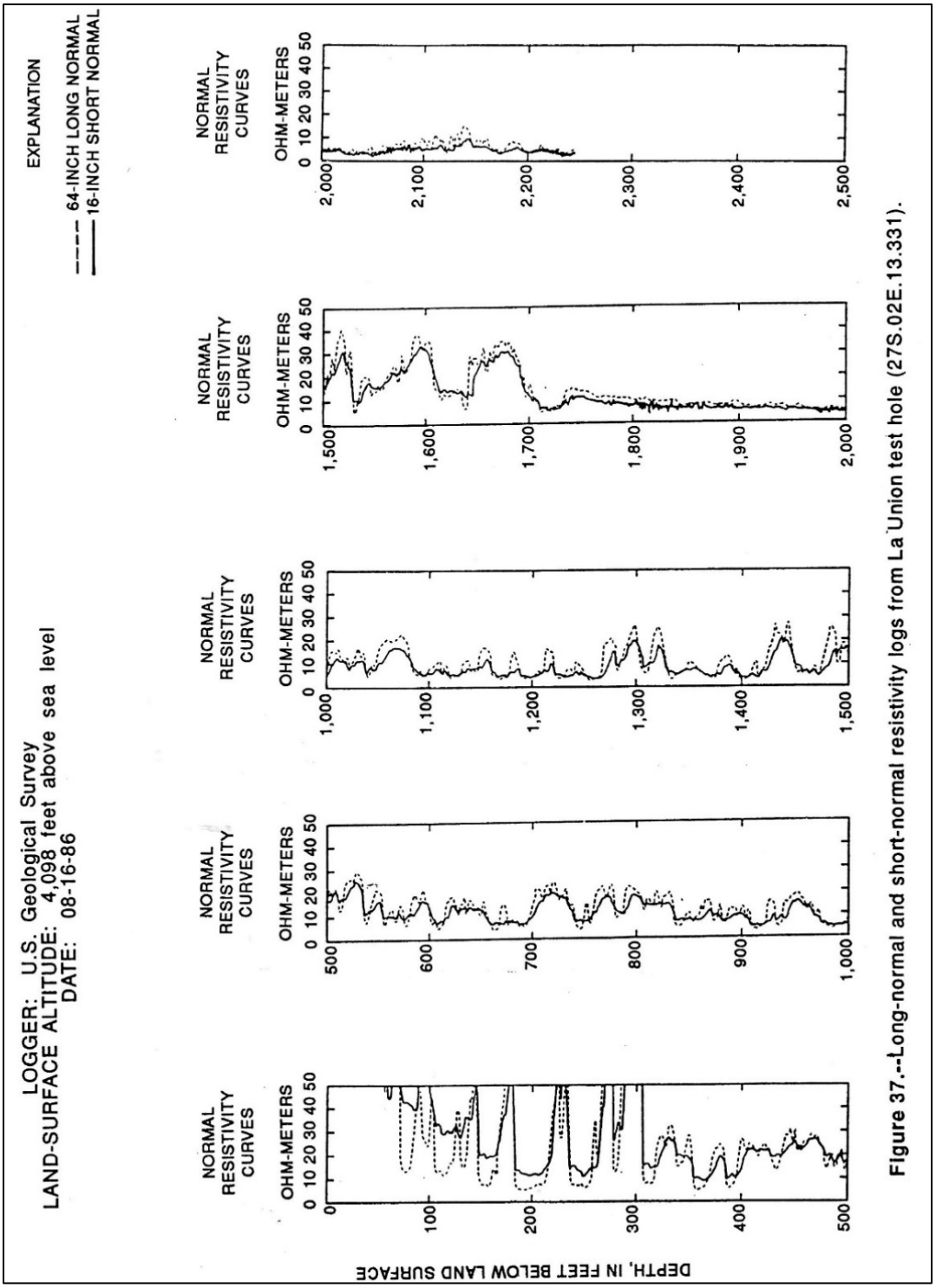

Figure 6-13 (Nickerson and Myers 1993, Fig. 37)**.** Electrical-resistivity log of USGS-EPWU La Union test hole (USGS-EPWU MT-3, **TBL. 1**, no. 242), with current interpretations of HSU contact depths (bgs): USF—/MSF2 - 530 ft (162 m), MS—2/LSF - 1,735 ft (529 m), and estimated L—F/Tls - 2,500-ft (762 m). Depth to water was 316.6 ft (96.5 m) in August 1986. *See* Hawley and Kennedy (2004, Pls. 4c, 4d, and A3): and **PLATES 5i, 5j,** and **5p.**

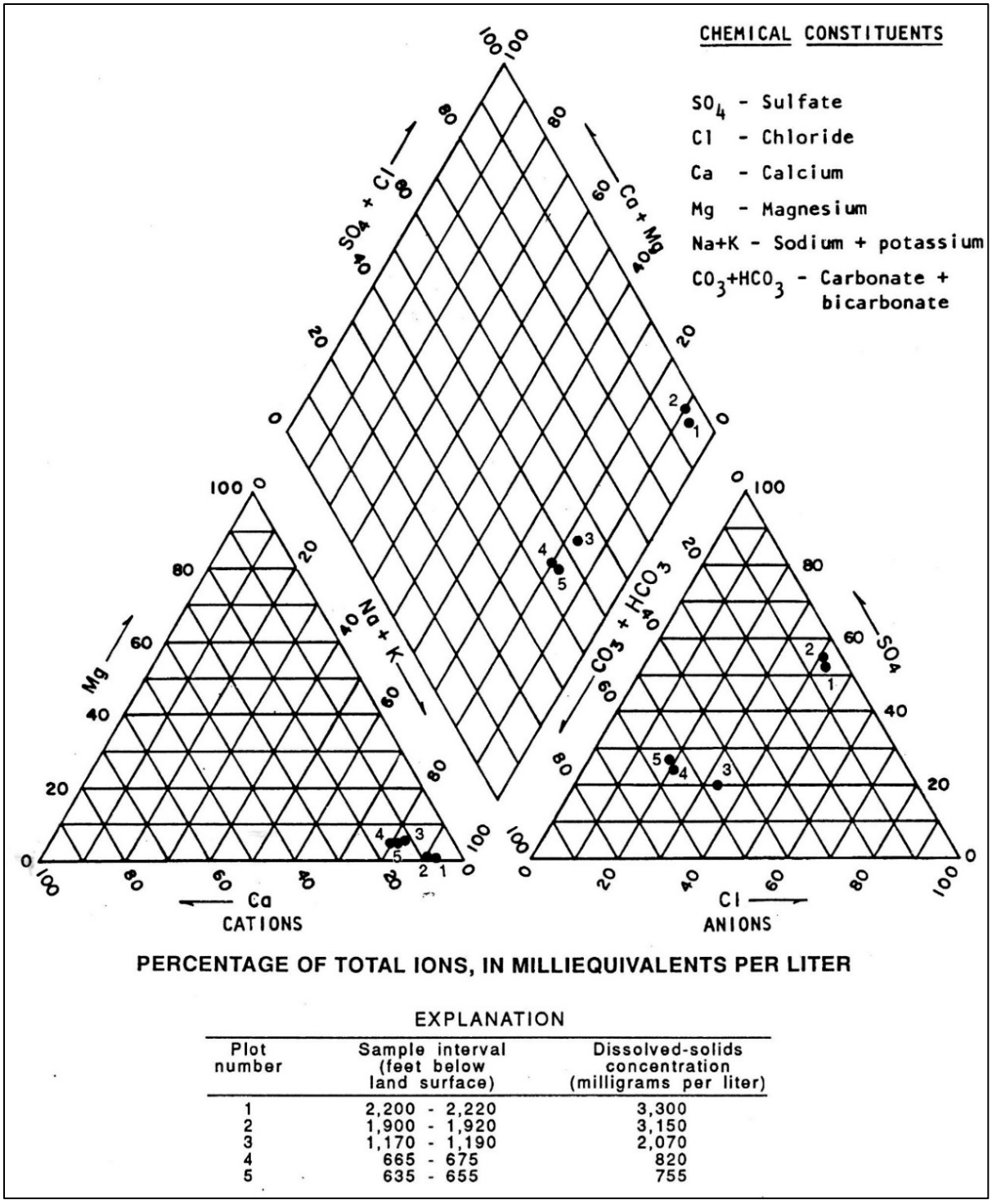

EXPLANATION

Plot number	Sample interval (feet below land surface)	Dissolved-solids concentration (milligrams per liter)
1	2,200 - 2,220	3,300
2	1,900 - 1,920	3,150
3	1,170 - 1,190	2,070
4	665 - 675	820
5	635 - 655	755

Figure 6-14 (Nickerson and Myers 1993, p. 63)**.** Chemical analyses of water from selected depth intervals in La Union test hole (USGS-EPWU MT-3, **TBL. 1**, no. 242). Samples from (1) lower part of HSU-LSF (LFA-9), (2) upper part of HSU-LSF (LFA-9), (3) middle part of HSU-MSF 2 (LFA-3), (4) upper and middle parts of HSU-MSF 2 (LFA-3), and (5) upper HSU-MSF2 (LFA-3). Water temperature and sample silica content (Celsius and Mg/L): (1) 30.5° and 45, (2) 32° and 22, (3) 30.5° and 42, (4) 28.5° and 37, and (5) 29 and 43 (*cf.* Nickerson and Myers 1993, Tbl. 2).

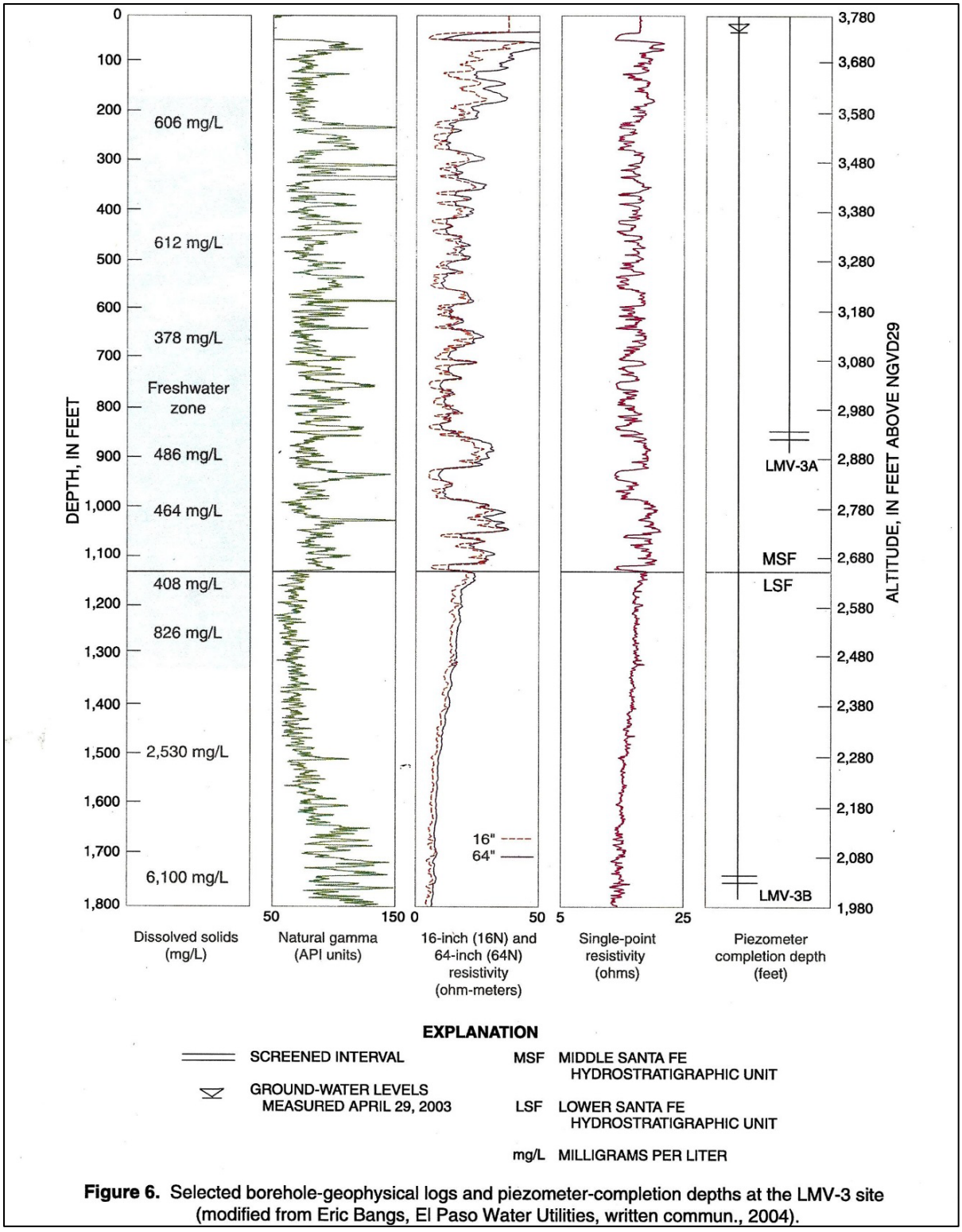

Figure 6. Selected borehole-geophysical logs and piezometer-completion depths at the LMV-3 site (modified from Eric Bangs, El Paso Water Utilities, written commun., 2004).

Figure 6-15 (Nickerson 2006, Fig. 6)**.** Selected borehole-geophysical logs and piezometer-completion depths at the LMV-3 site (**TBL. 1**, no. 248). Note that the transitional contact-depth between LFA*s 4 and 9* in HSU-LSF is here interpreted to be at about 1,330 ft (405 m) bgs.

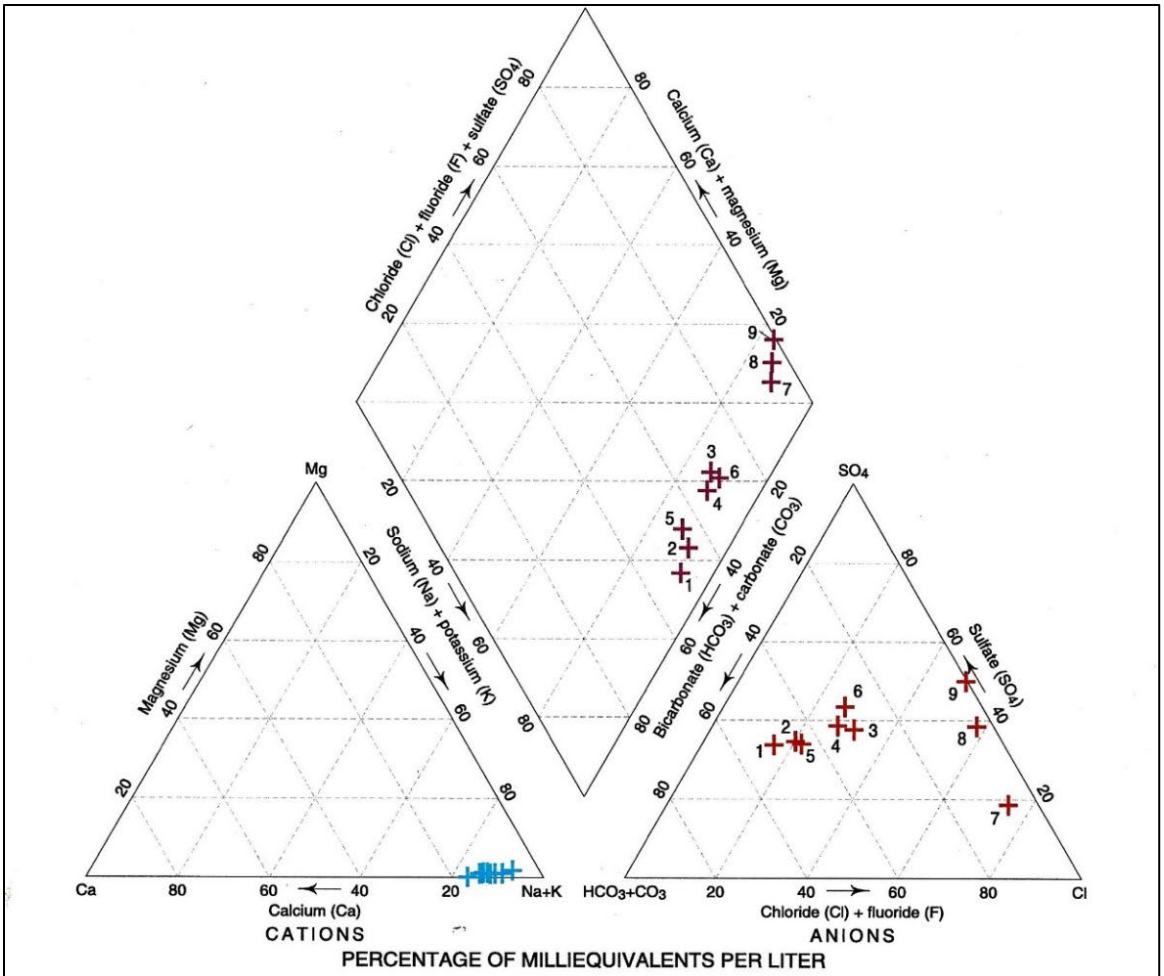

EXPLANATION

Plot number	Sample interval (feet below land surface)	Dissolved-solids concentration (milligrams per liter)	Sample type	Analyzing agency
1	190-210	606	Borehole	EPWU
2	450-470	612	Borehole	EPWU
3	640-660	378	Borehole	EPWU
4	870-890	486	Borehole	EPWU
5	990-1,010	464	Borehole	EPWU
6	1,130-1,150	408	Borehole	EPWU
7	1,250-1,270	826	Borehole	EPWU
8	1,470-1,490	2,530	Borehole	EPWU
9	1,745-1,755	6,100	Piezometer	USGS

Figure 6-16 (Nickerson 2006, Fig. 4)**.** Distribution of major constituents in groundwater-quality samples from selected depth intervals at the LMV-3 site (**TBL. 1**, no. 248). Sampled intervals by HSU and LFA: (1) 190-210 ft (58-61 m)−basal USF2 (LFA 3), (2) 450-470 ft (137-143 m)−upper MSF2 (LFA 3), (3) 640-660 ft (195-196 m)−lower MSF2 (LFA 3), (4) 870-890 ft (265-271 m)−MSF (LFA 4), (5) 990-1,010 ft (302-308 m)−basal MSF2 (LFA 3), (6) 1,130-1,150 ft (344-350 m)−upper LSF (LFA 4), (7) 1,250-1,270 ft (381-387 m)−upper LSF (LFA 4), (8) 1,470-1,490 ft (448-454 m)−LSF (LFA 9), and (9) 1,745-1,755 ft (532-535 m)−LSF (LFA 9). GW silica content (mg/L): (1) 43.6, (2) 44.7, (3) 44, (4) 44.6, (5**)** 43.8, (6) 30.1, (7) 22.5, (8) 29.5, and (9) 31.9 (*cf.* Nickerson 2006, Appendix Table 2, p. 22).

6.3.4c. Santa Teresa High (STH)

The Santa Teresa High (STH) has an area of 35.5 mi^2 (90 km^2) and is the southeastern-most MeB hydrogeologic subdivision that is located entirely in the United States (**Figs. 6-1** to **6-3, Tbls. 6-1** to **6.4**; **PLS. 5k** and **5p**; **APNDX. F: Pls. F2-2, F3-1i**, and **F4-1k**). It takes its provisional name from (1) the Santa Teresa Territorial Land Grant in the lower Mesilla Valley, and (2) the community of Santa Teresa and adjacent industrial-park on the UPRR [SPRR]. The STH was initially designated the Santa Teresa "bench" by Hawley and Kennedy (2004). However, due to its thick cover of SFG basin-fill (>1,400 ft/425 m) and fault-zone borders, the unit best fits in the MeB structural "High" category as defined herein (e.g., MBH and PSH; **Part**s **6.3.2** and **6.4.1**).

The transitional Santa Teresa High-Black Mountain Subbasin boundary is characterized by substantial thinning of SFG basin fill, and the pinch out of the Tlvs andesitic-volcanic cover on Tls siliciclastic sedimentary rocks (**Figs. 6-2** and **6-3**; **PLS. 5o**, and **5p**; *cf.* **Part 6.3.4b**). A shallowly buried southern segment of the Mesilla Valley fault zone (MVfz) forms the eastern structural boundary between the STH and the Anthony-Canutillo and Anapra-Oasis Benches (ACBn and AOBn, **6.3.5b and 5d**). The STH's southwestern boundary with El Milagro Subbasin (EMSB) is marked by the low scarp of the Mastodon fault zone (MDfz), which crosses the US-Mexico border south of Santa Teresa (**6.3.4d**; **Fig. 6-1**, **Tbl. 6-2**; **PLS. 5k** and **5p**).

From a subsurface-database perspective, the STH is the most intensively investigated part of the southern MeB (Wilson et al. 1981; Hawley and Kennedy 2004). Twenty-nine of the 32 original wells in the Santa Teresa ["Crowder"] well field are located within the STH, and information on 22 of the wells is included in **TABLE 1**. The following passage from Wilson and others (1981, p. 54) describes the aquifer-evaluation activities that were initiated in the early 1970s by the late Charles L. Crowder (1932-2018), who is regarded by many as the leading visionary in land- and water-resource development in this part of the US-Mexico Border region (Culbertson 2018, Kocherga 2018b, Pacheco 2018c, 2024b,c):

> The Santa Teresa well field, containing 32 wells, is located on the eastern edge of the West Mesa in T. 28 S., R. 2 and 3 E. At present (1981), pumps have not been installed in many of these wells. The wells range in depth from 190 to 618 feet* [58-188 m], and static water levels range from about 33 to 337 feet [10-103 m]. During a test in November 1974, well 28S.3E.28.114 [no. 20**] yielded 748 gallons per minute (Trauger and Stoneman, 1975).
>
> **A 1,980 ft (603.5 m) test hole that was drilled at the Well-14 site penetrated the entire thickness of SFG basin fill (**TBL. 1**, no. 261; **Fig. 6-17**).*
>
> ***About 2,600 ft (792 m) north of ST 24 (**TBL. 1**, no. 281, **Fig. 6-17**).*

Figure 6-17 is a previously unpublished "GENERALIZED GEOLOGIC CROSS-SECTION A-A', CROWDER WELL FIELD, SANTA TERESA, NEW MEXICO" (Brown and Caldwell, Fig. 4, *circa* 1975). It was contributed to the NM WRRI TAAP database by Thomas Maddock III in 2010. *See*

TABLE 1 for construction and hydrostratigraphic information on Santa Teresa (ST) Wells 5 (no. 264), 9 [19] (no. 266), 14 (no. 261), 21 (no. 280), 23 (no. 292), 24, and 29 (no. 265). Only Wells 21 and 23, which are located on the Anthony-Canutillo Bench (ACBn—MVfz footwall block, are outside the STH and southernmost BMSB area.

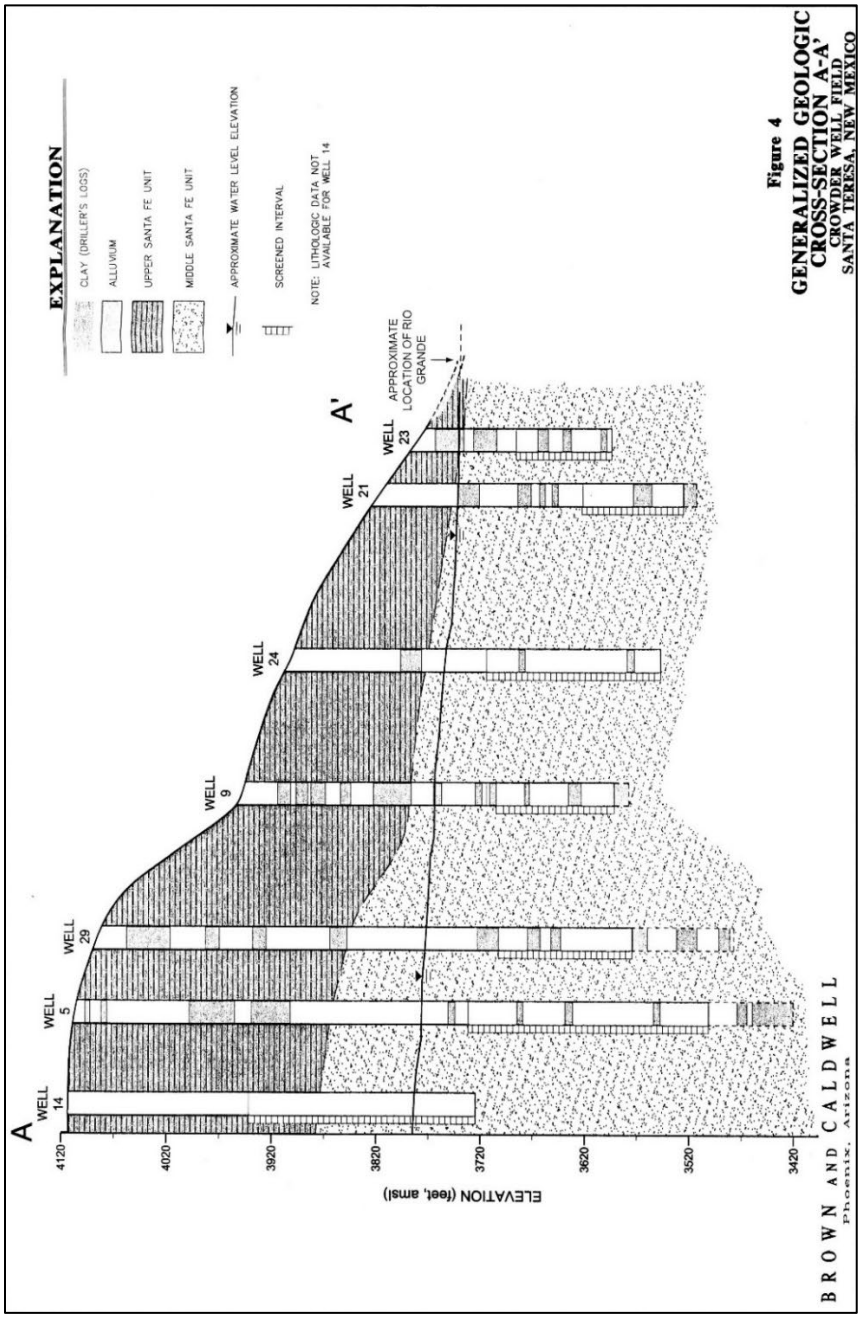

Figure 6-17. "GENERALIZED GEOLOGIC CROSS-SECTION A-A', CROWDER WELL FIELD, SANTA TEREI[ST]..." (Brown and Caldwell-unpublished, *ca.* 1975, Fig. 4). *Notes:* 1. Wells 21 and 23 are on the Anthony-Canutillo Bench (ACBn) just east of the MVfz. 2. 1,980 ft (603.5 m) test well at ST Well-14 site (*cf.* **Fig. 6-18**).

A 1,980-ft (603.5-m) test hole that was drilled for the C.L. Crowder Investment Company at the ST-14 site in March 1972 (**TBL. 1**, no. 261) is of special importance to this study. It is located about 0.9 mi SW of the former Strauss Land & Cattle Company Headquarters, and it is the only well in the southeastern MeB-West Mesa area that penetrates the complete SFG section. The HSU-LSF contact on Tlvs bedrock at a depth of about 1,820 ft (555 m) bgs. The borehole electrical-resistivity log for the test hole was digitized by R.P. Lozinsky in 1988, and initially published with provisional HSU assignments in Hawley and Lozinsky (1992, Pl. 9). It was republished with updated HSU notations by Hawley and Kennedy (2004) as part of their Plate A5, and it is included here in **Figure 6-18**. General hydrogeologic-section alignment is **QQ′** north of Lanark**,** and **PP′** in the Santa Teresa High area (**Fig. 1-4**). The short- and long-normal resistivity pair in the electric log (red and blue) show the presence of water-producing sand layers in the upper 1,200 ft (366 m) of saturated SFG basin fill, with the fresh/brackish-water transition occurring about 500 ft (150 m) below the water table. As noted in **Part 6.3.3b**, the electric-log *signatures* for SFG deposits and subjacent Tlvs bedrock in the test borings for ST-14 and Afton MT-1 (**TBL. 1**, no. 175) are very similar, even though they are about 22 mi (35 km) apart and are on opposite sides of the deeply buried Mid-basin High (*cf.* **Fig. 6-8**, and **APNDX. A5**: **Pl. EA-5**). This suggests that there is general SFG stratigraphic continuity at depth beneath much of the central and southeastern part of the West Mesa area (*cf.* **Fig. 6-2**).

6.3.4d. El Milagro Subbasin (EMSB)

El Milagro Subbasin (EMSB) is the southernmost hydrogeologic subdivision of the MeB, and only about one quarter of its 78.5 mi^2 (203 km^2) area is in the United States (**Figs. 6-1** to **6-3** [III-III′] and **Tbls. 6-1** to **6-4**; **PLS. 5l** and **5p**). Its respective eastern and western subbasin boundaries with the Sierra Juárez Uplift (SJU), and the South Mid-Basin and Potrillo-Sapello Highs (SMbH and PSH) are formed by the El Vergel and Sierra Sapello fault zones (EVfz and SSfz, **Tbl. 6-2**; *cf.* **Parts 5.1.5** and **5.1.6**). Its northeastern boundary with the STH is structurally well-defined by the Mastodon fault zone (MDfz), but its transitional southern border with the Méndez-Vergel Inflow Corridor (MVIC) has no distinct structural or topographic expression (**5.1.5**, *cf.* **Figs. 3-6**, **3-7a** and **3-7b**). It is here provisionally placed 4 to 6 km (2.5-3.7 mi) north of Mex. Federal Hwy. 2, which corresponds closely with the GW-basin's southern structural border as initially "defined" by Frenzel and Kaehler (1990-1992, Fig. 4; *cf.* **Figs. 1-6**, **6-1** and **6-2**; **PLS. 5p** and **5s**). Summary information on the construction and hydrostratigraphic relationships for 14 wells located in the EMSB or in contiguous areas is included in **TABLE 1** (well nos. 359, 362, 365, 367, 372, 376, 379, 385, 388, 390, 392-394, and 396). They range in depth from 300 to 985 ft (90 to 300 m). Sampled water quality in Wells 359, 367, 372 and 390 is in the 300 to 700 mg/L TDS range, and no water-quality data is available for Well 396.

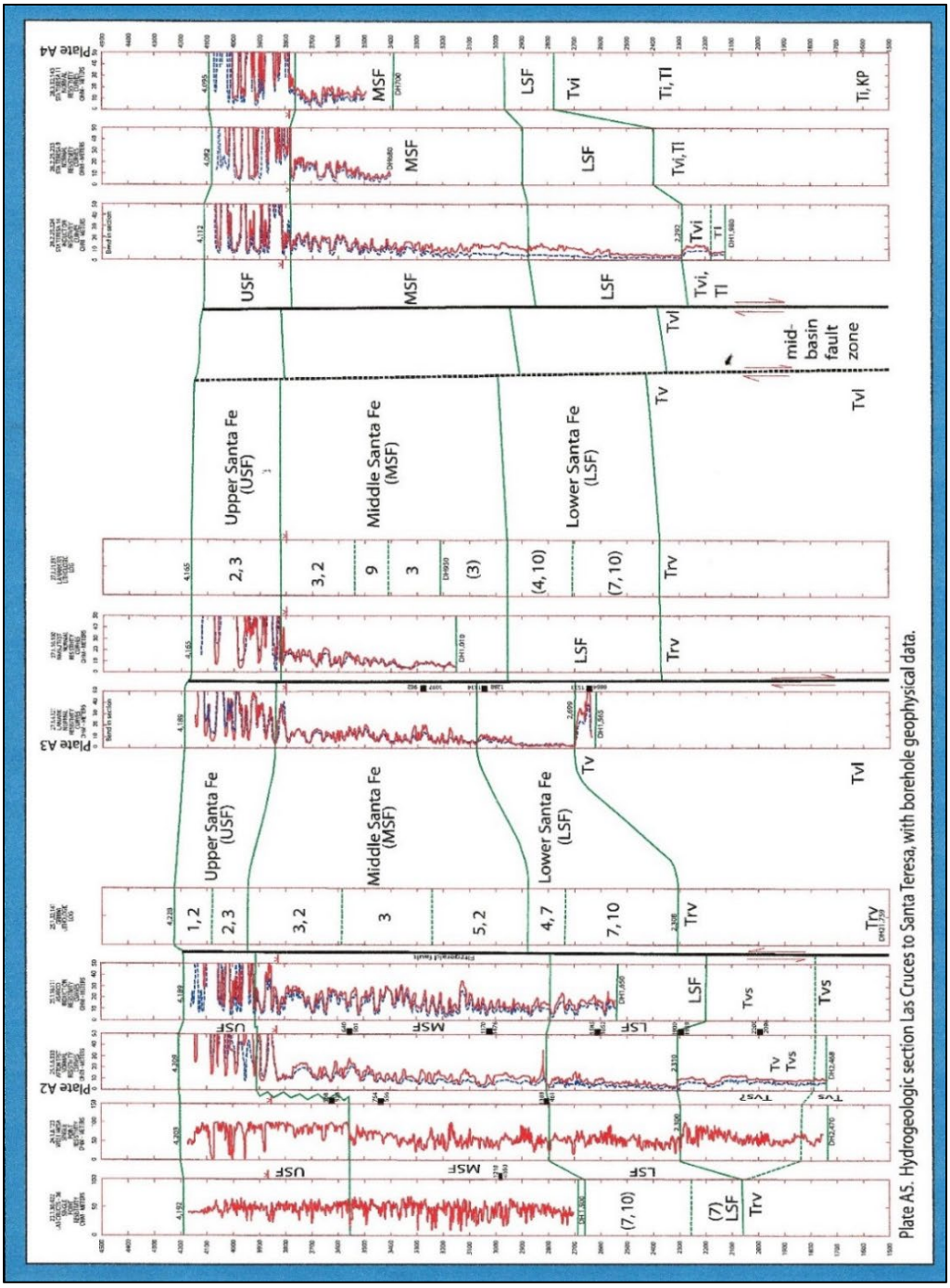

Figure 6-18 (Hawley and Kennedy 2005, Pl. A5)**.** Index hydrogeologic section showing positions of 11 key-well sites on the MeB West Mesa between I-10 and the Santa Teresa Industrial Park (*cf.* **Part 6.3.3b**). Well nos. and hydrogeologic-subdivision acronyms (**TBL. 1**) listed in N to S order: 93 (LC-36/FASB), 146 (USGS WM-Deep/FASB), 175 (Afton MT-1 [FASB], **Fig. 6-8**), 176 (ASARCO/FASB), 180 (Grimm et al. oil test/NMBH), 236 (Lanark MT-2**, Fig. 6-4** [NMBH]), 238 (NMSU test [NMBH]), 239 (Lanark-SPRR [NMBH]), 261 (ST-14 test [STH]), 266 (ST-9 [STH]), and 290 (ST-11 [STH]). Tl=Lower Tertiary sedimentary rocks, Tvl=Lower Tertiary volcanic rocks, Tvs=Lower Tertiary volcanic and sedimentary rocks, Ti=Lower and Middle Tertiary igneous-intrusive rocks, Tv=Lower and Middle Tertiary volcanic and igneous-intrusive rocks, and Trv=Lower and Middle Tertiary silicic volcanic rocks.

The El Milagro Subbasin is hydraulically linked with two neighboring GW basins:

1. The northeastern part of El Parabién Basin (EPB, **Part 6.4.2**) serves as a source of fresh- to moderately brackish GW recharge to the southeastern MeB-Lower MeV aquifer system via the Chontes-Milagro Inflow Corridor (CMIC) across the Potrillo-Sapello High (PSH, **6.4.1**; *cf.* **Part 7.6.2**).
2. The southwestern-most part of the Hueco Bolson (SWSB) may be an area where small amounts of brackish GW can flow into the southern EMSB via the Méndez-Vergel Inflow Corridor (see **Fig. 1-9**) (MVIC) (**Part 5.1.6**; *cf.* **7.5.2**).

As noted in Part **5.1.6**, the EMSB and the Méndez-Vergel Inflow Corridor (MVIC) have been recently proposed as the location of a new Mexican National Railroad section that connects with the Union Pacific RR in the Santa Teresa Industrial Park area (Pacheco 2022b-c; **Parts 1.1.2**).

In their detailed analysis of gravity-survey data in the southern part of the Study Area, Jiménez and Keller (2000, p. 82) found no evidence for the southern extension of a deep Mesilla RG-rift Basin in the El Milagro Subbasin area south of the International Boundary (*cf.* Jiménez and Keller 2000, Figs. 6 and 7; **Parts 3.6.1**, **6.4** and **6. 5; Figs. 3-7** to **3-9**):

> A significant point from a water-resources point of view is that the gravity anomalies show that the Mesilla Basin is separated from basins in Mexico by a structural high [*cf.* **5.7**]. In addition, the basins in Mexico are relatively small in areal extent suggesting that deep ground-water resources are limited.

As in adjacent parts of the Santa Teresa High (**6.3.4c**), the vadose zone is about 350 ft (107 m) thick and is composed of HSU-USF2 (ARG) deposits (mostly LFA 3). Saturated SFG thickness ranges from about 1,450 ft (442 m) at its northeastern border with the STH to 1,200 ft (366 m) at its southern transitional boundary with the Méndez-Vergel Inflow Corridor (MVIC) north of Mex. Hwy. 2 (**PLS. 5l**, **5p**, and **5s**). Saturated-thickness of HSU-USF2 (LFA 3) is about 300-ft (90 m), and the estimated thickness range of HSU-MSF2 (also LFA 3) is 550 to 750 ft (168-229 m) (**PL. 7**). The maximum inferred thickness of mostly piedmont facies in HSU-LSF (LFA 7) ranges from 450 to 700 ft (137-213 m). Lower Tertiary siliciclastic sedimentary rocks (Tls-**Tbl. 6-3**) underlie SFG basin fill throughout the EMSB area (**Figs. 6-2** and **6-3** [III-III′]). They represent deposits in the NW-trending Laramide Potrillo basin of early Cenozoic age that predated RG-rift development (**PLS. 5k**, **5l**, **5p** and **5s**; Seager 2004).

Several public water-supply wells in the new Junta Municipal de Agua y Saneamiento de Ciudad Juárez (JMASCJ) well field are also located in the EMSB (**Part 1.5**; **Fig. 1-13**, *cf.* Sheng et al. 2013, Villagran 2017a). As noted in **Part 1.5**, however, all subsurface data used in hydrogeologic-framework characterization throughout the northern "Acuífero Conejos-Médanos" area (**Figs. 1-11** to **1-13**) was

acquired prior to initial (2007) development of the JMASCJ well field (*cf.* **TBL. 1**, well nos. 357 to 395; INEGI 1983b, 2012, Hawley et al. 2000, **APNDS. C**, **D**, and **H**).

6.3.5. Hydrogeologic Subdivisions East of the Mesilla Valley fault zone (MVfz)

6.3.5a. Las Cruces Bench (LCBn)

The Las Cruces Bench (LCBn), with an area of about 38 mi^2 (98 km^2), is the northernmost MeB hydrogeologic subdivision located east of the Mesilla Valley fault zone (MVfz). The latter forms a shallowly buried, but still well-defined structural boundary between the LCBn and the northern parts of the Fairacres and Mesquite Subbasins (FASB and MSB) (**Figs. 6-1** to **6-3** [I-I′] and **Tbls. 6-1** to **6-4**; **PLS. 5d** to **5g**, and **5o**). The LCBn's eastern border with the Tortugas Uplift (TtU, **5.2.3**) is formed by a series of closely spaced, down-to-west faults, which are here informally designated the West Tortugas fault zone (TTfz-**Tbl. 6-2**). The northern and southern ends of the LCBn are located at points where the WTfz merges with the MVfz. The northernmost section of the WTfz forms the southwestern boundary of the Doña Ana Mountains Uplift (DAMU, **5.2.1**), and its southern segment borders the northwestern Fillmore Pass Corridor (FPC, **5.1.2**). As noted in **Part 5.2.3**, aquifers in much of the central Tortugas Mountain Uplift (TtMU) have significant GW geothermal-resource potential (*cf.* Gunaji et al. 1978, Bond et al. 1981, Chaturvedi 1981, Gross and Icerman 1983, Icerman and Lohse 1983, Cuniff 1986, Gross 1988, Ross and Witcher 1998; **TBL. 1**, 122-124).

Basin-fill is less than 1,400 ft (425 m) thick, and vadose-zone thickness is in the 30 to 200 ft (10-60 m) range. Saturated SFG deposits are primarily composed of interbedded medium- to fine-grained basin-floor facies (LFA 3) in HSUs-USF2 and MSF2, and fine- to coarse-grained piedmont facies in the MSF1/LSF HSU sequence (LFAs 5, 7 and 8; **PLS. 5d-5g** and **7**; *cf.* Taylor 1967, King et al. 1971). Estimated saturated-thickness of HSU-USF2 is in 100 to 600 ft (30-185 m) range, and the thickness range for unit MSF (LFA 7) is 200 to 600 ft (60-185 m). Thickness of underlying HSU-LSF (mostly LFA 8) ranges from 150 to 550 ft (46-168 m). Except for a small area of its southern end, silicic-volcaniclastic and epiclastic rocks of latest Eocene to middle Oligocene age (Tmrs-**Tbl. 6-3**) underlie SFG basin fill throughout the LCBn area (**Figs. 6-1** to **6-3** [I-I′] and **Tbls. 6-1** to **6-4**). Most bedrock units have OMU and DAMU caldera source areas (Seager 1981; Seager et al. 1987).

The eastern Las Cruces metropolitan district, the main NMSU Campus, and most of the Las Cruces Municipal Well Field are located in the north-central part of the LCBn (**Fig. 6-1**; *cf.* **Fig. 2-2** [**PL. 3**]; **TBL. 1**, nos. 102-114, 117-121, and 127; Wilson et al. 1981, Hawley and Kennedy 2004). Aquifers in this area include USF2 (LFA 2-3) deposits that are primarily recharged by seepage from the Alameda, Las Cruces and Tortugas Arroyo systems that cross the northern SJB-Talavera Subbasin (TSB) and have headwaters in the Organ Mountains Uplift (**Fig. 6-1**, **Tbl. 6-1**). Las Cruces Dam and its large reservoir capacity for temporary flood-water storage are of special interest because of their potential for a large-

scale ASR operation that would utilize the thick underlying HSU-USF2 (LFA 2-3) deposits for aquifer recharge and temporary GW storage (*cf.* **Parts 6.3.3b**, **7.5.1** and **8.5.4**). The zoned-earthfill structure is about 3 miles (6 km) long and is located south of US-70 and immediately east of I-25. It was originally designed to retard, but not permanently store runoff from the large Alameda and Las Cruces Arroyo watersheds.

6.3.5b. Anthony-Canutillo Bench (ACBn)

The Anthony-Canutillo Bench (ACBn), with an area of about 53 mi^2 (138 km^2), is the MeB's southeastern-most major hydrogeologic subdivision (**Figs. 6-1** to **6-3** [II-II′] and **Tbls. 6-1** to **6-4**; **PLS. 5i**, **5j**. and **5o**. The ACBn takes its compound name from two West Texas communities, Anthony and Canutillo, with Anthony's settlement dating back to initial construction of the Atchison & Santa Fe RR in 1881 (Julyan 1996, p. 18). The ACBn includes (1) rapidly expanding commercial and industrial developments at the northwestern edge of the El Paso metropolitan district, (2) large feed-lot operations in Doña Ana County, and (3) the EPWU Canutillo Well Field (e.g., **Fig. 2-2**; **PL. 3**; **TBL. 1**, nos. 322 to 348).

The MVfz (**Part 6.3.1b**) forms a shallowly buried, but still well-defined structural boundary between the ACBn and the Black Mountain Subbasin (BMSB), and the respective southern and northern parts of the Mesquite Subbasin and the Santa Teresa High (MSB and STH) (**Figs. 6-1** to **6-3** [II-II′] and **Tbls. 6-1** to **6-4**; **PLS. 5j**, and **5o**). Rather than being marked by a basin-boundary fault zone, the ACBn's eastern border is placed in an area just east of I-25 where saturated SFG basin fill wedges out against underlying bedrock units (K/P) of the Franklin Mountains Uplift (FMU, **5.1.3**). Its northern end is contiguous with the southwestern Fillmore Pass Corridor (FPC, **5.1.2**), and selection of its transitional southern boundaries with the Anapra-Oasis Bench (AOBn-SW) and Sunland Park outflow corridor (SPoc-SE) is based primary on Lower MeV geomorphic and shallow-aquifer characteristics (**PLS. 5k**, **5o**, and **7**).

Lower Cretaceous marine-sedimentary rocks with a local cover of Eocene nonmarine sandstones and siltstones form the primary bedrock units beneath the ACBn's SFG basin fill (Tls/K-**Fig 6-2** and **Tbl. 6-3**). The only exception is a small area at the northern end of the Bench where the basin fill is directly underlain by unit-Tlvs. The SFG is less than 1,500 ft (457 m) thick, and vadose-zone thickness ranges from 10 to 200 ft (3-60 m). Saturated-thickness of HSU-USF2 is usually less than 200 ft (60 m), but HSU-MSF2 (LFA 3) can locally be as much as 600 ft (183 m) thick. The general thickness range of underlying HSU-LSF deposits (mostly LFA 4) is from 100 to 600 ft (30-183 m).

SFG deposits are primarily composed of interbedded fine-grained basin-floor facies (LFA 3) in HSUs-USF2 and MSF2, and sand-dominant eolian facies are the primary component of HSU-LSF (LFA 4; **PLS. 5i**, **5j** and **7**; **APNDX. C2a** and **C2b** *cf.* Leggat et al. 1962, Cliett 1969, W.E. King et al. 1971,

Cliett and Hawley 1996, Hawley and Kennedy 2004). As noted in **Parts 3.7.1** and **4.2.1**, the most striking lithofacies type in HSU-LSF comprises thick deposits of well-sorted, fine to medium sand (LFA 4) that form the very productive "deep-aquifer" zone in the EPWU-Canutillo Well Field area (Hawley and Kennedy 2004; *cf.* **6.3.5** and **7.2.1**). The unit was first identified by Leggat and others (1962) in the ACBn area and later by Wilson and others (1981) beneath the central part of the MeV (*cf.* Hawley and Lozinsky 1992), and it has long been interpreted as deposits of an ancient dune-field complex that has contemporary analogs in the Great Sand Dunes of Colorado's San Luis Basin and the nearby Médanos de Samalayuca (**Figs**. **1-2** and **3-1**; *cf.* Cliett 1969, p. 212, Schmidt and Marston 1981, Valdez and Zimbelman 2020).

Nickerson (2006) also included background information on the most-recent EPWU-USGS cooperative efforts in the Anthony area (*cf.* **Parts 6.3.1** and **6.3.4a-4b**). The following passage from USGS Scientific Investigations Report 2005-5248 (p. 14) deals with hydrostratigraphic and hydrochemical relationships observed at the LMV-1 piezometer site, which is located in the eastern part of the Anthony-Canutillo Bench about 0.6 mi (1 km) south of the I-10—West Vinton Exit (**TBL. 1**, no. 344, **Figs. 6-20** and **6-21**):

> The LMV-1 site is located approximately 1 mile east-southeast of Vinton, Texas, along the eastern margin of the lower Mesilla Valley [**Pl. 5j**, **TBL. 1**, no. 344]. The borehole was drilled to a total depth of about 857 feet below land surface [e-resistivity log, with GW-sample depths on **Fig. 6-19**]. Piezometer LMV-1A is completed in the middle Santa Fe Group (MSF) hydrostratigraphic unit; the screened interval is from 280 to 290 feet below land surface. Piezometer LMV-1B is completed in the lower Santa Fe Group (LSF) hydrostratigraphic unit; the screened interval is from 640 to 650 feet below land surface. Dissolved-solids concentrations in water samples from the LMV-1 site range from 868 mg/L at 640 to 650 feet below land surface to 1,910 mg/L at 830 to 850 feet below land surface **[Fig. 6-20**]. The fresh-water zone with dissolved-solids concentrations of 1,000 mg/L or less is estimated to extend from about 430 to 660 feet below land surface. Slightly saline water appears to extend from the water table to the top of the freshwater zone and from the base of the freshwater zone to the bottom of the borehole. The predominant water type is sodium chloride sulfate, which may represent mixing with geothermal water along the eastern margin of the Mesilla Valley [**Fig. 6-1**, **Pl. 5j**]. . . .

Nickerson (2006, p. 14 and Tbl. 4) also states that:

> **1.** Water-quality samples collected by the USGS from the LMV [1 to 3] piezometers were analyzed for the stable isotopic ratios of $\delta^{2}H$, $\delta^{18}O$, and $\delta^{l3}C$. The isotopic composition of sample LMV-1A [the shallowest, 280-290 ft / 85.3-88.4 m piezometer] may represent source water from precipitation as mountain-front recharge along the Franklin Mountains
>
> **2.** ^{14}C in percent modern carbon (pmC) in sample LMV-1A is 6.74, and the "Corrected" [groundwater] age is 16,600 years before present [*cf.* **Part 6.3.4a**, **Table 6-5**].

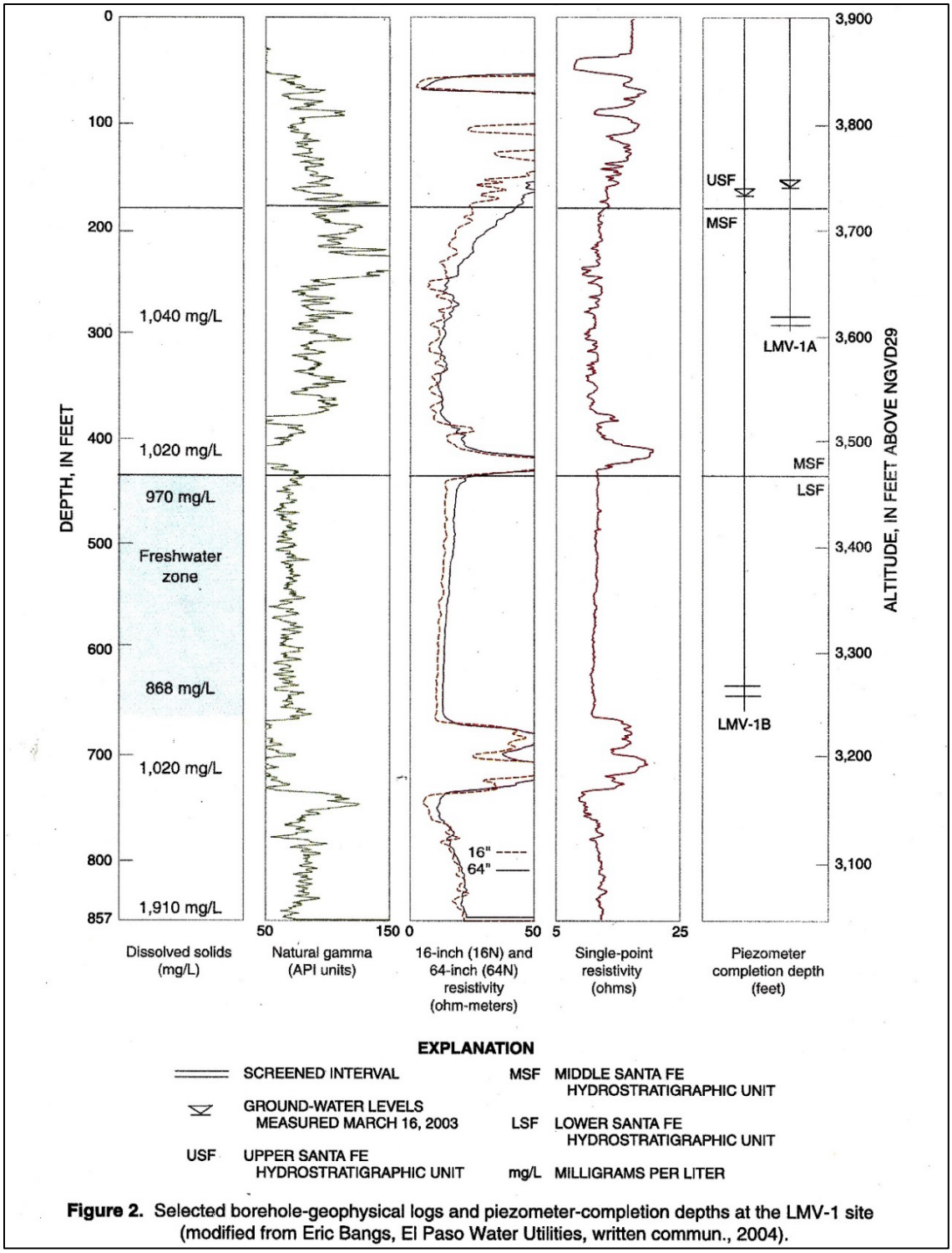

Figure 2. Selected borehole-geophysical logs and piezometer-completion depths at the LMV-1 site (modified from Eric Bangs, El Paso Water Utilities, written commun., 2004).

Figure 6-19 (Nickerson 2006, Fig. 2)**.** Selected borehole-geophysical logs and piezometer-completion depths at the LMV-1 site (**TBL. 1**, no. 344), with the base of the "Freshwater zone" at about 660 ft (200 m) bgs. Note also that the LFA 4/LSF 8, and LSF 8/LSF 9 contact depths in HSU-LSF are here interpreted to be also at about 660 ft (200 m) and 740 ft (226 m), respectively, and that the depth to Cretaceous bedrock (K) is at least 860 ft (262 m).

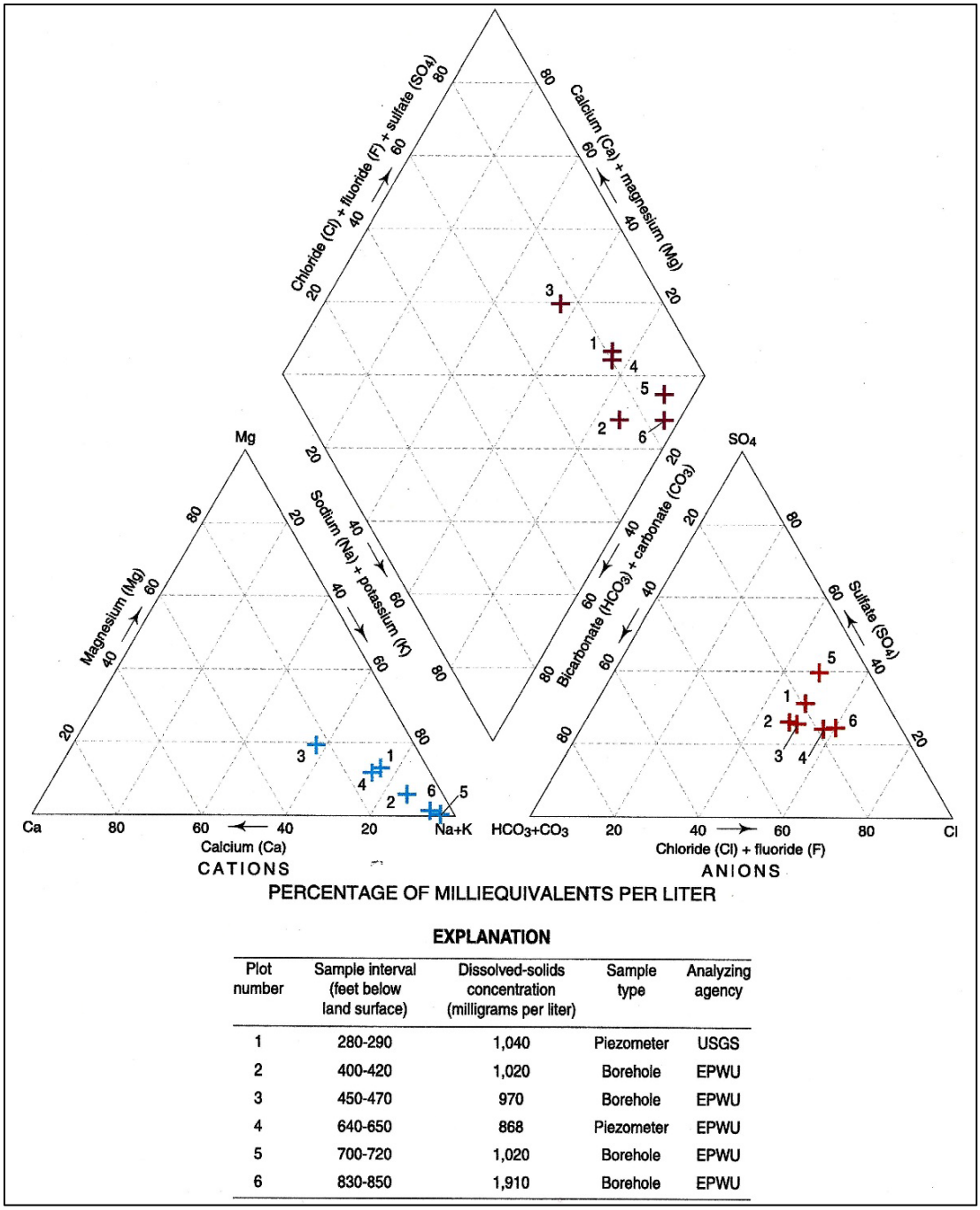

EXPLANATION

Plot number	Sample interval (feet below land surface)	Dissolved-solids concentration (milligrams per liter)	Sample type	Analyzing agency
1	280-290	1,040	Piezometer	USGS
2	400-420	1,020	Borehole	EPWU
3	450-470	970	Borehole	EPWU
4	640-650	868	Piezometer	EPWU
5	700-720	1,020	Borehole	EPWU
6	830-850	1,910	Borehole	EPWU

Figure 6-20 (Nickerson 2006, Fig. 3)**.** Distribution of major constituents in groundwater-quality samples from selected depth intervals at the LMV-1 site (**TBL. 1**, no. 344). Sampled intervals by HSU and LFA: (1) 280-290 ft (85-88 m)−middle MSF2 (LFA 3), (2) 400-420 ft (122-128 m)−basal MSF2 (LFA 3), (3) 450-470 ft (137-143 m)−upper LSF (LFA 4), (4) 640-650 ft (195-198 m)−LSF (LFA 4), (5) 700-720 ft (213-219.5 m)−lower LSF (LFA 8), and (6) 830-850 ft (253-259 m)−basal LSF (LFA 7). GW silica content (mg/L): (1) 15.69, (2) 21.3, (3) 24.1, (4) not sampled, (5) 28.7, and (6) 6.4 (Nickerson 2006, Appendix Table 2, p. 22).

6.3.5c. Anapra-Oasis Bench (AOBn)

The Anapra-Oasis Bench (AOBn) is the southeastern-most hydrogeologic subdivision of the MeB. More than half of its 53 mi^2 (138 km^2) area is located south of the International Boundary (**Fig. 6-1** to **6-3** [III-III′]**, Tbls. 6-1** to **6-4**; **PL. 5l**, and **APNDX. F: Pls. F3-1j** and **F4-1l**). It takes its compound name from (1) the border community of Anapra ("Spanish: this side of the river") on the SP[UP] RR and 1907-1914 US P.O. (Julyan 1996), and (2) the El Oasis ranch site that is located about 8 km (5 mi) to the SW in Chihuahua. The ACBn is bordered on the west by the Santa Teresa High (STH, **6.3.4c**) and El Milagro Subbasin (EMSB, **6.3.4d**), and their structural boundaries are formed, respectively, by the southern and northern segments of the Mesilla Valley and El Vergel fault zones (mVfz and EVfz, **Tbl. 6-2**).

The Anapra-Oasis Bench (AOBn) is bordered on the southeast by a piedmont area where saturated SFG basin-fill deposits wedge out against underlying Cretaceous sedimentary-rocks of the Cerro del Cristo Rey and Sierra Juárez Uplifts (CCRU and SJU), **Figs. 6-2** and **6-3**; **Tbl. 6-3**; **PL. 5l**; **Part**s **5.1.3** and **5.1.4**). Its northeastern border is located at the edge of the Mesilla Valley floor, which marks the southwestern boundaries of the ACBn and the Sunland Park Outflow Corridor (SPoc, **6.3.5d**). Lower Tertiary siliciclastic sedimentary rocks, which were deposited in the Laramide (pre-RG rift) Potrillo basin, form the primary bedrock units beneath the SFG deposits in the AOBn area (Tls-**Tbl. 6-3**). Because of their small size, the local bodies of intrusive andesite (Tli/Tlii) that are also present, cannot be depicted on the basin-scale (1:100,000) maps and cross-sections (Hoover et al. 1988; *cf.* **PLS. 2B** and **2C**, **Tbls. 3-1** and **3-2**, and **TBL. 2**).

Basin-fill is less than 1,000 ft (300 m) thick, and vadose-zone thickness is in the 30 to 300 ft (10-90 m) range. SFG deposits in the zone of saturation are primarily composed of interbedded medium- to fine-grained basin-floor facies (LFA 3) in HSUs-USF2, and fine- to coarse-grained piedmont facies are the dominant component of HSUs-MSF1 and LSF (LFA 7; **PLS. 5l** and **7**). Saturated-thickness of HSU-USF2 is less than 100 ft (30 m), but HSU-MSF2 (LFA 7) can locally be as much as 400 ft (122 m) thick. Thickness of underlying HSU-LSF deposits (also mostly LFA 7) is generally less than 200 ft (60 m).

Sayre and Livingston (1945, p. 35 and 36) described a well-exposed 235-ft (71.6-m) section of the upper "Santa Fe formation" in a SPRR cut 0.5 mi (0.8 km) west of Anapra (*cf.* Conover 1954, p. 23, 24; **APNDX. F: Pls. F3**-1j and **F4-1l**). W.S. Strain (1960, p. 156, 157) measured the upper 139 ft (42.4 m) of the same section, and collected fragments of fossil vertebrates from one "medium gravelly sand" layer in the lower part of the SFG section. In contrast to later workers, however, Strain correlated all but the upper 8.7 ft (2.7 m) of the section with his Fort Hancock Formation, and he considered that the Camp Rice Formation comprised no more than a thin veneer of ARG fluvial deposits (*cf.* Vanderhill 1986, Seager et al. 1987, Mack et al. 1968a, 1968b).

6.3.5d. Sunland Park Outflow Corridor (SPoc)

The Sunland Park Outflow Corridor (SPoc) has an area of about 13 mi^2 (33.5 km^2). It takes its provisional name from the community of Sunland Park (P.O. since 1960) and the Sunland Park Race Track (Julyan 1996). As noted in **Parts 6.3.5b** and **c**, the SPoc-AOBn boundary is located at the southwestern edge of the river-valley floor (**APNDX. F: Pls. F3-1j** and **F4-1l**). Its transitional northwestern border with the Anthony-Canutillo Bench (ACBn) is marked by gradual pinchout of SFG basin-fill deposits against Eocene igneous-intrusive, and Lower Tertiary and Cretaceous sedimentary bedrock units (Tlvs-Tls/K; **Figs. 6-2** and **6-3**, and **Tbls. 6-2** to **6-4**; **PLS. 5k** and **5o**). The Corridor's eastern boundary is located near I-10 in an area of valley-border to piedmont-slope transition where saturated basin-fill deposits wedge out against the subjacent Lower Tertiary igneous and sedimentary rocks of the western Franklin Mountains Uplift (FMU, **5.1.3**; **Fig. 6-2**; **PL. 5k**).

Combined river-valley fill (HSU-RA) and undivided SFG basin fill is less than 200 ft (60 m) thick, and vadose-zone thickness is usually in the 10 to 30 ft (3-10 m) range. SFG deposits are primarily composed of interbedded medium- to fine-grained basin-floor facies (LFA 3) in HSU-MSF2, and fine- to coarse-grained piedmont facies are the dominant component of HSU-MSF1 (LFA 7; **PLS. 5k, 5o** and **7**). Saturated-thickness of undivided HSU-MSF is less than 100 ft (30 m). Of special importance is the SPoc's role as a discharge area for a still poorly defined, pre-development GW flow system that included not only the "ground-watershed" of the MeB, but also a large part of the northern "Zona Hidrogeológica de Conejos Médanos" in north-central Chihuahua (**Figs. 1-12** and **1-14**; **PLS. 4** and **12**; *cf.* INEGI 2012).

The SPoc shallow-aquifer system provides the geohydrologic connection between the Rio Grande and the upwelling GW-flow regimes in contiguous parts of the Anthony-Canutillo and Anapra-Oasis Benches (ACBn and AOBn), both of which contribute to the predominantly surface-flow system in El Paso del Norte (El Paso Narrows) (**Figs. 3-10**, **6-2** and **6-3,** and **Tbls. 6-1** to **6-4**; **PL 5o**). The *damming* effect of the SPoc-EPdN valley/canyon constriction on the upwelling GW-flow and hydrochemical systems on the upstream side of the Mesilla Valley fault zone (MVfz) is quite substantial (**Fig. 1-6**, **PLS. 4** and **5o**; *cf.* Slichter 1905b, Toth 1963, Mills 2003, Phillips et al. 2003, Hawley and Kennedy 2004 [Figs. 5.2 and 5.3], Witcher et al. 2004 [Sections 2.8.1 and 2.9.2], Hogan et al. 2012, Moore et al. 2008, Teeple 2017, Villagran 2017a, Kubicki et al. 2021; **APNDX. H7.3**). Analogous structural/bedrock uplift controls that produce a pronounced upward-flow gradient on the local groundwater-flow regime have already been noted in the Tonuco Outflow Corridor (TNoc), which is located upstream from Selden Canyon (SCyn) (*cf.* **Part 6.2**). Hydrogeologic-framework controls on regional GW-flow systems in both outflow corridors are schematically illustrated on Hydrogeologic Section O-O′ (**PL 5o**).

6.4. EL PARABIÉN GW BASIN AND THE POTRILLO-SAPELLO HIGH

From a fluvial-geomorphic perspective, the southernmost MeB and EPB are within the southwestern part of an extensive fluvial-deltaic plain that was constructed by ARG distributaries during Pliocene to Early Pleistocene time (**Parts 3.5** and **3.7.2**; **Fig. 3-14**). Estimated thicknesses of the USF2-ARG deposits range from 300 ft to 600 ft (90-180 m). In such cases, accurate interpretations of hydrogeologic boundary conditions in underlying RG-rift basin fill and bedrock units are only possible when deep-borehole and geophysical-survey information is available (*cf.* **Figs. 1-4**, **1-11**, **1-12, 3-6**, **3-7**, **3-11, 3-12** and **6-22**; and **Parts 3.5.2**, **3.6**, **3.7**, **5.7.5** and **6.3.3e**; **PLS. 5k**, **5l**, **5p**, **5q**, **5r**, and **5s**).

As noted in **APPENDIX H6.2**, several recent USGS geohydrologic reports erroneously infer that the southern MeB merges southward with the "Acuífero Conejos-Médanos." The latter feature is better classified as a groundwater-resource management unit that includes a number of unmapped GW basins similar to those defined in the United States section of the Mesilla Basin region (**Figs. 1-1**, **1-11** and **6-1,** and **Tbl. 6-1**; *cf.* **Part 1.1.3**, Frenzel and Kaehler 1992, Nickerson and Myers 1993, Teeple 2017.). Aside from some binational historic-cultural and geopolitical impediments discussed in **APPENDIX H7**, much of the difficulty in reaching consensus in defining the southern hydrogeologic-subdivision boundaries of the Study Area is due to its basin-floor geomorphic setting that has yet to be affected by stream erosion or a significant amount of structural deformation (*cf.* **Parts 3.5** and **3.7.2**).

Figure 6-21 is an index map of the "International-Boundary Zone (IBZ)" as provisionally named in this study (**Part 1.8.2**). The southern Study Area is within the black rectangle, and the Mesilla and El Parabién GW Basins (MeB and EPB) are outlined in green and violet, respectively. Northern boundaries of the Acuífero Conejos-Médanos and the Zona Hidrogeológica de Conejos Médanos are shown, respectively, by dash-dot pink and solid yellow lines (**Figs. 1-1** and **1-11**). Study well-control points (**TBL. 1**) are shown with red dots, and 23 production wells (dk. red dots) in the new Junta Municipal de Agua y Saneamiento Cd. Juárez (JMASCJ) well field are located within the white oval (**Figs. 1-11** to **1-13**). Blue-gray shading shows the maximum extent of pluvial-Lake Palomas during its Late Pleistocene, 3,970 ft (1,210 m) high stands. The approximate position of the present GW-flow divide between EPdN-directed and El Barreal-directed underflow is shown with a dashed-blue line.

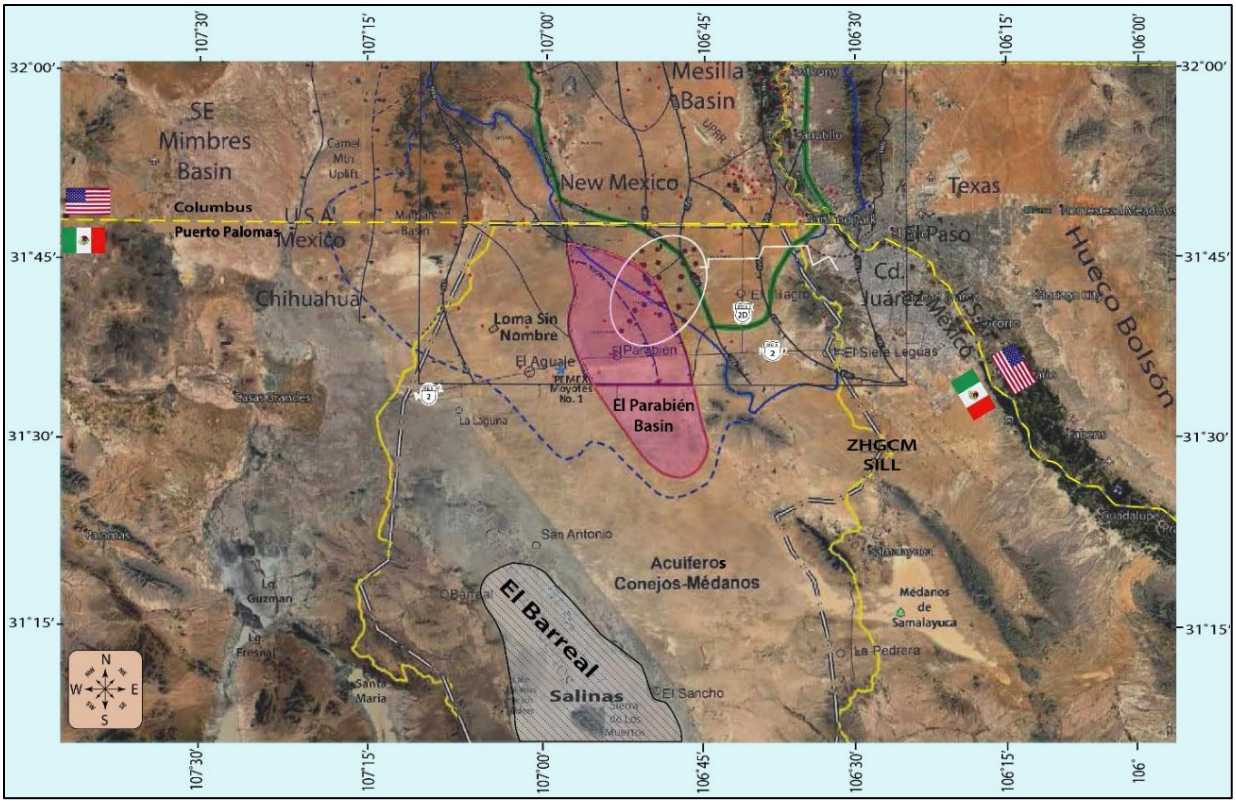

Figure 6-21. Index map of the "International-Boundary Zone (IBZ)" as provisionally defined in this investigation. It is located between the 31° and 32° N latitude and the 106°30' and 108° W longitude (*cf.* **Part 1.8.2**). 2018 Google Earth® image base.

6.4.1. El Parabién GW Basin (EPB)

The northern EPB is separated from the southern MeB by the provisionally named Potrillo-Sapello High (PSH). Both features have a thick cover of USF2-ARG deposits, and they were initially identified "based on the integrated analysis of gravity, drilling, geologic, and remote-sensing data" by Alberto Jiménez and G.R. Keller at the UTEP Pan American Center for Earth & Environmental Sciences-Geophysical Research Laboratory (**Parts 3.6.1**; **6.4.1** and **6.4.2**). According to Jiménez and Keller (2000, p. 80-82):

> The region of primary interest is situated immediately west of Ciudad Juárez. The definition and investigation of the gravity lows in this area was the chief aim of this study. These gravity lows correspond to a series of [RG-rift] basins west of the El Paso-Ciudad Juárez metroplex that may contain important water resources. . . .
>
> Relatively low gravity values (-160 to -170 [milligals] obtained in the El Parabién Ranch area [**Fig. 1-4**] indicate the presence of a deep basin containing sedimentary fill with a thickness of 2.2 km —7,218 ft - SFG/Tls*]. Here we name this feature as the El Parabién basin [p. 81-82, Figs. 7 and 6 (**Figs. 22a, 22b**); *cf.* **Part 3.6, Figs. 3-8a and 8b**] . . . .
>
> **The identical "feature" is named "BASIN DE LA MESILLA" in CONAGUA 2020 (p. 20, cross-section* B-B'; **Fig. 6-23**)

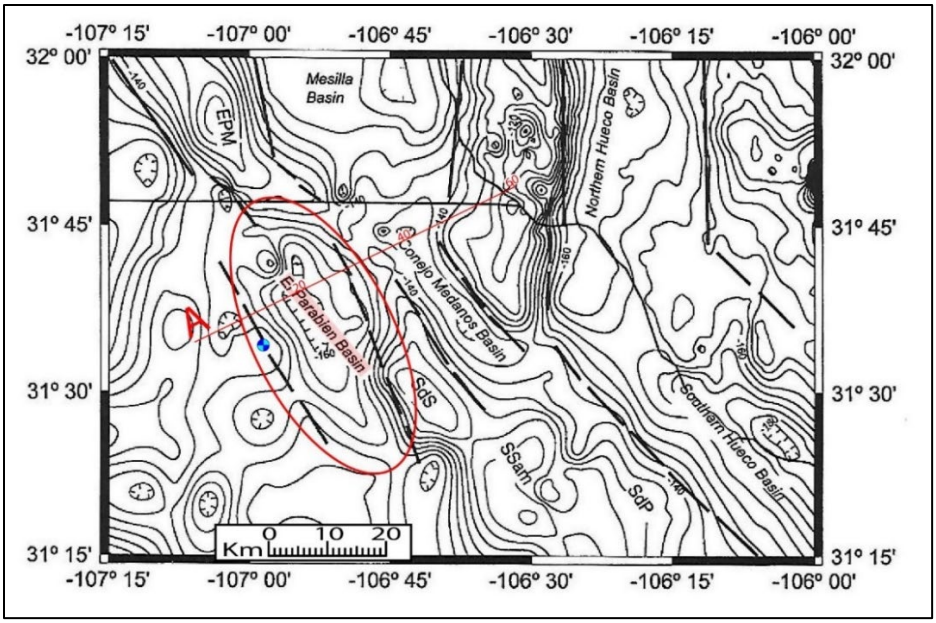

Figure 6-22a (adapted from Jiménez and Keller 2000, Fig. 7; reproduced with New Mexico Geological Society, Inc. permission)**.** Gravity map (4 milligal contour interval) with interpretations of major RG-rift basin extent that is "based on the integrated analysis of gravity, drilling, geologic, and remote-sensing data." EPM-East Potrillo Mountains, SdS-Sierra de Sapello [SSU], SSam-Sierra Samalayuca, and SdP-Sierra del Presidio. Profile A-red line (**Fig. 6-22b**), El Parabién Basin-red outline, and Pemex Moyotes No. 1-blue circle.

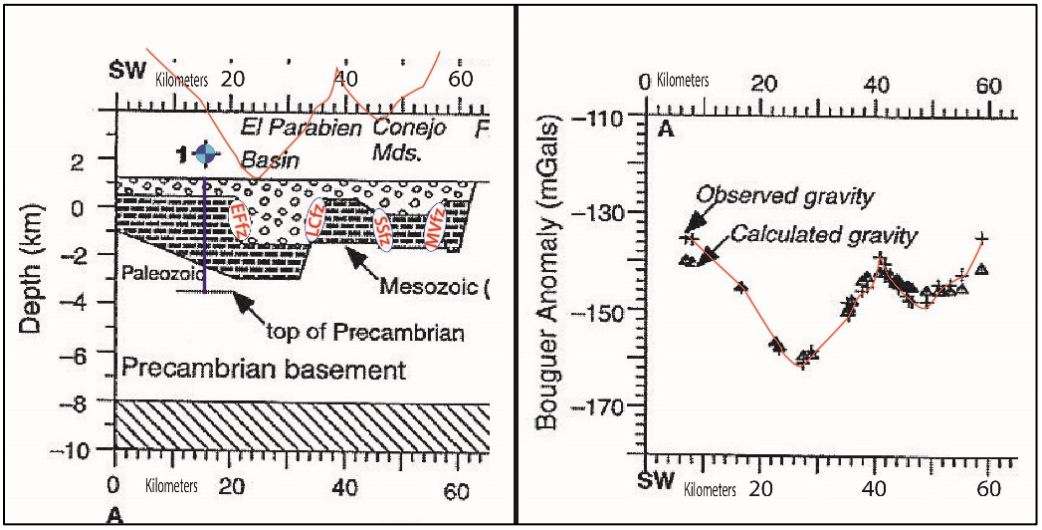

Figure 6-22b (adapted from Jiménez and Keller 2000, Fig. 6, p. 82; reproduction of original illustration with New Mexico Geological Society, Inc. permission)**.** Western part of computer model of gravity profile A-A' (right, and red line, right and left), and schematic geologic section (left), with Cenozoic Laramide and RG-rift basin fill shown by open polygons. Location of Profile A on **Fig. 22a**. Pemex Moyotes No.1-blue circle (**Part 5.6.4**). Fault zones (**Tbl. 6-2**): EFfz-El Faro, LCfz-Los Cuates, SSfz-Sierra Sapello, and MVfz-Mesilla Valley.

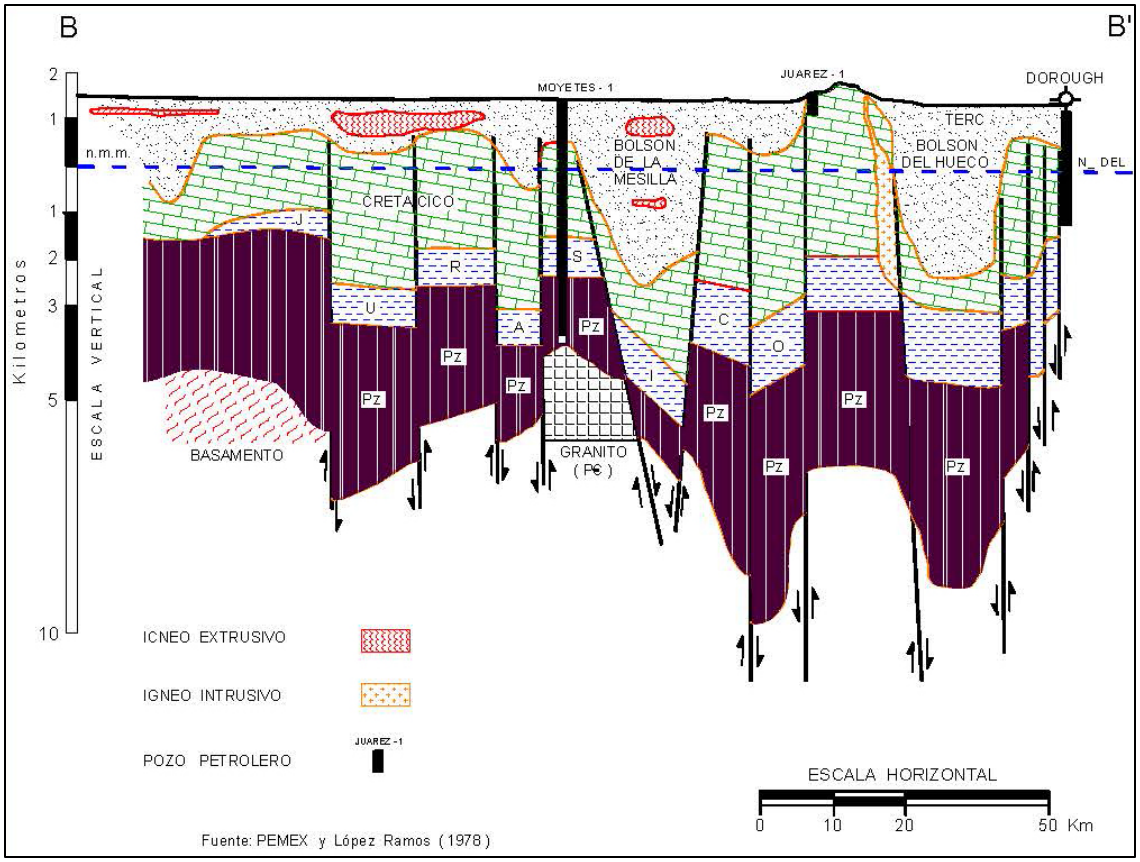

Figure 6-23 (CONAGUA 2020, p. 20)**.** Geologic Cross-Section (BB') of the IBZ (**Fig. 6-21**) that is located near 31°40-45' N, and extends from the Palomas volcanic field west of Puerto Palomas to the Hueco Bolson east of Ciudad Juárez. It shows regional stratigraphic and deep-seated structural relationships at a Vertical exaggeration (VE) of about 8x (*cf.* **Figs. 6-2** and **6-3** [**III-III'**]).

The structurally deepest part of El Parabién GW Basin (EPB) is located near Rancho El Parabién on Mexico Federal Highway 2, and about 19 km (12 mi) west of its junction with Federal Highway 2D (San Jerónimo-Santa Teresa bypass **Figs. 6-1** and **6-2a**, **b**). The EPB is structurally separated from the MeB's Kilbourne-Noria and El Milagro Subbasins (KNSB and EMSB) by the Potrillo-Sapello High (PSH; **Part 6.4.2**). Its western boundary with the El Aguaje Uplift (EAU) is formed by the buried El Faro fault zone (EFfz; **Part 5.7.5**). Jiménez and Keller (2000) found no evidence for a deep southern extension of the Mesilla GW Basin into Mexico (**Part 6.3.4d**), but they did identify a relatively shallow "Conejo Medanos Basin (**Fig. 6-22a**, **b**)"* that occupies most of the MeB-El Milagro Subbasin and Méndez-Vergel Inflow Corridor (**Parts 5.1.6** and **6.3.4d**).

This is neither the "Valle Conejos Médanos" (INEGI (1999, Fig. 5.3A-21), nor the "Acuífero Conejos-Médanos," the northern parts of which is shown on **Figure 6.-21 (cf.* **APNDX. H6.2**).

The EPB is provisionally divided into two subbasins on basis of known RG-rift structural features, which include the steep gravity gradients identified by Jiménez and Keller (2000; **Figs. 6-22a, b**;

Tbl. 6-2; **PL. 5s**). Their names have been taken from two centrally located Ranch sites (**Figs. 6-1** to **6-2** [III-III′] and **Tbls. 6-1** to **6-3**; **PLS. 5l**, and **5s**). The larger El Espejo Subbasin (EESB), with an area of about 158 km^2 (61 mi^2), occupies the deeper western part of the EPB and includes Rancho El Parabién. The Los Chontes Subbasin (LCSB), with an area of 126 km^2 (49 mi^2), forms a shallower part of the EPB that is located between the Potrillo-Sapello High (PSH) and the EESB. The Las Cuates fault zone (LCfz), which forms the EPB's structural boundary with the PSH, is relatively distinct in terms of both gravity-gradient inflection and fault displacement of surficial SFG deposits (**Figs. 6-2** and **6-3** [III-III′] and **6-22b**; **Tbls. 6-1** and **6-2**; **PLS. 5l** and **5s**; *cf.* **Parts 6.3.2b** and **6.3.3e**).

Estimated maximum thickness of SFG basin fill in the El Espejo Subbasin (EESB) ranges from 1,600-2,300 ft (490 to 700 m). In the Los Chontes Subbasin (LCSB) basin-fill thickness is in the 1,500 to 2000 ft (455-610 m) range. The vadose zone is 300 to 400 ft (90-120 m) thick throughout the EPB and is composed entirely of HSU-USF2 deposits (mostly ARG LFAs 2 and 3) (*cf.* Gutiérrez-Ojeda 2001). Estimated saturated-thickness of HSU-USF2 (LFA 3) in the EESB ranges from about 550 to 750 ft (170-230 m). Inferred, respective thickness ranges of HSUs MSF1 and LSF are 500 to 1,000 ft (150-300 m) and from 200 to 500 ft (60-150 m) in the EPB. (**PLS. 5l**, **5s**, and **7**). Saturated MSF and LSF deposits in the EESB and LCSB are here interpreted as being composed of basin-floor to distal-piedmont facies (LFAs 4 to 7) that are primarily sandy mudstone, sandstone and fine-conglomeratic sandstone.

The EPB serves as the primary GW underflow contributor (via the PSH/Chontes-Milagro Inflow Corridor) to the MeB transboundary-aquifer system that includes much of the El Milagro Subbasin and Anapra-Oasis Bench area (**Figs. 6-1**, **Tbl. 6-1**). Extended intervals of recharge to this very large GW reservoir, however, only occurred prior to 9 ka during the 3,944 to 3,970-ft (1,202 to 1,210-m) high stands of pluvial-Lake Palomas (Castiglia and Fawcett 2006, Tbl. 1; *cf.* **Parts 3.1.4** and **7.6.2**). The northeastern paleo-lake shoreline is located near the settlement of La Laguna within 5 mi (24 km) of the central EPB, and 25 mi (40 km) of the southwestern El Milagro Subbasin (EMSB) boundary (**Figs. 1-19**, **1-12**, and **6-21**; *cf.* **Part 3.1.4**). As a result of this "paleo-recharge" process, substantial quantities of fresh to moderately brackish GW are now stored in USF2/MSF2 aquifer zones that are located not only in the EPB, but also in adjacent parts of the Potrillo-Sapello High (PSH) and the MeB-El Milagro Subbasin (*cf.* **CHPT. 7**).

Nine of the new public water-supply wells operated by the Junta Municipal de Agua y Saneamiento de Ciudad Juárez (JMASCJ) are located in the EPB (**Fig. 6-21**; *cf.* **Part 1.2**). Subsurface hydrostratigraphic and hydrochemical information of reasonably good quality is only available for the upper 1,000 ft (300 m) of SFG section (**PL. 4**; **TBL. 1**, well nos. 364-366, 368, 373, 376, 379, 385, 388, 393 and 394). The widespread occurrence of fresh water (<1,000 mg/L TDS) in the HSU-USF2 aquifer zone of the El Parabién GW Basin and contiguous parts of the El Aguaje Uplift (EAU) is of special

relevance in this study. This is because it provides conclusive documentation of the regional GW-flow system with a Late Pleistocene, pluvial-Lake Palomas underflow source (**Figs. 1-9** and **6-21**; **PL. 5s; TBL. 1,** nos. 364-366, 368, 373, 376, 377, 379, 380, 382, 385, 386, 388, 393 and 394; *cf.* **Part 7.6**). Relatively low chloride values occur in the upper part of the USF2 freshwater-aquifer zone near Rancho El Parabién (Gutiérrez-Ojeda 2001), and chloride and TDS values in water sampled in well 382 (El Faro site) are 14.2 mg/L and 596 mg/L, respectively (INEGI 1983 [no. 26]; Hawley et al. 2000, Fig. 4-8); *cf.* **Part 7.6.2**, and **Figs. 7-19** and **7-20**).

6.4.2. Potrillo-Sapello High (PSH)

> A NW-trending series of gravity highs is associated with the East Potrillo Mountains, Sierra Sapello, Sierra Samalayuca, and Sierra del Presidio. A significant point from a water-resources point of view is that the gravity anomalies show that the Mesilla Basin is separated from the basins in Mexico by a structural high [Potrillo-Sapello High herein]. In addition, the basins in Mexico are relatively small in areal extent suggesting that the deep ground-water resources are limited [Jimenez and Keller, 2000, p. 82].

The Potrillo-Sapello High (PSH) is a deeply buried, structurally positive bedrock feature that extends between the East Potrillo and Sierra Sapello Uplifts, and separates the much-deeper southern Mesilla and northern El Parabién RG-rift depressions (**Figs. 1-5**, **6-2** and **6-3** [III-III′]; **PLS. 1B**, **1C**, **5l** and **5s**; *cf.* **Part 3.5.2**). The PSH has a NW-SE trend and is about 3 mi (5 km) wide, and its only topographic expression is a very low-relief watershed divide at the southwestern edge of the Mesilla GW Basin (**Figs. 1-9** and **6-21**). Overlying basin-fill thickness exceeds 1,000 ft (330 m) except where the PSH merges southward with the Sierra Sapello Uplift (SSU). The PSH is underlain by a sequence of Permian and Cretaceous marine-sedimentary rocks that are overlain by a northward-thickening body of non-marine siliciclastic rocks of Early Tertiary age (Tls/K/J/P-**Tbls. 3-2** and **3-3**; **Fig. 6-2**; **PLS. 5l**, **5q** and **5s**). It is here interpreted as a deeply buried remnant of the Laramide Potrillo uplift of early Cenozoic age (*cf.* Seager 2004, Averill and Miller 2013; *cf.* **Fig. 6-22a**).

The central section of the PSH merges northward with the South Mid-Basin High (SMbH, **6.3.2b**), and it is bounded on the northeast by the buried Noria fault and/flexure zone (NRfz, **Tbl. 1-2**), which marks the southwestern edge of the MeB's Kilbourne-Noria Subbasin (KNSB, **5.4.2** and **6.3.3e**). The PSH's eastern boundary with the MeB's El Milagro Subbasin (EMSB, **6.3.4d**) is formed by the northern segment of the Sierra Sapello fault zone (SSfz, **Tbl. 1-2**). The SSfz is also poorly defined in both a structural and topographic sense due to deep burial by Upper SFG deposits. The Las Cuates fault zone (LCfz), which forms the PSH's western structural boundary with El Parabién Basin (EPB), is much more distinct in terms of both gravity-gradient inflection and topographic expression of faulted surficial SFG deposits (**Figs. 6-1**, **6-2**, **6-22a**,**b**; **Tbl. 6-2**).

The PSH has two, provisionally named subdivisions: the La Joya Sector (PSH-LJS) and the Chontes-Milagro Inflow Corridor (PSH-CMIC). Their transitional boundary is located at the southern end of the Mid-Basin High (MbH) and in an area where predevelopment GW flow is sub-parallel to the US-Mexico Border (**Figs. 1-9** and **6-1**; and **PL. 4**). Ten of the new public water-supply wells operated by the JMASCJ are located in the EPB (**Figs. 1-13**, **6-1** and **6-22**; *cf.* **Parts 2.3.3** and **6.4.2**; INEGI 1983b, 2012, Villagran 2017a). Water sampled from the 200 to 300 m (656-984 ft bgs) depth zone in a nearby Secretaria de Recursos Hidráulicos (SRH) test well had a TDS content of 1,552 mg/L (**TBL. 1**, no. 362). The PSH-CMIC merges northwestward with the LJS and southward with the Sierra Sapello Uplift (SSU). While not expressed in surface topography, the "Inflow Corridor" name emphasizes its essential geohydrologic function as a conduit for underflow from the northern EPB to the El Milagro Subbasin (EMSB) of the MeB (*cf.* **Parts 6.3.4d**, **6.4.2** and **7.6**).

CHAPTER 7.
HYDROGEOLOGIC CONTROLS ON GROUNDWATER FLOW AND CHEMISTRY IN AQUIFER SYSTEMS OF THE MESILLA BASIN REGION

7.1. INTRODUCTION

This next-to-last section of the Report includes summaries of the Mesilla Basin region's (MBR's) hydrogeologic setting, and interpretations of available data on the GW-flow system in the Study Area (**Fig. 7-1**). Due to subject-matter complexity, some figures and tables from preceding Report chapters are repeated. Hydrogeologic controls on GW flow and chemistry are described in terms of (1) interactions of the Middle- to Late-Holocene Rio Grande and shallow groundwater-flow systems, (2) the hydraulic linkage between the Mesilla GW Basin and the two GW basins with which it is has direct interbasin-underflow connections: the Southern Jornada and El Parabién Basins (SJB and EPB; **Figs. 6-1**, **7-1** and **7-2**; and **Tbl. 6-1**). Information on Middle-Cenozoic to Late-Pleistocene stages of hydrogeologic-framework evolution is summarized in **Part 7.2**, and advancements in post-1945 GW-flow system characterization in the United States part of the Study Area are described in **Part 7.3**. Selections from reports on previous work in **Part 7.4** provide a pre-Rio Grande Project (RGP/1916) perspective on interactions between the Rio Grande and shallow GW-flow regimes. Hydrogeologic-framework controls on GW flow between the MeB and its interlinked GW basins and bordering uplifts in the United States are described in **Part 7.5**. Interpretations of hydrogeologic-framework controls on GW-flow contributions from adjacent parts of Chihuahua are summarized in **Part 7.6**.

The 2017 Google Earth® image-base for **Figure 7-1** illustrates the eastern Basin and Range (B&R) physiographic province terrain of the MBR. The NM WRRI Study Area is outlined in magenta; and locations of major basins of the southern RG-rift tectonic province are shown. Blue shading shows the approximate extent of the areas inundated by pluvial-Lakes Otero and Palomas at their respective Late Pleistocene high stands in New Mexico's Tularosa Basin and the Los Muertos Basin/El Barreal area of Chihuahua.

Figures 7-2a and **7-2b** are index maps for major geohydrologic features of the Study Area, with the respective boundaries of the Mesilla, southern Jornada, and El Parabien GW Basin outlined in green, orange, and violet. The regional GW-flow system is described in the context of a potentiometric-surface configuration that pre-dates installation of large-production wells for irrigation and M&I purposes after World War (WW) II. The static water level (swl) estimates for the United States part of the Study Area are based on the water-level contour map in Frenzel and Kaehler (1992, Pl. 1), which is "modified from Wilson and others, 1981, pl. 9." Hydrogeologic-framework controls on shallow-aquifer responses to river-flow conditions in inner-RG valley and canyon areas are described primarily in terms of water-development practices that predate the 1916 Rio Grande Project (RGP) activity (**Part 1.3**).

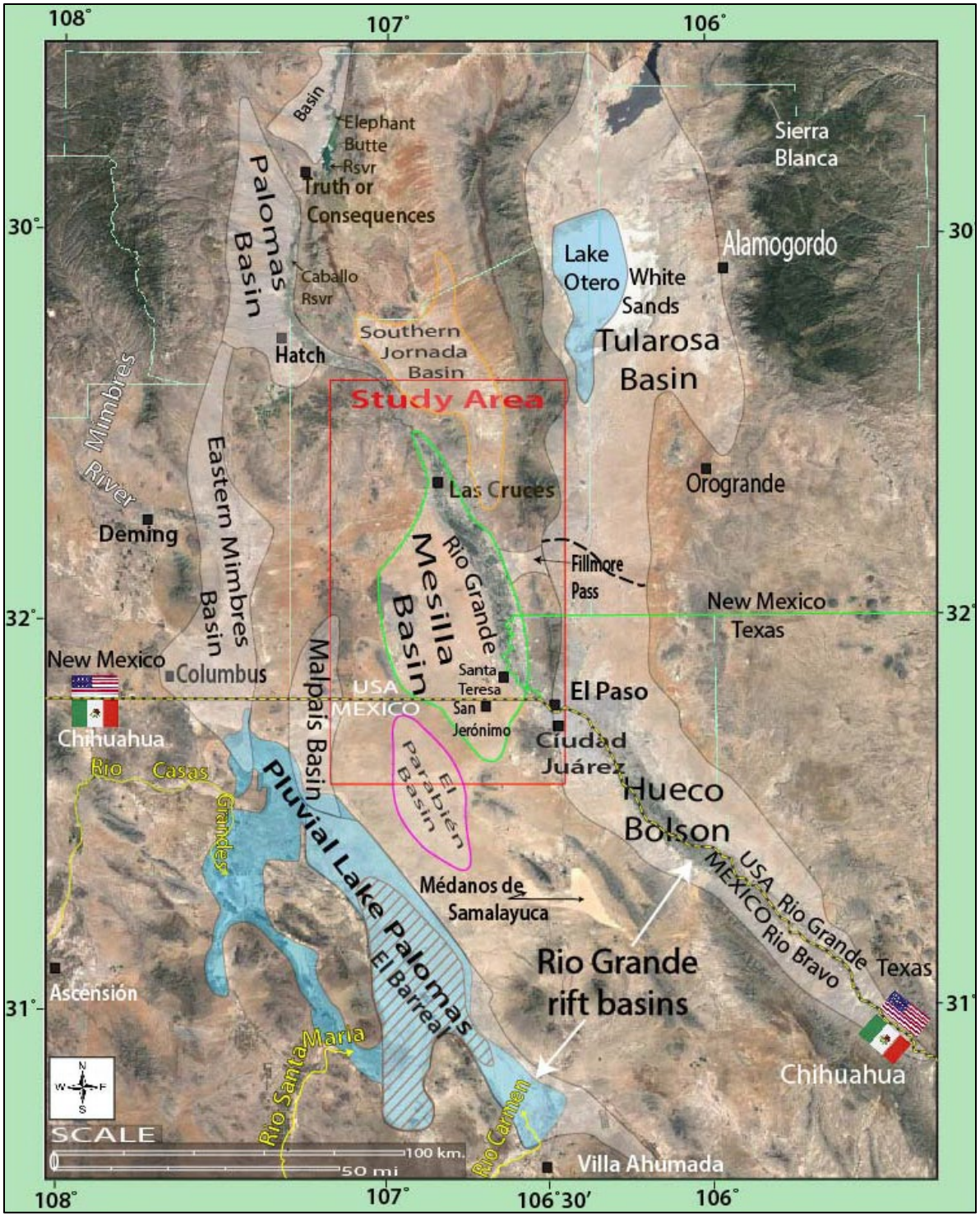

Figure 7-1. Index map of the binational/tristate Mesilla Basin region (MBR) that shows locations of the Study Area (magenta outline), major landscape features in the eastern B&R physiographic province, and basins of the southern RG-rift tectonic province (*cf.* **Figs. 7-2** and **7-5**). Blue shading shows the approximate extent of the areas inundated by pluvial-Lakes Palomas and Otero at their respective Late Pleistocene high stands in the Zona Hidrogeológica de Conejos Médanos (ZHGCM) basin complex, and the central Tularosa Basin. 2017 Google Earth® image-base.

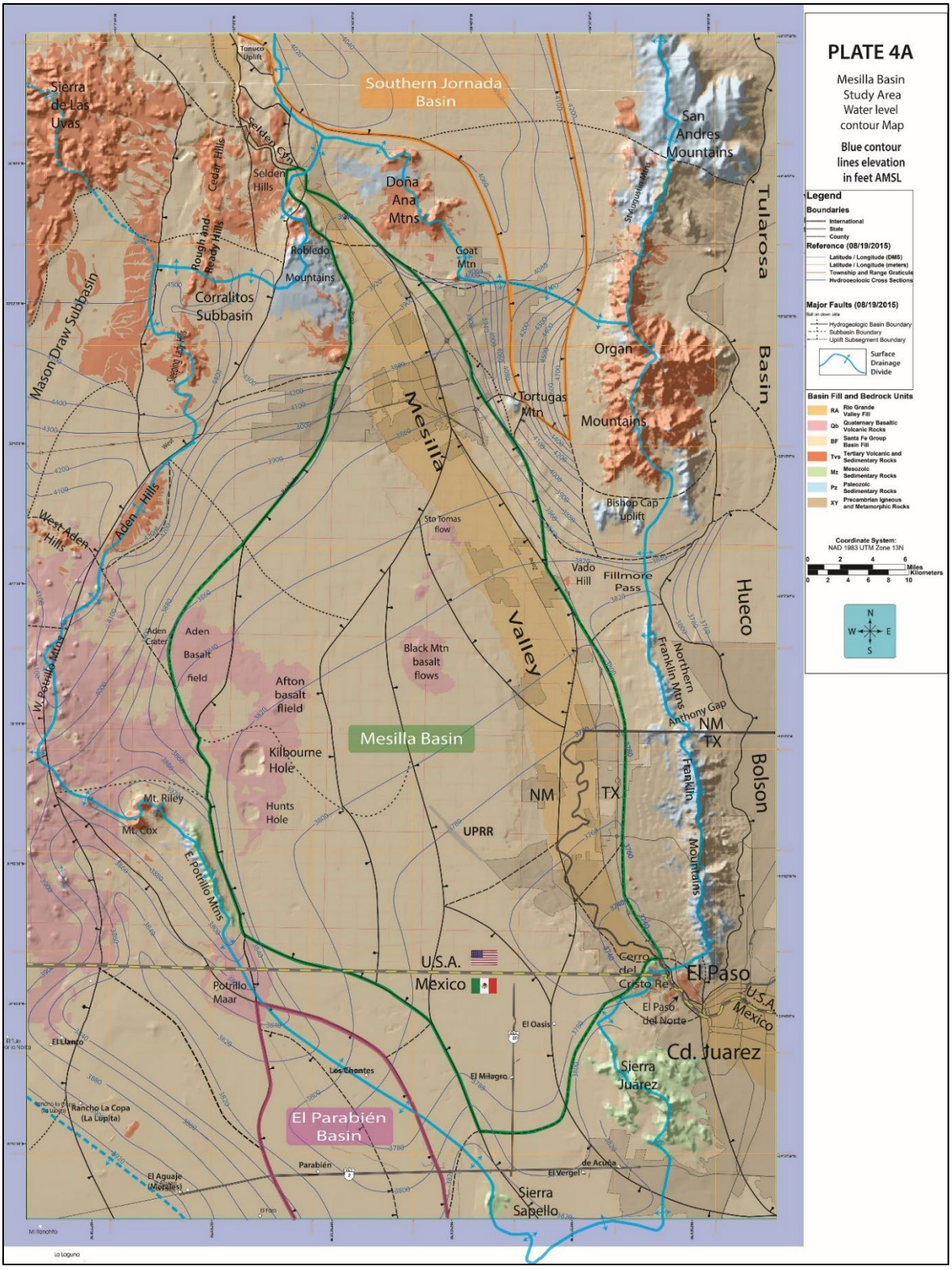

Figure 7-2a (page-size **PL. 4A).** Index map for major geohydrologic features of the NM WRRI Study Area (~1976 potentiometric-surface altitude in 10 and 100 ft amsl intervals). **PLATE 1** Hydrogeologic-Map DEM base.

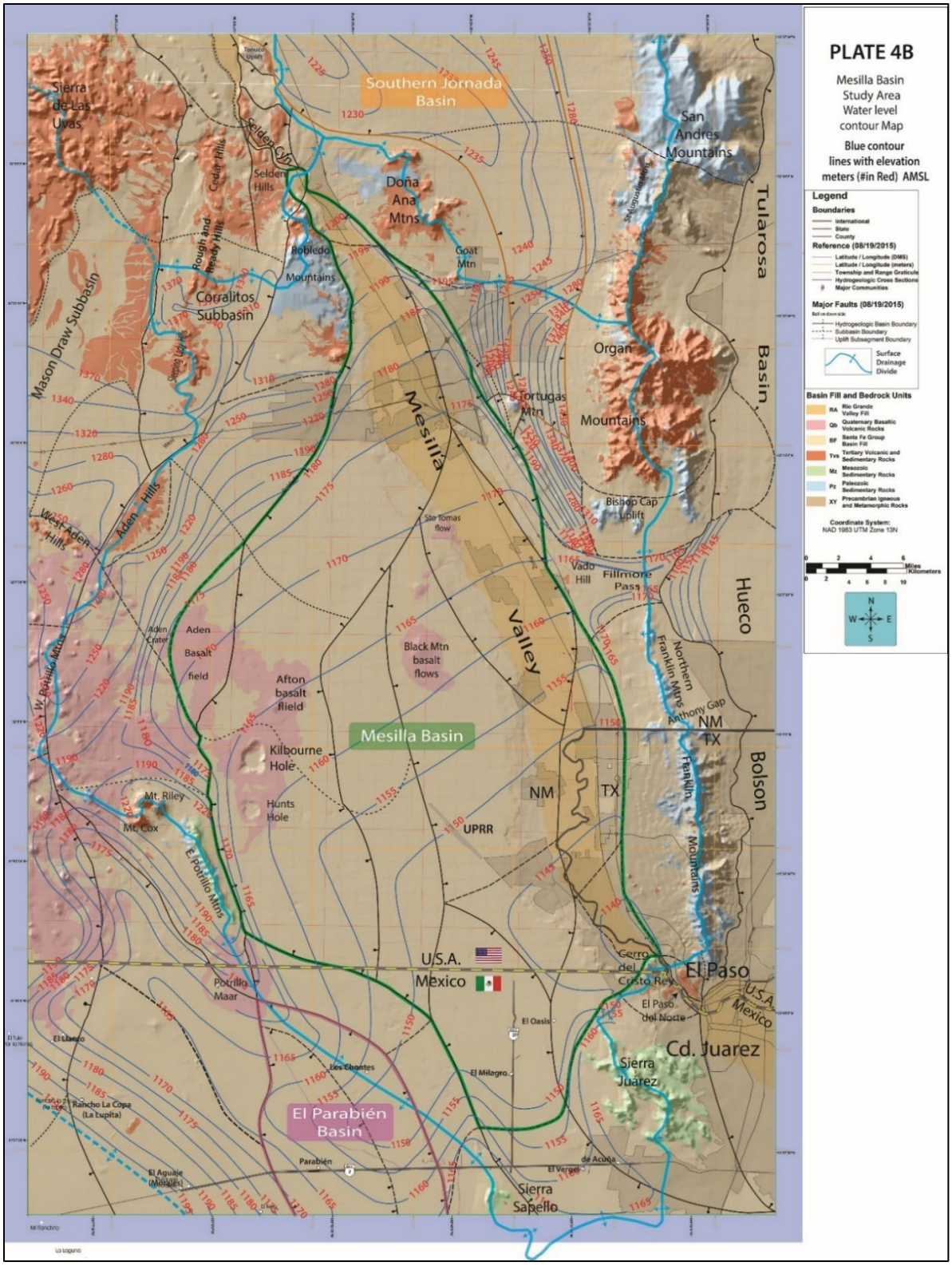

Figure 7-2b (page-size **PL. 4B).** Index map to major geohydrologic features of the NM WRRI Study Area (~1976 potentiometric-surface altitude in 5, 10, and 30 m amsl intervals). **PLATE 1** Hydrogeologic-Map DEM base.

Solid and dashed thick blue lines on **Figures 7-2a** and **7-2b** show locations of major surface-watershed divides. The approximate potentiometric-surface altitude is shown with (1) blue 10- and 100-ft amsl contours in **Figure 7-2a**, and (2) orange 5-, 10-, and 30-m amsl contours in **Figure 7-2b**. The dashed blue line with arrows in the map's southwestern corner shows the approximate position of the GW-flow divide between (1) flow directed toward the lower MeV and EPdN, and (2) and flow directed toward El Barreal in the Zona Hidrologíca de Conejos Médanos (ZHGCM; *cf.* Fig. 7.3; INEGI 2012; CONAGUA 2020, Fig. 5). It also marks part of the southern border of the Transboundary-Aquifer component of the Acuífero Conejos-Médanos (*cf.* **Parts 1.6.3**, **1.7** and **7.6.2**). Indirect GW-flow links with the Hueco Bolson, Cedar-Corralitos Upland Basin (CCUB), and Malpais Basin (MpB) are discussed in **Part 7.5**.

Figure 7-3 (page-size **PL. 11**) is an index map for the primary GW-management and geohydrologic units in Mexico and the United States south of 32° N latitude on a 2018 Google Earth® image-base. The El Parabién and southern Mesilla GW Basins are outlined in violet and green, respectively, and the Study Area border is in black. The black-dashed and white line is the "delineación oficial" of the "Acuífero Conejos-Médanos," and the larger "Zona Hidrogeológica de Conejos Médanos (ZHGCM)" is bounded with a solid yellow line (INEGI 2012). The provisionally named "International Boundary Zone (**Fig. 1-11**)" includes most of the "Acuífero Conejos-Médanos" area. Key-well sites are shown with red dots, and the dark red dots show locations of 23 production wells in the new Ciudad Juárez Junta Municipal de Agua y Saneamiento (JMASCJ) well field (*cf.* **PL. 3, TBL. 1**). The surface-watershed boundary of the southern MeB is in blue, and the area inundated by pluvial-Lake Palomas during its Late Pleistocene high stands has light-blue shading. The dashed-blue line shows the approximate position of the present GW-flow divide between NE-directed flow toward the lower MeV and EPdN, and SW-directed flow toward El Barreal in the ZHGCM. It also marks the southern border of the Transboundary-Aquifer component of the Acuífero Conejos-Médanos.

The dominant composition of aquifer and vadose-zone materials in SFG basin-fill and river-valley/canyon deposits in the Mesilla, Southern Jornada, and El Parabién GW Basins is described in terms of (1) Lithofacies Assemblages (LFAs), and (2) Hydrostratigraphic Units (HSUs) (**Figs. 7-4a**, **4b** and **7-5**, and **Tbls. 7-1** and **7-2**; **CHPTS. 4** to **6**). Related bedrock-lithologic, and structural boundary components of GW-basins and interbasin Uplifts are described in context of both interbasin and intra-basin flow (*cf.* **Figs. 7-9** and **7-10**; **PLS. 1B, 1C** and **5a-s**). Middle-Cenozoic to Late-Pleistocene stages of hydrogeologic-framework evolution are summarized in **Part 7.2**, and **Figure 7-5** shows general correlations between Cenozoic time-rock classes, and their lithostratigraphic and hydrostratigraphic equivalents.

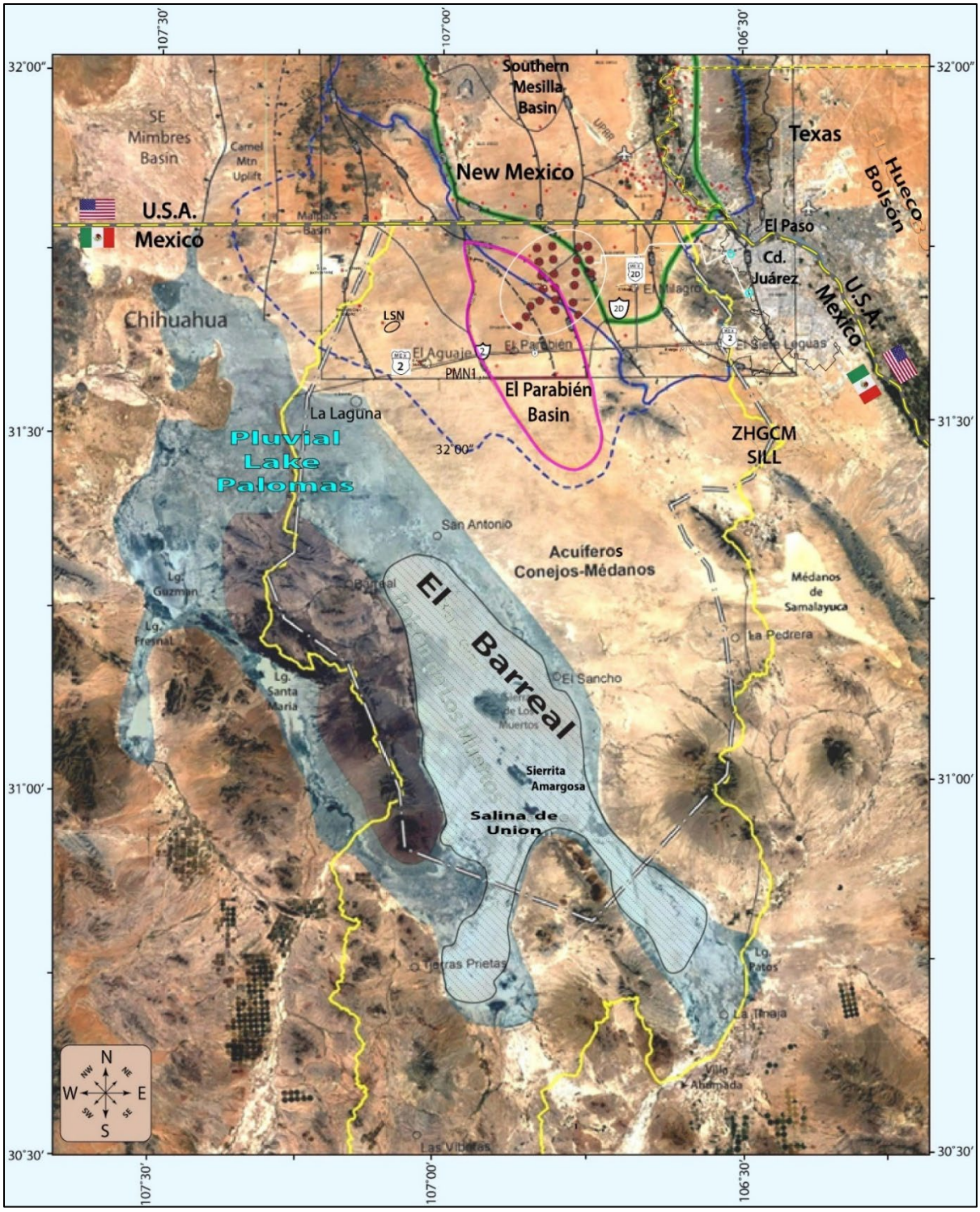

Figure 7-3 (page-size **PL. 11**)**.** Index map for major GW-management and geohydrologic units in Mexico and the United States that is compiled on a 2018 Google Earth® image-base. The El Parabién and southern Mesilla GW Basins are outlined in violet and green, and the Study Area border is in black. The black-dashed and white line is the "delineación oficial" of the "Acuífero Conejos-Médanos," and the larger "Zona Hidrogeológica de Conejos Médanos (ZHGCM)" is bounded with a solid yellow line (INEGI 2012).

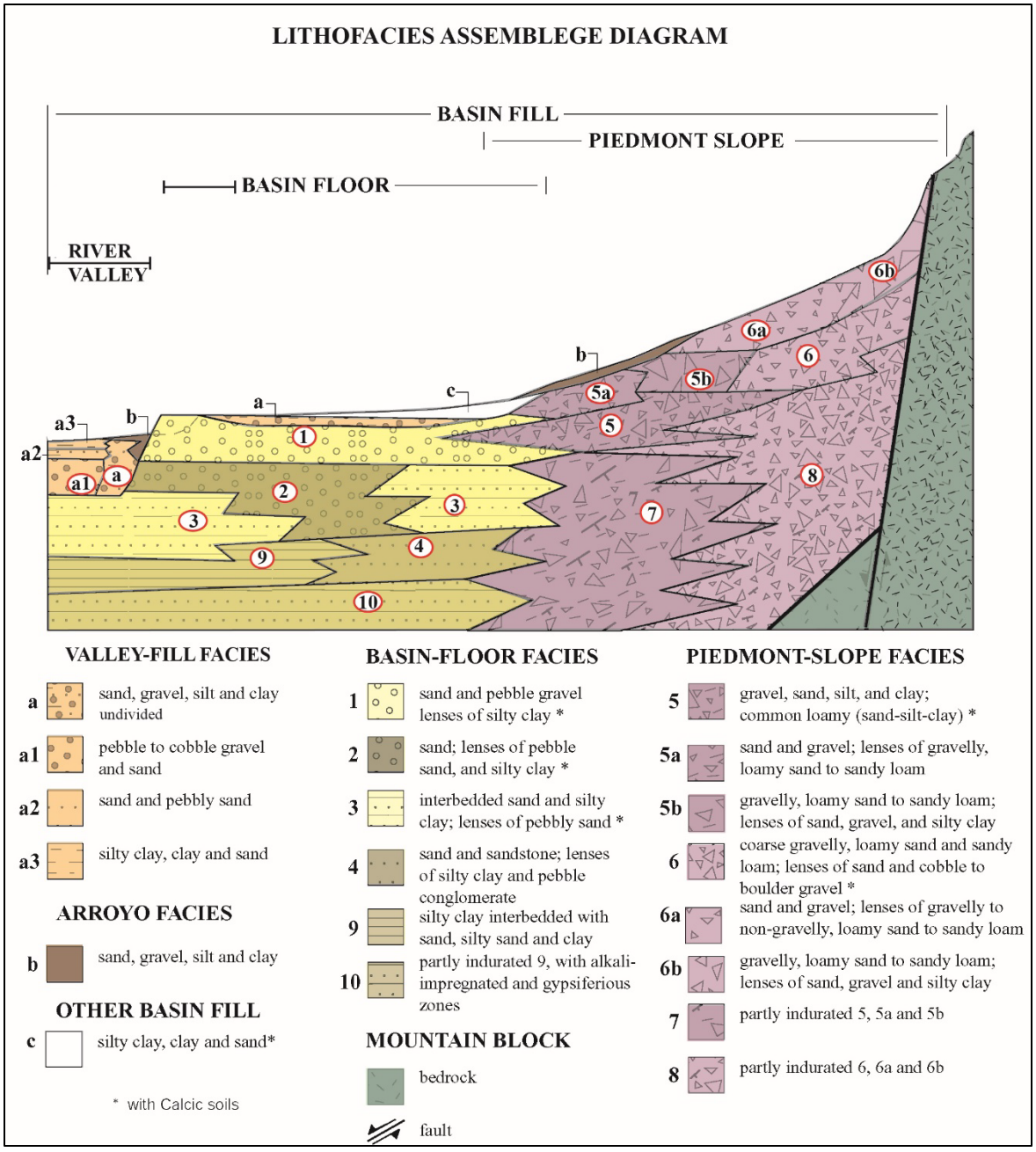

Figure 7-4a (modified from Hawley and Kernodle 2000, Fig. 5)**.** Schematic distribution patterns of major lithofacies assemblages (LFAs) in intermontane-basin and river-valley fills of the RG-rift province (*see* **Fig. 7-4b** and **Tbls. 7-1** and **7-2**).

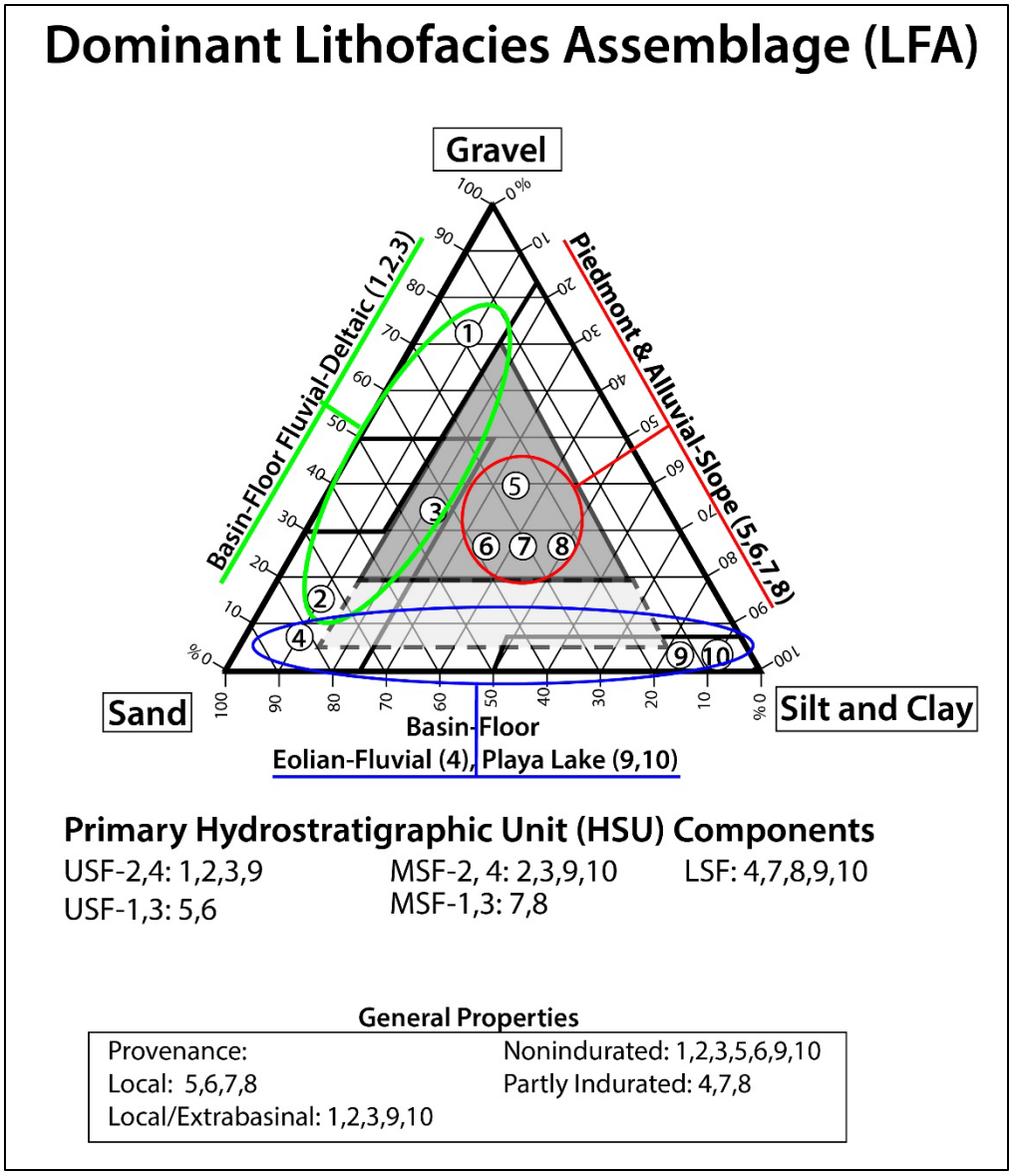

Figure 7-4b. Idealized triangular diagram of dominant textural classes in lithofacies assemblages (LFAs) 1 to 10, and primary LFA composition of SFG Hydrostratigraphic Units (HSUs)–USF/MSF/LSF (*cf*. **Fig. 4-3**, and **Tbls. 7-1** and **7-2**).

Table 7-1. Summary of Major Sedimentary Properties that Influence Groundwater-Flow and Aquifer-Production Potential of Lithofacies Assemblages (LFAs) 1 to 10 in Santa Fe Group Basin Fill. Modified from Haase and Lozinsky (1992). *cf.* Fig. 7-3 and Tbl. 7-1)

Lithofacies	Ratio of sand plus gravel to silt plus clay[1]	Bedding thickness (meters)	Bedding configuration[2]	Bedding continuity (meters)[3]	Bedding connectivity[4]	Hydraulic conductivity (K)[5]	Groundwater production potential
1	High	>1.5	Elongate to planar	>300	High	High	High
2	High to moderate	>1.5	Elongate to planar	>300	High to moderate	High to moderate	High to moderate
3	Moderate	>1.5	Planar	150 to 300	Moderate to high	Moderate	Moderate
4	Moderate to low*	>1.5	Planar to elongate	30 to 150	Moderate to high	Moderate	Moderate
5	Moderate to high	0.3 to 1.5	Elongate to lobate	30 to 150	Moderate	Moderate to low	Moderate to low
5a	High to moderate	0.3 to 1.5	Elongate to lobate	30 to 150	Moderate	Moderate	Moderate
5b	Moderate	0.3 to 1.5	Lobate	30 to 150	Moderate to low	Moderate to low	Moderate to low
6	Moderate to low	0.3 to 1.5	Lobate to elongate	130 to 150	Moderate to low	Moderate to low	Low to moderate
6a	Moderate	0.3 to 1.5	Lobate to elongate	30 to 150	Moderate	Moderate to low	Moderate to low
6b	Moderate to low	0.3 to 1.5	Lobate	<30	Low to moderate	Low to moderate	Low
7	Moderate*	0.3 to 1.5	Elongate to lobate	30 to 150	Moderate	Low	Low
8	Moderate to low*	>1.5	Lobate	<30	Low to moderate	Low	Low
9	Low	>5	Planar	>150	Low	Very low	Very low
10	Low*	>5	Planar	>150	Low	Very low	Very low

[1]High >2; moderate 0.5-2; low <0.5

[2]Elongate (length to width ratios >5); planar (length to width ratios 1-5); lobate (asymmetrical or incomplete planar beds).

[3]Measure of the lateral extent of an individual bed of given thickness and configuration.

[4]Estimate of the ease with which groundwater can flow between individual beds within a particular lithofacies. Generally, high sand + gravel/silt + clay ratios, thick beds, and high bedding continuity favor high bedding connectivity. All other parameters being held equal, the greater the bedding connectivity, the greater the groundwater production potential of a sedimentary unit.

[5]High 10 to 30 m/day; moderate, 1 to 10 m/day; low, <1 m/day; very low, <0.1 m/day.

*Significant amounts of cementation of medium to coarse-grained beds (as much as 50%)

Table 7-2. Summary of Major Sedimentary Properties that Influence Groundwater-Flow and Aquifer-Production Potential of Lithofacies Assemblages (LFAs) *a* to *c* in Post-SFG Deposits. Modified from Hawley and Kernodle (2000). *cf.* Fig. 7-3 and Tbl. 7-1)

Lithofacies	Ratio of sand plus gravel to silt plus clay[1]	Bedding thickness (meters)[3]	Bedding configuration[2]	Bedding continuity (meters)[3]	Bedding connectivity[4]	Horizontal hydraulic conductivity (K)[5]	Groundwater production potential
a	High to moderate	>1.5	Elongate to planar	>300	High to moderate	High to moderate	High to moderate
a1	High	>1.5	Elongate to planar	>300	High	High	High
a2	High to moderate	>1.5	Planar to elongate	150 to 300	Moderate to high	Moderate	Moderate
a3	Moderate to low	>1.5	Planar to elongate	30 to 150	Moderate to high	Moderate to low	Moderate to low
b	Moderate to low	0.3 to 1.5	Elongate to lobate	<300	Moderate	Moderate to low	Moderate to low
c	Low to moderate	0.3 to 1.5	Elongate to lobate	30 to 150	Low	Low	Low

[1]High >2;moderate 0.5-2; low <0.5

[2]Elongate (length to width ratios >5); planar (length to width ratios 1-5); lobate (lenticular or discontinuous planar beds).

[3]Measure of the lateral extent of an individual bed of given thickness and configuration.

[4]Estimate of the ease with which groundwater can flow between individual beds within a particular lithofacies. Generally, high sand + gravel/silt + clay ratios, thick beds, and high bedding continuity favor high bedding connectivity. All other parameters being held equal, the greater the bedding connectivity, the greater the groundwater production potential of a sedimentary unit.

[5] High, 10 to 30 m/day; moderate, 1 to 10 m/day; low, <1 m/day; very low, <0.1 m/day.

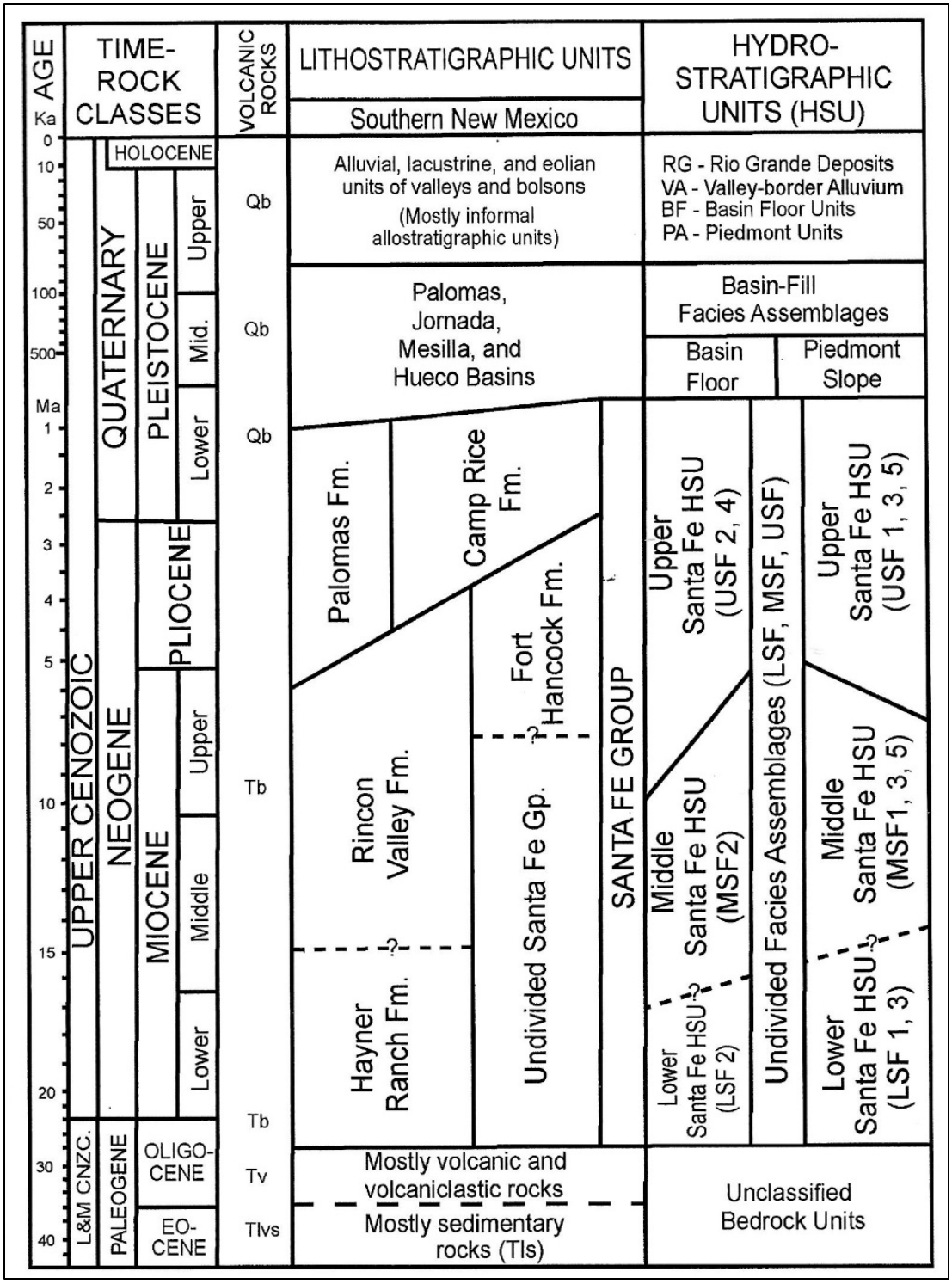

Figure 7-5 (modified from Hawley et al. 2009, Fig. 6)**.** Correlation diagram of major time-rock classes, and lithostratigraphic and hydrostratigraphic units of Cenozoic age in the southern RG-rift region of New Mexico, Texas, and Chihuahua. Bedrock units: Qb–Quaternary basalt, Tb–Tertiary mafic volcanics, and Tv–older Tertiary intermediate and silicic volcanics, and associated plutonic and sedimentary rocks Tvls and Tls. Detailed information on Middle and Upper Quaternary stratigraphic units is in **Part 3.8**).

7.2. REVIEW OF SANTA FE GROUP DEPOSITION AND ANCESTRAL RIO GRANDE DEVELOPMENT FROM A GW-FLOW SYSTEM PERSPECTIVE

Saturated parts of the Santa Fe Group (SFG) form the primary aquifer unit throughout the RG-rift tectonic province (**Parts 3.4** and **3.5**; Hawley and Kernodle 2000). SFG deposits in the Study Area, which are described in detail in **CHAPTER 6**, have saturated thicknesses that commonly exceed 1,000 ft (300 m) and are locally as much as 2000 ft (600 m) thick (**PLS. 5a** to **5s** and **7**; **TBL. 1**; *cf.* Leggat et al. 1962, Hawley et al. 1969, King et al. 1971, Wilson et al. 1981, Hawley and Kennedy 2004, Hawley et al. 2009). A provisional model of the topography, and dominant lithostratigraphic and structural components of the bedrock terrane that is buried by Santa Fe Group (SFG) basin fill is introduced in **Part 3.4 (Figs. 3-12** and **6-2** [**PL. 1B**]; **Tbls. 3-3** and **6-3**).

Most of the Mesilla Basin region's water supply is produced from unconfined to partly confined aquifer zones in Hydrostratigraphic Unit (HSUs) USF2 and MSF2 (**Fig. 7-4; TBLS. 1** and **2**). Poorly consolidated, sand-dominant fluvial facies (LFAs 2 and 3) are the primary aquifer constituents in both basal parts of HSU-USF2 and the more extensive deposits of HSU-MSF2 (**Figs. 7-3** and **7-6**, **Tbls**. **4-1** and **4-2**; **PLS. 5d** to **5l**, **5o** to **5s**, and **7**). Ancestral Rio Grande (ARG) lithofacies assemblages (LFAs 1 to 3) in HSU-USF2 form the most dynamic part of the GW-flow system because of their high transmissivity and good connection with the shallow alluvial-aquifer system (**HSU-RA**) in the northern and central parts of the inner Mesilla Valley (**Parts 6.3.1a, 6.3.3b** and **6.3.4**; **Figs. 7-3** and **7-6**, **Tbl. 7-1**, **PL. 5o**). Aquifers in piedmont-slope facies in HSUs USF1 and MSF1 (mostly LFAs 5 and 7) only serve as small GW-supply sources (e.g., for stock, domestic, and some suburban subdivisions).

The following primary hydrogeologic-framework components have been described in detail in **CHAPTERS 3** to **6**, and examples of subsurface relationships in the Rio Grande Valley/Canyon and "International-Boundary Zone (IBZ)" areas are illustrated in **Figures 7-6** and **7-7**:

1. Santa Fe Gp and RG Valley-Fill LFAs (**Part 4.2.1**; **Figs. 7-3** and **7-4**, and **Tbls. 7-1** and **7-2**).
2. SFG and RG Valley-Fill HSUs-(**Part 4.2.2**; **Figs. 7-3** and **7-4**, and **Tbls. 7-1** and **7-2**).
3. Bedrock-lithologic, and structural-boundary characteristics of GW-basins and interbasin Uplifts (**Part 3.4** and **CHAPTERS 5** and **6; PLS 2B** and **2C**).

Their collective influence on groundwater flow and chemistry in SFG basin-fill and river-valley-fill aquifer systems of the Mesilla Basin region is described here from two geologic-time perspectives: first, in terms of hydrogeologic-framework composition that, in some cases date back to the onset of RG-rift tectonism and SFG deposition (**Parts 3.4** to **3.7**), and second, with respect to geologic/geomorphic processes that have been active during and since the last glacial-pluvial stage of the Quaternary Period (about the past 70,000 years [70 ka], **Fig. 7-4**; **3.8** and **3.9**).

7.2.1. Deposition of Lower and Middle Santa Fe Hydrostratigraphic Units

Lithofacies Assemblages (LFAs 6 and 8 to 10) in Middle and Lower Santa Fe HSUs (MSF/LSF) are not significant aquifer components. This is mainly because of relatively fine-grained matrix, and age-related diagenetic properties of consolidation and cementation (e.g., LFAs 3, 7, 9 and 10; **Figs. 7-3** and **7-4**; **Tbl. 7-1**). The only important Lower Santa Fe aquifer unit comprises LFA 4 deposits that occur in the deep-subsurface beneath much of the Mesilla Valley between Mesquite and Canutillo (**APNDX. C2b** and **C2c**). The unit is composed primarily of fine to medium sand, with discontinuous sandstone zones, and is as much as 660 ft (200 m) thick (Leggat et al. 1962; Wilson and White 1985; Hawley and Kennedy 2004; Nickerson 2006). These sediments are interpreted as dune-field deposits associated with piedmont depositional tracts downwind from basin-floor plains occupied by large fluvial-fan and lacustrine complexes (*cf.* Cliett 1969, Wilson et al. 1981, Hawley and Lozinsky 1992). Present-day geomorphic analogs in the RG-rift province include at the Great Sand Dunes of Colorado's San Luis Valley and Los Médanos de Samalayuca (**Parts 3.7.1** and **6.3.5b**); **Fig**s. **1-2** and **7-3**; **PLS. 5g** to **5j** and **5o***; cf.* Berg 1969, Cliett 1969, Schmidt and Marston 1981, Wilson et al. 1981, Castillo et al. 1984, Langford 2002, Hawley and Kennedy 2004, Allen et al. 2009). Their role as active parts of the present-day GW-flow regime has yet to be adequately evaluated.

The Middle Santa Fe hydrostratigraphic unit (HSU-MSF) was deposited during a middle to late Miocene interval of accelerated basin subsidence and mountain-block uplift (**Part 3.7.1**). Basin-floor lithofacies assemblages (LFAs) 3 and 9 are the major components of HSU-MSF2 in the central parts of the Mesilla and El Parabién Basins that extend westward from the Franklin Mountains and Sierra Juárez piedmont slopes to the East Potrillo and El Aguaje Uplifts (**5.1.3**, **5.1.5**, **5.4.1** and **5.6.5**; **PLS. 5h-5l, 5o-5r**, and isopleth maps-**PLS. 7A** to **7C**). HSU-MSF2 is more than 1,000 ft (300 m) thick in the most-rapidly subsiding central-basin areas. Only the upper part of this generally fine-grained sequence has interbedded sand strata with significant fresh-water aquifer potential, and water quality is commonly slightly saline in productive-sand zones in the western parts of the MeB. The primary HSU-MSF2 lithofacies assemblage (LFA 3**)** was deposited in basin-floor alluvial-flat and fluvial-deltaic environments, and is a general correlative of the upper Rincon Valley and Fort Hancock Formations (**Fig**. **7-4,** and **Tbl. 7-1**).

7.2.2. Late Stages of Rift-Basin Filling and Initial SFG Aquifer System Development

All major structural components of the basin and bedrock uplifts of the present regional landscape had formed by Late Miocene time (10 to 5 Ma), with the Robledo and East Potrillo uplifts being the most recent to emerge as prominent mountain landforms (**Part 3.7.2**; *cf.* Seager et al. 2008, Mack et al. 2018a). There is no stratigraphic evidence, however, to suggest that surface-drainage systems exited the Mesilla Basin region during the 20 to 25 Ma interval of Lower and Middle SFG deposition (**Fig. 7-4**). Evolving

basins in the southern RG-rift region appear to have existed as a slowly aggrading, poorly integrated group of structural depressions until Early Pliocene time (~5 Ma) when a sediment-loaded Ancestral Rio Grande (ARG), with Southern Rocky Mountains headwaters, entered the northern part of the region (Mack 2004, Connell et al. 2005, Mack et al. 2006, Hawley et al. 2009, Koning et al. 2018).

Prior to initial RG-valley and canyon incision (~ 0.75 Ma), the ARG distributive fluvial system (DFS) delivered enormous quantities of water and sediment to the two major interlinked basin groups of the southern RG rift: the Southern Jornada–Mesilla–El Parabién–Florida-Mimbres group on the west, and the Tularosa Basin-Hueco Bolson group on the east (**Parts 3.5** and **3.7**; Hawley 1975; Gile et al. 1981; Seager et al. 1984 and 1987; Gustafson 1991; Seager 1995; Collins and Raney 2000; Averill and Miller 2013). The primary corridor connecting the two basin groups was Fillmore Pass between the Organ and Franklin Mountains (*cf.* **Parts 5.1.2** and **7.5.2**; Strain 1966, p. 11). The bulk of the Upper SFG was deposited by ARG distributaries that terminated in the three most actively subsiding RG-rift depressions (*sinks*) of the Mesilla Basin region: Tularosa Basin, Hueco Bolson, and Florida-Mimbres ("Los Muertos") subbasin (**Figs. 3-13** and **3-14**). Two of the basins remain endorheic (internally drained): the Tularosa and Los Muertos. Only the Hueco Bolson is now connected with the through-going Rio Grande-Bravo system with respect to both surface and subsurface flow (Connell et al. 2005; Hawley et al. 2009).

Infilling of the basin-floor areas with as much as 1,000 ft (300 m) of Upper SFG fluvial-deltaic deposits produced the low-relief La Mesa (geomorphic) surface, which extends southward to the northeastern edge of the El Barreal depression in the Zona Hidrogeológica de Conejos Médanos (ZHGCM) basin complex; and it is still only disrupted by the deep valleys and canyons of the Rio Grande/Bravo fluvial system (**Fig. 7-1**; **Parts 3.5** and **3.8**). The extent and basic geometry of the ARG-DFS is shown schematically in **Figure 7-6**., which illustrates the major role played by this complex distributary-channel network in deposition of the primary components of the Upper SFG aquifer system throughout the Mesilla Basin region (**Figs. 3-7**, **3-14**, and **3-15**). This portrayal of the ARG's terminal "distributive-drainage network" is based on a conceptual model of Rio Grande drainage-basin evolution developed by Hawley (1975), and Connell and others (2005) that used the J.R.L. Allen (1965, Fig. 1) system of fluvial "drainage net" classification (*cf.* Part **3.7.3**; Weissmann et al. 2011, Nichols 2015). The intermittent paleo-lake complex into which the ARG fluvial-deltaic distributaries discharged was named Lake Cabeza de Vaca (LCdV) by W.S. Strain (1966). Distal fluvial-deltaic and lacustrine facies deposited in the Hueco Bolson part of the LCdV basin complex are included in Strain's "type" Fort Hancock Formation, and disconformably overlying ARG fluvial facies comprise most of his Camp Rice Formation (*cf.* **Part 3.7.2b**; **Fig. 7-4**; Strain 1966 [p. 16-21], Gustavson 1991a).

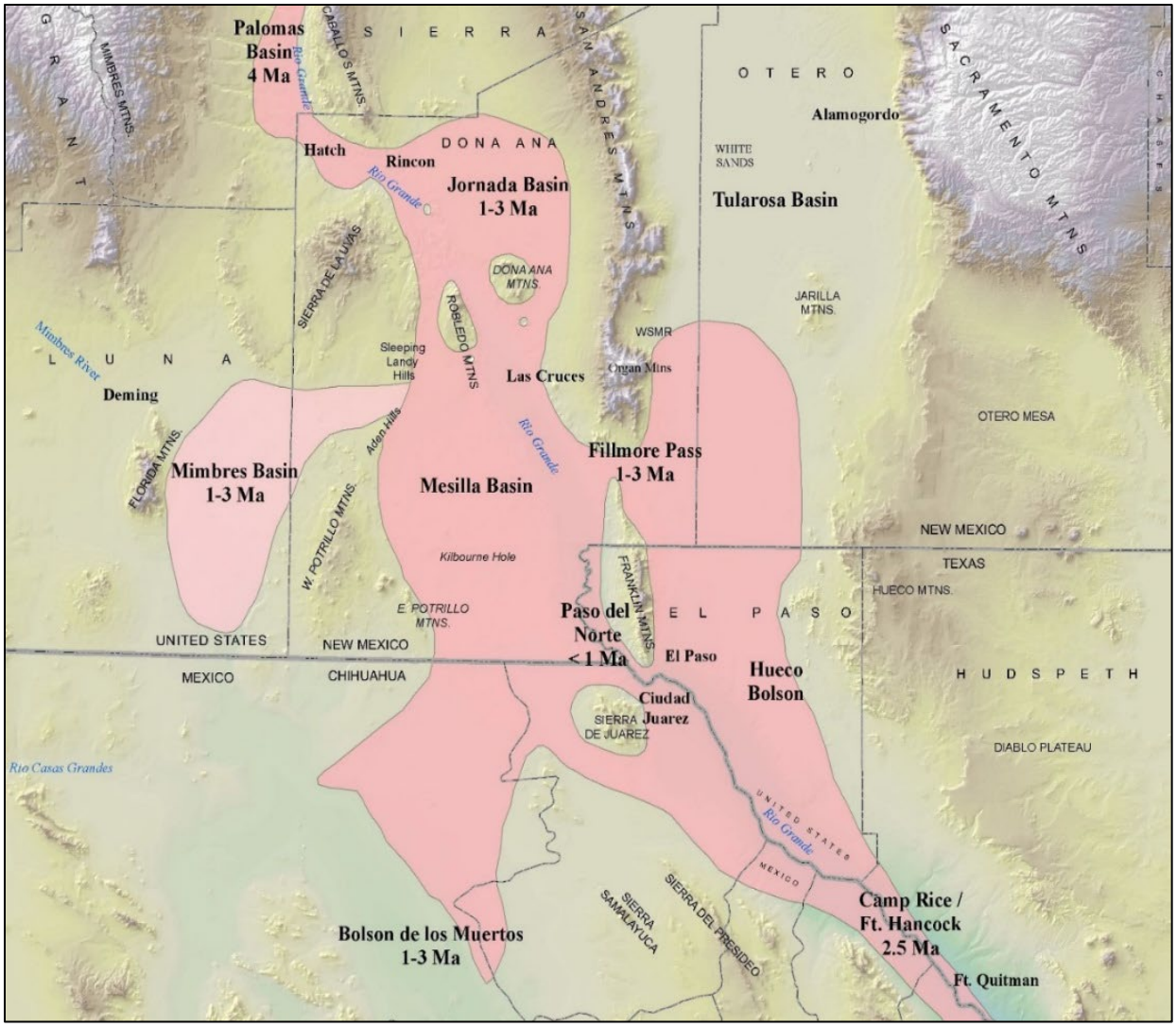

Figure 7-6 (Hawley et al. 2009, Fig. 9)**.** Schematic illustration (USGS DEM base) of the approximate area where fluvial and fluvial-deltaic deposits of the Ancestral Rio Grande (ARG) form the dominant Upper SFG basin-fill component. The primary distributary-channel network that spread out from an apex at the end of a trunk ARG channelbelt in the Palomas Basin northwest of Hatch is in dark pink, and a secondary ARG spill-out fluvial fan in eastern Mimbres Basin is in light pink. Million-yr (Ma) age ranges of major distributary channelbelts are based on geochronologic information available in 2008. The RG-rift "Bolson de los Muertos" complex of Chapin and Seager (1075) is located in the "Acuifero Conejos Médanos" section of the northern Zona Hidrogeológica de Conejos Médanos (**Figs. 1-10**, **1-11**, and **3-1**).

7.2.3. River-Valley and Canyon Entrenchment, Paleo-Lakes in Post-SFG Endorheic Basins, and Early-Stage GW-Flow System Evolution

Before about 0.75 Ma almost all of the SFG basin fill beneath the floors of the Southern Jornada, Mesilla and El Parabién Basins was in the zone of GW saturation, and most surface and subsurface flow was directed toward the endorheic Los Muertos Basin (**Fig. 7-7**; *cf.* Lee 1907, p. 22; **APNDX. C1b**). Mid- to Late-Pleistocene entrenchment of the present Rio Grande/Bravo valley and canyon system during four major glacial-pluvial stages led to (1) progressive drainage of aquifers in contiguous RG-rift basins, and (2) an ultimate water-table drop of 300 to 350 ft (~100 m) beneath the undissected basin-floor surfaces that occupy most of the Study Area (**Figs. 7-1**, **7-2**; *cf.* **7-9** and **7-10**; **PLS. 5a-5m** and **5p-5l**; *cf.* **Part 7.6**).

The final major interval of valley entrenchment and widening occurred sometime during marine oxygen-isotope stage (OIS) 2, which lasted from about 29 to 12 ka and included the last glacial maxima (Lisiecki and Raymo 2005; *cf.* Stein et al. 2006 [Fig. 2], Kottlowski 1958a, Hawley 1965, Hawley and Kottlowski 1969). During the past 12,000 yr, however, the entire river-valley floor from the Albuquerque-Santo Domingo Basin through the Hueco Bolson has back-filled about 60 to 100 ft (18-30 m) with coarse- to medium-grained channel deposits that have a thin veneer of fine- to medium-grained floodplain facies (HSU-RA, LFAs a1 to a3; **Tbl. 7-2**; **Part 4.2**).

The potentiometric-surface configuration and regional GW-flow boundary positions that are shown on **Figure 7-2** illustrate the general area where USF2-ARG channel networks now serve as very effective conduits for GW flow into, through, and out of the large GW reservoirs in the El Parabién and southern Mesilla Basins (*cf.* **Part 7.6.2**). In a present-day hydrogeologic-framework context, ARG-distributary channel deposits in Upper SFG basin fill (where still in the saturated zone), now function as an enormous system of high-permeability drains that deliver underflow recharge to the shallow aquifers of the Lower Mesilla Valley (*cf.* **Parts 3.5**, **3.7.3** and **3.9**).

Because of its hydraulic linkage with the Rio Grande Valley, the endorheic Zona Hidrogeológica de Conejos Médanos (ZHGCM) basin complex is the only part of the Mesilla Basin region that has any potential for producing significant amounts of subsurface recharge to the shallow GW-flow system in the Lower MeV upstream from EPdN (**Figs. 7-1**, **7-2** and **7-7** to **7-9**; **PLS. 5k**, **5l, 5o** and **5s [Hydrogeologic Se'tions K'K' "o "'L', O"-O''** and **S-S**']). Only during the past 350-400 ka, however, has entrenchment of the river's valley and canyon sections been deep enough (≤3,800-ft [1,160-m] amsl at EPdN) to produce the hydraulic gradient needed (≥0.0005) to allow GW discharge from Lake Palomas high stands to contribute significant amounts of recharge to alluvial aquifers at the lower end of the MeV (**Parts 3.8**, **3.9**, **6.3.5d** and **7.6.2**; **Figs. 3-13**, **3-14**; *cf.* Eastoe et al. 2008 [p. 744-745]).

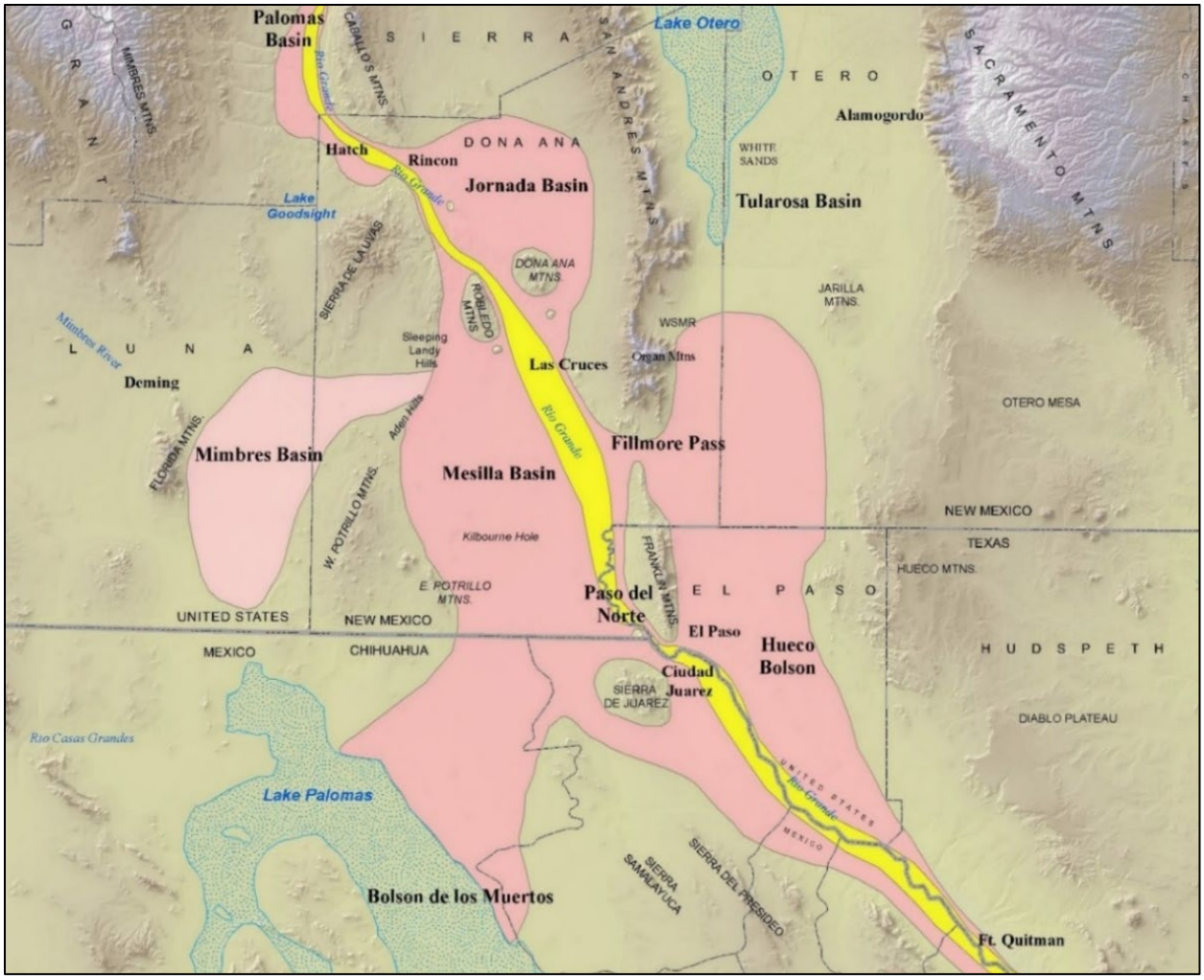

Figure 7-7 (Hawley et al. 2009, Fig. 10; *cf.* **Fig. 7-5).** Schematic illustration of major Quaternary-landscape features of the Mesilla Basin region. The approximate area covered by the Ancestral Rio Grande (ARG) distributary drainage network that spread out from a trunk-ARG channel system in the Palomas Basin is in pink. The Rio Grande/Bravo Valley and Canyon system is in yellow. The stipple pattern covers the basin-floor areas occupied by deepest Late Pleistocene stages of two large pluvial lakes: Palomas (NW Chihuahua) and Otero (Tularosa Basin). Remnants of the Early Pleistocene ARG fluvial-deltaic plain comprise parts of the "La Mesa geomorphic surface (Hawley and Kottlowski 1969)." The RG-rift "Bolson de los Muertos" complex of Chapin and Seager (1075) is located in the "Acuifero Conejos Médanos" section of the northern Zona Hidrogeológica de Conejos Médanos (**Figs. 1-10**, **1-11**, and **3-1**). USGS-DEM base.

7.3. INTERACTION OF THE RIO GRANDE AND SHALLOW GW-FLOW SYSTEMS IN THE PAST 6,000 YEARS

Surface- and subsurface-flow boundaries are related to active surficial-geomorphic processes, as well as to climate-process regimes of the Quaternary past. Boundary-conditions described herein include both surface-watershed and GW-underflow divides, with the former being primarily static and the latter including both static and dynamic features. Surface-watershed and GW-flow divides occupy essentially the same upland-landscape position where erosion-resistant bedrock forms the primary topographic control. This hydrogeologic setting characterizes most of the highland terrains in the United States part of the MBR, with one major exception – the West Potrillo Mountains – where Quaternary basaltic rocks bury SFG basin fill, and underlying bedrock terranes (**Parts 5.5** and **5.6**). Otherwise, GW flow-system divides follow the nearly continuous crests of the region's major mountain highlands (*cf.* **Figs. 2** and **3**). In the southern MBR, moreover, thick cover of USF2-ARG fluvial-deltaic deposits obscures bedrock and RG-rift structural feature that would otherwise mark watershed divides.

From a Middle Holocene to present-day perspective (~ the last 6 ka), intermittent seepage from the Rio Grande, which is now augmented by Rio Grande Project return-flow, has formed the primary source of fresh-water recharge to the shallow GW-flow system of the inner MeV and interlinked aquifers of the MBR (**Figs. 7-1**, **7-2** and **7-7**; *cf.* King et al. 1971, Wilson et al. 1981, Peterson et al. l984, Peterson and Wilson 1988, Frenzel and Kaehler 1992 [Fig. 15], Hawley and Kennedy 2004, Witcher et al. 2004, Teeple 2017 [p. 8], Ikard et al. 2021 and 2023, Pearson et al. 2022; *cf.* **Part 7.3.2**). Other than these river-derived contributions and the small amounts of mountain-block/front recharge from bordering highlands, fresh-water aquifer systems throughout the south-central New Mexico Border region have only been replenished by underflow from adjacent uplands and intermontane basins where groundwater quality is predominantly brackish.

7.3.1. Impacts of Elephant Butte Dam and the Rio Grande Project on the Hydrologic System

The complexity of pre-dam Rio Grande flow and shallow-aquifer recharge/discharge processes in a Late Holocene-Historic temporal context is illustrated in the background-summaries that follow (**Parts 7.3.4** and **7.3.5**). Emphasis here is on the river's inner-valley/canyon reaches between San Marcial near the head of Elephant Butte Reservoir and the southeastern Hueco Bolson near Fort Quitman (RG Project area: **Fig. 1-6**). Primary attention is on the timing of the low and/or no stream-flow intervals that occurred in the Historic period prior to Elephant Butte Dam completion and Rio Grande Project initiation in 1916 (*cf.* Mueller 1975 [Pt. 3.2.3] Esslinger 1996 and 1998, Kelley et al. 2007).

Elephant Butte Dam was completed on May 13, 1916. In an address at the dam's dedication on October 19, 1916, Arthur P. Davis, Director and Chief Engineer of the Reclamation Service, reviewed the reasons for its size and great storage capacity (Kelley et al. 2007, p. 539):

> There were evidences in the records - which were of considerable extent - that some years only about 200,000 acre-feet of water were discharged in this river and that in other years more than 2,000,000 acre-feet were discharged. Sometimes a series of those dry years occurred together, and at other times more than one of those wet years occurred in a series; and, looking over the ground and having studied that water supply, I made up my mind that the full utilization of this water supply could not be obtained without a reservoir of immense dimensions - one large enough, first, to hold the waters of those great years when 2,000,000 acre-feet were discharged, and to provide for evaporation and hold that water here until a dry year should come. . . .

USGS Hydrologist Clyde S. Conover described the early years of the Rio Grande Project in his pioneering study of "Ground-water conditions in the Rincon and Mesilla Valleys and adjacent areas in New Mexico (USGS WSP-1230, 1954, p. 17):"

> The Rio Grande Project (RGP) of the Bureau of Reclamation includes most of the valley lands of the Rio Grande in New Mexico and Texas from Caballo Dam southward to a point about 40 miles below El Paso, . . .a distance of about 130 miles [**Fig. 1-6**]. From Caballo Dam to Selden Canyon, a distance of about 30 miles, the Rio Grande flows in the Rincon Valley, which has a maximum width of about 2 miles. Below Selden Canyon the valley floor widens into the Mesilla Valley, which extends about 55 miles southeastward to "The Pass [EPdN]," 4 miles above El Paso. The Mesilla Valley is one of the larger widened areas along the Rio Grande and has a width of about 5 miles near Las Cruces. The El Paso Valley extends about 90 miles south[east]ward from El Paso and ranges in width from 4 to 6 miles, but only the upper 40 miles is included inIe [RGP]...
>
> The water for the Rio Grande Project is stored in Elephant Butte Reservoir, which has a capacity of 2,197,600 acre-feet, and in Caballo Reservoir, which has a capacity of 345,870 acre-feet, about 28 miles below Elephant Butte Dam. Water released from Caballo Reservoir is diverted into canals in the Rincon Valley by Percha Dam, about 2 miles below Caballo Dam; in the Mesilla Valley [by Leasburg Dam] at the head of the valley and by Mesilla Dam, about 5 miles southwest of Las Cruces; and in the El Paso Valley by the American Dam, about 3 miles northwest of El Paso. Water for the Mexican side of the El Paso Valley, generally referred to as the Valle de Juárez, is diverted at the International Dam, about 2 miles below the American Dam.

Andrea Glover of the IBWC (2018, p. 63) describes (1) the enormous scale of Rio Grande Project modifications of river-channel and contiguous-floodplain environments, and (2) the essential role played by effective reservoir-management in terms of maintaining delivery of a relatively constant supply of surface water to the GW basins downstream from Caballo Dam (**Fig. 1-7**; *cf.* **Parts 7.5** and **8.3.1b**, **APNDX. E3**; Burkholder 1919, Mueller 1975, Esslinger 1998, Flannigan 2007, and Kelley et al. 2007):

> The Convention of 1906 (34 Stat. 2953) requires that the United States (US) deliver an annual appropriation of water to Mexico at their Acequia Madre headgates in El Paso, TX (IBC, 1936, p. 2), and while the US Government owns Elephant Butte and Caballo Dams, prior to the Canalization Project they did not own the river channel. Measuring treaty water deliveries was almost impossible because of private water diversions along the 125 river mi (201 km) in the US. The unregulated flows also allowed Mexico to sometimes exceed their allotment (IBC, 1936, p. 3). Public Resolution No. 648, Act of June 4, 1936, authorized the canalizing of the Rio Grande from Caballo Dam, NM, to El Paso, TX. Construction began on January 15, 1938 and was completed in February 1943 . . . . The project was meant to establish a normal flow and flood

channel confined between parallel levees sized to carry the estimated maximum flood flows (IBC, 1935, p. 5). When the initial project was complete, 125.92 mi (202.6 km) of levee were constructed, almost 3300 ac (1334 ha) of floodway were leveled, the river was shortened by approximately 10 mi (16 km), and 7395 ac (2993 ha) of land were acquired at a total project cost of $2,996,052 (Baker, 1943, p. 4, 18, and 32).

The essential role played by the post-dam Rio Grande in maintaining the groundwater-flow regime throughout the Mesilla Valley is emphasized by Nickerson and Myers (1993, p. 10 [**Fig. 7-8**]):

> Rio Grande streamflow is the primary source of recharge to the aquifer system in the Mesilla Valley. Most recharge to the aquifer system is from Rio Grande seepage in losing reaches of the stream, seepage from irrigation canals, and infiltration of applied irrigation water. Recharge from precipitation and interbasin ground-water inflow is considered minor. The net transfer of water to or from the aquifer system by recharge and discharge mechanisms is related directly to Rio Grande streamflow and the volume of river water used for irrigation [Ikard et al. 2023]. . . .

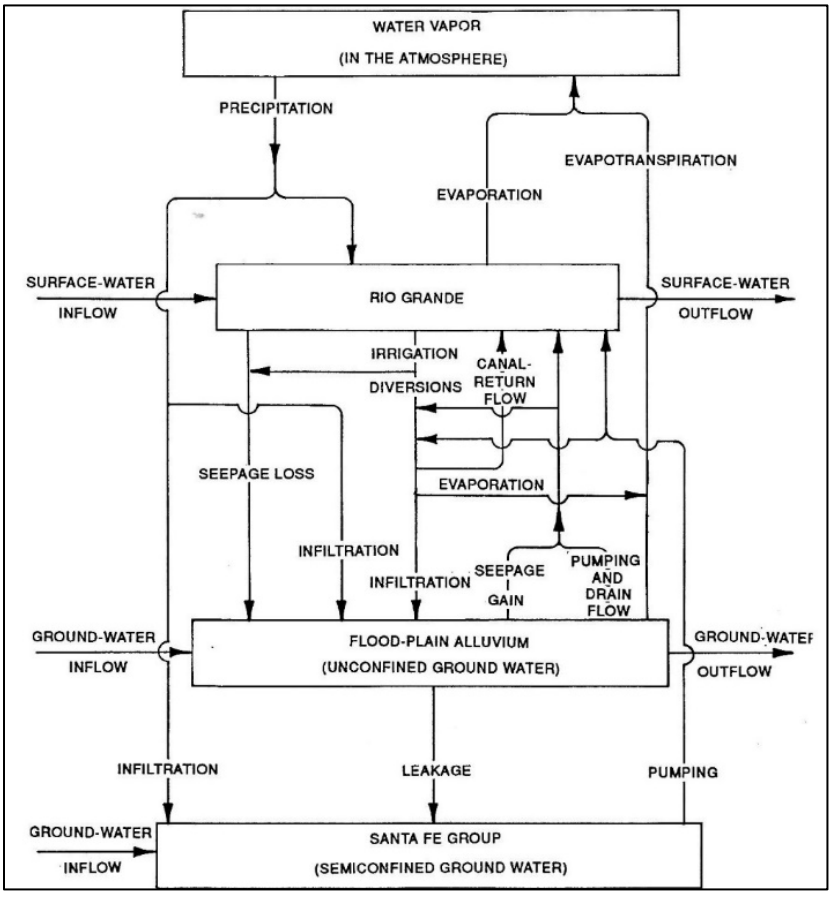

Figure 7-8 (FIG. 10 *in* Nickerson and Myers 1993)**.** Diagram showing the generalized circulation of water in the Rio Grande channel and floodplain area of the inner Mesilla Valley.

The following selections from Walton and others (1999, p. 42) further illustrate the complex nature of the shallow GW-flow system, in terms of variability in both water quantity and quality in a Rio Grande Project (1916 to present) context:

A. The Rio Grande flows through the Mesilla and Hueco bolsons in the El Paso-Ciudad Juárez area . . . . The sediments of the Mesilla Bolson are subdivided into four aquifers: the shallow aquifer, upper and lower intermediate aquifers, and the deep aquifer (Nickerson 1989 [1995, 2006]). The sources of recharge to the aquifers in the Mesilla Bolson include infiltration from the Rio Grande, irrigation canals, irrigation water spread in agricultural fields, and lateral flow from the La Mesa [West Mesa], New Mexico, area. Historically, the Rio Grande was a losing stream (indicating ground-water recharge) at the north end of the Mesilla Bolson [Valley] and a gaining stream (indicating discharge) at the south end near EI Paso. However, irrigation and municipal water use have changed this pattern to be more complex and seasonally variable. . . .

B. The quality and amount of recharge from the irrigated fields, leakage from irrigation canals, and ground-wa'er flow from' the La Mesa area . . . control water quality in the shallow aquifer of the Mesilla Bolson. Recharge in the shallow aquifer appears to be keeping pace with water usage (Hernandez, 1978; Peterson et al., 1984). Pumping from the deep aquifer has reversed the historical upward flow of low salinity water towards the surface. The present hydraulic gradient causes a downward migration of higher-salinity, shallow ground water into the intermediate aquifer. The quality of shallow ground water is thus of crucial importance to the long-term quality of water in the deeper aquifers. Shallow ground water tends to be brackish and may degrade water quality in the intermediate aquifer [*cf.* **Part 7.8.1b**].

The buildup of salinity in the shallow aquifer and, over time, the deeper aquifers is related to the interactions between surface waters and shallow ground water and is impacted by water use decisions. Currently, the system is irrigation dominated. River water is diverted at the north end of the Mesilla Bolson [Valley] and applied to fields. In the fields salts in the irrigation water are concentrated by evapotranspiration and additional salts are leached from . . . minerals in the soil. The salinity increase in the shallow ground water from irrigation is reduced by leakage of high quality waters from the canals. Hernandez (1978) examined the relationship between surface and ground water and found that salinity increased consistently as one moves down the river from the Elephant Butte Reservoir . . ., to the south end of the Hueco Bolson [*cf.* Wierenga 1979, Phillips et al. 2003, Witcher et al. 2004, Hogan et al. 2012, Teeple 2017, Kubicki et al. 2021] . . . .

7.3.2. Background on Hydrogeologic-Framework Characterization in the MBR

The hydrogeologic maps and cross-sections of the **PLATES 1** and **5** series (e.g., **Figs. 6-2**, **6-3, 7-9** and **7-10**) illustrate the complex nature of the hydrogeologic controls on surface- and subsurface-water flow and quality in the MBR. The 19 cross-sections in the **PLATE 5 (5a** to **5s)** series described in **Part 2.3.1** form fence-diagram array (*cf.* **Fig. 1-3**). Thirteen sections (A-A' to L-L' and S-S') have a general transverse-basin (W-E) orientation, and the other six (M-M′ to R-R′) are aligned approximately parallel to dominant NNW to SSE basin trends. The quasi-3-D graphic product portrays the functions of hydrogeologic-framework controls on GW-flow and chemistry at levels of detail that are much-more amenable to numerical modeling than has heretofore been possible. Each cross-section in the **PLATE 5** series was initially compiled at 1:100,000 scale at 1:1 and 5:1 vertical exaggeration. A mean sea-level (msl) base altitude allows full-depth display of most of the 395 deep-borehole records used in cross-section development (**TBL. 1**, **PL. 3**; *cf.* **Fig. 2-2**).

Figures 7-9 and **7-10** are page-size reproductions of down-RG valley/canyon and transverse hydrogeologic cross-sections (**PLS. 5o**, and **5i-5l** and **5s**) that extend, respectively, from (1) the lower part

of the Rincon Valley Basin to the western edge of the Hueco Bolson, and (2) across the northern and central parts of the International Boundary Zone (IBZ – **Figs. 1-10** and **7-5**; Sections O-O'-O"-O"', I-I' to L-L' and S-S'). Inset index maps on the left end of individual sections show their specific locations (*cf.* **Fig. 1-3**). The approximate pre-development water-table/potentiometric-surface altitude (**Fig. 7-2**) is shown by a blue line in each section's upper part.

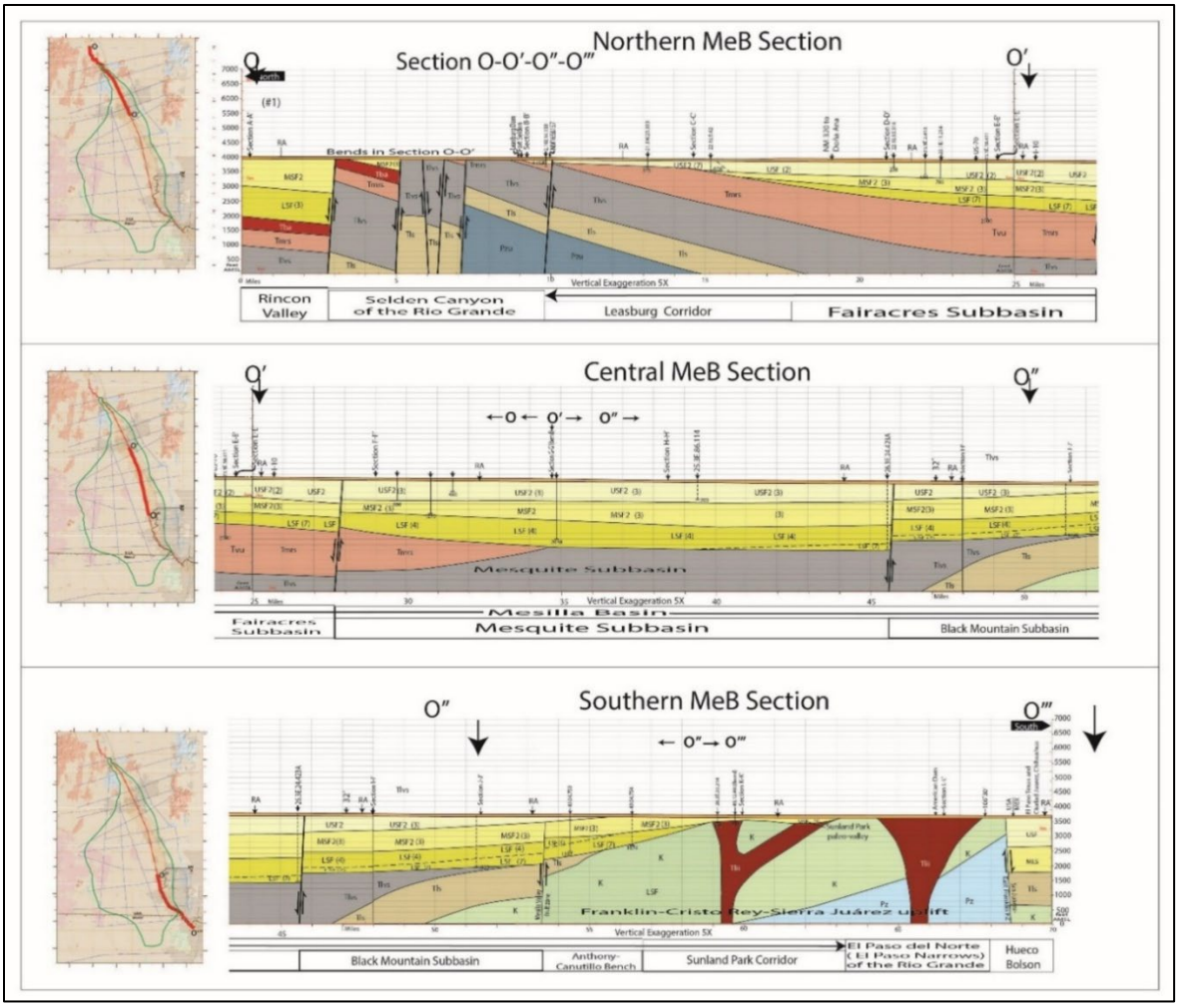

Figure 7-9. Page-size reproduction of **PLATE 5o** series of down RG Valley/Canyon (NNW to SSE) hydrogeologic cross-sections O-O'-O"-O"', with locations shown on inset index maps **(Fig. 1-3**). Base elevation-msl and VE-5x. The approximate pre-development water-table/potentiometric-surface is in the upper part of HSU-RA (orange) in each section (**Fig. 7-2**). Santa Fe Group (SFG) Hydrostratigraphic Units (HSUs) are shown with yellow shading, with lighter hues indicating best groundwater-production potential.

Thin (<30 m) Rio Grande alluvial deposits of latest Quaternary age (RA) are in orange on **Figures 7-9** and **7-10**. Santa Fe Group (SFG) Hydrostratigraphic Units (HSUs USF/MSF/LSF) are shown with yellow shading, with lighter hues indicating best groundwater-production potential. Underlying

bedrock units, in order of increasing age, comprise the following lithostratigraphic sequence (*cf.* **TBL. 2**): Latest Tlvs-Eocene volcaniclastic, epiclastic and volcanic rocks of intermediate composition (gray), Tli-Eocene intrusive igneous rocks of intermediate composition (red), Tls-Lower Tertiary siliciclastic sedimentary rocks (tan), K-Cretaceous marine sedimentary rocks (light green), Pz-Upper and Lower Paleozoic marine sedimentary rocks (dark and light blue), and XY-Proterozoic (Precambrian) igneous and metamorphic rocks (brown – only on **Fig. 7-10**).

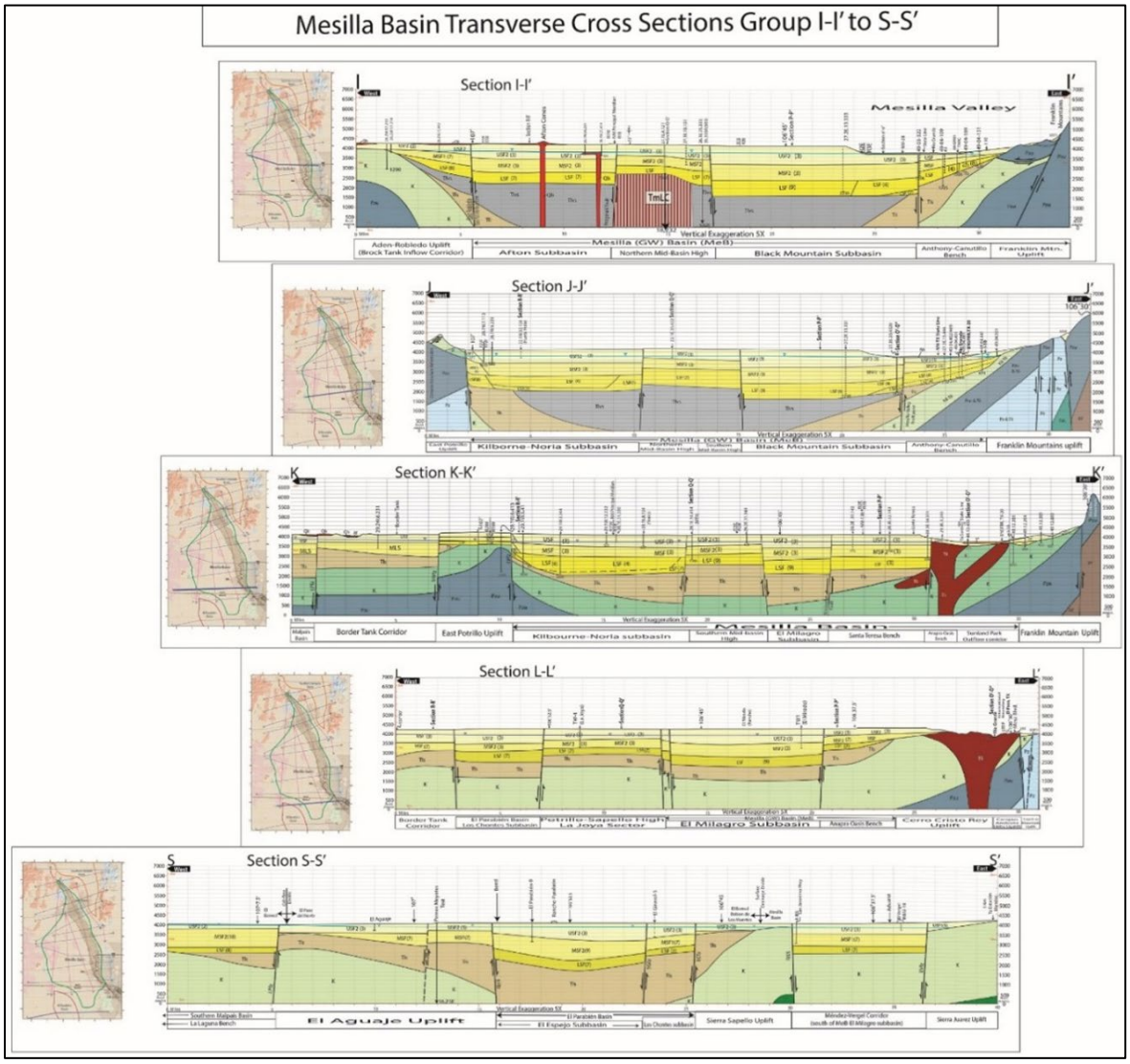

Figure 7-10. Page-size reproduction of **PLATE 5i** to **5l** and **5s** panel. Transverse (W to E) hydrogeologic cross-sections I-I' to L-L' and S-S' that span the northern and central parts of the International Boundary Zone (IBZ–**Fig. 7-5**), with section locations shown on **Fig. 1-3**, and panel inset index maps.

As noted in **Part 2.3.3**, the **PLATE 5o** (Section O-O', O'-O", O"-O"' series) was compiled to better illustrate the hydrologic linkage (via Selden Canyon and El Paso del Norte) between major

hydrogeologic-framework components in the Rincon Valley Basin (RVB) with those in the binational western Hueco Bolson (e.g., Hawley and Kennedy 2004, and Hawley et al. 2005 and 2009). The iterative process of cross-section design, which is described in detail in **APPENDIX A**, started with work done to support early-stage GW-flow modeling efforts in the Mesilla GW Basin (MeB) by Khaleel et al. 1983, Peterson and others (1984), and Frenzel and Kaehler (1992) (*cf.* Hawley 1984, Hawley and Lozinsky 1992, Nickerson and Myers 1992). Subsequently, more-detailed characterization of basin-scale hydrogeologic controls on GW flow and chemistry by Hawley and Kennedy 2004, Hawley and others (2005 and 2009), and Sweetkind (2017) have been used in a number of investigations of GW-flow, and related hydrochemical systems in the river valley/canyon reaches between Caballo Reservoir and Fabens, TX (e.g., Witcher et al. 2004, Hibbs and Merino 2007, Hogan et al. 2007 and 2012, Hutchinson and Hibbs 2007, Druhan et al. 2008, Eastoe et al. 2008 and 2010, Hibbs et al. 2015, Teeple 2017, Hanson et al. 2018, Kubicki et al. 2021). While they include isotope geochemical data of significant value, the merit of recent studies by Szynkiewicz and others (2015) and Garcia and others (2021) has been difficult to evaluate because these investigations do not appear to have utilized the above-described types of detailed hydrogeologic information.

7.3.3. "Paleohydrology" of an "Exotic" River—Inferences from Historic Accounts, Gaging-Station Records and Tree-Ring Proxies

A defining characteristic of the Historic record of Upper Rio Grande discharge between the Española Basin (at Otowi Gage) and the lower Hueco Bolson (near Fort Quitman) is its high variability, both in terms of annual and seasonal values, and river-channel/shallow-aquifer hydraulic-connectivity (e.g., Gunaji 1961, Taylor 1967, Richardson et al. 1972, Mueller 1975, Peterson et al. 1994, Peterson and Wilson 1988, Nickerson 1988, Frenzel and Kaehler 1992, Nickerson and Myers 1993, Ackerly 1999 and 2000, Witcher et al. 2004, USGS 1965, Western Water Assessment 2009, Hogan et al. 2012, Lehner et al. 2017, Teeple 2017a,b, Fuchs et al. 2019, Garcia et al. 2021, Kubicki et al. 2021, Davis 2022, Pearson et al. 2022, USGS-ND; and **Figs. 1-5**, **1-8**, **7-9**, **7-13** and **7-14**). Moreover, due to the occurrence of no-flow channel reaches at irregular intervals, the Historic Rio Grande in the Mesilla Basin region is now more properly classed as an intermittent stream rather than as a perennial one (**Part 3.2.3**).

According to Conover (1954, p. 16):

> The flow of the Rio Grande in this area in summer is maintained principally by releases from Elephant Butte and Caballo Reservoirs and in the winter by return drainage flow. Prior to the [1915] construction of Elephant Butte Dam the river was often dry for months at a time. Slichter (1905, p. 21) states that there was no water in the Rio Grande below El Paso for 9 months prior to August 25, 1904.

Historical anthropologist Neal Ackerly (1999, 2000) has taken two approaches in obtaining reasonable approximations of the long-term fluctuations in Upper Rio Grande discharge. In the first, Ackerly (1999) relied primarily on Historic narratives of onsite and remote observers, with the latter including an 1811 account of Baron Alexander von Humboldt about a 130 mi (>50 "leagues") reach of the river centered near El Paso de Norte (EPdN) that "became dry [for several weeks]" in 1752 (1999, p. 27). Ackerly's second (2000) approach involved use of tree-ring records, here the 1480 to 1964 "Fort Wingate series," with some calibration provided by 1896 to 1964 "San Marcial gauging station data," and he uses extended tree-ring records as "proxy data" in order to learn more "about long-term variability in the Rio Grande's flow" (2000, p. 1). USGS Water-Supply Papers 1312, 1732, 1932, and 2132 were the San Marcial Gauging Station reference sources, and cited information on the New Mexico regional tree-ring record included papers and database files by Drew (1972), Dean and Robinson (1978), Stockton and others (1983), Meko (1990), and Stockton (1990).

The effectiveness of this paleo-hydrologic approach has subsequently been demonstrated by research collaborations by dendrochronologists, paleoclimatologists, and hydrologists (e.g., Biodi et al. 2001, Grissino-Mayer et al. 2002, Western Water Assessment [WWA] 2009, Llewellyn and Vaddey 2013, Lehner et al. 2017, and Chavarria and Gutzler 2018; *cf.* Paskus 2020 [Chapt. 7]). The WWA (University of Colorado) "2008 Tree-ring reconstruction of streamflow and climate for the northern Rio Grande basin [from 1450-2002]," which includes proxy interpretations for flow past the Rio Grande gage near Otowi, NM, has already proven to be useful in interpreting of prehistoric floodplain-agricultural practices in the Albuquerque area (Love and Hawley 2010).

The following selections from Ackerly (1999, p. 27-28) exemplify the use of historical documents as a very effective tool for characterizing the pre-dam variability in the flow of an "exotic" river prior to the onset of any significant irrigation-agricultural activity in the Rio Grande basin above the Fort Quitman Gaging Station (**Fig. 1-7**; *cf.* Scurlock 1998):

> In his report on the 1850-1853 U.S. - Mexico Boundary Survey, John Bartlett [1854] commented (personal Narrative of Explorations and Incidents 1965 (reprint): 186-188):
>
> "The freshets that take place are owing to the melting of snows in the Rocky Mountains. These are not of yearly occurrence; for during the summers'of 1851 and '52, there were none. The river not only did not swell or overflow its banks, but in the former year it became quite dry near EI Paso, all the water being transferred to I acequias ... I was told by a gentleman at San Eleazario [sic], twenty-five miles below EI Paso, that the summer of 1852 was the first one in five years where there had been sufficient water to irrigate all the lands of that vicinity which had been put under cultivation."
>
> This implies that the river had been extraordinarily low or even dry (see below) each summer between 1847-1851. Remember, at this time the San Luis Valley of Colorado had barely been settled, Colorado was not using water from the Rio Grande in substantial amounts, and the Mesilla Valley had been occupied for less than a decade.

Similarly, W.W. Follett's (1898) publication "Equitable Distribution of Waters of the Rio Grande" contains the[se] comment[s]:

A. That the river went dry many years before the large use of water in Colorado began. The records show that in 1851 it [the Rio Grande] was dry as far north as Socorro, N. Mex. Again in 1860 or 1861 it was dry in the Mesilla Valley, and 1879 was the driest year of record prior to 1889, the flow ceasing nearly or quite as far north as Albuquerque. In 1889 it was dry for over four months at EI Paso, and this dry river was continuous farther north than Albuquerque (Pg. 100).

C. In 1889, for instance, the records show a large volume of water in the river at Del Norte [Colorado] and the channel dry from Albuquerque southward, while in 1894, with a very small amount in the river in the San Luis [Valley], it did not go dry at Albuquerque, but was dry thirty days for a long distance below there, and was not dry for any length of time in the Mesilla Valley (pg. 100).

The technical name for what is being described here is an "exotic" river in which flows typically diminish with distance from headwaters and/or ones in which surface flows periodically disappear beneath the bed of the river, only to reappear some distance downstream when (typically) impermeable subsurface dikes force water up toward the surface of the river's bed [*cf.* **PL 5o**].

In short, the Rio Grande did not always flow every year and certainly did not flow in the same amounts from year to year. Equally important, not all portions of the Rio Grande contained water even during the same year; instead, surface flows ceased in some parts of the river while other parts of the river continued to have surface water.

7.3.4. Use of Stable-Isotope Data to Identify Groundwater "Types" in Basin-Fill Aquifers and Pre-Dam River-Recharge Processes

Eastoe and others (2008, p. 737) use stable isotope data to distinguish four water types in the basin-fill aquifer system in the El Paso County/Ciudad Juárez part of the Hueco Bolson: "Two types [Groups A and B] relate to recharge from the Rio Grande: pre-dam (pre-1916) river water [Grp B] with oxygen-18 and deuterium ($\delta^{18}0$, δD, ‰) from (-11.9, -90) to (-10.1, -82), contrasts with present-day river water [Grp A] (-8.5, -74) to (-5.3, -56). Pre-dam water is found beneath the Rio Grande/Bravo floodplain and Ciudad Juárez, and is mixed with post-dam river water beneath the floodplain (*cf.* Hogan et al. 2012).

Two other types [Groups C and D] relate to recharge of local precipitation; evidence of temporal change of precipitation isotopes is present in both types. Recharge from the Franklin and Organ Mountains plots between (-10.9, -76) and (-8.5, -60) on the global meteoric water line (GMWL [global meteoric water line-Craig 1961a]), and is found along the western side of the Hueco Bolson, north [and east] of the Rio Grande (*cf.* Hibbs and Merino 2020, Kubicki et al. 2021). Recharge from the Diablo Plateau [on the basin's northeastern border] plots on an evaporation trend originating on the GMWL near (-8.5, -58). . . ." In their Hueco Bolson example, Eastoe and others (2008, p. 746) demonstrate that "recharge to regional aquifers in alluvial basins [like the MeB] can be dominated by stream-bed infiltration where the geology and local groundwater conditions are favorable." The following selections provide more detail on this study's purpose and conclusions (p. 746):

Groundwater isotope data for the Hueco Bolson and the adjacent region have been presented in several earlier articles. Kreitler et al. (1986[87]) and Fisher and Mullican (1990, 1997) published O, H, S and C stable isotope data, plus chemical analyses and ^{3}H and ^{14}C data for groundwater in the southeastern part of the basin in Hudspeth County. Anderholm and Heywood (2002) presented a similar suite of measurements for nine wells in El Paso County. . . . Other relevant isotope studies in the region include Witcher et al. (2004), with data for the Mesilla Basin, upstream of El Paso; and Phillips et al. (2003), with detailed O and H isotope data for surface water in the upper Rio Grande. In the groundwater studies, the origin of a group of samples of evaporated water with $\delta^{18}O$ values near -11 % remained unexplained [p. 738-1].

The previous work shows that useful isotope distinctions exist between native basin and river-derived groundwater types. In this study, the initial hypotheses were (1) that a systematic study of stable O and H isotopes would lead to an improved understanding of groundwater sources in the Hueco Bolson aquifer; (2) that the damming of the Rio Grande would generate an isotope effect related to residence time of Hueco Bolson groundwater; and (3) that the radioactive isotopes tritium [^{3}H] and carbon-14 would further refine the understanding of groundwater residence times. A sample set from supply wells in the Hueco Bolson aquifer (the deeper regional aquifer of the basin [**Group C**], as opposed to the shallow aquifer that is limited to the Rio Grande flood plain [**Group B**]) in west Texas and adjacent New Mexico and Chihuahua have been examined. The more general applications of the findings to aquifers downstream of major dams in other river basins were examined, along with the importance of mountain front/mountain block recharge relative to recharge from major streams in the alluvial aquifers of the Basin and Range province [p. 738-2].

The association of these [**Group B**] samples with the RGEL [Rio Grande Evaporation Line] . . . and with the area close to the Rio Grande . . . suggests that they are recharged river water. The low $\delta^{18}O$ and δD values of group B, however, are far from the range of values recorded in Rio Grande surface water since 2002. They resemble values at present found in the river as it enters the Albuquerque basin, 460 km [286 mi] upstream of El Paso (Phillips et al. 2003). According to the isotope data, group B cannot be generated from locally derived water (as indicated by mountain groundwater. . .) by any likely near-surface process such as mixing or evaporation. Fig. 6 indicates that the water with lowest $\delta^{18}O$ and δD values recharged prior to 1953. The ^{14}C data indicate maximum (i.e., uncorrected) residence times of 1,800 to 7,500 years for samples (sites [south of the river channel in the HB-SWSB-**Fig. 7-2**] . . .) with $\delta^{18}O$ <-11.6% [p. 244].

7.4. ADVANCES IN GW-FLOW SYSTEM CHARACTERIZATION—1946 to 2021

7.4.1. Early-Stage USGS and NM WRRI Investigations—1946 to 2007

Figures 7-11 to **7-13** illustrate early-stage development of water-table and/or potentiometric-surface maps that depict general GW-flow trends in the United States part of the Study Area. They comprise an invaluable history of groundwater-level measurements, most of which were made between 1946 and 1992 for USGS water-resources investigations. **Figure 7-11** is a facsimile copy of a section of Plate 1 *in* Clyde S. Conover's (1954) pioneering report on "Ground-water conditions in the Rincon and Mesilla Valleys . . ." which show the approximate 1947 water-table altitude in central and southern Doña Ana County (*cf.* **APNDX. C2a**). Estimated depths to water in the 300 to 400-ft and > 400-ft ranges shown, respectively, with light greenish yellow and green dotted patterns.

Even without water-table altitude information in Mexico, Conover (1954, Pl. 1) inferred that (1) GW-flow west of the East Potrillo Mountains was southward into Chihuahua, and (2) underflow was northeastward toward the lower MeV in the International Boundary area between Noria and Mastodon Sidings of the SPRR. The only significant interpretive-error on the Conover map is the placement of a water-table "mound" in the area of Black Mountain (Fig. 7-11). It is based on the assumption of the time that this local basaltic volcanic center of Middle- to Late-Pleistocene age was located on an older Cenozoic bedrock uplift (**Part 6.3.4b**, **Figs. 7-2** and **7-4**; *cf.* **6-2**, **PL. 1B**).

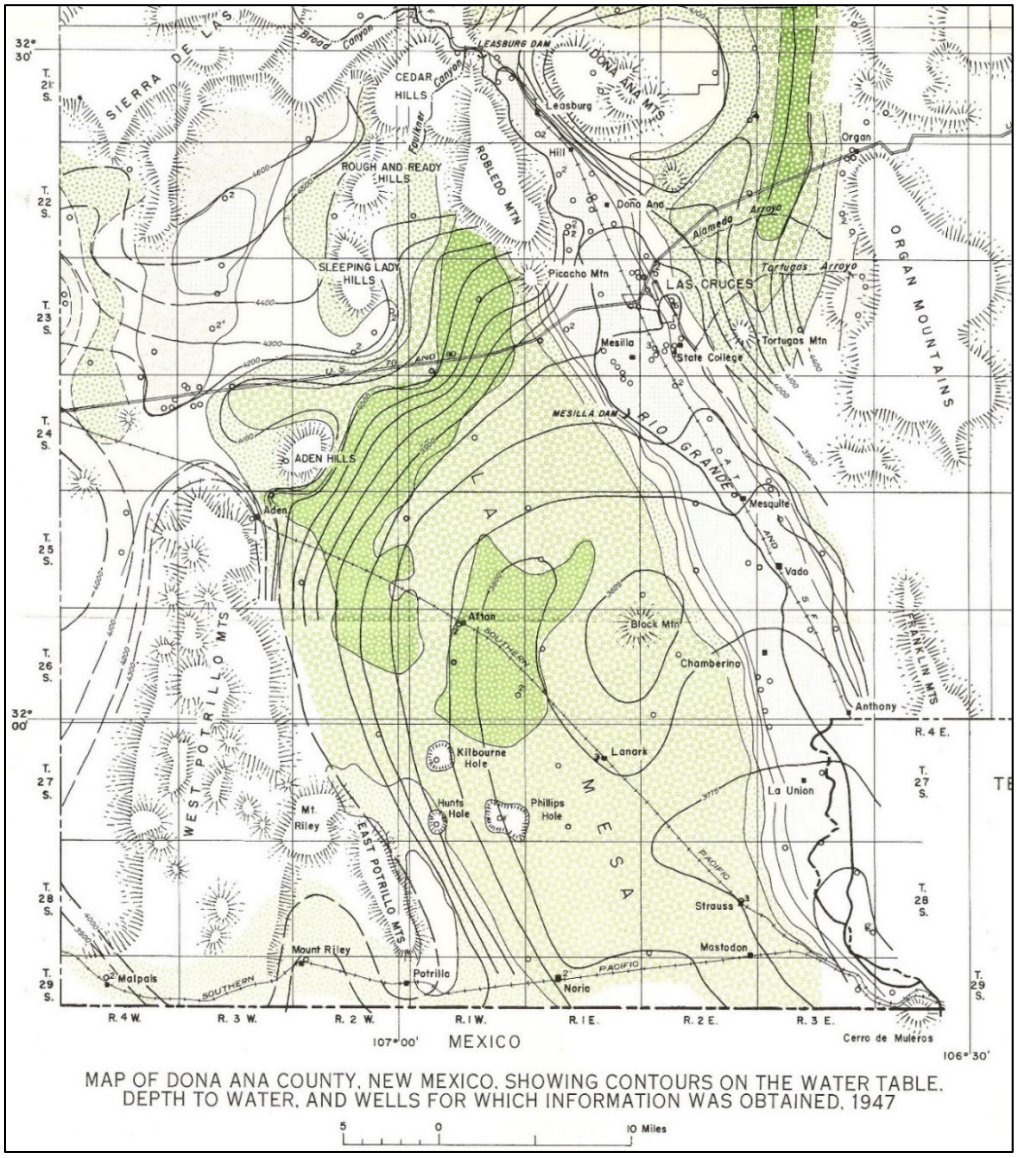

Figure 7-11 (facsimile copy of central and southern parts of Plate 1 *in* Conover 1954 [partial **PL. 9A**]). Map showing the approximate 1947 water-table altitude in central and southern Doña Ana County, with estimated depths to water in the 300 to 400 ft and > 400 ft ranges shown, respectively, with light greenish yellow and green dotted patterns.

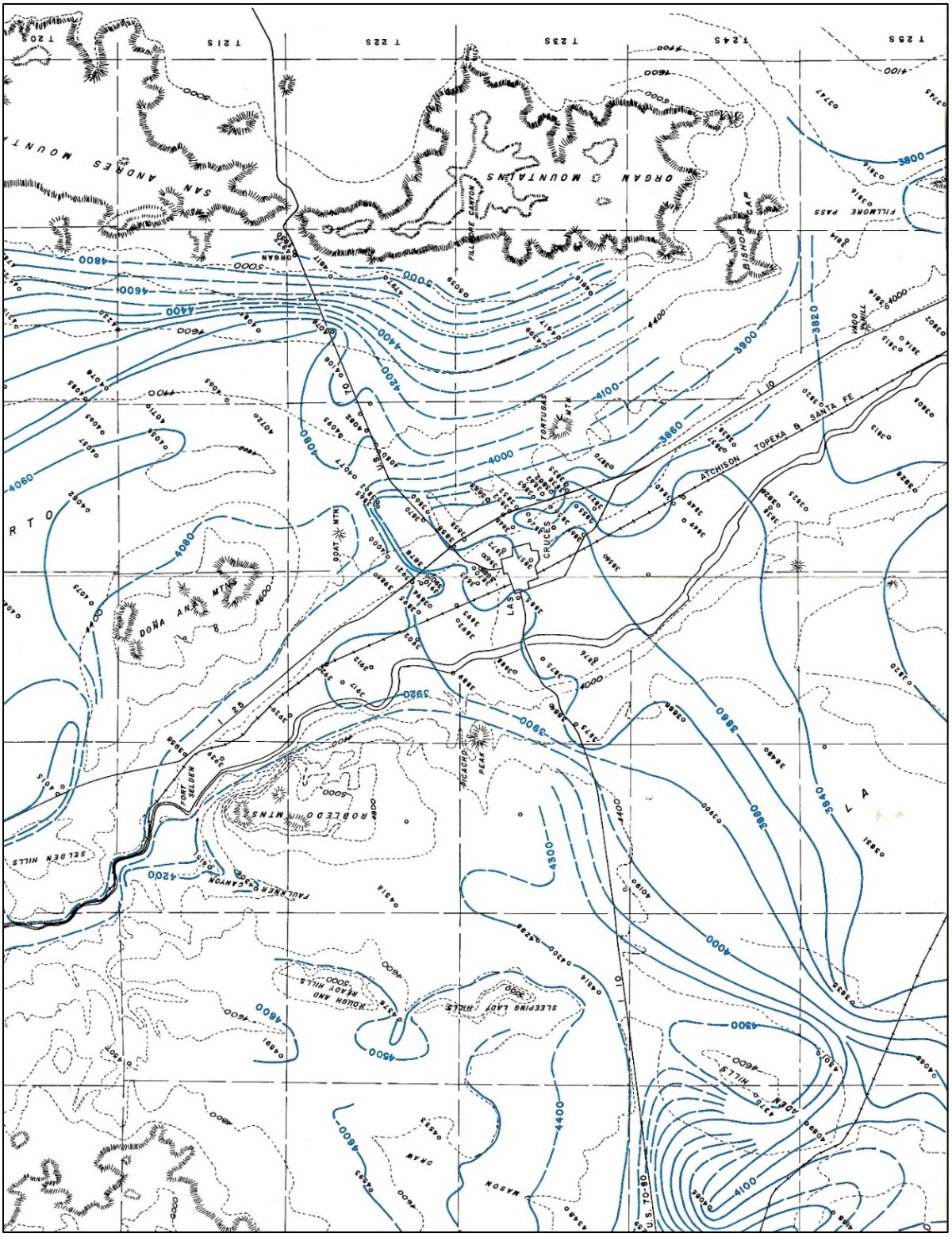

Figure 7-12a (middle part of **Pl. 9B**). Map showing approximate water-level (blue) and land-surface (black-dashed) altitude for the middle MeB and the southern end of the Southern Jornada Basin (King et al. 1971, PL. 1) 1965-1968 water-level compilation, with N to left map orientation. Note first recognition of Rincon Valley-directed GW flow in the SJB north of US-70.

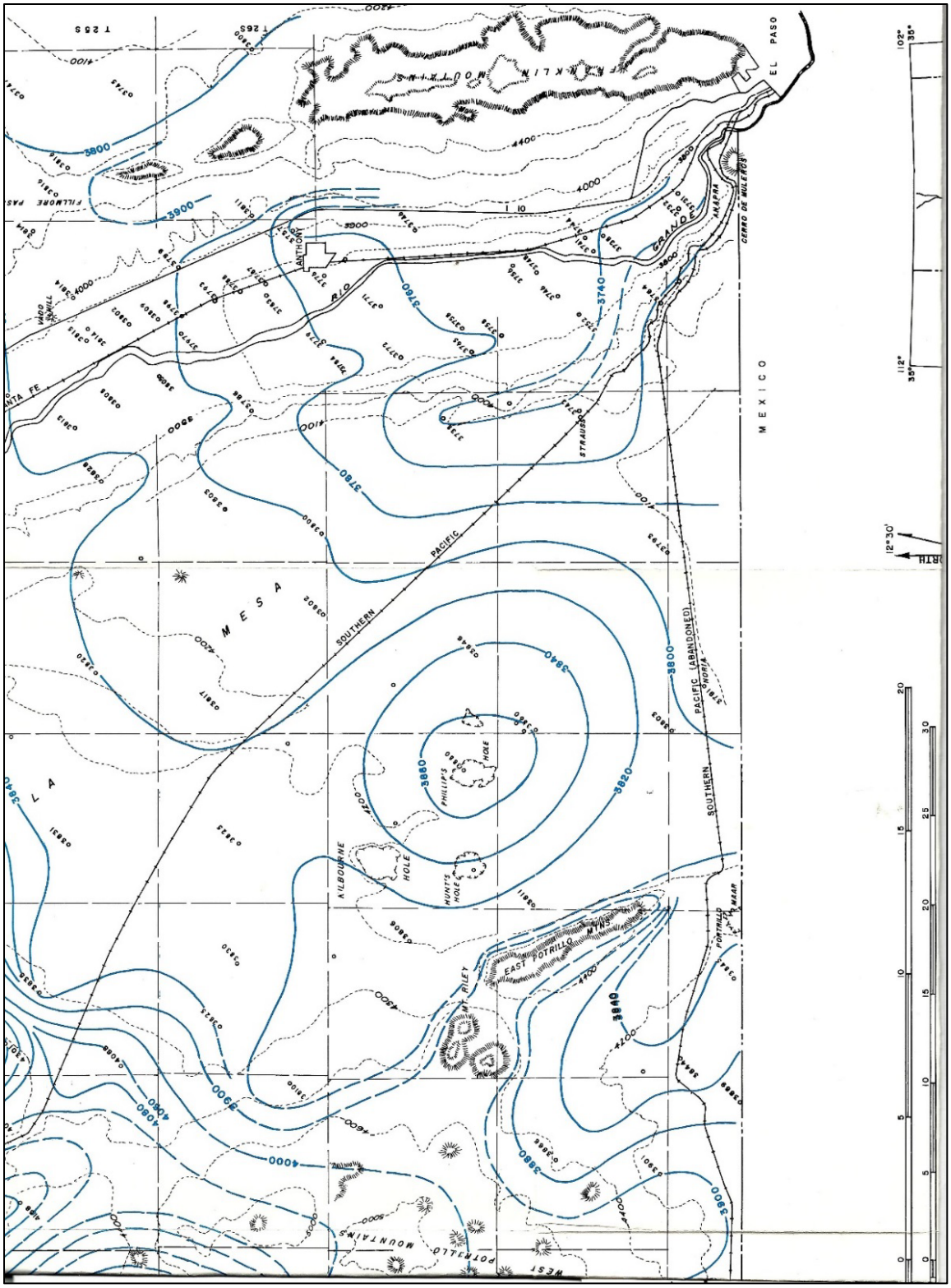

Figure 7-12b (lower part of **PL. 9B).** Map showing approximate water-level (blue) and land-surface (black-dashed) altitude in the southern Mesilla Basin area (King et al. 1971, PL. 1) 1965-1968 water-level compilation, with N to left map orientation. Note eastward GW-flow along the International Boundary zone east of the abandoned Noria Siding on the SPRR.

The above-cited USGS and NM WRRI groundwater investigations represent major advancements in the characterization of GW flow and chemistry throughout the U.S. part of the Mesilla Basin region. This is mainly because only a few prior GW-resource investigations had a strong conceptual base in terms of the geologic characterization of aquifer-system components (e.g., Knowles and Kennedy 1958, Leggat et al. 1962, Cliett 1969, W. King et al. 1971 [**Fig. 7-12**], and Wilson et al. 1981 [*cf.* **Fig. 7-13**]). Progress in development of potentiometric-surface maps and GW-flow concepts since the 1950s reflects (1) major advances in well-location and land-surface elevation control (e.g., aneroid barometric and 15-min quadrangle maps vs. contemporary GPS-platforms and GIS technology), (2) precision in depth-to-water measurements (e.g., chalked steel tape, electric-sounding devices, and analog-to-digital recorders), and (3) standardization of seasonal water-level measurement and water-sampling protocols. King and others (1969, 1971) were the first to apply contemporary hydrogeologic-framework concepts in their description of subsurface conditions in the Mesilla Basin and Rincon Valley area (**Figs. 7-12a** and **7-12b** [**PL. 9B**]). For example, they showed that a large part of the predevelopment GW flow in the Southern Jornada Basin (SJB) discharged to the Rincon Valley Basin (RVB) northwest of the Tonuco Mountains Uplift (**Figs. 7-2**, and **7-12a**). They also recognized the general eastward underflow component of the Transboundary GW-flow system in the United States part of the southern Study Area (**Figs. 7-2**, **7-7**, and **7-12b**).

Figure 7-13 (lower **PLATE 9C**) is a facsimile copy of the southern part of Plate 1 in Frenzel and Kaehler (1992). This slight modification of the 1976 USGS water-level map in C.A. Wilson and others (1981, Pl. 9) represents the first systematic compilation of baseline information on potentiometric-surface configuration in the Mesilla and Rincon-Palomas Groundwater Basins. Together with comprehensive maps and tabular databases, the Wilson and others 1981 report continues to serve as the primary resource document on predevelopment GW-flow and hydrochemical conditions in the region. Again, note the eastward GW flow that (1) has an ENE-directed component indicating a significant underflow contribution from north-central Chihuahua, (2) discharges in the shallow aquifer system of the Lower Mesilla Valley, and (3) immediately underlies the new Border Wall (**Figs. 1-11** to **1-14**, and **7-2** and **7-7**).

7.4.2. Transboundary Aquifer Assessment Program (TAAP) Contributions

Andrew Teeple's (2017a, b) "geophysics- and geochemistry-based assessment of the geochemical characteristics and groundwater-flow system of the U.S. part of the Mesilla Basin/Conejos-Médanos aquifer system" is a product of ongoing USGS Transboundary Aquifer Assessment Program (TAAP) investigations (*cf.* Sweetkind 2017 and 2018, Hanson et al. 2018, Fuchs et al. 2019, Kubicki et al. 2021, Robertson et al. 2022). **Figure 7-14** (Teeple 2017, Fig. 47) is representative of the new generation of USGS-TAAP water-level maps that utilized state-of-practice wellhead location/altitude control in recording "mean winter 2010-11 water-level altitudes measured in wells completed in the Santa Fe Group in the Mesilla Basin study area."

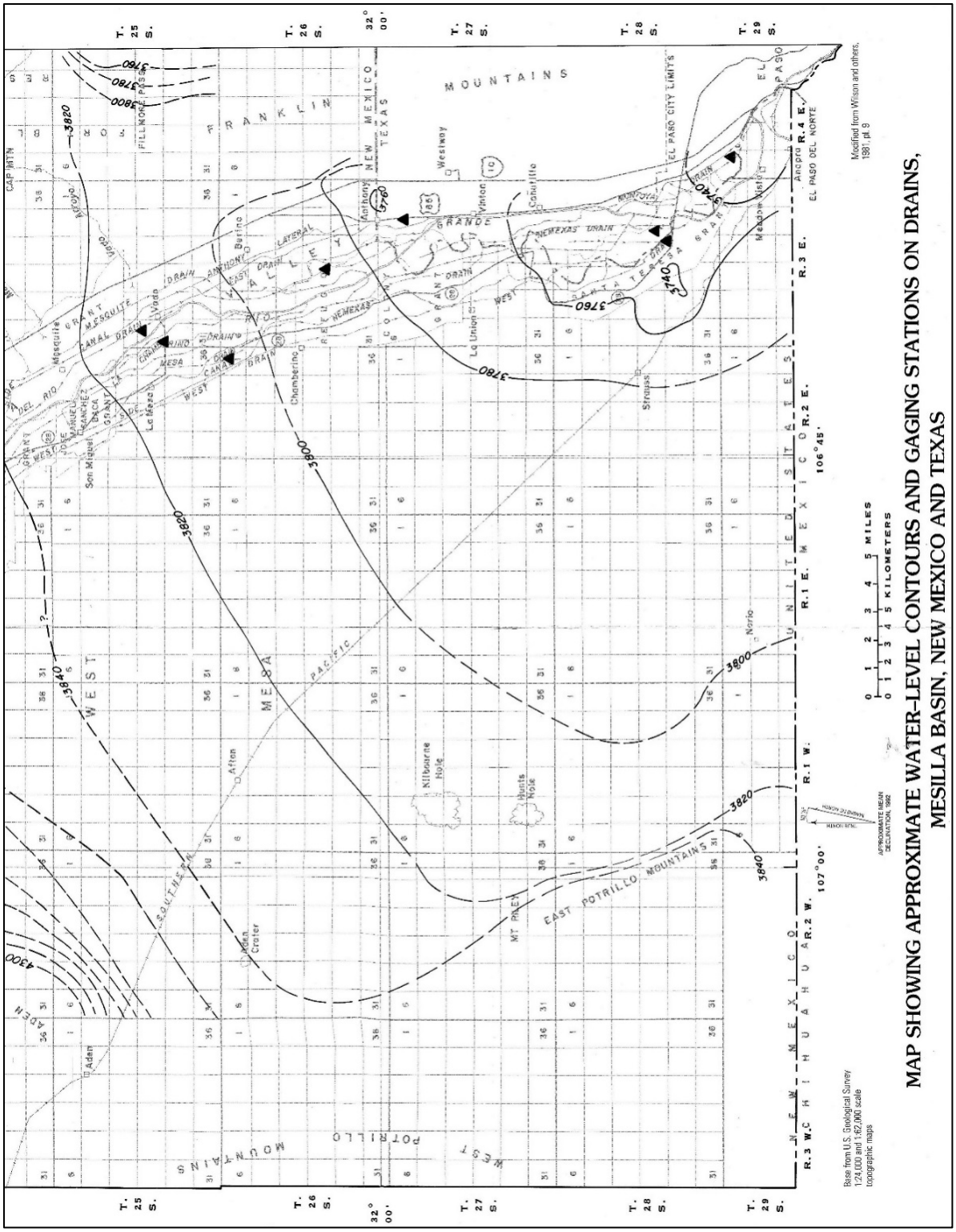

Figure 7-13 (southern part of **PL. 9C**)**.** Map showing approximate water-level contours, Mesilla Basin, New Mexico and Texas (modification of Wilson et al. 1981 [PL. 9] by Frenzel and Kaehler 1992 [PL. 1]). Compilation of water-level data through January 1976, with N to left map orientation. Note NE-directed GW flow from Mexico near the International Boundary.

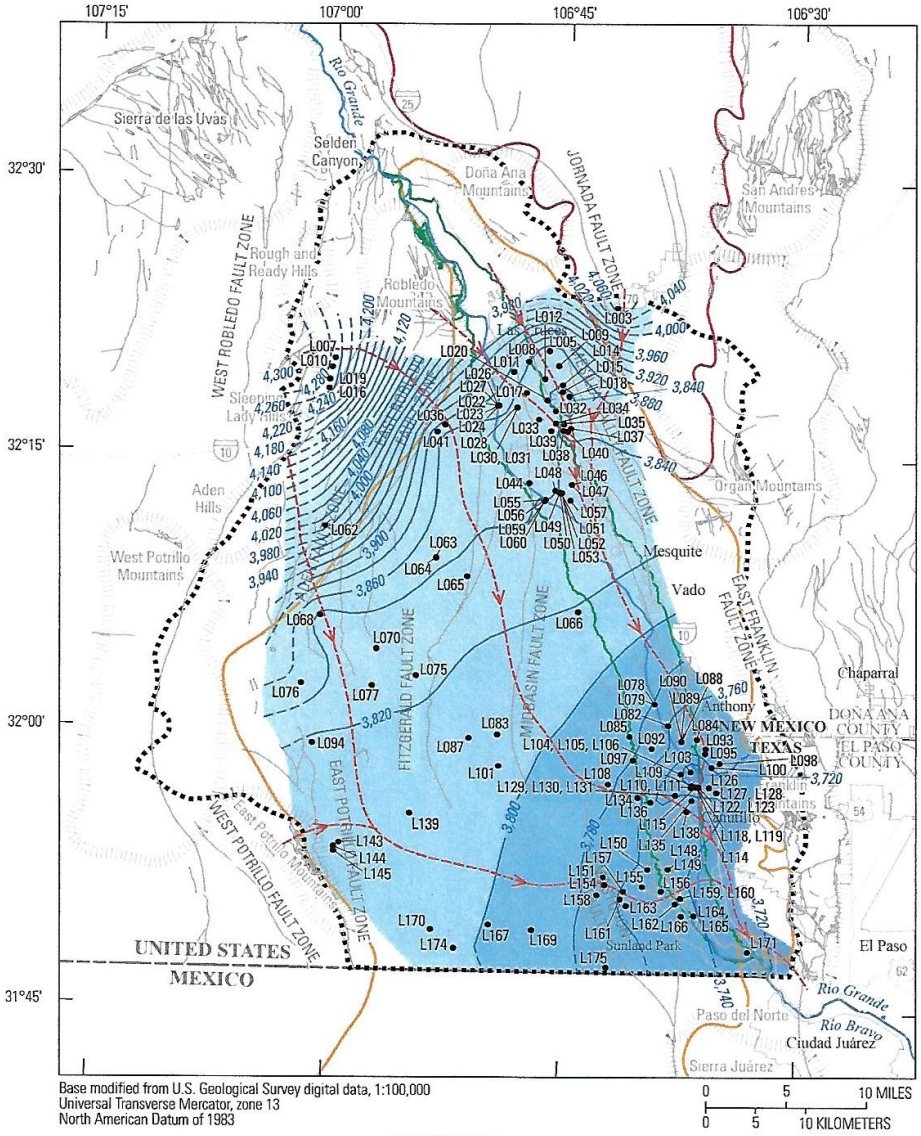

Figure 47. Potentiometric surface developed from mean winter water-level altitudes (November 2010 through April 2011) measured in wells completed in the Santa Fe Group in the Mesilla Basin study area in Doña Ana County, New Mexico, and El Paso County, Texas.

Figure 7-14 (Teeple 2017a, Fig. 47)**.** Potentiometric-surface map, with inferred GW-flow paths, developed from mean winter 2010-11 water-level altitudes measured in wells completed in the SFG aquifer system of Doña Ana County, NM and El Paso County, TX. Contour interval 20 ft. Note the ENE-directed GW flow that is sub-parallel to the International Boundary.

Seminal USGS contributions to the TAAP are also illustrated by Teeple's (2017a) work on groundwater age-dating and isotope chemistry, especially when being considered in the context of ongoing concerns about "groundwater sustainability" (*cf.* **Part 8.3** and **APNDX. E1**; and Ikard et al. 2021, Pepin et al. 2022, and Pearson et al. 2022):

7.4.2a Teeple 2017a (p. 81; *cf.* Fig. 7-14):

> Sources of water for the groundwater system within the study area consist of seepage from the Rio Grande, runoff and recharge within the mountains and uplifted areas, and inflows of upwelling groundwater from deep saline sources or from other aquifer systems. These sources of water were qualitatively analyzed and compared to previously published studies within the area (Frenzel and Kaehler, 1992; Nickerson and Myers, 1993; Witcher and others, 2004; S.S. Papadopulos and Associates, Inc., 2007). The predominant source of water for the groundwater system within the study area was the Rio Grande, with the other water sources [within the United States] contributing a small fraction of the total amount of water. Runoff and recharge within the mountains and uplifted areas (including mountain-front recharge contributed the least amount, consistent with the local climate and annual rainfall in the area . . . .

7.4.2b Teeple 2017b (p. 95):

> The ^{14}C age-dating results indicate the Rio Grande alluvium contained the youngest water and that the middle Santa Fe and lower Santa Fe contained the oldest water, results consistent with apparent groundwater age increasing with increasing depth. The groundwater sample results for ^{3}H [tritium] compared favorably to the apparent ^{14}C age-dates; most of the groundwater samples with ^{3}H concentrations that were greater than 1.6 TU ([tritium-unit] postbomb water) had modem ^{14}C apparent ages. All of the groundwater samples with ^{3}H concentrations of less than 0.6 TU were classified as older water with apparent ages of ^{14}C ranging from about 2,800 to 35,000 ^{14}C years before pres249rovin.].
>
> The groundwater sample results of δD and δ ^{18}O were compared with the groundwater sample results of ^{14}C age dating. Most of the groundwater samples classified as old groundwater (greater than 10,000 ^{14}C years BP) were also classified as isotopically lighter (δD values of less than -82.65 per mil), supporting the hypothesis that this water was recharged during the wet and cool climate of the Pleistocene [*cf.* Kubicki et al. 2021].
>
> The geochemistry data indicate that there was a complex system of multiple geochemical endmembers and mixing between these endmembers with recharge to the Rio Grande alluvium and Santa Fe HGUs [HSU-equivalent "Hydrogeologic Units"] composed mostly of seepage from the Rio Grande, inflows from deeper or neighboring water systems, and mountain-front [and mountain-block] recharge. The following distinct geochemical groups were determined in the study area: (1) seepage from the ancestral Rio Grande — groundwater older than 10,000 ^{14}C years BP (hereinafter referred to as the "ancestral Rio Grande geochemical group"), (2) seepage from the modern Rio Grande--groundwater younger than 10,000 ^{14}C years BP (hereinafter referred to as the "modern Rio Grande geochemical group"), (3) mountain-front [and block] recharge from the Organ and Robledo Mountains and from the highlands to the southwest (hereinafter referred to as the "mountain-front geochemical group"), (4) deep groundwater upwelling (herein after referred to as the "deep groundwater upwelling geochemical group"), and (5) unidentifiable source of freshwater, which could contain interbasin flow from the Jornada Basin (hereinafter referred to as the "unknown freshwater geochemical group"). . . .

7.5. HYDROGEOLOGIC CONTROLS ON INTERBASIN GW FLOW IN THE UNITED STATES PART OF THE STUDY AREA

The hydraulic-geometry of the Selden Canyon and El Paso del Norte bedrock-channel and floodplain constrictions preclude transmission of significant amounts of interbasin underflow (**Part 3.2.3**). Maximum saturated alluvial-fill cross-sections in either the SCyn or EPdN reaches do not exceed 26,500 ft^2 (2,500 m^2). With hydraulic gradients in the 0.001 to 0.002 range and estimated hydraulic conductivities (K_{hsat}) between 30 and 60 ft/day (10-20 m/day), maximum underflow discharge would approximate or be even less than the 81 ac-ft/yr (50 gpm, 0.11 cfs, 0.1 hm^3/yr) discharge rate first measured by Charles Slichter at the American Dam site in EPdN (Slichter 1905b, p. 13; *cf.* **7.3** [Conover 1954, p. 5-7], Frenzel and Kaehler 1992 [p. C33], Nickerson and Myers 1993 [p. 22], and Hawley and Kennedy 2004 [p. 73]); **APNDX. C1**). As also schematically illustrated in the northern and southern segments of **PLATE 5o**, the *damming* effect that the SCyn and EPdN constrictions impose on GW-flow regimes in aquifer systems immediate-upgradient basin-fill can be quite substantial (*cf.* Hubbert 1940, Toth 1963, Mills 2003, Phillips et al. 2003, Hawley and Kennedy 2004 [Figs. 5.2 and 5.3], Witcher et al. 2004, Moore et al. 2008, Garcia et al. 2021, Kubicki et al. 2021; **Parts 3.4.2a**, **3.4.2b** and **6.3.5d**; ***cf.*** **APNDX. H7**).

Essentially all water that now enters and leaves the MeV as surface flow is representative of the range in annual releases of Rio Grande Project water (**Fig. 7-15** [Frenzel and Kaehler 1992, Fig. 7]; *cf.* **Part 3.2.3**, **Fig. 3-6**). Based on early work of Lee 1907 (p. 32), the 1992 Frenzel and Kaehler GW-flow model (p. C38) assumed a pre-1916 average river-inflow from Selden Canyon to the MeV of 700 cfs (507,122 ac-ft/yr; 625.54 hm^3/yr). Most of the active subsurface flow in the MeB is restricted to the respective lower and upper parts of HSUs-USF2 and MSF2, especially where ARG deposits (LFAs 2 and 3) are a major aquifer constituent. This premise is based on (1) GW age and stable-isotope composition (**Part 7.3.3**), and (2) information presented in a predevelopment context on HSU and LFA hydraulic-conductivity and thickness properties of saturated SFG basin fill deposits (*cf.* Kubicki et al. 2021).

Significant transformations of the GW-flow system and its chemical composition in deeply buried aquifer zones, such as the “Deep Aquifer” of the Canutillo Well Field (HSU-LSF: LFA 4), have only occurred after the onset of large-scale pumping of deep M&I and irrigation in late 1950s (e.g., Leggat et al. 1962, Wilson et al. 1981, Gates et al. 1984, Wilson and White 1984, Nickerson 1989, Wade and Reiter 1994, Cliett and Hawley 1996, West 1996, Hutchison 2006). Observed and potential-future impacts of increased SFG-aquifer development in the International Boundary Zone (IBZ-**Fig. 7-7**), as well as in sections of the Study Area located in or adjacent to the MeV, are discussed in **Part 7.6**. Description of shallow-subsurface flow conditions in basin-bounding uplifts and basin-fill subcrop zones is primarily restricted to noting the influence of bedrock composition on GW quality (**Part 3.2.2**; Kubicki et al. 2021).

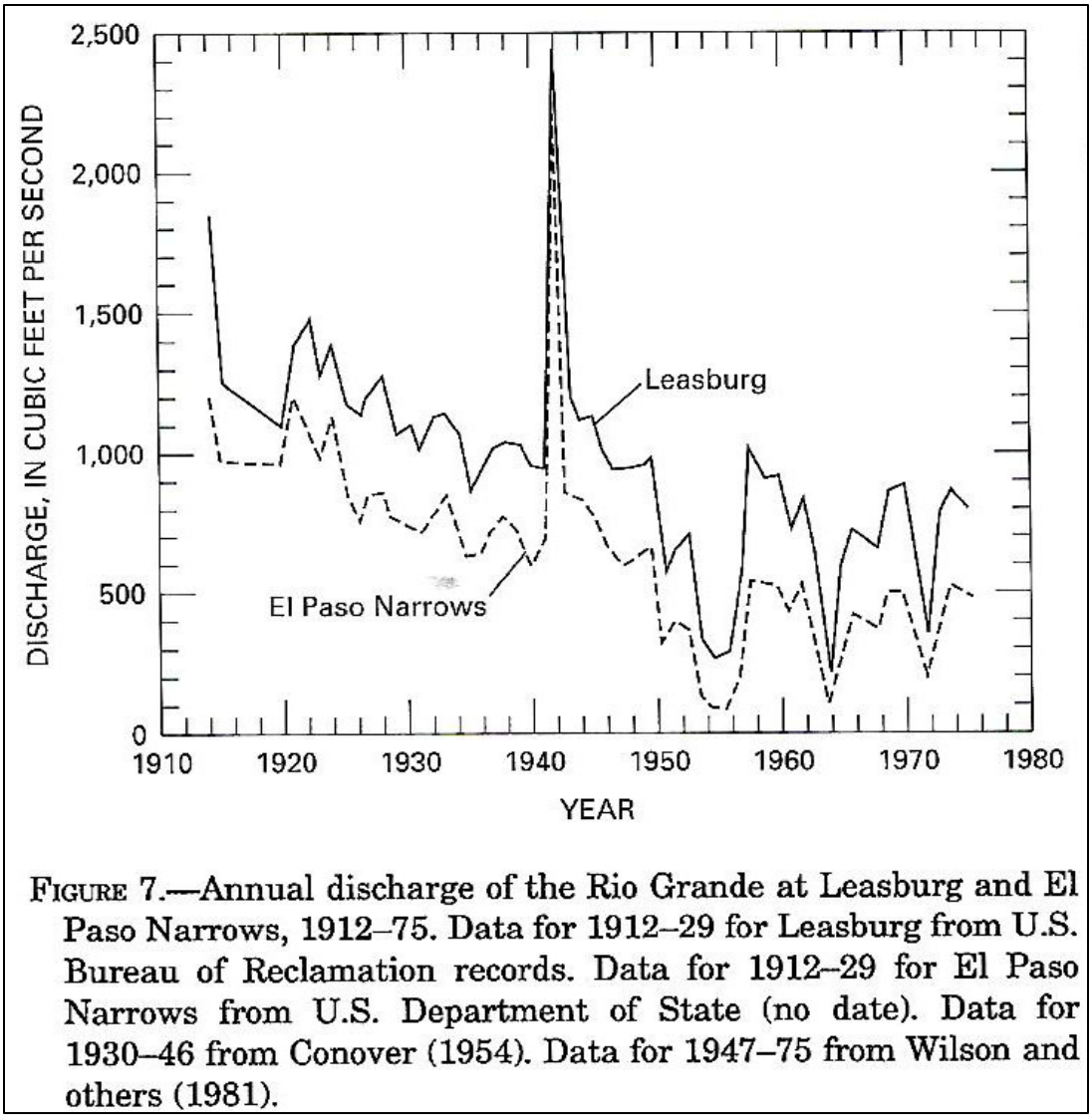

FIGURE 7.—Annual discharge of the Rio Grande at Leasburg and El Paso Narrows, 1912–75. Data for 1912–29 for Leasburg from U.S. Bureau of Reclamation records. Data for 1912–29 for El Paso Narrows from U.S. Department of State (no date). Data for 1930–46 from Conover (1954). Data for 1947–75 from Wilson and others (1981).

Figure 7-15. Facsimile copy of Figure 7 in Frenzel and Kaehler (1992) showing annual Rio Grande discharge at Leasburg Dam and El Paso Narrows (Courchesne Bridge Gaging Station).

Underflow relationships between the MeB and interlinked GW basins are summarized in the following Chapter sections: (1) between the Southern Jornada Basin and MeB (**Part 7.5.1**), (2) between the MeB and Western Hueco Bolson (**Part 7.5.2**), (3) contributions from the Cedar-Corralitos Upland Basin to the MeB (**Part 7.5.3**), (4) contributions from Western Basin-Boundary Uplifts to the MeB (**Part 7.5.4**), and (5) indirect contributions from the Malpais Basin-Border Tank Corridor Area to the binational southern MeB (**Part 7.5.5**).

7.5.1. GW-Flow Contributions from the Southern Jornada GW Basin to the MeB

As illustrated on **Figures 7-2** and **7-12a**, GW flow in the Isaacks Lake and Experimental Range Subbasins (ILSB and ERSB) of the Southern Jornada Basin (SJB) is northwestward toward a primary

discharge zone at the eastern edge of the Rincon Valley Basin (RVB; **Parts 5.2.2**, **6.1.1** and **6.1.2;** *cf.* Wilson et al. 1981 [Pl. 5], Shomaker and Finch 1996, Kambhammettu et al. 2010). The SJB and RVB in this area are separated by a shallowly buried, narrow ridge of lower SFG conglomerate and sandstone that connects the Tonuco Mountains and Rincon Hills Uplifts (Hawley et al. 2005, Pls. R1, R3 and R4e). GW-quality is predominantly brackish, and the very small amount that contributes to shallow-subsurface and RG-surface flow in the RVB-Tonuco Outflow Corridor (TNoc) returns to the MeB via Selden Canyon.

The SJB-Talavera Subbasin (TvSB) at the southern end of the Jornada del Muerto basin is in the Mesilla basin watershed with respect to both surface runoff and GW-flow (**Figs. 1-5**, **6-1**, and **7-2**; *cf.* Wilson et al. 1981 [Pl. 9], Teeple 2017 [Fig. 47]). Both the surface-watershed and GW-flow divides between the SJB-ILSB and TvSB are located near U.S. Hwy. 70 (**Figs. 7-2, 7-12a**; **PL. 9B**; **APNDX. F: Pls. F2-8** and **F3-2b**). The primary mountain-block recharge area for basin-fill aquifers of the SJB-TvSB and ILSB, as well as the MeB-LCBn, is in the igneous bedrock terrane of the Organ Mountains Uplift (OMU), which contributes a relatively small but still-significant amount of high-quality water to the GW-flow system. On the other hand, the relatively large watersheds in Upper Paleozoic marine-sedimentary rocks exposed in southern San Andres Mountain Uplift (SAMU) contribute not only mountain-block recharge of poor quality, but also gypsiferous fine-grained sediment to the thick SFG basin fill of the SJB-ERSB (*cf.* **Parts 5.1.1**, **5.2**, **6.1.3**, **6.3.5a** and **8.3.2**).

Most of the GW flow from TvSB to the MeB- Las Cruces Bench (LCBn) passes through gaps in the buried Tortugas Uplift (TtU; **Fig. 7-16** [Hawley 1984, pl. 5 and Frenzel and Kaehler 1992, Fig. 11]; **Parts 5.2**, **6.1.3** and **6.3.5**). Using **Figures 7-2** and **7-12a** for reference, westward GW-flow in the TvSB has a primary recharge source in the west-central Organ Mountains Uplift. Predevelopment interbasin GW flow terminated in the MeB-LCBn below the eastern edge of the Mesilla Valley (**Fig. 7-2**; **Tbl. 7-1**); however, much of this flow in now captured by pumping for suburban-domestic use in the TvSB. Frenzel and Kaehler (1992, Fig. 18), for example, estimate that the combined "mountain-front" recharge component to the northeastern MeB from the OMU and adjacent parts of the SJB-TvSB is about 3,767 ac-ft/yr (5.2 cfs, 4.65 hm^3/yr).

The segment of the TtU between the Doña Ana Mountains and Tortugas Mountain Uplifts (DAMU and TtMU) where most of the interbasin GW flow occurs is provisionally designated the North Tortugas inflow-corridor (NTic) herein (**Parts 5.2.1** and **5.2.3**; **Figs. 7-11a** and **7-15**). Hawley and Kennedy (2004, p. 75) used a Darcy-equation based calculation to estimate that "only a minor component of predevelopment flow (probably less than 850 ac-ft/yr [1.05 hm^3/yr])" discharged [from TvSB] to the Mesilla Valley through shallow gaps in the buried Doña Ana-Goat Mountain-Tortugas uplift near U.S. 70 (**Fig. 7-16**).

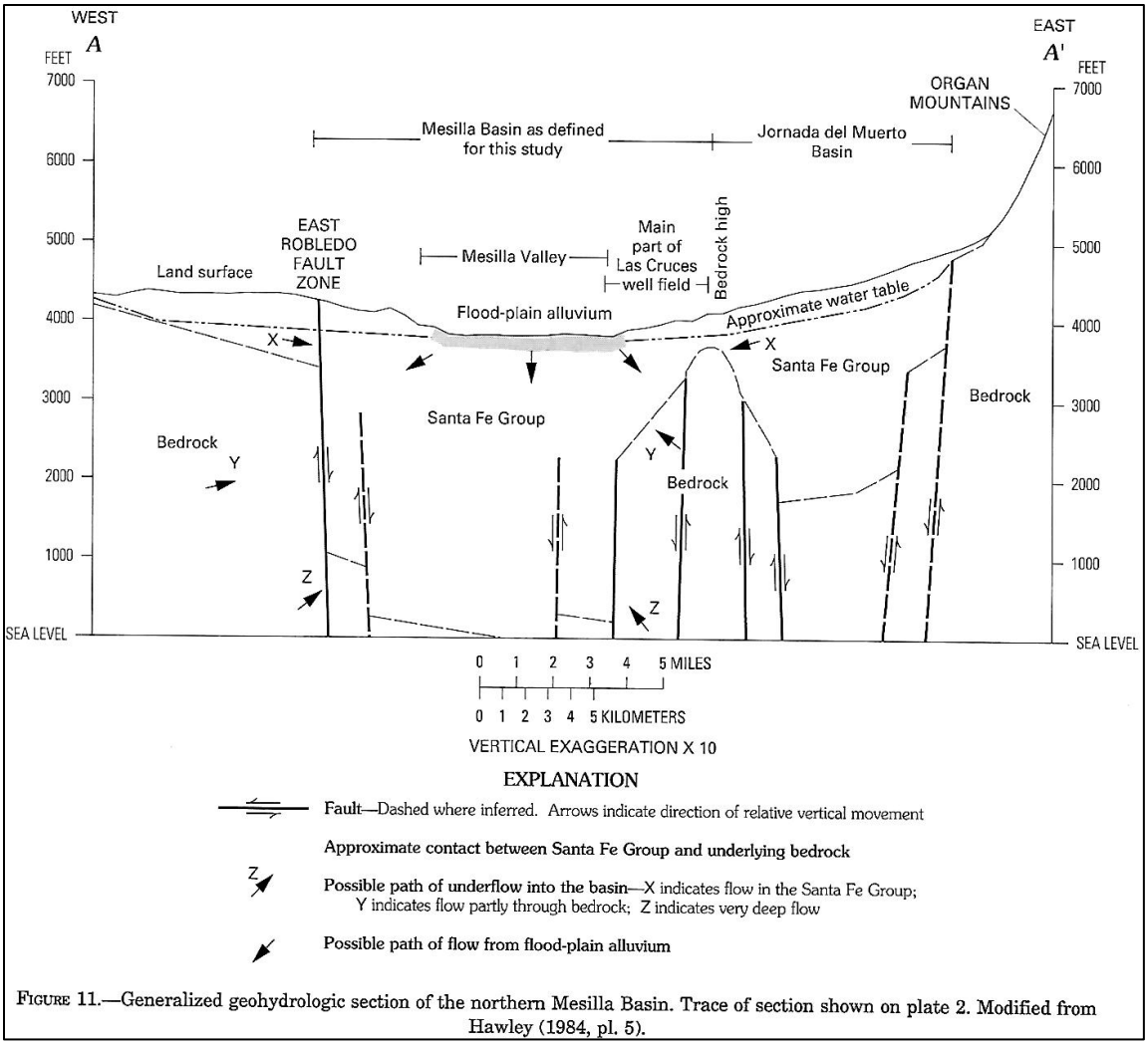

FIGURE 11.—Generalized geohydrologic section of the northern Mesilla Basin. Trace of section shown on plate 2. Modified from Hawley (1984, pl. 5).

Figure 7-16 (Frenzel and Kaehler 1992, fig. 11, modified from Hawley 1984 [pl. 5])**.** Schematic hydrogeologic section, in the approximate position of **PLATE 5e**, which extends ENE across the northern MeB and the Southern Jornada Basin (SJB) W of the Organ Mountains Uplift. The shallowly buried northern part of the Tortugas Uplift ("Jornada Horst" of Woodward and Myers 1996 [fig. 5]) separates the MeB-Mesilla Valley (MEV) from the SJB.

7.5.2. GW-Flow Relationships between the MeB and Western Hueco Bolson

The Organ-Franklin-Sierra Juárez mountain chain (OMU-FMU-CJU), which forms the Study Area's most-distinct hydrographic and hydrogeologic boundary combination, separates the Mesilla GW Basin (MeB) from the southwestern Tularosa Basin (SWTB) and western Hueco Bolson (WHB), (**Figs. 7-1** and **7-2** [**PL. 4**]; **Tbl. 7-1**). Basic structural and lithologic relationships are described in detail in **Parts 5.1.1** to **5.1.4**, and emphasis here is on interbasin or potential-interbasin GW-flow relationships. The western Hueco Bolson (WHB and SWHB), which is bordered by the Franklin Mountains and Sierra Juárez Uplifts (FMU and SJU), is the deepest structural basin of the southern RG-rift province (Knowles and Kennedy 1957; Mattick 1967; Lovejoy and Hawley 1978; Lovejoy and Seager 1978; Seager et al.

1987; Collins and Raney 2000; Hawley et al. 2009; **Figs 6-2** and **6-3** [II-II'], **Tbls. 6-1**and **6-3**; **PL. 5h**). The Bolson's western hydrogeologic boundary is formed by the active Franklin Mountains-Sierra Juárez fault zone (FMfz and SJfz, **Tbl. 6-2**; *cf.* Machette 1987, Keaton and Barnes 1995).

The east-central and southeastern MeB has direct geohydrologic/hydrogeologic connections with the western Hueco Bolson in three places (**Figs. 7-1, 7-2**, and **7-5**): (1) Fillmore Pass Corridor (FPC, **Part 5.1.2**) between the Franklin and Organ Mountains Uplifts (FMU and OMU), (2) El Paso del Norte (EPdN, **3.1.3c**), and (3) the Méndez-Vergel Inflow Corridor (MVIC), between the Sierra Juárez and Sierra Sapello Uplifts (SJU and SSU). Hydrogeologic-framework controls on a limited amount of brackish GW-flow into the MeB-El Milagro Subbasin (EMSB) through the MVIC were described in **Part 5.1.6**. The underflow source appears to be located primarily in an unnamed subbasin at southwestern edge of the Hueco Bolson that is bounded by the Sierra del Presidio and Sierra Samalayuca uplifts (**Figs. 6-22a** and **7-9**).

The 6-mi (10 km) long Fillmore Pass Corridor (FPC) connects the MeB-Mesquite Subbasin (MSB-**Part 6.3.4a**) with the northwestern Hueco Bolson (HB-NWSB) in an area adjacent to the latter's transitional boundary with the southwestern Tularosa Basin (SWTB, **Figs. 7-1** and **7-2**; *cf.* Meinzer and Hare 1916, Knowles and Kennedy 1957, Orr and R. White 1985, Orr and Myers 1986, Bedinger et al. 1989b, Orr and Risser 1992, Huff 2005, Hawley et al. 2009). During much of the late Pliocene and Early Pliocene, the FPC provided the primary conduit for both surface (ARG) and subsurface flow from the Mesilla Basin to the Hueco Bolson and southwestern Tularosa Basin (SWTB) (**Parts 3.4.1 and 5.1.2**; **Figs. 6-1** and **7-2**; *cf.* Strain 1966, Hawley et al. 1969, Seager 1981, Mack et al. 1996 and 1997, Lucas and Hawley 2002, Connell et al. 2005, Hawley et al. 2009). Once incision of the valleys and canyons of the through-going Rio Grande/Bravo was initiated, however, the FPC was transformed to a "wind-gap."

The FPC'I minimum width is about 2.5 mi (4 km), and its base is about 900 ft (275 m) below ground surface (**Fig. 6-1**, **PL. 5n**). The approximate cross-section area of saturated SFG deposits in the narrowest part of the FPC (mostly MSF2-LFA3) is about $7.5x10^6$ ft^2 ($0.7x10^6$ m^2), and an FPC aquifer unit with an average K_{hsat} of least 10 ft/day (3 m/day) would be able to transmit a significant amount of interbasin underflow (**Figs. 6-1**, **6-2** and **7-2**, and **Tbl. 7-3**; **PLS. 5h** and **5n**). During most of the Holocene Epoch differences in hydraulic head in adjacent parts of the Hueco Bolson (NWHB) and MeB-MeV have not been enough to allow a significant amount of interbasin underflow to occur in either direction (Frenzel and Kaehler 1992, C17). Orr and Risser (1992), for example, assign an underflow contribution of 260 ac-ft/yr (0.32 hm^3/yr) for the FPC in their northern Hueco Bolson GW-flow model, with most of it derived from mountain block/front recharge sources in the southernmost part of the OMU.

Paleohydrologic conditions in the southwestern Tularosa Basin (SWTB) and contiguous parts of the Hueco Bolson during the last glacial/pluvial-stage were very similar to those existing in the

northeastern Bolsón de los Muertos when it was occupied by pluvial-Lake Palomas about 29 to 12 ka (**Figs. 1-2**, **1-10**, **3-3** and **7-6**; **Parts 3.3.2** and **3.9**). During the 3,950 ft (1,204 m) high stands of pluvial-Lake Otero, which occurred as recently as 12 to 15 ka, large parts of the west-central Tularosa Basin floor were inundated, and GW levels would have been significantly higher than at present throughout much of the SWTB and NWHB (Allen 2005; Allen et al. al. 2009). The water-table altitude at the Hueco Bolson end of the Fillmore Pass Corridor during the last full-glacial/pluvial interval is conservatively estimated to have been about 3,925-ft (1196-m) amsl. At the same time, the water-table level in Mesilla Valley, which is located only 6 mi (10 km) to the west, was in the 3,725 to 3,750-ft (1,135-1,143-m) amsl altitude range (*cf.* **PL. 5h**). It is therefore reasonable to infer that at least some part of the western Hueco Bolson GW-flow system contributed a significant quantity of predominantly brackish underflow to the shallow-aquifer zone in the eastern Mesquite Subbasin (MSB) during the latest part of the Pleistocene Epoch.

7.5.3. GW-Flow Contributions from the Cedar-Corralitos Upland Basin to the Northwestern MeB

The Robledo Mountains Uplift (RMU, **Part 5.3.1a**) is a prominent horst-type structural uplift that separates the Cedar-Corralitos Upland Basin (CCUB) from the northern part of the MeB and MeV area (**PLS. 5c** and **5d**). Paleozoic marine carbonate and siliciclastic rocks form the bulk of the uplift. The Aden-Robledo Uplift (ARU, 5.3.1b) is shallowly buried southern extension of the RMUs where Paleozoic rocks are buried by a southward-thickening wedge of lower Cenozoic andesitic volcanic and volcaniclastic rocks, with the latter only being exposed in the Aden Hills Uplift (AHU, **Figs.7-1** and **7-2**, and **Tbls. 6-3** and **7-1**, **PL. 5e**). The East Robledo fault zone (ERfz), which marks the abrupt structural boundary between the RMU-ARU and the MeB-Fairacres Subbasin (FASB), is one of the most active fault systems in the southern RG-rift province (**Fig. 6-1** and **Tbl. 6-2**; Seager et al. 2008; Mack et al. 2018b). For example, fault displacement of lower-Pleistocene beds is this ERfz segment locally exceeds 300 ft (90 m) (**PL. 1C** [I-I′], and **PL. 5c** to **5e**).

The Corralitos Ranch Subbasin (CRSB) of the CCUB is bounded on the west by the Ward Tank fault zone (WTfz) and on the east by the West Robledo fault zone (WRfz). Both are major RG-rift extensional-tectonic features that have been active for much of Late Cenozoic time (**Tbl. 6-2**). Boundary uplifts to the west and east comprise, respectively, the Uvas-Goodsight Uplift (UGU) and the Robledo Mountains and Aden-Robledo Uplifts (RMU and ARU). In marked contrast to aquifer systems in other parts of the Study Area, the primary aquifer comprises silicic volcanic and interlayered sedimentary rocks of early- to mid-Cenozoic age instead of SFG basin fill (*cf.* unit Tmrs, **Tbl. 6-3**; Clemons 1976a).

CCUB-CRSB has topographic closure, however, surface- and subsurface-flow divide positions have heretofore not been well defined (**Parts 5.4.1** and **5.4.2**; **Fig. 7-2**, **Tbl. '-1**; **PLS. 1C [**I-I'**]**, **5b** to **5e**). The low-relief Sleeping Lady and Rough-and-Ready Hills, which form the core of the southern Cedar Hills (silicic-volcanic) vent zone, provide the primary bedrock topographic and structural control for the

flow-divide positions. Small amounts of surface-runoff discharges to a north-south aligned group of playas at the east-central edge of the subbasin (**Fig. 7-2, Tbl. 7-1**). Groundwater-flow is partitioned into three sectors of limited extent: (1) northward into the Cedar Hills Subbasin (CHSB), (2) southwestward toward the northeastern Mimbres GW Basin (MbB) (**Part 5.4.2b**), and (3) southeastward across the northern part of the Aden-Robledo Uplift to the MeB-Fairacres Subbasin (**Figs. 7-12a**, **7-16** and **7-17**; Frenzel and Kaehler fig. 11; Nickerson and Myers 1993, fig. 9; Teeple 2017, fig. 47).

Due to the presence of a small component of interbasin underflow linkage with the MeB, the CCUB-CRSB is in the *closed-drained* basin category of Hibbs and Darling (2005, **Fig. 4-1**). Its small watershed size and the absence of high-relief terrain in a Chihuahuan Desert landscape, however, prevents the CRSB being a substantial underflow-recharge contributor to GW-flow and hydrochemical systems in any of its neighboring GW basins from either a paleo-hydrologic or a present geohydrologic perspective (e.g., Myers and Orr 1985, p. 20-21). Frenzel and Kaehler (1992, fig. 18) estimate that the CRSB's underflow contribution to the MeB GW-flow system is less than 145 ac-ft/yr (0.2 cfs, ~0.18 hm^3/yr). The northern section of the Aden-Robledo Uplift (ARU) forms the primary site of interbasin underflow between the CCUB-Corralitos Ranch and the MeB-Fairacres Subbasins (CRSB and FASB), and it is provisionally named the South Robledo Inflow Corridor (SRic) herein.

The following observations by Frenzel and Kaehler (1992, p. C18) clearly support current interpretations of GW-flow conditions in the ARU-SRic and adjacent parts of the western MeB-FASB east of the East Robledo fault zone (ERfz; **Figs. 7-2** and **7-16**):

> The water-table gradient beneath the West Mesa averages about 4.5 feet per mile: approximately the same as in the Mesilla Valley. Near the edges of the Mesilla Basin, water flows into the basin from the surrounding highlands, and the water-table gradient is steeper in those places due to thinner aquifers and possibly [definitely] lower permeability. Near the East Robledo fault, where the transmissivity of the basin fill changes greatly, it might be expected that the water-table contours would have a kink in them as shown by the dashed and queried 3,840-, 3,860-, and 3,880-foot contours on Plate 1 [**Fig. 7-17**].

This well-documented example of the proper interpretation of Darcy Law hydraulic relationships is also supported by the winter of 1985 potentiometric-surface map of Nickerson and Myers (1993, Fig. 9; **Fig. 7-14**, *cf.* Teeple 2017, p. 77).

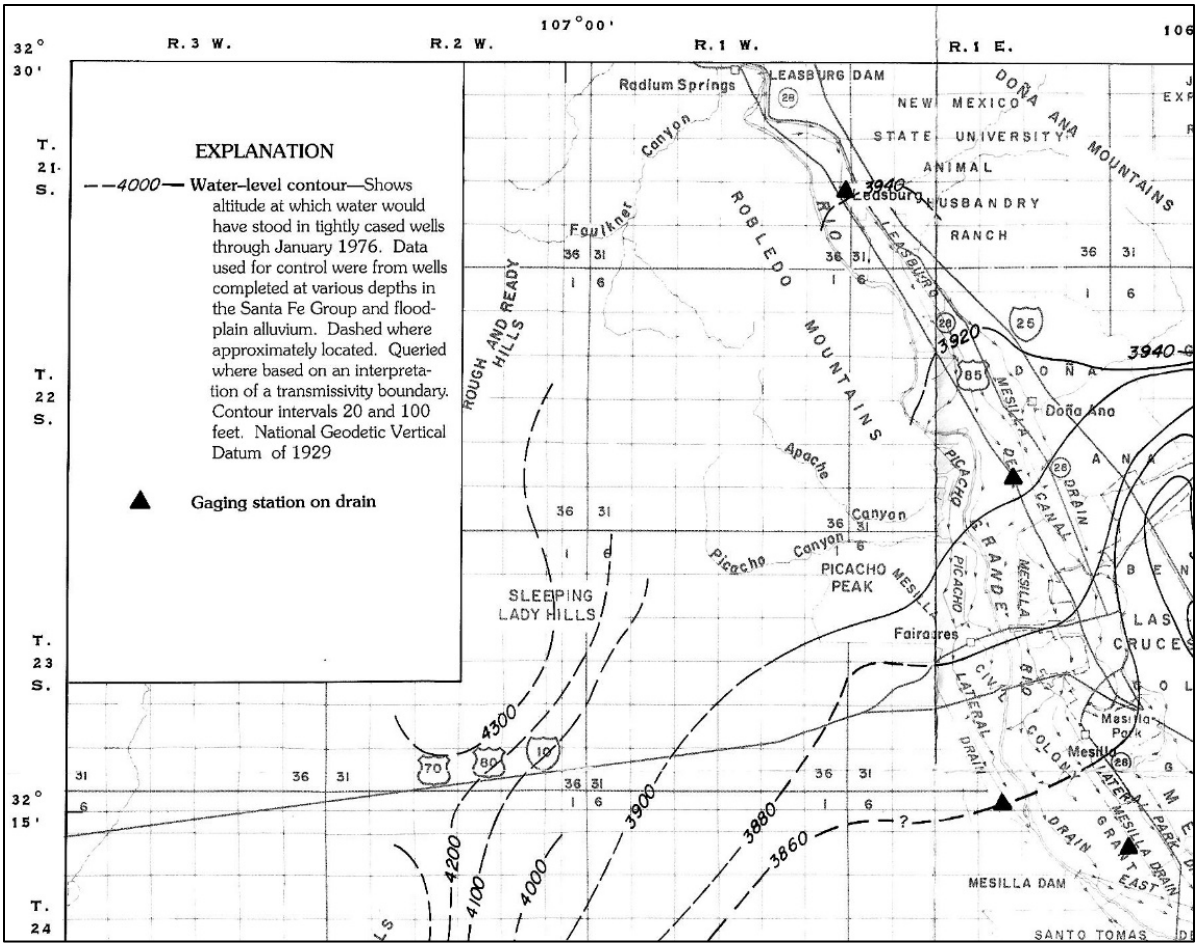

Figure 7-17 (upper-left part of **PL. 9C**)**.** Map showing approximate water-level contours [alt. in ft amsl] in the NW part of the MeB W of Las Cruces, NM (modification of Wilson et al. 1981 [PL. 9] by Frenzel and Kaehler 1992 [PL. 1]). This compilation of water-level data (through Jan. 1976) is the first potentiometric-surface map that accurately portrays interbasin GW flow in the upper SFG aquifer system in the East and West Robledo fault-zone area between the Robledo Mountains and Aden Hills Uplifts, and the Cedar-Corralitos Upland Basin and the MeB-Fairacres Subbasin (**Parts 5.4.2b** and **6.3.3b**; **Figs. 6-1**, **7-2**, **7-11, 7-12a**, **7-14** and **7-16**; **PL. 5d** [Hydrogeologic Section D-D']).

7.5.4. GW-Flow Contributions to the MeB from Western Basin-Boundary Areas

The only prominent highlands on the MeB's western border south of the Aden-Robledo Uplift comprise the East Potrillo Uplift (EPU-PRS, **5.4.1**) and the basaltic cinder cones of the West Potrillo Volcanic Field (**Part 5.6; Figs. 6-1** to **6-3** [II-II′], **Tbls. 6-1 and 6-2**; **PLS. 5i** to **5k**). As noted in **Part 5.6**, the basaltic rocks of West Potrillo Mountains, rather than being part of a RG-rift structural uplift, form a relatively thin cover on underlying SFG basin fill, and Middle- to Lower-Tertiary and Pre-Cenozoic bedrock units. Mid- to Lower-Tertiary volcanic and sedimentary rocks are exposed or shallowly buried in the West Aden Uplift (WAU) and the MbB-West Potrillo Bench (WPBn) at the west-central edge of the Study Area (**5.6.1**). There, and to the north, the drainage-divide position (surface and subsurface) between

the Mesilla and Mimbres hydrographic basins is essentially the same due to bedrock control on surface topography (**Fig. 6-2**). A distinct flow divide of this type also follows the crests of Mount Riley-Cox and the East Potrillo Mountains along the MeB's southwestern border (**Figs 7-5**; **PLS. 5j** and **5k**).

Determining both surface-watershed and GW-flow divide locations, however, remains problematic in the Malpais Basin (**Part 5.7.2**) and the Camel Mountain Uplift south of 32° N latitude (**Fig. 7-5**). Major contributing factors in the MpB include (1) poor definition of surface-drainage features, (2) absence of deep-well control and resulting lack of hydrostratigraphic information, and (3) depths-to-water commonly exceeding 500 ft (150 m, *cf.* King et al. 1971). The East Potrillo fault zone (EPfz, **Tbl. 6-3**) forms a distinct structural and hydrogeologic boundary between the Afton and Kilbourne-Noria Subbasins of the MeB (AfSB and KNSB) and adjacent parts of the EPU and the MeB-East Aden Bench (EABn) (**Parts 6.3.3c** to **6.3.3e**).

As in the Corralitos Ranch Subbasin (**Part 5.4.2b, 7.6.3**), the East Potrillo Uplift (EPU) at the MeB's western border has neither the altitude nor the areal extent needed to produce a substantial amount of mountain-front/block recharge to the MeB's aquifer system (**Figs. 7-2** and **7-9** [**PL. 5j**]). Frenzel and Kaehler (1992, Fig. 18), for example, limit the "mountain-front" recharge component from the EPU and adjacent parts of the West Potrillo Mountains (volcanic field) to less than 2,175 ac-ft/yr (3 cfs, 2.7 hm^3/yr). Primary sources of higher quality recharge that enters the MeB-KNSB via the Brock Tank inflow corridor (BTic) comprise (1) highlands underlain by Eocene (?) plutonic rocks of the Mount Riley-Cox intrusive center (Tmi-**Tbl. 6-3**), and (2) undifferentiated SFG basin fill and bedrock units that are buried by basalt flows of the West Potrillo Volcanic Field (**5.5.1** and **5.6**; **Figs 6-2** and **6-3** [II-II′]; **Tbl. 6-2**; **PL. 5k**; Seager 1989 and 1995; Hoffer 1976 and 2001b).

The Lower Cretaceous/Permian (K/P) bedrock terrane that is well exposed in the East Potrillo Mountains comprises marine-carbonate and siliciclastic sedimentary rocks with a high degree of structural deformation (Seager and Mack 1994; **PL. 5j**). Four deep exploration wells, three geothermal drilled for Hunt Energy Corp in 1980 and one oil and gas, provide relatively detailed stratigraphic and structural information on the East Potrillo Mountains fault block and contiguous parts of the Kilbourne-Noria Subbasin (KNSB; **TBL. 1**, nos. 257, 269, 297 and 298; **Parts 5.5 and 6.3.3e**). Subsurface conditions in the 7,346-ft (2,239-m) Pure Oil Co. No. 1-H Federal test well are described in Seager and Mack 1994, p. 24 (**TBL. 1**, no. 269). Unpublished logs (geologic, geophysical and temperature) of the geothermal test borings (nos. 257, 297 and 298), all of which had significant lost-circulation problems, document the existence of (1) a highly fractured, karstic bedrock-aquifer system, and (2) a potentially significant source of brackish-water recharge at the western edge of the KNSB (Snyder 1986).

The role played by the Cretaceous/Permian (K/P) bedrock terrane in terms of both brackish GW and geothermal-energy availability remains to be evaluated. The primary reservoir for this low-

temperature geothermal system and potential brackish-water resource includes a Lower Cretaceous and Middle Permian bedrock section that is at least 2,000 ft (610 m) thick in its upper part (**Parts 5.5.1** and **6.3.3e**; Fig. 7-9 [**PLS 5j** and **5k**]; *cf.* Thompson 1982, Witcher 1988, Seager and Mack 1994, Witcher 1995). However, unforeseen impacts of National Monument-status, Border Wall construction, and other yet-to-be resolved binational border security issues preclude any type of detailed subsurface-investigation activity that would be required for proper resource assessment (e.g., seismic and electro-magnetic surveys, and deep drilling; *cf.* **APNDX. H1**; **Part 1.8.3**; **Figs. 6-2** and **6-3**, **Tbl. 6-3**; Banerjee et al. 2018, Attanasio and Galvan 2019, Kocherga 2019b, Bixby and Smith 2020).

7.5.5. Indirect GW-Flow Contributions from the Malpais Basin to the Southern MeB

The Border Tank Corridor (BTC, **Part 5.6.3**) is located between the East Potrillo Uplift (EPU), the eastern Malpais Basin (MpB, **5.6.2**), and the northern El Aguaje Uplift **(**EAU, **5.6.4**). Its importance in this study relates to the fact that the BTC and adjacent basin and uplift areas, while not contiguous to the MeB, are part of a large subsurface-watershed that perennially contributes a small, but still significant amount of mostly brackish water to the Transboundary aquifer system of the northern El Parabién GW Basin (EPB) and southern MeB (**Figs. 7-2** and **7-7**; **Tbl. 7-1**; **PLS. 5k** and **5l**; *cf.* **Parts 6.3** and **6.4**).

The BTC's general position in the United States part of the Study Area was initially recognized by Conover (1954, **Fig. 7-11**), and its existence was verified by King and others (1971, **Fig. 7-12b**). Until this study, however, absence of an integrated model of the Transboundary area's hydrogeologic framework precluded even general characterization of its GW-flow regime. Detailed surface mapping and limited well control indicate that conglomeratic sandstone facies (LFA 7) of undivided SFG HSUs MSF1/LSF form the primary aquifer material (**Fig. 7-9** [**PL. 5k**]; Seager 1995, Sheet 3, FF′; and Seager 1989, Fig. 4; **TBL. 1**, nos. 303, 304, 311, 361-363, and 366). The basalt flows of the West Potrillo Volcanic Field that cover large parts of the MpB-Guzmans Lookout Subbasin (GLSB) are entirely in the vadose zone, are not significant aquifer units except at large hydromagmatic vent centers like the Potrillo and Malpais Maars (Hoffer 2001a and b).

As indicated by the underflow trends on the provisional potentiometric-surface map, the primary sources of recharge to BTC GW-flow regime include the southwestern slopes of the East Potrillo Uplift (EPU), and parts of the MpB-Guzmans Lookout Subbasin (**Figs. 6-1, 7-2** and **7-5**). The only significant source of mountain-block/front recharge is located on the southwestern slopes of the EPU's Potrillo-Mt. Riley Sector (PRS) (**Fig. 7-3** and **Tbl. 7-1**; **Fig. 7-10** [**PL. 5j**], Seager and Mack 1994, *cf.* **Part 5.7.3**). Cretaceous and Permian marine sedimentary rocks are exposed or shallowly buried in a large part of the EPU (**Fig. 6-2** and **Tbl. 6-3**; **Fig. 7-10** [**PLS. 5j** and **5k**]; **Part 7.5.5**). As described in more detail in **Part 7.6**, the regional flow-system's primary recharge sources to the southwest are associated with millennial-

scale drainage of parts of the SFG aquifer system in Mexico's "Zona Hidrogeológica de Conejos Médanos" that last received significant recharge during high stands of pluvial-Lake Palomas (**Fig. 7-6**).

7.6. HYDROGEOLOGIC CONTROLS ON INTERBASIN GW-FLOW IN THE INTERNATIONAL BOUNDARY ZONE

7.6.1. Background on Early-Stage Trans-International Boundary Aquifer Investigations

The scope of the present study precluded any detailed analysis of hydrogeologic and hydrochemical information in areas located south of the International Boundary that were acquired after 2000 (e.g., Hawley et al. 2000; *cf.* **Parts 1.8** and **7.6**; **Tbl. 1-3**; **Figs. 6-22, 7-2** and **7-5**). Two investigations that did involve limited binational research efforts were initiated in the early 1990s following enactment of the 1984-La Paz Agreement's "Integrated Environmental Plan for the Mexican-U.S. Border Area—Border XXI Program (**APNDX. H4.4.1**)."

The first study included a comprehensive "Transboundary aquifers and binational ground-water data base" exchange (Hibbs et al. 1997; **Fig. 7-18** [**PL. 10**]), but emphasis was on the Hueco Bolson, with work in the Mesilla Basin being limited to areas in the United States. Barry Hibbs, then with the Texas Water Development Board (TWDB), and Bobby Creel of the NM WRRI served as lead principal investigators. The U.S. Environmental Protection Agency-Region VI was the primary research-funding source (Interagency Contracts X-996343-01-0, X-996350-01-0, and X-996350-01-3; *cf.* Hibbs and 30 others 1998). While the report by Hibbs and others (1997) contains very little subsurface information of hydrogeologic value for binational parts of the Mesilla Basin region, it does include a map and CD-ROM cover-insert with an invaluable compilation of general information on regional groundwater quality in Stiff-diagram format (**Fig. 7-18a** and **7-18b** [**PL. 10** extract, TWDB 1997]).

Four color-coded total dissolved solid (TDS)-range categories are shown on **Figure 7-18**: blue—0 to 1,000 mg/L, green—1,000 to 3,000 mg/L, yellow—3,000 to 5,000 mg/L, and red—>5,000 mg/L. The TWDB Stiff diagrams for water sampled from the 40 wells in Chihuahua utilized a 1982 GW-chemistry database originally developed by the Secretaria de Recursos Hidráulicos (SRH, INEGI 1983b**;** *cf.* **PL. 10**, **TBL. 1**). Most samples were collected from domestic and livestock wells completed in SFG basin fill in the area west and south of Sierra Juárez. Because no local upland recharge sites exist, it is here inferred that low-chloride (<1,000 mg/L TDS) water from the seven sampled wells in the central part of **Figure 7-18a** had a pluvial-Lake Palomas GW-discharge source (*cf.* Rpt. **Part 7.7.2**).

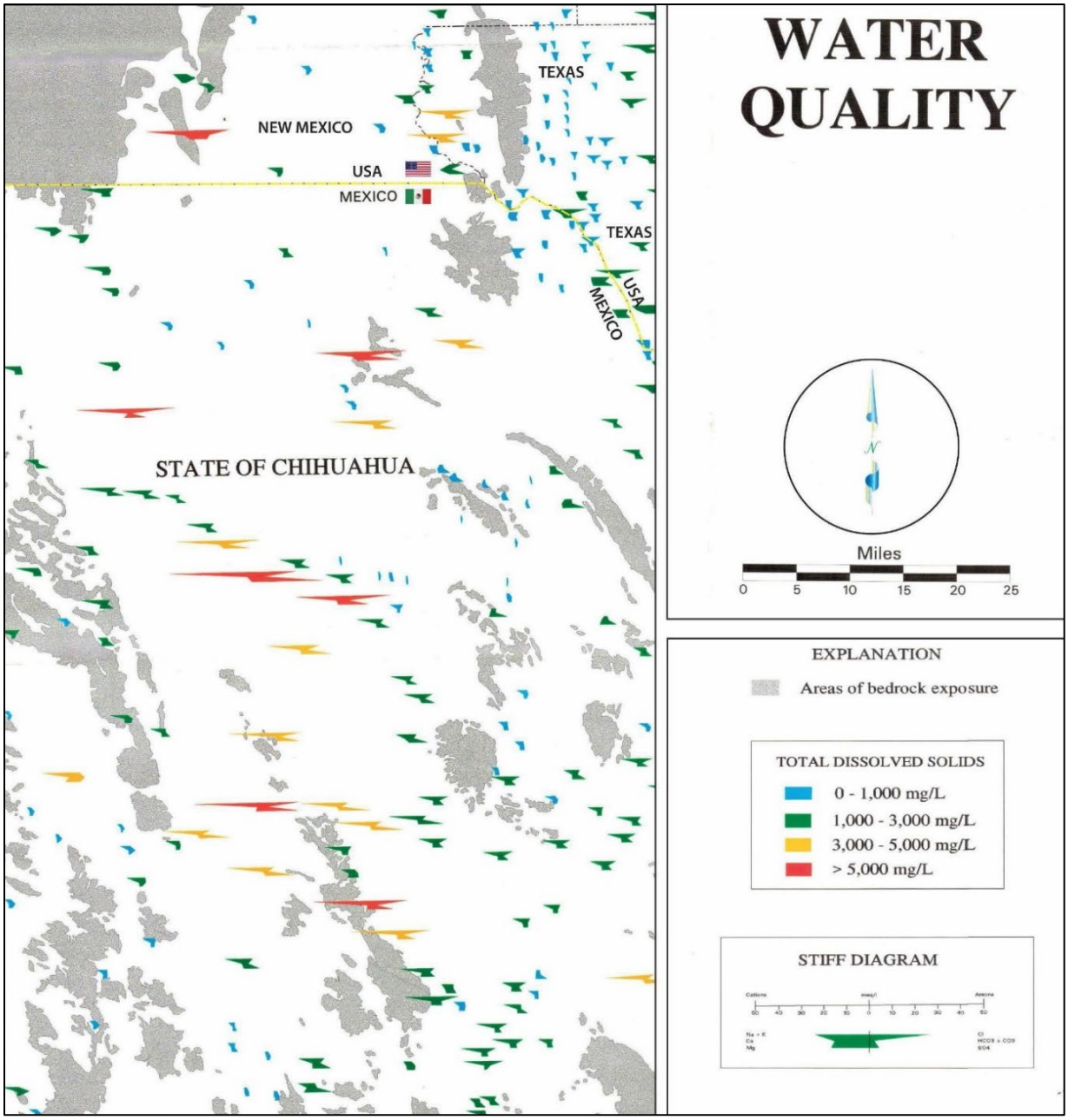

Figure 7-18. Facsimile copy of the Texas Water Development Board (TWDB) compilation of "Water Quality" data for the region west of El Paso/Ciudad Juárez in the west-central part of **PLATE 10** (Hibbs et al. 1997). Stiff diagram and TDS-class explanations are in the lower-right box**.** The high sodium-chloride-sulfate symbol in the upper center is for water sampled from the Los Argüeles well in the Sierra Sapello Uplift (6,020 mg/L TDS—**TBL. 1**, no. 283; INEGI 1883b, no. 29). Symbols for high sodium chloride content in the left center and upper left are for water sampled, respectively, in the Zona Hidrogeológica de Conejos Médanos (ZHGCM), and adjacent to the East Potrillo fault zone (EPfz). The latter sample was from well no. 256 (**TBL. 1**), with a reported TDS content of 4,770 mg/L (Anderholm 1992, p. C65).

The second, more-detailed NM WRRI report on the "Trans-International Boundary Aquifers in Southwestern New Mexico" covered the region between the Mesilla Basin and southeastern Arizona (Hawley et al. 2000; *cf.* Hibbs et al. 1999 and 2000, Kennedy et al. 2000; **APNDX. H4.4.2**). Piper-diagrams and ion-content maps for aquifer systems of the Mimbres Basin are included to illustrate general hydrochemical conditions in the southwestern-most part of the Study Area as reported in Hawley and others (2000, Chapt. 4, Figs. 4-5 to 4-9).

Figure 7-19 is a facsimile copy of their "Chloride in Wells" map **(**Fig. 4-8) that is based on analyses of water samples from wells in an area that extends westward into the lower Rio Casas Grandes basin and Laguna Guzman (**Fig. 7-5**; *cf.* INEGI 1983b, Hibbs et al. 1999). The map area designated "Bolson de los Muertos" includes parts of the northern Zona Hidrogeológica de Conejos Médanos (ZHGCM), the Malpais Basin, El Aguaje Uplift, and El Parabién Basin (**Figs. 1-9** and **1-12**). A Lake Palomas high-stand source for most of the fresh water stored in HSU-USF2/MSF2 aquifer zones of the northern El Parabién Basin—southern Mesilla Basin area is indicated by (1) the occurrence of low chloride values (14.2 mg/L Cl) and 596 mg/L TDS water sampled in well no. 382 [**TBL. 1**]), and (2) the general presence of ≤1,000 mg/L TDS water sampled in 14 other wells completed in the same HSUs (*cf.* **Figs. 2-5** and **7-18a**). **TBL. 1**, nos. 362, 364, 365, 367, 368, 373, 377, 379, 380, 382, 385, 387, 389, 393 and 394; Gutiérrez-Ojeda 2001 [p. 26]; **Part 6.4**).

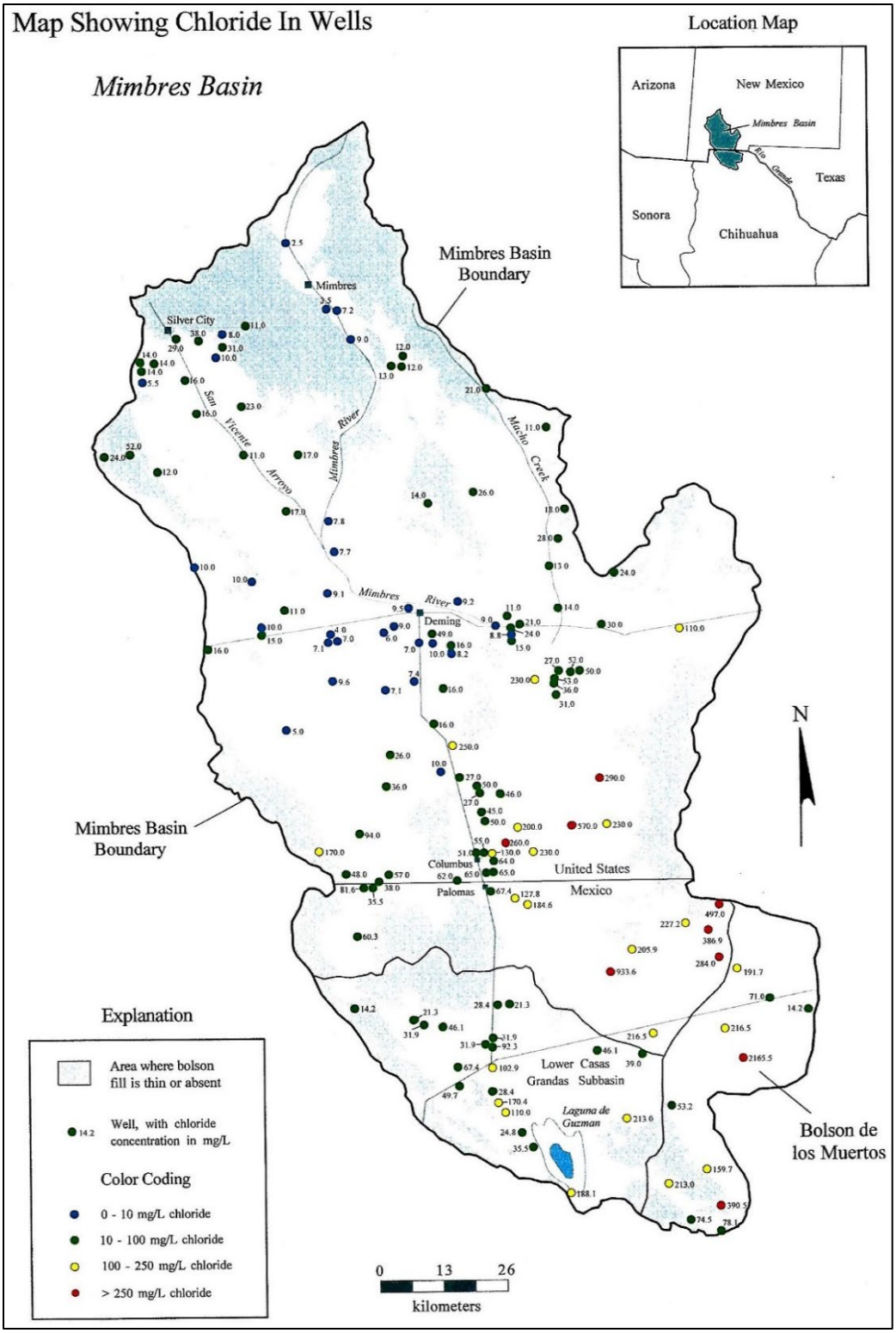

Figure 7-19. (Hawley et al. 2000, Fig. 4-8) Chloride concentrations (mg/L) of water from selected wells in the Mimbres Basin and contiguous parts of the Lower [Rio] Casas Grandes Subbasin and the Bolsón de los Muertos [El Aguaje Uplift, and Malpais and El Parabién Basins].

7.6.2. Provisional Assessment of Pluvial-Lake Palomas GW-Outflow Contributions to the Transboundary Aquifer System of the Southern Mesilla Basin Area

Because of the recurring presence of large pluvial lakes in the endorheic basins of northwestern Chihuahua during the mid- to late Quaternary Period, it is the only part of the Mesilla Basin region outside the central MeB with any potential for producing significant amounts of fresh to moderately brackish GW recharge to the aquifer systems of the IBZ (**Figs. 7-5** and **7-7; PLS. 5k**, **5l** and **5o**). Only during the past 0.4 Ma, however, has the altitude of the Lower MeV-EPdN reach been low enough (≤3,800 ft [1,160 m]) to produce the hydraulic gradient needed (≥0.0005) to permit significant amounts of underflow discharge from pluvial-lake high stands to reach the shallow aquifer system at the southern part of the MeV (**Figs. 7-2** and **7-5**; **Part 6.3.5d**; **Figs 7-9** and **7-10** [**PLS. 5o** and **5k**]).

Parts of the Zona Hidrogeológica de Conejos Médanos (ZHGCM) and adjacent lowlands that were inundated during the latest Pleistocene high stands of pluvial-Lake Palomas are shown with pale-blue shading on **Figure 7-5**. The lake's high-stand surface area is here estimated to have been at least 7,500 km^2 (2,900 mi^2), or about one-third the areal extent of Lake Erie, with the latter being much deeper. Both the hydrographic basin of Lake Palomas and that of its ephemeral lake-plain remnants (barreals-playas-lagunas-salinas) occupy a hydrographic basin with an area of at least 27,000 mi^2 (65,000 km^2). By way of comparison, the area of the Rio Grande drainage basin above Leasburg Dam (alt. 3,960 ft/1,207 m) is about 28,000 mi^2 (72,520 km^2) (USGS 1961, 2017; *cf.* **Figs. 1-3** and **1-5**; **Parts 3.2.3** and **3.3.2**).

A provisional but still conservative estimate of GW-outflow contribution to Transboundary Aquifer Systems of the IBZ during Lake Palomas high stands is about 8.76 x10^6 m^3 (7,100 ac-ft), with high-stand intervals lasting possibly as long as 10,000 yrs. The following assumptions were used in this Darcy-equation (Q=KIA) based calculation:

1. A saturated thickness of about 100 m (300 ft) in sand-dominant deposits of the HSU-USF2 ARG fluvial-deltaic facies in contiguous parts of the El Aguaje Uplift (EAU) and El Parabién GW Basin (EPB) during 1,210-m amsl (3,970-ft) high stands (*cf.* **Figs. 7-2**, **7-5**, and **7-10 [PL. 5s**]).
2. A 4,000,000 m^2 aquifer cross-section area (A) for a 40-km contact shoreline (*cf.* **Figs. 7-5** and **7-10**).
3. An average saturated hydraulic conductivity (K_{hsat}) of 6 m/day (20 ft/day) for sediments of primary LFA 3 composition (**Fig. 7-3**, **Tbls. 7-1** and **7-2**).
4. A 0.001 hydraulic gradient (I) for the GW-flow system between the eastern edge of Lake Palomas and the southern MeB, or about the same as present (**Figs. 7-2** and **7-5**).

The intermittent lakes in the ZHGCM-El Barreal area have not reached high-enough levels during the past 8,000 yrs (~1,195 m [3,920 ft]) to contribute significant amounts of (fresh to brackish) GW recharge to the Transboundary Aquifer System (*cf.* Castiglia and Fawcett 2006, Fig. 1B). The GW-flow divide (alt. ~1,210 m/3,970 ft) located between the El Aguaje and La Laguna well sites (**Fig. 7-5**) forms

the present no-flow boundary between NE-directed flow toward the lower Mesilla Valley and EPdN, and SW-directed flow toward El Barreal in the northeastern BdlM (**Figs. 7-5** and **7-10** [Sect. S-S′, **PL. 5s**]). As shown on **Figures 7-2** and **7-10**, the respective altitudes of the predevelopment water-table were about 1,194 m (3,918 ft) at El Aguaje and 1,192 m (3,910 ft) at La Laguna **(TBL. 1**, nos. 380 and 384).

By way of comparison, annual GW flow in SFG (HSU-USF2/MSF2) basin fill beneath a section of the International Boundary between the South Mid-Basin High (SMBH) and the lower end of the Mesilla Valley is conservatively estimated to have been about 2.19 x 10^6 m^3 (1,774 ac-ft) prior to JMASCJ Well Field operation (2010). The following assumptions were used in a provisional calculation of the annual Transboundary contribution of fresh to moderately brackish groundwater to the shallow aquifer system of the Sunland Park Outflow Corridor (SPoc):

1. A saturated thickness of about 100 m (300 ft) of LFA 3-dominant, HSU-USF2/MSF2 deposits that are primarily composed of ARG fluvial-deltaic facies (*cf.* **Fig. 7-7**).
2. A 1,000,000 m^2 (10.76 x 10^6 ft^2) aquifer cross-section area (A) that is based on a minimum cross-section width of 10 km (6-mi) (*cf.* **Figs. F7-2**, **7-5,** and **7-10 [PLS. 5k and 5l**]).
3. Hydraulic conductivities for sediments of primary LFA 3 composition are in the 3 to 10 m/day (10 to 33-ft/d) range, with an estimated average K_{hsat} of 6 m/day (20 ft/d) (**Fig. 7-3**, **Tbls. 7-1** and **7-2**).
4. A 0.001 hydraulic gradient (I) for the GW-flow system in the binational part of the MeB (**Fig. 7-2**).

7.7. CONCLUDING REMARKS ON THE TRANSBOUNDARY GW-FLOW SYSTEM

The interpretations presented herein on the age and chemical composition in the transboundary GW-system at the southern end of the Study Area, have now been confirmed by an "Investigation of the origin of Hueco Bolson and Mesilla Basin aquifers (US and Mexico) with isotopic data analysis" by Ana C. García-Vásquez and others (2022). With regards to tritium, an unstable isotope of hydrogen (^3H or T), they make the following observation (p. 8):

> This [non-significant tritium content] is an important finding because it indicates that the water present in this zone is not of recent origin, which demonstrates that there is no recharge in this zone. Furthermore, this study does not report any significant tritium concentrations in [the southern MeB and northern EPB part of] the Conejos Médanos Aquifer.

Stable isotopes for oxygen are ^{16}O, ^{17}O, ^{18}O, and for hydrogen are protium (^1H) and deuterium (^2H, D). When these isotopes are combined to form a water molecule, they also provide an isotopic composition that translates into a powerful hydrology tracer. A pair of isotopes commonly used in hydrology is the $\delta^{18}O$ combination, which is compared using the global meteoric water line (GMWL [*cf.* Craig 1961a]) to show the percentage of isotope present in the sample. With regards to $\delta^{18}O$, García-Vásquez and others (2022) observe that (p. 12):

In conclusion, the samples collected and analyzed by this study complete the description of the Hueco Bolson and the Mesilla/Conejos-Médanos Basin at the US-Mexico transboundary area. According to previous study results shown for Group 2, a stable isotope $\delta^{18}O$ concentration falls below the GMWL in the evaporated zone, which indicates that these are old waters that have undergone evaporation, horizontal infiltration, or dissolution processes. Moreover, groundwater values indicate that groundwater recharge sources include precipitation, bedrock fissure water, or both. Furthermore, results are consistent with findings by Eastoe et al. (2007), Teeple (2017), Hawley and Kottlowski (1969), Witcher et al. (2004), and . . . ., whose findings indicate that the groundwater is not recent and that it was recharged thousands of years ago when the climate was more humid, which could be the cause for the same isotopic content in the Hueco Bolson and Conejos-Médanos/Mesilla Basin aquifers near the Juárez Mountains.

In the description of their Study Area, García-Vásquez and others (2022) also note that (p. 4):

In regard to groundwater quality in the transboundary Mesilla/Conejos-Médanos Basin aquifer, Hawley and Swanson (2022. . .) [state] that the ongoing research has demonstrated that very large quantities of fresh to slightly saline water are stored in the basin-fill aquifer system, where most groundwater in storage is at least 11ka and was recharged during the last glacial/pluvial stage of the Late Pleistocene Epoch (~29 to 11 ka).

CHAPTER 8.
PROGRESS IN HYDROGEOLOGIC-FRAMEWORK CHARACTERIZATION, AND OPTIONS FOR LONG-TERM GROUNDWATER-RESOURCE DEVELOPMENT IN THE MESILLA BASIN REGION

8.1. OVERVIEW

Recent progress in hydrogeologic-framework characterization of the binational Mesilla Basin region (MBR) is summarized in this chapter of the Report (Fig. 7-1). Investigations of the "Hydrogeology of the Rio Grande Valley and Adjacent Intermontane Areas of Southern New Mexico" were initiated in 1965 as part of the new Water Resources Research Institute program at NMSU. According to W.E. King and others (1969, p. 5):

> In 1964, the Water Resources Research Act was passed by the United States Congress; and the Water Resources Research Institute of New Mexico, under the direction of H. R. Stucky, was established soon thereafter. The present investigation [in the MBR] was among the first to be funded by the institute. The field and laboratory work was begun in February 1965 and terminated in August 1968.
>
> The principal investigator, W. E. King, professor of geology at New Mexico State University, spent one quarter of his time through each academic year and three full months each summer on the investigation. He was responsible for supervision of the investigation and is accountable for many of the conclusions. Andrew M. Taylor served as a graduate assistant on the project from its inception through August 1967 and did much of the well logging and surface geology. Richard P. Wilson spent one year as a student assistant and is largely responsible for the drafting as well as much of the thought expressed in the water-table contour map (Pl. 1).
>
> John W. Hawley, areal geologist with the Soil Conservation Service, of the U.S. Department of Agriculture, suggested the investigation and cooperated in the study throughout (*cf.* King et al. 1971, p. 9-24); [**APNDX. C8a**]).

Report emphasis is on the challenges and opportunities for long-term groundwater (GW)-resource conservation in the Mesilla GW Basin (MeB) area of the MBR, which includes the Mesilla Valley (MeV) of the Rio Grande (RG). **Figure 8-1** is an index map of the southwestern New Mexico border region, with the NM WRRI Study Area (**Fig. 8-2**) in the beige rectangle. Major political boundaries and selected population centers are shown, respectively, with black dashed lines and small squares. The small inset map in the upper-left corner shows the location of the RG-rift tectonic province. Major intermontane basins in the southern part of RG rift are outlined in black, and the blue line shows the general position of the Rio Grande/Bravo channel. With the exception of the Malpais Basin (Seager 1989, 1995) and El Parabién Basin (Jiménez and Keller 2000), names and general outlines of RG-rift basins are from Hawley (1978, Sheet 2), and Seager and Morgan (1979, Fig. 1). Chihuahua's "Zona Hidrogeológica de Conejos Médanos (ZHGCM)," is shown with light-gray shading (INEGI 2012). The "Acuifero Conejos Médanos (ACM)" is a federal GW-resource management unit in Mexico occupies most of the northern ZHGCM (Fig. 7-4). It merges northeastward with the southern end of the Mesilla (GW) Basin.

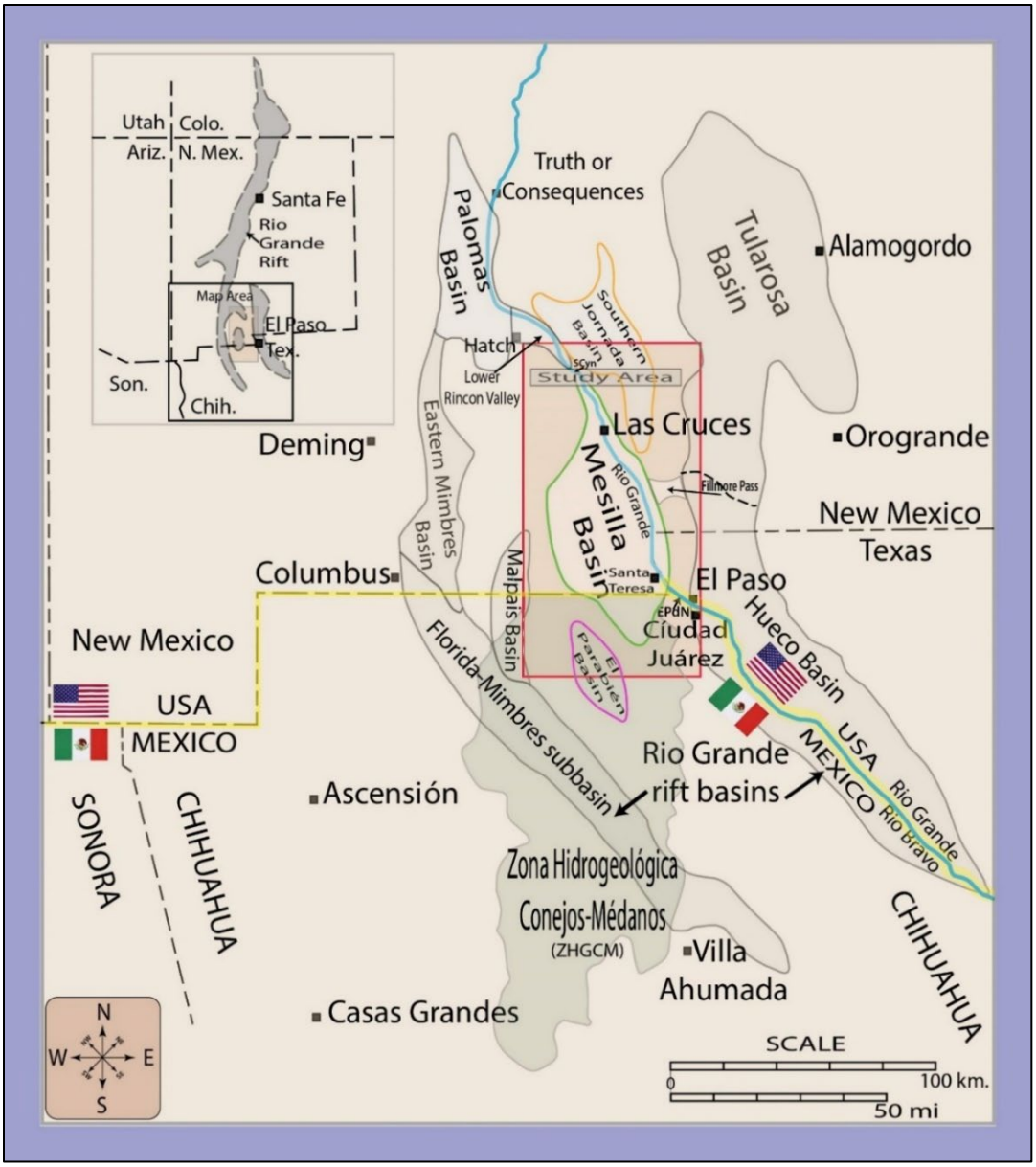

Figure 8-1. Index map for the US-Mexico borderlands region that covers parts of southern New Mexico, western Texas, northern Chihuahua, and northeastern Sonora. Major political boundaries and selected population centers are shown, respectively, with black dashed lines and small squares. The blue line shows the general position of the Rio Grande/Bravo channel; and the NM WRRI Study Area (**Fig. 1-3**) is outlined in magenta. The small inset map in the upper-left corner shows the location of the Rio Grande rift (RG-rift) tectonic province. Outlines of major structural basins in the southern RG-rift province are based on Seager and Morgan (1979, Fig. 1); and names and outlines of the El Parabién Basin, Malpais Basin, and Florida-Mimbres subbasin are from Jiménez and Keller (2000), Seager (1989), and Averill and Miller (2013), respectively. The southern Mesilla GW Basin extends into Chihuahua's "Zona Hidrogeológica de Conejos Médanos (ZHGCM)," which is shown with light-gray shading (**Fig. 7-3**; *cf.* **APNDX. H6.4**).

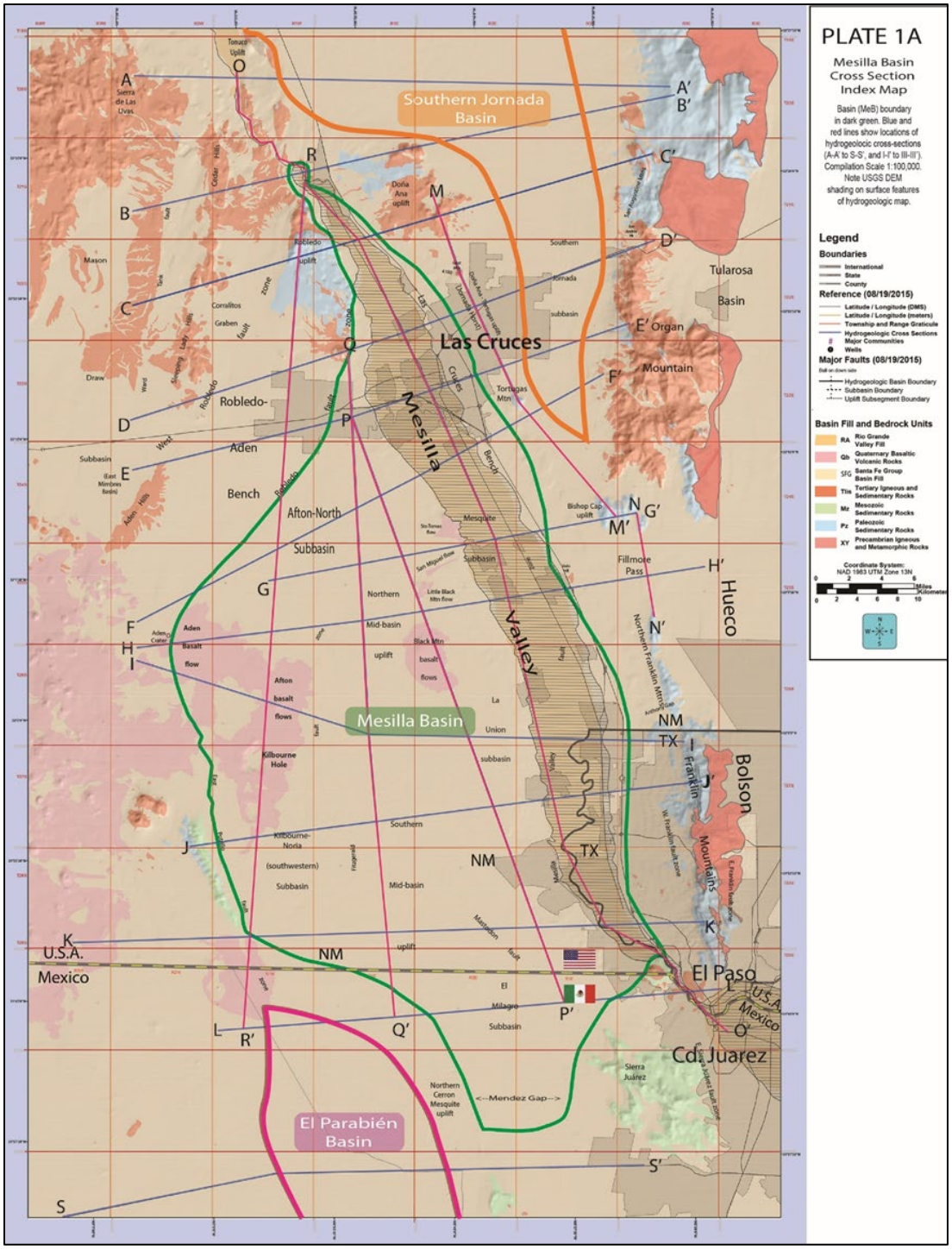

Figure 8-2 (page-size **PL. 1A**)**.** Study Area index map showing locations of the Mesilla, Southern Jornada, and El Parabién groundwater (GW) basins (MeB, SJB and EPB; outlined in green, orange and red, respectively). Also shown are the locations of hydrogeologic cross-section **A-A'** to **S-S'** (Report **PLATES 5a** to **5s**), major terrain features (incl. the Mesilla Valley, Selden Canyon and El Paso del Norte of the Rio Grande), and the Las Cruces and El Paso/Ciudad Juárez metropolitan centers. USGS DEM base, with UTM-NAD83 SI-system and latitude/longitude coordinates.

The NM WRRI Study Area index map (**Fig. 8-2**) has 10,000 m UTM-Zone 13 (NAD83) and latitude/longitude boundaries, and it is on a USGS DEM base. The boundary coordinates of the 3,350-mi^2 (8,675-km^2) Study Area are 3,504,000 m and 3,611,000 m northing, and 302,000 m and 367,000 m easting, respectively. The Mesilla, Southern Jornada, and El Parabién groundwater (GW) basins (MeB, SJB, and EPB) are outlined in green, orange, and red, respectively. Locations of Hydrogeologic Cross-Sections **A-A'** to **S-S' (PLS. 5a** to **5s**) are shown, as are the El Paso/Ciudad Juárez and Las Cruces metropolitan centers, with a 2020 population of almost 2.5 million.

8.1.1. Geographic Setting

The MBR is located in the Mexican Highland section of the Basin and Range (B&R) physiographic province. It includes parts of four Rio Grande (RG) rift-basin complexes that are hydrologically connected with the Rincon and Mesilla Valleys of the Rio Grande/Bravo fluvial system: the Southern Jornada, Hueco, El Parabién, and Zona Hidrogeológica Conejos Médanos (**Fig. 7-1** and **8-1**). Principal fluvial-geomorphic features include the Mesilla Valley (MeV), Selden Canyon (SCyn), and El paso del Norte (EPdN). Because presence of the through-flowing Rio Grande/Bravo system, the MBR is a major site of both irrigation-agriculture, and municipal and industrial (M&I) development. As such, the ever-increasing demands on its limited *fresh*-groundwater resources requires continued improvement of hydrogeologic characterization of aquifer systems, with the latter being defined in terms of lithologic composition, stratigraphic position, and bedrock and structural boundary conditions.

8.1.2. Chapter Content Summary

Study purpose and scope, and Report content are summarized in **Part 8.2**, and refinements in hydrogeologic-framework characterization that are required for the development of improved GW-flow and hydrochemical models are outlined in **Part 8.3**. **Part 8.4** includes brief reviews of (1) the Middle- to Late-Cenozoic evolution of RG rift and deposition of Santa Fe Group (SFG) basin-fill, and (2) the Mid- to Late-Quaternary development of the existing river-valley and canyon system. Emphasis is on (1) GW-flow system evolution that following initial development of the through-going Rio Grande/Bravo fluvial system, and (2) the Late Quaternary history of pluvial lakes that formed in hydraulically linked parts of the Los Muertos and Tularosa RG-rift basins (**Fig. 8-1**). **Part 8.5** offers a present-day perspective on GW-resource "sustainability" in the United States part of the MBR, and it includes an overview of potential long-term pumping effects on aquifer-framework properties.

Viable options for long-term development of aquifer systems in the U.S. part of the Mesilla GW Basin (MeB) are reviewed in **Part 8.6**. Emphasis of more site-specific discussions is on areas of the inner Mesilla Valley (MeV) and the MeB-West Mesa that are well suited for further GW-resource development, especially in relation to future (1) managed-aquifer recharge (MAR) operations, and (2)

brackish-GW (BGR) desalination and concentrate disposal. Potential sources of energy for BGR desalination in the West Mesa area are also briefly described in **Part 8.6**, with solar and geothermal energy getting special attention.

The "Concluding Remarks" in **Part 8.7** are made in the context of an idealistic, but still realistic "Design with Nature Now" approach to realities of climate change and the related challenges that groundwater-resources conservation will always face in this arid-semiarid region (*cf.* Steiner et al. 2019). Emphasis is on the immediate need for detailed information on deep-subsurface conditions in the MeB, with respect to not to only hydrogeology, but also geophysics and hydrochemistry.

8.2. REPORT CONTENT SUMMARY

8.2.1. Purpose, Scope of Work, and Chapter Content

The advances in conceptual-model development and hydrogeologic-framework characterization described in the Report and its eight Appendices are representative of the latest stage in efforts by the NM WRRI to ensure that essential baseline information on the region's groundwater resources is available to a diverse user group. The Report's format is designed to convey basic information on (1) the stratigraphy and lithologic character of basin-fill deposits, and (2) geohydrologic-boundary conditions at levels of detail appropriate for ongoing development of basin-scale numerical models of GW-flow and hydrochemical systems (here ~1:100,000 scale). Because of the Report's geoscience emphasis and its target-audience diversity, a glossary (**APNDX. G**) of 231 specialty terms is included.

The *geologic-materials* component of the hydrogeologic framework comprises the following integrated system of basin-fill sedimentary-lithofacies and bedrock-terrane classes (with Report **CHAPTERS** noted):

1. Lithofacies Assemblage (LFA) composition of the Upper, Middle, and Lower Santa Fe Group Hydrostratigraphic Units (HSUs) that comprise the bulk of the intermontane-basin fill in the RG-rift tectonic province (**CHAPTERS 3, 4** and **6**).
2. Bedrock composition and internal structural fabric of major inter-basin RG-rift and B&R province uplifts (e.g., San Andres**,** Organ, Franklin, Sierra Juárez, Doña Ana, Robledo, and East Potrillo) (*cf.* **CHAPTERS 3** and **5**).
3. Basin-border and intra-basin structural-boundary elements that primarily comprise RG-rift fault-zone (fz) components (*cf.* **CHAPTERS 3** and **6**).

While incorporating the results of multi-institutional hydrogeologic investigations that were initiated in the 1950s, this study also illustrates the iterative nature of all geoscience-based endeavors and the continuing need for additional field-based and laboratory research. Work completed to date is described in detail in the following Report Chapters:

1. The study's purpose, location, and scope of work, and details of Report organization are introduced in **CHAPTER 1**.
2. **CHAPTER 2** deals with GIS-related methods of Report preparation, such as (1) feature location, and (2) digital hydrogeologic map and cross-section compilation, and (3) subsurface data compilation, analysis, and interpretation.
3. The geologic and geomorphic setting is described in **CHAPTER 3** in terms of (1) Study Area location in the Basin and Range (B&R) physiographic and Rio Grande rift tectonic provinces, and the Chihuahuan Desert ecoregion, (2) the basic components of Upper Cenozoic Santa Fe Group (SFG) basin fill, and (3) the Mid- to Late Quaternary evolution of the present RG valley and canyon system and its alluvial-aquifers.
4. Hydrogeologic-framework controls on GW-flow and chemistry in a Basin and Range (B&R) and RG-rift provincial setting, are covered in **CHAPTERS 4, 6,** and **7** in terms of two primary aquifer-system components: lithofacies-assemblages (LFAs), and hydrostratigraphic units (HSUs). The latter components include (1) extensive and thick SFG basin fill, and (2) the alluvial fill of the inner RG Valley.
5. Bedrock compositional and structural boundary conditions associated with inter-basin mountain uplifts are described in **CHAPTERS 5**. Short descriptions of localities in and adjacent to the East Potrillo Uplift (EPU) with potential for desalination-concentrate and other types of wastewater management activities are also included in **CHAPTER 5** (e.g., **Parts 5.4.1a**, **5.6.2**, **5.6.3**).
6. Composition and hydraulic properties of aquifer and vadose-zone materials in individual hydrogeologic subdivisions of the Study Area are described in detail **CHAPTER 6**. The format of this chapter is designed to facilitate development of basin-scale numerical models of GW flow and chemistry. Hydrogeologic-framework controls on potential for GW-resource development in the United States part of the MeB, as well as its vulnerability for contamination are reviewed in Parts **6.3.2**, **6.3.3b-e**, **6.3.4a-d** (*cf.* **APNDX. E10**).
7. Framework controls on GW flow and chemistry are described in three temporal contexts in **CHAPTER 7**: Mid- to Late-Quaternary, Historic-Present, and Anthropogenic-near future. From a Late Quaternary-time perspective (~past 150 ka), the ultimate driving force for the *movement* of *subsurface water* relates to (1) the highly variable nature of Rio Grande discharge in terms of both flow and sediment load, (2) climate-controlled cycles of river-valley/canyon incision, and (3) correlative underflow-recharge contributions from large pluvial lakes in hydraulically linked parts of the Los Muertos and Tularosa RG-rift basins (**Fig. 8-1**). In order to be truly functional, the hydrogeologic-framework model must include *geologic-material* and RG-rift structural components that are associated with the *movement* of *subsurface water* in the *vadose* as well as *phreatic* zones.

8.2.2. APPENDIX-Content Summary

The scope and format of the main body of the Report did not permit inclusion of large amounts of essential supporting information, such as summaries of the pioneering contributions of special relevance to hydrogeologic investigations in the MBR. Much of the information of this type has been compiled as *stand-alone* documents, with cited-reference lists, in **APPENDICES A**, **C** to **E,** and **H**. Each is included in a separate electronic-file binder (PDF) in the Report DVD (also available online at https://nmwrri.nmsu.edu/publications/technical-reports/tr-reports/tr-363.html).

1. **APPENDIX A** includes background material on conceptual development of digital methods for hydrogeologic-framework characterization in the Mesilla Basin region since 1980.
2. **APPENDIX B** is a bibliography of more than 2,200 publications on topics that are related to hydrogeologic controls on groundwater-flow and hydrochemistry systems in the western US-Mexico Boundary region. The topic and subtopic alphanumeric codes assigned to each entry are designed to facilitate cross-referencing and EndNote® compilation.
3. **APPENDIX C** reviews major contributions to the hydrogeology, geohydrology, and hydrochemistry of the MBR (1890-2010), with emphasis on collaborative investigations by federal, state, and local agencies and organizations.
4. **APPENDIX D** includes facsimile reproductions of selections from published work on the Cenozoic geology, hydrogeology, geomorphology, and physical and cultural geography of the New Mexico-Chihuahua Border Region.
5. **APPENDIX E** is a **CHAPTER 8** addenda that provides background information on conservation of GW resources in the United States part of the MBR. Topics covered include: (1) "Sustainable" GW Development, (2) the rather nebulous concept of "resilience" in a groundwater-resource-management context, (3) GW mining, (4) Rio Grande Project water management, (5) potential impacts of climate change on water-resource availability, (6) vulnerability to aquifer and vadose-zone contamination, and (7) challenges facing future GW-resource conservation.
6. **APPENDIX F** is a compilation of selected images and photographs (satellite, aerial, and ground) of the New Mexico-Texas-Chihuahua border region: (1) Apollo, Gemini, and Landsat photographs and images, (2) aerial-photo views of Study Area landscapes, and (3) ground-photos of major Hydrostratigraphic Units and Lithofacies Assemblages in Santa Fe Group basin fill and alluvial deposits of the Rio Grande Valley.
7. **APPENDIX G** is a glossary of more than 240 scientific and technical terms. The compilation is designed to provide ready access to definitions of a large number of specialized geologic and hydrologic terms, most of which are in common usage in reports on basin-fill aquifer systems in the Basin and Range physiographic province.

8. **APPENDIX H** supplements found in **Part 1.5** contain detailed background information on (1) the 1680 to present history of water-resource development, and (2) the conservation of shared GW resources in Transboundary aquifer systems of the Paso del Norte region. Binational research collaborations, many of which have had NM WRRI support since 1964, get special attention. The most recent of these postdate 1994 implementation of EPA-La Paz Agreement Title XXI. It also includes a UACJ translation of selections on the geohydrology of northern Chihuahua from Estudio Hidrológico del Estado de Chihuahua (INEGI 1999).

8.2.3. Preparation and Content of Illustrations and Tables

As in previous investigations, syntheses of available hydrogeologic information for the Mesilla Basin region have been presented primarily from a geology-based perspective (e.g., Hawley and Lozinsky 1992, Hawley and Kennedy 2004, Hawley et al. 2000, 2005 and 2009). However, maps and cross-sections in those reports retained much of the cartographic detail present in their 1:100,000-1:125,000 scale geologic-map sources (e.g., Seager et al. 1987, Seager 1995, and Collins and Raney 2000). Because of inherent geologic-map-unit complexities, however, this approach has proven to be inappropriate for digital hydrogeologic-framework characterizations that need to mesh as effectively as possible with contemporary geohydrologic and hydrochemical numerical modeling platforms (*cf.* **Part 2.3**; Sweetkind 2017, 2018, Sweetkind et al. 2017, Teeple et al. 2017, Hanson et al. 2018).

A distinctive feature of the cartographic products in this Report is the reduced complexity and expanded-graphic display of the lithologic, stratigraphic, and structural features that form the basic framework components of an intermontane-basin and river-valley aquifer systems (*cf.* **Part 2.3.1**). Accordingly, lithofacies-assemblage (LFA), hydrostratigraphic-unit (HSU), and structural-boundary elements are now combined in much-less complex hydrogeologic-unit categories that are designed to be compatible with current MODFLOW-compatible software like Leapfrog®.

TABLE 1 is an Excel®-Spreadsheet compilation of records of 395 *Key Wells* in the Binational Study Area, with location, construction, and hydrostratigraphic-interpretive information. **TABLE 1A** includes lists of published and unpublished sources of borehole records, and names and acronyms for hydrogeologic subdivisions shown on maps and cross-sections are listed on **TABLE 1B**.

The Report's primary graphic component comprises eight **PLATES**. Their content and methods of preparation are summarized in **Part 2.4**. **PLATES 1** to **8** were initially compiled at a map scale of 1:100,000, and each is designed for electronic-file access in the Report DVD (and online), as well as 11 x 17-inch format printing. The 10,000 m (100 km^2) UTM-SI grid system is used in combination with latitude/longitude and township-range (USA) coordinates for feature location. Much of the base-line

geological and geophysical information used in **PLATE 1**-derivative map and cross-section preparation was obtained from a report on detailed-reconnaissance work on "Rift Basin Structure of the Border Region . . ." by the Geophysical Research Center at UTEP (e.g., Jiménez and Keller 2000, **Part 3.6**).

Locations of the 395 key wells that are the primary source of subsurface hydrogeologic information used in this study are shown on **PLATE 3** (**Fig. 1-1—**page-size). Well selection was based mainly on (1) depth and quality of the hydrostratigraphic and hydrochemical database, and (2) accuracy of predevelopment static water-level (swl) information. Well-location index numbers correspond to 395 entries in **TABLE 1** (**Parts 1.4.2** and **2.3.2**). **PLATES 4A** and **4B** (**Figs. 1-9** and **1-9b**) are index maps to major geohydrologic features of the Study Area (**Fig. 7-2**). Major surface-watershed divides are shown by solid and dashed thick blue lines. Thin blue contour lines (20 and 100 ft on **PLATE 4A**, and 5, 10, and 30 m on **PLATE 4B**) are approximations of *pre-development* (1976) potentiometric-surface altitudes. The dashed blue line with arrows in the southwest corners of the maps show the approximate position of the regional GW-flow divide between El Paso del Norte-directed flow, and ZHGCM (El Barreal)-directed flow (**Part 7.1**; **Fig. 8-3**; *cf.* **Parts 1.6.3**, **1.7** and **7.6.2**).

New hydrogeologic map and cross-section products include structure-contour maps of HSU and bedrock-bounding surfaces (4), and pre-development potentiometric-surface approximation. Perhaps the most innovative contribution of the investigation are the three volumetric (isopleth) maps (**PLS. 7A** to **7C**) that show the primary lithofacies-assemblage composition of the saturated parts of the Upper/Middle/Lower SFG Hydrostratigraphic Unit sequence in each hydrogeologic subdivision of the Study Area's major GW basins**.** They are designed for use in *next-generation* groundwater-flow and hydrochemical model development, and their digital format facilitates cartographic updates. They are general equivalents of the volume-element or "voxel" units that were recently designed for use in the MBR by Donald Sweetkind of the USGS (Sweetkind 2017 and 2018 [p. 60]; *cf.* Journel and Huijbregts 1978, Geosoft 2016). The map series also provides a provisional hydrogeologic-framework interpretation in an area in Chihuahua that includes the new JMASCJ well field (e.g., **Fig. 6-21**).

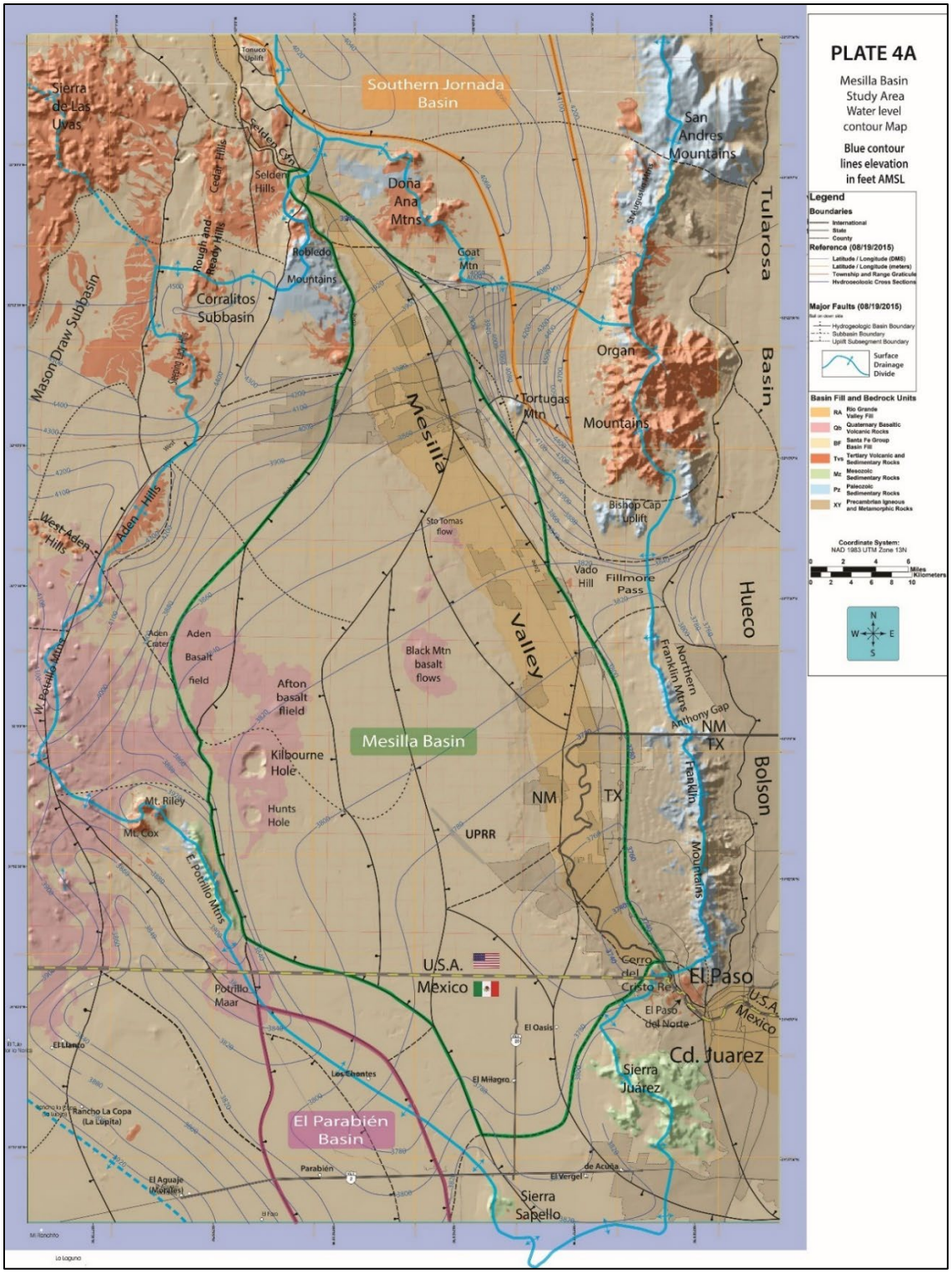

Figure 8-3 (page-size **PL. 4A).** Index map for the Study Area's primary geohydrologic features on a **PLATE 1** hydrogeologic-map base. The approximate pre-development (~1976) potentiometric-surface altitude (amsl) is shown with 20- and 100-ft contours. Major surface-watershed divides are shown by solid and dashed thick blue lines. The dashed blue line with arrows in the map's SW corner marks the approximate boundary between EPdN- and ZHGCM (El Barreal)-directed GW flow.

8.3. MAJOR GEOLOGIC FEATURES OF THE MESILLA BASIN REGION

8.3.1. Regional Geologic Setting

The Mesilla Basin region (MBR – **Figs. 7-1**) is in the Mexican Highland section of the eastern Basin and Range (B&R) physiographic province, and it is located at the southern end of the Rio Grande rift (RG-rift) tectonic province (**Fig. 8-1**). The sub-continental scale of the RG-rift province is shown on the smaller inset map in **Figure 8-1**. The inherent complexity and deep-seated nature of the major structural components of Rio Grande rift basins and their bordering bedrock uplifts requires that their characterization in a detailed hydrogeologic context be based on a variety of direct and indirect methods of surface and subsurface investigation (e.g., surface mapping, borehole-sample logging, and geophysical and geochemical surveys; *cf.* **PL. 1** to **PL. 7** series). Former Head of the UTEP Geophysical Laboratory, G.R. Keller describes some aspects of this multi-disciplinary process in a seminal 2004 review paper titled, "Geophysical constraints on the crustal structure of New Mexico (2004, p. 450):"

> Seismic reflection, gravity, and drilling data have delineated the many large, deep basins that form the upper crustal expression of the [RG] rift. Initially, the primary emphasis was on gravity studies (e.g., Cordell, 1976, 1978; Ramberg et al., 1978; Birch, 1982). However, the petroleum industry has released a considerable amount of seismic reflection data for research purposes, and [a] series of papers that focus on the [RG-] rift basins and include many seismic reflection profiles is [cited] in Keller and Cather (1994). In general, the basins are asymmetrical and more complex structurally than their surface expression would suggest [*cf.* **Part 3.6**; and Seager and Morgan (1979), and Averill andr (2013)].

8.3.2. Hydrogeologic Subdivisions

Synthesis of geophysical-survey and deep-borehole information now permits identification and subdivision of the Study Area's major GW basins at a level of detail that has heretofore not been possible (*cf.* **CHPTS. 3** and **6**, **TBL. 1**). **Figure 8-4** is a Study Area index map showing locations of the major hydrogeologic subdivisions that now can be defined in the context of a more-detailed conceptual model of the MBR's tectonic setting. The Mesilla GW Basin (MeB) is in blue shades, and the Mesilla Valley of the Rio Grande is in dark blue. The Southern Jornada and El Parabién GW Basins (SJB and EPB) are in light green and pink, respectively. SCyn and EPdN show the respective locations of Selden Canyon and El Paso del Norte. Solid and dashed black lines mark the boundaries of interbasin-uplift and intrabasin subdivisions. Acronyms for hydrogeologic-subdivision categories, including fault zones (lines with bar and ball symbols), are listed in **Tables 8-1** and **8-2** [**TBLS. 2** and **3**].

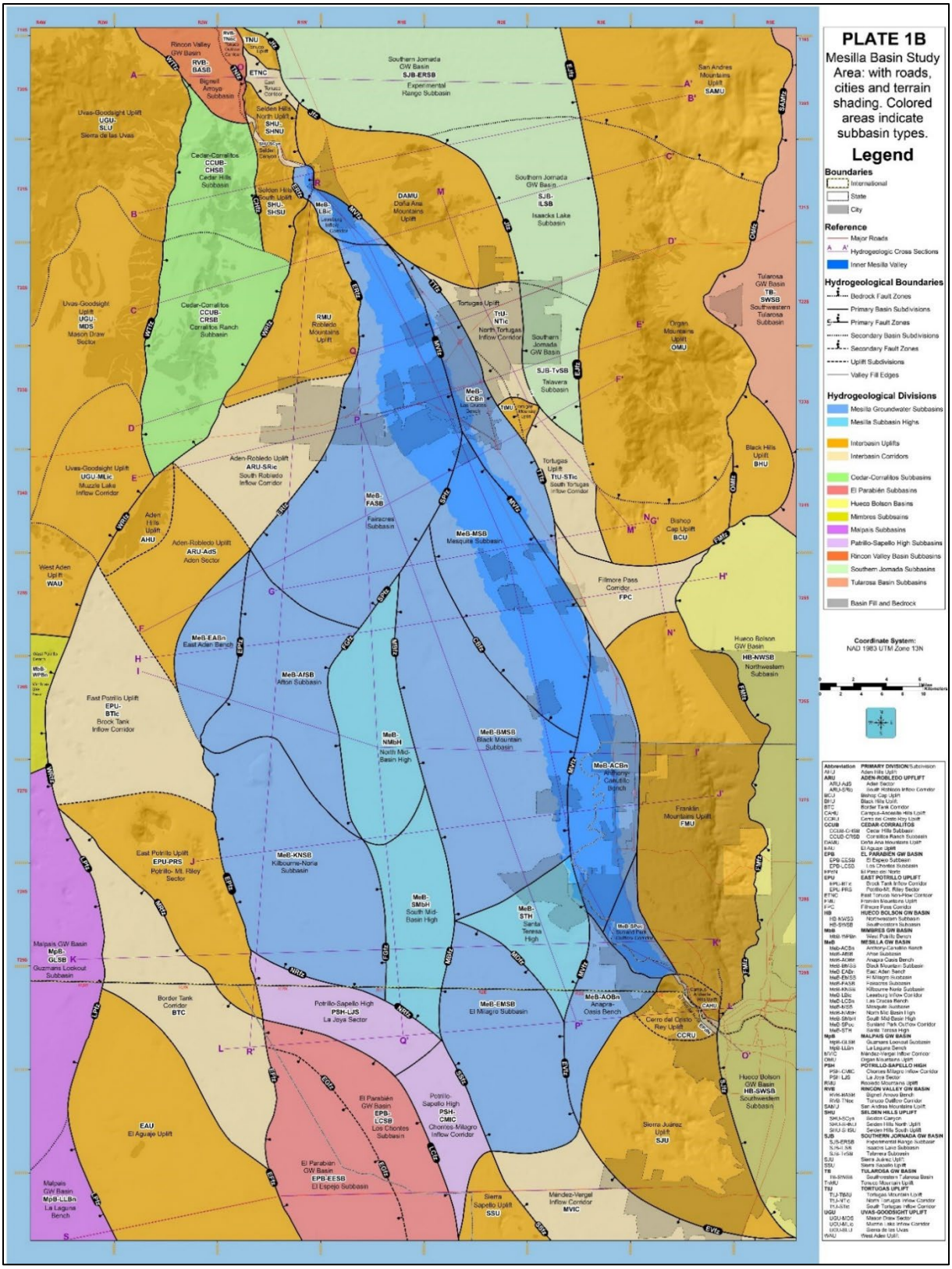

Figure 8-4 (page-size **PL. 1B).** Index map for the Study Area's major hydrogeologic subdivisions on USGS DEM base (PL. 1). Explanations of subdivision names and acronyms are on **Tables 8-1** and **8-2**.

Table 8-1. Names and Acronyms of Hydrogeologic Subdivisions shown on Maps, Cross-Sections, and the Well-Information Spreadsheet (Fig. 8-2; PLS. 1 to 8, TBLS. 1 and 2)

ACRONYM	RIO GRANDE (RG) VALLEY AND CAnYONS (NARROWS)
EPdN	El Paso del Norte (Cyn)
MeV	Mesilla Valley
SCyn	Selden Canyon (Cyn)
EPJV	El Paso-Juárez Valley

ACRONYM	MESILLA GW BASIN (MeB)	SUBDIVISION (AREA in km²)
MeB-ACBn	Mesilla Basin	Anthony-Canutillo Bench (138)
MeB-AfSB	Mesilla Basin	Afton Subbasin (180)
MeB-AOBn	Mesilla Basin	Anapra-Oasis Bench (72.7)
MeB-BMSB	Mesilla Basin	Black Mountain Subbasin (353)
MeB-EABn	Mesilla Basin	East Aden Bench (70.7)
MeB-EMSB	Mesilla Basin	El Milagro Subbasin (203)
MeB-FASB	Mesilla Basin	Fairacres Subbasin (382)
MeB-KNSB	Mesilla Basin	Kilbourne-Noria Subbasin (278)
MeB-LBic	Mesilla Basin	Leasburg Inflow Corridor (25.4)
MeB-LCBn	Mesilla Basin	Las Cruces Bench (97.5)
MeB-MSB	Mesilla Basin	Mesquite Subbasin (228)
MeB-NMbH	Mesilla Basin	North Mid-Basin High (143)
MeB-SMbH	Mesilla Basin	South Mid-Basin High (121)
MeB-STBn	Mesilla Basin	Santa Teresa high (89.5)
MeB-SPoc	Mesilla Basin	Sunland Park Outflow Corridor (33.4)

ACRONYM	OTHER GW BASINS (B)	SUBDIVISION
EPB	El Parabién Basin (N-part—Drains to MeB)	
EPB-EESB	El Parabién Basin	El Espejo Subbasin (158)
EPB-LCSB	El Parabién Basin	Los Chontes Subbasin (126)
HB	Hueco Bolson (W-edge—Receives inflow from MeB through EPdN)	
HB-NWSB	Hueco Bolson	Northwestern Subbasin
HB-NWSB	Hueco Bolson	Southwestern Subbasin
MbB	Mimbres Basin (No-flow boundary with MeB; surface and subsurface flow to Zona Hidrogeológica Conejos Médanos (ZHGCM)	
MbB-WPBn	Mimbres Basin	West Potrillo Bench
MpB	Malpais GW Basin (E-edge—connects with BTC, MbB, and LMB)	
MpB-GLSB	Malpais Basin	Guzmans Lookout Subbasin (SB)
MpB-LLBn	Malpais Basin	La Laguna Bench (Bn)
RVB	Rincon Valley GW Basin (Drains to MeB through SCyn)	
RVB-BASB	Rincon Valley Basin	Bignell Arroyo Subbasin (47.2)
RVB-TNoc	Rincon Valley Basin	Tonuco Outflow Corridor (5)
SJB	Southern Jornada GW Basin (Drains to MeB and RVB)	
SJB-ERSB	Southern Jornada Basin	Experimental Range Subbasin (264)
SJB-ILSB	Southern Jornada Basin	Isaacks Lake Subbasin (164)
SJB-TvSB	Southern Jornada Basin	Talavera Subbasin (68.2)
SWTB	Southwestern Tularosa Basin	

ACRONYM	UPLAND GW BASIN	SUBDIVISION
CCUB	Cedar-Corralitos Upland Basin (UB)	
CCUB-CHSB	Cedar-Corralitos	Cedar Hills Subbasin (96.2)
CCUB-CRSB	Cedar-Corralitos	Corralitos Ranch Subbasin (205)

Table 8-1. (concluded) Names and Abbreviations of Basin/Inter-Basin Subdivisions

ABBREVIATION	INTERBASIN HIGH (IBH)	SUBDIVISION
PSH	Potrillo-Sapello High (163)	
PSH-LJS		La Joya Sector (93.5)
PSH-CMIC		Chontes-Milagro Inflow Corridor (69.5) (EPB-LCSB to MeB-EMSB)

ABBREVIATION	INTERBASIN UPLIFT (U)	SUBDIVISION
AHU	Aden Hills Uplift	
ARU	Aden-Robledo Uplift	
ARU-AdS	Aden-Robledo Uplift	Aden Sector (S)
ARU-SRic	Aden-Robledo Uplift	South Robledo Inflow Corridor (145)
BCU	Bishop Cap Uplift	
BHU	Black Hills Uplift	
CAHU	Campus-Andesite Hills Uplift	
CCRU	Cerro del Cristo Rey Uplift	
CMU	Camel Mountain Uplift	
DAMU	Doña Ana Mountains Uplift	
EAU	El Aguaje Uplift (310)	
EPU	East Potrillo Uplift	
EPU-BTic	East Potrillo Uplift	Brock Tank Inflow Corridor (227)
EPU-PRS	East Potrillo Uplift	Potrillo-Mt. Riley Sector (S)
FMU	Franklin Mountains Uplift	
OMU	Organ Mountains Uplift	
RMU	Robledo Mountains Uplift	
SAMU	San Andres Mountains Uplift	
SHU	Selden Hills Uplift	
SJU	Sierra Juárez Uplift	
SSU	Sierra Sapello Uplift (41)	
TNU	Tonuco Uplift	
TtU	Tortugas Uplift	
TtMU	Tortugas Uplift	Tortugas Mountain Uplift (U)
TtU-NTic	Tortugas Uplift	North Tortugas Inflow Corridor (63.5)
TtU-STic	Tortugas Uplift	South Tortugas Inflow Corridor (59.2)
UGU	Uvas-Goodsight Uplift	
UGU-SLU	Uvas-Goodsight Uplift	Sierra de las Uvas (U)
UGU-MDS	Uvas-Goodsight Uplift	Mason Draw Sector (S)
UGU-MLic	Uvas-Goodsight Uplift	Muzzle Lake Inflow Corridor (ic, to the Mimbres Basin-MbB)
WAU	West Alden Uplift	

ABBREVIATION	INTER-BASIN GROUNDWATER-FLOW CORRIDORS
BTC	Border Tank Corridor (214) (Malpais Basin to El Parabién Basin underflow)
ETNC	East Tonuco Corridor (13.5) (Jornada Basin to Rincon Valley Basin underflow)
FPC	Fillmore Pass Corridor (73.7) (Mesilla Basin-Hueco Bolson—potential inter-basin underflow)
MVIC	Méndez-Vergel Corridor (115) (possible Hueco Bolson to Mesilla Basin underflow)

Table 8-2. Names and Acronyms for Boundary-Fault Zones* of the Study Area's Major GW Basins (TBL. 3; PLS. 1, 2, 5 and 9; and Tbl. 8-1)

Map-Unit Acronyms and Names	Bordering Hydrogeologic-Map Subdivisions (Fig. 6-1, Tbl. 6-1)
Southern Jornada Basin (SJB)	
West Side	
Jfz—Jornada fz (**A1**, **B2**, **C1**)*	ERSB/SDMU-ETC-DAMU, ILSB/DAMU, TSb/TtU
East Side	
EJfz—East Jornada fz (**A3**, **B3**, **C2**)	ERSB/SAMU, ILSB/OMU, TSB/OM
Mesilla Basin (MeB)	
MeB Border	
West Side (N to S)	
ERfz—East Robledo fz (**A1**, **b1**, **C2**)	LBic/RMU, FaSB/RMU—ARU-RS
EPfz—East Potrillo fz-S (**A1**, **B1**, **C1-2**)	KNSB/EPU-BTic, KNSB/EPU-PRS
NRfz—Noria fz (**A3**, **B3**, **C2, C4**)	KNSB/PSH-LJS, SMbH/PSH-LJS
SSfz—Sierra Sapello fz (**A3**, **B3**, **C3-4**)	EMSB/PSH-CMIC
East Side (N to S)	
MVfz—Mesilla Valley fz-N (**A3**, **B3**, **C2**)	LBic/DAMU,
TTfz—Tortugas fz (**A3**, **B3**, **C2**)	LCBn/DAMU, LCBn/TtU, LCBn/FPC
MVfz—Vado Hill Segment (**A3**, **B3**, **C2**)	MSB/FPC
MeB Interior (Intra-Basin)	
North and West of Mid-Basin High (MBH)	
MVfz—Mesilla Valley fz-C (**A3**, **B4**, **C2**)	FASB/LCBn
SPfz—San Pablo fz (**A3**, **B3**, **C2**)	FASB/MSB, FASB/BMSB, FASB/NMBH
FGfz—Fitzgerald fz (**A2**, **B2**, **C2**)	AfSB/nMbH, KNSB/SMBH
EPfz—East Potrillo fz-N (**A2**, **B4**, **C2**)	AfSB/EABn.
East of Mid-Basin High (MbH)	
MVfz—Mesilla Valley fz-S (**A3**, **B4**, **C2**)	MSM/ACBn, BMSB/ACBn, STBn/ACBn, STH/AOBn
CBfz—Chamberino fz (**A2**, **B2**, **C3**)	MSB/BMSB
MBfz—Mid-Basin fz (**A3**, **B3**, **C4**)	BMSB/NMBH, BMSB/SMBH, EMSB/SMBH
MDfz—Mastodon fz (**A1**, **B2**, **C2**)	EMSB/STBn
EVfz—El Vergel fz-N (**A3**, **B4**, **C2**)	EMSB/AOBn
El Parabién Basin (EPB)	
West Side	
EFfz—El Faro fz (**A2**, **B4**, **C1**)	LCSB/BTC
East Side	
LCfz—Las Cuates fz (**A2**, **B2**, **C1**)	EESB/BTC, EESB/EAU
El Parabién Basin Interior (Intra-Basin)	
EGfz—El Girasol fz (**A2**, **B2**, **C2**)	EESB/LCSB

**Qualitative Fault-Zone Attributes*

A. Plio-Pleistocene (<5 Ma) Fault-Zone Activity: A1. High, A2. Moderate, A3. Low

B. Fault-Zone Topographic Definition: B1. High, B2. Moderate, B3. Low, B4. Buried

C. Fault-Zone Subsurface Definition (e.g., borehole and/or geophysics):

C1. High, C2. Moderate, C3. Low, C4. Deeply Buried

Figure 8-5 (page-size **PL. 2B**) schematically portrays the topography, and primary stratigraphic and structural components of the bedrock terrane that is buried by basin-fill deposits within the Study Area (**Fig. 8-2**). The structure-contour intervals on the bedrock surface are 25, 50, and 100 m, and the red lines show locations of three schematic geologic cross-sections (I-I′ to III-III′) on **Figure 8-5** (**PL. 1C**). The latter shows general subsurface relationships to a depth of 10,000 ft (3 km) bmsl at about 2.5 vertical exaggeration (VE). The map and cross-sections represent the first effort to create an approximation of the base of the RG-rift basin fill and associated aquifer systems in this part of the RG rift. It is based on a synthesis of available geological and geophysical information that has been acquired since the 1962 initiation of detailed hydrogeological studies in the MBR. Explanations of stratigraphic-unit names and acronyms are also listed on **Table 8-3**. The Mesilla GW Basin boundary is in green, with map-unit subdivisions defined in **Table 8-3**. The general position of the deeply buried "Lanark igneous-intrusive complex (TmLC)," which forms the central part of the Mid-Basin High, is also shown (*cf.* **PLS. 5i** and **5q**; **Part 6.3.2a**; Clemons 1993).

Section I-I′ (**Fig. 8-6**) shows basic bedrock geologic relationships in the northern MeB/MeV and southern part of the Southern Jornada Basin (SJU).

Section II-II′ (**Fig. 8-6**) illustrates these basic geologic relationships in a central MeB area that includes the deeply buried Lanark intrusive complex (TmLC) that forms much of the central Mid-Basin High (MeB-MBH; **Part 6.3.2a**).

Section III-III′ (**Fig. 8-6**) shows basic geologic relationships in an area located about 5 mi (8 km) south of the International Boundary.

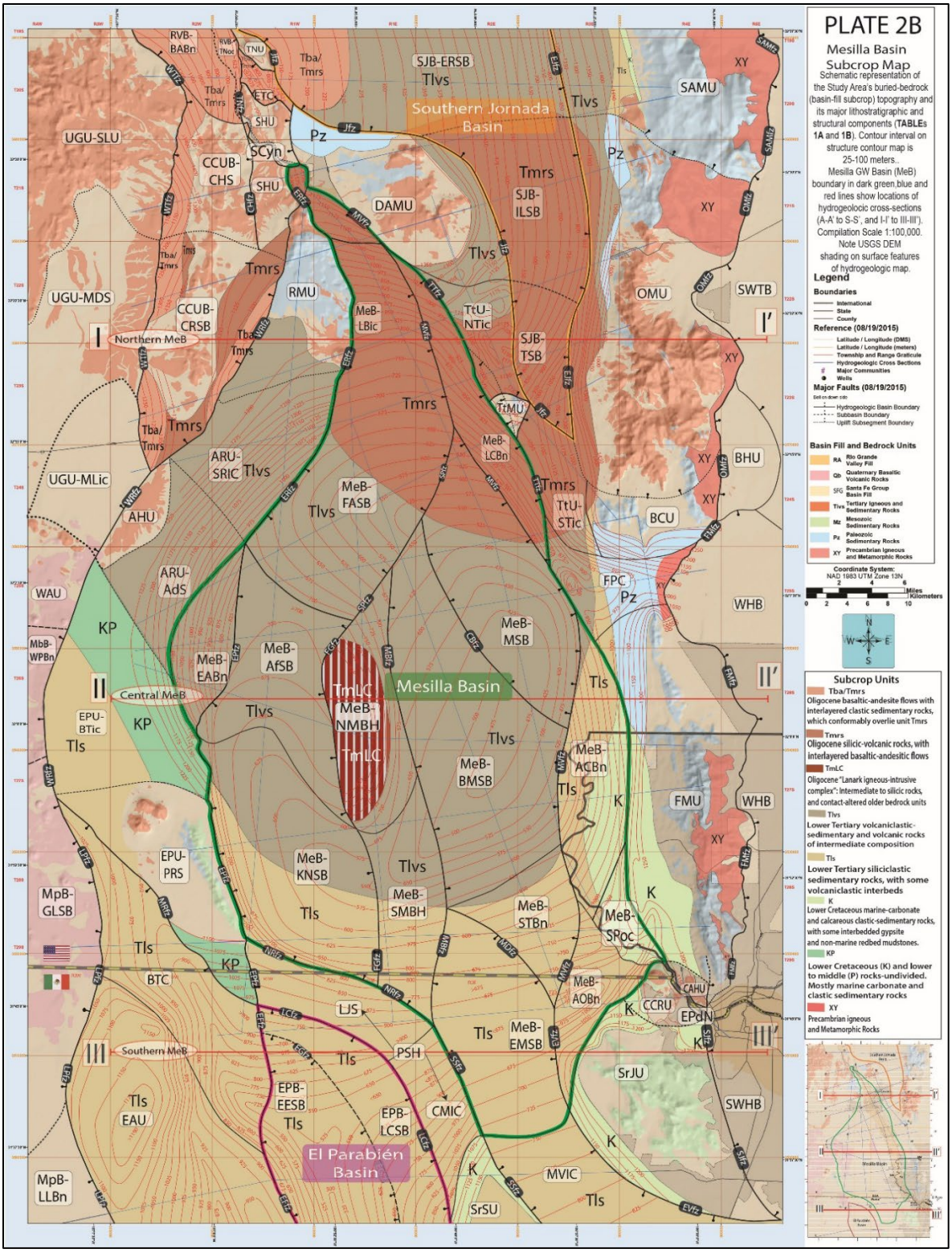

Figure 8-5 (page-size **PL. 2B).** Schematic depiction of basin-fill subcrop topography, and primary lithostratigraphic and structural components in the NM WRRI Study Area. **PLATE 1** Hydrogeologic-Map base, with explanation on **Table 8-3**. Structure contours are at 25, 50, and 100 m intervals, and W-E red lines show locations of cross-sections I-I′ to III-III′ (**Fig. 8-6**).

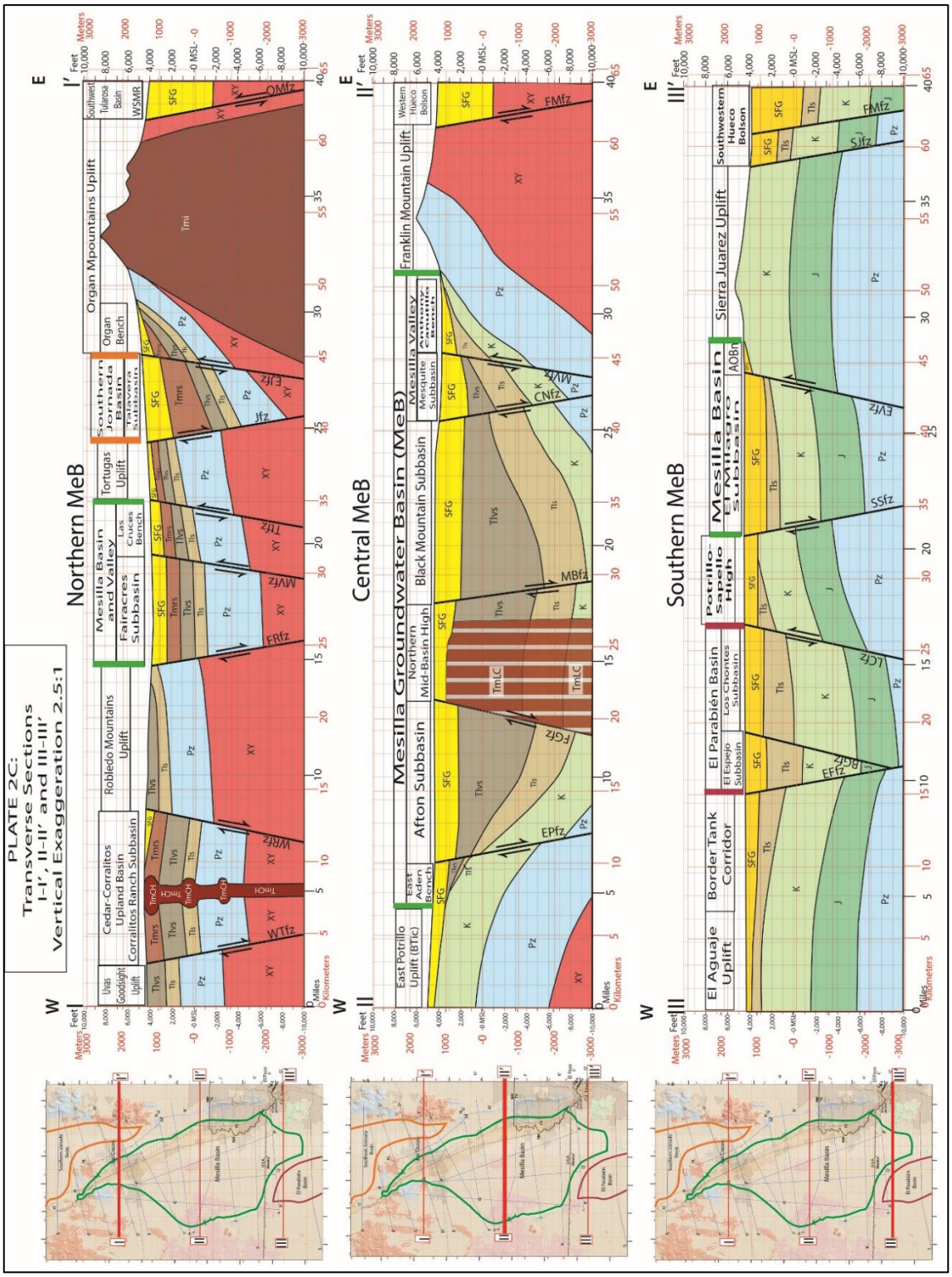

Figure 8-6 (page-size **PL. 2C**)**.** Schematic geologic cross-sections I-I' to III-III', which show major subsurface stratigraphic and structural relationships in the central and southern parts of the NM WRRI Study Area. Explanation on **Table 8-3**, with geologic-section locations on **Figure 8-5**.

Table 8-3. Explanation of Lithostratigraphic Units on Figures 8-5 and 8-6

Rio Grande (RG) Rift Basin Fill (Upper Oligocene to Lower Pleistocene)

SFG Santa Fe Group Hydrostratigraphic Units (HSUs)-Undivided. Includes alluvial deposits of the inner Rio Grande Valley (**RA**), and thin, but locally extensive basaltic volcanics (**Qb**). Mostly middle to late Quaternary age

Middle to Lower Tertiary Igneous Extrusive/Intrusive and Non-marine Sedimentary Rocks

Tba Basaltic andesite lava flows and vent-zone units, with interlayered mudstones, sandstones and conglomerates volcanic rocks—late Oligocene Uvas Basaltic Andesite correlative

TmCH Cedar Hills vent zone. N-S aligned series of flow-banded rhyolite domes and feeder conduits intruded into the Cedar-Corralitos Upland Basin stratigraphic sequence—Oligocene

TmLC Lanark Complex—Intermediate to silicic igneous-intrusive complex that forms central part of the Northern Mid-Basin High and is buried by at least 1,500 ft (455 m) of SFG basin fill—Oligocene (*cf.* **PLS. 2, 5i** and **5q**; Phillips-Sunland oil test: **TBL. 1**, no. 237; Clemons 1993)

Tmrs Silicic pyroclastic and volcaniclastic rocks—Oligocene, mainly rhyolite and latite ashflow tuffs and tuffaceous sandstones, with some capping basaltic-andesite flows (**Tba**)

Tmi Intermediate to silicic (felsitic) plutonic rocks in the Organ and Doña Ana Mountains, and Mt. Riley-Cox and **TmLC** areas, including monzodiorite to syenite stocks—Oligocene and Late Eocene (Seager et al. 1987, Clemons 1993, Seager 1995)

Tlvs Volcaniclastic and epiclastic-sedimentary rocks, and local basal gypsite beds, with andesitic to dacitic flows and breccias—Eocene Palm Park and Rubio Peak Fm correlative that is exposed in uplifts flanking much of the northern and central Study Area. The unit is about 3,880 ft (1,183 m) thick in the Mobile-Grimm oil test (**PLs 5q**, **TBL. 1**, no. 180; Clemons 1993).

Tls Mostly siliciclastic sedimentary rocks, sandstones, mudstones, and conglomerates with minor or no volcanic constituents. General correlative of lower Eocene/Paleocene Love Ranch/Lobo Fms. The unit is about 7,000 ft (2,134 m) thick in the Mobil-Grimm oil-test well (**TBL. 1**, no. 180). An inferred correlative sequence of siliciclastic rocks is at least 1,000 ft (330 m) thick in the Pemex-Moyotes oil-test well (**PL. 5s**, **TBL. 1**, no. 397; Clemons 1993, Jiménez and Keller 2000)

Mesozoic Sedimentary Rocks-Mostly Marine, and Commonly Structurally Deformed

K Lower Cretaceous marine rocks-undivided. Sandy to shaly limestone, coquina limestone, silty shale, calcareous sandstone, and limestone-pebble conglomerate, with local occurrences of gypsite beds. Approximately 1550 to 2200 ft (470-670 m) thick were exposed in the Sierras Juárez and Sapello, Cerro Cristo Rey, and the East Potrillo Mountains. 1,050 ft (320 m) penetrated in the Grimm oil-test well (**TBL. 1**, no. 180). In the Pemex-Moyotes oil-test well, the Lower Cretaceous section is 5,512 ft (1,680 m) thick (**PL. 5s**, **TBL. 1**, no. 397)

J Jurassic marine rocks-undivided: limestone, shale, and gypsite, with local occurrences of halite beds beneath the southeastern-most part of the Study Area. Present in the shallow subsurface but not exposed in Sierra Sapello. A 3,380 ft (1,130 m) thick Jurassic section was penetrated in the Pemex-Moyotes oil-test well between Permian (**P**) and Lower Cretaceous (**K**) rocks (**PL. 5s**, **TBL. 1**, no. 397)

Paleozoic Sedimentary Rocks-Mostly Marine, and Commonly Structurally Deformed

Pz Paleozoic rocks, **Pzu/Pzl**-undivided

Pzu Upper Paleozoic (Pennsylvanian and Permian) rocks-undifferentiated: primarily limestone and redbed mudstones, with shale, sandstone, and some gypsite

Pzl Middle and Lower Paleozoic rocks-undivided: Middle Paleozoic (Devonian and Mississippian)—primarily limestone, with shale. Lower Paleozoic (Cambrian-Ordovician-Silurian)—primarily limestone and dolomite, with thin basal sandstone

Proterozoic (Precambrian) Rocks

XY Igneous and metamorphic rocks-undivided

8.4. SUMMARY OF HYDROGEOLOGIC-FRAMEWORK DEVELOPMENT AND GROUNDWATER FLOW-SYSTEM EVOLUTION

8.4.1. Major Middle-to-Late Cenozoic Stages of Hydrogeologic-Framework Development

A unique aspect of this study has involved state-of-practice, digital characterization of the Mesilla Basin region's (MBR's) hydrogeologic framework. *Geologic-material* and RG-rift *structural* component are integrated with the relatively dynamic parts of the hydrogeologic framework that portray the *movement* of *subsurface water* in broad range of geologic-time contexts (primarily the past million years [Ma] in the case of the MeB). From the perspective of *geologic-material* composition and hydraulic functions, about 30 Ma of framework development is here described in terms of an eight-stage conceptual model of intermontane-basin evolution in a southern RG-rift tectonic setting (**Figs. 8-5** and **8-6,** and **Tbl. 8-4**).

8.4.2. Quaternary Groundwater-Flow System Evolution

With respect to hydrogeologic-framework controls on groundwater flow and chemistry in the MBR (the central theme of **CHAPTER 7**), deep river-valley and canyon entrenchment during the Middle and Late Pleistocene produced an almost complete reversal in the southward-directed GW-flow system of Pliocene and Early Pleistocene age in much of the MBR (**Figs. 7-3**, **8-3** and **8-7**). The other prominent hydrogeologic features of the MBR's intermontane-basin landscape are the parts of the Bolson de los Muertos and Tularosa Basin that were inundated during high stands of pluvial-Lakes Palomas and Otero in the last Pleistocene glacial stage (about 29-11 ka; **Parts 7.2.2** and **7.6.2**). During the past 400 to 500 ka, relatively short intervals of valley and canyon cutting coincided with at least four major stages of Pleistocene glaciation in the river's Rocky Mountain headwaters' region, and partial back-filling of valley floors was associated with longer interglacial intervals (**Parts 3.7.3**, **3.7** and **3.9**).

The general potentiometric-surface configuration and GW-flow boundary positions that are shown on **Figures 8-3** illustrate how saturated parts of the USF2-ARG distributary-channel networks would function as an enormous system of high-permeability conduits (*cf.* **Figs. 3-14** and **7-6**). Under proper hydraulic conditions, the latter would be able to deliver large volumes of GW recharge to the shallow aquifer systems of the inner-Mesilla Valley area between Anthony, NM/TX and El Paso del Norte (**Fig. 7-2**; *cf.* **Parts 6.3.4b-c** and **6.3.5b-d**). In addition, such deposits serve as efficient pathways for outflow from residual GW reservoirs in the Transboundary Aquifer system that were periodically replenished by GW discharge from pluvial-Lake Palomas during Late-Pleistocene glacial stages.

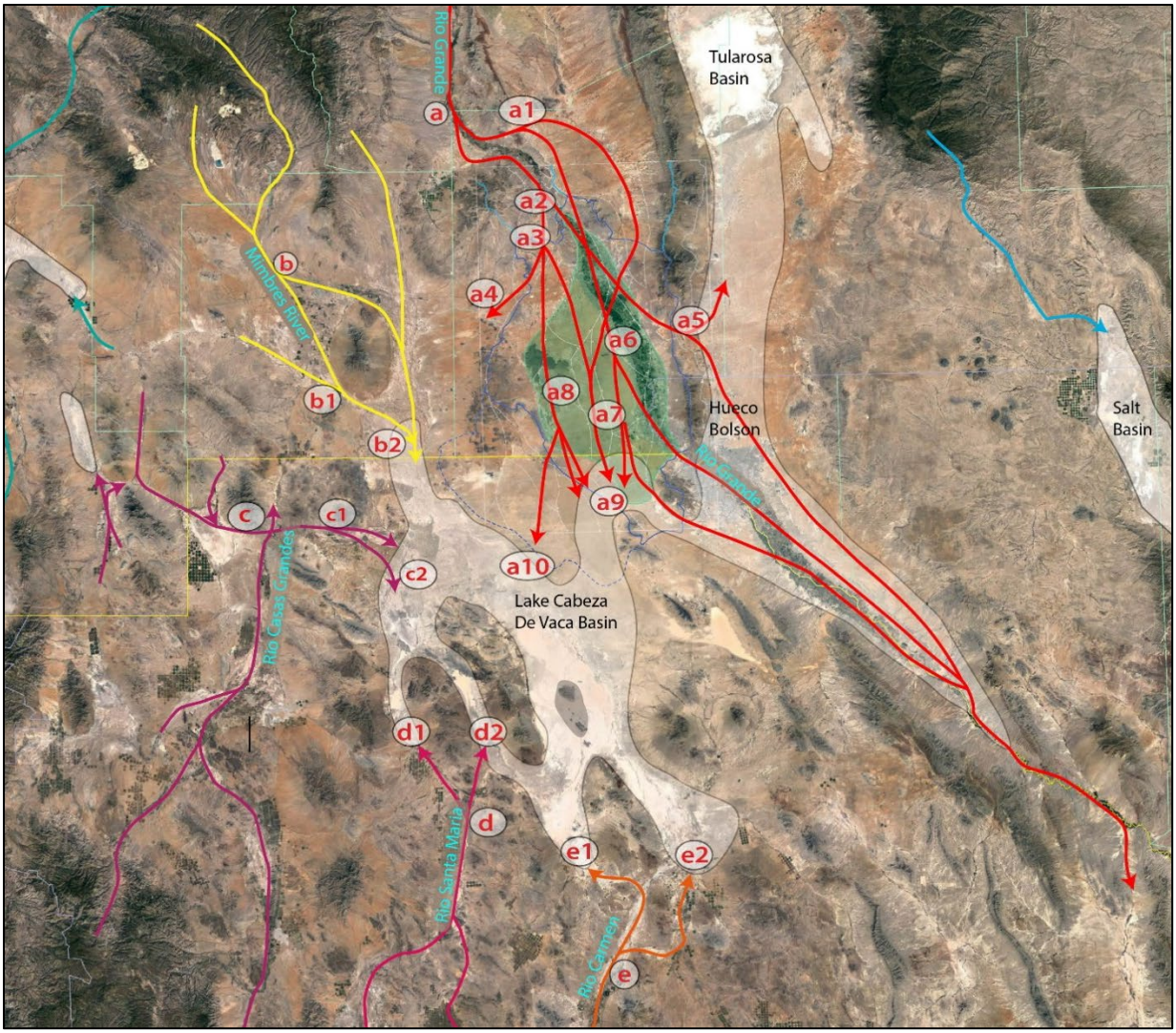

Figure 8-7 (adapted from Hawley 1975, Fig. 2)**.** Pliocene and Early Pleistocene depositional setting of the ARG distributive fluvial system (DFS-red lines) that terminated in the paleo-Lake Cabeza de Vaca (LCdV) complex of W.S. Strain (1966, 1971). The Mesilla GW Basin is shown in green. ARG deposits in the Upper SFG Hydrostratigraphic Unit (HSU-USF2) comprise the region's most-productive aquifers. Explanations of symbols for general positions of distributive-fluvial system (DFS)-apices, ancestral-river channelbelt-segments, and LCdV fluvial-deltaic termini are in **Table 3-4**. The location of Fillmore Pass and the DFS apex of the ARG "Camp Rice Fan Delta" of Seager (1981, Fig. 84) is shown with an **a5**. The Rios Casas Grandes (violet), Santa Maria and Carmen (pink and orange), and the Mimbres River (yellow) remain as the primary surface- and subsurface-flow contributors to ephemeral lake-plain remnants of pluvial-Lake Palomas in the Zona Hidrogeológica Conejos Médanos (ZHGCM) area: Lagunas Guzman, Santa Maria and Patos, and El Barreal-Salinas de Uníon. Only small parts of the Mesilla Basin and Hueco Bolson have surface-flow connection with Rio Grande at present (Hawley et al. 2000 and 2009). 2018 Google Earth® image base.

Table 8-4. Explanation of Figure 3-15 Alpha-Numeric Symbols for Pliocene and Early Pleistocene Distributive Fluvial Systems (DFSs) of Ancestral Rivers with Fluvial-Deltaic Termini in the Paleo-Lake Cabeza de Vaca (LCdV) Complex

---

A. APEX AREA OF THE ANCESTRAL RIO GRANDE-CAMP RICE FM DFS (ARG-DFS) IN THE SOUTHERN JORNADA BASIN, HUECO BOLSON, AND LOS MUERTOS BASIN (BdLM) —RED LINES

A1. Eastern Rincon Valley head of the ARG-DFS distributary-channel complex in the Southern Jornada Basin.

A2. Upper Selden Canyon head of the ARG-DFS distributary-channel complex in the central and eastern Mesilla Basin area.

A3. Lower Selden Canyon head of the ARG-DFS distributary-channel complex in the western Mesilla Basin area.

A4. Cedar-Corralitos Basin head of the ARG-DFS distributary-channel complex in the northwestern Mesilla and northeastern Mimbres Basin areas.

A5. Fillmore Pass head of the ARG-DFS distributary-channel complex in the western Tularosa Basin and northwestern Hueco Bolson area (**Fig. 1-15**, Seager 1981 [Fig. 84]).

A6. South-central Mesilla Basin head of the ARG-DFS distributary-channel complex in the El Parabién Basin-Paso del Norte area.

A7. Southeastern Mesilla Basin head of the ARG-DFS distributary-channel complex in the El Parabién Basin, Méndez-Vergel Corridor, and southwestern Hueco Bolson area.

A8. Southwestern Mesilla Basin head of the ARG-DFS distributary-channel complex in the El Parabién Basin and the northeastern LCdV-BdLM.

A9. South-central termini of ARG-DFS fluvial-deltaic distributaries in the northeastern LCdV-BdLM.

A10. Southwestern termini of ARG-DFS fluvial-deltaic distributaries in the northwern LCdV-BdLM.

B. APEX AREA OF THE ANCESTRAL RIO MIMBRES-UPPER GILA GP DFS (ARM-DFS—YELLOW LINES) IN THE NORTHERN LCdV-BdLM

B1. Southeastern Mimbres Basin head of the ARM-UGDFS fluvial-deltaic distributaries.

B2. Southern termini of ARM-DFS fluvial-deltaic distributaries in the norrn LCdV-BdLM.

C. APEX AREA OF THE ANCESTRAL RIO CASAS GRANDES-BOCA GRANDE DFS (ARCG-DFS—VIOLET LINES) IN THE NORTHWESTERN LCdV-BdLM

C1. Head of ARCG-BGDFS fluvial-deltaic distributaries in the northwestern LCdV-BdLM

C2. Eastern termini of ARCG-DFS fluvial-deltaic distributaries in the northwern LCdV- BdLM

D. APEX AREA OF THE ANCESTRAL RIO SANTA MARIA DFS (ARSM-DFS—PINK LINES) IN THE SOUTHWESTERN LCdV-BdLM

D1. Eastern termini of ARSM-DFS fluvial-deltaic distributaries south of Laguna Santa Maria.

D2. Western termini of ARSM-DFS fluvial-deltaic distributaries south ofguna Fresnal

E. APEX AREA OF THE ANCESTRAL RIO CARMEN DFS (ARC-DFS—ORANGE LINES) IN THE SOUTHEASTERN LCdV-BdLM

E1. Eastern termini of ARC-DFS fluvial-deltaic distributaries in the southeastern LCdV-BdlM near Villa Ahumada and Laguna Patos.

E2. Western termini of ARC-DFS fluvial-deltaic distributaries northwest of Carrizal in the southeastern LCdV-BdLM

The other prominent hydrogeologic features of the MBR's intermontane-basin landscape are the parts of the Bolson de los Muertos and Tularosa Basin that were inundated during high stands of pluvial-Lakes Palomas and Otero in the last Pleistocene glacial stage (about 29-12 ka; **Fig. 8-8**; **Parts 7.2.2** and **7.6.2**). During the past 400 to 500 ka, relatively short intervals of valley and canyon cutting coincided with at least four major stages of Pleistocene glaciation in the river's Rocky Mountain headwaters' region, and partial back-filling of valley floors was associated with longer interglacial intervals (**Parts 3.7.3**, **3.7** and **3.9**).

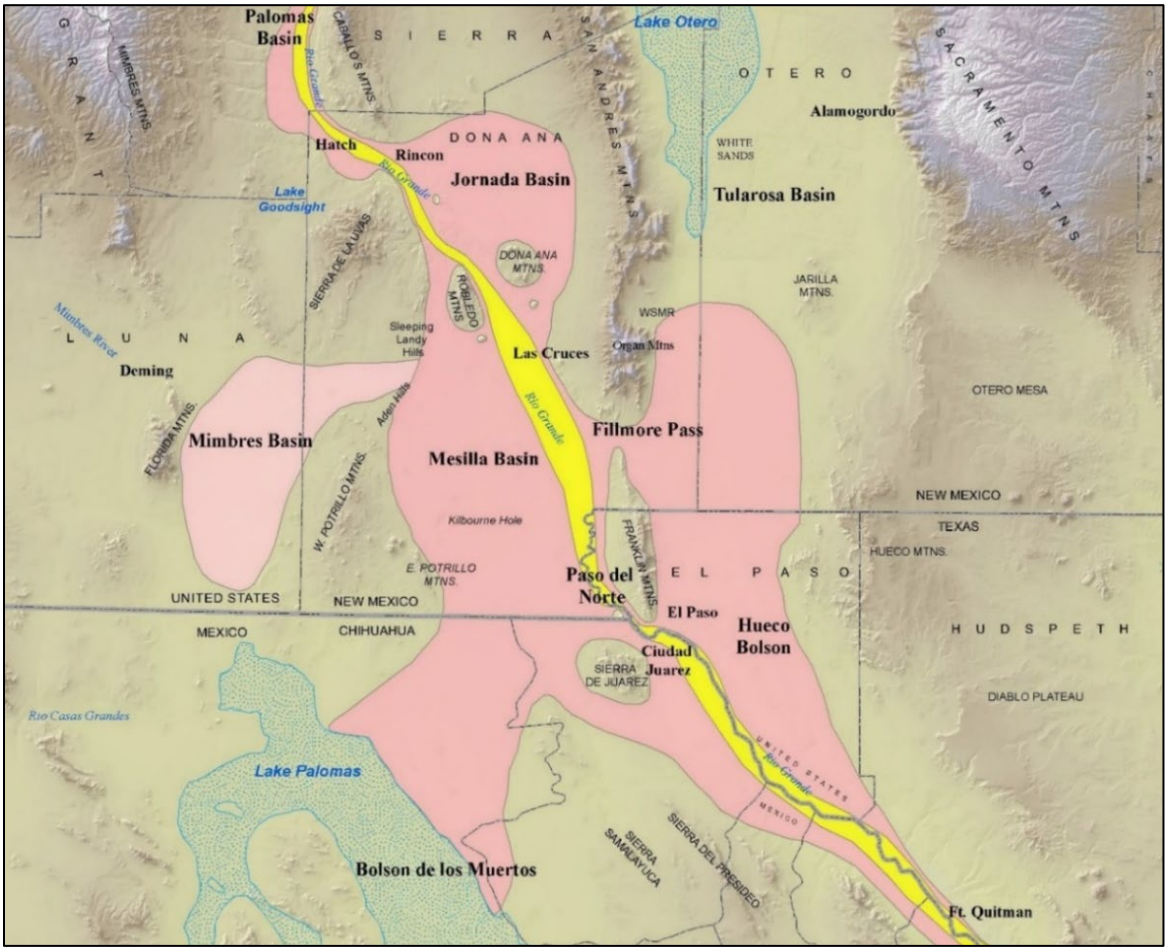

Figure 8-8 (Hawley et al. 2009, Fig. 10; USGS DEM base)**.** Schematic depiction of major Quaternary-landscape features of the Mesilla Basin region. The approximate area covered by the Ancestral Rio Grande (ARG) distributary drainage network that spread out from a trunk-ARG channel system in the Palomas Basin is in pink. The deeply entrenched Rio Grande/Bravo Valley and Canyon system is in yellow. The stipple pattern covers the basin-floor areas occupied by deepest Late Pleistocene stages of two large pluvial lakes: Palomas (Los Muertos basin area) and Otero (Tularosa Basin). Remnants of Early Pleistocene, ARG fluvial-deltaic plain comprise the "La Mesa geomorphic surface (Hawley and Kottlowski 1969)." The RG-rift "Bolson de los Muertos/Los Muertos Basin" complex of Chapin and Seager (1975) is located in the "Acuifero Conejos Médanos" section of the northern Zona Hidrogeológica de Conejos Médanos (**Figs. 1-10**, **1-11**, and **3-3**).

Table 8-5. Major Stages of Hydrogeologic-Framework Development during the Past 30 Ma

1. Deposition of the Late Oligocene to Mid-Miocene, Lower Santa Fe Group (SFG) deposits in endorheic, early-stage RG-rift basins. Partly consolidated, sand-dominant eolian and piedmont-alluvial facies are the primary components of deep aquifers that are presently known to occur beneath the east-central Mesilla Valley (MeV).
2. Deposition of the Mid- to Late-Miocene, Middle SFG basin fill in actively subsiding RG-rift basins during a transitional period of Upper RG drainage-basin evolution from endorheic to early-stage exorheic. Thick, partly consolidated, sand-dominant eolian and alluvial/fluvial facies of the Middle SFG Hydrostratigraphic-Unit (MSF2) are the primary aquifer-system components beneath the central and southern parts of the Mesilla GW Basin (MeB).
3. Deposition of Pliocene and Lower Pleistocene, Upper SFG basin fill during an interval marked by presence of an Ancestral Rio Grande (ARG) fluvial-deltaic system that terminated in endorheic paleo-lake basins of the Hueco Bolson-Mesilla Basin-Zona Hidrogeológica de Conejos Médanos (ZHGCM) region. Sand-dominant ARG fluvial facies of Hydrostratigraphic-Unit USF2 are the primary aquifer-system component beneath the north-central part of the MeB.
4. The MeV is part of series of deep canyon and valleys cut by the Rio Grande-Bravo during at least four major intervals of fluvial erosion that correlate with Pleistocene glacial/interglacial cycles. Valley and canyon incision began about 0.75 Ma soon after integration of a through-going river that discharged in the Gulf of Mexico, with headwaters in the southern Rocky Mountain region (**Part 4.5**).
5. Intervals of river-valley/canyon entrenchment coincided with major mid- to late-Pleistocene glacial-interglacial cycles with 100 to 150 ka periodicity, which are generally correlative with cyclic formation of large pluvial lakes in adjacent parts of the endorheic Palomas and Los Muertos RG-rift basins. Conversely, interglacial stages, like the present Holocene Epoch (past 12 ka) are characterized by partial alluvial backfilling of inner river-valley/canyon areas, and they are generally coeval with intervals of ephemeral-lake plain formation aggradation in neighboring endorheic basins.
6. The final interval of deep, RG-valley/canyon incision occurred during the last full-glacial stage (~12 to 29 thousand years ago). At that time the river-channel in the Sunland Park-Courchesne Bridge reach was about 25 m lower that it is now (alt. ~1106-m amsl), and the water table altitude at the northeast edge of pluvial-Lake Palomas about 60 km to the southwest was about 1,210-m amsl (**Part 7.6.2**).
7. By the Early Holocene interglacial stage, however, discharge and sediment-load conditions in all but the river's headwater reaches were no longer conducive significant incision of the valleys and canyons of Middle and Lower Rio Grande/Bravo system, and the river's channel/floodplain base level (its associated water table) has remained in an essentially quasi-equilibrium (graded) position for at least the last 9,000 years.
8. Accelerating global-climate and associated regional-environmental changes may have already signaled the end of the well-documented glacial-interglacial cycles of the Quaternary Period, and the beginning of a recently proposed "Anthropocene Epoch"* in about 1950 CE. If so, planning horizons for water-resource management in this "Era of Uncertainty" are now only in the multi-decade range at best (e.g., Kahneman and Tversky 1974 and 1996, Crutzen and Stoermer 2000, Glennon 2002, Hawley 2005, Taleb 2010, Lewis 2016, Meixner et al. 2016, Jamail 2019, Overpeck and Udall 2020, Siegel 2020, Williams et al. 2020a, Brannen 2021, Davis 2021a-e, Zalasiewicz et al. 2021, C. Allen 2022; *cf.* **Tbl. 1-3**, **APNDX. G**).
   ***Anthropocene (a provisional name proposed by Crutzen and Stoermer 2000 [cf. Zalasiewicz et al. 2021]); https://www.nytimes.com/2024/03/05/climate/anthropocene-epoch-vote-rejected.html?unlocked_article_code=1.aU0.Yoaa.8m5-c7KcfueD&smid=em-share*

8.5. CHALLENGES TO LONG-TERM GW-RESOURCE DEVELOPMENT IN THE U.S. PART OF THE MESILLA BASIN REGION

Prospects for long-term GW-resource development are especially problematic in dryland areas like the Mesilla Basin region (MBR) where (1) both surface- and subsurface-water supplies are limited, (2) watershed-runoff conditions related to regional and basin-scale climate change remain uncertain, (3) the population now exceeds two million, and (4) binational and tristate institutional structures play a key role in water resources management (**Part 8.3**; **APNDS. E** and **H**). In this respect, evaluation of options for GW-resource development should only be regarded as starting points in an intensive, expensive, and time-consuming iterative process of hydrogeologic-framework characterization. This is a case where positive or negative outcomes are best classed qualitatively as being in one of three broad conceptual categories: (1) possible to highly probable, (2) highly improbable but still possible, and (3) hydrogeologically impossible (*cf.* **APNDX. E3.3:** Black Swan Events).

8.5.1. The Rather Nebulous Concepts of Resilience and Groundwater Sustainability in the Context of Climate-Change and Resource-Management Realities

> "Reality is that which, when you stop believing in it, doesn't go away." **Philip K. Dick**
> https://en.wikipedia.org/wiki/Philip_K._Dick

Architect and urban planner Jon Penndorf* offers a contemporary view on "Resilience" *in* "Adapting for the effects of climate change:" Urban Land (2018), v. 77, no. 3, p. 78:

> The prospect of a changing climate and the natural impacts that accompany it must be met by each of us. Resilience means working with—instead of fortifying against—nature and the greater community. Resilience requires us to understand the patterns of how the natural environment works. And it demands that we design a built environment that aligns with those mechanisms for the long-term viability of humanity's investment [*cf.* McHarg 1969].
> **Jon Penndorf, FAIA, is a Senior Associate in the Washington, DC office of Perkins & Will, where he serves as Sustainability Leader and Project Manager. A member of the AIA Committee on the Environment (COTE) Advisory Group and regional representative to the AIA Strategic Council, he works to push the Institute and its members forward on the topic of resilience.*
> *https://aiau.aia.org/instructors/penndorf.*

8.5.2. The "Groundwater Sustainability" Concept (Alley, Reilly, and Franke, 1999, U.S. Geological Survey Circular 1186, p. 3):

> Perhaps the most important attribute of the concept of ground-water [groundwater] sustainability is that it fosters a long-term perspective to management of ground-water resources. Several factors reinforce the need for a long-term perspective. First, ground water is not a nonrenewable resource, such as a mineral or petroleum deposit, nor is it completely renewable in the same manner and time frame as solar energy. Recharge of ground water from precipitation continually replenishes the ground-water resource but may do so at much smaller rates than the rates of ground-water withdrawals. Second, ground-water development may take place over many years; thus, the effects of both current and future development must be considered in any water-management strategy. Third, the effects of ground-water pumping tend to manifest themselves

> slowly over time. For example, the full effects of pumping on surface-water resources may not be evident for many years after pumping begins. Finally, losses from ground-water storage must be placed in the context of the period over which sustainability needs to be achieved. Ground-water withdrawals and replenishment by recharge usually are variable both seasonally and from year to year. Viewing the ground-water system through time, a long-term approach to sustainability may involve frequent temporary withdrawals from ground-water storage that are balanced by intervening additions to ground-water storage [*cf.* Alley and Leake 2004, Alley and Alley 2017].

It is important to emphasize that most, GW-sustainability models appear to assume that only water of "fresh" quality (i.e., <1,000 mg/L TDS) is being considered. Groundwaters in productive aquifers of arid semiarid temperate regions, however, can have salinities that are significantly higher than 1,000 mg/L TDS (Stanton et al. 2017; *cf.* **Parts 1-1** and **8-2**). For example, slightly saline brackish groundwater (BGW - 1,000 to 3,000 mg/L TDS range) is the primary component of some productive basin-fill aquifers of the Mesilla Basin region (*cf.* **PL. 10D**, **Figs. 7-17** and **7-18**). In such cases, producible slightly saline BGW is here considered to be a major asset rather than a liability, especially where (1) state-of-practice R-O desalination technology is an environmentally and economically viable option, (2) effective strategies for desal-concentrate management are readily available, and (3) suitable hydrogeologic conditions for managed-aquifer recharge (MAR)* exist (EPW-ND, Archuleta 2010, NRC 2012, TWDB 2010 and 2015, Erlitski and Craver 2020, Wolf et al. 2020).

**Managed aquifer recharge (MAR): The practice of increasing, by artificial means, the amount of water that enters a groundwater reservoir (synonymous with the older term artificial recharge; NGWA 2014).*

Circumstances contributing to uncertainty in predictions of Long-Term GW-resource availability in the United States part of the MBR include: (1) a geographic setting in an arid/semiarid region where this already finite resource is subject to ever-increasing anthropogenic and climatic stresses, (2) impediments associated with binational/tristate issues of a legal, political, and socio-economic nature, and (3) the current absence of realistic assessment of the enormous costs that will be required for successful implementation of any plans for future large-scale aquifer-system development.

Prior to Elephant Butte Dam construction and initial "Rio Grande Project" deliveries in 1916, MBR aquifer systems were recharged by river-channel seepage (Historically intermittent), with a much smaller component derived from local ephemeral streams (arroyos) with large-upland watersheds (**Part 7.3**; Fig. 7-8; *cf.* Ikard et al. 2021, 2023). Much of the GW-reservoir in and near the Rincon, Mesilla and El Paso Valleys is now used conjunctively with "Rio Grande Project" surface water for irrigation-agriculture (I-Ag). Near river-valley floors, upper parts of the basin-fill aquifer system currently receives intermittent to perennial recharge from three primary sources: (1) Rio Grande Project irrigation return flow, (2) treated municipal wastewater, and (3) inflow from GW in basin-fill storage. "Project water" deliveries through canals, laterals, and increasingly efficient field-application practices are here considered to be essential for the long-term GW-resource availability (*cf.* Beene et al. 2020, Davis 2020f-

h, 2021b). However, the reliability of these deliveries is affected by: (1) ever-increasing water-user demands on the upstream Rio Grande watershed, (2) competition between I-Ag, and municipal and industrial (M&I) users of the limited fresh-GW reserves, and (3) the 21st Century realities of global climate change (**APNDX. E2.3**).

At increasing distances away from the inner Mesilla Valley, the percentage of the underflow contribution of older water stored in SFG basin fill and subjacent bedrock units also increases. Much of it is brackish (1,000-10,000 mg/L TDS), and it was only effectively recharged during glacial cycles with multi-millennial periodicity (*cf.* **Parts 5.3.2** and **5.4.1a**). For example, all of the effective recharge to aquifer systems in the southern MeB occurred more than 12,000 years ago during Late Pleistocene high stands of pluvial-Lake Palomas in northwestern Chihuahua. Nonetheless, opportunities clearly remain for long-term GW-resource development due to seven primary factors, most of which have significant hydrogeologic-framework component:

1. The fluvial origin, sedimentary composition, and great thickness of the RG-rift basin-SFG aquifer media (**CHPTS. 3**, **4** and **6**).
2. The quantity and quality of fresh to moderately brackish water stored in the SFG aquifer system (**CHPTS. 6** and **7**).
3. The substantial recharge role played by Rio Grande Project (RGP) water (**CHPT. 7**).
4. The material and human infrastructure involved in RGP and earlier-generation crop-irrigation activity (**APNDX. E**).
5. Optimum locations for managed aquifer recharge (MAR), and aquifer storage and recovery (ASR) activity (**CHPTS. 3** and **6**).
6. Optimum locations for desalination-plant and concentrate-management facilities (**CHPTS. 3**, **5** and **6**).
7. Many optimum sites for future solar-energy development, existing ones for natural-gas fueled electricity generation, some potential for future wind- and geothermal-energy projects (**CHPTS. 3**, **5** and **6**; *cf.* Robinson-Avila 2020a, b, Garland 2020).

A very effective conservation program, involving both surface-water and groundwater resources, was initiated by the El Paso Water Utility in the 1980s, and advanced systems of storm-water management are now in place for the urban/suburban watersheds of Las Cruces as well as El Paso (e.g., Garza et al. 1980; Knorr 1988, Knorr and Cliett 1985; Buszka et al. 1994; Archuleta 1995, 2010; Sheng 2005; El Paso Water ND). While significant progress has been from a surface-water perspective, existing RG-Compact provisions may still limit the options for managed aquifer-recharge (MAR) activity in the United States part of the MBR (*cf.* **APNDX. E8.2**). Hydrogeologic conditions beneath much of central

Ciudad Juárez are also ideal for a future large-scale MAR project, and there are no "RG-Compact" constraints on water-resource development (*cf.* **APNDX. H3.9**). On the other hand, advanced systems of storm-water management have yet to be developed for the large (~150 km^2/ 95 mi^2) urban/suburban watershed that includes much of eastern front of Sierra de Juárez.

8.6. VIABLE PROSPECTS FOR LONG-TERM GW-RESOURCE DEVELOPMENT IN THE UNITED STATES PART OF THE MESILLA GW BASIN

8.6.1. Background

The large size and river-connected nature of the SFG aquifer system in the MeB was first described in a hydrogeologic context by W.E. King and others (1969). Soon after its publication, Professor John W. Clark, P.E., former NMSU Civil Engineering Department Chair*, advised the report's authors not to be too optimistic in their estimates of the size and production potential of the reservoir's potable-GW component. He recognized that, while long-term aquifer-system development might be possible in terms of water quantity, its initial fresh-water component would eventually be replaced by progressively more-saline water derived from drainage of GW reservoirs in contiguous intermontane-basin and upland areas.

Second Director of the NM WRRI. In the late 1960s Prof. Clark provided independent civil-engineering consulting services for the C.L. Crowder Investment Company during the planning stages for Santa Teresa area development. (Part 6.3.4c**; cf. Pacheco 2018c).*

The following estimate** of the amount "of freshwater [that] could be pumped in the West Mesa" area was made for the NM Office of the State Engineer by C.A. Wilson and others (1981, p. 59):

> Assuming that the specific yields of the sand layers is 15 percent and that 60 percent of the freshwater zone is sand, about 34 million acre feet [42,000 hm^3] of freshwater could be pumped in the West Mesa. Additional water may be derived from clay unit in the aquifer. The very large volume of slightly saline water that lies beneath the freshwater zone is not considered in this calculation although this water may be suitable for some purposes.

While allowing for a very large Rio Grande Project (seepage-) recharge component to the shallow aquifer system in the MeV (**Fig. 7-9**), no geohydrologic work in the MeB has ever shown that the river has been the major contributor of recharge to basin-fill aquifers of the western part of the West Mesa area (**Parts 7.4.1**, **7.4.2**, and **8.4.2**; e.g., Frenzel and Kaehler 1992, Nickerson and Myers 1993, Teeple 2017).

***The estimate includes an assumption of freshwater-aquifer thickness that was based on their interpretation of "vertical electrical-resistivity sounding" geophysical surveys in the MeB West Mesa area (cf. Jackson 1976, and Nickerson and Myers 1993 [p. 55]).*

Hawley and Kennedy (2004, p. 76-77) made this preliminary estimate of aquifer "storage and production potential" in the MeB area as defined herein (**Figs. 8-2** and **8-3**):

> The most productive aquifers in the 1,100-mi^2 Mesilla "groundwater" basin are formed by 1) unconsolidated to weakly indurated basin fill of the upper and middle Santa Fe HSUs, and 2) overlying Mesilla Valley fill deposited by the Rio Grande (HSU RA). The total saturated thickness of the latter unit rarely exceeds 60 ft; while the *upper* and *middle* Santa Fe units extend from about 600 to 1,600 ft below the water table in the structurally deepest parts of the basin (. . .). Limiting assumptions used in this study for preliminary estimates of available water stored in the basin-fill aquifers of the Mesilla Basin: 1) the estimated average thickness of the unconfined to semi-confined part of the system is about 200 ft in an inner-basin area of about 1,000 mi^2, 2) specific yield is 0.1, and 3) quality is potable (or fresh, <1,000 mg/L TDS). If these assumptions prove to be valid, then our estimate of available water in storage is about 13 million ac-ft. Based on review of data in the Frenzel and Kaehler (1992) flow model, Balleau (1999, p. 46) estimated that about 14 million ac-ft of available fresh water is stored in the upper 100 ft of saturated fill in the West Mesa area (about 360,000 acres [145,690 hectares] in NM).
>
> Estimated average thickness of fill that is saturated with fresh to slightly saline water (< 3,000 mg/L TDS) is about 1,000 ft in the deepest parts of the Mesilla Basin. Since the areal extent of the deeper subbasins is about 750 mi^2, there could be as much as 480 million ac-ft of saturated, poorly consolidated basin fill in the central and eastern parts of the Mesilla Basin. As noted above, essentially all of the aquifer zones more than 200 ft below the potentiometric surface are confined or semiconfined. So even if an assumed "available porosity" value of 10% proves to be reasonable, there will always be large variation in our estimates of the amount of recoverable groundwater (as much as 50 million ac-ft [62,000 hm^3]), given the constraints imposed by technology, economics, environmental concerns, and socio-political forces.

The amount of economically recoverable water in the 500 to 3,000 mg/L TDS range in the upper part of the SFG aquifer system in the West Mesa section of the MeB is here estimated to be at least 30 million ac-ft (37,000 hm^3) (**Fig. 1-5**, *cf.* **Part 6.3**). Basic assumptions for this estimate include: A West Mesa area of about 500 mi^2 (1,300 km^2) with a 1000-ft (300-m) average saturated-zone thickness, unconfined to leaky-confined aquifer conditions, a specific yield (*Sy*) of 0.1, long-term increase in storivity (*S*) from a 1 x 10^{-4} base value to one approaching the *Sy* range (*cf.* West 1996, p. 22-23). Even allowing for a large Rio Grande Project (seepage-) recharge component to the shallow aquifer system in the MeV (**Fig. 7-9**), however, neither the Frenzel and Kaehler (1992) study nor any subsequent work suggests that the river has been the significant recharge contributor to SFG basin-fill aquifers of the western part of the MeB-West Mesa.

By way of comparison, C.A. Wilson and others (1981, p. 59) made the following estimate of how much "fresh [ground]water could be pumped in the West Mesa" area:

> Assuming that the specific yields of the sand layers is 15 percent and that 60 percent of the freshwater zone is sand, about 34 million acre feet [42,000 hm^3] of freshwater could be pumped in the West Mesa. Additional water may be derived from clay unit in the aquifer. The very large volume of slightly saline water that lies beneath the freshwater zone is not considered in this calculation although this water may be suitable for some purposes.*
>
> **Freshwater thickness is based on interpretation of first-generation "vertical electrical-resistivity sounding" surveys in the MeB West Mesa area (Jackson 1976; cf. Nickerson and Myers 1993 [p. 55])*

Estimates of aquifer storage capacities in the above-cited quantity ranges are also being made by water-resource economists and climatologists in their ongoing independent research on the potential impacts of climate change on parts of the Mesilla Basin region where groundwater and surface-water are "managed conjunctively." Ward and others (2019) developed and applied a basin-scale hydroeconomic optimization model of surface-water and groundwater use, which included the Mesilla Aquifer and Hueco Bolson. The study was designed to assess economic costs associated with several potential policies that could be implemented to support sustained aquifer protection.

The Ward (Ward et al. 2019) model incorporated several thousand pieces of data and optimized several hundred thousand variables to discover least-cost aquifer-protection measures, so considerable simplification of the aquifer/river system and institutions were required to make the model manageable. One major simplification of a non-hydrogeologic nature has been to approximate each aquifer as consisting of a large bucket full of aquifer material, an approach that has been done by a number of peer-reviewed published works in recent years (Maxwell and Miller 2005; Rassam et al. 2008; Rosero et al. 2011). The hydroeconomic modeling of Ward and others was based on estimates of the groundwater storage capacity and impacts of pumping for the Mesilla Aquifer and Hueco Bolson (their Fig. 1, and Tbls. 1 and 2; *cf.* Hawley et al. 2001, Hawley and Kennedy 2004, and Sheng 2013). Modeling assumptions for their "Mesilla Aquifer" include (1) an "Aquifer Storage Capacity" of 50,000,000 ac-ft (~61,675 hm^3), (2) a "storage coefficient" value of 0.10, and (3) a 1,100 mi^2 (2,850 km^2) "Plan View Area" of the "aquifer material," which includes SFG basin fill as defined by Hawley and Kennedy (2004).

Unlike the detailed assessment of the economically recoverable brackish-groundwater (BGW) reserves in the western Hueco Bolson that has been completed by El Paso Water (EPU), however, no entity to date has made the time-consuming and expensive attempt to quantify just how much BGW lies beneath the freshwater zone in the MeB's West Mesa area (*cf.* **Part 8.5.2**; Hutchison 2006, Hawley et al. 2009, Archuleta 2010, EPW-ND).

8.6.2. Potential Long-Term Pumping Effects on Aquifer-Framework Properties

The above-cited estimates of the large volumes of fresh to moderately brackish water in storage in the SFG aquifers of the central and western MeB illustrate challenges that face long-term GW-resource development throughout the Study Area. With use of state-of-practice well-development technology, it would be quite possible to extract (*mine*) 10 to 20 million ac-ft (12,335-24,670 hm^3) of nonrenewable fresh to moderately brackish water out of the SFG aquifer system in less than 100 years. The long-term challenge involves finding economically and environmentally viable ways to extend that relatively short timeline into a long-term sustainable GW-production process.

As noted in **Part 7.6.2**, pumping in the new Ciudad Juárez Junta Municipal de Agua y Saneamiento (JMASCJ) Well Field area already may be intercepting a significant part of the better-

quality GW in basin-fill storage that was initially recharged by Late Pleistocene underflow-discharge from pluvial-Lake Palomas (**Figs. 7-3**, **7-6** and **7-7**). While small static-water level declines have been reported in the few USGS monitoring wells that are located near the International Boundary, the aggregate effect of an increasing number of wells that tap the large thicknesses of semi-confined SFG aquifers in the eastern part of the IBZ on GW quantity and quality has not yet been accessed. As of the end of 2020, moreover, neither land-surface subsidence nor water-quality deterioration has been detected in the MeB north of the International Boundary.

One significant geotechnical problem encountered in actively developed GW basins relates to groundwater-pumping effects on aquifer-framework properties (*cf.* **APNDX. E3.1.1**):

> Land subsidence is a gradual settling or sudden sinking of the Earth's surface due to subsurface movement of soil or rocks. . . .
>
> Although subsidence can and does occur on geologic time scales as a result of natural forces, in this chapter we confine our discussion to subsidence that happens on a human time scale due to human actions. . . .
>
> The most serious and widespread type of land subsidence is that which occurs in response to the mining of groundwater and resultant compaction of aquifers. . . . Fluid withdrawal causes head to decrease that in turn causes effective stress to increase. The response of a compressible porous medium to increases in effective stress is compaction.
>
> *From Chapter 9 in "Introduction to Hydrogeology" by David Deming (2002, p. 240).*

Prudent consideration of the impacts of long-term pumping effects on framework properties of partly consolidated basin-fill aquifers (such as those in many parts of the MeB) involves recognition that the operation of groups of deeply penetrating, high-capacity wells may result in significant amounts of aquifer-media compaction/consolidation (*cf.* Poland et al. 1975, Helm 1982, 1984, 1994a, 1994b, Hanson 1989, Sheng and Helm 1994, Haneberg 1995, Haneberg and Friesen 1995, West 1996, Carpenter 1999, Burbey 1999, 2001, Galloway et al. 1999, Sheng et al. 2003, Bell et al. 2008). While land-subsidence and earth-fissure phenomena that are commonly associated with GW-pumping have yet to be reported in any part of the Study Area, their future appearance in parts of the Mesilla and Southern Jornada GW Basins that have experienced large potentiometric-surface declines is definitely possible (e.g., MacMillan et al. 1976, Land and Armstrong 1985, Abernathy and Small 1986, Kernodle 1992a, Heywood 1995, 2003, Shomaker and Finch 1996).

One hydrogeologic-framework feature of SFG deposits beneath the MeB-West Mesa (La Mesa) surface that mitigates against near-term aquifer-media compaction is their degree of overconsolidation. While site-specific studies have yet to be done in the MeB, initial work completed in a very similar hydrogeologic setting in the Albuquerque Basin indicates that major geotechnical problems related to aquifer-media compaction can be avoided through prudent long-term well field operation. Because of its seminal nature, the following extended summary of the Albuquerque Basin study by NM Bureau of

Geology Engineering Geologist, W.C. Haneberg (*former Kentucky State Geologist*) is included here (Haneberg 1995, p. 90):

> . . . . [T]here is no convincing evidence of widespread land subsidence in the Albuquerque area despite heavy pumping and water-level decreases that locally exceed 50 m (see Thorn et al., 1993 for water-level decline maps). In contrast, water-level decreases of 35 m and less have produced widespread land subsidence and earth fissures in the Mimbres Basin south of Deming, New Mexico (Contaldo and Mueller, 1991; Haneberg and Friesen, 1995). The most likely explanation for the lack of subsidence in and around Albuquerque is that the upper Santa Fe Group aquifer system is overconsolidated, meaning that in the past the aquifer system has been subjected to greater lithostatic stress than it is being subjected to today. Holzer (1981) has shown that if an aquifer system has been overconsolidated, land subsidence is minimal until the reduction in effective confining stress brought about by ground-water overdraft exceeds the preconsolidation stress, which is the maximum effective stress to which the system has been subjected in the past. Because the groundwater exerts an up-ward-directed buoyant force on the aquifer skeleton, a reduction in water level (and therefore pore-water pressure) is mechanically equivalent to an increase in the weight of the overlying sediments. Once the preconsolidation stress is exceeded, according to the data collected by Holzer (1981), land subsidence occurs rapidly.
>
> The postulated overconsolidation of the upper Santa Fe Group aquifer system is probably a result of the Pleistocene incision of the Rio Grande valley, which produced geomorphic features such as the Llano de Albuquerque-a relic of the pre-incision basin floor-and stream terraces well above the current river level [*Hueco Bolson floor and Mesilla Basin-West Mesa hydrogeologic analogs*]. The difference in elevation between the Llano de Albuquerque and the modern river level suggests that as much as 100 m of sediment may have been removed from the center of the basin. Assuming that the pre-incision water table had the same relationship with the ground surface as did the Holocene predevelopment water table, the difference between the preconsolidation stress and the current effective lithostatic stress for the upper Santa Fe Group aquifer system should be equal to the buoyant unit weight of the basin fill multiplied by the depth of incision or, equivalently, the change in water-table elevation.
>
> Because the saturated unit weight of unconsolidated siliciclastic sediments is about twice the unit weight of water, the stress difference is approximately equal to the pressure at the base of a column of water equal in height to the inferred depth of incision (i.e., on the order of 100 ±20 m H_20 or 1000 ±200 kPa). The low values are obtained by using a saturated bulk density of 1,800 kg/m^3 the average values are obtained by using a saturated bulk density of 2000 kg/m^3 and the high values are obtained by using a saturated bulk density of 2,200 kg/m^3. Therefore, it appears that there is little potential for widespread subsidence in the immediate future. Over the long term, however, there is a considerable potential for widespread land subsidence if drawdown approaches the 80- to 120-m range. It must be emphasized, however, that the preconsolidation stress estimates given above are based on subjective geomorphic criteria and are therefore imprecise and highly speculative. More accurate estimates of the preconsolidation stress, which are necessary to adequately assess the subsidence potential, can be obtained either by laboratory testing of samples or by continuing to withdraw groundwater and noting the amount of draw down that is necessary to induce widespread land subsidence in the Albuquerque area [*in a similar MeB hydrogeologic setting*].

8.6.3. Inner Mesilla Valley Area

The Mesilla Valley (MeV) floor is the only part of the MeB where (1) a large perennial to intermittent stream is present, and (2) the water-table remains within 100 ft (30-m) of the land surface (e.g., Nelson and Holmes 1914, Conover 1954, Richardson et al. 1972, Wilson et al. 1981; *cf.* **Fig. 8-4**; **Parts 3.2.3b**, **3.8** and **7.4.1**). As documented in the following *Historical Note*, irrigation agriculture on the river floodplain dates back to the late Spanish Colonial-early Republic of Mexico era (*cf.* **APNDX. H 3.2.6**):

> BRAZITO settlement; 5 mi (8 km) S of Las Cruces. The Spanish *brazito* means "little arm," or "tributary": and the name of this Hispanic settlement on the Rio Grande has been attributed to "arms," or branches, of the river marshlands near the site, though the name also has been interpreted to mean "little bend on the river." . . . . About 1822 the *Brazito Land Grant,* extending 8 miles along the Rio Grande S. of Las Cruces, was made to Juan Antonio García [de Noriega]. . . . (Julyan 1996, p. 49).

While some groundwater was used for crop irrigation prior to Rio Grande Project (RGP) development, widespread supplemental use of groundwater for crop and orchard irrigation did not start until the 1950s (*cf.* Barker 1898, Follett 1898, Slichter 1905b, Lee 1907, Nelson and Holmes 1914, Conover 1954, C.A. Wilson et al. 1981, Esslinger 1996, Walton et al. 1999). According to Esslinger (1998, p.101-102):

> Throughout the history of the [Rio Grande] Project, there has been an increasing use of groundwater to supplement the supply of surface water available from the Rio Grande. This use of groundwater commenced at least as early as 1940s and probably earlier. In the early and mid-1950s, the Rio Grande Project in New Mexico suffered water shortages because of a series of droughts in the watershed of the upper Rio Grande in Colorado and New Mexico and because of the up-stream use of water in excess of Rio Grande Compact entitlements. This severely impaired the ability of the members of the irrigation district to continue to grow crops with surface water, and led to increased groundwater pumping in the early and mid-1950s. Most of these wells have been drilled into thelllow aquifer which constitutes the Rio Grande alluvium, and others have been drilled into the underlying aquifer known as the Santa Fe Formation [Group] (*cf.* **APNDX. E3.3.5**).

RGP surface-water delivery to the Rio Grande Project (RGP) continues its essential function as the primary recharge contributor to the MeV's shallow aquifer system (**Fig. 1-6**; **APNDX. E3.3.8**). From a Historic and cultural perspective, one rarely mentioned resource is the multi-generational *Human Infrastructure* that has existed in the Mesilla and Rincon Valley area since the Civil War, and which remains available for meeting many of current and future water-resource management challenges. Beene and others (2020, **Part 7.3.1**) offer a contemporary perspective on the essential geohydrologic role that irrigation agriculture continues to play in terms of "feedbacks of irrigator decisions, hydrologic change and long-term water planning [in the] Mesilla Valley."

8.6.3a. Options for Long-Term GW-Resource Development

The Mesilla Valley (MeV) is of primary of interest in all GW-resource assessments because of two basic hydrogeologic-framework components (**Parts 3.2.3** and **8.4.1**):

1. It includes the only river-channel and floodplain area in the southern New Mexico region that has perennial source of high-quality surface flow from a 28,000 mi^2 (72,520 km^2) watershed with headwaters in the Southern Rocky Mountains province (*cf.* **Parts 3.1.5a** and **7.4.1**).
2. It is also the only large area where Rio Grande-alluvial fill (HSU-RA) is hydraulically well-connected with great thicknesses of SFG basin fill that forms the MeB's primary aquifer system (*cf.* **Figs. 7-2, 7-15** 'nd **8-2** 'Sections'C-C' to J-J' and O-O']; **PLS. 5c** to **5j** and **5o**).

As noted in **Part 3.2.3**, two key factors in long-term availability of both surface- and subsurface water-resource in GW basins downstream from Caballo Dam involve (1) the enormous scale of RGP modifications of river-channel and contiguous-floodplain environments, and (2) the essential role played by efficient reservoir-management practices in terms of storage in and deliveries from Elephant Butte and Caballo Reservoirs (e.g., **Fig. 1-8**; *cf.* Esslinger 1996 and 1998, Glover 2018 [p. 63], **Part 8.5.2a**; **APNDX. E3**). While the material and human infrastructure is already in place, the major challenge facing future generations of project managers involves finding an optimum balance between competing reservoir uses that (1) minimize evaporative losses and maximize downstream deliveries or (2) maximize evaporative losses and permit at least seasonal recreational activity. When placed in the context of 1938 Rio Grande Compact delivery obligations, strategies for water-resource management throughout the Upper RG-Basin will also be faced with similar challenges (e.g., Walton et al. 1999, Ortega-Klett 2000, Flannigan 2007, Hernandez 2012b-c, Bryan 2020, Davis 2020a-d, Pacheco 2020c, Davis 2021a-b, Bryan 2023).

The following review of opportunities for and challenges facing future groundwater-resource development in the MeV is presented from the perspective of the two inner-valley hydrogeologic settings where irrigation-agricultural and M&I activities are concentrated: (1) the channel and floodplain of the Rio Grande, and (2) contiguous valley-border areas (**Parts 6.3.1**, **6.3.3** and **6.3.4**). While not covered in this discussion, the vulnerability of the shallow aquifer systems of the inner Mesilla Valley to anthropogenic contamination is an ever-present challenge (*cf.* **APNDX. E5**).

8.6.3b. Hydrogeologic Factors Affecting Surface-Water and GW Connectivity in the MeV

Emphasis here is on hydrogeologic subdivisions of eastern MeB where the thin alluvium of the Mesilla Valley floor and valley-border alluvial deposits (HSUs-RA and VA) are superimposed on thick, saturated SFG basin fill. They comprise, in north-to-south order '**Fig. 8-2** Section O-O'-O" [**PL. 5o**]):

1. Fairacres Subbasin (FASB-**6.3.3b**), and contiguous parts of the Las Cruces Bench (LCBn-**6.3.5a**).
2. Mesquite Subbasin (MSB-**6.3.4a**), and contiguous parts of the Las Cruces Bench and the Anthony-Canutillo Bench (ACBn-**6.3.5b**).
3. Black Mesa Subbasin (BMSB-**6.3.4b**), and contiguous parts of the Anthony-Canutillo Bench.

Because of their proximity to the inner valley of the Rio Grande, the Fairacres Subbasin (FASB), the Las Cruces Bench (LCBn), and the Mesquite and Black Mesa Subbasins (MSB and BMSB) are the only parts of the MeB where significant amounts of river-sourced GW recharge to the SFG aquifer system can occur (**Parts 6.3.3b**, **6.3.4a, b** and **6.3.5a**; **Tbl. 8-1**; **F'g. 8-2** 'Sections'C-C' to J-J' and O-O']; **PLS. 5c** to **5j** and **5o**; *cf.* Teeple 2017, Fig.47). It is also important to note that the FASB and MSB have indirect linkage to sources of good-quality, mountain-front recharge in the western Organ Mountains uplift (OMU-**5.1.1**).

Hydrogeologic factors affecting surface/subsurface-water connectivity on the MeV floor are schematically illustrated from a basin-scale down-valley perspective on **PLATE 5o**, and from a transverse-valley perspective on **PLATES 2A, 5c** to **5k** (e.g., **Figs. 7-9, 7-10** 'nd**''-2**: Secti'ns O-O''O", and C-C' to K-K'). Observed shallow-subsurface relationships in parts of Fairacres Subbasin (FASB-**Part 6.3.3b**) that are cr'ssed by'Sections C-C' to E-E' (**PLS. 5c** to **5e**) show that saturated, coarse grained basal-channel facies of HSU-RA are in direct contact with sand-dominant channel facies of HSU-USF2 in most of the Subbasin area (e.g., LFA2, *cf.* **Figs. 4-3** and **7-3**, **Tbls. 7-3** and **7-4**). While adjacent parts of the Mesquite Subbasin (MSB-**6.3.3c**) share the same overall hydrogeologic-setting, the HSU-USF2 deposits that underlie HSU-RA are composed primarily of the interbedded sand and silt-clay fluvial sediments of LFA3 (**PLS. 2A, 5o**, **5f-5h**; **Figs. 7-9, 7-10** 'nd''**-2**: Sect'ons O-O'-O" and F-F' to H-H').

Results of channel-seepage investigations reported by Nickerson (1998) and Teeple (2017) further document that MeV-floor area within the Fairacres and Mesquite Subbasins have been and will continue to be the optimum localities for recharge of the shallow aquifer system through utilization of innovative irrigation practices (including intermittent fallowing). As noted in **APNDX. E5.2**, however, this is also one of the most vulnerable parts of the Study Area with respect to GW-contamination potential (e.g., Creel et al. 1998, Kennedy 1999, Walker et al. 2015). In the Black Mesa Subbasin (BMSB-**6.3.4b**), the hydraulic connection between HSU-RA deposit and underlying USF2 basin fill is progressively less effective in a down-valley direction. Here, the HSF-USF2 section is erosionally truncated and fine-grained LFA-3 interbeds are more common (**PLS. 5o**, **5j** and **5k**; **Figs. 7-'** a'' **8-2**:'Sections'O'-O", I-I' and J-J'). Similar conditions prevail east of the Mesilla Valley fault zone (MVfz) in the adjacent parts of the Anthony-Canutillo Bench (ACBn-**6.3.5b**).

Further south in the southern ACBn and the Sunland Park outflow corridor (SPoc-6.3.5d), deep-well control and hydrochemical investigations demonstrate that Rio Grande Project irrigation practices

and river-flow are not effective aquifer-recharge mechanisms (**PLS. 2A, 5o** and **5k**; **Figs. 7-'** a'' **8-2**: Se'tions O'-O'' and K-K'). Rather, historic records of deep-well performance and GW quality show that (1) pre-development hydraulic head increased with depth, and (2) recharge contribution from the regional (partly Transboundary) GW-flow system had a significant upwelling component (*cf.* Leggat et al. 1962, Wilson et al. 1981, Frenzel and Kaehler 1992, Phillips et al. 2003, Hawley and Kennedy 2004, Witcher et al. 2004, Hogan et al. 2007 and 2012, Teeple 2017, Kubicki et al. 2021; **APNDS. C2** and **H8.4**).

8.6.3c. Managed Aquifer Recharge (MAR) Potential in Mesilla Valley Border Areas

Hydrogeologic-framework hydrochemical conditions are especially suited for managed aquifer recharge (MAR) activity in eastern and western parts of the Mesilla Valley (MeV) border where thick Upper SFG-ARG deposits (USF2: LFA 1-3) has a very thin or no cover of alluvial-valley fill, and direct-recharge from river-channel or tributary-arroyo seepage is seasonably available (e.g., Whitworth 1995, Bouwer 2002). In addition, each area includes ideal sites for both high-yield M&I water-supply well location, and water-treatment facility construction (e.g., Wolf et al. 2020). As noted in **Part 6.3.3b**, USF2: LFA 1-3 basin fills in the Fairacres Subbasin (FASB) and adjacent parts of the Mesquite Subbasin (MSB) have optimum MAR potential, especially in the Mesilla Valley-border area west of Mesilla Dam because of its proximity to the Rio Grande and the Stahmann Pecan Orchard complex (*cf.* **PL. 5d**, **APNDX. F: PLS. F3-1**).

The most favorable general locality for MAR operations is located in the north-central part of the LCBn in an area that includes the eastern Las Cruces metropolitan district, the main NMSU Campus, and most of the Las Cruces Municipal Well Field (*cf.* **Part 6.3.5a**; **Figs. 6-1** and **2-2** [**PL. 3]**; **TBL. 1**, nos. 102-114, 117-121, and 127; Wilson et al. 1981, Hawley and Kennedy 2004). Aquifers in this area comprise USF2 (LFA 2-3) deposits that are recharged primarily by seepage from the braided-channel networks of the Alameda, Las Cruces, Tortugas, and Fillmore Arroyos that traverse the Tortugas Uplift (TtU) and SJB-Talavera Subbasin (TSB), and have headwaters in the highest parts of the Organ Mountains Uplift (OMU; **Fig. 6-1**, **Tbl. 6-1; APNDX. F: PLS. F3-2c**). A very promising site for a MAR pilot project is in the large reservoir basin adjacent to Las Cruces Dam, a zoned-earthfill structure that is located south of US-70 and immediately east of I-25. The Dam is about 3 miles (6 km) long and was originally designed to retard storm runoff from the Alameda and Las Cruces Arroyo watersheds. The reservoir basin is of special interest because most of it is excavated in high-permeability HSU-USF2 (LFA 1-2) deposits that are ideally suited for temporary GW storage and recovery-well siting (*cf.* **Parts 1.3**, **4.2**, **7.5.1** and **8.4.1**).

8.6.4. Options for GW-Resource Development in the Mesilla GW Basin-West Mesa Area

From both hydrogeologic and climate-future perspectives (Dunbar et al. 2022), the challenges that face any type of GW-resource development in the 500 mi^2 (1,300 km^2) West Mesa area of the MeB are illustrated by the relative lack of detail in the hydrogeologic-subdivision descriptions (*cf.* **Parts 6.3.2** to **6.3.4)**. The pressing need for more accurate characterization of subsurface conditions is demonstrated in **Table 8-6** in which only 14 of the widely spaced boreholes have any high-quality information on hydrogeological, geophysical, and hydrochemical conditions in even the upper part of the SFG basin fill (e.g., **PL. 3** and **TBL. 1**; **Figs. 6-4** to **6-14**, **6-17** and **6-18**). In marked contrast to work in New Mexico, efforts to characterize basin-fill deposits from a GW-resource perspective have been underway in the Texas part of the Mesilla Basin-Hueco Bolson region for decades (e.g., Sayre and Livingston 1946, Knowles and Kennedy 1958, Leggat et al. 1962, Davis and Leggat 1965, Cliett 1969, Gates and Stanley 1976, Alvarez and Bruckner 1980, Buszka et al. 1994, Hutchinson 2006, Hawley et al. 2009, and El Paso Water [EPW] ND). Until work of this type is complete in the New Mexico part of the MeB, prudent GW-resource development will not be possible on a multi-generational Human-time scale. Above all, future management of the area's basin-fill aquifers must include effective water-conservation practices, such as MAR projects and a variety of proactive GW-pollution control measures.

Table 8-6. Number of Deep-Borehole Control Points in Selected Hydrogeologic Subdivisions of the MeB-West Mesa area (*cf.* PL. 3, Fig. 8-2, Tbl. 8-1 and TBL. 1)

6.3.2 Mid-Basin High (MBH)
- **6.3.2a.** North Mid-Basin High (NMBH) – 4 (**TBL. 1**, nos. 178-179, 180, 236, and 237; **Fig. 6-18**)
- **6.3.2b.** South Mid-Basin High (SMBH) – 1 (**TBL. 1**, no. 257, **Fig. 6-10**)

6.3.3a-e. Basin subdivisions north and west of the Mid-Basin High.
- **6.3.3b** Fairacres Subbasin (FASB) – 4 (**TBL. 1**, nos. 93, 146, 175, and 176; **Fig. 6-18**)
- **6.3.3c** Afton Subbasin (AfSB) – 0
- **6.3.3e** Kilbourne-Noria Subbasin (KNSB) – 2 (**TBL. 1**, nos. 295 and 296, **Fig. 6-10**)

6.3.4a-d. Basin subdivisions between the Mid-Basin High and Mesilla Valley fault zone
- **6.3.4b** Black Mountain Subbasin (BMSB) – 1 (**TBL. 1**, no. 242)
- **6.3.4c** Santa Teresa High (STH) – 2 (**TBL. 1**, no. 251, **Fig. 6-18**)

Due to the proximity to recharge sites in the MeV and the presence of large fresh-water reservoirs, MeB-West Mesa sites with greatest potential for long-term groundwater development are located in the northern Fairacres Subbasin and the Black Mountain Subbasin (FASB-**Part 6.3.3b** and BMSB-**6.3.3d**; *cf.* **Figs. 7-2** and **8-2**; **PLS. 5e** to **5j** and **5p**). On the other hand, while very large volumes of water in the 500 to 3,000 mg/L TDS range are stored in basin-fill aquifers in the western part of the MeB, none have received significant amounts of recharge from the Upper Rio Grande basin during at least the past 350 thousand years (**Parts 7.3** and **8.3**). This area includes much of the Mid-Basin High

(MBH-**6.3.2a** and **2b**) and three deep structural basins between it and the East Robledo and East Potrillo fault zones (ERfz and EPfz): (1) Southwestern Fairacres Subbasin (FASB-**6.3.3b**), (2) Afton Subbasin (AfSB-**6.3.3c**), and (3) Kilbourne-Noria Subbasin (KNSB-**6.3.3e**). The primary source of perennial GW recharge is from stored brackish water of Late Pleistocene age in basin-fill and contiguous bedrock terranes (**Figs. 7-6, 7-12** to **7-15**; **Parts 5.3**, **5.4,** and **7.5.3** to **7.5.5**; *cf.* King et al. 1971, Frenzel and Kaehler 1992, Teeple 2017).

8.6.5. Optimal Hydrogeologic Settings for Brackish GW (BGW) Development

As noted in the **Parts 1.1.1** and **8.4.1b**, all surface and subsurface waters in the fresh to moderately brackish range (<5,000 mg/L TDS) are here considered as assets rather than liabilities. This is definitely the case in parts of the Mesilla, Hueco and Tularosa Basins, where brackish groundwater (BGW) in the 1,000 to 3,000 mg/L TDS range is ideally suited for high-recovery reverse-osmosis (RO) membrane desalination (Hightower 2003, LGB–Guyton Associates 2003, TWDB 2015, Gude 2016, Erlitski and Craver 2020; *cf.* **Part 7.7.2**). The 27.5 mg/d (97.3 mL/d) Kay Bailey Hutchison desalination plant operated by El Paso Water (EPW) in the western Hueco Bolson provides an operating model for BGW desalination from an SFG-aquifer source that is hydrogeologically nearly identical to the MeB West Mesa aquifer system (Hawley and Kennedy 2004; Hutchison 2006; Hawley et al. 2009; Archuleta 2010; EPW-ND). Moreover, MeB-West Mesa aquifers with significant potential for GW production also include many optimal sites for future managed aquifer recharge (MAR) operations, such as those already applied with success in SFG aquifers of the western Hueco Bolson (*cf.* Knorr and Cliett 1985, Knorr 1988, Buszka et al. 1994, Archuleta 2010, EPW-ND). In addition to RO-membrane treatment, it is important to note that major advances are being made in other areas of desalination technology, many of which are designed to (1) operate at wide range of input-output scales, and (2) deal with a variety of concentrate-management options (*cf.* Davis 2020e).

Most of the remaining challenges to multi-scale BGW-resource development are associated with the legal and institutional impediments that will always exist in any binational, arid/semiarid region with such political and socio-economic complexity (e.g., Hawley and Swanson 2022). As indicated by the information in **Table 8-6**, moreover, no studies have been completed to date in the New Mexico part of the MeB for the express purpose of estimating either the amount of available BGW, or the production-capacity and life of wells that would tap into a BGW reservoir. Previous water-resource investigations have focused on the availability of fresh groundwater for a wide variety of agricultural, domestic, and M&I uses (*cf.* **APNDX. C**). With respect to irrigation-agriculture, moreover, the processing and disposal costs involved would make use of desalinated BGW unfeasible for food-crop and orchard irrigation

Emphasis here is on the Hydrogeologic Subdivisions of the MeB-West Mesa area that have (1) large inferred BGW reserves in aquifer storage, and (2) thick HSU-USF2/MSF2 basin fill that is

composed primarily of sand-dominant (LFA *2* and *3*) material with saturated hydraulic conductivities (Khsat) that range from 10 to 30 ft/day (3 to 10 m/day) (*cf.* **Fig. 7-7, PLS. 5f-k** and **7A-B**; **Parts 6.3.2a-b, 6.3.3b-e**, and **6.4b-d**). The more-productive BGW reservoirs, moreover, are expected to have relatively long-life expectancies due to progressive expansion into contiguous aquifer systems, many of which are already subject to pumping and increasing depletion of their freshwater component (*cf.* **Part 1.4.2**).

BGW produced from the southern MeB-West Mesa area could be processed at a proposed desalination plant that would be located near the Santa Teresa Industrial Park (**Part 6.3.4c**). As noted above, this facility's design and scale would be similar to that of the existing Kay Bailey Hutchison plant in the Hueco Bolson (e.g., EPW-ND, Archuleta et al. 2010). In this case, site selection and planning for plant construction could proceed with minimum delay. In addition, economically and environmentally viable sites for concentrate management activity, such as those described by Archuleta (2010, p. 27-28), are located at the western edge of the MeB in and adjacent to the East Potrillo Uplift (EPU) (**Parts 5.4.2** and **5.6.3**). Because of the potential for additional BGW production from the thick, HSU-USF2/MSF2 aquifer zones in the West Mesa area west of Las Cruces (CoLC, **Part 6.3.3b**), it also will be prudent to start planning for construction of a smaller-scale desalination plant near the site of CoLC Well No. 36 (**TBL. 1**, no. 96; *cf.* P.D.C. Mack 1985, Myers and Orr 1986, Nickerson and Myers 1993).

8.6.6. Sources of Energy for Groundwater Desalination and Other Purposes

Potential sources of energy for GW desalination in the MeB West Mesa include natural gas, nuclear, solar, wind, geothermal, and hydrogen. With the exception of wind and hydrogen, energy from all these sources is now being used for a variety of other M&I purposes in the Mesilla Basin region (Clayton et al. 2014), and energy from natural gas and solar sources is currently being supplied by the Public Service Company of New Mexico (PNM) and El Paso Electric Company (Robinson-Avila 2020a [p.15]; 2021a, b). Natural gas is the only readily available source of nonrenewable energy in the immediate MeB vicinity, and a well supplying the large PNM Afton Station electric-power plant in the North Mid-Basin High (NMBH) area has been in operation since 2006 (*cf.* **Part 6.3.2a**, **TBL. 1**, no. 178; **Tbl. 8.2**).

8.6.6a. Geothermal

The potential for development of the geothermal-energy resources of the basins and bordering bedrock uplands of the MBR has long been recognized, and new technology has transformed this potential into an economically viable option (Swanberg 1975; Gross and Icerman 1983; Icerman and Lohse 1983; Snyder 1986; Ross and Witcher 1998; Witcher 2010; Witcher and Mack 2018; Robinson-Avila 2023a-d; Boetel 2024a; Gleason 2024a, b). Of special relevance to this investigation, moreover, is the more-detailed documentation of geothermal-resource availability in "Salinity contributions from

geothermal waters to the Rio Grande and shallow aquifer system in the transboundary Mesilla Basin (Pepin et al. 2022)."

8.6.6b. Hydrogen

The viability of the use of hydrogen (H^2) as a major source of energy to produce electricity, heat, and automotive power is still being investigated (Norvelle 2021; Polich 2021; Robinson-Avila 2021c- e; McBranch 2023; Romero 2023). Technologies for two sources of H^2 production are now in early stages of development: (1) "Blue hydrogen" that is extracted from methane (CH^4), and (2) "Green hydrogen," which has no emissions and is produced by splitting water (H^2O) by electrolysis. The latter process, however, requires large quantities of electricity and fresh water, with the latter already in short supply the Mesilla GW Basin, as well as in many or places with similar geohydrologic settings in the American Southwest. "Blue hydrogen," on the other hand," is easy to extract, but large amounts of the "greenhouse gas" CO^2 is produced in the process. In this case, large-scale application of "Carbon Capture and Storage (CCS)" technology will be required to ensure the economic and environmental viability of "Blue hydrogen" production. This definitely should not pose a problem in New Mexico, however, as stated by New Mexico Tech Physics Professor, Dr. Van Romero in a recent op-ed piece in the Albuquerque Journal (2023, p. A9):

> CCS technology is not new in New Mexico. New Mexico Tech, along with the University of Utah, Los Alamos National Lab, Sandia National Lab, and Pacific Northwest National Lab, have studied the storage of carbon dioxide by injecting 1.5 million metric tons of carbon dioxide into geologic formations over the 20-year course of the study. The goal was to ensure the long-term safety of the carbon storage, ensuring that we can safely extract energy from blue hydrogen without concern about adding to the growing carbon crisis.
>
> Mother Nature also shows us that natural carbon dioxide deposits, discovered in [northeastern] New Mexico in 1917 in a formation known as the Bravo Dome, have been successfully stored for over a million years. The Bravo Dome is one of nine known natural occurring reservoirs of carbon dioxide in the United States that stretch from Montana to New Mexico to Mississippi. Clearly, Mother Nature has demonstrated that carbon dioxide can be permanently sequestered in geologic formations. There is no reason to believe that new carbon storage projects will have different outcomes.

8.6.6c. Solar

While still in initial stages of development, solar energy is now the most promising 21st Century renewable energy resource in mid-latitude, arid to semiarid intermontane-basin and plateau-plains regions of North America (Muñoz-Meléndez et al. 2012, p. 211; *cf.* Robinson-Avila 2020a, 2020e, 2020h, 2021a, b). Sparsely populated Chihuahuan-Desert terrains of this type are the dominant landscape features of the Mesilla Basin region (*cf.* **Figs. 1-13** and **14**; **Part 3.3**). Perhaps the most significant challenge that solar energy now faces relates to an international trade dispute that may have a major impact on the essential-component supply chain (Robinson-Avila 2022d-g). Development of the region's wind- and geothermal-

energy also has some potential. Many favorable sites for both wind-farm and geothermal well-field location, however, are now in places with restricted access due to current federal-government environmental regulations, or International-Boundary security concerns (*cf.* **5.4.1**, **5.4.2** and **5.6.1**; **APNDX. H**).

8.7. CONCLUDING REMARKS

8.7.1. Recommendations for Future Hydrogeologic Investigations in the MBR

Recommendations for future hydrogeologic investigations in the MBR must be made in the context of the myriad 21st Century challenges that face water-resources conservation in an arid/semiarid region where the impact of climate change is a reality not a supposition (e.g., **APNDX. E4**). As noted in **Part 8.6.1**, any type of long-term GW-resource development throughout the Mesilla GW Basin (MeB), but especially in the West Mesa area (**Parts 6.3.2** to **6.3.4**), faces major challenges related to the availability of adequate-funding sources.* While the science and technology used in characterization of deep-subsurface conditions are well-developed in the fields of oil and natural-gas exploration, this is clearly not the case when detailed assessment of groundwater- and geothermal-reservoirs is concerned. In **Table 8-6**, for example, only 14 widely spaced boreholes are listed that have any good-quality information on geohydrologic, geophysical, and hydrochemical conditions in the SFG basin fill (e.g., **PLS. 3** to **5** and **7**, and **TBL. 1**; **Figs. 6-4** to **6-14**, **6-17** and **6-18**). In marked contrast to the New Mexico section of the MeB, well-funded efforts to acquire this type information have been underway in the Texas parts of the western Hueco Bolson, and southeastern Mesilla Basin for decades (e.g., Knowles and Kennedy 1958, Leggat et al. 1962, Gates et al. 1984, Archuleta 1995, 2010, El Paso Water ND).

**The 60 million dollars that has recently been invested by the U.S. Department of Interior "to address drought resiliency in the Rio Grande south of Elephant Butte" Reservoir, while primarily allocated for improved surface-water management, will be of significant benefit to managed-acquifer recharge in many parts of the MBR. (Cook 2024)*

Because of the test-well drilling and logging expenses involved, estimated costs for detailed hydrogeologic-framework characterization in just the Mesilla Valley (MeV) and West Mesa parts of the MeB are conservatively in the 25-to-50-million-dollar range. Only when information of this quality is available, however, can planning for prudent GW-resource management be possible from a multi-generational Human-time perspective. Above all, such plans must involve effective water-conservation practices that must include a variety of proactive GW-pollution control measures (*cf.* **APNDX. E**).

8.7.2. A "Design with Nature Now" Approach to GW-Resource Development in the MBR

An idealistic, but still realistic, "Design with Nature Now" approach to planning for long-term natural-resource development applies directly to future development of the MBR's GW resources (Steiner et al. 2019). The concept is succinctly summarized by three co-editors of a collection of papers compiled

in honor of visionary landscape architect and planner, Ian L. McHarg on the 50th Anniversary of the publication of his classic "Design with Nature" (*cf.* McHarg 1969):

> **What does it mean to design with nature now?**
>
> Renowned for his book "Design with Nature" Ian L. McHarg (1920-2001) was one of the most influential environmental planners and landscape [a]rchitects of the 20th century.
>
> By "design with nature" McHarg meant that the way we occupy and modify the earth is best when it is planned and designed with careful regard to both the ecology and the character of the landscape. In this way, he argued that our cities, industries and farms could avoid major natural hazards and become truly regenerative. More deeply, McHarg believed that by living with rather than against the more powerful forces and flows of the landscape, communities would gain a stronger sense of place and identity.
>
> McHarg did more than write and talk about these ideas. He developed practical planning and design techniques to make them real, and then he put his theory into action around the world.
>
> McHarg was prescient and his philosophy and idealism underpin the [McHarg] Center's mission to this day. But, in a world as complex and fluctuating as todays, we must continually ask: what do we mean by design, and what we mean by nature?
>
> We consider nature to be an all-inclusive, evolving system of which humans have substantial yet incomplete scientific and cultural knowledge. We believe terrestrial nature, i.e., 'the landscape' is best understood as simultaneously an ecosystem and a cultural system—a recognition that urban agglomeration economies and rural processes of extraction and transport now form a planetary network.
>
> Carefully reading the landscape in this way is the prerequisite for consciously designing our future; using artistic creativity and scientific intelligence to shape the landscape in the best long-term interest of all living things.
>
> After centuries of mistakenly believing we could exploit the landscape without consequence (design without nature) we have now entered an age of extreme climate change marked by rising seas, resource depletion, desertification, ecosystem migration, and unprecedented rates of species extinction. Set against the global phenomena of accelerating consumption, ubiquitous urbanization and rising inequity, these environmental changes are impacting everyone, everywhere. Adapting our cities and their infrastructure to these conditions of rapid environmental change is the central design and planning challenge of the 21st century.
>
> The McHarg Center's purpose is to meet this challenge by providing a platform for environmental and social scientists, planners, designers, policy makers, developers and communities to unite and to research and design new ways of improving the ecological performance and quality of life in cities and towns worldwide.
>
> As we begin to understand the true complexity and holistic nature of the earth system, and begin to appreciate humanity's impact within it, we can build a new identity for society as a constructive part of nature. This is ethical. This is optimistic. This is a necessity.
>
> This is what it means to "design with nature".* **
>
> **Richard Weller, Frederick Steiner, and Billy Fleming—McHarg Center at the University of Pennsylvania, Weitzman School of Design*
> *https://mcharg.upenn.edu/what-does-it-mean-design-nature-now-0*
>
> ***References cited in the Report and/or **APPENDIX E** that relate (directly or indirectly) to the "Design with Nature Now" topic*: Newell 1963, McPhee 1989, Reisner 1993, Boulton et al. 2002, Glennon 2002, Taleb 2010, Kolbert 2014, Lewis 2018, Penndorf 2018, Alley and Alley 2017 and 2020, Overpeck and Udall 2020, Paskus 2020, Siegel 2020, Williams et al. 2020, Zalasiewicz et al. 2021, Brannen 2022, Dunbar et al., 2022.

CITED REFERENCES IN NM WRRI-TCR 363

Alphanumeric Topical Cross-Referencing Codes for APPENDIX B Entries

Abernathy, G.H., and Small, F.P., 1986, Field measurements of stress changes in an aquifer matrix during pumping cycles-Final Report to S.E. Reynolds, N.M. Interstate Streams Commission: Civil, Agricultural and Geological Engineering Department, N.M. State University, 99 p. **(H1, H2, H3)**

Adams, D.C., and Keller, G.R., 1994, Crustal structure and basin geometry in south-central New Mexico, *in* Keller, G.R., and Cather, S.M., eds., Basins of the Rio Grande rift: Structure, stratigraphy and tectonic setting: Geological Society of America Special Paper 291, p. 241-255. **(C2b, C4)**

Ackerly, N.W., 1999, The evolution of the Rio Grande, *in* Ortega Klett, C.T., ed., Proceedings of the 43rd Annual New Mexico Water Conference: Water Challenges on the Lower Rio Grande. New Mexico Water Resources Research Institute, Report No. 310, p. 26-32. *This is an excellent introduction to the historical river-flow record.* **(B2, B3)**

Ackerly, N.W., 2000, Paleohydrology of the Rio Grande, *in* Ortega Klett, C.T., ed., Proceedings of the 44th Annual New Mexico Water Conference: The Rio Grande Compact: It's the law! New Mexico Water Resources Research Institute, Report No. 312, p. 113-123. **(B2, B3)**

Ackermann, H.D., Pankratz, L.W., Klein, D.P., 1994, Six regionally extensive upper-crustal refraction profiles in southwest New Mexico: U.S Geological Survey Open-File Report 94-965, 6 p. *See Klein 1995.* **(C4)**

Adorno, R., and Pautz, P.C., editors and translators, 1999, Álvar Núñez Cabeza de Vaca, "*Relation* of 1542," *in* Álvar Núñez Cabeza de Vaca: His Account, His Life, and the Expedition of Pánfilio de Narváez: Lincoln, University of Nebraska Press, 212 p. ISBN 13: 9780803264168 **(B3)**

Akhtar, A., 2021, The Singularity is here – Artificially intelligent advertising technology is poisoning our societies: The Atlantic Dispatches-Opening Argument, v. 328, no. 5, p. 17-21. **(A2)**

Albritton, C.C., Jr., and Smith, J.F., Jr., 1965, Geology of the Sierra Blanca area, Hudspeth County, Texas: U.S. Geological Survey Professional Paper 594-J, 131 p. **(C2a, D1, F1)**

Albuquerque Journal (ABQ Jrnl), 2019, Union Pacific upgrading facility in Santa Teresa: Albuquerque Journal–METRO & NM, May 5, 2019, p. C2. **(A3)**

Albuquerque Journal (ABQ Jrnl), 2020, New runway finished at Doña Ana Jetport: Albuquerque Journal–METRO & NM, Nov 24, 2020, p. A8. **(A3)**

Al-Garni, M.A., 1996, Direct current resistivity investigation of groundwater in the lower Mesilla Valley, New Mexico and Texas: Colorado School of Mines, master's thesis, 126 p. *See Zohdy et al. 1976.* **(C4, H2)**

Allen, B.D., 2005, Ice Age lakes in New Mexico, *in* Lucas, S.G., Morgan, G.A., and Zeigler, K.E., eds., New Mexico's Ice Ages: New Mexico Museum of Natural History and Science Bulletin 18, 107-114. https://geoinfo.nmt.edu/staff/allen/documents/IceAgeLakesNM.pdf **(C1, I2)**

Allen, B.D., Love, D.W., and Myers, R.G., 2009, Evidence for late Pleistocene hydrologic and climatic change from Lake Otero, Tularosa Basin, south-central New Mexico: New Mexico Geology, v. 31, no. 1, p. 9-25. **(C1, I1, I2)**

Allen, C.D., 2022, IV. Climate change: Terrestrial ecosystem responses and feedbacks to water resources in New Mexico in New Mexico, *in* Dunbar, N.W., Gutzler, D.S., Pearthree, K.S., and Phillips, F.M., eds., Climate Change in New Mexico Over the Next 50 Years: Impacts on Water Resources: NM Bureau of Geology and Mineral Resources Bulletin 164, p. 37-53. **(B3, C1)**

Allen, J.R.L., 1965, A review of the origin and characteristics of recent alluvial sediments: Sedimentology (Special Issue), v. 5, no. 2, p. 91-191. **(D1)**

Alley, W.M., ed., 2013, Five-year interim report of the United States – Mexico Transboundary Aquifer Assessment Program: 2007-2012: U.S. Geological Survey Open-File Report 2013-1059, 31 p. **(A2, D1, F1)**

Alley, W.M., and Alley, R., 2013, Too hot to touch – The problem of high-level radioactive waste: New York, Cambridge University Press, 370 p., ISBN 978-1-107-03011-4 www.cambridge.org/alleyalley **(A2, D1, E2c)**

Alley, W.M., and Alley, R., 2017, High and Dry – Meeting the challenges of the world's dependence on groundwater: New Haven, CT, Yale University Press, 304 p., ISBN 978-0-300-22038-4 **(A2, D1)**

Alley, W.M., and Alley, R., 2020, The war on the EPA – America's endangered environmental projections: Lanham, MD, Rowman & Littlefield, 287 p., ISBN 978-1-5381-3151-3. *See Chapters 9 and 10: "Toxic Chemicals" and "The Forever Chemicals."* **(A2, D1, E2c)**

Alley, W.M., and Leake, S.A., 2004, The journey from safe yield to sustainability: Ground Water, v. 42, no. 1, p. 12-16. **(A2, D1)**

Alley, W.M., Reilly, T.M., and Franke, O.L., 1999, Sustainability of ground-water resources: U.S. Geological Survey Circular 1186, 79 p. **(A2, D1)**

Almada, F.R., 1968, Diccionario de historía, geografía, y biografía Chihuahuenses (2nd ed.): Chihuahua, México, Universidad de Chihuahua, 378 p. **(A1, A2, B3, C, F3)**

Alvarez, H.J., and Buckner, A.W., 1980, Ground-water development in the El Paso region, Texas, with emphasis on the resources of the lower El Paso Valley: Texas Department of Water Resources Report 246, 346 p. **(H1)**

Amato, J.F., Mack, G.H., Jonell, T.N., Seager, W.R., and Upchurch, G.I., 2017, Onset of the Laramide orogeny and associated magmatism in southern New Mexico based on U-Pb geochronology: Geological Society Of America Bulletin. v. 129, p. 1209-1226. **(C2b)**

Anderholm, S.K., 1985, Clay-size fraction and powdered whole-rock X-ray analyses of alluvial basin deposits in central and southern New Mexico: U.S. Geological Survey Open-File Report 85-163, 18 p. **(C2a, H2)**

Anderholm, S.K., and Heywood, C.E., 2003, Chemistry and age of ground water in the southwestern Hueco Bolson, New Mexico and Texas: U.S. Geological Survey Water-Resources Investigations Report 02-4237, 16 p. **(H2)**

Anderson, R.E., 1971, Thin-skin distention in tertiary rocks of southeastern Nevada: Geological Society of America, Bulletin, v. 82, no. 1, p. 43-58. *See Stewart 1971.* **(C2a)**

Anning, D.W., and Konieczki, A.D., 2005, Classification of hydrogeologic areas and hydrogeologic flow systems in the Basin and Range Physiographic Province: U.S. Geological Survey Professional Paper 1702, 37 p. **(D1)**

Anthony, E.Y., and Poths, J., 1992. The surface exposure dating and magma dynamics, the Potrillo Volcanic Field, Rio Grande Rift, New Mexico: Geochimica et Cosmochimica Acta, v.56, p. 4105-4108. **(C2b, C4)**

Araurjo-Mendieta, J., and Casar-González, R., 1987, Estratigrafía y sedimentología del Jurásico Superior en la cuenca de Chihuahua, norte de México: Revista del Instituto Mexicano del Petróleo, v. 19, no. 1, p. 6-29. **(F1)**

Archuleta, E.G., 1995, Effective water planning for the Las Cruces/El Paso/Juárez area, *in* Ortega-Klett, C.T., ed., Proceedings of the 39th Annual New Mexico Water Conference, N.M. Water Resource Research Institute Report 290, p. 245-259. **(E2, F1)**

Archuleta, E., 2010, How cooperative planning and technology have led to successful water management in the Paso del Norte region: Journal of Transboundary Water Resources, v. 1, p. 11-30. https://nmwrri.nmsu.edu/publications/pub-documents/JTWR-Book.pdf **(E2)**

Armour, J., Fawcett, P.J., and Geissman, J.W., 2002, 15 k.y. paleoclimatic and glacial record from Northern New Mexico: Geology, v. 30, no. 8, p. 723-726. **(C1)**

Associated Press, 2019, Report raises alarms over Arizona's water supply: Albuquerque Journal-NATION, Sunday, October 27, 2019, p. A4. **(A3)**

Attanasio, C., 2019, Trump's threat to close border stirs fears of economic harm - Warnings of layoffs, shortages and grocery store price increases: Albuquerque Journal–NATION, Tuesday, April 2, 2019, p. A4. **(A3)**

Attanasio, C., and Galvan, A., 2019, Work on more border wall starts on 46-mile stretch west of Santa Teresa and Arizona – Funds come through Trump executive order: Albuquerque Journal–METRO & NM, Sunday, August 25, 2019, p. A11. **(A3)**

Averill, M.G., 2007, A lithospheric investigation of the southern Rio Grande rift: University of Texas at El Paso, doctoral dissertation, 213 p. **(C2b, C4)**

Averill, M.G., and Miller, K.C., 2013, Upper crustal structure of the southern Rio Grande rift: A composite record of rift and pre-rift tectonics, *in* Hudson, M.R., and Grauch, V.J.S., eds., New Perspectives on Rio Grande Rift Basins: From Tectonics to Groundwater: Geological Society of America Special Paper 494, p. 463-474. doi: 10.1130/2013.2494(17) **(C2b, C4)**

Avila, V.M., Doser, D.I., Dena-Ornelas, O.S., Moncada, M.M., and Marrufo-Cannon, S.S., 2016, Using geophysical techniques to trace active faults in the urbanized northern Hueco Bolson, West Texas, USA, and northern Chihuahua, Mexico: Geosphere, v. 12, no. 1, p. 264-280. **(C2b, C4)**

Bahr, T. 1998, An overview of New Mexico's water resources, *in* Herrera, E., Bahr, T.G., Ortega Klett, C.T., and Creel, B.J., eds., Water resources issues in New Mexico: New Mexico Journal of Science, v. 38. p. 3-34. https://nmwrri.nmsu.edu/publications/miscellaneous-reports/m-documents/m26.pdf **(E2)**

Baker, W.W., 1943, Final report on the construction of the canalization feature of the Rio Grande Canalization Project: International Boundary Commission (IBC), p. 4, 16, 18, 32. *See Glover 2018.* **(B3, E2)**

Baldridge, W.S., 2004, Pliocene-Quaternary volcanism in New Mexico and a model for genesis of magmas in continental extension, *in* Mack, G.H., and Giles, K.J., eds., The Geology of New Mexico: A geologic history: New Mexico Geological Society, Special Publication 11, p. 312-330. **(C2b, C4)**

Baldridge, W.S., Keller, G.R., Haak, V., Wendtland, E., Jiracek, G.R., and Olsen, K.H., 1995, Rio Grande rift, *in* Olsen, K.H., ed., Continental rifts: Evolution, structure, tectonics: Developments in Tectonics 25: Amsterdam, Elsevier, p. 233-275. **(C2b)**

Baldwin, B., 1956, The Santa Fe group of north-central New Mexico: New Mexico Geological Society, Guidebook 35, p. 115-121. **(D1)**

Baldwin, B., 1963, Part 2 – Geology, *in* Spiegel, Z.E., and Baldwin, B., Geology and water resources of the Santa Fe area, New Mexico: U.S. Geological Survey, Water-Supply Paper 1525, p. 21-89. **(D1)**

Ball, G.P., Robertson, A.J., and Medina Morales, K., 2020, Seepage investigation of the Rio Grande from below Leasburg Dam, Leasburg, New Mexico, to above El Paso, Texas, 2018: U.S. Geological Survey Scientific Investigations Report 2019-5140, 16 p. **(H3)**

Balleau, W.P., 1999, Groundwater modeling in the lower Rio Grande, *in* Ortega Klett, C.T., ed., Proceedings of the 43rd Annual New Mexico Water Conference: Water Challenges on the Lower Rio Grande. New Mexico Water Resources Research Institute, Report No. 310. p. 46-58. **(H3)**

Banerjee, S., Cook, J., and Truett, S., 2018, The border wall endangers the future of humanity and nature: Albuquerque Journal–OPINION–EDITORIAL, Sunday, August 19, 2018, p. A13. **(A3)**

Baptey, M.M., 1955, Alkali metasomatism and petrology of some keratophyres: Geology Magazine, v. 92, no. 2, p. 104-126. **(G1)**

Barker, F.C., 1898, Irrigation in Mesilla Valley, New Mexico: U.S. Geological Survey Water-Supply and Irrigation Paper 10, 51p. **(G1)**

Barry, R.G., 1983, Late Pleistocene climatology, *in* Porter, S.C., ed., Late Quaternary environments of the United States, volume 1, The Late Pleistocene: Minneapolis, University of Minnesota Press, p. 390-407. **(C1)**

Barry, T., and Sims, B., 1994, The challenge of cross-border environmentalism: The U.S.-Mexico case: Albuquerque, NM, Resource Center Press, 121 p. ISBN 0-911213-45-7 **(A2, B3, E3)**

Barry, T., Browne, H., and Sims, B., 1994, The great divide: The challenge of U.S.-Mexico Relations in the 1990s: New York, Grove Press, 452 p. ISBN 0-8021-1559-4 **(B3, E3)**

Bartlett, J.R., 1854, Personal narrative of expeditions and incidents in Texas, New Mexico, California, Sonora, and Chihuahua, connected with the United States and Mexican Boundary Commission during the years 1850-1853: New York, D. Appleton and Company, 2 vols., 1130 p. [1965 reprint, Glorieta, NM, Rio Grande Press]. **(B3)**

Basler, J.A., and Alary, L.J., 1968, Quality of shallow ground water in the Rincon and Mesilla Valley, New Mexico and Texas: U.S. Geological Survey Open-File Report 68-7, 30 p., 5 figs. **(G2, H2)**

Beck, R.W., 2004, Guidance Manual for Reverse Osmosis Desalination Facility Permitting Requirements in Texas**:** Prepared for Texas Water Development Board, November 23, 2004, 86 p. **(C4, E2)**

Bedinger, M.S., Sargent, K.A., and Langer, W.H., eds., 1989b, Studies of geology and hydrology in the Basin and Range province, southwestern United States, for isolation of high-level radioactive waste – Characterization of the Rio Grande region, New Mexico and Texas: U.S. Geological Survey Professional Paper 1370-C. 48 p. **(F2, H3)**

Beehner, T.S., 1990, Burial of fault scarps along the Organ Mountains fault, south-central New Mexico: Bulletin of the Association of Engineering Geologists, v. 27, no. 1, p. 1-19. *See Gile 1991.* **(C2b, C3, C4)**

Beene, D., Fuchs, E., Rinehart, E., and Lin, Y. (Abstract), 2020, Feedbacks of irrigator decisions, hydrologic change and long-term water planning, Mesilla Valley, N.M.: Program with abstracts, Water, Energy, and Policy in a Changing Climate Conference, National Groundwater Association (NGWA), Albuquerque, NM, February 24-25, 2020. **(E2)**

Bell, J.W., Amelung, F., Ramelli, A.R., and Blewitt, G., 2008, Permanent scatterer InSAR reveals seasonal and long-term aquifer-system response to groundwater pumping and artificial recharge: Water Resources Research, v. 44, W02427. **(D1)**

Bennett, M.R., Bustos, D., Pigati, J.S., Springer, K.B., Urban, T.M., Holliday, V.T., Reynolds, S.C., Budka, M., Honke, J.S., Hudson, A.M., Fenerty, B., Connelly, C., Martinez, P.J., Santucci, V. L., and Odess, D., 2021, Evidence of humans in North America during the Last Glacial Maximum, 2021, Science, v. 373, issue 6562, p. 1528-1531. **(B2, C1, I2)**

Berg, E.L., 1969, Geology of Sierra de Samalayuca, Chihuahua, Mexico: New Mexico Geological Society Guidebook 20, p. 176-182. **(C2a, F3)**

Berggren, W.A., Hilgen, F.J., Langereis, C.O., Kent, D.V., Obradovich, J.D., Raffi, I., Raymo, M.E., and Shackleton, N.J., 1995, Late Neogene chronology: New perspectives in high-resolution stratigraphy: Geological Society of America Bulletin, v. 107, p. 1272-1287. **(B1)**

Bestelmeyer, B.T., Duniway, M.C., James, D.K., Burkett, L.M., and Havstad, K., 2013, A test of critical thresholds and their indicators in a desertification-prone ecosystem: more resilience than we thought: Ecology Letters, v. 16, p. 339-345. **(C1)**

Bestelmeyer, B.T., Peters, D.C., Archer, S.R., Browning, D.M., Okin, G.S., Schooley, R.L., and Webb, N.P., 2018, The grassland-shrubland regime shift in the southwestern United States: Misconceptions and their implications for management: Bioscience, v. 68, no. 9, p. 678-690. **(C1)**

Betancourt, J.L., Van Devender, T.R., and Martin, P.S., eds., 1990, Packrat Middens: The last 40,000 years of biotic change: University of Arizona Press, 467 p. **(B1, C1)**

Birch, F., 1982, Gravity models of the Albuquerque Basin: Rio Grande Basin, New Mexico: Geophysics, v. 47, p. 1185-1197. **(C4)**

Birkeland, P.W., 1984, Presentation of the Kirk Bryan Award to Leland H. Gile, John W. Hawley, and Robert B. Grossman, *in* Medals and Awards for 1983: Geological Society of America, v. 95, p. 1003-1004. **(A2)**

Bixby, K., and Smith, D., 2020, Ongoing border wall construction has risks: Albuquerque Journal–OPINION–EDITORIAL, Sunday, April 5, 2020, p. A11. **(A3)**

Blair, T.C., Clark, J.S., and Wells, S.G., 1990, Quaternary continental stratigraphy, landscape evolution, and application to archaeology: Jicarilla piedmont and Tularosa graben floor, White Sands Missile Range, New Mexico: Geological Society of America Bulletin, v. 102, p. 748-759. **(C2b)**

Blásquez, L.L., 1959, Hidrogeológica de las regiones desérticas de México: Universidad Nacional Autónoma de México, Anales del Instituto de Geología, Tomo XV, 172 p. **(F3)**

Boetel, R., 2024a, State's hot-spring geology could unlock energy: Albuquerque Journal–BUSINESS OUTLOOK, Monday, March 25, 2024, p. 2. **(A3)**

Bond, G.N., Boucher, J.H., Eriksen, W.T., Hudson, S.L., and Kaiser, B.D., 1981, A direct application of geothermal energy at L'EGGS Plant, Las Cruces, New Mexico: U.S. Department of Energy, Idaho Operations Office, Report DOE/ID/12047-3. **(C4)**

Boulton, G.S., Peacock, J.D., and Sutherland, D.G., 2002, Quaternary, Chapter 15: *in* Trewin, N.H., ed., The Geology of Scotland (4th edition, 576 p.): London, The Geological Society, p. 409-430. **(C1, D1)**

Bouwer, H., 2002, Artificial recharge of groundwater: Hydrogeology and engineering: Hydrogeology Journal (2002) v. 10, p. 121-142. **(D2, E2b)**

Brand, D.C., 1937, The natural landscape of northwestern Chihuahua: University of New Mexico Press, 74 p. **(B2, C, C1, C2a, F3)**

Brannen, P., 2021, The dark secrets of the Earth's deep past – The geologic record suggests that climate models are missing something truly frightening: The Atlantic, v. 327, no. 2, p. 60-75. **(B1, C1)**

Brown and Caldwell, circa 1975, Generalized geologic cross-section A-A', Crowder Well Field, Santa Teresa Fig. 4: 2010 contribution to NM WRRI TAAP database by Thomas Maddock III**. (H1)**

Bryan, K., 1909, Geology in the vicinity of Albuquerque: University of New Mexico Bulletin 51, Geological Series, v. 3, no. 1, 24 p. **(G1, I3)**

Bryan, K., 1923, Erosion and sedimentation in the Papago country, Arizona: U.S. Geological Survey, Bulletin 730-B, p. 19-90. **(C2a, A2)**

Bryan, K., 1938, Geology and groundwater conditions of the Rio Grande depression in Colorado and New Mexico, *in* [U.S.] National Resources Committee, Regional Planning part VI – The Rio Grande joint investigations in the upper Rio Grande basin in Colorado, New Mexico, and Texas, 1936-1937: U.S. Government Printing Office, Washington, D.C., v. 1, part 2, p. 197-225. **(D1, G2, I3)**

Bryan, S.M., Associated Press, 2020, Climatologist: Dry Areas in Southwest getting dryer – Precipitation declines as temperatures rise: Albuquerque Journal–METRO & NM, Sunday, September 27, 2020, p. A12, A13. **(A3)**

Bryan, S.M., Associated Press, 2023, US judge recommends settlement over Rio Grande--Calls it consistent with a water-sharing agreement among NM, Texas, Colorado: Albuquerque Journal, Thursday, July 6, 2023, p. A3-A4. **(A3)**

Buffington, L.C., and Herbel, C.H., 1965, Vegetation changes on a semidesert grassland range: Ecological Monographs, v. 35, p. 139-164. **(C1)**

Bull, W.B., 1968, Alluvial fans: Journal of Geological Education, v. 16, p. 101-106. **(D1)**

Bull, W.B., 1977, The alluvial fan environment: Progress in Physical Geography, v. 1, p. 222-270. **(D1)**

Bulloch, H.F., Jr., and Neher, R.E., 1980, Soil Survey of Doña Ana County area, New Mexico: U.S. Soil Conservation [Natural Resource] Service, 177 p. **(C3)**

Burbey, T.J., 1999, Effects of horizontal strain in estimating specific storage and compaction in confined and leaky systems: Hydrogeology Journal, v. 7, p. 521-532. **(D1)**

Burbey, T.J., 2001, Storage coefficient revisited: Is purely vertical strain a good assumption?: Ground Water, v. 39, no. 3, p. 458-464. **(D1)**

Burkholder, J.L., 1919, Drainage works of the Rio Grande Irrigation Project: Engineering News Record, v. 83, p. 543-549. **(E2)**

Burrows, R.H., 1909, Geology of northern Mexico: Mining and Scientific Press, v. 99, no. 9 (whole no. 2562, 28 Aug.), p. 290-294; continued as "Geology of northeastern Mexico," in v. 99, no. 10 (4 Sept.), p. 324-327. **(C2a, F3, G1)**

Bustos, D., Jakeway, J., Urban, T.M., Holliday, V.T., Fenerty, B., Raichlen, D.A., Budka, M., Reynolds, S.C., Allen, B.D., Love, D.W., Santucci, V.L., Odess, D., Willey, P., McDonald, H.G., and Bennett, M.R., 2018, Footprints preserve terminal Pleistocene hunt? Human-sloth interactions in North America: Science Advances [AAAS], v. 4, issue 4, 6 p. **(B2, C1, I2)**

Buszka, P.M., Brock, R.D., and Hooper, R.P., 1994, Hydrogeology and selected water-quality aspects of the Hueco Bolson aquifer at the Hueco Bolson Recharge Project area, El Paso, Texas: U.S. Geological Survey, Water-Resources Investigations Report 94-4092, 41 p. **(E2b, F2)**

Callahan, C.J., 1973, Aden Basalt Volcanic Depressions, Doña Ana County, New Mexico: University of Texas at El Paso, master's thesis, 82 p. **(C2a)**

Callahan, C., and Terrazas, C., 1971, Topographic map-Potrillo Maar area, Chihuahua, Mexico; scale-1:12,000 and 10 ft contour interval; *with annotations on* Geology by Chester Callahan, and *plane-table* Topography by Chuck Terrazas [unpublished map prepared for the University of Texas at El Paso, Department of Geology]: C. Callahan to J. Hawley letter transmittal of 7/1/1981. **(C2a)**

Campos-Enriquez, J.O., Ortega-Ramírez, J., Alariste-Vilchis, D., Cruz-Gática, R., and Cabral-Cano, E., 1999, Relationship between extensional tectonic style and paleoclimatic elements at Laguna El Fresnal, Chihuahua Desert, Mexico: Geomorphology, v. 28, p. 75-94. **(C1, C2b, F3, I2)**

Cantú-Chapa, C.M., Sandoval-Silva, R., and Arenas-Partida, R., 1985, Evolución sedimentaria del Cretácico Inferior en el norte de México; Revista Instituto Mexicano del Petróleo, v. 17, no. 2, p. 14-37. **(C2a, F3)**

Carciumaru, D.D., 2005, Structural geology and tectonics of the northern Chihuahua trough: University of Texas at El Paso, doctoral dissertation, 99 p. **(C2b, F3)**

Carpenter, M.C., 1999, South-Central Arizona – Earth fissures and subsidence complicate development of desert water resources, *in* D. Galloway., D.R. Jones, and S.E. Ingebritzen, eds., Land subsidence in the United States: U.S. Geological Survey Circular 1182, p. 65-78. **(D1)**

Castiglia, P.J., 2002, Late Quaternary climate history of the pluvial Lake Palomas system, Chihuahua, Mexico: University of New Mexico, master's thesis, 161 p. **(B2, C1, F3, I2)**

Castiglia, P.J., and Fawcett, P.J., 2006, Large Holocene lakes and climate change in the Chihuahuan Desert: Geology, v. 34, no. 2, p. 113-116. *Seminal paper; but they still do not recognize the major contribution of Mimbres Basin/River system to pluvial Lake Palomas*. **(B2, C1, F3, I2)**

Castillo, R.C., Cortes, A., Morales, P., Romero, G., and Villegas, R., 1984, A survey of groundwater flow using deuterium and oxygen-18 as tracers, in Samalayuca Dunes Northern Mexico: Revista Mexícanos de Física, v. 30, no. 4, p. 147-155. **(F3, H2, H3)**

CH2MHill, 2013, Distal Mesilla conceptual site model prepared for the United States Army Corps of Engineers: Technical Report, 224 p. **(E2c, F1, H1, H2)**

Chapin, C.E., 1971, The Rio Grande rift, Part I: Modifications and additions: Guidebook of the San Luis Basin, Colorado, New Mexico Geological Society, Guidebook 22, p. 191-201. **(C2a, I3)**

Chapin, C.E., 1979, Evolution on the Rio Grande rift – A summary, *in* Riecker, R.E., ed., Rio Grande rift: Tectonics and magmatism: Washington, D.C., American Geophysical Union, p. 1-5. **(C2a)**

Chapin, C.E., and Cather, S.M., 1994, Tectonic setting of the axial basins of the northern and central Rio Grande Basin, New Mexico, *in* Keller, G.R., and Cather, S.M., eds., Basins of the Rio Grande Rift – Structure, stratigraphy, and tectonic setting. Geological Society of America, Special Paper 291, p. 5-25. **(C2b, I3)**

Chapin, C.E., and Seager, W.R., 1975, Evolution of the Rio Grande rift in the Socorro and Las Cruces areas: New Mexico Geological Society, Guidebook 26, p. 297-321. **(C2a, I3)**

Chaturvedi, L., 1981, New Mexico State University geothermal production well: N.M. Energy Institute Technical Completion Report, 48 p. **(C4, H1, H2)**

Chavarria, S.B., and Gutzler, D.S., 2018, Observed changes in climate and streamflow in the upper Rio Grande basin: Journal of the American Water Resources Association, v. 54, no. 3, p. 644-659. **(C1)**

Chávez, O.E., 2000, Mining of Internationally Shared Aquifers: The El Paso-Juárez Case, 40 Natural Resources Journal, v. 40, issue 2 (The La Paz Symposium on Transboundary Groundwater Management on the U.S. - Mexico Border), p. 237-260. **(E2, E3)**

Chávez-Quirarte, R., 1986, Stratigraphy and structural geology of Sierra de Sapello, Northern Chihuahua, Mexico: University of Texas at El Paso, doctoral dissertation, 167 p. **(C2a, F3)**

Christensen, J.H., Hewitson, B., Busuioc, A., Chen, A., Gao, X., Held, I., Jones, R., Kolli, R.K., Kwon, W.T., Laprise, R., Magana Rueda, V., Mearns, L., Menendez, C.G., Raisanenvj, J., Rinke, A., Sarr, A., and Whetton, P., 2007, Regional Climate Projections, Chapter 11 *in* Solomon, S., Qin, D., Manning, M., Chen, Z., Marquis, M., Averyt, K.B., Tignor, M., and Miller, H.L., eds., Climate Change 2007: The Physical Science Basis: Contribution of Working Group I to the Fourth Assessment Report of the Intergovernmental Panel on Climate Change; Cambridge, UK and NY: Cambridge University Press. **(C1)**

Clayton, M.E., Kjellsson, J.B., and Webber, M.E., 2014, Can renewable energy and desalination tackle two problems at once? EARTH, November/December 2014, p. 60-65. **(E2a)**

Clemons, R.E., 1976a, Geology of east half of Corralitos Ranch Quadrangle, Doña Ana County, New Mexico: New Mexico Bureau of Mines and Mineral Resources, Geologic Map 36, two sheets, scale 1,24,000. **(C2a)**

Clemons, R.E., 1977, Geology of west half of Corralitos Ranch Quadrangle, Doña Ana County, New Mexico: New Mexico Bureau of Mines and Mineral Resources, Geologic Map 44, two sheets, scale 1,24,000. **(C2a, H1)**

Clemons, R.E., 1979, Geology of Good Sight Mountains and Uvas Valley, southwest New Mexico: New Mexico Bureau of Mines and Mineral Resources, Circular 169, 31 p. *First map of Lake Goodsight* **(C2a, H1, I2)**

Clemons, R.E., 1993, Petrographic analysis of Cenozoic-Mesozoic-Permian well cuttings from two exploration wells in south-central New Mexico: New Mexico Bureau of Mines and Mineral Resources, Circular 203, 28 p. **(C2b, H1)**

Clemons, R.E., and Seager, W.R., 1973, Geology of Souse Springs Quadrangle, Doña Ana County, New Mexico: New Mexico Bureau of Mines and Mineral Resources, Bulletin 100, 31 p. **(C2a)**

Clemons, R.E., Hawley, J.W., Hoffer, J.M., and Seager, W.R., 1975, Las Cruces to the Sierra de las Uvas and Aden volcanic area and return: New Mexico Geological Society Guidebook 26, p. 17-34. **(C2a)**

Cliett, T., 1969, Groundwater occurrence of the El Paso area and its related geology: New Mexico Geological Society Guidebook 20, p. 209-214. **(H1)**

Cliett, T., and Hawley, J.W., 1996, General geology and groundwater occurrence of the El Paso area, *in* Ortega-Klett, C.T., ed., Proceedings of the 40th Annual New Mexico Water Conference, New Mexico Water Resource Research Institute Report 297, p. 51-56. **(H1, H2)**

Coe, R.S., Singer, B.S., Pringle, M.S., and Zhao, X., 2004, Matuyama–Brunhes reversal* and Kamikatsura event on Maui: paleomagnetic directions, 40Ar/39Ar ages and implications: Earth and Planetary Science Letters, v. 222, p. 667-684. **776 ka* **(B1)**

Collins, E.W., and Raney, J.A., 1991, Tertiary and Quaternary structure and paleotectonics of the Hueco Basin, Trans-Pecos Texas and Chihuahua, Mexico: The University of Texas at Austin, Bureau of Economic Geology, Geological Circular GC 91-2, 44 p. **(C2b)**

Collins, E.W., and Raney, J.A., 1994a, Impact of late Cenozoic extension on Laramide overthrust belt and Diablo platform margins, northwestern Trans-Pecos Texas: New Mexico Bureau of Mines and Mineral Resources Bulletin 150, p. 71-81. **(C2b)**

Collins, E.W., and Raney, J.A., 1994b, Tertiary and Quaternary tectonics of the Hueco Bolson, Trans-Pecos Texas and Chihuahua, Mexico, *in* Keller, G.R., and Cather, S.M., eds., Basins of the Rio Grande Rift – Structure, stratigraphy, and tectonic setting: Geological Society of America Special Paper 291, p. 265-282. **(C2b)**

Collins, E.W., and Raney, J.A., 1997, Quaternary faults within intermontane basins of northwest Trans-Pecos Texas and Chihuahua, Mexico: The University of Texas at Austin, Bureau of Economic Geology Report of Investigations No. 245, 59 p. **(C2b)**

Collins, E.W., and Raney, J.A., 2000, Geologic map of west Hueco Bolson, El Paso region, Texas: The University of Texas at Austin, Bureau of Economic Geology, Miscellaneous Map No. 40, scale 1:100,000. **(C2b, F1)**

Collins, E., Haller, K.M., and Machette, M.N., compilers, 2015, Fault number 900, East Franklin Mountains fault, *in* Quaternary fault and fold database of the United States: U.S. Geological Survey website, accessed June 24, 2021 at https://earthquakes.usgs.gov/hazards/qfaults **(Cªb, C4)**

CONAGUA, 2015a, Actualización de la Disponibilidad Media Anual de Agua en el Acuífero Conejos Médanos (0823), Estado de Chihuahua: Subdirección General Técnica, México DF, p. 1-32. **(F3)**

CONAGUA, 2015b, Actualización de la Disponibilidad Media Anual de Agua en el Acuífero Valle de Juárez (0833), Estado de Chihuahua: Subdirección General Técnica, México DF, p. 1-36. **(F3)**

CONAGUA, 2020, Actualization de la Inibilidad Media Anual de Agua en el Acuifero Conejos-Medanos (0823) Estado de Chihuahua, *in* Subdireccion General Tecnica Gerencia de Aguas Subterraneas; Comisión Nacional del Agua: Mexico City, Mexico, 36 p. https://sigagis.conagua.gob.mx/gas1/Edos_Acuiferos_18/chihuahua/DR_0823.pdf. **(F3)**

Connell, S.D., Hawley, J.W., and Love, D.W., 2005, Late Cenozoic drainage development in the southeastern Basin and Range of New Mexico, southeasternmost Arizona and western Texas, *in* Lucas, S.G., Morgan, G., and Zeigler, K.E., eds., 2005, New Mexico's Ice Ages: New Mexico Museum of Natural History & Science Bulletin No. 28, p. 125-150. **(C2b, I1, I3)**

Connell, S.D., Love, D.W., and Dunbar, N.W., 2007, Geomorphology and stratigraphy of inset fluvial deposits along the Rio Grande Valley in the central Albuquerque Basin: New Mexico Geology, v. 29, no. 1, p. 13-31. **(C2b, D1, I3)**

Connell, S.D., Smith, G.A., Geissman, J.W., and McIntosh, W.C., 2013, Climatic controls on nonmarine depositional sequences, Albuquerque Basin, Rio Grande rift, north-central New Mexico, *in* Hudson, M.R., and Grauch, V.J.S., eds., New Perspectives on the Rio Grande rift: from tectonics to groundwater: Geological Society of America, Special Publication, p. 483-485. **(C1, I3)**

Conover, C.S., 1954, Ground-water conditions in the Rincon and Mesilla Valleys and adjacent areas in New Mexico: U.S. Geological Survey Water-Supply Paper 1230, 200 p. **(G2)**

Contaldo, G.J., and Mueller, J.E., 1991, Earth fissures of the Mimbres Basin, southwestern New Mexico: New Mexico Geology, v. 13, p. 69-74. **(D1, H1)**

Cook, C., 2024, Haaland announces $60M investment in water – Money to address drought resiliency in the Rio Grande south of Elephant Butte: Albuquerque Journal, Saturday May 11, 2024, p. A1, A5. **(A3, E2b)**

Cope, E.D., 1884, On the distribution of the Loup Fork formation in New Mexico: Proceedings of the American Philosophical Society, v. 21, 308-309. *Earliest mention of presence of "Santa Fe beds" in lower RG Valley near T or C.* **(C2a, G1)**

Cordell, L., 1975, Combined geophysical studies at Kilbourne Hole maar, New Mexico: New Mexico Geological Society Guidebook 26, p. 269-271. **(C2a, C4)**

Cordell, L., 1976, Aeromagnetic and gravity studies of the Rio Grande graben in New Mexico between Belen and Pilar: New Mexico Geological Society, Special Publication 6, p. 62-70. **(C4)**

Cordell, L., 1978, Regional geophysical setting of the Rio Grande rift: Geological Society of America Bulletin 89, p. 1073-1090. **(C4)**

Córdoba, D.A., 1969a, Geología del área de Cerro de Muleros o Cristo Rey, Esca315rovin43,000: [Inset map on] Hoja Ciudad Juárez 13R-a (3): Carta Geológica de México, escala 1:100,000, *Reprinted as back-cover insert in Córdoba and others, 1969*. **(C2a, F3)**

Córdoba, D.A., 1969b, Hoja Ciudad Juárez 13 R-a (3) con Resumen de la Geología de la Hoja Ciudad Juárez de Chihuahua: Universidad Nacional Autónoma de México, Instituto Geología, Carta Geología de México, Serie de 1:100,000. *Reprinted as back-cover insert in Córdoba and others, 1969*. **(C2a, F3)**

Córdoba, D.A., 1969c, Mesozoic stratigraphy of northeastern Chihuahua, Mexico: New Mexico Geological Society Guidebook 20, p. 91-101. **(C2a, F3)**

Córdoba, D.A., Rodríguez-Torres, R., and Guerrero-García, J., 1970, Mesozoic stratigraphy of the northern portion of the Chihuahua Trough, *in* The Geologic Framework of the Chihuahua Tectonic Belt: Symposium in honor of Professor Ronald K. DeFord: West Texas Geological Society and University of Texas at Austin, p. 83-97. **(C2a, F3)**

Córdoba, D.A., Wengerd, S.A., and Shomaker, J.W., eds., 1969, Guidebook of the Border Region: New Mexico Geological Society Guidebook 20, 218 p. *See Road Log Section, p. 1-38.* **(C2a)**

Craig, H., 1961a, Isotopic variation in meteoric waters: Science, v. 133, p. 1702-1703. **(D1)**

Creel, B.J., 2010, Research needs in the U.S. portion of the Rio Grande watershed: Journal of Transboundary Water Resources, v. 1, p. 31-41. https://nmwrri.nmsu.edu/publications/pub-documents/JTWR-Book.pdf **(C1, E2, E3)**

Creel, B.J., Hawley, J.W., Kennedy, J.F., and Granados Olivas, A., 2006, Groundwater resources of the New Mexico-Texas-Chihuahua border region, *in* Anderson, K.S.J., ed., Science on the Border: N.M. Journal of Science, v. 44. p. 11-29. **(F1, H1)**

Creel, B.J., Sammis, T.W., Kennedy, J.F., Sitze, D.O., Asare, D., Monger, H.C., and Samani, Z., 1998, Ground-water aquifer sensitivity assessment and management practices evaluation for pesticides in the Mesilla Valley: New Mexico Water Resources Research Institute Technical Completion Report 305, 50 p. https://nmwrri.nmsu.edu/publications/technical-reports/tr-reports/tr-305.html **(E2c, H2)**

Crilley, D.M., Matherne, A.M., Thomas, N., and Falk, S.E., 2013, Seepage investigations of the Rio Grande from below Leasburg Dam, Leasburg, New Mexico, to above American Dam, El Paso, Texas, 2006-13: U.S. Geological Survey Open-File Report 2013-1233, 34 p. **(H3)**

Crutzen, P.J., and Stoermer, E.F., 2000. The "Anthropocene:" IGBP Global Change Newsletter, v. 41, p. 17-18. **(B1, B3, C1)**

Culbertson, M.C., 2018, Remembering Charlie Crowder, who worked to build a bi-national border industrial complex: NMPolitics.net, 4 p. **(A2)**
Cuniff, R.A., 1986, New Mexico State University, Geothermal Exploratory Well, DT-3; Final completion report: New Mexico State University Physical Science Laboratory (Las Cruces, NM-88003-3458), 151 p. **(C4, H2)**
Cunningham, E.E.B., Long, A., Eastoe, C.J., and Bassett, R.L., 1998, Migration of recharge waters downgradient from the Santa Catalina Mountains into the Tucson Basin aquifer: Hydrogeology Journal, v. 6, no. 1, p. 94-103. **(D2, H3)**
Daggett, P.H., and Keller, G.R., 1987, Complete Bouguer anomaly map of east half of Las Cruces and northeast El Paso 1º x 2º sheets, Sheet 3, *in* Seager, W.R., Hawley, J.W., Kottlowski, F.E. and Kelley, S.A., Geology of east half of Las Cruces and northeast El Paso 1º x 2º sheets, New Mexico: New Mexico Bureau of Mines and Mineral Resources, Geologic Map 57, scale 1:125,000. **(C4)**
Daggett, P.H., and Keller, G.R., 1995, Complete Bouguer anomaly map of southwest quarter of Las Cruces and El Paso 1º x 2º sheets, Sheet 3, *in* Seager, W.R., Geology of the southwest quarter of the Las Cruces and northwest El Paso 1º x 2º sheets: New Mexico Bureau of Mines and Mineral Resources, Geologic Map 60, scale 1:125,000. **(C4)**
Daggett, P.H., Keller, G.R., Morgan, P., and Wen, C.L., 1986, Structure of the southern Rio Grande rift from gravity interpretation: Journal of Geophysical Research, v. 91, n. B6, p. 6157-6167. **(C4)**
Dailey, D., 2021, Paso del Norte in 1817: From the Report of Father Juan Rafael Rascón: Southern New Mexico Historical Review, Volume XXVIII (January 2021), p. 1-9. http://www.donaanacountyhistsoc.org **(B3)**
D'Ammassa, A., Las Cruces Sun-News, 2021, Herrell calls for wall to be finished – New Mexico congresswoman leads delegation of Republican lawmakers to the border: Albuquerque Journal, Monday, April 14, 2021, p. A1, A2. **(A3)**
Daniel B. Stephens and Associates, Inc. (DBSAI), 2010, Evaluation of Rio Grande salinity San Marcial, New Mexico to El Paso, Texas: Report (pdf) prepared for the New Mexico Interstate Stream Commission and New Mexico Environment Department, June 30, 2019, 202 p. **(C4, E2, H2)**
Darling, B.K., Hibbs, B.J., and Sharp, J.M., Jr., 1998, Environmental isotopes as indicators of the residence time of ground waters in the Eagle Flat and Red Light Draw Basins of Trans-Pecos, Texas: West Texas Geological Society Publication no. 98-105, p. 259-270. **(C1, H2, H3)**
Darling, B.K., Hibbs, B.J., and Sharp, J.M., 2017, Integrations of carbon-14 and Oxygen-18 as a basis for differentiating between Late Pleistocene and post-Pleistocene groundwater ages along flow paths of two West Texas bolson aquifers: Geological Society of America 129th Annual Meeting, Abstracts with Programs, v. 49, no. 7. ISSN 0016-7592 **(B2, C1, H2, H3)**
Darton, N.H., 1916a, Explosion craters: Science Monthly, v. 3, no. 4, p. 417-430. **(C2a, D1, G1)**
Darton, N.H., 1916b, Geology and underground water of Luna County, New Mexico: U.S. Geological Survey Bulletin 618, 188 p. **(D1, G1)**
Darton, N.H., 1922, Geologic structure of parts of New Mexico: U.S. Geological Survey Bulletin 726-E, p. 173-275. **(C2a)**
Darton, N.H., 1928a, Geologic map of New Mexico: U.S. Geological Survey, scale 1:500,000. **(C2a, D1)**
Darton, N.H., 1928b, Red beds and associated formations within New Mexico with outline of the geology of the state: U.S. Geological Survey, Bulletin 794, 356 p. **(C2a, D1)**
Darton, N.H., 1933, Guidebook of the western United States, Part F, The Southern Pacific Lines, New Orleans to Los Angeles. U.S. Geological Survey Bulletin 845. 304 p., 29 route maps. [West TX, and Southern NM and AZ: p. 120-160]. **(B3, C2a, F2, G1)**
Davidson, S.K., Hartley, A.J., Weissmann, G.S., Nichols, G.J., and Scuderi, L.A., 2013, Geomorphic elements on modern distributive fluvial systems: Geomorphology, v. 180-181, p. 82-85. **(D1)**
Davidson, T.T., 1998, Groundwater recharge: The legal realities of keeping the hydrologic system whole, *in* Herrera, E., Bahr, T.G., Ortega Klett, C.T., and Creel, B.J., eds., Water resources issues in New Mexico: New Mexico Journal of Science, v. 38. p. 35-53. https://nmwrri.nmsu.edu/publications/miscellaneous-reports/m-documents/m26.pdf **(E2b, E3)**
Davie, W., Jr., and Spiegel, Z., 1967, Geology and water resources of Las Animas Creek and vicinity, Sierra County, New Mexico: New Mexico State Engineer Hydrographic Survey Report, 44 p. **(C2a, G2, H1)**
Davis, M.E., and Leggat, E.R., 1965, Reconnaissance investigation of the ground-water resources of the upper Rio Grande basin, Texas, *in* Reconnaissance investigations of the ground-water resources of the Rio Grande basin, Texas: Texas Water Commission Bulletin 6502, p. U1-U99. **(G2, H1)**
Davis, T., 2019a, Report: NM water stress level extremely high: Albuquerque Journal, Monday, August 12, 2019. **(A3)**

Davis, T., 2019b, Aquifer on the rebound – Water levels up 30-40 feet; San Juan Project, conservation credited: Albuquerque Journal, Saturday, August 24, 2010, p. A1, A2. **(A3, E2b)**
Davis, T., 2020a, Texas, Colorado give NM the OK to use stored water – Permission for emergency use by the state last granted in the 1950s: Albuquerque Journal, Saturday, July 18, 2020, p. A1, A4. **(A3)**
Davis, T., 2020b, Agencies look to acquire more water for minnow – Interstate Stream Commission OKs $100K for potential lease: Albuquerque Journal, Friday, July 24, 2020, p. B1. **(A3)**
Davis, T., 2020c, Emergency water release a short-term solution – Rio Grande in ABQ would have been dry by now, while northern NM in dire straits: Albuquerque Journal, Saturday, August 8, 2020, p. A8, A9. **(A3)**
Davis, T., 2020d, With river on life support, water debt looms: Albuquerque Journal, Friday, August 14, 2020, p. A7, A8. **(A3)**
Davis, T., 2020e, Planning for New Mexico's water future – 50-plan will support existing research projects: Albuquerque Journal, Monday, August 17, 2020, p. A1, A6. **(A3)**
Davis, T., 2020f, Cuba [NM] counts on new facility to treat its brackish water – Technology converts extracted minerals to fertilizer: Albuquerque Journal, Monday, August 31, 2020, p. A1, A2. **(A3)**
Davis, T., 2020g, Tracking every last drop – New technology aims to get better water data to farmers: Albuquerque Journal, Saturday, October 10, 2020, p. A10. **(A3)**
Davis, T., 2020h, Dry as a bone – 2021 to be a critically low water supply year: Albuquerque Journal, Saturday, November 12, 2020, p. A5. **(A3)**
Davis, T., 2020i, Rio Grande Compact states jiggle duties – Nearly all of New Mexico is experiencing severe drought: Albuquerque Journal, Saturday, November 13, 2020, p. A8. **(A3)**
Davis, T., 2021a, NM will pay farmers to stop groundwater use – Plan hopes to understand how aquifer system reacts to scenarios: Albuquerque Journal, Saturday, January 2, 2021, p. A1, A5. **(A3)**
Davis, T., 2021b, Drought-stricken NM getting little help from winter storms – Snowpack below average across state; northern mountains fare slightly better: Albuquerque Journal, Sunday, January 10, 2021, p. A8-A9. **(A3)**
Davis, T., 2021c, Rio Grande in *Peril* – NM water manager warn communities to prepare for bleak future: Albuquerque Journal, Monday, February 1, 2021, p. A8-A9. **(A3)**
Davis, T., 2021d, Fire, rain a bad mix – UNM study shows impacts on Western watersheds: Albuquerque Journal, Saturday, June 5, 2021, p. A1, A3. **(A3, C1)**
Davis, T., 2021e, 'We're sounding the alarm' on water flow, Elephant Butte managers say: Albuquerque Journal, Sunday, June 20, 2021, p. A1, A16. **(A3)**
Davis, T., 2021f, Rio Grande to 'Rio Sand'? – Iconic river may go dry through ABQ this summer: Albuquerque Journal, Saturday, June 26, 2021, p. A1-A2. **(A3)**
Davis, T., 2021g, In 50 years: Hotter, Drier – New Mexico's changing climate spells uncertainty for water: Albuquerque Journal, Friday July 23, 2021, p. A1-A2. **(A3)**
Davis, T., 2021h, Rio Grande goes with monsoon flow – Rains ease fears of river drying, but farmers still face irrigation woes: Albuquerque Journal, Thursday August 12, 2021, p. A1-A2. **(A3)**
Davis, T., 2022c, 'Status quo is not an option' for Rio Grande: Albuquerque Journal, Wednesday July 27, 2022, p. A1-A2. **(A3)**
Dean, J.S., and Robinson, W.J., 1978, Expanded tree-ring chronologies for the southwestern United States: University of Arizona, Laboratory of Tree-Ring Research, Chronology Series III. **(B2, B3, C1)**
DeAngelo, M.V., and Keller, G.R., 1988, Geophysical anomalies in southwestern New Mexico: New Mexico Geological Society, Guidebook 39, p. 71-75. **(C4)**
Deason, M.G., 1998, An historical overview of playas and other wetland/riparian areas of "Nuevo Mexico," *in* Herrera, E., Bahr, T.G., Ortega Klett, C.T., and Creel, B.J., eds., Water resources issues in New Mexico: New Mexico Journal of Science, v. 38. p. 189-218. https://nmwrri.nmsu.edu/publications/miscellaneous-reports/m-documents/m26.pdf **(B3, C1)**
DeBrine, B., Spiegel, Z., and Williams, D., 1963, Cenozoic sedimentary rocks in Socorro Valley, New Mexico: New Mexico Geological Society Guidebook 14, p. 123-131. **(C2a)**
deBuys, W., 2011, A great aridness: Climate change and the future of the American Southwest: New York, Oxford University Press, 369 p. ISBN: 9780199778928 **(C1)**
Decker, E.R., and Smithson, S.B., 1975, Heat flow and gravity interpretation across the Rio Grande rift in southern New Mexico and west Texas: Journal of Geophysical Research, v. 80, no. 17, p. 2542-2552. **(C4)**
DeHon, R.A., 1965, Maare of La Mesa: New Mexico Geological Society, Guidebook 16, p, 204-209. **(C2a)**
DeHon, R., and Earl, R., 2018a, Reassessment of features in the Aden Crater lava flows, Doña Ana County, New Mexico: New Mexico Geology, v. 40, p. 17-26. **(C2b)**

DeHon, R.A., and Earl, R.A., 2018b, The Aden lava flows, Doña Ana County, New Mexico: N.M. Geological Society, Guidebook 69, p. 197-202. **(C2b)**
Deming, D., 2002, Introduction to hydrogeology: New York, The McGraw-Hill Book Companies, Inc., 468 p. ISBN 0-07-232622-0 **(D1)**
Deming, D., and Bredehoeft, J.D., 2002, Groundwater at the U.S. Geological Survey, 1879-2000, *in* Introduction to hydrogeology: New York, The McGraw-Hill Book Companies, Inc., p. 8-11. **(D1)**
Denny, C.S., 1941, Quaternary geology of the San Acacia area, New Mexico: Journal of Geology, v. 49, no. 3, p. 225-260. **(C2a)**
Dethier, D.P., 2001, Pleistocene incision rates in the western United States calibrated using Lava Creek B tephra: Geology, v. 29, no. 9, p. 783-786. **(C2b, I3)**
Dickerson, P.W., 2013, Tascotal Mesa transfer zone – An element of the Border Corridor transform system, Rio Grande rift of West Texas and adjacent Mexico, *in* Hudson, M.R., and Grauch, V.J.S., eds., New Perspectives on Rio Grande Rift Basins: From Tectonics to Groundwater: Geological Society of America Special Paper 494, p. 475-500. doi: 10.1130/2013.2494(18) **(C2b)**
Dickinson, W.R., 2002, The Basin and Range Province as a composite extensional domain: International Geology Review, v. 44, p. 1-38. **(C2b)**
Dickinson, W.R., Klute, M.R., and Swift, P.N., 1986, The Bisbee Basin and its bearing on late Mesozoic paleogeographic and paleotectonic relations between the Cordilleran and Caribbean regions, *in* Abbott, P.L. (ed.), Cretaceous Stratigraphy Western North America, Society of Economic Paleontologists and Mineralogists, Pacific Section, Book 46, p. 51-62. **(C2a, C2b)**
Dick-Peddie, W.A., 1993, New Mexico vegetation - past, present, and future: University of New Mexico Press, 244 p. **(C1)**
Dimond, D., 2021, The future of the 'big, beautiful' border wall is dim: Albuquerque Journal–OPINION–EDITORIAL, Saturday, January 2, 2021, p. A11. **(A3)**
Doty, G.C., 1963, Water-supply development at the National Aeronautics and Space Agency-Apollo Propulsion System Development Facility, Doña Ana County, New Mexico: U.S. Geological Survey, Open-File Report 63-29, 40 p. **(C2a, H1)**
Douglas, M.W., Maddox, R.A., Howard, K., and Reyes, S., 1993, The Mexican monsoon: Journal of Climate, v. 6, p. 1665-1677. **(C1)**
Drew, L.G., ed., 1972, Tree-ring chronologies of western North America, II. Arizona, New Mexico, and Texas: University of Arizona, Laboratory of Tree-Ring Research, Chronology Series I. **(B2, B3, C1)**
Drewes, H., and Dyer, R., 1993, Geologic map and structure sections of the Sierra Juárez, Chihuahua, Mexico: U.S. Geological Survey Miscellaneous Investigations Map I-2287, scale 1:12,500. **(C2b, F3)**
Druhan, J.L., Hogan, J.F., Eastoe C.J., Hibbs, B.J., and Hutchison, W.R., 2008, Hydrogeologic controls on groundwater recharge and salinization: a geochemical analysis of the northern Hueco Bolson aquifer, Texas, USA: Hydrogeology Journal, v. 16, no. 2, p. 281-296. **(D2, H1, H2)**
Dunbar, N.W., 2005, Quaternary volcanism in New Mexico, *in* Lucas, S.G., Morgan, G., and Zeigler, K.E., eds., New Mexico's Ice Ages: New Mexico Museum of Natural History & Science Bulletin No. 28, p. 95-106. **(C2b)**
Dunbar, N.W., Gutzler, D.S., Pearthree, K.S., Phillips, F.M., Bauer, P.W., Allen, C.D., DuBois, D., Harvey, M.D., King, J.P., McFadden, L.D., Thomson, B.M., and Tillery, A.C., 2022, Climate Change in New Mexico Over the Next 50 Years: Impacts on Water Resources: NM BG and MR Bulletin 164, 218 p. **(B3, C1)**
Dunham, K.C., 1935, The geology of the Organ Mountains, with an account of the geology and mineral resources of Dona Ana County, New Mexico: New Mexico Bureau of Mines and Mineral Resources, Bulletin 11, 272 p. **(C2a, G1)**
Dyer, R., 1987, First day, Part A; Road log from El Paso/Ciudad Juárez via Villa Ahumada, El Sueco to Ciudad Chihuahua, *in* Excursión Geológica, Libreto Guía de Caminos, Sociedad Geológica Mexicana, Universidad Autónoma de Chihuahua, and the University of Texas at El Paso, p. 2-30. **(C2a, F1)**
Dyer, R., 1989, Structural geology of the Franklin Mountains, West Texas, *in* Muehlberger, W.R., and Dickerson, P.W., Structure and stratigraphy of Trans-Pecos Texas: 28th International Geological Congress, Field Trip Guidebook T317, p. 65-70. **(C2a)**
Eakin, T.E., Price, D., and Harill, J.R., 1976, Summary appraisals of the nation's ground-water resources – Great Basin region: U.S. Geological Survey Professional Paper 813-G, 37 p. **(D1)**
Eames, A.J., 1930, Report on ground-sloth coprolite from Dona Ana County, New Mexico: American Journal of Science, v. 119, p. 353-356. **(B2, C1)**

Eastoe, C., and Towne, D., 2018, Regional zonation of groundwater recharge mechanisms in alluvial basins of Arizona: Interpretation of isotope mapping: Journal of Geochemical Exploration, v. 194, p. 135-145. **(D2, H2, H3)**

Eastoe, C.J., and Wright, W.E., 2019, Hydrology of mountain blocks in Arizona and New Mexico as revealed by isotopes in groundwater and precipitation: Geosciences, v. 9, article 461. **(C1, D2, H2, H3)**

Eastoe, C.J., Hutchison, W.R., Hibbs, B.J., Hawley, J., and Hogan, J.F., 2010, Interaction of a river with an alluvial basin aquifer: Stable isotopes, salinity and water budgets: Journal of Hydrology, v. 395, p. 67-78. **(H1, H2)**

Eastoe C.J., Hibbs, B.J., Granados Olivas, A., Hogan, J.F., Hawley, J., and Hutchison, W.R., 2008, Isotopes in the Hueco Bolson aquifer, Texas (USA) and Chihuahua (Mexico): Local and general implications for recharge sources in alluvial basins: Hydrogeology Journal, v. 16, no. 4, p. 737-747. **(H1, H2)**

El Paso Water (EPW), ND, Water Resources-El Paso Water: https://epwater.org/our_water/water_resources **(E2, E2a, E2b, F2)**

Erlitski, R., and Craver, D. (Abstract), 2020, High-Recovery for Quick Recovery: Desalination solves multiple challenges to a community in need: Program with abstracts, Water, Energy, and Policy in a Changing Climate Conference, National Groundwater Association (NGWA), Albuquerque, NM, February 24-25, 2020. **(E2a)**

Esslinger, G.L., 1996, Water development on the Lower Rio Grande: The Elephant Butte Project, *in* Ortega Klett, C.T., ed., Reaching the Limits: Stretching the Resources of the Lower Rio Grande, Proceedings of the 40th Annual New Mexico Water Conference: New Mexico Water Resources Research Institute Report No. 297, p. 13-19. **(B3, E2, E3)**

Esslinger, G.L., 1998, Water politics in southern New Mexico: New Mexico Journal of Science, v. 38. p. 83-103. https://nmwrri.nmsu.edu/publications/miscellaneous-reports/m-documents/m26.pdf **(E2, E3)**

Fenneman, N.M., 1931, Physiography of the western United States: New York, McGraw- HI Book Co., 534 p. **(C)**

Fenneman, N.M., and Johnson, D.W., 1946, Physiographic divisions of the conterminous U.S. – Get this data set: U.S. Geological Survey, accessed June 9, 2016, at http://water.usgs.gov/lookuIetspatial?physio **(C)**

Fergusson, E., 1973 [1959], New Mexico: A pageant of three peoples; second edition with Introduction by Paul Horgan: University of New Mexico Press, Albuquerque, 408 p. ISBN 0-8263-0271-8 **(B3)**

Feth, J.H., and Whitehead, H.C., 1964, Chemical composition of rain, dry fallout, and bulk precipitation at Menlo Park, California, 1957-1959: Journal of Geophysical Research, v. 69, p. 3319-3333. **(C1, C3, D1)**

Fisher, R.S., and Mullican, W.F. III, 1990, Integration of ground-water and vadose zone geochemistry to investigate hydrochemical evolution: A case study in arid lands of the northern Chihuahuan Desert, Trans-Pecos Texas: University of Texas at Austin, Bureau of Economic Geology, Geological Circular GC 90-5, p. 1-36 **(F2, H1, H2)**

Fisher, R.S., and Mullican, W.F. III, 1997, Hydrochemical evolution of sodium-sulphate and sodium-chloride groundwater beneath the northern Chihuahuan Desert, Trans-Pecos Texas, USA: Hydrogeology Journal, v. 5. p. 4-16. **(F2, H1, H2)**

Flannigan, K.G., 2007, Surface water management: Working within the legal framework: Natural Resources Journal, v. 47, no. 3, p. 515-523. *1938 Rio Grande Compact* **(B3, E2, E3)**

Fleck, J., 2013, Texas fires shot in water war – Lawsuit claims N.M. has drained the Rio Grande: Albuquerque Journal, Wednesday, January 9, 2013, p. A1, A2. **(A3, E3)**

Fleck, J., 2016, Water is for fighting over, and other myths about water in the West: Washington, DC, Island Press, 264 p. ISBN: 9781610916790 (**A3, E2**)

Fleischhauer, H.L., Jr. and Stone, W.J., 1982, Quaternary geology of Lake Animas, Hidalgo County, New Mexico: New Mexico Bureau of Mines and Mineral Resources, Circular 174, 25 p. **(C2a, I2)**

Flores Mata, G., 1970, Informe de Actividades, mayo 1967-septiembre 1970, Anexos 3: Mapa de Grandes Grupos de Suelos del Edo. De Chihuahua de acurdo al Sistema de FAO/UNESCO/SRH, [y] Anexos 4. De 319 cuerdo al sistema Americano de la 7a, Aproximación: Secretaria de Recursos Hidráulicos, Jefatura Irrigación y Control de Ríos, Dirección de Agrología, Serie Estudios Publicación Numero 1, 33 p. **(C3, F3)**

Follett, W.W., 1898, Rio Grande Waters – Equitable distribution of waters of the Rio Grande: Message to the President of the United States: 55th Congress, 2nd Session, U.S. Senate Document No. 229, Washington, D.C., US Government Printing Office, 289 p. **(B3, D1, E3)**

Fox, W.J., 1975, The Broad Canyon Dam: New Mexico Geological Society Guidebook 26, p. 181. **(C2a)**

Frenzel, P.F., and Kaehler, C.A., 1990, Geohydrology and simulation of ground-water flow in the Mesilla Basin, Doña Ana County, New Mexico and El Paso County, Texas; *with a section on Water quality and geochemistry by S.K. Anderholm*: U.S. Geological Survey Open-file Report 88-305, 179 p. **(F2, H2, H3)**

Frenzel, P.F., and Kaehler, C.A., 1992, Geohydrology and simulation of ground-water flow in the Mesilla Basin, Doña Ana County, New Mexico and El Paso County, Texas, *with a section on Water quality and geochemistry by S.K. Anderholm*: U.S. Geological Survey Professional Paper 1407-C, 105 p. **(F2, H2, H3)**
Frye, J.C., and Willman, H.B., 1962, Morphostratigraphic units in Pleistocene stratigraphy: American Association of Petroleum Geologists Bulletin, v. 46, p. 112-113. **(D1)**
Galloway, D., Jones, D.R., and Ingebritzen, S.E., eds., 1999, Land subsidence in the United States: U.S. Geological Survey Circular 1182, 177 p. **(D1)**
Galloway, W.E., 2005, Gulf of Mexico Basin depositional record of Cenozoic North American drainage basin evolution: International Association of Sedimentologists, Special Publication 35, p. 409-423. **(D1, I3)**
Galton, F., 1892, Inquiries into human faculty and its development (2nd Edition-Macmillan): New York, Dutton (1911), 302 p. **(A2)**
Galvan, A., 2020, Feds give 65 acres for border wall project – Land transfer done for infrastructure use: Albuquerque Journal–METRO & NM, Friday, July 24, 2019, p. B 2. **(A3)**
Gámez, J., Ranis, M., and Eppes, M., 2021, Bringing art to your science and thus your science to the people: Joining visual culture and scientific evidence: GSA Today, v.1, no. 8, p. 13. **(D1)**
Garcia, S., Louvat, P., Gaillardet, J., Nyachoti, S., and Ma, L., 2021, Combining uranium, boron, and strontium isotope ratios ($^{234}U/^{238}U$, $\delta\ ^{11}B$, $^{87}Sr/^{86}Sr$) to trace and quantify salinity contributions to Rio Grande river in Southwestern United States. Frontiers in Water, v. 2, article 575216, 24 p. **(C4, H2)**
Garcia-Vasquez, A.C., Granados-Olivas, A., Samani, Z., and Fernald, A., 2022, Investigation of the origin of Hueco Bolson and Mesilla Basin aquifers (US and Mexico) with isotopic data analysis: Water, v. 14 (526), 17 p. **(F1)**
Garland, M., 2020, Growing the wind industry is smart – Projects provide jobs and clean power: Albuquerque Journal – NM'S ENERGY FUTURE, Monday, March 16, 2020, p. A11. **(A3)**
Garza, S., Weeks, E.P., and White, D.E., 1980, Appraisal of potential for injection-well recharge of the Hueco bolson with treated sewage effluent – Preliminary study of the northeast EI Paso area, Texas: U.S. Geological Survey Open-file report 80-1106, 37 p. **(E2b, F2, H2)**
Gates, J.S., and Stanley, W.D., 1976, Hydrologic interpretation of geophysical data from the southeastern Hueco Bolson, El Paso and Hudspeth Counties, Texas: U.S. Geological Survey Open-File Report 76-650, 37 p. **(C4, F2, H1)**
Gates, J.S., White, D.E., and Leggat, E.R., 1984, Preliminary study of aquifers of the lower Mesilla Valley in Texas and New Mexico by model simulation: U.S. Geological Survey Water Resources Investigations Report 84-4317, 21 p. **(H1, H3)**
Geosoft, 2016, Oasis montaj application help system: Geosoft. http://www.geosoft.com/products/oasis-montaj/ VOXEL modeling **(D1, E2)**
Gibbard, P.L., Head, M.J., Walker, M.J.C., and the Subcommission on Quaternary Stratigraphy, 2010, Formal ratification of the Quaternary System/Period and the Pleistocene Series/Epoch with a base at 2.58 Ma: Journal of Quaternary Science, v. 25, p. 96-102. **(B1)**
Gile, L.H., 1961, A classification of ca horizons in soils of a desert region, Doña Ana County, New Mexico: Soil Science Society of America Proceedings, v. 25, no. 1, p. 52-61. **(C3)**
Gile, L.H., 1966a, Coppice dunes and the Rotura soil: Soil Science Society of America Proceedings, v. 30, p. 657-660. **(C3)**
Gile, L.H., 1967, Soils of an ancient basin floor near Las Cruces, New Mexico: Soil Science, v. 103, no. 4, p. 265-276. **(C3)**
Gile, L.H., 1986, Late Holocene displacement along the Organ Mountains fault in southern New Mexico – a summary: New Mexico Geology, v. 8, no. 1, p. 1-4. **(C2a, C3)**
Gile, L.H., 1987a, A pedologic chronology of Kilbourne Hole, southern New Mexico: I. Soils in tuff; II. Time of the explosions: Soil Science Society of America Journal, v. 51, p. 746-760. **(C2a, C3)**
Gile, L.H., 1990, Chronology of lava and associated soils near San Miguel, New Mexico: Quaternary Research, v. 33, p. 37-50. **(C2b, C3)**
Gile, L.H., 1991, Discussion, burial of fault scarps along the Organ Mountains fault, south-central New Mexico: Bulletin of the Association of Engineering Geologists, v. 27, no. 3, p. 325, 326. *See Beehner 1990.* **(C2b, C3)**
Gile, L.H., 1994b, Soils, geomorphology, and multiple displacements along the Organ Mountains fault in southern New Mexico: New Mexico Bureau of Mines and Mineral Resources Bulletin 133, 91 p. **(C2b, C3)**
Gile, L.H., 1999, Eolian and associated pedogenic features of the Jornada Basin floor, southern New Mexico: Soil Science Society of America Journal, v. 63, p. 151-163. **(C3)**

Gile, L.H., and Grossman, R.B., 1979, The Desert Project Soil Monograph: U.S. Department of Agriculture, National Technical Information Service, Document No. PB80-13534, Springfield, VA 22161, 984 p. **(C3)**
Gile, L.H., and Hawley, J.W., 1966, Periodic sedimentation and soil formation on an alluvial-fan piedmont in southern New Mexico: Soil Science Society of America Proceedings, v. 30, p. 261-268. **(C2a, C3)**
Gile, L.H., and Hawley, J.W., 1972, The prediction of soil occurrence in certain desert regions of the southwestern United States: Soil Science Society of America Proceedings, v. 36, no. 1, p. 119-124. **(C2a, C3)**
Gile, L.H., Gibbens, R.P., and Lenz, J.M., 1998, Soil-induced variability in root systems of creosotebush (Larrea tridentata) and tarbush (Flourensia cernua): Journal of Arid Environments, v. 39, p. 57-78. **(C1, C3)**
Gile, L.H., Hawley, J.W., and Grossman, R.B., 1981, Soils and geomorphology in the Basin Range area of southern New Mexico – Guidebook to the Desert Project: New Mexico Bureau of Mines and Mineral Resources, Memoir 39, 222 p. https://geoinfo.nmt.edu/publications/monographs/memoirs/39/ **(C2a, C3)**
Gile, L.H., Peterson, F.F., and Grossman, R.B., 1966, Morphological and genetic sequences of carbonate accumulation in desert soils: Soil Science, v. 101, no. 5, p. 347-360. **(C3)**
Gile, L.H., Hawley, J.W., Grossman, R.B., Monger, H.C., Montoya, C.E., and Mack, G.H., 1995, Supplement to the Desert Project Guidebook, with emphasis on soil micromorphology: New Mexico Bureau of Mines and Mineral Resources, Bulletin 142, 96 p. **(C2b, C3)**
Gile, L.H., Monger, H.C., Grossman, R.B., Ahrens, R.J., Hawley, J.W., Peterson, F.F., Gibbens, R.P., Lenz, J.M., Bestelmeyer, B.T., and Nolen, B.A., 2007, A 50th Anniversary Guidebook for the Desert Project: Lincoln, NE, U.S. Department of Agriculture, Natural Resources Conservation Service, National Soil Survey Center, 279 p. **(C1, C2b, C3)**
Giles, G.C., and Pearson, J.W., 1998, Characterization of hydrostratigraphy and groundwater flow on the southwestern San Andres Mountains pediment, NASA-JSC White Sands Test Facility: New Mexico Geological Society Guidebook 49, p. 317-325. **(H1, H3)**
Gleason, M., 2024a, Tech Outlook: NM Tech's Shari Kelley explains geothermal energy: Albuquerque Journal–BUSINESS OUTLOOK, Monday, March 25, 2024, p. 6. **(A3)**
Gleason, M., 2024b, 'The Earth is always hot'– Geothermal advancements, incentives could help NM meet renewable energy goals: Albuquerque Journal–BUSINESS OUTLOOK, Monday, March 25, 2024, p. 10-12. **(A3)**
Glennon, R., 2002, Water follies: Groundwater pumping an' the fate of America's fresh waters – Chapter 15. The Tragedy of Law and the Commons [p. 209-224]: Washington DC, Island Press, 314 p. ISBN 1-55963-223-2 **(A2, E2)**
Glover, A., 2018, Levees of the Hatch and Mesilla Valleys: N.M. Geological Society Guidebook 69, p. 63-64. *See Baker 1943.* **(B3, E2)**
Goff, F., and Gardner, J.N., 2004, Late Cenozoic geochronology of volcanism and mineralization in the Jemez Mountains and Valles caldera, north-central New Mexico, *in* Mack, G.H., and Giles, K.J., eds., The Geology of New Mexico: A geologic history: New Mexico Geological Society, Special Publication 11, p. 295-312. **(B1, C2b)**
Gómez, F., 1983, Geology of Sierra del Aguila, northern Chihuahua, Mexico, *in* Geology and Mineral Resources of North-Central Chihuahua: El Paso Geological Society, Guidebook 1983 Field Conference, p. 261-267. **(C2a, F3)**
Gradstein, F.M., Ogg, J.G., Schmitz, M., and Ogg, G., eds., 2012, The geologic time scale 2012: Amsterdam, Elsevier, 1176 p. Paperback ISBN: 9780444594259 **(B1)**
Granados Olivas, A., 2000, Relationships between Landforms and Hydrogeology in the Lower Casas Grandes Basin, Ascension, Chihuahua, Mexico: New Mexico State University, doctoral dissertation, 292 p. **(E1, F3, H1)**
Granados Olivas, A., 2010, Future solutions: Research needs in the Mexican section of the Rio Grande (Bravo) watershed: Journal of Transboundary Water Resources, v. 1, p. 147-157. https://nmwrri.nmsu.edu/publications/pub-documents/JTWR-Book.pdf **(E2, F3)**
Granados Olivas, A., 2022, Los recursos hidrológicos en cuencas transfronterizas entre México y Estados Unidos: El Paso del Norte y la gobernanza binacional del agua: Universidad Autónoma de Chihuahua y Universidad Autónoma de Ciudad Juárez, 324 p. ISBN 978-607-536 **(A2, B3, F1)**
Granados Olivas, A., and Kretzschmar, T., 2001, Uso de sistemas de información Geográfica y sistemas de teledetección en la identificación y mapeo de potenciales zonas de recarga hacia acuíferos del Desierto Chihuahua: VIII Reunión Nacional sobre Sistemas de Captación de Agua de Lluvia, Cd. Chihuahua, Chih., SEMARNAT [Mexico]. 17 p. **(D2, E1, F3)**

Granados Olivas, A., and Monger, H.C., 1999, Remote Sensing Technology for Development Planning Along the U.S.-Mexico Border: Hydrogeology and Geomorphology, *in* Herrera, E. and Mexal, J., eds., Ensuring Sustainable Development of Arid Lands Through Time: Las Cruces, New Mexico Academy of Science Journal, v. 39, p. 123-137. **(E1, E2, F1)**

Granados Olivas, A., Brown, C., Greenlee, J., Creel, B., Hawley, J.W., Kennedy, J., Dena-Ornelas, O., and Hurd, B., 2006, Geographic information systems at the Paso del Norte region. The academic accomplishments and challenges for a Transboundary water resources GIS cooperation, *in* Anderson, K.S.J., ed., Science on the Border: New Mexico Journal of Science, v. 46, p. 45-56. **(E1, F1)**

Grandin, T., 2006, Thinking in pictures - and other reports from my life with autism: New York, Vintage Books, 270 p. ISBN-13: 978-0-307-27565-3 **(A2)**

Grauch, V.J.S., and Connell, S.D., 2013, New perspectives on the geometry of the Albuquerque Basin, Rio Grande rift, New Mexico: Insights from geophysical models of rift-fill thickness, *in* Hudson, M.R., and Grauch, V.J.S., eds., New Perspectives on Rio Grande Rift Basins: From Tectonics to Groundwater: Geological Society of America Special Paper 494, p. 427-462. **(C2b, C4)**

Grauch, V.J.S., and Hudson, M.R., 2007, Guides to understanding the aeromagnetic expression of faults in sedimentary basins: Lessons learned from the central Rio Grande rift: Geosphere, v. 3, no. 6, p. 596-623. **(C2b, C4)**

Gries, J.G., 1979, Problems of delineation of the Rio Grande rift into Chihuahua tectonic belt of northern New Mexico, *in* Riecker, R.E., ed., Rio Grande rift: Tectonics and magmatism: Washington, D.C., American Geophysical Union, p. 107-113. **(C2a, F1)**

Gries, J.G., and Haenggi, W.T., 1970, Structural evolution of the eastern Chihuahua Tectonic Belt, *in* The Geologic Framework of the Chihuahua Tectonic Belt: Symposium in honor of Professor Ronald K. DeFord, West Texas Geological Society and University of Texas at Austin, p. 119-137. **(C2a, F1)**

Grissino-Mayer, H., Baisan, C.H., Morino, K.A., and Swetnam, T.W., 2002, Multi-century trends in past climate for the Middle Rio Grande Basin, AD 622-1992: Final report submitted to the USDA Forest Service, Albuquerque, NM. Laboratory of Tree-Ring Science, Report 2002/6. **(B2, C1)**

Groat, C.F., 1970, Geology of Presido Bolson, Presidio County, Texas and adjacent Chihuahua, Mexico: University of Texas at Austin, doctoral dissertation, 167 p. **(C2a, F1, I3)**

Groat, C.F., 1972, Presido Bolson, Trans-Pecos Texas and adjacent Mexico: Geology of a desert basin aquifer system: Texas Bureau of Economic Geology Report of Investigation, 76, 46 p. **(C2a, F1, I3)**

Gross, J., and Icerman, L., 1983, Subsurface investigations for the area surrounding Tortugas Mountain, Doña Ana County, New Mexico: New Mexico Energy Research and Development Institute, Interim Report NMERDI 2-67-2238 (2), 70 p. **(C4, H1)**

Gude, V.G., 2016, Desalination and sustainability - An appraisal and current perspective: Water Research, v. 89, p. 87-106. **(E2a)**

Guerrero, J.C., 1969, Stratigraphy of Banco de Lucero, State of Chihuahua, *in* The Border Region, New Mexico Geological Society Guidebook 20, p. 171-172. **(C2a, F3)**

Gunaji, N.N., 1961, Ground-water conditions in Elephant Butte Irrigation District: Las Cruces, New Mexico State University, Engineering Experiment Station, 43 p. **(H2, H3)**

Gunaji-Klement & Associates, 1994, Water quality and availability plan for Miner's Ridge Subdivision in Dona Ana County, New Mexico: Report prepared for: Mr. George B. Rawson, Pueblo Builders, Inc., P.O. Box 1286, Las Cruces, NM 88004 *by* Gunaji-Klement & Associates, Engineers & Geologists, P.O. Box 5008, Las Cruces, NM 88003, 19 p., *with* 1. Clemons, C.E., 1994, Report on lithologic analysis of cuttings from well in NE ¼ Sec. 22, T23S, R3E, and 2. SW Geophysical Services, Inc., 9/26/1994, Borehole geophysical logs: SP, Electrical Resistivity, Gamma Ray, and Neutron. **(H1, H2)**

Gunaji-Klement & Associates, 2001, Sonoma Ranch Golf Course Well Completion Report: Submitted to: Mr. George B. Rawson, Sonoma Ranch Development Company, P.O. Box 936, Las Cruces, NM 88004 *by* Gunaji-Klement & Associates, Consulting Engineers, P.O. Box 5008, Las Cruces, NM 88003-5008, 19 p., *with* SW Geophysical Services, Inc., 7/17/2001, Borehole geophysical logs: SP, Electrical Resistivity, and Temperature. **(H1, H2)**

Gunaji, N.N., Thode, E.F., Chaturvedi, L., Walvekar, A., LaFrance, L., Swanberg, C.A., and Jiracek, G.R., 1978, Geothermal application feasibility study for the New Mexico State University campus: New Mexico Energy Institute at New Mexico State University, Technical Report NMEI 13 - Contract 76-205, 118 p. **(C4, H2)**

Gustavson, T.C., 1991a, Arid basin depositional systems and paleosols: Fort Hancock and Camp Rice Formations (Pliocene-Pleistocene) Hueco Bolson, West Texas and adjacent Mexico: The University of Texas at Austin, Bureau of Economic Geology, Report of Investigations No. 198, 49 p. **(C2b, C3, I3)**

Gutiérrez-Ojeda, C., 2001, Aquifer recharge estimation at Mesilla Bolson and Guaymas aquifer systems, Mexico, *in* IAEA, eds., Isotope based assessment of groundwater renewal in water scarce regions: IAEA-TECDOC-1246, Vienna, International Atomic Energy Agency, p. 23-44. *See Secretaria de Recursos Hidráulicos 1988, Pozo no. 9-El Parabién*. **(F3, H2, H3)**

Gutzler, D.S., 2005, Once and future climates in New Mexico and North America; the icehouse and the hothouse anti-analogues, *in* Lucas, S.G., Morgan, G.A., and Zeigler, K.E., eds., New Mexico's Ice Ages: New Mexico Museum of Natural History and Science Bulletin 18, 107-114. **(C1)**

Gutzler, D.S., 2020, New Mexico's climate in the 21st Century – A great change is underway: New Mexico Earth Matters, Summer 2020, p. 1-5 **(C1)**

Gutzler, D.S., and Robbins, T.O., 2011, Climate variability and projected change in the western United States: regional downscaling and drought statistics: Climate Dynamics, v. 37, no. 5, p. 835-849. **(C1)**

Haase, C.S., and Lozinsky, R.P., 1992, Estimation of hydrologic parameters, *in* Hawley, J.W., and Haase, C.S., compilers, Hydrogeologic framework of the northern Albuquerque Basin: New Mexico Bureau of Mines and Mineral Resources, Open File Report 387, p. VI-1–VI-3. **(D1)**

Hackett, O.M., 1972, Presentation of the O.E. Meinzer Award to George Burke Maxey, with response by George B. Maxey, in Medals and Awards for 1971: Geological Society of America, v. 83, no. 6, p. xxv-xxviii. **(A2, D1)**

Haenggi, W.T., 2001, Tectonic history of the Chihuahua trough, Mexico, and adjacent USA; Part I, The pre-Mesozoic Setting: Boletín de Sociedad Geológica Mexicana, Tomo 54, p. 28-66. **(C2b, F3)**

Haenggi, W.T., 2002, Tectonic history of the Chihuahua trough, Mexico, and adjacent USA; Part II, Mesozoic and Cenozoic: Boletín de Sociedad Geológica Mexicana, Tomo 55, p. 38-74. **(C2b, F3)**

Hall, S.A., 2005, Ice Age vegetation and flora of New Mexico, *in* Lucas, S.G., et al., eds., New Mexico's Ice Ages: New Mexico Museum of Natural History & Science Bulletin No. 28, p. 171-183. **(B2, C1)**

Halpenny, L.C., Babcock, J.A., and Greene, D.K., 1972, Basic data report, ASARCO La Mesa test production water well: Tucson, AZ, Water Development Corporation Open-File Report, 40 p. **(C2a, H1, H2, H3)**

Hamblock, J.H., Andronicos, C.L., Miller, K.C., Barnes, G.C., Ren, M., Averill, M.G., and Anthony, E.Y., 2007, A composite geologic and seismic profile beneath the southern Rio Grande rift in New Mexico, based on xenolith mineralogy, temperature, and pressure: Tectonophysics, v. 442, issues 1-4, p. 14-48. **(C2b, C4)**

Hammond, G.P., and Rey, A., 1953, Don Juan de Oñate, colonizer of New Mexico, 1595-1628; Coronado Quarto Centennial Publications, 1540-1940, Albuquerque, Vol. II: Albuquerque, University of New Mexico Press, 1187 p. *May 4, 1498 Oñate party leaves EPdN and enters NM (p. 95).* **(B3)**

Hamway, S., 2020a, Recycling company to expand in Santa Teresa – Texas firm has 11 plants in US, Mexico: Albuquerque Journal–BUSINESS, Wednesday, February 19, 2020, p. A10-A11. **(A3, E2c)**

Hamway, S., 2020b, Taiwanese firm plans move to Santa Teresa – Relocation part of trend for manufacturers to set up sites near customers: Albuquerque Journal–BUSINESS, Tuesday, December 8, 2020, p. A8. **(A3)**

Haneberg, W.C., 1995, Depth-porosity relationships and virgin specific storage estimates for the upper Santa Fe Group aquifer system, central Albuquerque Basin, New Mexico: New Mexico Geology, v. 17, no. 4, p. 62-71. **(D1)**

Haneberg, W.C., and Friesen, R.L., 1995, Tilts, strains, and ground-water levels near an earth fissure in the Mimbres Basin, New Mexico: Geological Society of America Bulletin, v. 107, p. 316-326. **(D1, H1)**

Hanson, R.T., 1989, Aquifer-system compaction, Tucson Basin, and Avra Valley, Arizona: U.S. Geological Survey Water-Resources Investigations Report 88-4172, 69 p. **(D1)**

Hanson, R.T., McLean, J.S., and Miller, R.S., 1994, Hydrogeologic framework and preliminary simulation of ground-water flow in the Mimbres Basin, southwestern New Mexico: U.S. Geological Survey Water-Resources Investigations Report 94-4011, 118 p. **(F2, H1, H3)**

Hanson, R.T., Ritchie, A.B., Boyce, S.E., Galanter, A.E., Ferguson, I.A., Flint, L.E., and Henson, W.R., 2018, Rio Grande transboundary integrated hydrologic model and water-availability analysis, New Mexico and Texas, United States, and Northern Chihuahua, Mexico: U.S Geological Survey Open-File Report 2018-1091, 185 p. **(F1, H3)**

Harbour, R.L., 1972, Geology of the northern Franklin Mountains, Texas and New Mexico: U.S. Geological Survey, Bulletin 1298, 129 p. **(C2a)**

Hardin, G., 1968, The tragedy of the commons: Science, v. 162, p.1243-1247. **(D1)**

Harris, L.G., 1996, The Developers: Controlling the Lower Rio Grande 1890-1980, *in* Ortega Klett, C.T., ed., Reaching the Limits: Stretching the Resources of the Lower Rio Grande, Proceedings of the 40th Annual New Mexico Water Conference: New Mexico Water Resources Research Institute Report No. 297, p. 7-12. **(A2, B3, E2, E3)**

Harris, L.G., 2012, Whose water is it anyway? Anatomy of the water war between El Paso, Texas and New Mexico, *in* Ortega Klett, C.T., ed., One hundred years of water wars in New Mexico: Santa Fe, Sunstone Press, p. 227-253. ISBN: 978-0-86524-902-5 **(A2, B3, E2, E3)**

Hartley, A.J., Weissmann, G.S., Nichols, G.J, and Warwick, G.L., 2010, Large distributive fluvial systems, characteristics, distribution, and controls on development: Journal of Sedimentary Research, v. 80, issue 2, p. 167-183. **(D1)**

Hathaway, D.L., 2011, Transboundary groundwater policy: Developing approaches in the western and southwestern United States. Journal of the American Water Resources Association (JAWRA), v. 47, no. 1, p. 103-113. **(E2, F1)**

Hawley, J.W., 1962, Late Pleistocene and recent geology of the Winnemucca segment of the Humboldt River Valley, Nevada: University of Illinois at Urbana-Champaign, doctoral dissertation, 220 p. **(D1)**

Hawley, J.W., 1965, Geomorphic surfaces along the Rio Grande Valley from El Paso, Texas to Caballo Reservoir, New Mexico: New Mexico Geological Society, Guidebook 16, p. 188-198. **(C2a)**

Hawley, J.W., 1969a, Geology and its relation to the hydrologic system, *in* King, W.E., Hawley, J.W., Taylor, A.M., and Wilson, R.P., Hydrogeology of the Rio Grande Valley and adjacent intermontane areas of southern New Mexico: New Mexico Water Resources Research Institute, WRRI Report 6, p. 19-47; *cf. King, W.E., and others, Geology and ground-water resources of central and western Doña Ana County, New Mexico: New Mexico Bureau of Mines and Mineral Resources, Hydrologic Report 1, p. 9-24, 61-62.* **(C2a, H1)**

Hawley, J.W., 1969b, Notes on the geomorphology and late Cenozoic geology of northwestern Chihuahua: New Mexico Geological Society Guidebook 20, p. 131-142. **(C2a, F3)**

Hawley, J.W., compiler, 1970, Cenozoic stratigraphy of the Rio Grande Valley area, Doña Ana County, New Mexico: El Paso Geological Society, Guidebook 4, 49 p. **(C2a, F2)**

Hawley, J.W., 1975a, Quaternary history of Doña Ana County region, south-central New Mexico: New Mexico Geological Society Guidebook 26, p. 139-150. **(C2a, F1, I3)**

Hawley, J.W., 1975b, The desert soil-geomorphology project: New Mexico Geological Society, Guidebook 26, p. 183-185. **(A2, C3)**

Hawley, J.W., compiler, 1978, Guidebook to the Rio Grande rift in New Mexico and Colorado: New Mexico Bureau of Mines and Mineral Resources, Circular 163, 241 p. **(A2, C2a, C4)**

Hawley, J.W., 1984, Hydrogeologic cross sections of the Mesilla Bolson, New Mexico and Texas: New Mexico Bureau of Mines and Minerals Resources, Open-file Report 190, 10 p. *Appendix in Peterson, D.M., Khaleel, R., and Hawley, J.W., 1984.* **(H1)**

Hawley, J.W., 1986, Physiographic provinces [and] landforms of New Mexico, *in* Williams, J.L., ed., New Mexico in Maps (2nd edition): University of New Mexico Press, p. 23-31. **(C2a)**

Hawley, J.W., 1993, Geomorphic setting and late Quaternary history of pluvial-lake basins in the southern New Mexico region: New Mexico Bureau of Mines and Mineral Resources Open-File Report 391, 28 p. **(C2b, I1)**

Hawley, J.W., 2005, Five million years of landscape evolution in New Mexico: An overview based on two centuries of geomorphic conceptual-model development, *in* Lucas, S.G., et al., eds., New Mexico's Ice Ages: New Mexico Museum of Natural History & Science Bulletin No. 28, p. 9-93. **(A1, A2, C2b, F1, I1, I3)**

Hawley, J.W., 2014b, Biographical profile of Oscar E. Meinzer, *in* Kues, B.S., Lewis, C.J., and Lueth, V.W., A brief history of geological studies in New Mexico: New Mexico Geological Society, Special Publication 12, p. 117-119 (*cited references 209-230*). **(A2)**

Hawley, J.W., 2020, A Hydrogeologic perspective on groundwater conservation in the northern Rio Grande basin, New Mexico, Texas, and Chihuahua—2014 Albert E. Utton Memorial Lecture, in Sheely, M., ed. Proceedings, 59th Annual New Mexico Water Conference, Santa Fe, NM., p. 59-84, with 28 pptx-slide pdf on CD-ROM. **(D1, F1, H1)**

Hawley, J.W., and Gile, L.H., 1966, Landscape evolution and soil genesis in the Rio Grande region, southern New Mexico: Friends of the Pleistocene, Rocky Mountain Section, Guidebook 11th Field Conference; Las Cruces, NM State University Agronomy Department, Special Publication, 74 p. **(C2a, C3)**

Hawley, J.W., and Granados Olivas, A., 2012, Progress report on development of an annotated bibliography for transboundary aquifer systems of the Mesilla Basin-Paso del Norte area, New Mexico, Texas, and Chihuahua, *in* Aquifers of West Texas-Theme Session T5: Geological Society of America, Abstracts with Programs, v. 44, no. 1, p. 38, No.199147 on CD/ROM. **(A1, F1)**

Hawley, J.W., and Haase, C.S., 1992, compilers, Hydrogeologic framework of the northern Albuquerque Basin: New Mexico Bureau of Mines and Mineral Resources, Open-file Report OF-387, 74 p., 8 Appendices, Glossary. **(D1)**

Hawley, J.W., and Kennedy, J.F., 2004, Creation of a digital hydrogeologic framework model of the Mesilla Basin and southern Jornada del Muerto Basin: New Mexico Water Resources Research Institute Report No. 332, 105 p., with plates and appendix on CD ROM. https://nmwrri.nmsu.edu/publications/technical-reports/tr-reports/tr-332.html **(F1, H1)**

Hawley, J.W., and Kernodle, J.M., 2000, Overview of the hydrogeology and geohydrology of the northern Rio Grande basin – Colorado, New Mexico, and Texas, *in* Ortega-Klett, C.T., ed., Proceedings of the 44th Annual New Mexico Water Conference: New Mexico Water Resources Research Institute Report 312, p. 79-102. **(D1)**

Hawley, J.W., and Kernodle, J.M., 2008, Early contributions to arid-zone hydrogeology in the eastern Basin and Range region: Ground Water, v. 46, no. 3, p. 510-516. **(A2, B3, D1)**

Hawley, J.W., and Kottlowski, F.E., 1969, Quaternary geology of the south-central New Mexico border region, *in* Border Stratigraphy Symposium: New Mexico Bureau of Mines and Mineral Resources, Circular 104, p. 89-115. **(C2a)**

Hawley, J.W., and Longmire, P.A., 1992, Site characterization and selection, *in* Reith, C.C. and Thomson, B.M., eds., Deserts as Dumps? The disposal of hazardous materials in arid ecosystems: University of New Mexico Press, p. 57-99. **(C2b, D1, E2c)**

Hawley, J.W., and Love, D.W., 1981, Overview of geology as related to environmental concerns in New Mexico, *in* Wells, S.G., and Lambert, W., eds., Environmental geology and hydrology in New Mexico: NM Geological Society, Special Publication No 10, p. 1-10. **(A2, E2)**

Hawley, J.W., and Lozinsky, R.P., 1992, Hydrogeologic framework of the Mesilla Basin in New Mexico and western Texas: New Mexico Bureau of Mines and Mineral Resources, Open-File Report 323, 55 p. **(H1)**

Hawley, J.W., and Seager, W.R., 1969, Description of Santa Fe Group measured sections: Appendix A, *in* Hawley, J.W., and five others, The Santa Fe Group in the south-central New Mexico border region New Mexico Bureau of Mines and Mineral Resources, Circular 104, p. 68-76. **(C2a)**

Hawley, J.W., and Swanson, B.H. (Abstract), 2020, Hydrogeologic framework of the International Boundary Zone of the Mesilla Basin region: Program with abstracts, Water, Energy, and Policy in a Changing Climate Conference, National Groundwater Association (NGWA), Albuquerque, NM, February 24-25, 2020. **(H1)**

Hawley, J.W., and Swanson, B.H., 2022, Conservation of shared groundwater resources in the binational Mesilla Basin-El Paso Del Norte Region – A Hydrogeological Perspective, in Granados Olivas, Alfredo, coordinador, Los Recursos Hidrológicos en Cuencas Transfronterizas entre México y los Estados Unidos: El Paso del Norte y la Gobernanza Binacional de Agua [Hydrological Resources in Transboundary Basins between Mexico and the United States: El Paso del Norte and the Binational Water Governance]: Universidad Autónoma de Ciudad Juárez y Universidad Autónoma de Chihuahua, p. 202-323. ISBN 978-607-536 **(F1, H1)**

Hawley, J.W., and Wilson, W.E. III, 1965, Quaternary geology of the Winnemucca area, Nevada: Desert Research Institute, University of Nevada, Reno, Technical Report No. 5, 66 p. **(D1)**

Hawley, J.W., Bachman, G.O., and Manley, K., 1976, Quaternary stratigraphy in the Basin and Range and Great Plains provinces, New Mexico and western Texas, *in* Mahaney, W.C., ed., Quaternary stratigraphy of North America: Stroudsburg, PA, Dowden, Hutchinson, and Ross, Inc., p. 235-274. **(A1, A2, D1, I1, I3)**

Hawley, J.W., Haase, C.S., and Lozinsky, R.P., 1995, An underground view of the Albuquerque Basin, New Mexico, *in* Ortega-Klett, C.T., ed., Proceedings of the 39th Annual New Mexico Water Conference, New Mexico Water Resource Research Institute Report 290, p. 37-55. **(D1)**

Hawley, J.W., Kambhammettu, B.V.N.P., and Creel, B.J., 2010, Digital hydrogeologic-framework model of the San Francisco River basin, west-central New Mexico and east-central Arizona: New Mexico Water Resources Research Institute Report No. 354, 51 p., 7 tables and 5 figures, with 3 plates and Appendix on CD ROM. https://nmwrri.nmsu.edu/publications/technical-reports/tr-reports/tr-354.html **(D1, H1)**

Hawley, J.W., Kennedy, J.F., and Creel, B.J., 2001, The Mesilla Basin aquifer system of New Mexico, West Texas and Chihuahua – An overview of its hydrogeologic framework and related aspects of groundwater flow and chemistry, *in* Mace, R.E., Mullican, W.F. III, and Angle, E.S., eds., Aquifers of West Texas: Texas Water Development Board Report 356, p. 76-99. **(H1)**

Hawley, J.W., Seager, W.R., and Clemons, R.E., 1975, Las Cruces to north Mesilla Valley, Cedar Hills, San Diego Mountain and Rincon area: New Mexico Geological Society Guidebook 26, p. 35-53. **(C2a)**

Hawley, J.W., Kennedy, J.F., Granados Olivas, A., and Ortiz, M.A., 2009, Hydrogeologic framework of the binational western Hueco Bolson-Paso del Norte area, Texas, New Mexico, and Chihuahua: Overview and progress report on digital model development: New Mexico Water Resources Research Institute Report No. 349, 45 p., 2 pls. https://nmwrri.nmsu.edu/publications/technical-reports/tr-reports/tr-349.html **(F1, H1)**

Hawley, J.W., Kennedy, J.F., Ortiz, M.A., and Carrasco, S., 2005, Creation of a digital hydrogeologic framework model of the Rincon Valley and adjacent areas of Dona Ana, Sierra and Luna Counties NM: New Mexico Water Resources Research Institute, Addendum to Report No. 332 on CD ROM. https://nmwrri.nmsu.edu/publications/technical-reports/tr-reports/tr-332.html **(H1)**

Hawley, J.W., Wilson, W.E., Cartwright, K., Swinderman, J., and Farvolden, R.N., 1961, Progress report on the geologic phase of the Humboldt River Project for Field Season 1960, *in* Progress Report, Humboldt River Research Project – A State-Federal Cooperative Program: Carson City, Nevada State Department of Conservation and Natural Resources, p. 26-32. **(D1)**

Hawley, J.W., Kottlowski, F.E., Seager, W.R., King, W.E., Strain, W.S. and LeMone, D.V., 1969, The Santa Fe Group in the south-central New Mexico border region, *in* Border Stratigraphy Symposium: New Mexico Bureau of Mines and Mineral Resources, Circular 104, p. 52-76. **(C2a, F1)**

Hawley, J.W., Hibbs, B.J., Kennedy, J.F., Creel, B.J., Remmenga, M.D., Johnson, M., Lee, M.M., and Dinterman, P., 2000, Trans-International Boundary aquifers in southwestern New Mexico: New Mexico Water Resources Research Institute, prepared for U.S. Environmental Protection Agency-Region 6 and International Boundary and Water Commission; Technical Completion Report-Interagency Contract X-996350-01-3, 126 p. https://nmwrri.nmsu.edu/publications/pub-external-pages/trans-international-boundary-aquifers-in-southwest-new-mexico.html **(C2b, D1, F1, I2)**

Hayden, F.V., 1873, First, second, and third annual reports of the United States Geological Survey of the Territories for the years 1867, 1868, and 1869: Publication of the Hayden Survey, Washington, DC, Government Printing Office, 261 p. **(B3, D1)**

Haynes, C.V., Jr., 1968, Geochronology of late Quaternary alluvium, *in* Morrison, R.B., and Wright, H.W., Jr., eds., Means of correlation of Quaternary successions: University of Utah Press, INQUA VII Congress, v. 8, p. 591-631. **(B2, C2a)**

Hayton, R.D., 1978a, Institutional policies for U.S.-Mexico groundwater management: Natural Resources Journal, v. 18, no. 1 (Symposium on U.S.-Mexican Transboundary Resources, Part II), p. 201-212. **(E2, E3, F1)**

Hayton, R.D., 1978b, The ground water legal regime as instrument of policy objectives and management requirements, *in* ANNALES JURIS AQUARUM II: Caracas, Venezuela; 2nd International Conference on Water Law and Administration (Feb. 1976), p. 8-14. **(E2, E3, F1)**

Heilweil, V.M., and Brooks, L.E., eds., 2011, Conceptual model of the Great Basin carbonate and alluvial aquifer system: U.S. Geological Survey, Scientific Investigations Report 2010-5193, 191 p., 2 pls., data. **(D1, D2)**

Helm, D.C., 1982, Conceptual aspects of subsidence due to fluid withdrawal, *in* Narasimhan, T.N., ed., Recent trends in hydrogeology: Geological Society of America, Special Paper 189, p. 103-139. **(D1)**

Helm, D.C., 1984a, Analysis of sedimentary skeletal deformation in a confined aquifer and the resulting drawdown: American Geophysical Union, Water Resources Monograph 9, Groundwater Hydraulics, p. 29-82. **(D1)**

Helm, D.C., 1984b, Field-based computational techniques for predicting subsidence due to fluid withdrawal; *in* Holzer, T.L., ed., Man-induced land subsidence: Geological Society of America, Reviews in Engineering Geology VI: Groundwater Hydraulics, p. 1-22. **(D1)**

Helm, D.C., 1994a, Hydraulic forces that play a role in generating fissures at depth: Bulletin of the Association of Engineering Geologists, v. 16, no. 3, p. 293-304. **(D1)**

Helm, D.C., 1994b, Horizontal aquifer movement in a Theis-Theim confined system: Water Resources Research, v. 30, p. 953-964. **(D1)**

Hennings, P.H., 1994, Structural transect of the southern Chihuahua fold belt between Ojinaga and Aldama, Chihuahua, Mexico: Tectonics, v. 13, p. 1445-1460. **(C2b, F3)**

Henry, C.D., 1979, Geologic setting and geochemistry of thermal water and geothermal assessment, Trans-Pecos Texas: Texas Bureau of Economic Geology, Report of Investigations 96, 48 p. **(C2a, F1, H1, H2)**

Henry, C.D., and Gluck, J.K., 1981, A preliminary assessment of the geologic setting, hydrology, and geochemistry of the Hueco Tanks geothermal area, Texas and New Mexico: University of Texas at Austin, Bureau of Economic Geology, Geological Circular 81-1, 48 p. **(C2b, H1, H2)**

Henry, C.D., and Price, J.G., 1985, Summary of the tectonic development of Trans-Pecos Texas: University of Texas at Austin, Bureau of Economic Geology, Miscellaneous Map No. 36, scale 1:500,000, text 8 p. **(C2a, F1)**

Herbel, C.H., and Gile, L.H., 1973, Field moisture regimes and morphology of some arid-land soils in New Mexico, *in* Bruce, R.R., and Stelly, M., eds., Field soil-water regime: Soil Science Society of America, Special Publication No. 5, p. 119-152. **(C1, C3)**

Hernandez, J.W., 1978, Interrelationships of ground and surface water quality in the El Paso-Juárez and Mesilla Valleys: Natural Resources Journal, v. 18, no. 1 (Symposium on U.S.-Mexican Transboundary Resources, Part II), p. 1-9. **(F1, H2)**

Hernandez, J.W., 2012a, Preface, *in* Ortega Klett, C.T., ed., One hundred years of water wars in New Mexico: Santa Fe, Sunstone Press, p. 9. ISBN: 978-0-86524-902-5 **(B3, E3)**

Hernandez, J.W., 2012b, Conflicts in the division of New Mexico's share of the Colorado River, *in* Ortega Klett, C.T., ed., One hundred years of water wars in New Mexico: Santa Fe, Sunstone Press, p. 202-211. ISBN: 978-0-86524-902-5 **(B3, E3)**

Hernandez, J.W., 2012c, Ready to Fight: Steve Reynolds-Institution-Engineer-Litigator, *in* Ortega Klett, C.T., ed., One hundred years of water wars in New Mexico: Santa Fe, Sunstone Press, p. 52-65. ISBN: 978-0-86524-902-5 **(B3, E3)**

Hernandez, J.W., 2012d, Water wars during our Territorial years, *in* Ortega Klett, C.T., ed., One hundred years of water wars in New Mexico: Santa Fe, Sunstone Press, p. 19-28. ISBN: 978-0-86524-902-5 **(B3, E3)**

Herrick, C.L., 1900, The geology of the White Sands of New Mexico: Journal of Geology, v. 8, p. 112-128. **(B2, C1, G1, I2)**

Hester, C.M., and Coleman, J., 2014, Between an uncomfortable position and an absurd one: Groundwater, v. 52, no. 5, p. 645-646. **(D1, H3)**

Heywood, C.E., 1995, Investigation of aquifer-system compaction in the Hueco basin, Texas, USA, in 5th International symposium on land subsidence, Delft, Netherlands, October, 1995: International Association of Hydrological Sciences Publication 234, p. 35-45. **(C2b, C4, D1)**

Heywood, C.E., and Yager, R.M., 2003, Simulated ground-water flow in the Hueco Bolson, an alluvial-basin aquifer system near El Paso, Texas: U.S. Geological Survey Water Resources Investigations Report 02-4108, 27 p. **(F1, H3)**

Hibbs, B.J., and Darling, B.K., 2005, Revisiting a classification scheme for U.S.-Mexico alluvial basin-fill aquifers: Ground Water, v. 43, no. 5, p. 750-763. **(D1, D2, F1)**

Hibbs, B., and Merino, M., 2007, Discovering a geologic salinity source in the Rio Grande aquifer: Southwest Hydrology: v. 6, p. 20-23. **(F1, H1, H2)**

Hibbs, B., and Merino, M., 2020, Reinterpreting models of slope-front recharge in a desert basin: Geosciences, v. 10, no. 297, 20 p. Licensee MDPI, Basel, Switzerland. **(F1, H1, H2)**

Hibbs, B.J., Lee, M.M., and Hawley, J.W., 1999, Evolution of hydrochemical facies in the Mimbres Basin aquifer system: A transboundary resource, *in* Hydrological issues of the 21st Century: Ecology, Environment, and Human Health: American Institute of Hydrology, Hydrological Science and Technology, v. 15, no. 1-4, p. 52-65. **(F1, H1, H2)**

Hibbs, B., Eastoe, C., Hawley, J., and Granados, A., 2015, Multiyear study of the binational Hueco Bolson Aquifer reformulates key conceptual models of groundwater flow, *in* Water is not for gambling: Utilizing science to reduce uncertainty: Proceedings 2015 UCOWWR/NIWR/CUAHSI Annual Conference, Universities Council on Water Resources, p. 81-86. https://ucowr.org/ **(F1, H1, H2)**

Hibbs, B.J., Lee, M.M., Hawley, J.W., and Kennedy, J.F., 2000, Some notes on the hydrogeology and ground-water quality of the Animas basin system, southwestern New Mexico: New Mexico Geological Society, Guidebook 51, p. 227-234. **(F1, H1, H2)**

Hibbs, B., Phillips, F., Hogan, J., Eastoe, C., Hawley, J., Granados, A., and Hutchison, B., 2003, Hydrogeologic and Isotopic Study of the Groundwater Resources of the Hueco Bolson Aquifer El Paso/Juárez Area: Hydrological Science and Technology, v. 19, no. 1-4, p. 109-119. **(F1, H1, H2)**

Hibbs, B.J., Creel, B.J., Boghici, R., Hayes, M., Ashworth, J., Hanson A., Samani, Z., Kennedy, J.F., Hann, P., and Stevens, K., 1997, Transboundary Aquifers of the El Paso/Ciudad Juárez/Las Cruces Region: U.S. Environmental Protection Agency, Region 6; Technical Contract Report - Interagency Contracts X-996343-01-0 and X-996350-01-0, prepared by the Texas Water Development Board and the New Mexico Water Resources Research Institute, variously paged. *See TWDB, 1997, Appendix C–G.I.S. coverages, metadata descriptions, [and] groundwater data sets on CD-ROM, with Water Quality map insert on back-cover.* https://nmwrri.nmsu.edu/publications/publications.html **(F1, H1, H2)**

Hibbs, B., Boghici, R., Ashworth, J., Hayes, M., Peckham, D., Guillen, R., Fuentes, O., Laloth, N., Morales, M., Maldonado, A., Creel, B., Kennedy, J., Hanson, A., Samani, Z., Nunez, F., Lemus, R., Moreno, G., Rascon, E., Kuo, R., Waggoner, S., Ito, C., Robinson, J., Valdez, J., Little, D., Rascon, A., Reyes, A., Williams, K., Vaughan, M., Cabra, O., Kelly, T., King, C., 1998, Transboundary aquifers and binational ground-water data base, City of El Paso/Ciudad Juárez area; Base de datos binacíonal del acuífero transfronterízo, de Ciudad Juárez, Chih./El Paso, Tex.: first binational aquifer report and data base sanctioned by the governments of the United States and Mexico, 47 p. + appendices and CD-ROM. Participating agencies; International Boundary and Water Commission, U.S. Environmental Protection Agency, Texas Water Development Board, New Mexico Water Resources Research Institute, Comisión Internacíonal de Limites y Aguas, Comisión Nacional del Agua, Junta Municipal de Agua y Saneamiento de Ciudad Juárez. **(F1, H1, H2)**

Hiebing, M.S., 2016. Using geochemistry and gravity data to pinpoint sources of salinity in the Rio Grande and fault networks of the Mesilla Basin, University of Texas at El Paso, master's thesis, 104 p. **(C4, H2)**

Hiebing, M.S., Doser, D., Avila, V., and Ma, L., 2018, Geophysical Studies of Fault and Bedrock Control on Groundwater Geochemistry within the Southern Mesilla Basin, West Texas and Southern New Mexico, Geosphere, v. 14, no. 4, p. 1912-1934. **(C4, H2)**

Hightower, M., 2003, Desalinization of inland brackish water: Issues and concerns: Southwest Hydrology, v. 2, no. 3, p. 18-19. **(E2a)**

Hill, R.T., 1896, Descriptive topographic terms of Spanish America: National Geographic, v. 7, p. 291-302. **(A1, B3, C2a, F1)**

Hill, R.T., 1900, Physical geography of the Texas region: U.S. Geological Survey Topographical Atlas Folio 3, 12 p. **(B3, C2a, G1)**

Hoffer, J.M., 1970, Petrology and mineralogy of the Campus Andesite pluton, El Paso, Texas: Geological Society of America Bulletin, v. 81, p. 2129-2136. **(C2a)**

Hoffer, J.M., 1971, Mineralogy and petrology of the Santo Tomas-Black Mountain basalt field, Potrillo volcanics, south-central New Mexico: Geological Society of America Bulletin, vol. 82, no. 3, p. 603-612. **(C2a)**

Hoffer, J.M., 1976, Geology of the Potrillo basalt field, south-central New Mexico: New Mexico Bureau of Mines and Mineral Resources, Circular 149, 30 p. **(C2a)**

Hoffer, J.M., 2001a, Geology of Potrillo Maar, southern New Mexico and northern Chihuahua, Mexico, *in* Crumpler, L.S., and Lucas, S.G., eds., Volcanology in New Mexico: New Mexico Museum of Natural History and Science, Bulletin 18, p. 137-140. **(C2b, F1)**

Hoffer, J.M., 2001b, Geology of the West Potrillo Mountains, *in* Crumpler, L.S., and Lucas, S.G., eds., Volcanology in New Mexico: New Mexico Museum of Natural History and Science, Bulletin 18, p. 141-145. **(C2b)**

Hoffer, J.M., Penn, B.S., Quezada, O.A., and Morales, M.A., 1998, Qualitative age relationships of Late Cenozoic cinder cones, southern Rio Grande rift, utilizing cone morphology and Landsat thematic imagery: New Mexico Geological Society Guidebook 49, p. 123-128. **(C2b, E1, F2)**

Hogan, J., Phillips, F., Eastoe, C., Lacey, H., Mills, S., and Oelsner, G., 2012, Isotopic tracing of hydrological processes and water quality along the upper Rio Grande, USA, *in* Monitoring Isotopes in Rivers: Creation of the Global Network of Isotopes in Rivers (GNIR): Tecdoc 1673, International Atomic Energy Agency, Vienna, Austria, p. 111-136. **(D2, H2, H3)**

Hogan, J.F., Phillips, F.M., Mills, S.K., Hendrickx, J.M.H., Ruiz, J.T., Chesley, J.T., and Asmeron, Y., 2007, Geologic origins of salinization in a semi-arid river: The role of sedimentary basin brines: Geology, v. 35, no. 12, p. 1063-1066. **(D2, H2, H3)**

Holliday, V.T., and Miller, D.S., 2013, The Clovis landscape, Chapter 13, p. 221-245, *in* Graf, K.E., Ketron, C.V., and Waters, M.R., eds., Paleoamerican Odyssey, Center for the Study of the First Americans, Department of Anthropology, Texas A&M University, 573 p. ISBN-13: 978-0-615-82691-2 **(B2, C1, C3)**

Hoidale, G.B., Smith, S.M., Blanco, A.J., and Barber, T.L., 1967, A study of atmospheric dust: Atmospheric Science Laboratory, White Sands Missile Range, New Mexico, ECOM Report No. 5067, 132 p. **(C1, C3)**

Holzer, T.L., 1981, Preconsolidation stress on aquifer systems in area of induced land subsidence: Water Resources Research, v. 17, p. 693-704. **(D1)**

Hoover, D.B., and Tippens, C.L., 1975, A reconnaissance audio-magnetotelluric survey at Kilbourne Hole, New Mexico: New Mexico Geological Society Guidebook 26, p. 277-278. **(C4)**

Hoover, J.D., Ensendot, S.E., Barnes, C.G., and Dyer, R., 1988, Early Trans-Pecos magmatism: Petrology and geochemistry of Eocene intrusive rocks of the El Paso area: New Mexico Geological Society, Guidebook 39, p. 109-118. **(C2a, F1)**

Hornberger, G.M., Raffensperger, J.P., Wiberg, P.L., and Eshleman, K.N., 1998, Elements of physical hydrology: The Johns Hopkins University Press, 302 p. *See Glossary, p. 277-292*. ISBN 0-8018-5856-9 **(A1, D2)**

Horst, J., McDonough, J., and Houtz, E., 2020, Understanding and managing the potential by-products of PFAS destruction, *in* Advances in Remediation Solutions: Groundwater Monitoring & Remediation, v. 20, no. 2, p. 17-27. **(E2c)**

Houghton, J., 2004, Global Warming: The Complete Briefing (3rd edition): Cambridge University Press, 351 p. **(A2, C1)**

Hu, X.C., Andrews, D.Q., Lindstrom, A.B., Bruton, T.A., Schaider, L.A., Grandjean, P., Lohmann, R., Carignan, C.C., Blum, A., Balan, S.A., Higgins, C.P., and Sunderland, E.M., 2016, Detection of Poly- and Perfluoroalkyl Substances (PFASs) in U.S. Drinking Water Linked to Industrial Sites, Military Fire Training Areas, and Wastewater Treatment Plants: Environmental Science & Technology Letters, v. 3, no. 10, p. 344-350. Published online 2016 Aug 9. doi: 10.1021/acs.estlett.6b00260 **(E2c)**

Hubbert, M.K., 1940, The theory of groundwater motion: Journal of Geology, v. 48, p. 785-944. **(D1)**

Hudson, M.R., and Grauch, V.J.S., 2013, Introduction, *in* Hudson, M.R., and Grauch, V.J.S., eds., New Perspectives on Rio Grande Rift Basins: From Tectonics to Groundwater: Geological Society of America Special Paper 494, p. v-xii. **(A2, C2b, C4)**

Huff, G.F., 2004, An overview of the hydrogeology of saline groundwater in New Mexico, *in* Ortega Klett, C.T., ed., Proceedings of the 49th Annual New Mexico Water Conference: Water desalination and reuse strategies for New Mexico. New Mexico Water Resources Research Institute Report 336, p. 21-34. **(D1, E2a, H2)**

Huff, G.F., 2005, Simulation of ground-water flow in the basin-fill aquifer of the Tularosa Basin, south-central New Mexico, predevelopment through 2040: U.S. Geological Survey, Scientific Investigations Report 2004-5197, 98 p. **(H3)**

Hundley, N., 1966, Dividing the waters: A century of controversy between the United States and Mexico: University of California Press, 266 p. **(B3, E3, F1)**

Hunt. A., and Morgan, G.S., 2022, Coprolites in caves: Late Pleistocene coprofaunas of the American Southwest and their significance, *in* Morgan. G.S. et al., eds., Late Cenozoic Vertebrates from the American Southwest: A tribute to Arthur H. Harris: New Mexico Museum of Natural History and Science, Bulletin 88, p. 343-359 **(B2, C1)**

Hurd, B., Brown, C., Greenlee, J., Granados Olivas, A., and Hendrie, M., 2006, Assessing water-resource vulnerability for arid watersheds: GIS-based research in the Paso del Norte region, *in* Anderson, K.S.J., ed., Science on the Border: New Mexico Journal of Science, v. 46, p. 203-235. **(E1, E2, F1)**

Hutchison, W.R., 2006, Groundwater management in El Paso, Texas: The University of Texas at El Paso, Center for Environmental Resource Management, doctoral dissertation, 329 p. **(H1, H2, H3)**

Hutchison, W.R., and Hibbs, B.J., 2008, Ground water budget analysis and cross-formational leakage in an arid basin: Ground Water, v. 46, no. 3, p. 384-395. **(H1, H2, H3)**

Icerman, L., and Lohse, R.L., 1983, Geothermal low-temperature reservoir assessment in Doña Ana County, New Mexico: New Mexico Energy Research and Development Institute Report 2-69-2202, 188 p. **(C4, H2)**

Ikard, S., Teeple, A, and Humberson, D., 2021, Gradient self-potential logging in the Rio Grande to identify gaining and losing reaches across the Mesilla Valley: Water, v. 13, issue 10, Article 1331, 21 p. **(C4, H3)**

Ikard, S.J., Carroll, K.C., Rucker, D.F., Teeple, A.P., Tsai, C.-H., Payne, J.D., Fuchs, E.H., and Jamil, A., 2023, Geoelectric Monitoring of the Electric Potential Field of the Lower Rio Grande before, during, and after Intermittent Streamflow, May-October, 2022: Water, v. 15, no. 1652, 47 p. **(C4, H3)**

INEGI, 1983a-cj, Ciudad Juárez H13-1, Cartas Edafológica: Instituto Nacional de Estadística, Geografía e Informática, SPP Programación y Presupuesto. Dirección General de Geografía del Territorio Nacional. Escala 1:250,000. **(C3, F3)**

INEGI, 1983b-cj, Ciudad Juárez H13-1, Cartas Geológica: Instituto Nacional de Estadística, Geografía e Informática, SPP Programación y Presupuesto. Dirección General de Geografía del Territorio Nacional. Escala 1:250,000. **(F3)**

INEGI, 1983c-cj, Ciudad Juárez H13-1, Cartas Hidrológica de Aguas: Instituto Nacional de Estadística, Geografía e Informática, SPP Programación y Presupuesto. Dirección General de Geografía del Territorio Nacional. Escala 1:250,000. **(F3)**

INEGI, 1995, Ciudad Juárez H13-1, Espacio mapa a Ciudad Juárez, Hoja H13-1; EOSAT Inc. Images, fecha de las imágenes de Febrero a Abril 1993: Instituto Nacional de Estadística, Geografía e Informática, SPP Programación y Presupuesto. Dirección General de Geografía del Territorio Nacional. Escala 1:250,000. **(E1**, **F3)**

INEGI, 1999, Estudio Hidrológico del Estado de Chihuahua: Instituto Nacional de Estadística, Geografía e Informática; Dirección General de Difusión, Aguascalientes, México, 222 p. ISBN 970-13-2077-8 **(F3)**

INEGI, 2012, Zona Hidrogeológica Conejos-Médanos: Instituto Nacional de Estadística y Geografía, Edificio Sede, Av. Héroe de Nacozari Sur 2301, Fraccionamiento Jardines del Parque, 20276, Aguascalientes, Aguascalientes; DR©2012, Impreso en México. www.inegi.org.mx; atencion.usuarios@inegi.org.mx **(F3)**

International Boundary Commission (IBC), 1935, Final Report: Control and canalization of the Rio Grande, Caballo Dam, New Mexico to El Paso, Texas: p. 5. *See Glover 2018*. **(E2)**

International Boundary Commission (IBC), 1936, Final Report: Control and canalization of the Rio Grande, Caballo Dam site, New Mexico to Courchesne Bridge at El Paso, Texas: p. 2-3. *See Glover 2018*. **(E2)**

International Boundary and Water Commission (IBWC), 2010, Hydrogeological activities in the Conejos-Medanos/Mesilla Basin Aquifer, Chihuahua Phase I: Prepared by the International Boundary and Water Commission, and Mexican Geological Survey, v. 1, 109 p. *See INEGI 2012.* **(F1)**

International Boundary and Water Commission (IBWC), 2011, Acuífero Conejos-Médanos: Binational Waters map. https://www.ibwc.gov/wp-content/uploads/2022/12/Conejos_Medanos_Aquifer.jpg **(E1**, **F3)**

Izett, G.A., and Obradovich, J.D., 1994, 40Ar/39Ar age for the Jaramillo Normal Subchron and the Matuyama/Brunhes geomagnetic boundary: Journal Geophysical Research, v. 99, p. 2925-2934. **(B1, C2b)**

Izett, G.A., and Wilcox, R.E., 1982, Map showing localities and inferred distributions of the Huckleberry Ridge, Mesa Falls, and Lava Creek Ash Beds (Pearlette family ash beds) of Pliocene and Pleistocene age in the western United States and southern Canada: U.S. Geological Survey, Miscellaneous Investigations Map I-1325, scale 1:4,000,000. **(B1, C2a, I3)**

Izett, G.A., Obradovich, J.D., and Mehnert, H.H., 1988, The Bishop ash bed (middle Pleistocene) and some older (Pliocene and Pleistocene) chemically similar ash beds in California, Nevada and Utah: U.S. Geological Survey, Bulletin 1675, 37 p. **(B1, C2b)**

Jackson, D.B., 1976, Schlumberger soundings in the Las Cruces, New Mexico, area: U.S. Geological Survey Open-File Report 76-231, 170 p. **(C4)**

Jackson, D.B., and Bisdorf, R.J., 1975, Direct-current soundings on the La Mesa Surface near Kilbourne and Hunt Holes, New Mexico: New Mexico Geological Society Guidebook 26, p. 273-275. **(C2a, C4)**

Jackson, D., ed., 1966, The Journals of Zebulon Montgomery Pike, with letters and related documents: University of Oklahoma Press; 2 Volume facsimile; v. 1, 464 p.; v. 2, 449 p. **(B3)**

James, H.L., 1969, History of the United States-Mexican boundary survey – 1848-1855: New Mexico Geological Society Guidebook 20, p. 40-55. **(B3, F1)**

Jarvis, M.D., Buck, B., and Witcher, J.C., 1998, Quaternary paleospring deposits at San Diego Mountain in south-central New Mexico: New Mexico Geological Society Guidebook 49, p. 71-74. **(C1, C4, H1, H2)**

Jarvis, T., Giordano, M., Puri, S., Matsumoto, K., and Wolf, A., 2005, International borders, ground water flow, and hydroschizophrenia, Ground Water, v. 43, p. 764-770. **(D1, E3)**

Jasechko, S., Lechler, A., Pausata, F.S.R., Fawcett, P.J., Gleeson, T., Cendón, D.I., Galeewsky, J., LeGrande, A.N., Risi, C., Sharp, Z.D., Welker, J.M., Werner, M., Yoshimura, K., 2015. Late-glacial to late-Holocene shifts in global precipitation $\delta^{18}O$: Climate Past, v. 11, p. 1375-1393. **(B2, C1)**

Jiménez, A.J., and Keller, G.R., 2000, Rift basin structure in the border region of northwestern Chihuahua: New Mexico Geological Society Guidebook 51, p. 79-83. **(C2b, C4, F1**, **H1)**

Jochems, A.P., 2017, Geologic map of the Arroyo Cuervo 7.5-minute quadrangle, Doña Ana and Sierra Counties, New Mexico: New Mexico Bureau of Geology and Mineral Resources, Open-File Geologic Map OF-GM 261, scale 1:24,000. **(C2b)**

Jochems, A.P., and Morgan, G.S., 2018, A stable isotope record from paleosols and groundwater carbonate of the Plio-Pleistocene Camp Rice Formation, Hatch-Rincon Basin, southern New Mexico: N.M. Geological Society Guidebook 69, p. 109-117. **(C1, C2b, C3)**

Journel, A.G., and Huijbregts, C.J., 1978, Mining geostatistics: New York, Academic Press, 600 p. VOXEL modeling **(D1, E2)**

Julyan, R., 1996, The place names of New Mexico: University of New Mexico Press, 385 p. **(A1, B3)**

Junge, C.E., and Werby, R.T., 1958, The concentration of chloride, sodium, potassium, calcium, and sulfate in rain water over the United States: Journal of Meteorology, v. 15, p. 417-425. **(C1, C3, D1)**
Kahn P.A., 1987, Geology of Aden Crater, Dona Ana County, New Mexico: University of Texas at El Paso, master's thesis, 89 p. **(C2a)**
Kahneman, D., and Tversky, A., 1974, Judgement under uncertainty: Heuristics and biases: *Science,* vol. 185, issue 4157, pp. 1124-1131. **(A2, D1)**
Kahneman, D., and Tversky, A., 1996, On the reality of cognitive illusions: Psychological Review, v. 103, no. 3, p. 582-591. *See Lewis 2017.* **(A2, D1)**
Kambhammettu, B.V.N.P., Allena, P., and King, J.P., 2010, Simulation of groundwater flow in the southern Jornada Del Muerto Basin, Doña Ana County, New Mexico: New Mexico Water Resources Research Institute Report No. 352, prepared for Lower Rio Grande Water Users Organization (LRGWUO), 63 p. https://nmwrri.nmsu.edu/publications/technical-reports/tr-reports/tr-352.html **(H1, H3)**
Keaton, J.R., 1993, Maps of potential earthquake hazards in the urban area of El Paso, Texas: U.S. Geological Survey, technical report prepared under contract 1434-92-G-2171, 87 p. **(C2b, C4)**
Keaton, J.R., and Barnes, J.R., 1995, Paleoseismic evaluation of the East Franklin Mountains fault, EI Paso, Texas: Technical report to U.S. Geological Survey, under Contract 1434-94-G-2389, December 1995. *See Collins and others, 2015.* **(C2b, C4)**
Keaton, J.R., Barnes, J.R., Scherschel, C.A., and Monger, H.C. (abstract), 1995, Evidence for episodic earthquake activity along the East Franklin Mountains fault, EI Paso, Texas: Geological Society of America Abstracts with Programs, v. 27, no. 4, p. 17. **(C2b, C4)**
Keigwin, L.D., Klotsko, S., Zhao, N., Reilly, B., Giosan, L., and Driscoll, N.W., 2018, Deglacial floods in the Beaufort Sea preceded Younger Dryas cooling: Nature Geoscience, v. 11, no. 8, p. 599-604. **(A2, C1)**
Keller, G.R., 2004, Geophysical constraints on the crustal structure of New Mexico, *in* Mack, G.H., and Giles, K.J., eds., The Geology of New Mexico: A geologic history: New Mexico Geological Society, Special Publication 11, p. 439-456. **(C2b, C4)**
Keller, G.R., and Cather, S.M., eds., 1994, Basins of the Rio Grande rift: Structure, stratigraphy and tectonic setting: Geological Society of America Special Paper 291, 304 p. **(C2b, C4)**
Kelley, S.A., and Chapin, C.E., 1997, Cooling histories of mountain ranges in the southern Rio Grande rift based on apatite fission-track analysis – A reconnaissance survey: New Mexico Geology, v. 19, p. 1-14. **(C2b)**
Kelley, S.A., and Matheny, J.P., 1983, Geology of Anthony quadrangle, Doña Ana County, New Mexico: New Mexico Bureau of Mines and Mineral Resources, Geologic Map 54, scale 1:24,000. **(C2a)**
Kelley, S., Augusten, I., Mann, J., and Katz, L., 2007, History of Rio Grande reservoirs in New Mexico: Legislation and litigation: Natural Resources Journal, v. 47, no. 3, p. 525-613. **(B3, E2)**
Kelley, V.C., 1952, Tectonics of the Rio Grande depression of central New Mexico: New Mexico Geological Society, Guidebook 3, p. 92-105. (**C2a**)
Kendy, E., 2003, The false promise of sustainable pumping: Ground Water, v. 41, no. 1, p. 2-4. **(D1)**
Kennedy, J.F., 1999, Aquifer sensitivity assessment for the Lower Rio Grande, *in* Ortega Klett, C.T., ed., Proceedings of the 43rd Annual New Mexico Water Conference: Water Challenges on the Lower Rio Grande. New Mexico Water Resources Research Institute, Report No. 310. p. 84-104. **(E2c)**
Kennedy, J.F., and Hawley, J.W., 2003, Late Quaternary paleohydrology of a linked pluvial-lake and Ancestral Rio Grande system, Paso Del Norte Region, Southwestern USA And Northern Mexico *in* Shaping the Earth, a Quaternary Perspective: XVI INQUA Congress (July 23-30, 2003), Desert Research Institute, Reno, NV, Programs with Abstracts, p. 181. **(F1, H1, I2)**
Kennedy, J.F., Hawley, J.W., and Johnson, M., 2000, The hydrogeologic framework of basin-fill aquifers and associated ground-water-flow systems in southwestern New Mexico – An overview: New Mexico Geological Society Guidebook 51, p. 235-244. **(F1, H1, I2)**
Kernodle, J.M., 1992a, Results of simulations by a preliminary numerical model of land subsidence in the El Paso, Texas, area: U.S. Geological Survey, Water-Resources Investigations Report 92-4037, 35 p. **(D1, H3)**
Kernodle, J.M., 1992b, Summary of U.S. Geological Survey ground-water-flow models of basin-fill aquifers in the southwestern alluvial basins region, Colorado, New Mexico, and Texas: U.S. Geological Survey Open-file Report 90-361, 81 p. **(D2, H3)**
Kernodle, J.M., McAda, D.P., and Thorn, C.R., 1995, Simulation of Ground-water Flow in the Albuquerque Basin, Central New Mexico: U.S. Geological Survey, Water Resources Investigations Report 94-4251, 114 p. (**D1, D2**)
Keyes, C.R., 1905, Geology and underground water conditions of the Jornada del Muerto, New Mexico: U.S. Geological Survey, Water-Supply and Irrigation Paper 123, 42 p. **(G1)**

Khatun, S., Doser, D.I., Imana, E.C., and Keller, G.R., 2007, Locating faults in the southern Mesilla Bolson, west Texas and southern New Mexico, using 3-D modeling of precision gravity data: Journal of Environmental & Engineering Geophysics, v. 12, p. 149-161. **(C2b, C4)**

King, J.E., 1991, Early and Middle Quaternary vegetation, *in* Smiley, T.L., and four others, Quaternary paleoclimates, *in* Morrison, R.B., ed., Quaternary non-glacial geology; Conterminous U.S.: Boulder, CO, Geological Society of America, The Geology of North America, v. K-2, p. 19-26. **(B1, C1)**

King, J.P., 2022, VII. Changes in surface-water and groundwater supplies and impacts on agricultural, industrial, and municipal users, *in* Dunbar, N.W., Gutzler, D.S., Pearthree, K.S., and Phillips, F.M., eds., Climate Change in New Mexico Over the Next 50 Years: Impacts on Water Resources: NM Bureau of Geology and Mineral Resources Bulletin 164, p. 81-89. **(B3, C1)**

King, W.E., 1973, Hydrogeology of La Mesa, Doña Ana County, New Mexico, *in* Guidebook to the geology of south-central Doña Ana County, New Mexico: El Paso Geological Society 7th Annual Field Trip, p. 56-67. **(H1)**

King, W.E., and Kelley, R.E., 1980, Geology and paleontology of Tortugas Mountain, Doña Ana County, New Mexico: New Mexico Geology, v. 2, no. 3, p. 33-35. **(C2a)**

King, W.E., Hawley, J.W., and Cliett, T.E. (Abstract), 1971, Santa Fe Group and Rio Grande Valley-fill aquifers in the south-central New Mexico border region: Geological Society of America, Abstracts with Programs, v. 3, no. 3, p. 239-240. **(C2a, F1, H1)**

King, W.E., Hawley, J.W., Taylor, A.M., and Wilson, R.P., 1969, Hydrogeology of the Rio Grande Valley and adjacent intermontane areas of southern New Mexico: New Mexico Water Resources Research Institute Miscellaneous Report No. M6, 141 p. https://nmwrri.nmsu.edu/publications/miscellaneous-reports/m-documents/m6.pdf **(F2, H1, H2)**

King, W.E., Hawley, J.W., Taylor, A.M., and Wilson, R.P., 1971, Geology and ground-water resources of central and western Doña Ana County, New Mexico: New Mexico Bureau of Mines and Mineral Resources, Hydrologic Report 1, 64 p. **(F2, H1, H2)**

Kisner, J., 2022, Hanya Yanagihara's haunted America – Her new novel experiments with alternative versions of history, upending personal and national destinies: The Atlantic-Culture & Critics, v. 329, no. 1, p. 86-88. **(A2)**

Klein, D.P., 1995, Structure of the basins and ranges, southwest New Mexico, and interpretation of seismic velocity sections: U.S Geological Survey Open-File Report 95-406, 60 p. (with plates by Adams, G.A., and Hill, P.L., scale 1:250,000 and 1:500,000). **(C4, F2)**

Knorr, D.B., 1988, City of El Paso ground water recharge project, *in* Ortega Klett, C.T., ed., Ground Water Management, Proceedings of the 32nd Annual New Mexico Water Conference: New Mexico Water Resources Research Institute Report No. 229, p. 87-101. **(D2, E2b)**

Knorr, D.B., and Cliett, T., 1985, Proposed groundwater recharge at El Paso, Texas, *in* Asano. T., ed., Artificial recharge of groundwater: Boston, Butterworth Publishers, p. 425-479. **(D2, E2b)**

Knowles, D.B., and Kennedy, R.A., 1958, Ground-water resources of the Hueco Bolson northeast of El Paso, Texas: U.S. Geological Survey, Water-Supply Paper 1426, 186 p. **(F2, G2)**

Knowlton, D.R., 1939, Unitization–Its progress and future, drilling and production practice: American Petroleum Institute Report 39, p. 630-639. **(D1)**

Knutti, R., Rogelj, J., Sedláček, J., and Fischer, E.M., 2016, A scientific critique of the two-degree climate change target: Nature Geoscience, v. 9, p. 13. **(C1)**

Kocherga, A., 2017, Visiting envoy promotes NAFTA's importance: Albuquerque Journal-BUSINESS SECTION, Friday, November 17, 2017, p. B1-B2. **(A3)**

Kocherga, A., 2018a, Dedicated lane serves Foxconn – Mexican electronics plant utilizes quick Santa Teresa border crossing: Albuquerque Journal BUSINESS, SECTION, Friday, February 2, 2018, p. A14-A15. **(A3)**

Kocherga, A., 2018a, Dedicated lane serves Foxconn – Mexican electronics plant utilizes quick Santa Teresa border crossing: Albuquerque Journal–BUSINESS, Friday, February 2, 2018, p. A14-A15. **(A3)**

Kocherga, A., 2018c, Little panic in pecan region – Measured concern so far among southern NM's nut orchards, with little immediate impact, *in* NM feels tariff's bite: Albuquerque Journal–BUSINESS, Friday, May 7, 2018, p. B11-B12. **(A3)**

Kocherga, A., 2018d, Meat packer brings 1295 jobs to Sunland Park: Albuquerque Journal–BUSINESS, Saturday, July 14, 2018, p. A12-A13. **(A3)**

Kocherga, A., 2018e, NM border visionary Charlie Crowder dies: Albuquerque Journal–UPFRONT, Friday, August 10, 2018, p. A1, A16. **(A3)**

Kocherga, A., 2018f, Study surveys border opportunities: Albuquerque Journal–BUSINESS, Wednesday, August 15, 2018, p. A10. **(A3)**
Kocherga, A., 2018g, Border summit focuses on trade turmoil-NAFTA update due Mexico's Zedillo says: Albuquerque Journal–BUSINESS, Thursday, August 16, 2018, p. A10-A11. **(A3)**
Kocherga, A., 2018h, Bustling cross-border trade topic of lecture – Jerry Pacheco to share insights of years working in Santa Teresa: Albuquerque Journal–BUSINESS, Wednesday, August 22, 2018, p. A10. **(A3)**
Kocherga, A., 2019b, Trump tweets threat to shut down border – New Mexicans say closure could threaten business, tourism: Albuquerque Journal, Saturday, March 30, 2019, p. A1, A4. **(A3)**
Kocherga, A., 2019h, Border Contradictions – Southern New Mexico farmer wants a wall – and more workers: Albuquerque Journal–ON THE BORDER, Sunday, September 29, 2019, p. A1, A4 and A5. **(A3)**
Kolbert, E., 2014, The sixth extinction – An unnatural history: New York, Henry Holt and Company, LLC, 219 p. ISBN 798 0-8050-9311-7 **(B1, C1)**
Konikow, L.F., and Leake, S.A., 2014, Depletion and capture: Revisiting "the source of water derived from wells." Ground Water, v. 52 (suppl. 1), p. 100-111. **(D1, H3)**
Koning, D.J., and Read, A.S., 2010, Geologic map of the southern Española Basin, Santa Fe County, New Mexico: New Mexico Bureau of Geology and Mineral Resources, Open-file Report 531. **(B1, D1)**
Koning, D.J., Jochems, A.P., and Cikoski, C., 2015, Geologic map of the Skute Stone Arroyo 7.5-minute quadrangle, Sierra County, New Mexico: New Mexico Bureau of Mines and Mineral Resources, Open-File Geologic Map 252, scale 1:24,000. CD-ROM. **(C2b)**
Koning, D.J., Jochems, A.P., Heizler, M.T., 2018, Early Pliocene paleovalley incision during early Rio Grande evolution in southern New Mexico: New Mexico Geological Society Guidebook 69, p. 93-108. *Repository: 2018001.* **(C2b)**
Kortemeier, C.P., 1982, Occurrence of Bishop Ash near Grama, New Mexico: New Mexico Geology, v. 4, no. 2, p. 22-24. **(B1, C2a)**
Kottlowski, F.E., 1953, Tertiary-Quaternary sediments of the Rio Grande Valley in southern New Mexico: New Mexico Geological Society, Guidebook 4, p. 30-41, 144-148. **(C2a)**
Kottlowski, F.E., 1958a, Geologic history of the Rio Grande near El Paso: West Texas Geological Society, Guidebook 1958 Field Trip, Franklin and Hueco Mountains, Texas, p. 46-54. *N.M. Bureau of Mines and Mineral Resources, Reprint Series No. 1. Reprint produced with permission of the West Texas Geological Society, Inc.* **(C2a, F1)**
Kottlowski, F.E., 1958b, Lake Otero-second phase formation of New Mexico's gypsum dunes: Geological Society of America Bulletin, v. 69, no. 12, p. 1733-1734. **(C2a, I2)**
Kottlowski, F.E., 1960, Reconnaissance geologic map of Las Cruces 30-minute quadrangle: New Mexico Bureau of Mines and Mineral Resources, Geologic Map 14. **(C2a)**
Kottlowski, F.E., 1965a, Facets of the Late Paleozoic strata of southwestern New Mexico: New Mexico Geological Society, Guidebook 16, p., 141-147. **(C2a)**
Kottlowski, F.E., and Hawley, J.W., 1975, Las Cruces to southern San Andres Mountains and return: New Mexico Geological Society Guidebook 26, p. 1-16. **(C2a)**
Kottlowski, F.E., Foster, R.W., and Wengerd, S.A., 1969, Key oil tests and stratigraphic sections in southwest New Mexico: New Mexico Geological Society, Guidebook 20, p. 186-196. **(C2a)**
Kreitler, C.W., Raney, J.A., Nativ, R., Collins, E.W., Mullican, W.F. III, Gustavson, T.C., and Henry, C.D., 1987, Siting a low-level radioactive waste disposal facility in Texas, volume four – Geologic and hydrologic investigations of the State of Texas and University of Texas lands: University of Texas at Austin, Bureau of Economic Geology, final report prepared for the Low-Level Radioactive Waste Disposal Authority under contract no. IAC (86-87)-1722, 330 p. **(C2a, E2c, F2, H1, H2)**
Krider, P.R., 1998, Paleoclimatic significance of late Quaternary lacustrine and alluvial stratigraphy, Animas Valley, New Mexico, Quaternary Research, v. 50, p. 283-289. **(B2, C1, F1, I2)**
Kubicki, C., Carroll, K.C., Witcher, J.C., and Robertson, A., 2021, An Integrated Geochemical Approach for Defining Sources of Groundwater Salinity in the Southern Rio Grande Valley of the Mesilla Basin, New Mexico and West Texas, USA: New Mexico Water Resources Research Institute Report No. 388, 40 p., 3 Appendices. https://nmwrri.nmsu.edu/publications/technical-reports/tr-reports/tr-388.html **(F2, H1, H2, H3)**
Kues, B.S., 2014a, Biographical profile of N.H. Darton, *in* Kues, B.S., Lewis, C.J., and Lueth, V.W., A brief history of geological studies in New Mexico: New Mexico Geological Society, Special Publication 12, p. 97-98 (*cited references 209-230*). **(A2)**

Kues, B.S., 2014b, Biographical profile of Willis T. Lee, *in* Kues, B.S., Lewis, C.J., and Lueth, V.W., A brief history of geological studies in New Mexico: New Mexico Geological Society, Special Publication 12, p. 91-92 (*cited references 209-230*). **(A2)**
Land, L.F., and Armstrong, C.A., 1985, A preliminary assessment of land-surface subsidence in the El Paso area, Texas: U.S. Geological Survey Water Resources Investigations Report 85-4155, 96 p. **(C4, D1, H3)**
Laney, R.L., Raymond, R.H., and Winnika, C.C., 1978, Maps showing water-level declines, land subsidence, and earth fissures in south-central Arizona: US. Geological Survey Water-Resources Investigations 78-83, 2 sheets, scale 1:125,000. **(C4, D1, H3)**
Lang, W.B., 1943, Gigantic drying cracks in the Animas Valley, New Mexico: Science, v. 98, p. 593-594. **(G2, I2)**
Langford, R.P., 2002, Playa lake shorelines and the Holocene history of the White Sands dune field. New Mexico Geological Society Guidebook 53, p. 45-47. **(I2)**
Langman, J.B., and Ellis, A.S., 2013, Geochemical indicators of interbasin groundwater flow within the southern Rio Grande Valley, southwestern USA: Environmental Earth Science v. 68, p. 1285-1303. **(C4, H2, H3)**
Lansford, R.R., Lucero, D., Gore, C., Wilken, W.W., Nedom, R., Lucero, A.A., and Schultz, J., 1997, Irrigation water sources and cropland acreages in New Mexico, 1994-1996: New Mexico State University, Agricultural Experiment Station Technical Report 29. **(E2)**
Laplace, P.S., 1825, Essai Philosophique sur les Probabilités, fifth edition. New York, Springer. Translated by A.I. Dale 1995; *See Miller and Gelman 2020.* **(A2, D1)**
Lawton, T.E., 2004, Upper Jurassic and lower Cretaceous strata of southwestern New Mexico and northern Chihuahua, Mexico, *in* Mack, G.H., and Giles, K.J., eds., The Geology of New Mexico: A geologic history: New Mexico Geological Society Special Publication 11, p. 153-168. **(C2b, F1)**
LBG–Guyton Associates, 2003, Brackish groundwater manual for Texas regional water planning groups: Texas Water Development Board, 188 p. http://www.twdb.texas.gov/publications/reports/contracted_reports/doc/2001483395.pdf **(D1, E2a)**
Leavy, B.D., 1987, Surface-exposure dating of young volcanic rocks using *in situ* buildup of cosmogenic isotopes: Socorro, New Mexico Institute of Mining and Technology, doctoral dissertation, 167 p. **(B1, C2a)**
Lee, E., and Ganster, P., eds., 2012, The U.S.-Mexican border environment: Progress and challenges for sustainability: Southwest Consortium for Environmental Research and Policy, SCERP Monograph Series, no. 16, 453 p., ISBN: 0-925613-53-3 **(E2, E3)**
Lee, M., Associated Press, 2022, NM seeks opportunity in Texas border disruptions – State backs proposal for rail line through Santa Teresa crossing; Albuquerque Journal–METRO & NM, Friday, May 6, 2022, p. A7. *See Stevenson, M., 2022.* **(A3)**
Lee, W.T., 1907a, Afton Craters of southern New Mexico: Geological Society of America Bulletin, v. 18, p. 211-220. **(C2a, F2, G1)**
Lee, W.T., 1907b, Water resources of the Rio Grande Valley in New Mexico: U.S. Geological Survey, Water-Supply Paper 188, 59 p. **(C2a, F2, G1)**
Leeder, M.R., 1998, Lyell's Principles of Geology: foundations of sedimentology, *in* Blundell, D.J., and Scott, A.C., eds., Lyell: the past is the key to the present: Geological Society of London, Special Publication 143, p. 97-110. **(D1)**
Leeder, M.R., Mack, G.H., Peakall, J., and Salyards, S.L., 1996, First quantitative test of alluvial stratigraphic models: Southern Rio Grande rift, New Mexico: Geology, v. 24, no. 1, p. 87-90. **(C2b, I3)**
Leggat, E.R., 1962, Development of ground-water of the El Paso district, Texas: 1955-60, Progress Report No. 8: Texas Water Commission, Bulletin 6204, 56 p. **(F2, G2)**
Leggat, E.R., Lowry, M.E., and Hood, J.W., 1962, Ground-water resources of the lower Mesilla Valley, Texas and New Mexico: Texas Water Commission, Bulletin 6203, 191 p. **(F2, G2, H1, H2)**
Lehner, F., Wahl, E.R., Wood, A.W., Blatchford, D.B., and Llewellyn, D., 2017, Assessing recent declines in Upper Rio Grande runoff efficiency from a paleoclimatic perspective: Geophysical Research Letters, v. 44, p. 4124-4133. **(B2, C1, I3)**
LeMone, D.V., and Lovejoy, E.M.P., eds., 1976, El Paso Geological Society symposium on the stratigraphy and structure of the Franklin Mountains: El Paso Geological Society, Quinn Memorial Volume, 250 p. **(C2a)**
Lewis, M., 2016, The undoing project – A friendship that changed our minds: New York, W.W. Norton & Company, 362 p. ISBN 978-0-393-25459-4. *See Chapter 4: Errors, and Kahneman and Tversky (1974 and 1976).* **(A2, D1)**
Lewis, M., 2018, The fifth risk: New York, W.W. Norton & Company, 219 p. ISBN 978-1-324-00264-2 **(A2)**
Lim, X., 2019, Tainted water: The scientists tracing thousands of fluorinated chemicals in our environment: Nature, v. 566, no. 7742, p. 26-29. **(E2c)**

Limón-González, M., 1986, Evaluación geológico--geoquimica de la provincia de Chihuahua: Asociación Mexicana de Geólogos Petroleros, Boletín, Tomo XXXVIII, p. 3-58. **(C2a, C4, F3)**
Linthicum, K., Fry, W., and Minjares, G., 2020, US urges Mexico to reopen border factories – Mexican heath officials warn premature start could lead to widespread deaths: Albuquerque Journal–BUSINESS, Saturday, May 2, 2020, p. A6. **(A3)**
Lisiecki, LE., and Raymo, M.E., 2005, A Plio-Pleistocene stack of 57 globally distributed benthic $\delta^{13}O$ records: Paleoceanography, v. 20, issue 1. **(B1, B2)**
Littlefield, D.R., 2000, The history of the Rio Grande Compact of 1938, *in* Ortega Klett, C.T., ed., Proceedings of the 44th Annual New Mexico Water Conference: The Rio Grande Compact: It's the Law!: New Mexico Water Resources Research Institute Report No. 312, p. 21-28. **(E3)**
Llewellyn, D., and Vaddey, S., 2013, West-wide climate risk assessment: Upper Rio Grande impact assessment: U.S. Bureau of Reclamation, Upper Colorado Region, 169 p. https://www.usbr.gov/watersmart/baseline/docs/urgia/URGIAMainReport.pdf **(B2, B3, C1, D1)**
Lloyd, W.J., 1982, Growth of the municipal water system in Ciudad Juárez, Mexico: Natural Resources Journal, v. 22, p. 943-954. **(E2, F3)**
Lloyd, W.J., and Marston, R.A., 1985, Municipal and industrial water supply in Ciudad Juárez, Mexico: American Water Resources Association, Water Resources Bulletin, v. 21, no. 5, p. 841-849. **(E2, F3)**
Long, A., Hansen, R.M., and Martin, P.S., 1974, Extinction of the Shasta Ground Sloth: Geological Society of America Bulletin, v. 85, p. 1843-1848. **(B2, C1)**
Longmire, P.A., Gallaher, B.M., and Hawley, J.W., 1981, Geologic, geochemical and hydrological criteria for disposal of hazardous wastes in New Mexico, *in* S.G. Wells, and W. Lambert, eds., 1981, Environmental geology and hydrology in New Mexico: New Mexico Geological Society Special Publication 10, p. 93-102. **(E2c)**
Lorenz, E., 1963, Deterministic non-periodic flow: Journal of the Atmospheric Sciences, v. 20, no. 2, p. 130-141. **(C1, D1)**
Lorenz, E., 1976, Nondeterministic theories of climate change: Quaternary Research, v. 60, issue 4, p. 495-506. **(C1, D1)**
Love, D.W., and Hawley, J.W., 2010, Geology of the Montano Site Complex- Chapter 3 (p. 3-1 to 3-32); and Data synthesis, interpretation and summary-Chapter 13: The nature of the agricultural system (p. 13-5 and 13-6), *in* Report on 1988 data recovery at the Montano Site Complex, LA 33223; City of Albuquerque, New Mexico, and Subsequent analysis of collections (NMCRIS No. 116852). Report No. CEC-2009-12, submitted by Criterion Environmental Consulting, 4801 Lang Avenue NE, Suite 110, Albuquerque, NM 87109. Submitted to: Wilson & Company, Inc. 4900 Lang Avenue NE, Albuquerque, NM 87109, and City of Albuquerque, One Civic Plaza NW, Albuquerque, NM 87102. March 22, 2010. **(B2, C1, C3, I3)**
Love, D.W., and Seager, W.R., 1996, Fluvial fans and related basin deposits of the Mimbres drainage: New Mexico Geology, v. 18, p. 81-92. **(C2b, I2)**
Love, D.W., Allen, B.D., Scholle, P.A., and Bustos, D., 2020, White Sands National Park, *in* Scholle, P.A., Ulmer-Scholle, D.S., Cather, S.M., and Kelley, S.A., eds., The Geology of Southern New Mexico's Parks, Monuments, and Public Lands: N.M. Bureau of Geology and Mineral Resources, 404 p. ISBN: 978-1-883905-48-4 **(C2b, I2)**
Lovejoy, E.M.P., 1973, Evolution of the western boundary fault, Franklin Mountains, Texas: American Association of Petroleum Geologists Bulletin, v. 57, no. 9, p. 1766-1776. **(C2a)**
Lovejoy, E.M.P., 1976a, Geology of Cerro de Cristo Rey uplift, Chihuahua and New Mexico: New Mexico Bureau of Mines and Mineral Resources Memoir 31, 84 p. **(C2a, F1)**
Lovejoy, E.M.P., 1976b, Neotectonics of the southeast end of the Rio Grande rift along the Mesilla Valley fault zone and the course of the Rio Grande, El Paso, Texas, in Symposium on the stratigraphy of the Franklin Mountains: El Paso Geological Society, Quinn Memorial Volume, p. 123-138. **(C2a)**
Lovejoy, E.M.P., ed., 1979, Sierra de Juárez, Chihuahua, Mexico: Structure and history: El Paso Geological Society, Special Publication, 59 p. **(C2a, F3)**
Lovejoy, E.M.P. and Hawley, J.W., 1978, Southern rift guide 1, El Paso to New Mexico-Texas state line, *in* Hawley, J.W., compiler, Guidebook to Rio Grande rift in New Mexico and Colorado: New Mexico Bureau of Mines and Mineral Resources Circular 163, p. 57-71. **(C2a)**
Lovejoy, E.M.P., and Seager, W.R., 1978, Discussion of structural geology of Franklin Mountains, *in* Hawley, J.W., compiler, Guidebook to Rio Grande rift in New Mexico and Colorado: New Mexico Bureau of Mines and Mineral Resources, Circular 163, p. 68-69. **(C2a)**

Lozinsky, R.P., 1986, Geology and late Cenozoic history of the Elephant Butte area, Sierra County, New Mexico: New Mexico Bureau of Mines and Mineral Resources, Circular 187, 40 p. **(C2a)**

Lozinsky, R.P., and Hawley, J.W., 1986, The Palomas Formation of south-central New Mexico – A formal definition: New Mexico Geology, v. 8, no. 4, p. 73-82. **(C2a, I3)**

Lozinsky, R.P., Harrison, R.W., and Lekson, S.H., 1995, Elephant Butte – Eastern Black Range region: Journeys from desert lakes to mountain ghost towns: New Mexico Bureau of Mines and Mineral Resources, Scenic Trips to the Geologic Past No. 16, 169 p. *Building of Elephant Butte Dam, p. 60-65.* **(B2, B3, C2b)**

Lucas, S.G., and Hawley, J.W., 2002, The Otero Formation, Pleistocene lacustrine strata in the Tularosa Basin, southern New Mexico: New Mexico Geological Society Guidebook 53, p. 277-283. **(C2b, I2)**

Lucas, S.G., Krainer, K., Spielmann, J.A., and Durney, K., 2010, Cretaceous stratigraphy, paleontology, petrography, depositional environments, and cycle stratigraphy at Cerro de Cristo Rey, Doña Ana County, New Mexico: New Mexico Geology, v. 32, no. 4, p. 103-130. **(C2b, F1)**

Lucas, S.G., Morgan, G.S, Estep, J.W., Mack, G.H., and Hawley, J.W., 1999, Co-occurrence of the Proboscideans Cuvieronius, Stegomastodon, and Mammuthus in the Lower Pleistocene of Southern New Mexico: Journal of Vertebrate Paleontology, v. 19, no. 3, pp. 595-597. **(B1, C1)**

Luedke, R.G., and Smith, R.L., 1991, Quaternary volcanism in the western conterminous United States, in Morrison, R.B., ed., Quaternary non-glacial geology; Conterminous U.S.: Boulder, CO, Geological Society of America, The Geology of North America, v. K-2, p. 75-92. **(C2b)**

Lueth, V., Goodell, P.C., and Heizler, M.T., 1998, Geochemistry, geochronology, and tectonic implications of jarosite mineralization in the northern Franklin Mountains, Dona Ana County, New Mexico : New Mexico Geological Society Guidebook 49, p. 309-315. **(C2b)**

Lynch, D.J., Sheridan. M.B., and Kim, S.M. (The Washington Post), 2019, Trump secures revised replacement for NAFTA: Albuquerque Journal–NATION, Wednesday, December 11, 2019, p. A6. **(A3)**

Mace, R.E., Mullican, W.F. III, and Angle, E.S., eds., 2001, Aquifers of West Texas: Texas Water Development Board Report 356, 272 p. **(D1, F2)**

Machette, M.N., 1985, Calcic soils of the southwestern United States, *in* Weide, D.L., ed., Quaternary soils and geomorphology of the American Southwest: Geological Society of America Special Paper 203, p. 1-21. **(C2a, C3)**

Machette, M.N., 1987, Preliminary assessment of paleoseismicity at White Sands Missile Range, southern New Mexico: Evidence for recency of faulting, fault segmentation, and repeat intervals for major earthquakes in the region: U.S. Geological Survey, Open-File Report 87-444, 46 p. **(C2a, C4)**

Machette, M., Thompson, R., Marchetti, D., and Smith, R.S.U., 2013, Evolution of ancient Lake Alamosa and integration of the Rio Grande during the Pliocene and Pleistocene, *in* Hudson, M.R., and Grauch, V.J.S., eds., New Perspectives on Rio Grande Rift Basins: From Tectonics to Groundwater: Geological Society of America Special Paper 494, p. 1-20. doi: 10.1130/2013.2494(01) **(C2b, C3, I3)**

Macías-Coral, M., Samani, Z., and Martinez, S.L., 2006, Two countries-one common problem: How to deal with dairy manure along the United States-Mexico border, *in* Anderson, K.S.J., ed., Science on the Border: N.M. Journal of Science, v. 44. p. 89-97. **(E2c)**

Maciejewski, T.J., and Miller, K.C., 1998, Geophysical interpretation of subsurface geology, pediment of the San Andres Mountains to the Jornada del Muerto Basin, New Mexico: New Mexico Geological Society Guidebook 49, p. 101-106. **(C2b, C4)**

Mack, G.H., 2004, Middle and late Cenozoic crustal extension, sedimentation, and volcanism in the southern Rio Grande rift, Basin and Range, and southern Transition Zone of southwestern New Mexico, *in* Mack, G.H., and Giles, K.J., eds., The Geology of New Mexico: A geologic history: New Mexico Geological Society Special Publication 11, p. 389-406. **(C2b, I3)**

Mack, G.H., 2018, Authigenic opal and calcite beds in axial-fluvial sediment of the Camp Rice Formation (Pliocene-lower Pleistocene), Rincon Hills – Third-day Road Log from Las Cruces to Rincon Hills: N.M. Geological Society Guidebook 69, p. 39-45. **(C2b)**

Mack, G.H., and McMillan, N.J., 1998, Second-day road log from Las Cruces to Selden Canyon, Broad Canyon, and Rincon Arroyo: New Mexico Geological Society Guidebook 49, p. 23-34. **(C2b)**

Mack, G.H., Dunbar, N., and Foster, R., 2009, New sites of 3.1-Ma pumice beds in axial-fluvial strata of the Camp Rice and Palomas Formations, southern Rio Grande rift: New Mexico Geology, v. 31, no. 2, p. 31-37. **(C2b, I3)**

Mack, G.H., Kottlowski, F.E., and Seager, W.R., 1998, The stratigraphy of south-central New Mexico: New Mexico Geological Society Guidebook 49, p. 135-154. **(C2b, I3)**

Mack, G.H., Love, D.W., and Seager, W.R., 1997, Spillover models for axial rivers in regions of continental extension: The Rio Mimbres and Rio Grande in the southern Rio Grande rift, USA. Sedimentology, v. 44, p. 637-652. **(C2b, I3)**

Mack, G.H., Salyards, S.L., and James, W.C., 1993, Magnetostratigraphy of the Plio-Pleistocene Camp Rice and Palomas formations in the Rio Grande rift of southern New Mexico: American Journal of Science, v. 293, p. 49-77. **(B1, C2b, I3)**

Mack, G.H., Seager, W.R., and Kieling. J., 1994, Late Oligocene and Miocene faulting and sedimentation, and evolution of the southern Rio Grande rift, New Mexico, USA: Sedimentary Geology, v. 92, p. 79-96. **(C2b)**

Mack, G.H., McIntosh, W.C., Leeder, M.R., and Monger, H.C., 1996, Plio-Pleistocene pumice floods in the ancestral Rio Grande, southern Rio Grande rift, USA: Sedimentary Geology, v. 103, p. 1-8. **(B1, C2b, I3)**

Mack, G.H., Nightengale, A.L., Seager, W.R., and Clemons, R.E., 1994, The Oligocene Goodsight-Cedar Hills half graben near Las Cruces, and its implications on the evolution of the Mogollon-Datil volcanic field and to the southern Rio Grande rift: New Mexico Geological Society Guidebook 45, p. 135-143. **(C2b)**

Mack, G.H., Salyards, S.L., McIntosh, W.C., and Leeder, M.R., 1998, Reversal magnetostratigraphy and radioisotopic geochronology of the Plio-Pleistocene Camp Rice and Palomas formations, southern Rio Grande rift: New Mexico Geological Society Guidebook 49, p. 229-236. **(B1, C2b, I3)**

Mack, G.H., Cole, D.R., James, W.C., Giordano, T.H., and Salyards, S.L., 1994, Stable oxygen and carbon isotopes of pedogenic carbonate as indicators of Plio-Pleistocene paleoclimate in the southern Rio Grande rift, south-central New Mexico: American Journal of Science, v. 294, p. 621-640. **(B1, C1, C3)**

Mack, G.H., Hampton, B.A., Seager, W.R., Ramos, F.C., and Witcher, J.C., 2018a, Las Cruces Country III: Socorro, NM, N.M. Geological Society, Inc. Guidebook 69, 219 p. ISBN 1-58546-108-3 **(C2b)**

Mack, G.H., Ramos, F.C., Hampton, B.A., Seager, W.R., and Witcher, J.C., 2018b, Geologic Evolution of Southern New Mexico: Second-day Road Log from Las Cruces to the Northwestern Doña Ana Mountains and West-central Robledo Mountain: N.M. Geological Society, Guidebook 69, p. 15-29. **(C2b)**

Mack, G.H., Ramos, F.C., Hampton, B.A., Seager, W.R., and Witcher, J.C., 2018c, The Doña Ana Caldera and Regional Outflow Sheets: First-day Road Log from Las Cruces to Southern Doña Ana Mountains and Point of Rocks: N.M. Geological Society, Guidebook 69, p. 1-13. **(C2b)**

Mack, G.H., Seager, W.R., Leeder, M.R., Perea-Arlucea, M., and Salyards, S.L., 2006, Pliocene and Quaternary history of the Rio Grande, the axial river of the southern Rio Grande rift, New Mexico, USA: Earth-Science Reviews, v. 77, p. 141-162. **(C2b, I3)**

Mack, G.H., Jones, M.C., Tabor, N.J., Ramos, F.C., Scott, S.R., and Witcher, J.C., 2012, Mixed geothermal and shallow meteoric origin of opal and calcite beds in Pliocene-lower Pleistocene axial-fluvial strata, southern Rio Grande rift, Rincon Hills, New Mexico, U.S.A.: Journal of Sedimentary Research, v. 82, p. 616-631. **(C2b, C4, H2)**

Mack, P.D.C., 1985, Correlation and provenance of facies within the upper Santa Fe Group in the subsurface of the Mesilla Valley, southern New Mexico: New Mexico State University, master's thesis, 137 p. **(H1)**

MacMillan, J.R., Naff, R.L., and Gelhar, L.W., 1976, Prediction and numerical simulation of subsidence associated with proposed groundwater withdrawal in the Tularosa Basin, New Mexico: International Association of Hydrological Sciences, Publication No. 121, Proceedings of the Anaheim Symposium, p. 600-608. **(D1, H3)**

Maker, H.J., Neher, R.E., Derr, P.H., and Anderson, J.U., 1971, Soil Associations and land classifications for irrigation, Doña Ana County: New Mexico State University Agricultural Experiment Station, Research Report 183, 40 p. **(C3)**

Maksim, N., 2016, An integrated geophysical survey of Kilbourne Hole, southern New Mexico: Implications for near surface exploration of Mars and the Moon: University of Texas at EI Paso, doctoral dissertation, 80 p. **(C2b, C4)**

Mandel, S., 1979, Problems of large-scale groundwater development, *in* Back, W., and Stephenson, D.A., eds., Contemporary hydrology – The George Burke Maxey Memorial Volume: Journal of Hydrology, v. 43, no. 1/6, p. 439-443. *Seminal discussion of groundwater mining.* **(D1)**

Mandelbrot, B., 1982, The fractal geometry of nature: New York, W.H. Freeman and Company, 480 p. ISBN-10: 0716711869 **(D1)**

Manning, A.K., 2011, Mountain-block recharge, present and past, in the eastern Española Basin, New Mexico, USA: Hydrogeology Journal, v. 19, no. 2, p. 379-397. **(D2, H3)**

Markovich, K.H., Manning, A.H., Condon, L.E., and McIntosh, J.C., 2019. Mountain-block recharge: A review of current understanding: Water Resources Research, v. 55, p. 8278-8304. **(D2, H2)**

Markovich, K.H., Condon, L.E., Carroll, K.C., Purtschert, R., and McIntosh, J.C., 2021. A mountain-front recharge component characterization approach combining groundwater age distributions, noble gas thermometry, and fluid and energy transport modeling: Water Resources Research, v. 57, p. 1-21. **(D2, H2)**

Márquez-Alameda, A., coordinador del volumen, 1992, Historía general de Chihuahua I – Geología, geografía y arqueología: Universidad Autónoma de Ciudad Juárez y Gobierno del Estado Chihuahua, 307 p. **(A1, B1, B2, F3)**

Mattick, R.E., 1967, A seismic and gravity profile across the Hueco bolson, Texas: U.S. Geological Survey, Professional Paper 575-D, p. D85-D91. **(C2a, C4)**

Maxey, G.B., 1964, Hydrostratigraphic units: Journal of Hydrology, v. 2, no. 2, p. 124-129. **(D1)**

Maxey, G.B., 1968, Hydrogeology of desert basins: Ground Water, v. 6, no. 5, p. 1-22. **(D1)**

Maxey, G.B., and Eakin, T.E., 1949, Ground water in White River Valley, White Pine, Nye, and Lincoln Counties, Nevada: Nevada State Engineer's Office, Water Resources Bulletin 8, 59 p. **(D1, D2)**

Maxey, G.B., and Jameson, C.H., 1948, Geology and water resources of Las Vegas, Pahrump, and Indian Springs Valleys, Clark and Nye Counties, Nevada: Nevada State Engineer's Office, Water Resources Bulletin 5, 121 p. **(D1)**

Maxey, G.B., and Shamberger, H.A., 1961, The Humboldt River Research Project in Nevada, *in* Ground water in arid zones: International Association of Scientific Hydrology, Publication No. 57, p. 437-454. **(D1)**

McAda, D.P., and Barrow, P., 2002, Simulation of ground-water flow in the Middle Rio Grande basin between Cochiti and San Acacia, New Mexico: U.S. Geological Survey Water-Resources Investigations Report 02-4200, 81 p. **(D1)**

McCalpin, J.P., 2006, Quaternary faulting and seismic source characterization in the EI Paso-Juárez metropolitan area; Collaborative research with the University of Texas at EI Paso, Program Element II: Evaluate Urban Hazard and Risk, final Technical Report, National Earth Quake Hazards Reduction Program U.S. Geological Survey, 68 p. **(C2b, C4, F1)**

McCord, J.T. and Stephens, D.B., 1999, Contrasts in regional and local-scale heterogeneity in relation to ground-water supply and contamination in the Albuquerque Basin: New Mexico Geological Society Guidebook 50, p. 401-408. **(D1, E2c)**

McCray, J.E., Kirkland, S.L., Siegrist, R.L., and Thyne, G.D., 2005, Model parameters for simulating the fate and transport of on-site wastewater nutrients, Ground Water, v. 43, no. 4, p. 628-639. **(E2c)**

McDonald, H.G., 2022, Paleoecology of the extinct Shasta ground sloth. *Nothrotheriops shastensis* (Xenarthra, Notrotheridae): The physical environment, *in* Morgan. G.S. et al., eds., Late Cenozoic Vertebrates from the American Southwest: A tribute to Arthur H. Harris: New Mexico Museum of Natural History and Science, Bulletin 88, p. 22-44. **(B2, C1)**

McFadden, L.D., 2013, Strongly dust-influenced soils and what they tell us about landscape dynamics in vegetated aridlands of the Southwestern United States: Geological Society of America, Special Paper 500, p. 501-532. **(C3)**

McHarg, I.L., 1969, Design with Nature: New York, NY, Doubleday/Natural History Press, 197 p. ISBN-13: 978-0471114604. *See Steiner et al. 2019.* **(A2, E2)**

McKay, D., Perea, S., and Gallagher, M., 2020, NM races to stay ahead of coronavirus curve: Albuquerque Journal, Saturday, March 14, 2020, p. A1, A8. **(A3)**

McKee, S., 2022, As AI progresses, keep humanity in mind: Albuquerque Journal–BUSINESS OUTLOOK, Monday, January 24, 2022, p. 1, 5. **(A3)**

McLay, C.D., Dragden, R., Sparling, G., and Selvarajah, N., 2001, Predicting groundwater nitrate concentrations in a region of mixed agricultural land use: a comparison of three different approaches: Environmental Pollution, v. 115, p. 191-204 **(E2c)**

McMillan, N.J., 2004, Magmatic record of Laramide subduction and transition to Tertiary extension: Upper Cretaceous through Eocene igneous rocks of New Mexico, *in* Mack, G.H., and Giles, K.J., eds., The Geology of New Mexico: A geologic history: New Mexico Geological Society Special Publication 11, p. 249-270. **(C2b)**

McPhee, J., 1989, The Control of Nature: New York, Farrar, Strauss and Giroux, 272 p. ISBN: 0-374-52259-6 **(A2, E2)**

Meinzer, O.E., 1922, Map of the Pleistocene lakes of the Basin and Range province and its significance: Geological Society of America Bulletin, v. 33, p. 541-552. **(B2, C1, D1, I1)**

Meinzer, O.E., 1923b, Outline of ground water hydrology, with definitions: U.S. Geological Survey Water-Supply Paper 494, 71 p. **(A1, D1)**

Meinzer, O.E., and Hare, R.E., 1915, Geology and water resources of the Tularosa Basin, New Mexico: U.S. Geological Survey Water-Supply Paper 343, 317 p. **(B2, C1, C2a, D1, G1, I2)**

Meixner, T., Manning, A.H., Stonestrom, D.A., Allen, D.M., Ajami, H., Blasch, K.W., Brookfield, A.E., Castro, C.L., Clark, J.F., Gochis, D.J., Flint, A.L., Neff, K.L., Niraula, R., Rodell, M., Scanlon, B.R., Singha, K., and Walvoord, M.A., 2016, Implications of projected climate change for groundwater recharge in the western United States: Journal of Hydrology, v. 534, p. 124-138. **(C1, D2)**

Meko, D.M., 1990, Inferences from tree rings on low frequency variations in runoff in the interior western United States, *in* Proceedings of the Sixth Annual Pacific Climate Workshop: Sacramento, California Department of Water Resources, Interagency Ecological Studies Program, Technical Report 23, p. 123-127. **(B2, B3, C1)**

Merry, R.W., 2009, A country of vast designs – James K. Polk, the Mexican War, and the Conquest of the American Continent: New York, Simon & Schuster Paper Back edition, 576 p. **(A2, B3)**

Metcalf, A.L., 1967, Late Quaternary mollusks of the Rio Grande Valley, Caballo Dam to El Paso, Texas: El Paso, Texas Western Press, University of Texas at El Paso, Science Series No. 1, 62 p. **(B2, C1, C2a)**

Metcalf, A.L., 1969, Quaternary surface sediments and mollusks--southern Mesilla Valley, New Mexico and Texas: New Mexico Geological Society Guidebook 20, p. 158-164. **(B2, C1, C2a)**

Metcalfe, S., Bimpson, A., Courtice, A.J., and O'Hara, S., 1997, Climate change at the monsoon/westerly boundary in northern Mexico: Journal of Paleolimnology, v. 17, p. 155-171. **(B2, C1, F3, I2)**

Metcalfe, S., Say, A., Black, S., McCullock, R., and O'Hara, S., 2002, Wet conditions during the last glaciation in the Chihuahuan Desert, Alta Babícora basin, Mexico: Quaternary Research, v. 57, p. 91-101. **(B2, C1, F3, I2)**

Mifflin, M.D., 1968, Delineation of Groundwater Flow Systems in Nevada: University of Nevada-Reno, Desert Research Institute, Technical Report Series H-W, Hydrology and Water Resources Publication 4, 109 p. **(D1, D2)**

Mifflin, M.D., 1988, Region 5, Great Basin, *in* Back, W., Rosenshein, J.S., and Seaber, P.R., eds. Hydrogeology – The Geology of North America: Geological Society of America, Decade of North American Geology, v. 0-2, p. 69-78. **(D1, D2)**

Mifflin, M.D., and Hess, J.W., 1979, Regional carbonate flow systems in Nevada: Journal of Hydrology, v. 43, p. 217-237. **(D1, D2)**

Miller, J.B., and Gelman, A., 2020, Laplace's theories of cognitive illusions, heuristics and biases: Statistical Science, v. 35, no. 2, p. 159-170. **(A2, D1)**

Mills, S.K., 2003, Quantifying salinization of the Rio Grande using environmental tracers: New Mexico Institute of Mining and Technology, master's thesis, 397 p. **(E2a, H2)**

Minnis, M., 2015, Al Utton – Aztec Eagle: Albuquerque, NM, Utton Transboundary Resources Center, 347 p., ISBN 978-0-578-16455-7 **(A2, E3)**

Molina, C., 1997, Stratigraphy and structure of the Sierra Samalayuca, northern Chihuahua, Mexico: University of Texas at El Paso, master's thesis, 135 p. **(C2b, F3)**

Moncada-Gutierrez, M., 2016, A Geophysical investigation at Potrillo Maar: University of Texas at EI Paso, master's thesis, 47 p. **(C4, F1)**

Monger, H.C., 1993, Soil-geomorphic and paleoclimatic characteristics of the Fort Bliss Maneuver Areas, southern New Mexico and western Texas: U.S. Army Air Defense Artillery Center, Fort Bliss; Directorate of Environment; Environment Management Division, Cultural Resources Branch; Historic and Natural Resources Report No. 10, 233 p. **(C3)**

Monger, H.C., Daugherty, L.A., and Gile, L.H., 1991, A microscopic examination of pedogenic calcite in an Aridisol of southern New Mexico, *in* Occurrence, characteristics, and genesis of carbonate, gypsum, and silica accumulation in soils: Soil Science Society of America Special Publication No. 26, p. 37-60. **(C3)**

Monger, H.C., Gile, L.H., Hawley, J.W., and Grossman, R.B., 2009, The Desert Project – An analysis of aridland soil-geomorphic processes: New Mexico State University Agricultural Experiment Station Bulletin 798, 76 p. **(A2, C2b, C3)**

Monreal, R., and Longoria, J., 1999, A revision of the Upper Jurassic and Lower Cretaceous stratigraphic nomenclature for the Chihuahua trough, north-central Mexico: Implications for lithocorrelations, *in* Bartolini, C., Wilson, J.L., Lawton, T.F. (eds.), Mesozoic Sedimentary and Tectonic History of North-Central Mexico: Geological Society of America, Special Paper 340, p. 69-92. **(C2b, F3)**

Moore, S.J., Bassett, R.L., Liu, B., Wolf, C.P., and Doremus, D., 2008, Geochemical tracers to evaluate hydrogeologic controls on river salinization: Ground Water, v. 46, no. 3, p. 489-501. **(E2a, F2, H2)**

Moorhead, M.L., ed., 1954, Josiah Gregg [1844], Commerce of the prairies: University of Oklahoma Press, 469 p. **(A2, B3)**
Moorhead, M.L., 1958, New Mexico's royal road, trade and travel on the Chihuahua Trail: University of Oklahoma Press, 234 p. **(A2, B3)**
Morgan, G.S., 2022, Moles of the genus *Scalopus* (Mammalia: Soricomorpha: Talpidae) from the late Pliocene and early Pleistocene (Blancan) of New Mexico, *in* Morgan. G.S. et al., eds., Late Cenozoic Vertebrates from the American Southwest: A tribute to Arthur H. Harris: New Mexico Museum of Natural History and Science, Bulletin 88, p. 139-155 **(B1, C1)**
Morgan, G.S., and Lucas, S.G., 2003, Mammalian bio chronology of Blancan and Irvingtonian (Pliocene and early Pleistocene) faunas from New Mexico: Bulletin of the American Museum of Natural History, v. 278, p. 269-320. **(B1, C1)**
Morgan, G.S., and Lucas, S.G., 2005, Pleistocene vertebrates in New Mexico from alluvial, fluvial, and lacustrine deposits, *in* Lucas, S.G., et al., eds., New Mexico's Ice Ages: New Mexico Museum of Natural History & Science Bulletin No. 28, p. 185-231. **(B1, C1)**
Morgan, G.S., Hulbert, H.C., Jr., Gottlieb, E.S., Amato, J.M., Mack, G.H., Jonell, T.N., 2017, The tapir *Tapirus* (Mammalia: Perissodactyla) from the late Pliocene (early Blancan) Tonuco Mountain Local Fauna, Camp Rice Formation, Doña Ana County, southern New Mexico: New Mexico Geology, v. 39, no. 2, p. 28-39. **(C1, C2b)**
Morrison, R.B., 1969, Photointerpretive mapping from space photographs of Quaternary geomorphic feature and soil associations in northern Chihuahua and adjoining New Mexico and Texas: New Mexico Geological Society Guidebook 20, p. 116-129. **(C2a, C3, E1, F1, I2)**
Morrison, R.B., 1991, Quaternary geology of the southern Basin and Range province, *in* Morrison, R.B., ed., Quaternary non-glacial geology; Conterminous U.S.: Boulder, CO, Geological Society of America, The Geology of North America, v. K-2, p. 353-371. **(C2b, I1)**
Moyer, D.L., Anderholm, S.K., Hogan, J.F., Phillips, F.M., Hibbs, B.J., Witcher, J.C., Matherne, A.M., and Falk, S.E., 2013, Knowledge and understanding of dissolved solids in the Rio Grande – San Acacia, New Mexico, to Fort Quitman, Texas, and plan for future studies and monitoring: U.S. Geological Survey Open-File Report 2013-1190, 55 p. **(C4, F1, H2)**
Mueller, J.E., 1975, Restless river: International law and the behavior of the Rio Grande: Texas Western Press, University of Texas at El Paso, 155 p. **(A2, B3, E2, F1)**
Mumme, S.P., 1994, The North American Free Trade Agreement: The Environmental Side Agreement and Parallel Bilateral Border Accords: Transboundary Resources Report, v. 8, no. 3, p. 1-3. **(E2, E3, F1)**
Mumme, S.P., 2000, Minute 242 and beyond: Challenges and opportunities for managing transboundary groundwater on the Mexico-US Border: Natural Resources Journal, v. 40, no. 2, p. 341-378. **(E2, E3, F1)**
Mumme, S.P., 2010, Environmental governance in the Rio Grande watershed: Binational institutions and the transboundary water crisis – An agenda for strengthening binational water governance along the Rio Grande: Journal of Transboundary Water Resources, v. 1, p. 43-68. https://nmwrri.nmsu.edu/publications/pub-documents/JTWR-Book.pdf **(E2, E3, F1)**
Muñoz-Meléndez, G., Quintero-Núñez, M., and Sweedler, A., 2012, Energy for a sustainable border region in 2030, *in* Lee, E., and Ganster, P., The U.S.-Mexican border environment: Progress and challenges for sustainability: Southwest Consortium for Environmental Research and Policy, SCERP Monograph Series, no. 16, San Diego State University Press, p. 289-325. **(E2, E3, F1)**
Myers, R.G., and Orr, B.R., 1986, Geohydrology of the aquifer in the Santa Fe Group, northern West Mesa of the Mesilla Basin near Las Cruces, New Mexico: U.S. Geological Survey, Water-Resources Investigations Report 84-4190, 37 p. **(C2a, H1)**
National Ground Water Association (NGWA), 2010, Brackish groundwater: Westerville, Ohio, National Ground Water Association information brief, 4 p., accessed March 8, 2013. **(D1, E2a)**
National Ground Water Association (NGWA), 2014, Best suggested practices for aquifer storage and recovery: 601 Dempsey Rd., Westerville OH 43081-8978, NGWA Press. 21 p. ISBN 1-56034-026-6 **(D1, E2b)**
National Ground Water Association (NGWA), 2019a, NEWSLINE–NGWA supports legislation to create national to PFAS crisis: Groundwater Monitoring & Remediation, v. 39, issue 3, p. 6. **(D1, E2c)**
National Ground Water Association (NGWA), 2019b, NEWSLINE–Congress introduces a flurry of PFAS legislation: Groundwater Monitoring & Remediation, v. 39, issue 3, p. 7. **(D1, E2c)**
National Ground Water Association (NGWA), 2019c, NEWSLINE–NSF Standards add PFOA and PFOS reduction claims requirements: Groundwater Monitoring & Remediation, v. 39, issue 3, p. 7. **(D1, E2c)**

Naus, C.A., 2002, Conceptual model of the bolson-fill aquifer, Soledad Canyon area, Doña Ana County, New Mexico: New Mexico Geological Society Guidebook 53, p. 309-318. **(C2b, H1)**
Nelson, J.W., and Holmes, L.C., 1914, Soil Survey of the Mesilla Valley, New Mexico-Texas: U.S. Department of Agriculture, Bureau of Soils, Washington, D.C., U.S. Government Printing Office, 39 p. map scale 1:63,360. *Shallow depth to water table shown in large no. soil-test borings.* **(C3, G1)**
Neuendorf, K.K.E., Mehl, J.P., Jr., and Jackson, J.A., 2005, Glossary of Geology (fifth edition): Alexandria, VA, American Geological Institute, 779 p. **(A1)**
Newell, N.D., 1963, Crises in the History of Life: Scientific American, v. 208, no. 2, p. 76-92. **(B1, C1)**
Nichols, G., 2015, Stratigraphic architecture of fluvial distributive systems in Basins of internal drainage: Search and Discovery Article #51145 (2015), 42 p. pdf. *For related information contact author directly at Nautilus Ltd, Hermitage, Berkshire, United Kingdom.* g.nichols@nautiuswold.com **(D1)**
Nickerson, E.L., 1986, Selected geohydrologic data for the Mesilla Basin, Doña Ana County, New Mexico and El Paso County, Texas: U.S. Geological Survey Open-File Report 86-75, 59 p. **(H1)**
Nickerson, E.L., 1989, Aquifer tests in the flood-plain alluvium and Santa Fe Group at the Rio Grande near Canutillo, El Paso County, Texas: U.S. Geological Survey Water-Resources Investigations Report 89-4011, 29 p. **(H3)**
Nickerson, E.L., 1995, Selected geohydrologic data for the Mesilla ground-water basin, 1987 through 1992 water years, Doña Ana County, New Mexico and El Paso County, Texas: U.S. Geological Survey Open-File Report 95-111, 123 p. **(H1)**
Nickerson, E.L., 1998, U.S. Geological Survey seepage investigations of the Lower Rio Grande in the Mesilla Valley, *in* Ortega Klett, C.T., ed., Proceedings of the 43rd Annual New Mexico Water Conference: Water Challenges on the Lower Rio Grande. New Mexico Water Resources Research Institute, Report No. 310, p. 59-68. **(H3)**
Nickerson, E.L., 2006, Description of piezometers and ground-water-quality characteristics at three new sites in the Lower Mesilla Valley, Texas, and New Mexico: U.S. Geological Survey Scientific Investigations Report 2005-5248, 27 p. **(H1, H2)**
Nickerson, E.L., and Myers, R.G., 1993, Geohydrology of the Mesilla ground-water basin, Doña Ana County, New Mexico, and El Paso County, Texas: U.S. Geological Survey Water-Resources Investigations Report 92-4156, 89 p. **(H1, H2)**
NMOSE-GIS, NM Office of the State Engineer – GIS-Geographic Information System, webpage: https://www.ose.state.nm.us/GIS/index.php **(E1)**
Nordt, L., 2003, Late Quaternary fluvial landscape evolution in desert grasslands of northern Chihuahua, Mexico: Geological Society of America Bulletin, v. 115, no. 5, p. 596-606. **(B2, C1, C2b, F3)**
North American Commission on Stratigraphic Nomenclature (NACOSN), 2005, North American Stratigraphic Code: The American Association of Petroleum Geologists Bulletin, v. 89, p. 1547-1591. **(D1)**
Norvelle, N.R., 2021, NM just can't make the economics of hydrogen work: Albuquerque Journal–OPINION-LOCAL VOICES, Thursday, December 2, 2021, p. A13. **(A3)**
O'Donnell, J.E., Martinez, R., and Williams, J., 1975, Telluric current soundings near Kilbourne and Hunt Holes, New Mexico: New Mexico Geological Society Guidebook 26, p. 279-270. **(C4)**
Omernik, J.M., 2004, Perspectives on the nature and definition of Ecological Regions: Environmental Management. p. 34 – Supplement 1, p. 27-38. **(C1)**
Ordóñez, E., 1936, Physiographic provinces of Mexico: American Association of Petroleum Geologists Bulletin, v. 20, no. 10, p. 1277-1307. **(C, F3)**
Ordóñez, E., 1942, Las provincias fisiográficas de México: Revista Geografía de Instituto Panamericano Geografía e Historia, tomo. 1, nos. 2-3. **(C, F3)**
Orr, B.R., and Myers, R.G., 1986, Water resources in basin-fill deposits in the Tularosa Basin, New Mexico: U.S. Geological Survey Water Resources Investigations Report 85-4219, 94 p. **(H1, H2)**
Orr, B.R., and Risser, D.W., 1992, Geohydrology and potential effects of development of freshwater resources in the northern part of the Hueco Bolson, Doña Ana and Otero Counties, New Mexico, and El Paso County, Texas: U.S. Geological Survey Water-Resources Investigations Report 91-4082, 92 p. **(H1, H2)**
Orr, B.R., and White, R.R., 1985, Selected hydrologic data from the northern part of the Hueco Bolson, New Mexico and Texas: U.S. Geological Survey Open-File Report 85-696, 88 p. **(H1)**
Ortega Klett, C.T., ed., 2000, The Rio Grande Compact: It's the Law: Proceedings of the 44th Annual New Mexico Water Conference, New Mexico Water Resources Research Institute Report No. 310, 199 p. **(B3, E2, E3)**
Ortega Klett, C.T., ed., 2012, One hundred years of water wars in New Mexico: Santa Fe, Sunstone Press, 288 p. ISBN: 978-0-86524-902-5 **(A2, E2, E3)**

Ortega-Ramírez, J.R., Valiente-Banuet, A., Urrutia-Fucugauchi, J., Mortera-Gutierrez, C.A., and Alvarado-Valdéz, G., 1998, Paleoclimatic changes during the late Pleistocene-Holocene in Laguna Babícora, near the Chihuahuan Desert, Mexico: Canadian Journal of Earth Science, v. 35, p. 1168-1179. **(B2, C1, F3, I2)**

Ortiz, D., Lange, K.M., and Beal, L.V., 2001, Water resources data, New Mexico, Water Year 2000, volume 1. The Rio Grande Basin, the Mimbres River Basin, and the Tularosa Valley Basin: U.S. Geological Survey Water-Data Report NM-00-1, 411 p. **(D1)**

Orville, P.M., 1963, Alkali exchange between vapor and feldspar phases: American Journal of Science, v. 261, p. 201-237. **(D1)**

Overpeck, J.T, and Udall, B., 2020, Climate change and aridification of North America: Proceedings of the National Academy of Sciences of the United States of America (PNAS), v. 117, no. 22, p. 11856-11858. **(C1, D1)**

Pacheco, J., 2008, Foxconn can sharply alter border economy: Albuquerque Journal–BUSINESS OUTLOOK-International Trade, Monday, August 11, 2008, p. 9. **(A3)**

Pacheco, J., 2010, Infrastructure benefits both sides of the border: Albuquerque Journal–BUSINESS OUTLOOK-I Business Across the Border, Monday, May 24, 2010, p. 20. **(A3, E2, F1)**

Pacheco, J., 2011, A train ride to economic advancement: Albuquerque Journal–BUSINESS OUTLOOK-Business Across the Border, Monday, October 24, 2011, p. 5. **(A3)**

Pacheco, J., 2012, Southern N.M. rail project vast in impact: Albuquerque Journal–BUSINESS OUTLOOK-Business Across the Border, Monday, January 9, 2012, p. 3. **(A3)**

Pacheco, J., 2017a, Assaults on NAFTA can't dim the demand for trade: Albuquerque Journal–BUSINESS OUTLOOK, Monday, October 23, 2017, p. 9, 13. **(A3)**

Pacheco, J., 2017b, Mexican envoy expresses concerns for NAFTA-Part 1: Albuquerque Journal–BUSINESS OUTLOOK, Monday, December 4, 2017, p. 15. **(A3)**

Pacheco, J., 2018c, Visionaries transformed NM-Mexico border area: Albuquerque Journal–BUSINESS OUTLOOK, Monday, August 27, 2018, p. 12-13. **(A3)**

Pacheco, J., 2019a, Border walls useful in places, but not in others: Albuquerque Journal–BUSINESS OUTLOOK, Monday, February 11, 2019, p. 19, 21. **(A3)**

Pacheco, J., 2019f, The impressive impact of trade with Mexico: Albuquerque Journal–BUSINESS OUTLOOK, Monday, September 9, 2019, p. 3. **(A3)**

Pacheco, J., 2019g, USMCA aka NAFTA2 still awaits Congress: Albuquerque Journal–BUSINESS OUTLOOK, Monday, December 2, 2019, p. 10. **(A3)**

Pacheco, J., 2020a, Fight coronavirus chaos with communication: Albuquerque Journal–BUSINESS OUTLOOK, Monday, April 6, 2020, p. 8. **(A3)**

Pacheco, J., 2020b, 2008 conference foresaw pandemic challenge: Albuquerque Journal–BUSINESS OUTLOOK, Monday, May 18, 2020, p. 8. **(A3)**

Pacheco, J., 2020c, Collaboration needed to keep rivers flowing: Albuquerque Journal–BUSINESS OUTLOOK, Monday, October 5, 2020, p. 8. **(A3)**

Pacheco, J., 2020e, From Russia to DACA: Global wishes for '21 – Global trade wish list for '21: Albuquerque Journal–BUSINESS OUTLOOK, Monday, December 28, 2020, p. 16-17. **(A3)**

Pacheco, J., 2021a, Texas energy grid crisis affected Mexico, trade: Albuquerque Journal–BUSINESS OUTLOOK, Monday, March 8, 2021, p. 8. **(A3)**

Pacheco, Jerry, 2021e, Loosened borders welcome news for region: Albuquerque Journal–BUSINESS OUTLOOK, Monday, November 1, 2021, p. 12. **(A3)**

Pacheco, J., 2022a, Borderplex statistics show major economic activity: Albuquerque Journal–BUSINESS OUTLOOK, Monday, January 17, 2022, p. 12. **(A3)**

Pacheco, J., 2022b, Texas govs' border boondoggle helped nothing: Albuquerque Journal–BUSINESS OUTLOOK, Monday, April 25, 2022 p. 8. **(A3)**

Pacheco, J., 2022c, Border flub cost US GDP hundreds of millions: Albuquerque Journal–BUSINESS OUTLOOK, Monday, May 9, 2022 p. 4. **(A3)**

Pacheco, J., 2024b, Part 1: The slow start to the Santa Teresa Port: Albuquerque Journal–BUSINESS OUTLOOK, Monday, April 8, 2024, p. 13. **(A3)**

Pacheco, J., 2024c, Part 2: Santa Teresa Port of Entry has found success after slow start: Albuquerque Journal–BUSINESS OUTLOOK, Monday, April 22, 2024, p. 15. **(A3)**

Padovani, E.R., 1987, The ground truth from crustal xenoliths; a multifaceted approach, *in* Noller, J.S., Kirby, S.H., and Nielson-Pike. J.E., eds., Geophysics and petrology of the deep crust and upper mantle: Washington, DC, US Geological Survey, p. 40-43. **(C2a, C4)**

Padovani, E.R., and Reid, M.R., 1989, Field guide to Kilbourne Hole maar: New Mexico Bureau of Mines and Mineral Resources Memoir 46, p. 174-185. **(C2a)**
Paige, S., and Darton, N.H., 1916, Descriptions of the Silver City Quadrangle, New Mexico: United States Geological Survey, Geologic Atlas Folio 199, 10 p. **(C2a, G1)**
Paine, J.G., and Collins, E.W., 2002, Evaluating potential groundwater resources on State Lands in El Paso County, Texas using airborne geophysics: Report prepared by the University of Texas Bureau of Economic Geology for the General Land Office under contract no. 02-306R, 87 p. **(C4, F2)**
Palacios-Fest, M.R., Carreño, A.L., Ortega-Ramírez, J.R., and Alvarado-Valdéz, G., 2002, A paleoenvironmental reconstruction of Laguna Babícora, Chihuahua, Mexico based on ostracode paleoecology and trace element shell chemistry: Journal of Paleolimnology, v. 27, p. 185-206. **(B2, C1, F3, I2)**
Panagopoulos, G.P., Antonakos, A., and Lambrakis, N.J., 2006, Optimization of the DRASTIC method for groundwater vulnerability assessment via the use of simple statistical methods and GIS: Hydrology Journal, v. 14, no. 6, p. 894-911. **(E2c)**
Paskus, L., 2020, At the Precipice – New Mexico's Changing Climate: University of New Mexico Press, 200 p. ISBN 978-0-8263-5911-7 **(A2, C1)**
Pazzaglia, F.J., 2005, River responses to Ice Age (Quaternary) climates in New Mexico, *in* Lucas, S.G., et al., eds., New Mexico's Ice Ages: New Mexico Museum of Natural History & Science Bulletin No. 28, p. 115-124. **(C2b, I3)**
Pazzaglia, F.J., and Hawley, J.W., 2004, Neogene (rift flank) and Quaternary geology and geomorphology, *in* Mack, G.H., and Giles, K.J., eds., The Geology of New Mexico: A geologic history: New Mexico Geological Society Special Publication 11, p. 407-438. **(C2b)**
Pearson, E.A., Rucker, D.F., Tsai, C-H., Fuchs, E.H., Carroll, K.C. 2022, Electrical resistivity monitoring of lower Rio Grande River-Groundwater intermittency: Journal of Hydrology, v. 613. 13 p. **(C4, H3)**
Peipert, T., and Peterson, B., ASSOCIATED PRESS, 2021, Where's the snow? Rockies winter starts with a whimper – Denver sees high temps in the 70s; drought threatens the region's low water supply: Albuquerque Journal, Saturday, December 4, 2021, p. A8. **(A3)**
Penndorf, J., 2018, Adapting for the effects of climate change: Urban Land, v. 77, no. 3, p. 75-78. **(C1, E3)**
Pepin, J.D., Robertson, A.J., and Kelley, S.A., 2022, Salinity contributions from geothermal waters to the Rio Grande and shallow aquifer system in the transboundary Mesilla Basin (United States)/Conejos-Médanos (Mexico) Basin: Water, v. 14, issue 1, article 33, 24 p. **(C4, H2, H3)**
Perez-Arlucea, M., Mack, G., and Leeder, M., 2000, Reconstructing the ancestral (Plio-Pleistocene) Rio Grande in its active tectonic setting, southern Rio Grande Rift, New Mexico, USA: Sedimentology, v. 47, p. 701-720. **(C2b, I3)**
Pérez de Villagrá, Don Gáspar, 1962, A History of New Mexico, Alcalá – 1610 (Translated by Gilberto Espinosa, F.D. Hodge, ed.): Glorieta, NM, The Rio Grande Press, 308 p. *p. 21, May 4 1498 Oñate party leaves EPdN and enters NM.* **(B3)**
Peterson, D.M., and Wilson, J.L., 1988, Variably saturated flow between streams and aquifers: New Mexico Water Resources Research Institute Report No. 233, 289 p. https://nmwrri.nmsu.edu/publications/technical-reports/tr-reports/tr-233.html **(D2, H3)**
Peterson, D.M., Khaleel, R., and Hawley, J.W., 1984, Quasi three-dimensional modeling of groundwater flow in the Mesilla Bolson, New Mexico: New Mexico Water Resources Research Institute Report No. 178, 185 p. https://nmwrri.nmsu.edu/publications/technical-reports/tr-reports/tr-178.html **(H1, H3)**
Phillips, F., 2018, Climate change denial the real 'fake news:' Albuquerque Journal–OPINION–EDITORIAL SCIENCE AND CLIMATE, Sunday, July 8, 2018, p. A11. **(A3, C1)**
Phillips, F.M., Hall, G.E., and Black, M.E., 2011, Reining in the Rio Grande – People, Land, and Water: University of New Mexico Press, 252 p. **(A2, B3, C1, D1, E3)**
Phillips, F.M., Hogan, J.F., Mills, S.K., and Hendrickx, J.M.H., 2003, Environmental tracers applied to quantifying causes of salinity in arid-region rivers: Preliminary results from the Rio Grande, southwestern USA, *in* Alsharhan, A.S., and Wood, W.W., eds., Water resources perspectives: Evaluation, management and policy: Amsterdam, Elsevier, p. 327-334. **(D2, H2)**
Plummer, L.N., Bexfield, L.M., Anderholm, S.K., Sanford, W.E., and Busenberg, E., 2004, Geochemical characterization of ground-water flow in the Santa Fe Group aquifer system, Middle Rio Grande Basin, New Mexico: U.S. Geological Survey Water-Resources Investigations Report 03-4141,369 p., with CD-ROM. **(D1, D2, H3)**
Poland, J.F., Lofgren, B.E., Ireland, R.L., and Pugh, R.G., 1975, Land subsidence in the San Joaquin Valley, California, as of 1972: U.S. Geological Survey Professional Paper 437-H, 78 p. **(D1)**

Polich, J., 2021, Is blue hydrogen the bridge to a greener future: Albuquerque Journal, Monday, November 22, 2021, p. 12. *See Robinson-Avila, K., 2021c, NMSU powers up with clean energy.* **(A3)**
Poppa, T., 1985, Vast water under Mexico's sands?: El Paso Herald-Post (Metro), Thursday, February 14, 1985. **(A3, F3)**
Powell, J.W., 1885, On the Organization of Scientific Work of the General Government: Extracts from the testimony taken by the Joint Commission of the Senate and House of Representatives to "consider the present organization of the Signal Service, Geological Survey, Coast and Geodetic Survey, and the Hydrographic Office of the Navy Department, with the view to secure greater efficiency and economy of administration." Washington, Government Printing Office, 468 p. **(C, D1, E2)**
Quigley, W., 2011, Border area primed to fuel growth: Albuquerque Journal–BUSINESS, Thursday, March 24, 2011, p. B4. **(A3)**
Ramberg, I.B., Cook, F.A., and Smithson, S.B., 1978, Structure of the Rio Grande rift in southern New Mexico and West Texas based on gravity interpretation: Geological Society of America Bulletin, v. 89, no. 1, p. 107-123. **(C2a, C4)**
Ramos, F.C., and Heizler, M.T., 2018, Age relationships of volcanic rocks in the Doña Ana Mountains: New Mexico: Geological Society, Guidebook 69, p. 159-163. **(C2b)**
Ramos, F.C., Hampton, B.A., Seager, W.R., and Mack, G.H., 2018c, Cenozoic Igneous Activity in the Organ Mountains: Third-day (A) road log from Las Cruces to Dripping Springs Recreation Area, Organ Mountains: New Mexico Geological Society Guidebook 69, p. 31-37. **(C2b)**
Randel, W.J., 2018, The seasonal fingerprint of climate change – Satellite data provide evidence for human impacts on the seasonal temperature cycle: Science, v. 361, p. 227-228. **(C1)**
Rango, A., 2006, Snow: The real water supply for the Rio Grande basin, *in* Anderson, K.S.J., ed., Science on the Border: New Mexico Journal of Science, v. 44. p. 99-118. **(C1, F1)**
Rao, B.K., 1988, Digital Model of Groundwater Flow in the Southern Jornada del Muerto Basin, New Mexico: New Mexico State Engineer Report TDH-88-7, 10 p. **(H3)**
Reeder, H.O., 1957, Ground water in Animas Valley, Hidalgo County, New Mexico: New Mexico State Engineer Office, Technical Report No. 11, 101 p. **(G2, I2)**
Reeves, C.C., Jr., 1965, Pluvial Lake Palomas, northwestern Chihuahua, Mexico, and Pleistocene geologic history of south-central New Mexico: New Mexico Geological Society Guidebook 16, p. 199-203. **(C2a, F3, I2, I3)**
Reeves, C.C., Jr., 1969, Pluvial Lake Palomas, northwestern Chihuahua, Mexico: New Mexico Geological Society Guidebook 20, p. 143-154. **(C2a, C4, F3, I2, I3)**
Reeves, C.C., Jr., and DeHon, R.A., 1965. Geology of Potrillo maar, New Mexico and northern Chihuahua, Mexico: American Journal of Science, v. 263, p. 401-409. **(C2a, F1)**
Reheis, M.C., Goodmacher, J.C., Harden, J.W., McFadden, L.D., Rockwell, T.K., Shroba, R.R., Sowers, J.M., and Taylor, E.M., 1995, Quaternary soils and dust deposition in southern Nevada and California: Geological Society of America Bulletin, v. 107, p. 1003-1022. **(C3)**
Reisen, M., 2020, Wall goes up along NM border – Neighbors see both side of structure: Albuquerque Journal, Sunday, October 11, 2020, p. A1, A9. **(A3)**
Reisen, M., 2021, Border wall comes to a halt – Immigrant advocate hail Biden's swift action: Albuquerque Journal, Sunday, January 31, 2021, p. A1, A4 and A5. **(A3)**
Reisner, M., 1993, Cadillac desert: The American West and its disappearing water (revised and updated edition): New York, Penguin Books, 592 p. **(A2, B3, C1)**
Reiter, M., and Barroll, M.W., 1990, High heat flow in the Jornada del Muerto: A region of crustal thinning in the Rio Grande rift without upper crustal extension: Tectonophysics, v. 174, p. 183-195. **(C4)**
Reiter, M., and Wade, S.C., 1994, A hydrothermal study to estimate vertical groundwater flow in the Canutillo Well Field, between Las Cruces and El Paso: New Mexico Water Resources Research Institute Report No. 282 https://nmwrri.nmsu.edu/publications/technical-reports/tr-reports/tr-282.html **(C4, H3)**
Reiter, M., Shearer, C., and Edwards, C.L., 1978, Geothermal anomalies along the Rio Grande rift in New Mexico: Geology, v. 6, no. 2, p. 85-88. **(C4)**
Reiter, M., Edwards, C.L., Hartman, H., and Weidman, C., 1975, Terrestrial heat flow along the Rio Grande rift, New Mexico and southern Colorado: Geological Society of America, Bulletin, v. 86, no. 2, p. 811-818. **(C4)**
Reiter, M., Edwards, C.L., Mansure, A.J., and Shearer, C., 1978, Heat-flow data and major geologic features along the Rio Grande rift in New Mexico, *in* Guidebook to Rio Grande rift in New Mexico and Colorado: New Mexico Bureau of Mines and Mineral Resources, Circular 163, p. 234. **(C4)**

Respasch, M., Karlstrom, K., Heizler, M., and Pecha, M., 2017, Birth and evolution of the Rio Grande fluvial system in the past 8 Ma: Progressive downward integration and the influence of tectonics, volcanism, and climate: Earth-Science Reviews, v. 168, p. 113–164. **(C2b, I3)**

Reyes Cortés, I.A., 1992, Geología de Chihuahua, *in* Márquez-Alameda, A., Coordinador del volumen, 1992, Historía general de Chihuahua I – Geología, geografía y arqueología: Universidad Autónoma de Ciudad Juárez y Gobierno del Estado Chihuahua, p. 45-101. **(C2b, F3)**

Richardson, G.B., 1909, Description of the El Paso quadrangle, Texas: U.S. Geological Survey Geological Atlas, El Paso folio, ser. no. 116, 11 p. **(G1)**

Richardson, G.L., Gebbard, T.G., Jr., and Brutsaert, W.F., 1972, Water-table investigation in the Mesilla Valley: Las Cruces, New Mexico State University, Engineering Experiment Station Technical Report 76, 206 p. **(H3)**

Ricketts, J.W., Amato, J.M., and Gavel, M.M. 2021, The origin and tectonic significance of the Basin and Range – Rio Grande rift boundary in southern New Mexico, USA: GSA Today, v. 31, no. 10, p. 4-10. **(C2b, C4)**

Ríos, A.Á., 1999, Capirotada: A Nogales memoir: University of New Mexico Press, 145 p. ISBN 0-8263-20093-7 **(A2, B3)**

Rioux, M., Farmer, G.L., Bowring, S.A., Wooton, K.M., Amato, J.M., Coleman, D.S., and Verplanck, P., 2016, The link between volcanism and plutonism in epizonal magma systems: High-precision U-Pb geochronology from the Organ Mountains caldera and batholith: New Mexico: Contributions to Mineralogy and Petrology, v. 171, p. 1-22. **(C2b)**

Risser, D.W., 1988, Simulated water-level and water-quality changes in the bolson-fill aquifer, Post Headquarters Area, White Sands Missile Range, New Mexico: U.S. Geological Survey Water-Resources Investigations Report 87- 4152, 71 p. **(H1, H2)**

Rivera, A., 2021a, Knowledge capsules on TBA − Transboundary Aquifer -vs- Transboundary Groundwater; Transboundary zoning: to zone or not to zone, and Sustainable use of groundwater within a transboundary aquifer context: IAHG-TBA Commission Newsletter; v. 2, issue 1, p. 10-11 **(D1, E3)**

Rivera, A., 2021b, What should we manage, aquifers or groundwater? Guest Editorial: Groundwater, v. 59, issue 5, p. 2. **(D1, E3)**

Robertson, A.J., Matherne, A-M, Pepin, J.D., Ritchie, A.B., Sweetkind, D.S., Teeple, A.P., Granados-Olivas, A., García-Vásquez, A.M., Carroll, K.C., Fuchs, E.H. Fuchs, and Galanter, A.E., 2022, Mesilla/Conejos-Médanos Basin: U.S.-Mexico Transboundary Water Resources: Water, v. 14, article 134, 36 p. (**F1**)

Robinson, W., 1970, Ft. Wingate tree-ring sequence (NM031). **(B2, B3, C1)**

Robinson-Avila, K., 2020a, Race to carbon-free generation is on – NM utilities are making plans for wholesale energy transition: Albuquerque Journal–BUSINESS OUTLOOK: Charging ahead–THE FUTURE OF ENERGY, Monday, February 10, 2020, p. 12-15. **(A3)**

Robinson-Avila, K., 2020b, NM gas production up significantly: Albuquerque Journal–BUSINESS OUTLOOK: Charging ahead – THE FUTURE OF ENERGY, Monday, February 10, 2020, p. 18-23. **(A3)**

Robinson-Avila, K., 2020c, Bringing NM's grid into the 21st Century – Bill provides tools for planning, financing grid update: Albuquerque Journal–BUSINESS OUTLOOK, Monday, March 2, 2020, p. 4-5. **(A3)**

Robinson-Avila, K., 2020d, Coronavirus could threaten NM trade – Border companies stock up on inventory, monitor virus spread: Albuquerque Journal, Saturday, March 7, 2020, p. A1, A6. **(A3)**

Robinson-Avila, K., 2020e, Electric Rise in Wind, Solar – NM striding to 2020 renewable energy goal of 20% with several new projects on tap or online: Albuquerque Journal–BUSINESS OUTLOOK, Monday, June, 2020, p. 10-11. **(A3)**

Robinson-Avila, K., 2020f, More firms are setting up shop at Santa Teresa: Albuquerque Journal–BUSINESS OUTLOOK: Charging ahead – THE FUTURE OF ENERGY, p. A9-A24, Monday, September 14, 2020, p. 10-13. **(A3)**

Robinson-Avila, K., 2020g, Trade with Mexico up as Asia, Europe falters: Albuquerque Journal–BUSINESS OUTLOOK: Charging ahead – THE FUTURE OF ENERGY, p. A9-A24, Monday, September 14, 2020, p. 11-14. **(A3)**

Robinson-Avila, K., 2020h, Rise in Wind, Solar – NM leaders look to build a renewable grid that's resilient too: Albuquerque Journal–BUSINESS OUTLOOK, Monday, November 9, 2020, p. 10-11. **(A3)**

Robinson-Avila, K., 2021a, Confronting the climate crisis – NM, US poised for a sea change in policy, massive mobilization: Albuquerque Journal–BUSINESS OUTLOOK, Monday, January 11, 2021, p. 11-13. **(A3)**

Robinson-Avila, K., 2021b, Biden expected to pursue ambitious climate agenda: Albuquerque Journal–BUSINESS OUTLOOK, Monday, January 11, 2021, p. 11, 13. **(A3)**

Robinson-Avila, K., 2021c, NMSU powers up with clean energy – Power system a 'living lab:' Albuquerque Journal, Monday, October 18, 2021, p. A1-A2. See *Polich, J., 2021, Is blue hydrogen the bridge to a greener future?* **(A3)**

Robinson-Avila, K., 2021d, Santa Teresa ignites Border economy – NMSU study shows $1.1B annual impact, nearly 6,000 jobs: Albuquerque Journal–BUSINESS OUTLOOK, Monday, November 15, 2021, p. 10-13. **(A3)**

Robinson-Avila, K., 2021e, BayoTech's first production hub to be located in Albuquerque – Local startup built world's initial compact hydrogen generator: Albuquerque Journal, Saturday, December 4, 2021, p. A1, A8. See *Norvelle (2021), and Polich (2021).* **(A3)**

Robinson-Avila, K., 2022a, Hydrogen at the forefront – State is front and center in nationwide debate on pros and cons of hydrogen: Albuquerque Journal–BUSINESS OUTLOOK, Monday, January 17, 2022, p. 10-14. **(A3)**

Robinson-Avila, K., 2022b, Hydrogen-based aviation takes off **-** Company will build factory at the Sunport, employ 500: Albuquerque Journal, Friday, March 11, 2022, p. A1, A6. **(A3)**

Robinson-Avila, K., 2022c, Border boom pushes record NM exports to $5.4 billion – Last year, state hit a new annual high in global sales, exports to Mexico: Albuquerque Journal, Thursday March 24, 2022, p. A1, A3 **(A3)**

Robinson-Avila, K., 2022d, Trade dispute threatens NM solar markets – Projects canceled, prices jumping, thousands of jobs are at stake: Albuquerque Journal, Tuesday, April 19, 2022, p. A1, A4. **(A3)**

Robinson-Avila, K., 2022e, Heinrich leads charge to end solar trade debate – Petition for new tariffs on some Asian imports could lead to US layoffs: Albuquerque Journal, Thursday, April 21, 2022, p. A1, A5. **(A3)**

Robinson-Avila, K., 2022f, Solar industry in crisis over US trade dispute – NM sees layoffs, cancelled projects over US trade dispute: Albuquerque Journal, Thursday, May 12, 2022, p. A1, A3. **(A3)**

Robinson-Avila, K., 2022g, Dispute threatened PNM power supplies – Solar project delays worsen shortage estimates for summer 2023: Albuquerque Journal, Thursday, May 12, 2022, p. A1, A3. **(A3)**

Robinson-Avila, K., 2023a, Digging into NM's geothermal potential – Tax breaks, grants and loans are proposed to encourage use of this hot new technology: Albuquerque Journal, Wednesday, January 18, 2023, p. A6. **(A3)**

Robinson-Avila, K., 2023b, Geothermal makeovers could gain ground in New Mexico – UNM and other institutions consider technology to heat, cool campus buildings: Albuquerque Journal, Monday, January 31, 2023, p. A1, A7. **(A3)**

Robinson-Avila, K., 2023c, On the Cusp of a Geothermal Renaissance – New technology unlocks massive geothermal energy potential, including in New Mexico: Albuquerque Journal–BUSINESS OUTLOOK, Monday, January 31, 2023, p. 10-12, 14. **(A3)**

Robinson-Avila, K., 2023d, Sandia pumping up geothermal research: Albuquerque Journal–BUSINESS OUTLOOK, Monday, January 31, 2023, p. 11, 13. **(A3)**

Robinson-Avila, K., and Narvaiz, M., 2023, Autoparts maker coming to NM – Hota Industrial Manufacturing to build new factory at Santa Teresa: Albuquerque Journal, Wednesday, July 5, 2023, p. A1, A8. **(A3)**

Robinson-Avila, K., and Villagran, L., 2014, Santa Teresa catching fire – Companies flock to border industrial parks as Union Pacific opens massive transshipment station, *in* Boom on the Border: Albuquerque Journal, Monday, April 14, 2014, p. A1, A8. **(A3)**

Romero, V., 2023, Harnessing power of hydrogen critical to state's energy transition: Albuquerque Journal–OPINION, Friday, July 21, 2023, p. A9. **(A3, E2)**

Rosholt, J.N., Coleman, S.M., Stuiver, M., Damon, P.E., Naeser, C.W., Naeser, N.D., Szabo, B.J., Muhs, D.R., Liddicoat, J.C., Forman, S.L., Machette, M.N., and Pierce, K.L., 1991, Dating methods applicable to the Quaternary, *in* Morrison, R.B., ed., Quaternary non-glacial geology; Conterminous U.S.: Boulder, CO, Geological Society of America, The Geology of North America, v. K-2, p. 45-74. **(B1)**

Ross, H.P., and Witcher, J.C., 1998, Self-potential surveys of three geothermal areas in the southern Rio Grande rift, New Mexico: New Mexico Geological Society Guidebook 49, p. 93-100. **(C4)**

Ross, I., Kalve, E., McDonough, J., Hurst, J., Miles, J., and Pancras, T., 2019, *in* Bell, C.H., Gentile, M., Kalve, E., Ross, I., Horst, J., and Suthersan, S., eds., Per- and polyfluoroalkyl substances: Boca Raton, FL, CRC Press, p. 85-257. *See USEPA 2019.* **(E2c)**

Rugeley, T., 2020, Epic Mexico: A History from Earliest Times: University of Oklahoma Press, 270 p. ISBN-13: 978-0806167077 **(B2, B3)**

Ruhe, R.V., 1962, Age of the Rio Grande Valley in southern New Mexico, Journal of Geology, v. 70, p. 151-167. **(C2a)**

Ruhe, R.V., 1964, Landscape morphology and alluvial deposits in southern New Mexico: Annals of the Association of American Geographers, v. 54, p. 147-159. **(C2a, C3)**
Ruhe, R.V., 1967, Geomorphic surfaces and surficial deposits in southern New Mexico: New Mexico Bureau of Mines and Mineral Resources, Memoir 18, 65 p. **(C2a, C3)**
Ruleman, C.A., Hudson, A.M., Thompson, R.A., Miggins, D.P., Paces, J.B., and Goerhring, B.M., 2019, Middle Pleistocene formation of the Rio Grande Gorge, San Luis Valle, south-central Colorado and north-central New Mexico, USA: Process, timing, and downstream implications: Quaternary Science Reviews, v. 223, no. 105846, p. 1-48. **(I3)**
Ryder, P.D., 1996, Ground water atlas of the United States – Segment 4, Oklahoma, Texas: U.S. Geological Survey Hydrologic Investigations Atlas 730-E, 20 p. **(D1)**
Sálaz Márquez, R.D., 2004, Epic of the Greater Southwest: New Mexico · Texas · California · Arizona · Oklahoma · Colorado · Utah · Nevada: Box 10515, Alameda, NM 87184, Cosmic House, 620 p. ISBN 0-932492-06-1 **(A2, B3)**
Sanchez, R., Rodriguez, L., and Tortajada, C., 2018, Transboundary aquifers between Chihuahua, Coahuila, Nuevo Leon and Tamaulipas, Mexico, and Texas, USA: Identification and categorization, *in* Rivera, A. and Candela, L., eds., Special Issue on International Shared Aquifer Resources Assessment and Management: Journal of Hydrology: Regional Studies, v. 20, p. 74-102. **(E3, F1)**
Sanford, W.E., Plummer, L.N., McAda, D.P., Bexfield, L.M., and, Anderholm, S.K., 2004, Hydrochemical tracers in the Middle Rio Grande basin, USA: 2. Calibration of a groundwater-flow model: Hydrogeology Journal, v. 12, no. 4, p. 389-407. **(H2, H3)**
Sarna-Wojcicki, A.M., and Davis, J.O., 1991, Quaternary tephrochronology, *in* Morrison, R.B., ed., Quaternary non-glacial geology; Conterminous U.S.: Boulder, CO, Geological Society of America, The Geology of North America, v. K-2, p. 93-116. **(B1, C2b)**
Sayre, A.N., and Livingston, P., 1945, Ground-water resources of the El Paso area, Texas: U.S. Geological Survey Water-Supply Paper 919, 190 p. **(D1, F2, G2)**
Scanlon, B.R., 2004, Evaluation of methods of estimating recharge in semiarid and arid regions in the southwestern U.S., *in* Hogan, J.E., Phillips, F.M., and Scanlon, B.R., eds., Groundwater recharge in a desert environment: the southwestern United States: Washington, DC, American Geophysical Union, Water Science and Application 9, p. 235-254. **(D2)**
Schmid, W., King, J.P., and Maddock, T.M. III, 2009, Conjunctive surface-water/groundwater model in the southern Rincon Valley using MODFLOW-2005 with the Farm Process: New Mexico Water Resources Research Institute and Texas Water Resources Institute Report 350, 53 p. https://nmwrri.nmsu.edu/publications/technical-reports/tr-reports/tr-350.html **(H3)**
Schmidt, R.H., Jr., 1973, A geographical survey of Chihuahua: El Paso, Texas Western Press (UTEP), Southwestern Studies Monograph No. 37, 63 p. **(C1, C2a, F3)**
Schmidt, R.H., Jr., 1979, A climatic delineation of the "real" Chihuahuan Desert region: Phytologia, v. 44, p. 129-133 **(C1, F1)**
Schmidt, R.H., 1992, Chihuahua, tierra de contrastas geográficos: Geografía, *in* Márquez-Alameda, A., Coordinador del volumen, 1992, Historía general de Chihuahua I – Geología, geografía y arqueología: Universidad Autónoma de Ciudad Juárez y Gobierno del Estado Chihuahua, p. 45-101. **(C2b, F3)**
Schmidt, R.H., Jr., and Marston, R.A., 1981, Los Medanos de Samalayuca, Chihuahua, Mexico: New Mexico Journal of Science, v. 21, no. 2, p. 21-27. **(C2a, F3)**
Scholle, P.A., Ulmer-Scholle, D.S., Cather, S.M., and Kelley, S.A., eds., 2020, The Geology of Southern New Mexico's Parks, Monuments, and Public Lands: New Mexico Bureau of Geology and Mineral Resources, 404 p. **(C2b)**
Schumm, S.A., 1965, Quaternary paleohydrology, *in* Wright, H.E., Jr. and Frey, D.C., eds., The Quaternary of the United States: Princeton University Press, p. 783-794. **(C, D1)**
Schumm, S.A., 1968, Speculations concerning paleohydrologic controls on terrestrial sedimentation: Geological Society of America Bulletin, v. 79, p. 1573-1588. **(C, D1)**
Schumm, S.A., 1977, The fluvial system: New York, John Wiley and Sons-Interscience, 338 p. **(A2, D1)**
Schwennesen, A.T., 1918, Ground water in the Animas, Playas, Hachita, and San Luis Basins, New Mexico: U.S. Geological Survey Water-Supply Paper 422, 152 p. **(D1, F2, G1, I2)**
Scurlock, D., 1998, From the Rio to the Sierra: An environmental history of the Middle Rio Grande basin: U.S. Department of Agriculture, Rocky Mountain Research Station, Forest Service General Technical Report, RMRS-GTR-5, 440 p. **(B3, C1)**

Seager, R., Ting, M., Held, I., Kushnir, Y., Lu, J., Vecchi, G., Huang, H-P., Harnik, N., Leetmaa, A., Lau, N-C., Li, C., Velez, J., and Naik, N., 2007, Model Projections of an Imminent Transition to a More Arid Climate in Southwestern North America: Science, v. 316, issue 5828, p. 1181-1184. **(C1)**
Seager, W. R., 1975a, Cenozoic tectonic evolution of the Las Cruces area, New Mexico: New Mexico Geological Society, Guidebook 26, p. 241-250. **(C2a)**
Seager, W.R., 1975b, Geologic map and sections of south half of San Diego Mountain quadrangle, New Mexico: New Mexico Bureau of Mines and Mineral Resources, Geologic Map 35, scale 1:62,500. **(C2a)**
Seager, W.R., 1981, Geology of the Organ Mountains and southern San Andres Mountains, New Mexico: New Mexico Bureau of Mines and Mineral Resources, Memoir 36, 97 p. **(C2a)**
Seager, W.R., 1987, Caldera-like collapse at Kilbourne Hole Maar, New Mexico: New Mexico Geology, v. 9, no. 4, p. 69-73. **(C2a)**
Seager, W.R., 1989, Geology beneath and around the West Portrillo basalts, Doña Ana and Luna Counties, New Mexico: New Mexico Geology, v. 11, no. 3, p. 53-59. **(C2a)**
Seager, W.R., 1990, Eagle nest-Granite Hill area, Luna County, New Mexico – A new look at some old rocks: New Mexico Geology, v. 12, no. 1, p. 1-7 and 19. **(C2b)**
Seager, B. [W.R.], 1994, Russell E. Clemons, 1930-1994: New Mexico Geology, v. 16, no. 4, p. 78 **(A2)**
Seager, W.R., 1995, Geology of southwest quarter of Las Cruces and northwest El Paso 1º x 2º sheets: New Mexico Bureau of Mines and Mineral Resources, Geologic Map 60, scale 1:125,000. **(C2b, C4)**
Seager, W.R., 2004, Laramide (late Cretaceous to Eocene) tectonics of southwestern New Mexico, *in* Mack, G.H., and Giles, K.J., eds., The Geology of New Mexico: A geologic history: New Mexico Geological Society, Special Publication 11, p. 183-202. **(C2b)**
Seager, W.R., and Clemons, R.E., 1975, Middle to late Tertiary geology of the Cedar Hills-Selden Hills area, New Mexico: New Mexico Bureau of Mines and Mineral Resources, Circular 133, 24 p. **(C2a)**
Seager, W.R., and Hawley, J.W., 1973, Geology of Rincon quadrangle, New Mexico: New Mexico Bureau of Mines and Mineral Resources, Bulletin 101, 56 p., map scale 1:24,000. **(C2a)**
Seager, W.R., and Hawley, J.W., 1987, Geologic sections and gravity profiles through the east half of Las Cruces and northeast El Paso 1º x 2º sheets, New Mexico, *in* Seager, W.R., Hawley, J.W., Kottlowski, F.E. and Kelley, S.A., Geology of east half of Las Cruces and northeast El Paso 1º x 2º sheets, New Mexico: New Mexico Bureau of Mines and Mineral Resources, Geologic Map 57, scale 1:125,000. **(C2a, C4)**
Seager, W.R., and Mack, G.H., 1991, Geology of Garfield Quadrangle, Sierra and Doña Ana Counties, New Mexico: New Mexico Bureau of Mines and Mineral Resources, Bulletin 128, 27 p., map scale 1:24,000. **(C2b)**
Seager, W.R., and Mack, G.H., 1994, Geology of the East Potrillo Mountains and vicinity, Doña Ana County, New Mexico: New Mexico Bureau of Mines and Mineral Resources, Bulletin 113, 27 p. **(C2b)**
Seager, W.R., and Mack, G.H., 2018, Geology of the Doña Ana Mountains, south-central New Mexico: A summary: N.M. Geological Society, Guidebook 69, p. 71-81. **(C2b)**
Seager, W.R., and Morgan, P., 1978a, Stop S3, Leasburg Dam-Radium Springs overlook discussion, *in* Hawley, J.W., and Seager, W.R., 1978, New Mexico-Texas State Line to Elephant Butte Reservoir – Guidebook to Rio Grande Rift in New Mexico and Colorado: New Mexico Bureau of Mines & Mineral Resources, Circular 163, p. 75-78. **(C2a, C4)**
Seager, W.R., and Morgan, P., 1978b, Stop S5, San Diego [Tonuco] Mountain discussion, *in* Hawley, J.W., and Seager, W.R., 1978, New Mexico-Texas State Line to Elephant Butte Reservoir – Guidebook to Rio Grande Rift in New Mexico and Colorado: New Mexico Bureau of Mines & Mineral Resources Circular 163, p. 82-83. **(C2a, C4)**
Seager, W.R., and Morgan, P., 1979, Rio Grande rift in southern New Mexico, west Texas and northern Chihuahua, *in* Riecker, R.E., ed., Rio Grande rift, tectonics and magmatism: Washington D.C., American Geophysical Union, p. 87-106. **(C2a, C4)**
Seager, W.R., Clemons, R.E., and Hawley, J.W., 1975, Geology of Sierra Alta Quadrangle, Doña Ana County, New Mexico, New Mexico Bureau of Mines and Mineral Resources, Bulletin 102, 56 p., map scale 1:24,000. **(C2a)**
Seager, W.R., Hawley, J.W., and Clemons, R.E., 1971, Geology of San Diego Mountain area, Doña Ana County, New Mexico: New Mexico Bureau of Mines and Mineral Resources, Bulletin 97, 38 p., map scale 1:24,000. **(C2)**

Seager, W.R., Hawley, J.W., and Mack, G.H., 2015 [1995 revision], Geologic map of Hatch 7.5-minute quadrangle, Doña Ana County, New Mexico: New Mexico Bureau of Mines and Mineral Resources, Open-File Geologic Map 213, scale 1:24,000. CD-ROM. http://geoinfo.nmt.edu/publications/maps/geologic/ofgm/ **(C2b)**

Seager, W.R., Kottlowski, F.E., and Hawley, J.W., 1976, Geology of Doña Ana Mountains, New Mexico: New Mexico Bureau of Mines and Mineral Resources, Circular 147, 36 p., 2 tables, 13 figs., 3 sheets, scale 1:24,000. **(C2a)**

Seager, W.R., Kottlowski, F.E., and Hawley, J.W., 2008, Geologic Map of the Robledo Mountains and vicinity, Doña Ana County, New Mexico: New Mexico Bureau of Mines and Mineral Resources, Open-File Report 509, scale 1:24,000, CD-ROM. http://geoinfo.nmt.edu/publications/maps/geologic/ofgm/ **(C2b)**

Seager, W.R., Mack, G.H., and Lawton, T.F., 1997, Structural kinematics and depositional history of a Laramide uplift-basin pair in southern New Mexico: Implications for development of intraforeland basins: Geological Society of America Bulletin, v. 107, p. 1389-1401. **(C2b)**

Seager, W.R., Thacker, J.O., and Kelley, S.A., 2021, Geologic map of the Selden Canyon 7.5 minute quadrangle, Doña Ana County, New Mexico: New Mexico Bureau of Geology and Mineral Resources Open-File Geologic Map OF-GM-290, scale 1:24,000. **(C2b)**

Seager, W.R., Clemons, R.E., Hawley, J.W., and Kelley, R.E., 1982, Geology of northwest part of Las Cruces 1º x 2º sheet, New Mexico: New Mexico Bureau of Mines and Mineral Resources Geologic Map, GM-53, scale 1:125,000, 3 sheets. **(C2a)**

Seager, W.R., Hawley, J.W., Kottlowski, F.E., and Kelley, S.A., 1987, Geologic map of east half of Las Cruces and northeast El Paso 1º x 2º sheets, New Mexico: New Mexico Bureau of Mines and Mineral Resources, Geologic Map, GM-57, scale 1:125,000, 3 sheets. **(C2a)**

Seager, W.R., Kelley, S.A., Thacker, J.O., and Kelley, R.E., 2023, San Diego Mountain: A "Rosetta Stone" for Interpreting the Cenozoic Tectonic Evolution of South-Central New Mexico: New Mexico Geology, v. 44, no. 2, p. 23-62. **(C2b, I3)**

Seager, W.R., Mack, G.H., Raimonde, M.S., and Ryan, R.G., 1986, Laramide basement-cored uplift and basins in south-central New Mexico: New Mexico Geological Society Guidebook 37, p. 123-130. **(C2a)**

Seager, W.R., Shafiqullah, M., Hawley, J.W., and Marvin, R.F., 1984, New K-Ar dates from basalts and the evolution of the southern Rio Grande: Geological Society of America Bulletin, v. 95, no. 1, p. 87-99. **(C2a, I3)**

Secretaria de Programación y Presupuesto (SPP), 1981, Carta Hidrológica: Aguas Subterráneas, Chihuahua: Escala 1:1,000,000. **(F3)**

Secretaria de Agricultura y Recursos Hidráulicos (SARH), 1988, Resultados de las perforaciones por la S.A.R.H. en la zona de Conejos Médanos, Chihuahua – Programa de exploración: SARH Departamento de Aguas del Subsuelo, Anexos 2 y 3. *See Gutiérrez-Ojeda 2001, p. 26*. **(F3, H1)**

Self, S., Heiken, G., Sykes, M.L., Wohletz, K., Fisher, R.V., and Dethier, D.P., 1996, Field excursions to the Jemez Mountains, New Mexico: New Mexico Bureau of Mines and Mineral Resources, Bulletin 134, 72 p. **(B1, C2b)**

Servicio Geológico Mexicano (SGM), 2011, Hydrogeological activities in the Conejos-Médanos aquifer, State of Chihuahua, Phase I: Servicio Geológico Mexicano, v. 1, 109 p. **(F3, H1)**

Sharp, J.M., Jr., 2001, Regional groundwater flow systems in basins in Trans-Pecos Texas, *in* Mace, R.E., Mullican, W.F. III, and Angle, E.S., eds., Aquifers of West Texas: Austin, Texas Water Development Board Report 356, p. 66-75. **(D1, D2)**

Sheng, Z., 2005, An aquifer storage and recovery system with reclaimed wastewater to preserve native groundwater resources in El Paso, Texas: Journal of Environmental Management, v. 75, issue 4, p. 367-377. (**E2b, E2c**)

Sheng, Z., 2013, Impacts of groundwater pumping and climate variability on groundwater availability in the Rio Grande Basin: Ecosphere, v. 4, no. 1, p. 1-25. **(E2, F1, H3)**

Sheng, Z., and Devere, J., 2005, Understanding and managing the stressed Mexico-USA transboundary aquifer in the Hueco bolson aquifer in the El Paso del Norte region as a complex system: Hydrogeology Journal, v. 13, no. 5-6, p. 813-825. **(E2, F1)**

Sheng, Z., and Helm, D.C., 1994, Displacement discontinuity modeling of fissuring caused by ground-water withdrawal, *in* Siriwardane, H.J., and Zaman, M.M., eds., Proceedings of the 8th International Conference on Computer Methods and Advances in Geomechanics, Morgantown, WV, USA: Rotterdam, Netherlands, A.A. Balkema, p. 1263-1268. **(D1)**

Sheng, Z., Helm, D.C., and Li, J., 2003, Mechanisms of earth fissuring caused by groundwater withdrawal: Journal of Environmental Geosciences, v. 9, no. 4, p. 313-324. **(D1)**

Sheng, Z., Darr, M., King, J.P., Bumgarner, J., and Michelsen, A., 2013, Mesilla Basin/Conejos-Médanos section of the Transboundary Aquifer Assessment Program, *in* Alley, W.M., ed., Five-year interim report of the United States-Mexico Transboundary Aquifer Assessment Program: 2007-2012: U.S. Geological Survey Open-File Report 2013-1059, 31 p. (**D1, F1**)

Shomaker, J.W., and Finch, S.T., Jr., 1996, Multilayer ground-water flow model of southern Jornada del Muerto Basin, Doña Ana County, New Mexico, and predicted effects of pumping wells LRG-430-S-29 and -S-30. Albuquerque, New Mexico: John Shomaker & Associates, Inc., 26 p., 5 tables, 20 figures. **(H3)**

Siegel, D., 2008, Reductionist hydrogeology: ten fundamental principles: Hydrological Processes, v. 22, p. 4967-4970. **(D1)**

Siegel, D.J., 2020, The future of geoscience in the context of emerging climate disruption: GSA Today, v. 30, no. 2, p. 4-5. **(B3, C1**, **D1)**

Siegel, D.J., and Hinchey, E.J., 2019, Big data and the curse of scale: Groundwater, v. 57, no. 4, p. 505. **(D1)**

Sinno, Y.A., Daggett, P.H., Keller, G.R., Morgan, P., and Harder, S.H., 1986, Crustal structure of the southern Rio Grande rift determined from seismic refraction profiling: Journal of Geophysical Research, v. 91, p. 6,143-6,156. **(C2a, C4)**

Slichter, C.S., 1905b, Observations on ground waters of the Rio Grande valley: U.S. Geological Survey Water-Supply and Irrigation Paper 141, 83 p. **(G1)**

Smiley, T.L., Bryson, R.A., King, J.E., Kukla, G.J., and Smith, G.I., 1991, Quaternary paleoclimates, *in* Morrison, R.B., ed., Quaternary non-glacial geology; Conterminous U.S.: Boulder, CO, Geological Society of America, The Geology of North America, v. K-2, p. 13-44. **(B2, C1)**

Smith, G.A., 1994, Climatic influences on continental deposition during late-stage filling of an extensional basin, southeastern Arizona: Geological Society of America Bulletin, v. 106, p. 1212-1228. **(B1, C1, C2b)**

Smith, G.A., 2000, Recognition and significance of streamflow-dominated piedmont facies in extensional basins: Basin Research, v. 12, p. 399-411. **(D1)**

Smith, G.A., Wang, Y., Cerling, T.E., and Geissman, J.W., 1993, Comparison of a paleosol-carbonate isotope record to other records of Pliocene-early Pleistocene climate in the western United States: Geology, v. 21, p. 691-694. **(C1, C2b)**

Smith, G.I., 1966, Geology of Searles Lake – A guide to prospecting for buried continental salines, *in* Second Symposium on Salt, Cleveland, Northern Ohio Geological Society, p. 167-180. **(D1**, **I1)**

Smith, G.I., and Street-Perrott, F.A., 1983, Pluvial lakes of the western United States, *in* Porter, S.C., ed., Late Quaternary environments of the United States, volume 1, The Late Pleistocene: University of Minnesota Press, p. 190-212. **(B2, C1, I1)**

Smith, M., 2021, Christmas Eve on the Border – Santa Fe resident finds kindness among officers on both sides: Albuquerque Journal–OPINION–EDITORIAL, Sunday, January 3, 2021, p. A13. **(A3)**

Snyder, J.T., 1986, Heat flow in the southern Mesilla Basin, with an analysis of East Potrillo geothermal system, Doña Ana County, New Mexico: New Mexico State University, master's thesis, 252 p. **(C4, F2, H1)**

Sociedad Geológico Mexicana, A.C. (SGM), 1985, Plano geológico minero, Chihuahua, Mexico: Sociedad Geológico Mexicana, A.C., Delegación Chihuahua, Escala 1:500,000. **(C2a**, **F3)**

Sonnichsen, C.L., 1968, Pass of the North, four centuries on the Rio Grande: The University of Texas at El Paso, Texas Western Press, 469 p. *See comments on **EPdN** reach on pp.14-17, 29, 79, 89-91,106-107,132,135-136,147,262, 282-284.* **(A2, B3)**

Spagat, E., 2020, Contracting laws for Border Wall will be waived – Homeland Security says move will speed construction: Albuquerque Journal–METRO & NM, Wednesday, February 19, 2020, p. A7-A8. **(A3)**

Spagat, E., 2021, Biden halts Border Wall building after Trump's final surge: Albuquerque Journal–NATION, Friday, January 22, 2021, p. A3. **(A3)**

Spaulding, W.G., and Graumlich, L.J., 1986, The last pluvial climatic episode of southwestern North America: Nature, v. 320, p. 441-444. **(B2, C1)**

Spaulding, W.G., Leopold, E.B., and Van Devender, T.R., 1983, Late Wisconsin paleoecology of the American Southwest, *in* Porter, S.C., ed., Late Quaternary Environments of the United States, volume 1, The Late Pleistocene: University of Minnesota Press, p. 259-293. **(B2, C1)**

S.S. Papadopulos & Associates, Inc. (SSPA), 1987, Hydrogeologic evaluation of proposed appropriation of ground water from the Lower Rio Grande Underground Basin by the City of El Paso: S.S. Papadopulos & Associates, Inc., main report prepared for the State of New Mexico, variously paged. **(H1, H3)**

SSURGO, 2002/2003: Soil Survey Geographic Database of the National Resources Conservation Service (NRCS) for Doña Ana County, provided by the Elephant Butte Irrigation District. **(C3)**

Stanton, J.S., Anning, D.W., Brown, C.J., Moore, R.B., McGuire, V.L., Qi, S.L., Harris, A.C., Dennehy, K.F., McMahon, P.B., Degnan, J.R., and Böhlke, J.K., 2017, Brackish groundwater in the United States: U.S. Geological Survey Professional Paper 1833, 185 p. **(D1, E2a)**

Stein, R., Kanamatsu, T., Alvarez-Zarikian, C., Higgins, S.M., Channell, J.E.T., Aboud, E., Ohno, M., Acton, G.D., Akimoto, K., Bailey, I., Bjørklund, K.R., Evans, H., Nielsen, S.H.H., Fang, N., Ferretti, P., Gruetzner, J., Guyodo, Y.J.B., Hagino, K., Harris, R., Hatakeda, K., Hefter, J., Judge, S.A., Kulhanek, D.K., Nanayama, F., Rashid, H., Sierro Sanchez, F.J., Voelker, A., and Zhai, Q., 2006, North Atlantic Paleoceanography: The Last Five Million Years: Eos Transactions American Geophysical Union, v. 87, issue 13, p. 129-133. **(B1, B2, C1)**

Steiner, F.R., Weller, R., M'Closkey, K., and Fleming, B., eds., 2019, Design with nature now: Cambridge, MA, Lincoln School for Land Policy – Columbia University Press, 368 p. ISBN: 9781558443938. *See McHarg 1969 and* https://mcharg.upenn.edu/what-does-it-mean-design-nature-now-0 **(A2, E2)**

Stevenson, M., ASSOCIATED PRESS, 2022, Mexico favors NM over Texas – Rail link moved to Santa Teresa: Albuquerque Journal–BUSINESS, Wednesday, May 4, 2022, *See Lee, M., 2022.* p. A11. (**A3**)

Stewart, J.H., 1971, Basin and Range structure, a system of horsts and grabens produced by deep-seated extension: Geological Society of America, Bulletin, v. 82, p. 1019-1044. **(C2a)**

Stewart, J.H., 1998, Regional characteristics, tilt domains, and extensional history of the late Cenozoic Basin and Range province, western North America: Geological Society of America, Special Paper 323, p. 47-74. **(C2b)**

Stockton, C.W., 1990, Climatic, hydrologic, and water-supply inferences from tree rings: Civil Engineering Practice, p. 37-52. **(B3, C1, D1)**

Stockton, C.W., Quinlan, P.T., and Boggess, W.R., 1983, Climate change and surface-water availability in the Upper Rio Grande basin, *in* Region and State Water Resources Planning and Management: American Water Resources Association, p. 311-321. **(B3, C1)**

Stonestrom, D.A., Constantz, J., Ferré, T.P.A., and Leake, S.A., eds., 2007, Ground-water recharge in the arid and semiarid southwestern United States: U.S. Geological Survey Professional Paper 1703, 414 p. **(A2, D2)**

Strain, W.S., 1966, Blancan mammalian fauna and Pleistocene formations, Hudspeth County, Texas: Texas Memorial Museum, Bulletin 10, 55 p. **(B1, C2a)**

Strain, W.S., 1969, Late Cenozoic strata of the El Paso-Juárez area: New Mexico Geological Society Guidebook 20, p. 155-157. **(C2a)**

Strain, W.S., 1971, Late Cenozoic bolson integration in the Chihuahua tectonic belt, *in* The geologic framework of the Chihuahua tectonic belt: West Texas Geological Society, Publication No. 71-59, p. 167-173. **(C2a)**

Stuart, C.J., and Willingham, D.L., 1984, Late Tertiary and Quaternary fluvial deposits in the Mesilla and Hueco bolsons, El Paso area, Texas: Sedimentary Geology, v. 38, p. 1-20. **(C2a)**

Suthersan, S., Quinnan, J., Horst, J., Ross, I., Kalve, E., Bell, C., and Pancras, T., 2016a, Making strides in management of "Emerging Contaminants," *in* Advances in Remediation Solutions: Groundwater Monitoring & Remediation, v. 36, no. 1, p. 16-25. *See Fig. 1 and USEPA 2015.* **(E2c)**

Suthersan, S., Horst, J., Ross, I., Kalve, E., Quinnan, J., Houtz, E., and Burdick, J., 2016b, Responding to "emerging contaminant" impacts: Situation managements, *in* Advances in Remediation Solutions: Groundwater Monitoring & Remediation, v. 36, no. 3, p. 22-32. **(E2c)**

Swanberg, C.A., 1975, Detection of geothermal components in ground waters of Doña Ana County, southern Rio Grande rift, New Mexico: New Mexico Geological Society Guidebook 26, p. 175-180. **(C4)**

Swanberg, C.A., 1979, Chemistry of thermal and nonthermal groundwaters in the Rio Grande rift and adjacent tectonics provinces, *in* Riecker, R.E., ed., Rio Grande rift, tectonics and magmatism: Washington D.C., American Geophysical Union, p. 279-288. **(C4)**

Sweet, A.T., and Poulson, E.N., 1933, Soil Survey of the Rincon area, New Mexico: U.S. Department of Agriculture, Bureau of Chemistry and Soils, Series 1930, no. 5, 24 p., map scale 1:63,360. *Shallow depth to water table shown in large number of soil-test borings.* **(C3, H1)**

Sweetkind, D.S., 2017, Three-dimensional hydrogeologic framework model of the Rio Grande transboundary region of New Mexico and Texas, USA, and northern Chihuahua, Mexico: U.S. Geological Survey Scientific Investigations Report 2017-5060, 49 p. **(H1)**

Sweetkind, D.S., 2018, Digital 3D geologic framework of the Las Cruces area: New Mexico Geological Society Guidebook 69, p. 60-62. **(H1)**

Sweetkind, D.S., Hanson, R.T., Ritchie, A.B., and Hawley, J.W., 2017, Data release of Three-Dimensional Hydrogeologic Framework Model of the Rio Grande Transboundary Region of New Mexico and Texas, USA and Northern Chihuahua, Mexico: U.S. Geological Survey data release. **(H1)**

Swetnam, T.W., and Betancourt, J.L., 1998, Mesoscale disturbance and ecological response to decadal climate variability in the American Southwest: Journal of Climate, v. 11, p. 3128-3147. **(B2, C1)**

Székely, A. [Ambassador], 2010, Albert E. Utton Memorial Lecture (2003): Journal of Transboundary Water Resources, v. 1, p. 189-198. https://nmwrri.nmsu.edu/publications/pub-documents/JTWR-Book.pdf **(E3, F1)**

Szynkiewicz, A., Borrok, D.M., Ganjegunte, G.K., Skrzypek, G., Ma, L., Rearick, M.S., and Perkins, G.B. 2015b, Isotopic studies of the Upper and Middle Rio Grande. Part 2- Salt loads and human impacts in south New Mexico and west Texas: Chemical Geology, v. 14, p. 336-350. **(B3, E2a)**

Taleb, N.N., 2010, The Black Swan: the impact of the highly improbable (second edition), with a new section: On robustness & fragility: New York, Random House Trade Paperbacks, 444 p. ISBN 978-0-8129-7381-5 **(A2, D1)**

Tamayo, J.L., 1968, Geografía moderna de México (Quinta edición revisada): México, D.F., Editorial F. Trillas, S.A., 382 p. *See Las regiones geomorphícas – Sierra Madre Occidental (p. 43) and Altiplanicie Septentrional (p. 52-53); Vertientes interiores endorriceicas – cuencas de las Lagunas Guzman, Santa María y Patos (p. 142-143), and Chihuahua-Potosinense Provincia biótica (p. 162).* **(A2, F3)**

Taylor, A.M., 1967, Geohydrologic investigations in the Mesilla Valley, New Mexico: New Mexico State University, master's thesis, 130 p. **(H1, H3)**

Teclaff, L.A., 1982, Principles of transboundary pollution control: Mexico-Symposium on Anticipating Transboundary Resource Needs and Issues in the U.S.-Mexico Border Region to the Year 2000: Natural Resources Journal, v. 22, p. 1065-1079. **(E2c, E3)**

Tedford, R.H., 1981, Mammalian biochronology of the late Cenozoic basins of New Mexico: Geological Society of America Bulletin, Part I, v. 92, p. 1008-1022. **(B1, C2a)**

Teeple, A.P., 2017a, Geophysics- and geochemistry-based assessment of the geochemical characteristics and groundwater-flow system of the U.S. part of the Mesilla Basin/Conejos-Médanos aquifer system in Doña Ana County, New Mexico, and El Paso County, Texas, 2010-12: U.S. Geological Survey Scientific Investigations Report 2017-5028, 183 p. **(C4, H2)**

Teeple, A.P., 2017b, Time-domain electromagnetic data used in the assessment of the U.S. part of the Mesilla Basin/Conejos-Médanos Aquifer System in Doña Ana County, New Mexico, and El Paso County, Texas: U.S. Geological Survey data release. **(C4)**

Texas Water Development Board (TWDB), 1997, Appendix C – G.I.S. coverages, metadata descriptions,[and] groundwater data sets on CD-ROM, with Water Quality map* insert on back-cover; *in* Hibbs and 9 others, Transboundary Aquifers of the El Paso/Ciudad Juárez/Las Cruces Region: U.S. Environmental Protection Agency, Region 6; Technical Contract Report- Interagency Contracts X-996343-01-0 and X-996350-01-0, prepared by the Texas Water Development Board and the New Mexico Water Resources Research Institute, variously paged. **Map includes Stiff diagrams color-coded for four total dissolved solids classes [0-1,000, 1,000-3,000, 3,000-5,000, and >5,000 mg/L] for more than 200 wells in Doña Ana and Otero Counties, NM; El Paso and Hudspeth Counties, TX, and contiguous parts of Chihuahua.* https://nmwrri.nmsu.edu/publications/publications.html **(F1, H2)**

Texas Water Development Board (TWDB), 2015, Brackish resources aquifer characterization system (BRACS): Texas Water Development Board Web site, http://www.twdb.texas.gov/innovativewater/bracs/ **(E2a)**

Thomas, H.E., and Leopold, L.B., 1964, Ground Water in North America: Science, v. 143, no. 3610, p. 1001-1003. **(C1, D1)**

Thompson, J.C., Kreitler, C.W., and Young, M.H., 2020, Exploring groundwater recoverability in Texas, maximum economically recoverable storage: Texas Water Journal, v. 11, no. 1, p. 152-171. **(D1, H3)**

Thompson, R.N., Ottley, C.J., Smith, P.M., Pearson, D.G., Dickin, A.P., Morrison, M.A., and Gibson, S.A., 2005, Source of the Quaternary alkalic basalts, picrites and basanites of the Potrillo Volcanic Field, New Mexico, USA: Lithosphere or convecting mantle?: Journal of Petrology, v. 46, issue 8, p. 1603-1643. **(C2b, C4)**

Thompson, R.S.C., Van Devender, T.R., Martin, P.S., Foppe, T., and Long, A., 1980, Shasta ground sloth. (*Nothrotheriops shastensis* Hoffstetter) at Shelter Cave, New Mexico: Environment and extinction: Quaternary Research, v. 14, p. 360-376. (**B2**, **C1**)

Thompson, S. III, 1982a, Oil and gas exploration wells in southwestern New Mexico, *in* Drewes, H, ed., Cordilleran overthrust belt, Texas to Arizona: Rocky Mountain Association of Geologists, Guidebook to Field Conference, v.1, p. 137-153. **(C2a)**

Thompson, S. III, 1982b, Oil and gas exploration wells in southwestern New Mexico, *in* Powers, R.B., ed., Geologic studies of the Cordilleran thrust belt: Rocky Mountain Association of Geologists Guidebook to Field Conference, v. 2, p. 521-536. **(C2a)**

Thompson, S. III, and Bieberman, R.A., 1975, Oil and gas exploration wells in Doña Ana County, New Mexico: New Mexico Geological Society Guidebook 26, p. 171-174. **(C2a)**
Thompson, S. III, Tovar, J.C., and Conley, J.N., 1978, Oil and gas exploration wells in the Pedregosa Basin: New Mexico Geological Society Guidebook 29, p. 331-342. **(C2a, F1)**
Thomson, B.M., and McQuillan, D.M., 1984, Nitrate contamination of groundwater in Albuquerque, *in* W.J. Stone, compiler, Selected papers on water quality and pollution in New Mexico: New Mexico Bureau of Mines and Mineral Resources, Hydrologic Report 7, p. 204-216. **(E2c)**
Thorn, C.R., McAda, D.P. and Kernodle, J.M., 1993, Geohydrologic framework and hydrologic conditions in the Albuquerque Basin, central New Mexico: U.S. Geological Survey, Water-Resources Investigations Report 93-4149, 106 p. (**D1, D2**)
Thornbury, W.D., 1965, Regional geomorphology of the United States: New York, John Wiley and Sons, 609 p. **(C)**
Tight, W.G., 1905, Bolson plains of the Southwest: American Geologist, v. 36, p. 271-284. **(C)**
Tillery, S., and King, J.P., 2006, MODFLOW-2000 Farm Package Case Study: Southern Rincon Valley, New Mexico: Technical Report prepared for the U.S. Army Corps of Engineers, New Mexico State University, Department of Civil & Geological Engineering, January 2006. **(H3)**
Tillery, S., Sheng, Z., King, J.P., Creel, B., Brown, C., Michelsen, A., Srinivasan, R., and Granados Olivas, A., 2009, The development of a coordinated database for water resources and flow model in the Paseo del Norte watershed (phase III) – Part II, availability of flow and water quality data for the Rio Grande Project area: New Mexico Water Resources Research Institute Report No. 348, Part II, and Texas Water Resources Institute Technical Report 359, Part II, 14 p https://nmwrri.nmsu.edu/publications/technical-reports/tr-reports/tr-348-i.html **(H2, H3)**
Tillman, F.D., Pool, D.R., and Leake, S.A., 2015, The effect of modeled recharge distribution on simulated groundwater availability and capture: Groundwater, v. 53, no. 3, p. 378-388. **(D2)**
Tolman, C.F., 1909, Erosion and deposition in southern Arizona bolson region: Journal of Geology, v. VII, no. II, p. 136-163. **(C2a, D1)**
Tolman, C.F., 1937, Ground Water: New York, McGraw-Hill Book Co., Inc. 593 p. **(A2, C, D1)**
Topper, R., and Rein, K.G., 2017, Considerations for subsurface water storage in Colorado: Rocky Mountain Water, May 2017, p. 22-25. **(E2b)**
Tovar-R, J., Vázques, H., Lozano, S., 1978, Interpretación integrada geológica-geofísica, porción norte de Chihuahua: Asociación Mexicana de Geólogos Petroleros, Boletín, Tomo XXX, p. 59-132. **(C2a, C4, F3)**
Towle, J.N., and Fitterman, D.V., 1975, Geomagnetic variations at Kilbourne Hole, New Mexico: New Mexico Geological Society Guidebook 26, p. 281. **(C4)**
Trauger, F.D., and Doty, G.C., 1965, Ground water – Its occurrence and relation to the economy and geology of southwestern New Mexico: New Mexico Geological Society Guidebook 16, p. 215-227. **(E2, F2, G2)**
Trauger, F.D., and Stoneman, D.L., 1975, Geohydrology of the Santa Teresa area, Doña Ana County, New Mexico: *prepared by* Earth Environmental Consultants, Inc., Albuquerque, NM *for* C.L. Crowder Investment Company, 44 p. *including tables and well logs* **(F2, H1, H2, H3)**
Turner, S., 2019, Study: Border agents, illegal crossings harm environment: Albuquerque Journal, Tuesday, September 24, 2019, p. A1, A5. **(A3)**
Turner, S., 2020a, 30 miles of replacement border wall complete in New Mexico: Albuquerque Journal – METR0 & NM, Saturday, February 29, 2020, p. A7, A8. **(A3)**
Turner, S., 2020b, Wildlife groups sue over border wall funding: Albuquerque Journal, Thursday, May 13, 2020, p. A6. **(A3)**
Underwood, J.R., Jr., 1980, Physiographic features, Trans-Pecos region: New Mexico Geological Society Guidebook 31, p. 57-58. **(C2a, F1)**
United States and Mexico, 1907, Convention between the United States and Mexico Equitable Distribution of the Waters of the Rio Grande: Signed at Washington, May 21, 1906: Ratification advised by the Senate, June 26, 1906; ratified by the President, December 26, 1906; ratified by Mexico, January 5, 1907; ratifications Exchanged at Washington, January 16, 1907, and proclaimed, January 16, 1907: Washington, DC; U.S. Government Printing Office, 3 p. **(E3, F1)**
U.S. Bureau of Reclamation (USBOR), 2011, Reclamation – Managing water in the West – Rio Grande Project. **(E2, F2)**
U.S. Census Bureau, 2015, American Fact Finder. **(E2)**
U.S. Center for Disease Control (CDC-MMWR), 1997, Epidemiologic notes and report on human led absorption – Texas: Morbidity and Mortality Weekly Report (MMWR), September 19, 1997, v. 46, no. 37, p. 871-877. **(E2c)**

U.S. Environmental Protection Agency (USEPA), 2003a, The Concentrated Animal Feeding Operation (CAFO) Revised Rule. **(E2c)**
U.S. Environmental Protection Agency (USEPA), 2003b, Standards for use or disposal of sewage sludge- Final Rule: EPA 40CFR, Part 503, 48, p. 851-852. **(E2c)**
U.S. Environmental Protection Agency (USEPA), 2015c, The third unregulated contaminant monitoring rule (UCMR3): data summary. **(E2c)**
U.S. Environmental Protection Agency (USEPA), 2019, Per- and polyfluoroalkyl substances (PFAS) action plan-EPA Publication 100K20002. **(E2c)**
U.S. Geological Survey, 1961, Surface water supply of the United States – Part 8, Western Gulf of Mexico basins; U.S. Geological Survey Water-Supply Paper 1612, p. 411-413. **(D1)**
U.S. Geological Survey, 1965, Magnitude and frequency of floods in the United States – Part 8, Western Gulf of Mexico basins; U.S. Geological Survey Water-Supply Paper 1682, p. 418-422. **(D1)**
U.S. Geological Survey, 2017, U.S. Geological Survey National Water Information System: https://dx.doi.org/10.5066/F7P55KJN **(D1, E2)**
US-MX TAA (United States-Mexico Transboundary Aquifer Act), 2006, Public Law no. 109-448, 120 Statute 3328, Cornell University Law School Legal Information Institute, p. S.214-15. https://www.law.cornell.edu/topn/united_states-mexico_transboundary_aquifer_assessment_act **(E3, F1)**
U.S. Natural Resources Committee, 1938, The Rio Grande Joint Investigation in the Upper Rio Grande Basin in Colorado, New Mexico, and Texas: Washington, D.C., U.S. Government Printing Office, 566 p. **(B3, D1, G1)**
U.S. Reclamation Service, 1914, Maps of Mesilla Valley, showing various known river channels: U.S. Department of Interior, Bureau of Reclamation, Rio Grande Project. **(B3, E1, G1)**
University of Texas, 2005, Rio Grande-Río Bravo studies: Center for Research in Water Resources, accessed July 2014 at https://www.census.gov/quickfacts/ **(E2, F1)**
Updegraff, C.D., and Gelhar, L.W., 1978, Parameter estimation for a lumped-parameter ground-water model of the Mesilla Valley, New Mexico: New Mexico Water Resources Research Institute Report No. 97, 69 p. https://nmwrri.nmsu.edu/publications/technical-reports/tr-reports/tr-097.html **(H3)**
Utton, A.E., 1983, Some International Aspects of Groundwater Development in the Mexico-United States Frontier Region: UNM School of Law, Natural Resources Center Report to The Governor's Law Study Committee, 58 p. **(E3, F1)**
Utton, A.E., 1996, Remarks made by Professor Al Utton upon receiving an award of appreciation at the 40th Annual Water Conference, *in* Ortega Klett, C.T., ed., Reaching the Limits: Stretching the Resources of the Lower Rio Grande, Proceedings of the 40th Annual New Mexico Water Conference: New Mexico Water Resources Research Institute Report No. 297, p. 7-12. **(E3, F1)**
Utton, A.E., and Atkinson, C.K., 1979, International groundwater management: The case for the Mexico-United States frontier: New Mexico Water Resources Research Institute Report No. 109, 130 p. https://nmwrri.nmsu.edu/publications/technical-reports/tr-reports/tr-109.html **(E3, F1)**
Utton, A.E., and Atkinson, C.K., 1981, International groundwater management: The case for the Mexico-United States frontier, *in* Teclaff, L.A., and Utton, A.E., eds., International Groundwater Law: New York, Oceana Publications, Inc., p. 175-188. **(E3, F1)**
Utton, A.E., and Atkinson, C.K., 1983, La Administración Internacional de Aguas Subterráneas: El Caso de la Región Fronteriza México-Estados Unidas: Boletín Mexicano de Derecho Comparado - UNAM Instituto de Investigación Jurídicas: Nuevo Serie, Año XVI, Mayo-Agosto de 1983, No. 47. **(E3, F1)**
Valdez, A., and Zimbelman, J.R., 2020, Great Sand Dunes, *in* Lancaster, N. and Hesp, P., eds., Inland Dunes of North America. Dunes of the World: Cham, Switz., Springer, p. 1-10. **(A2, C2b)**
Valentine, J.A., 2012, Adjudications: Managing water wars in New Mexico, *in* Ortega Klett, C.T., ed., One hundred years of water wars in New Mexico: Santa Fe, Sunstone Press, p. 29-51. **(E3)**
Van Denburgh, A.S., 1996, Memorial to John H. Feth: Geological Society of America Memorials, v. 27, December, 1965. *See Feth et al. 1961 and 1965, and Feth 1964.* **(A2)**
Vanderhill, J.B., 1986, Lithostratigraphy, vertebrate paleontology, and magnetostratigraphy of Plio-Pleistocene sediments in the Mesilla Basin, New Mexico: University of Texas at Austin, doctoral dissertation, 311 p. **(B1, C1, C2a)**
Van Devender, T.R., 1990, Late Quaternary vegetation and climate in the Chihuahuan Desert, United States and Mexico, *in* Betancourt, J.L., Van Devender, T.R., and Martin, P.S., eds., Packrat middens, the last 40,000 years of biotic change: University of Arizona Press, p. 104-133. **(B2, C1)**

Van Devender, T.R., 1995, Desert grassland history: Changing climates, evolution, biogeography, and community dynamics, *in* McClaren, M.P., and Van Devender, T.R., and Martin, P.S., eds., The desert grassland: University of Arizona Press, p. 68-99. **(B2, C1)**

Van Devender, T.R., Thompson, R.S., and Betancourt, J.L., 1987, Vegetation history of the deserts of southwestern North America: The nature and timing of the late Wisconsin-Holocene transition, *in* Ruddiman, W.F., and Wright, H.E., Jr., eds., North America and adjacent oceans since the last glaciation: Geological Society of America, p. 323-352. **(B2, C1)**

Van West, C.R., Windes, T.C., Levine, F., Grissino-Mayer, H.D., and Salzer, M.W., 2013, The role of climate in early Spanish-Native American interactions in the US Southwest, *in* Mathers, C., Mitchem, J.M., and Haecker, C.M., eds., Native and Spanish New Worlds – Sixteenth-Century Entradas in the American Southwest and Southeast (Amerind Studies in Anthropology Series): University of Arizona Press, p. 81-98. **(B2, C1)**

Vespermann, D., and Schmincke, H., 2000, Scoria cones and tuff rings, *in* Sigurdsson, H., ed., Encyclopedia of volcanoes, New York, Academic Press, p. 683-694. **(A1)**

Villagran, L. 2017a, Reflecting on my years of covering borderlands: Albuquerque Journal, Wednesday, June 14, 2017, p. A9, A16. **(A3)**

Villagran, L., 2017b, Two nations, one aquifer – Border water at risk: Albuquerque Journal, Sunday, June 25, 2017, p. A1, A8, A9. **(A3)**

Vitarelli, D.C., 2021, Eruptive volume, and explosion energy estimated from Kilbourne Hole Maar, south-central New Mexico (Abstract): New Mexico Geology, v. 43, no. 1, p. 12-13. **(C2b)**

Wade, S.C., and Reiter, M., 1994, Hydrothermal estimation of vertical ground-water flow, Canutillo, Texas: Ground Water, v. 32, no. 5, p. 735-742. **(C4, H3)**

Waggoner, W.K., 1990, Petrology and geochemistry of mantle-derived lavas from Potrillo maar, New Mexico: University of Texas at El Paso, Senior Honors thesis, 69 p. **(C2b, C4)**

Wagner, J.D.M., Cole, J.E., Beck, J.W., Patchett, P.J., Henderson, G.M., Barnett, H.R., 2010. Moisture variability in the southwestern United States linked to abrupt glacial climate change. Nature Geoscience, v. 3, p. 110-113. **(B2, C1)**

Wahi, A.K., Hogan, J.F., Ekwurzel, B., Baillie, M.N., Eastoe, C.J., 2008. Geochemical quantification of semiarid mountain recharge. Ground Water v. 46, p. 414-425. **(D2, H2, H3)**

Walker, J.D., and Geissman, J.W., compilers, 2009, Commentary – 2009 Geologic Time Scale: GSA Today, v. 19, no. 4/5, p. 60-61. **(B1)**

Walker, J.S., Brown, C., and Fernald, S., 2015, Use of the *DRASTIC* Model to evaluate groundwater pollution sensitivity from on-site wastewater systems in the Mesilla Basin: New Mexico Water Resources Research Institute Report No. 367, 98 p. https://nmwrri.nmsu.edu/publications/technical-reports/tr-reports/tr-367.html **(E2c)**

Walker, M.J.C., Head, M.J., Berkelhammer, M., Bjorck, S., Cheng, H., Cwynar, L., et al., 2018, Formal ratification of the subdivision of the Holocene Series/Epoch (Quaternary System/Period): two new Global Boundary Stratotype Sections and Points (GSSPs) and three new stages/subseries: Episodes, v. 41, no. 4, p. 213-223. **(B1, B2, C1)**

Waltemeyer, S.D., 2001, Estimates of mountain-front streamflow available for potential recharge to the Tularosa Basin, New Mexico: U.S. Geological Survey Water-Resources Investigations Report 01-4013, 8 p. **(D1, D2)**

Waltemeyer, S.D., 2008, Analysis of the magnitude and frequency of peak discharge and maximum observed peak discharge in New Mexico and surrounding areas: U.S. Geological Survey Scientific Investigations Report 2008-5119, 105 p. **(D1, D2)**

Walton, J., Ohlmacher, G., Utz, D., and Kutianawala, M., 1999, Response of the Rio Grande and shallow ground water in the Mesilla Bolson to irrigation, climate stress, and pumping: Environmental & Engineering Geoscience, v. 5, no. 1, p. 41-50. **(H2, H3)**

Wang, L., Jiang, W.Y., Jiang, D.B., Zou, Y.F., Liu, Y.Y., Zhang, E.L., Hao, Q.Z., Zhang, D.G., Zhang, D.T., Peng, Z.Y., Xu, B., Yang, X.D., and Lu, H.Y., 2018, Prolonged heavy snowfall during the Younger Dryas: Journal of Geophysical Research: Atmospheres, v. 123, no. 24. **(A2, C1)**

Ward, F.A., 1998, Economics of water conservation, *in* Herrera, E., Bahr, T.G., Ortega Klett, C.T., and Creel, B.J., eds., Water resources issues in New Mexico: New Mexico Journal of Science, v. 38. p. 127-139. https://nmwrri.nmsu.edu/publications/miscellaneous-reports/m-documents/m26.pdf **(E2)**

Ward, F.A., Mayer, A.S., Garnica, L.A., Townsend, N.T., and Gutzler, D.S., 2019, The economics of aquifer protection plans under climate water stress: New insights from hydroeconomic modeling: Journal of Hydrology, v. 576, 667-684. **(E2)**

Wasiolek, M., 1995, Subsurface recharge to the Tesuque aquifer system from selected drainage basins along the western side of the Sangre de Cristo Mountains near Santa Fe, New Mexico. U.S. Geological Survey Water Resources Investigations Report 94-4072, 43 p. **(D2, H3)**

Webb, D.S., 1969, Facets the geology of the Sierra del Presidio area, north-central Chihuahua: New Mexico Geological Society Guidebook 20, p. 182-186. **(C2a)**

Weber, D.J., 1982, The Mexican frontier 1821-1846: The American Southwest under Mexico: University of New Mexico Press, 416 p., ISBN 0-8263-0603-9 **(B3)**

Weber, R.H., 1964, Cenozoic volcanic rocks of Socorro County: New Mexico Geological Society Guidebook 14, p. 132-143. **(C2a)**

Weissmann, G., Hartley, A., and Nichols, G., 2011, Alluvial facies distribution in continental sedimentary basins – Distributive fluvial systems, *in* Davidson, S., Leleu, S., and North, C., eds., Rock to rock record: The preservation of fluvial sediments and their subsequent interpretation: SEPM (Society for Sedimentary Geology), v. 79, p. 327-355. ISBN: 978-1-56576-305 **(D1)**

Wen, C-L., 1983, A study of bolson-fill thickness in the southern Rio Grande rift, southern New Mexico, west Texas and northern Chihuahua: University of Texas at Austin, master's thesis, 74 p. **(C4, F1)**

West, F., 1996, The Mesilla Valley: A century of water resources investigations, *in* Ortega Klett, C.T., ed., Reaching the Limits: Stretching the Resources of the Lower Rio Grande, Proceedings of the 40th Annual New Mexico Water Conference: New Mexico Water Resources Research Institute Report No. 297, p. 21-28. **(D1, H3)**

Western Water Assessment (WWA), 2009, Rio Grande TreeFlow 2008 Tree-ring reconstruction of streamflow and climate for the Rio Grande basin and adjacent basins [including Rio Grande near Otowi, NM from 1450-2002]: University of Colorado at Boulder. **(B2, B3, C1, D1)**

Whitworth, T.M., 1995, Hydrochemical computer modeling of proposed artificial recharge of the upper Santa Fe Group aquifer, Albuquerque New Mexico: New Mexico Geology, v. 17, no. 4, p. 72-78. **(D2, E2b)**

Wierenga, P.J., 1979, Soil salinity and cotton yields as affected by surface and trickle irrigation: New Mexico Water Resources Research Institute Report No. 106, 212 p. https://nmwrri.nmsu.edu/publications/technical-reports/tr-reports/tr-106.html **(H2, H3)**

Wierenga, P.J., Hills, R.G., and Hudson, D.B., 1991, The Las Cruces Trench Site: Experimental Results and One-Dimensional Flow Predictions. Water Resources Research, v. 27, p. 2695-2705. **(D2, H3)**

Wierenga, P.J., Hudson, D.B., Hills, R.G., Porro, I., Kirkland, M.R., and Vinson, J., 1990, Flow and Transport at the Las Cruces Trench Site; Experiment 1 and 2: U.S. Nuclear Regulatory Commission Report, NUREG/CR-5607, 413 p. **(D2, H3)**

Wilkins, D.W., 1986, Geohydrology of the Southwest Alluvial Basins, Regional Aquifer-systems analysis in parts of Colorado, New Mexico, and Texas: U.S. Geological Survey Water Resources Investigations Report 84-4224, 61 p. **(D1, F2)**

Wilkins, D.W., 1998, Summary of the southwest alluvial basins regional aquifer-system analysis in parts of Colorado, New Mexico, and Texas: U.S. Geological Survey Professional Paper 1407-A, 49 p. **(D1, F2)**

Williams, A.P., Cook, E.R., Smerdon, J.E., Cook, B.I., Abotzoglou, J.T., Bolles, K., Baek, S.H., Badger, A.M., and Livneh, B., 2020a, Large contribution from anthropogenic warming to an emerging North American megadrought: Science, v. 368, issue 6488, p. 314-318. **(B3, C1)**

Williams, T.R., and Bedinger, M.S., 1984, Selected geologic and hydrologic characteristics of the Basin and Range province, western United States--Pleistocene lakes and marshes: U.S. Geological Survey Miscellaneous Investigations Series Map I-1522-D, scale 1:2,500,000. **(I1)**

Williams, W.J.W., 1999, Evolution of Quaternary intraplate mafic lavas using ^{3}He surface exposure and ^{40}Ar/^{39}Ar dating, and detailed elemental He, Sr, Nd, and Pb isotopic signatures: Potrillo Volcanic Field, New Mexico, U.S.A., and San Quintín Volcanic Field, Baja California Norte, México: University of Texas at El Paso, doctoral dissertation, 195 p. **(B1, C2b, C4)**

Williams, W.J.W., and Poths, J., 1994, The Potrillo Volcanic Field, southern Rio Grande rift: ^{3}He surface exposure dates and petrogenetic considerations: New Mexico Geology, v. 16, p. 81. **(B1, C2b, C4)**

Wilson, C.A., and White, R.R., 1984, Geohydrology of the central Mesilla Valley, Doña Ana County, New Mexico: U.S. Geological Survey, Water-resources Investigations Report 82-444, 144 p. **(H1, H2)**

Wilson, C.A., White, R.R., Orr, B.R., and Roybal, R.G., 1981, Water resources of the Rincon and Mesilla Valleys and adjacent areas, New Mexico: New Mexico State Engineer Technical Report 43, 514 p. **(H1, H2)**

Wilson, J.L., and Guane, H., 2004, Mountain-block hydrology and mountain-front recharge, *in* Groundwater recharge in a desert environment: the southwestern United States: Washington, DC, American Geophysical Union, Water Science and Application 9, p. 113-137. **(D2)**
Wilson, L., 1981, Potential for ground-water pollution in New Mexico: New Mexico Geological Society, Special Publication No. 10, p. 47-54. **(E2c)**
Wilson, L., Anderson, S.T., Jenkins, D.N., and Cristiano, C., 1979, Program for the statewide monitoring of ground-water quality in New Mexico: unpublished final report on file in the office of New Mexico Environmental Improvement Division, Santa Fe, New Mexico, 180 p. **(E2c)**
Winograd, I.J., and Thordarson, W., 1975, Hydrogeologic and hydrogeochemical framework, South-Central Great Basin, Nevada-California, with special reference to the Nevada Test Site: U.S. Geological Survey Professional Paper 712-C, 126 p. **(D1)**
Witcher, J.C., 1988, Geothermal resources of southwestern New Mexico: New Mexico Geological Society Guidebook 39, p. 191-197. **(C4, F2, H2, H3)**
Witcher, J.C., 1995, A geothermal resource database of New Mexico. Southwest Technology Development Institute, New Mexico State University, 28 p. **(C4, H1, H2)**
Witcher, J.C., 1998, The Rincon SLH 1 geothermal well: New Mexico Geological Society Guidebook 49, p. 35-40. **(C2b, C4, H1, H2)**
Witcher, J.C., 2010, Geothermal greenhouse heating at Radium Springs, New Mexico: New Mexico Bureau of Geology and Mineral Resources, Lite Geology, p. 12-13. **(C4, H2)**
Witcher, J.C., and Mack, G.H., 2018, Masson Farm Geothermal Greenhouses at Radium Springs: Third-day (C) Road Log from Las Cruces to Geothermal Greenhouses of the Masson Farm at Radium Springs: N.M. Geological Society Guidebook 69, p. 47-51. **(C2b, C4, H2)**
Witcher, J.C., King, J.P., Hawley, J.W., Kennedy, J.F., Williams, J., Cleary, M., and Bothern, L., 2004, Sources of Salinity in the Rio Grande and Mesilla Basin Groundwater: New Mexico Water Resources Research Institute Report No. 330, 168 p., with appendices and plates on CD ROM. https://nmwrri.nmsu.edu/publications/technical-reports/tr-reports/tr-330.html **(C2b, E2a, H1, H2)**
Wolf, C., Ewing, A., and Yuhas, K. (Abstract), 2020, Securing water supply for Albuquerque, New Mexico using managed aquifer recharge: Program with abstracts, Water, Energy, and Policy in a Changing Climate Conference, National Groundwater Association (NGWA), Albuquerque, NM, February 24-25, 2020. **(E2b)**
Wood, M.K., 2012, Future water wars in New Mexico, *in* Ortega Klett, C.T., ed., One hundred years of water wars in New Mexico: Santa Fe, Sunstone Press, p. 262-282. ISBN: 978-0-86524-902-5 **(E3)**
Woodburne, M.O., and Swisher, C.C. III, 1995, Land mammal high resolution geochronology, intercontinental overland dispersals, sea level, climate, and vicariance, *in* Geochronology, time scales, and global stratigraphic correlation: SEPM Special Publication, no. 54, p. 335-364. **(B1, B2, C1)**
Woodward, D., and Duval R., 1996, United States-Mexico Border Area, as delineated by a shared-water resource perspective - Fact sheet 1: United States Department of the Interior U.S.-Mexico Border Field Coordinating Committee, 4 p. **(E2, F1)**
Woodward, D.G., and Myers, R.G., 1997, Seismic investigation of the buried horst between the Jornada del Muerto and Mesilla ground-water basins near Las Cruces, Doña Ana County, New Mexico: U.S. Geological Survey Water-Resources Investigations Report 97-4147, 45 p. **(C4, H1)**
Woodward, L.A., Callender, J.F., Seager, W.R., Chapin, C.E., Gries, J.C., Schaffer, W.L. and Zilinski, R.E., 1978, Tectonic map of the Rio Grande rift region in New Mexico, Chihuahua, and Texas, *in* Hawley, J.W., compiler, Guidebook to the Rio Grande rift in New Mexico and Colorado: New Mexico Bureau of Mines and Mineral Resources Circular 163, Sheet 2, approx. scale 1:1,000,000. **(C2a)**
Worrall, F., and Kolpin, D.W., 2004, Aquifer vulnerability to pesticide pollution – Combining soil, landuse and aquifer properties with molecular descriptors: Journal of Hydrology, v. 293, no. 1-4, p. 191-204. **(E2c)**
Wright, H.E., Jr., 1946, Tertiary and Quaternary geology of the lower Puerco area, New Mexico: Geological Society of America Bulletin, v. 57, p. 383-456. **(G2)**
Yeh, T.C. (T.-C. Jim), Khaleel, R., and Carroll, K.C., 2015, Flow through heterogeneous geologic media: New York, Cambridge University Pres., 343 p. ISBN 978-1-107-07613-6 **(A1, D2)**
York, J.C., and Dick-Peddie, W.A., 1969, Vegetation changes in southern New Mexico during the past hundred years, *in* McGinnies, W.G. and Goldman, B.J., Arid lands in perspective: University of Arizona Press, p. 155-166. **(B3, C1)**
Zalasiewicz, J., Waters, C.N., Williams, M., and Summerhayes, C., eds., 2019. The Anthropocene as a geological time unit: A guide to the scientific evidence and current debate, Cambridge University Press, 361 p. **(B1, B2, B3, C1, D1)**

Zalasiewicz, J., Waters, C.N., Ellis, E.C., Head, M.J., Vidas, D., Steffen, W., Thomas, J.A., Horn, A., Summerhayes, C., Leinfelder, R., McNeill, J.R., Gałuszka, A., Williams, M., Barnosky, A.D., Richter, D. deB., Gibbard, P.L., Syvitski, J., Jeandel, C., Cearreta, A., Cundy, A.B., Fairchild, I.J., Rose, N.L., Ivar do Sul, J.A., Shotyk, W., Turner, S., Wagreich, M., and Zinke J., 2021, The Anthropocene: comparing its meaning in geology (chronostratigraphy) with conceptual approaches arising in other disciplines: AGUPUBS Online Library, Wiley.com, 44 p. **(B1, B2, B3, C1, D1)**

Zohdy, A.A.R., Bisdorf, R.J., and Gates, J.S., 1976, Schlumberger soundings in the lower Mesilla Valley of the Rio Grande, Texas and New Mexico: U.S. Geological Survey Open-File Report 76-324, 77 p. *See Al-Garni 1996.* **(C4)**

Zohdy, A.A.R., Jackson, D.B., Mattick, R.E., and Peterson, D.L., 1969, Geophysical survey for ground water at White Sands Missile Range, New Mexico: U.S. Geological Survey Open-File Report 69-326, 144 p. **(C4)**

Zwanzinger, J.A., 1990a, Nuevos conceptos de la estratigrafía mesozoica de Chihuahua, *in* Goodell, P.C., García-Gutiérrez, C., and Reyes-Cortés, I., eds., Symposium on Energy Resources of the Chihuahua Desert: Universidad Autónoma de Chihuahua, Chihuahua, México. **(C2b, F3)**

Zwanzinger, J.A., 1992, New concepts in Mesozoic stratigraphy of Chihuahua, *in* Goodell, P.C., Garcia-Gutiérrez, C., and Reyes-Cortés, I., eds., Energy Resources of the Chihuahua Desert region: El Paso Geological Society, p. 77-124. **(C2b, F3)**

APPENDIX B Topic/Subtopic Categories, with Alphanumeric Cross-Reference Codes

A. Bibliographies, Dictionaries, Glossaries, Biographies, Reviews, and News Items
- A1. Bibliographies, Dictionaries, and Glossaries
- A2. Biographies and Reviews
- A3. News Items

B. Time: Geologic, Prehistoric, and Historic
- B1. Geologic and Prehistoric Time
- B2. Prehistoric Perspective: US Southwest and Northern Mexico
- B3. Historic Perspective: US Southwest and Northern Mexico

C. Environmental, Physiographic, and Geologic Setting
- C1. Climatic, Hydrographic, Ecologic, and Paleoenvironmental Setting
- C2. Geologic and Geomorphic Setting
  - C2a. Geologic and Geomorphic Setting: Pre-1990
  - C2b. Geologic and Geomorphic Setting: Post-1989
- C3. Soil-Geomorphic Relationships and Soil Surveys
- C4. Geophysical/Geochemical Data and Interpretations

D. Basic Hydrogeologic Concepts
- D1. Conceptual Models, Definitions, and Regional Overviews
- D2. Groundwater-Flow Systems, Including Recharge

E. GIS/Remote Sensing and GW-Resource Management/Planning
- E1. GIS/Remote Sensing
- E2. Resource Management/Planning
  - E2a. Desalination
  - E2b. Recharge and Recovery
  - E2c. Groundwater-Quality Projection and Waste Management
- E3. Legal and Environmental Issues and Constraints

F. Transboundary Regional Hydrogeology and Geohydrology
- F1. Binational
- F2. USA
- F3. México

G. Early Documents on Mesilla Basin Regional Aquifer Systems (1858-1970)
- G1. 1858 to 1935
- G2. 1935 to 1970

H. Contemporary Documents on Mesilla Basin Regional Aquifer Systems
- H1. Hydrogeology
- H2. Hydrochemistry
- H3. Flow Models

I. Paleohydrology: Ancestral Fluvial and Pluvial Lake Systems
- I1. Regional Overviews
- I2. Transboundary Region Paleohydrologic Systems
- I3. Evolution of the Rio Grande Fluvial System